12-11-2013 12:00 AM

Potential for Measurement of Mesospheric Ozone Density from Overdense Meteor Trains with a Monostatic Meteor Radar

Reynold E. Sukara
The University of Western Ontario

Supervisor
Dr. Wayne Hocking
The University of Western Ontario

Graduate Program in Physics
A thesis submitted in partial fulfillment of the requirements for the degree in Master of Science

Potential for Measurement of Mesospheric Ozone Density from Overdense Meteor Trains with a Monostatic Meteor Radar

(Thesis format: Monograph)

by

Reynold E. Sukara

Department of Physics and Astronomy
Graduate Program in Physics

A thesis submitted in partial fulfillment
of the requirements for the degree of
Master of Science

The School of Graduate and Postdoctoral Studies
The University of Western Ontario
London, Ontario, Canada

Abstract

Thermally ablating meteoroids, colliding with the Earth's atmosphere, leave a high temperature trail containing extremely energetic metallic ions and electrons. A well recognized, but unresolved, anomaly associated with ambipolar diffusion of meteor trains, which is more dominant in overdense meteors, takes place in the initial post-adiabatic train expansion. In this work, a newly proposed mechanism explaining this anomaly involving hyperthermal chemical reactions is presented. Data from the SKiYMET meteor radar system, deployed at latitudinally dispersed locations, were used to determine ozone density in the upper atmosphere by analyzing diffusion of overdense meteor trains. The results obtained in this study are in line with satellite measurements of ozone density. Moreover, it was demonstrated that backscatter can detect a direct signature of the newly discovered hyperthermal chemical reactions in overdense meteor trains. The hypothesis proposed in this thesis, suggesting the possibility of measuring the upper atmosphere ozone density using backscatter radar, has been validated.

Key words: ozone, radar, overdense meteors, mesosphere, hyperthermal chemistry, ambipolar diffusion

Dedication

To my Family

Acknowledgments

Finally a part of the journey is over. While the old adage says that it is not the destination, but the journey that matters, I would respectfully disagree with it. Not because it is incorrect, but because in the world we live in, it is only numbers and results that matter, and not much else. That being said, doing another master's degree, this time in the Department of Physics and Astronomy at Western, has taught me many things, but most of them not related to physics.

I am grateful to my family for their patience and support. Next, I am grateful to my supervisor, Dr. Wayne K. Hocking, for trusting me with the project of this magnitude and difficulty, for giving me the opportunity to do it in the first place and for many productive discussions. I also extend my thanks my advisory committee, Dr. John deBruyn and Dr. Richard Holt.

I would like to thank those who I think also contributed to the work and results in this thesis, directly or indirectly, whether they know it or not. Thus, first I would like to acknowledge IACPES, York University, without whose financial support this project would not have been possible, and Carol Weldon, the program coordinator. Next, I would like to thank Dr. Jack Baggaley (New Zealand), who despite serious health problems was maintaining communication with me. On the same note, I want to acknowledge kindness and professionalism of Dr. Richard Wayne (UK), Dr. Shaun Carl (Belgium), Dr. Yutaka Matsumi (Japan) and Dr. James Burkholder (US) who tried to help me with O(1D) chemistry. If I ever end up in academia, these guys are true role models. Special thanks go to Dr. John Plane in UK for his immense help when discussing the O_2 (delta) chemistry. I would like to sincerely thank Dr. Anne Smith for her help and kindness to provide ozone satellite data from Smith et al. (2013). In addition, I would like to thank Dr. David Tarasick for his help in putting me in touch with Dr. Smith.

I do not want to forget to thank Dr. Secco for offering me to start my PhD with him immediately after the completion of this project.

My thanks also goes to Marcial Garbanzo for his advice when it comes to programing. Last but not least, I would also like to emphasize the multifaceted role of the administrative personnel in the Physics Department, especially Jodi and Clara. Thank you for your kindness and support.

Table of Contents

List of Tables

List of Figures

List of Appendices

Chapter 1

If we knew what it is we were doing,
it would not be called research, would it?

- Albert Einstein

1. Introduction and Background

1.1 History

The study of meteors and associated phenomena is not a recent undertaking. Ancient peoples, from the old to the new world have been closely aware of the "falling stars" which played a significant role in many aspects of people's lives as documented in ancient religious and similar texts (e.g. Figure 1.1).

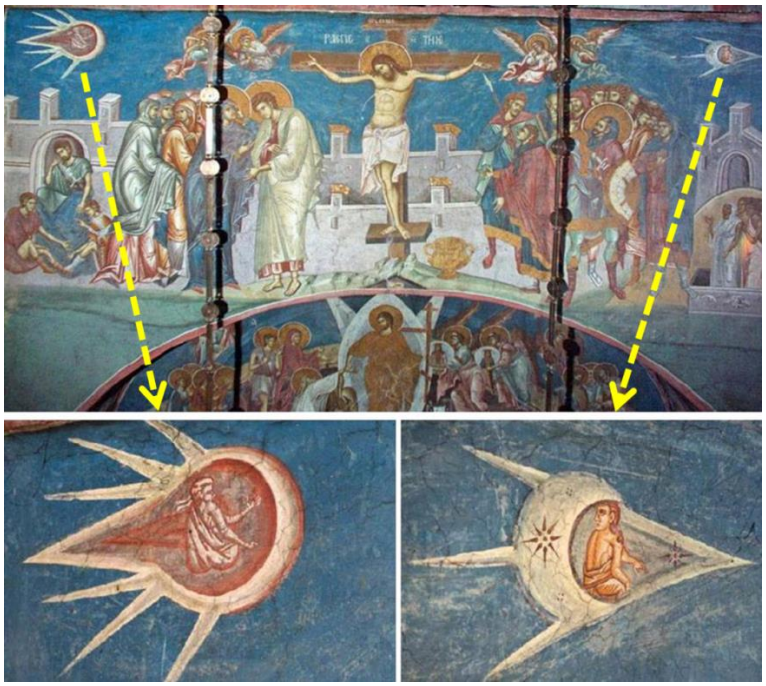

Figure 1.1: Strange religious fresco entitled "The Crucifixion" from Serbian Monastery Decani, Kosovo, painted in 1350 by an unknown artist, likely depicting the religious interpretation of the observed meteor phenomena (Credit: http://www.xfacts.com/old/).

In more recent history, the extensive renewed interest for meteor research was initiated by the spectacular Leonid meteor storm of 1833 (Burke, 1986) (Figure 1.2).

Figure 1.2: A famous depiction of the November 13, 1833 meteor storm. The original painting was executed around 1887 by the Swiss painter Karl Jauslin under the instructions of the Seventh-day Adventist minister Joseph Harvey Waggoner, who had witnessed the storm from rural eastern Pennsylvania when he was aged 13. The figure shows the Adolf Völlmy engraving that was published in April 1888 in The *Signs of the Times*, a weekly publication of the Seventh-day Adventist Church. The association of the Leonid storm with the apocalyptic opening of the sixth seal (Revelation 6.13 and Matthew 24.3) was stressed (Credit: http://star.arm.ac.uk/leonid/).

However, it was not until the advent of the modern observational and experimental techniques, such as radar, that has enabled revolutionary understanding of the meteor phenomena, its origins and dynamics. Maxwell's ground-breaking work on electricity and magnetism, followed by Hertz's confirmation of the existence of the radio waves in 1887 and the subsequent radio work of Marconi led Heaviside and Kennelly to propose the existence of the conductive layer in the upper atmosphere that we know today as the ionosphere.

The first radar device to monitor the ionosphere was constructed by the Breit and Tuve in 1926, and it can be said that ionospheric research was instrumental in further development and evolution of the meteor radar. Meteor observations using radar were first conducted in the 1940s. However, it was not until the World War II that radar research experienced the fastest development following the invention of magnetron cavity by British scientists. When Edward Appleton and his team from the Radio Research Board of the British Department of Scientific and Industrial Research used war-surplus radar to study meteors, it opened a new page in meteor research. They concluded that meteors cause abnormal bursts of ionization as they enter the ionosphere (Appleton and Naismith, 1947), thereby confirming the Hantaro Nagaoka hypothesis about meteors and the ionosphere (Nagaoka, 1929). Following the World War II, pioneers like Sir Bernard Lovell, John A. Clegg, John G. Davies, and in Canada, Donald R. W. McKinley and Peter M. Millman among others in the field paved the way for the modern research of meteors using radar techniques. During the early fifties, meteor trails were being used to investigate the high altitude winds, turbulence and even used in long distance meteor burst communication (Weitzen and Ralston, 1988).

This brief historical note does not do justice to all of the pioneers who contributed to the development of radar and its application to meteor research. Therefore, interested readers are directed to several outstanding historical review texts of the radar research by Hey and Stewart (1947), Swords (1986), Buderi (1996) and Watson (2009). Additionally, two comprehensive reviews of the historical meteor research by Kirinov (1960) and Burke (1982) in addition to McKinley (1961) are recommended for a further reading.

1.2 Meteor Fundamentals

The interplanetary space in the solar system is not an empty void. It is filled with cosmic dust and particles of various sizes (Brownlee, 1985) that frequently cross paths with Earth's orbit and subsequently enter the atmosphere at speeds ranging from 11.5 km/s to 72.5 km/s (Baggaley, 2002). However, most particles enter the atmosphere at speeds ranging from 15 km/s to 35 km/s. A particle moving through space, prior to entering the Earth's atmosphere, is defined as a meteoroid. There are two primary sources of meteoroids impacting the Earth's atmosphere (Ceplecha et al., 1998; Williams, 2002). The first one is sublimating comets as they orbit the sun and are responsible for periodic meteor showers. The second source of meteoroids, which may substantially vary in sizes and composition, and which cross Earth's orbit intermittently, originates from the asteroid belt (Figure 1.3), beyond Mars (Murad and Williams, 2002) and share the orbital plane with the planetary bodies in the solar system.

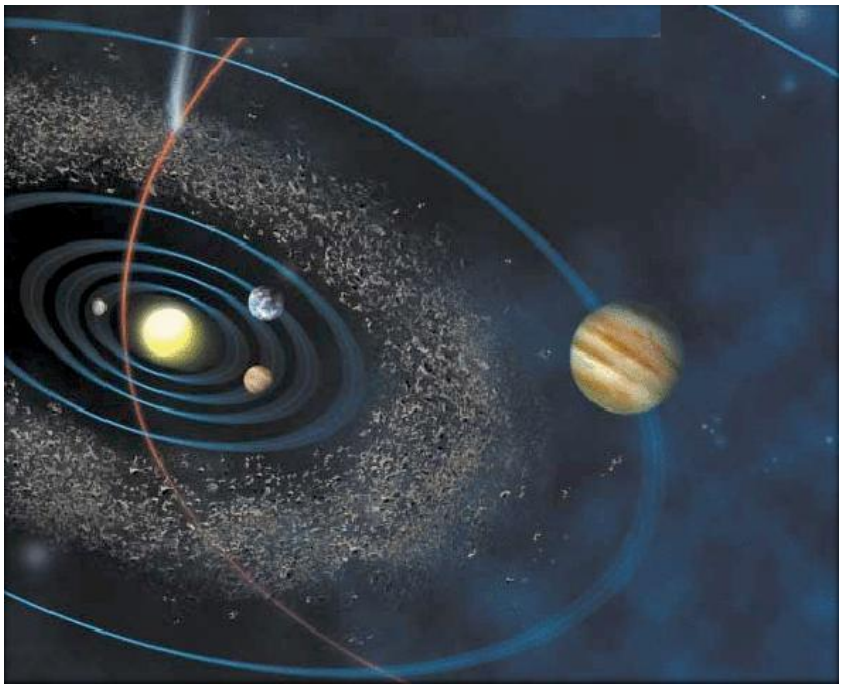

Figure 1.3: Illustrative representation of the asteroid and cometary sources of meteoroids (http://www.britastro.org/radio/projects/DM-Meteor.temp/meteors.html).

Upon entering the Earth's atmosphere, a meteoroid's hypervelocity collisions with the atmospheric constituents cause frictional heating, resulting in sputtering, evaporation, ablation and fragmentation among the primary ways of meteoroid mass loss. The luminous phenomena that results from collisional de-excitation of the ablated meteoroid atoms and excited atmospheric molecules are defined as *meteors*, a term that originates from ancient Greek and means "*things in the air*". In cases when the meteoroid is sufficiently big, and when it does not burn up in the atmosphere and reaches the ground, it is designated as a meteorite (Figure 1.4).

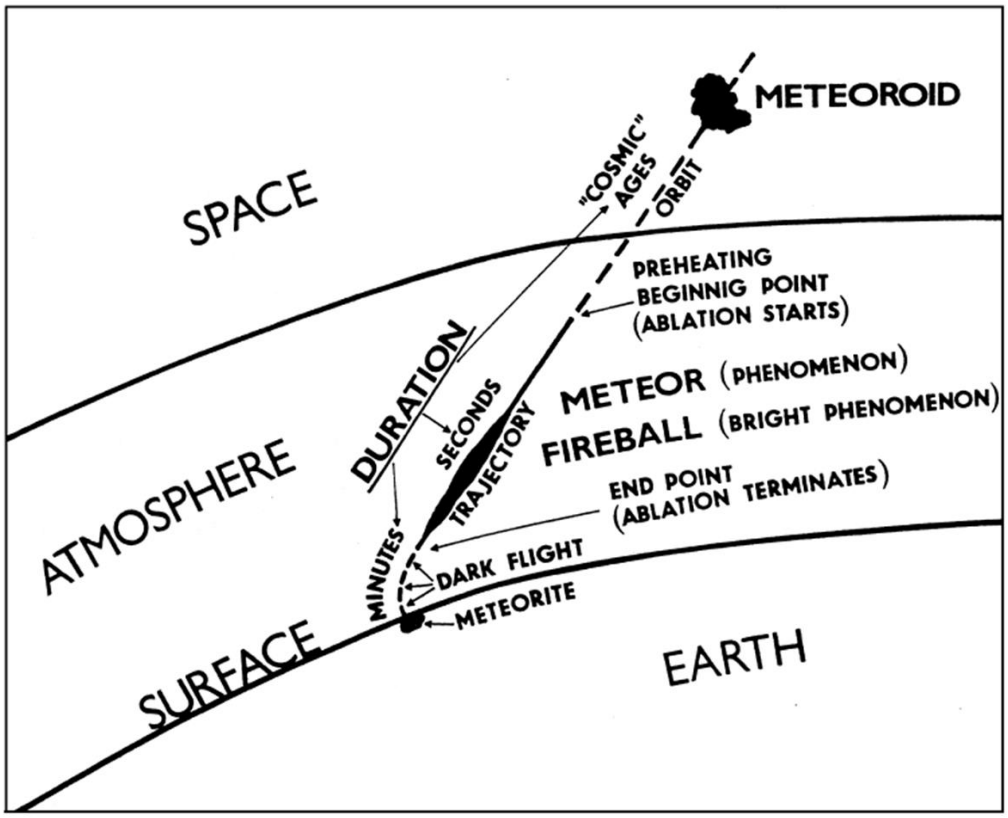

Figure 1.4: Basic terminology for meteors (Ceplecha et al. 1998).

The role of the Poynting-Robertson effect (Wyatt and Whipple, 1950) and the radiation pressure, while very small, contribute to the influx of the Earth's crossing particles. The primary classification arranges meteors into two groups: (i) meteor showers which have spatially and temporally repeating properties, and (ii) sporadic meteors, which are

considered dominant in numbers and in atmospheric mass influx. An apparent diurnal variation in meteor numbers occurs because of the Earth's daily rotation along its orbit, where meteors are swept up in highest numbers during the early morning hours (Figure 1.5).

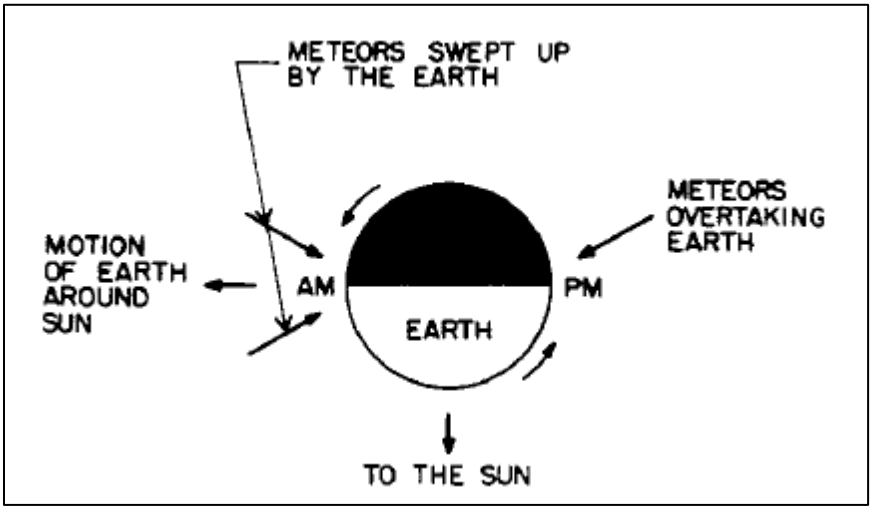

Figure 1.5: Diurnal variation of meteor rates. In the evening only meteors overtaking Earth are observed and in the morning, meteors with orbital directions opposite to that of Earth and the showers with the same orbital direction are observed (from Sugar, 1964).

While the estimates of the mass influx of the space dust and debris entering the atmosphere vary considerably (McBride et al., 1999), recent conservative estimates suggest that about 200,000 t/year of extra-terrestrial material enters Earth's atmosphere daily (Hughes, 1997).

Depending on the mass, velocity and primarily composition, preheating of the particle in the Earth's atmosphere begins at around 150 km. However the ablation and resulting luminous phenomenon occur between 60 and 120 km (Figure 1.6).

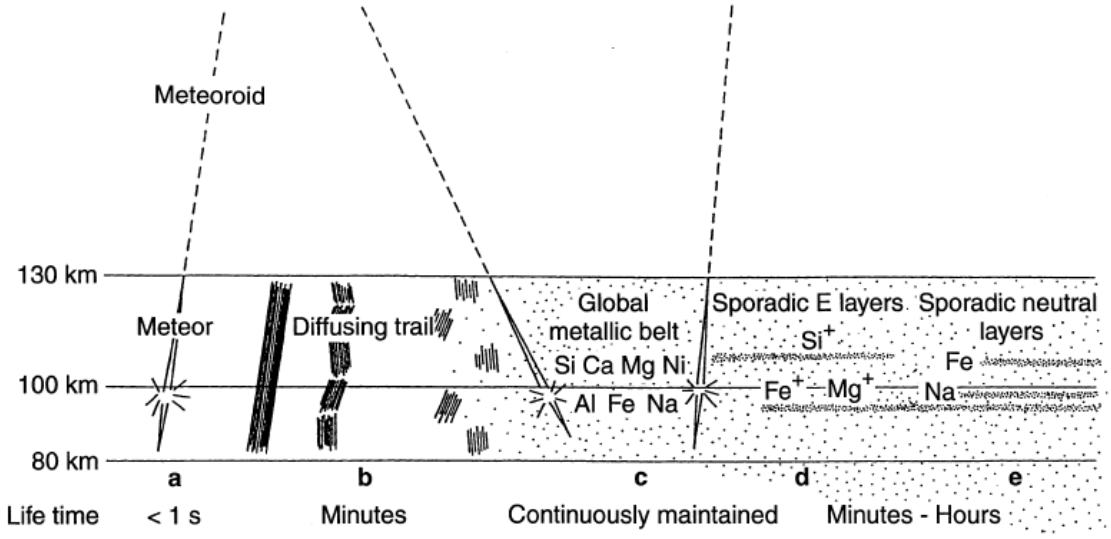

Figure 1.6: The illustration of the process of meteoroid ablation and particle deposition in the atmosphere. a) The ablation process resulting in luminous phenomena. b) The meteor trail can be observed for minutes, depending on the mode of observation. c) The constant influx of the particles and dust maintains continuous metallic layer in the upper atmosphere. d) Illustration of the downward drift of the metallic layer constituents. d) Formation of ionized sporadic E layers as a result of the downward transport of the ionized particles. e) Sporadic neutral layer can from simultaneously (Pellinen-Wannberg et al. 1998).

Meteors are observed and studied by visual techniques, lidar, satellites, rockets (meteor trails) and radar, which is the primary instrument used for data collection in this study. The substantial review of the mentioned methods is given in McKinley (1961) and Murad and Williams (2002). Here, however, only a review of radar theory and methods will be given further consideration as a primary tool of this study. Notably, while all the mentioned methods have their advantages and drawbacks, radar is the Swiss army knife of meteor study, as it collects data continuously and it is not weather dependant. Moreover, it is an excellent tool for the monitoring of meteor mass influx, altitudes, trajectories and velocities. Radar can observe ablating meteoroids down to the lower limit of 80 μm in size (Pellinen-Wannberg et al. 1998), as these are still large enough to generate the required ionisation trails. These very small particles, during the process of ablation and ionized trail formation, are generally considered underdense meteors, and

will be discussed later in the text; however they are not the focus of this work. In general, particles smaller than 20 μm reradiate the heat more efficiently and never reach temperatures required for melting and ablation. Beside its primary role, meteor radar has been used to investigate the turbulence and gravity waves in the mesosphere, and has been utilized by Hocking et al. (1997) and Hocking (1999) who has developed a novel technique of measuring temperature in the region of the mesopause boundary. Moreover, meteor trains observed by radar, allow measurements of the complex dynamics in the upper atmosphere (Marsh and Baggaley, 2001).

While most particles impacting the Earth's atmosphere are below 10^{-3} m, the peak in the size distribution is around 10^{-4} m (Kalashnikova, 2000; Havnes and Sigernes, 2005). For the meteoroids with velocities in excess of 30 km/s the heights with the strongest ablation are between 90 and 105 km, while in the lower speed regime below 30 km/s most ablation occurs between 75 and 90 km.

In simple terms, the meteor trail consists of ions and electrons, where the former are responsible for the reflection of radio waves, thus enabling the radar detection. Below 95 km in altitude, beside the ionic diffusion, which is the primary mechanism of the trail expansion, the chemistry plays a significant role in removal of electrons from the meteor train. The collisional deionization and complex set of chemical processes and reaction with the atmospheric constituents are still subject of great interest in the scientific community. Coinciding with the meteor region between 80 km and 95 km altitude is the secondary ozone maxima, exhibiting significantly increased concentration of O_3 which diverges from theoretical predictions. Owing to its high reactivity, ozone chemically interacts with the ions in the meteor trail and consequently plays an instrumental role in the removal of electrons through the set of relatively fast proceeding chemical reactions which are height and subsequently density dependent.

Consequently, chemical interaction between metallic ions in primarily overdense meteor trains and ambient atmosphere, especially ozone, contributing to the accelerated removal of electrons from the meteor trail and significantly exceeding the rates of ionic (or

hereafter referred as ambipolar) diffusion, may be used to determine ozone density in the upper atmosphere with the meteor radar (Jones et al., 1990).

The study of meteors and meteor trains is as relevant as ever for a wide spectrum of reasons. Those reasons include for example the fundamental necessity of ensuring the safety of the space faring transports and protection of both civilian and military orbital assets facing the risk of micrometeoroid impact. At the other end of the spectrum, meteors in the atmosphere contribute to better understanding of the formation conditions and evolution, as well as fundamental composition of the solar system and beyond.

1.3 Aim and Overview of the Thesis

The work in this thesis was initiated in an attempt to illuminate the reasons for the absence of clear explanation for the anomalous behaviour of the ambipolar diffusion of meteor trains as observed with backscatter meteor radars and continuously well documented in the literature for the past several decades. Furthermore, the main hypothesis motivating this investigation was centered around the idea that ozone (directly or indirectly) is the main participant in chemical reactions with meteoric ions in the immediate stages of the meteor train formation in the upper atmosphere between 80 km and 95 km. Accordingly, the primary goal of this thesis was to explore the such potential role of ozone chemistry during the initial meteor trail expansion and investigate the possibility of using backscatter meteor radar observation of overdense meteor trains electron diffusion as a reliable technique for determination of ozone density in the upper atmosphere. The brief introduction, given in the previous sections, is intended to present in a condensed way the idea and the concept of the meteor studies to the reader. However, it is far from being able to encompass the depth and the extent of the field of meteor studies. The hope is that the remaining chapters will bring the field of meteor research closer to the reader while staying on the course and exploring the novel ideas and hypothesis behind this work.

Consequently, the thesis is organized in such way where the second chapter deals with fundamental concepts of meteor physics, starting with meteor ablation, distinction between overdense and underdense meteors, meteor radar and related issues, such as initial radius, and concludes with a brief discussion about ozone in the upper atmosphere and review of previous efforts aimed of measuring its density profile.

Chapter three describes the methodology deployed in this work, and introduces the radar sites from which data was collected. It describes in detail the technical aspects of data processing and computational details which were used in determining the ozone density in the upper atmosphere.

The results are given in chapter four encompassing all radar sites, and finally chapter five discusses outstanding issues and future research options aimed at further refining the results and concepts presented in this work, and discusses the viability of a commercial application of the developed technique for upper atmospheric ozone measurements.

Chapter 2

No man is wise enough by himself.

- Titus Maccius Plautus

2. Meteor Physics

2.1 Ablation Fundamentals

Starting from the first principles, early authors such as Whipple (1943), Öpik, (1958), McKinley (1961), among others, developed the fundamentals of meteor dynamics that are the foundation of modern meteor physics. While the ablation theory has evolved since then, the question of the meteoroid densities still remains only partially resolved.

At the end of the Second World War, based on earlier observations, Herlofson (1948) was among the first to qualitatively describe the meteoric ablation as a result of hypervelocity collisions with atmospheric molecules. He assumed that the meteoroid collides with a specific atmospheric molecule only once. However, complications arise because, as subsequently noted by many authors, the ablating particle doesn't always behave as a solid body and such cases need to be addressed by other means (McKinley, 1961). There are two basic flow regimes that must be considered when dealing with meteoric ablation. The first case is when the "mean free path" of the air molecules at the specific altitude in the atmosphere is greater than the assumed radius of the meteoroid, in which instance the impact momentum and the energy are transmitted to the ablating particle through the direct collision with the air molecule. In this case no aerodynamic cushion is formed and the heat transfer from impacting atmospheric molecules is extremely high. This leads to rapid heating and subsequent ablation, sputtering and fragmentation (Öpik, 1958). This flow regime is applicable when the Knudsen number (Figure 2.1), which is essentially the ratio of the mean free path in the atmosphere to the characteristic dimension of the particle, is larger than 10 (Campbell-Brown and Koschny, 2004). The second regime exists when the meteoroids have a radius that exceeds the "mean free path", and where aerodynamic cushioning, with thickness of several atomic layers, is formed, affecting the coefficient of the heat transfer and the subsequent depth of

atmospheric penetration (Öpik, 1958). In this flow regime the Knudsen number is below 0.01 (Ceplecha et al. 2000).

Moreover, major studies of meteoric ablation that assume single particle dynamics and a classic model of conservation of energy and momentum, along with meteor light curves, have shown that the theory doesn't always entirely correspond to the observation (Campbell-Brown and Koschny, 2004, and references therein). However, Ceplecha et al. (1998) concluded that 73% of meteors investigated to date can be described well under the framework of single-body theory. Close study of the meteoroid ablation is important as its rate reveals mass deposition, momentum and energy release, thus further illuminating additional physical and chemical properties.

Here, the focus will be on the case of sputtering and ablation, while fragmentation will not be considered in-depth, as the work in this thesis revolves around the very narrow and specific subcategory of the meteors that may reside on the boundary of having characteristics of the both aforementioned flow regimes. These meteors are better known in radio science as overdense and will be discussed in much more detail later in the text, along with considerations of their significance.

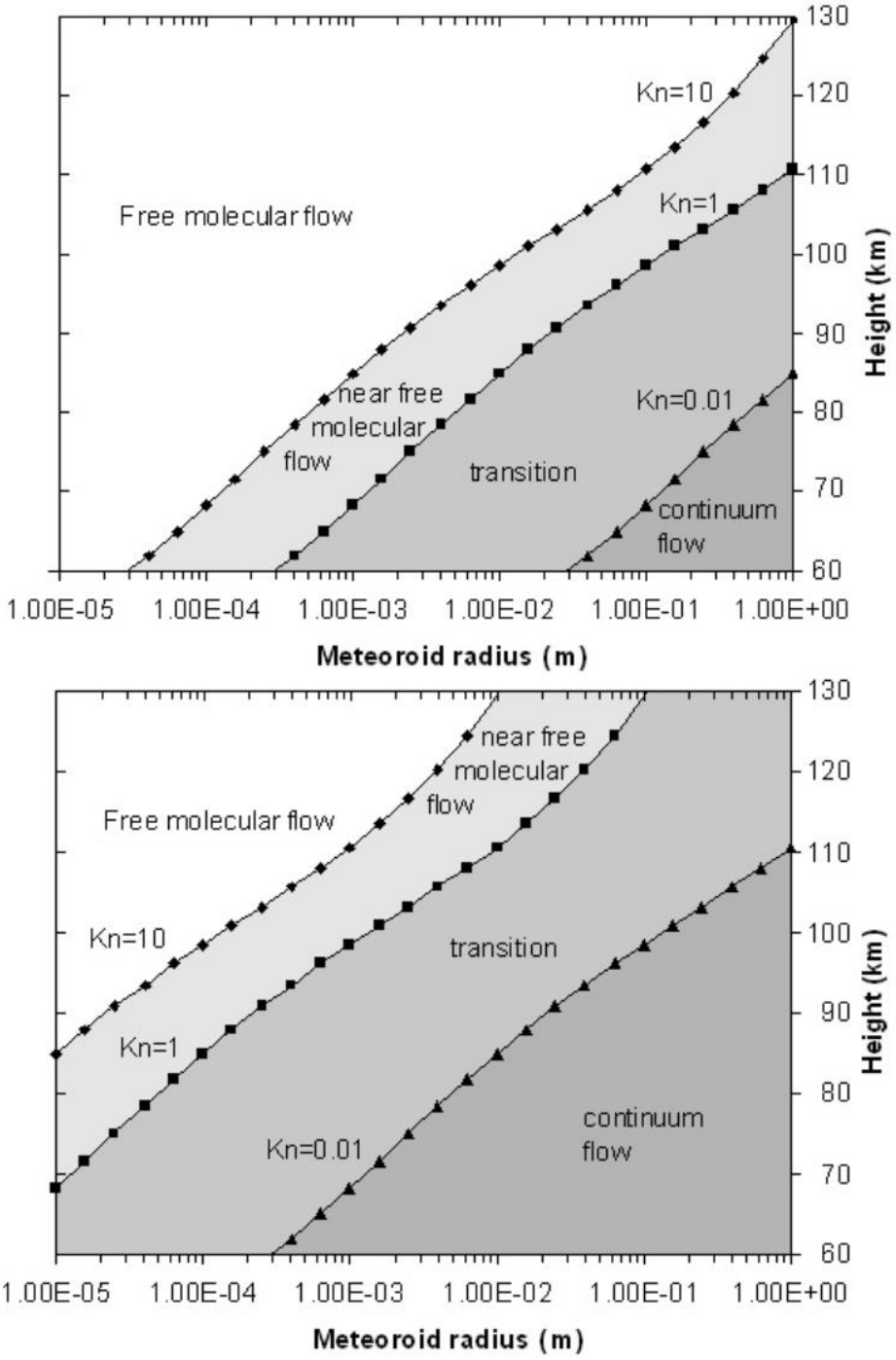

Figure 2.1: Top plot: flow regimes for meteoroids between 10^{-5} m and 1 m diameter, assuming no increase in density over the atmospheric density. Bottom plot: flow regimes assuming intensive ablation increases the density by a factor of 100 (Campbell-Brown and Koschny, 2004).

2.1.1 Meteor Sputtering

Fundamentally, the first stage of meteor ablation is preheating that occurs below 150 km altitude, and generally will depend on the size, velocity and the composition of the particle.

It is during this stage that mass loss of the meteoroid is due to the sputtering process. While particles with the lower mass limit of ~10^{-15} kg and in the size range of ~10^{-6} m cannot be heated efficiently to initiate ablation, they are still susceptible to sputtering (Popova, 2004). Extensive treatment of the subject of the sputtering was performed recently by Hill et al. (2005) and Rogers et al. (2005). Their approach has origins in the theoretical treatment of the gas-grain interactions in the interstellar medium first considered by Tielens (1994) and in an experimental study by Mizutani and Nishimatsu (1998). The mechanism of sputtering involves the loss of individual atoms during the high speed collisional process (Opik, 1958) and has been also studied by Lavedinets and Shushkova (1970), Brosch et al. (2001) and Coulson and Wickramasinghe (2003). The colliding atmospheric molecule transfers kinetic energy to the atoms on the surface of the meteoroid and dislodges it from the lattice. This may subsequently cause collisional chain reactions, dislodging several more meteoroid atoms from the surface region. The sputtering yield depends on the specific properties of the impacted particle and the incident angle, and it also depends on the atmospheric mass density and the individual atomic mass of the impacting atmospheric molecule. Sputtering will be the dominant mechanism for the mass loss if the particles have high velocities (above 30 km/s), low density and low mass (~10^{-12} kg) and originate from comets. Thus, it is considered as the main mechanism for the destruction of micrometeoroids or interstellar dust that intercepts the Earth's orbit (Rogers et al., 2005). Essentially, the atom will escape the lattice of the hosting surface only if it has sufficient energy to overcome the surface potential barrier. That energy is defined as the surface binding energy U_o. Therefore, for a given projectile and target, the minimum projectile energy to induce sputtering, also defined as the threshold energy (E_{th}) (Anderson and Bay, 1981), can be expressed:

$$E_{th} = \frac{U_0}{\beta(1-\beta)} \quad for \ \frac{M_1}{M_3} \leq 0.3, \tag{2.1}$$

$$E_{th} = 8U_0(M_1/M_2)^{1/3} \quad for \ M_1/M_2 > 0.3, \tag{2.2}$$

where M_1 is the projectile mass and M_2 is the mean molecular mass per atom of the target. Then the maximum fractional energy transfer β (not the same as the ionization coefficient β discussed later in the text) that is possible in the direct elastic collision can be written as:

$$\beta = \frac{4M_1M_2}{(M_1+M_2)^2} \tag{2.3}$$

It is now possible to define sputtering yield $Y(E,\theta)$. This parameter describes the mean number of sputtered particles per impacting molecule and depends on the physical characteristics of the target, various properties of the impacting molecule and the incident atom energy and the incident angle (Rogers et al., 2005). The sputtering yield for normal incidence, valid for $E > E_{th}$ is given by:

$$Y(E,\theta=0) = \frac{3.56}{U_0}\frac{M_1}{M_1+M_2}\frac{Z_1Z_2}{\sqrt{Z_1^{2/3}+Z_2^{2/3}}} \times \alpha\frac{R_p}{R}s_n(\gamma)\left[1-\left(\frac{E_{th}}{E}\right)^{2/3}\right] \times \left(1-\frac{E_{th}}{E}\right)^2 \tag{2.4}$$

where Z_1 is the atomic number of the impacting atom/molecule and Z_2 is the atomic number of the impacted meteoroid atom. The parameter α depends on the ratio of the atomic masses and is expressed as $\alpha = 0.3(M_2/M_1)^{2/3}$. The ratio $\frac{R_p}{R}$ is a correction factor and it is the ratio between the mean projected range to the mean penetrated path length and was approximated by Bohdansky (1984) as:

$$\frac{R_p}{R} = \left(K\frac{M_1}{M_2} + 1\right)^{-1} \tag{2.5}$$

According to Tielens et al. (1994), K is a "free parameter" which is dependent on the target material. Finally, the universal function $s_n(\gamma)$, discussed in much detail in Tielens et al. (1994) depends on the Coulomb interaction and is approximated by Matsunami et al. (1980) and Rogers et al. (2005) as:

$$s_n = \frac{3.441\sqrt{\gamma}\ln(\gamma + 2.718)}{1 + 6.35\sqrt{\gamma} + \gamma(-1.708 + 6.6882\sqrt{\gamma}\,)} \quad (7) \tag{2.6}$$

and

$$\gamma = \frac{M_2}{M_1 + M_2}\frac{a}{Z_1 Z_2 e^2}E \tag{2.7}$$

where e is the elementary charge, and the screening length for the interaction potential between the nuclei a obtained by Tielens et al. (1994) and can be expressed as:

$$a = \frac{0.885a_0}{\sqrt{Z_1^{2/3} + Z_2^{2/3}}} \tag{2.8}$$

Here, a_0 is the Bohr radius. However, the energy term in equations (2.4) and (2.8) is just the kinetic energy of the impacting atom and it must be calculated in cgs units. For the further simplification of this approach, the reader is directed to (Vondrak et al., 2008). Finally, the magnitude at which the meteoroid atoms are sputtered can be written as:

$$\frac{dN_{sp}}{dt} = 2Av\left(\frac{m}{\rho_m}\right)^{2/3}\sum n_i Y_i(E, \theta = 0) \tag{2.9}$$

The number density is denoted by n_i and Y_i is the sputtering yield of the i_{th} different impacting atmospheric molecule respectively. McKinley (1961) describes the shape factor of the meteoroid which is denoted here as *A*, and the factor of 2 is used to account for the angular dependence of the sputtering yield. Then the mass rate of change of the sputtering meteoroid is given by Rogers et al. (2005):

$$\left(\frac{dm}{dt}\right)_{sp} = -2M_2 Av\left(\frac{m}{\rho_m}\right)^{2/3}\sum n_i Y_i(E,\theta=0), \tag{2.10}$$

For meteoroids which have sufficient size density and velocity such that they result in formation of visual meteors, sputtering is not a significant contributor to the overall mass loss; however, it is an important precursor that still needs to be taken into consideration.

2.1.2 Meteor Ablation

When the particle surface reaches the melting point and ablation is initiated at lower altitudes, the meteoric atoms will ablate differentially, starting with most volatile ones first, while refractory elements ablate last (McNeil et al., 1998; William and Murad, 2002; Vondrak et al., 2008). Generally, the ablation is initiated when the meteoroid surface temperature reaches the minimum of 1850 K (Figure 2.2), however ablating temperatures may exceed several thousand degrees, depending on the mass, velocity, composition and entry angle.

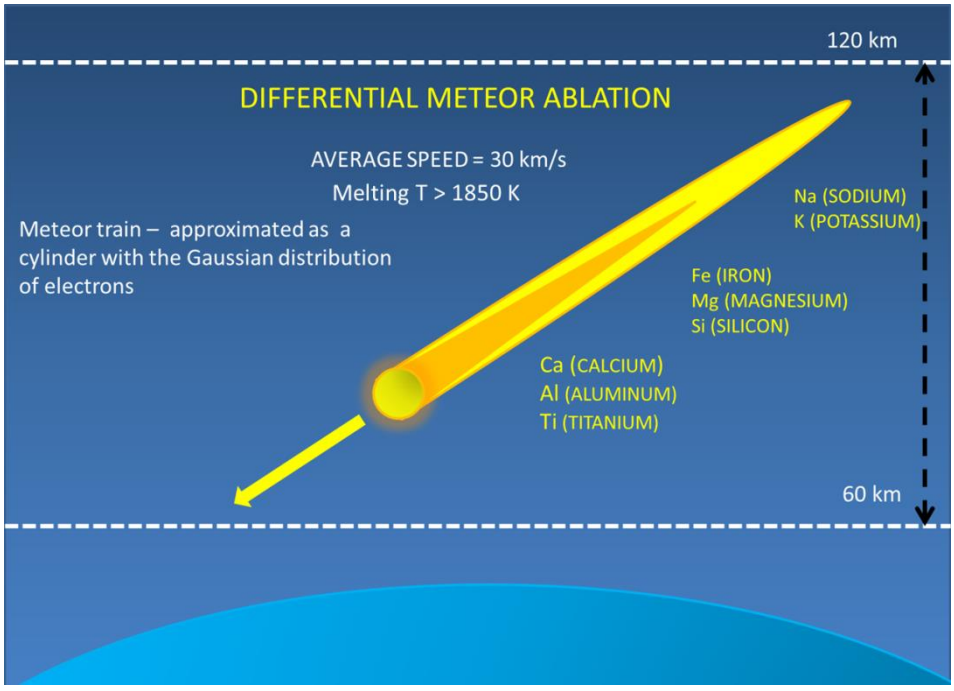

Figure 2.2: Depiction of meteor ablation as a function of height where volatiles such as Na and K ablate first, followed by Fe, Mg and Si, and Ca. Al and Ti ablate last.

The ablation efficiency depends on the atmospheric mass density. While Öpik (1958) and McKinley (1961) have given a comprehensive treatment of the subject, the most complete treatment is given by Bronshten (1983). It must be also noted that the energy required to completely vaporize a solid particle is several orders of magnitude smaller than the initial kinetic energy of the meteor (Zinn et al., 2004). For the purpose of completeness, the comprehensive treatment of the deferential ablation given by Vondrak et al. (2008) combined with some of the earlier outstanding works, will be reviewed here to illustrate the ablative processes.

As the ablating meteoroid travels through the atmosphere, its height from the surface z changes in time and is a function of the zenith angleχ:

$$\frac{dz}{dt} = -V\cos\chi(t) \tag{2.11}$$

Assuming free molecular flow and an approximately spherical shape of the particle with radius R impacting atmospheric column, the expression for the loss of momentum resulting from collisions is:

$$\frac{dV}{dt} = -\Gamma V^2\frac{3\rho_a}{4\rho_m \mathrm{R}} + \rho_m g \tag{2.12}$$

Here, V is the velocity of the particle, g is the gravitational acceleration. The dimensionless "free molecular drag" is denoted by Γ and has a value between 0.5 and 1 (Hughes, 1978). This parameter expresses the efficiency of the momentum transfer between the particle and the impacting atmospheric molecules. The sphericity of the particle is assumed because the particle is expected to rotate rapidly during the atmospheric entry thus creating the spherical effect (Hawkes and Jones, 1978). As noted earlier (Bronshten, 1983), and emphasised more recently (Brown et al., 1994), for larger meteoroids the aerodynamic cap would need to be included in calculations.

Thermal energy received by the meteoroid from the impacting atmospheric molecule is balanced by the radiative loss, temperature increase, melting, phase transitions and

vaporization of the meteoritic atoms (Vondrak et al., 2008 and references therein). Then the energy conservation is written as:

$$\frac{1}{2}\pi R^2 V^3 \rho_a \Lambda = 4\pi R^2\, \varepsilon\sigma(T^4 - T_{env}^4) + \frac{4}{3}\pi R^3\, \rho_m C \frac{dT}{dt} + L\frac{dm}{dt} \qquad (2.13)$$

where the parameter Λ is dimensionless and represents the free molecular heat transfer coefficient. It describes the amount of the incident kinetic energy which is transferred to the meteoroid. The left hand side here is just a frictional heating term that is balanced on the right hand side by the loss of energy through radiative loss ($4\pi R^2\, \varepsilon\sigma(T^4 - T_{env}^4)$), the energy used to increase the meteoroid temperature ($\frac{4}{3}\pi R^3\, \rho_m C \frac{dT}{dt}$) and the last term ($L\frac{dm}{dt}$) represents the heat lost in the transfer of particle mass into gas phase. Here, ε is the emissivity coefficient; σ is the Stefan-Boltzmann constant and the T and T_{env} are the temperatures of the particle surface and the atmospheric surrounding. The specific heat of the meteoroid is C and L is the latent heat of vaporization.

During the period before the onset of ablation, the heat loss due to evaporation is relatively small. However, in the high temperatures limit, evaporation plays a more dominant role in mass loss. The mass loss rate can be then calculated (as per Markova et al., 1986; Love and Brownlee, 1991; Mc-Neil et al., 1998 and Vondrak et al., 2008) by applying Langmuir evaporation. This approach assumes that the rate of evaporation into a vacuum is equal to the rate of evaporation needed to balance the rate of uptake of a species *i* in a closed system. The rate of mass release of species *i* with molecular weight μ_i, from the meteoroid with area *S* (Vondrak et al., 2008) is given by:

$$\frac{dm_i^A}{dt} = \gamma p_i S \sqrt{\frac{\mu_i}{2\pi k_b}} \qquad (2.14)$$

Where γ is the probability that the molecule remains "stuck" to the surface of the meteoroid, post collision, while p_i is the thermodynamic equilibrium pressure of species *i* in the gas phase. The superscript A refers to ablation and S (below) refers to sputtering. Therefore total mass loss due to the ablation is just a sum over all gas-phase components:

$$\frac{dm}{dt} = \sum_i \frac{dm_i^A}{dt} \tag{2.15}$$

If the fragmentation is ignored then the total mass loss rate from sputtering and ablation is expressed as:

$$\frac{dm}{dt} = \frac{dm^A}{dt} + \frac{dm^S}{dt} \tag{2.16}$$

This model of differential ablation has been verified and observed experimentally by Janches et al. (2008). The ablated material forms a trail of some initial radius closely behind the meteor head, and it contains stripped metallic ions and electrons in a quasi-neutral arrangement. The collisional and chemical processes with the surrounding atmosphere are instrumental in de-excitation of the high energy species, resulting in a luminous phenomenon and spectral emissions. Meteor radar detects the electrons in the trail. However, at this point the question of meteor ionization has to be addressed first, as even after decades of research there is still the unresolved problem of the meteor ionization coefficient and related parameters discussed in the next section.

2.2 Meteor Trail Ionization and β-Coefficient

Both theoretical and experimental work of the pre and post Second World War investigators (e.g. Herlofson, 1948; Greenhow and Hawkins, 1952; Greenhow and Neufeld, 1957) have shown that the maximum ionization, and hence electron production in a meteor trail, occurs at distinct atmospheric heights and is related to the size, velocity and composition of the meteoroid. Moreover, early comparisons of the visual and radio observations of meteor trail showed that there are variations and a deviation from the expected theoretical values of the electrons in the meteor trail. This is related to the ablation theory, covered in the previous section, which explains maximum mass loss in the specific atmospheric regions, as a function of meteor physical properties. The ablated atoms expelled from the boiling surface of the main body of the meteoroid have the same or greater initial velocity as a meteoroid and consequently a kinetic energy up to several hundred electron volts. Taking in consideration the visual magnitude (M_v) of the meteor,

derived from optical astronomy, researchers obtained the expression for the luminous intensity (*I*) (McKinley, 1961):

$$M_v = 6.8 - 2.5log_{10}I \tag{2.17}$$

where *I* is in watts. While a pedantic degree of precision is absent, based on the range of correction factors that must be applied, such as atmospheric absorption and zenith angle, this is a very important parameter for evaluating ionization. The most recent work by Weryk and Brown (2013a, 2013b) seeks to improve the above expression and has achieved significant progress. The luminous intensity, in term of mass loss and velocity, assumed to be closely proportional to the transfer of kinetic energy during ablation and in the spectral range 4500 to 5700 A (Davies and Hall, 1963), can be written as:

$$I = -\frac{1}{2}\tau_I \frac{dm}{dt} V^2 \tag{2.18}$$

where *V* is velocity and τ_I is the dimensionless luminous efficiency factor, generally difficult to constrain (Öpik,1958). The portion of kinetic energy that drives ionization is assumed to be proportional to the kinetic energy loss of the ablated atoms (McKinley, 1961). Utilizing this relationship, it is then possible to relate the number of the electrons produced in the meteor trail per unit length and give the expression for the energy of the ionization created per unit time:

$$qV\eta = -\frac{1}{2}\tau_q \frac{dm}{dt} V^2 \tag{2.19}$$

Here, η is the mean ionization potential per specific atom and τ_q is the dimensionless ionization-efficiency factor (McKinley, 1961). Using the classic mass change expression from McKinley (1961), the electron production rate per unit length can be easily derived. However McKinley's efforts in defining the mean ionization potential per specific atom were mirrored by the British researchers from the Jordell Bank organization who have defined the *ionization coefficient β* as a probability that a single ablated atom with mass μ would produce a free electron. Then as a function of β the equation for the number of electrons per unit length in the meteor trail is:

$$q = -\frac{\beta}{\mu V}\frac{dm}{dt} \tag{2.20}$$

It is then possible to relate the τ_q and β in the following way:

$$\tau_q = \frac{2\eta}{\mu V^2}\beta \tag{2.21}$$

McKinley (1961) related luminous efficiency factor and ionization efficiency factor and obtained $\tau_q/\tau_I \sim V^2$. Notably, the work by Weryk and Brown (2013a, 2013b) has made significant progress in improving the relation between β and τ_I. While the value of β has been subject of discussion and even disagreement for the past several decades, the value derived by Kaiser (1953) of ~0.1 seems to be the most accepted. Following Kaiser's work, the seminal investigation in understanding the ionization coefficient was conducted by Verniani and Hawkes (1964) and Verniani (1965), where they obtained β as a function of meteor velocity and also considered β for overdense meteors. The importance of understanding the nature of the ionization coefficient (or ionization probability) and deriving the most accurate value β is critical to meteor radar research as the radar technique of observing meteor phenomena principally depends not only on the meteor properties, but also on the properties and efficiency of the meteor trail ionization.

However, the significance of the work by other authors in the field, especially early contributions must be acknowledged. A strong relationship between the luminosity and ionization on one hand, and meteor mass and velocity on the other, was noted by Whipple (1955). Fialko (1959) for instance, further refined the relationship between the ionization coefficient and strength of the radio echo signal and meteor velocity. Davies and Hall (1963) investigated the efficiencies of the luminous and ionizing processes in the meteor trail using simultaneous photographic and radio echo observations. Further incremental improvement to the initial meteor ionization theory by Herlofson (1948) was performed by Furman (1960, 1961, 1964 and 1967). Among the noteworthy achievements of Furman's later work is the mathematical derivation of collisional ionization of the in situ atmospheric molecules by the ablating meteoric atom, in an early attempt to explain the forbidden oxygen emission at 5577Å. It should be remarked at this

point that even now in the 21st century, the access to the range of quality scientific literature from the old Soviet Union is still limited, and that is a significant loss for the global scientific community at large. However, the politics and policy are not the subject of this work, and aforementioned remark is intended to raise the reader's attention to the problem that still persists today.

Additionally, using the height of the maximum ionization obtained from the radar technique only, Rumi (1979) derived a way to evaluate the ionization coefficient from the value of maximum number of electrons ablated per unit length in the specific height region (q_{max}). The expression for beta then is:

$$\beta = 9.4 \cdot 10^5 \frac{q_{max} cos^2 \chi H}{p_{max}^3 v^6} \tag{2.22}$$

where H is the scale height at maximum pressure p_{max} (found in the tables of the U.S. Standard Atmosphere) and the zenith angle is denoted by χ. The importance of this formula in interpreting the results obtained here will be discussed in the following chapters.

Jones (1998) calculated the ionization coefficient theoretically taking into consideration all earlier relevant research. His results are valid for faint meteors with velocity $V \leq 35\ km/s$ and in analytic form beta is expressed as $\beta \approx 9.4 \cdot 10^{-6}(V-10)^2 V^{0.8}$. Recent work by Pecinová and Pecina (2008) has resulted in analytical expression for β for higher velocities.

When the ionization coefficient is known, it becomes relatively easy to calculate other meteor properties from the meteor radar echoes and optical studies (McKinley, 1961; Bronshten, 1983). At this point, it is prudent to review the basics of meteor radar theory, before discussing the remaining aspects of the meteor physics.

2.3 Meteor Radar Theory and Fresnel Diffraction

2.3.1 Application to Underdense Meteor Trains

For more than a half a century, meteor radars have been at the forefront of investigation of the meteor phenomena. The peak of meteor radio research was in the 1950s and the 1960s, where for instance in the period between 1951-1960 over 300 papers had been published on the topic (Sugar, 1964). The meteor observations have been carried out predominantly in the range of frequencies between 20 MHz and 70 MHz (Cervera, 1996), however infrequent research has been done with the frequencies as low as 2 MHz (Steel and Elford, 1991) and as high as 900 MHz (Wannberg et al, 2011). Limited by the frequency, the maximum altitude boundary for meteor radar is around 110 km. Here the basis of the radio echo is reviewed along with the issues that accompany meteor radar methodology. A comprehensive description of the meteor radar theory was given by McKinely (1961) and reviewed by Ceplecha et al. (1998) and briefly discussed by Baggaley (2002). Closely related, a recent and comprehensive review of the MST radar development and studies in the period between 1997 and 2008 was given by Hocking (2011).

In this section the backscatter radar theory is discussed in some detail as the backscatter radar is the primary tool deployed in this work (Figure 2.3). However a similar theory applies to the forward scatter and it is relatively similar as it can be seen from (e.g. McKinley, 1961; Foschini, 1997). The most important difference between the two types of radar is that backscatter radar emits short pulses and the transmitter and receiver are spaced relatively close to each other while forward scatter radar emits continuous waves and the transmitter and receiver are separated by considerable distances. The foundation of the radar theory is the electromagnetic radiation and scattering. As indicated earlier in the text, radar “sees” electrons in the meteor trail, as they behave as Hertzian dipoles. On the basis of the electron trail density, it is possible to differentiate between underdense and overdense meteor trains, discussed in detail further in the text. In the context of Hertzian dipole, one may recall the characteristic angular frequency of electrons, derived

from the equation of motion of electron (see Mitchner and Kruger, 1973), can be written as:

$$\omega_p = \sqrt{\frac{n_e e^2}{\epsilon_0 m_e}} \tag{2.23}$$

where m_e is the mass of the electron, n_e is electron volume density, e is elementary electron charge and ϵ_0 is the vacuum dielectric constant.

In order to present the meteor radar theory coherently and following the historical evolution of the field from the work of Herlofson (1951) and onward, underdense trains will be considered first. For now, before the more rigorous discussion about underdense and overdense meteors is initiated, it should suffice to say that in the former, the electron line density is sufficiently low, such that radio waves penetrate the trail and each electron behaves as an individual scatterer. Overdense trails exhibit a different behavior. Their initial electron line density is so high that the trail behaves as a metallic cylinder and the radio waves cannot penetrate the meteor trail surface (Jones and Collins, 1974; Jones and Jones, 1990).

Before proceeding further it should be remarked that the distribution of energy reflected by the meteor trail depends on the ionization distribution in the trail volume, spatial orientation of the trail, radar wavelength, polarization of the incident wave in respect to the trail and generally atmospheric dynamics in the specific region of the atmosphere (Sugar, 1964).

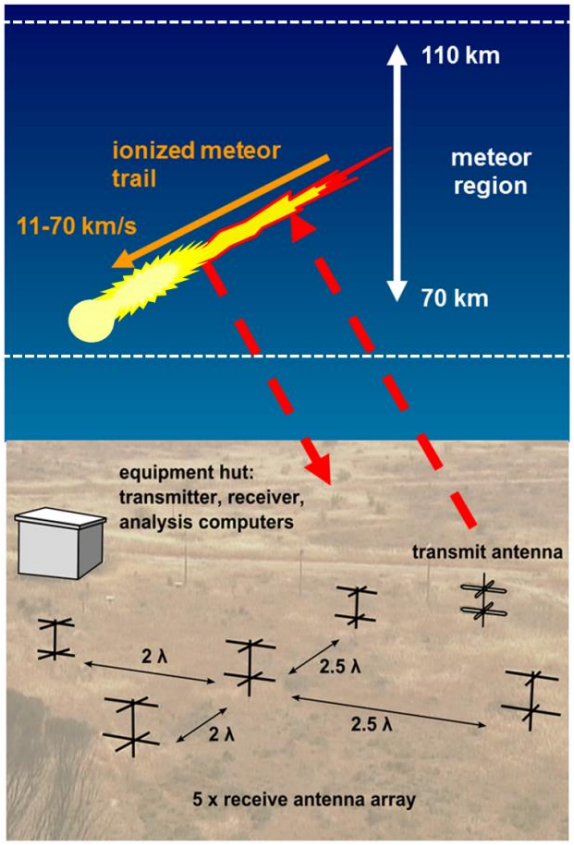

Figure 2.3: Illustration of the typical meteor radar setup.
(Credit: http://www.chemphys.adelaide.edu.au/atmospheric/instrumentation/radar_meteor)

The following analysis of the fundamentals of the radio scatter from meteor trails is closely based on the treatment of the subject by McKinley (1961); Cervera (1996); Badger (2002).

First, the scattering cross section of the free electron is defined as:

$$\sigma_e = 4\pi r_e^2 sin^2\gamma \qquad (2.24)$$

where e and r_e are the charge and radius of electron, respectively, and γ is the angle between the electric field vector of the incident wave and the line of sight to the receiver. For the full backscatter, the value of the electron scattering cross section is approximately 1×10^{-28} m^2.

At some distance *R* from the radar transmitter, the power flux of the incident wave at a point on the trail can be written as:

$$\phi_i = \frac{P_T G}{4\pi R^2} \tag{2.25}$$

The returned radar signal power, in terms of the single electron scattering is expressed as follows:

$$\Delta P_R = \frac{P_T G}{4\pi R^2} \frac{\sigma_e}{4\pi R^2} \frac{G\lambda^2}{4\pi} = \frac{G^2 P_T \lambda^2 \sigma_e}{64\pi^3 R^4} \tag{2.26}$$

where P_T and P_R are transmitted and received power respectively; *G* is the gain of the matched antenna and receiver, relative to an isotropic radiator in the free space. Distance from the transmitter is denoted with *R*, while λ and σ_e are the wavelength and electron scattering cross-section respectively. This expression is valid if an identical antenna is used for signal reception, where the absorbing area of the antenna is given by $A_a = G\lambda^2/4\pi$ and impedances are matched. Sugar (1964) gives this expression in terms of the individual transmitter and receiver gain.

It is also convenient to express the equation (2.26) as the power flux of backscattered radiation from a single electron (Cervera, 1996; Badger, 2002), thus:

$$\phi_e = \phi_i \frac{\sigma_e}{4\pi R^2} = \phi_i \left(\frac{r_e}{R}\right)^2 \tag{2.27}$$

The assumption is made that the electrons have Gaussian distribution in the underdense meteor trail and the scattering is entirely in phase, without influence of the geomagnetic field (valid only at higher radar frequencies). Moreover, it is assumed for the purpose of calculations that electrons are in a line element *ds* (McKinley, 1961). Additionally, it is taken that the trail radius is much smaller than the wavelength and that the secondary and radiative effects can also be also neglected. Then the peak amplitude of the field vector due to a single scattering electron in the trail is $E_0 = q\sqrt{(2Z_0\phi_e)}ds$, where Z_0 is the wave impedance of free space.

The returned wave has now traveled a distance of 2R, and therefore has a modulation factor of $e^{i\left(2\pi ft-\frac{4\pi R}{\lambda}\right)}$. Rewriting $\frac{2\pi}{\lambda} = k \; and \; 2\pi f = \omega$, the modulation factor can be written as $e^{i(\omega t-2kR)}$. Consequently, when R changes as a function of time, phase modulation of the wave is produced and the instantaneous amplitude of the echo signal received from the electrons in the element *ds* is given by:

$$dE_R = q\sqrt{(2Z_0\phi_e)}\int e^{i(\omega t-2kR)}\,ds \tag{2.28}$$

The electron density q per unit length is taken in front of the integral because it is assumed to be constant in the trail. Then the amplitude of total field from all electrons contribution in the trail between s_1 and s at the antenna (Figure 2.4) is expressed:

$$E_R = q\sqrt{(2Z_0\phi_e)}\int_{s_1}^{s} e^{i(\omega t-2kR)}\,ds \tag{2.29}$$

The use of the approximation $R \approx R + s^2/2R_0$ and transformation $x = 2s/\sqrt{R_0\lambda}$ is required because the integral above is difficult to evaluate. Remarkably, using the approximation for R above, the error is very small (*for a trail length of 10km and R_0=100km the error is about 0.001%* (Cervera, 1996)).

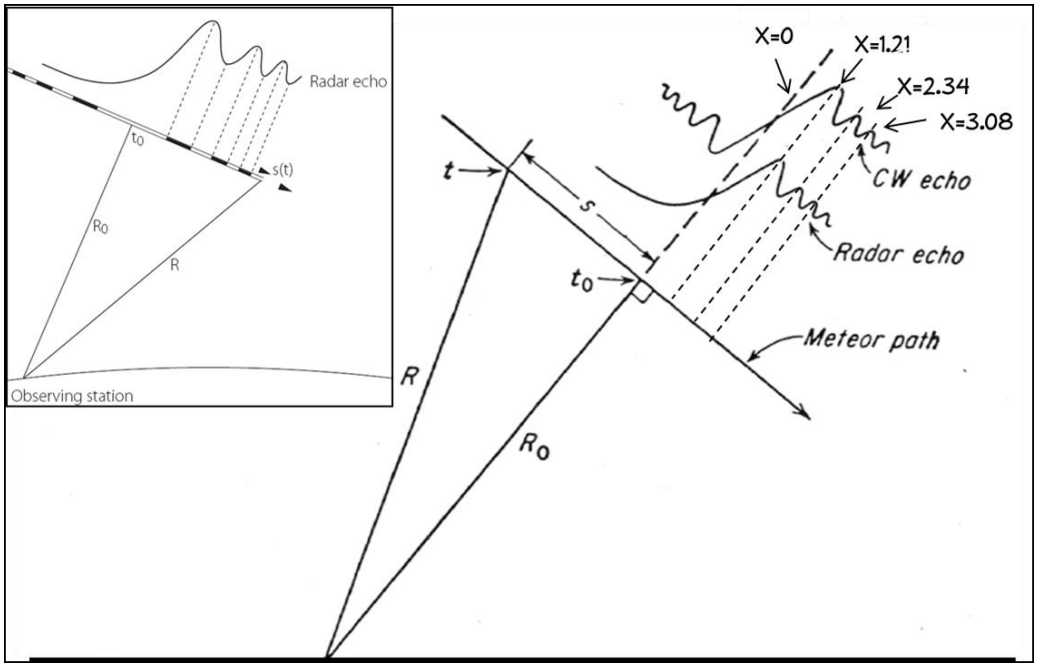

Figure 2.4: The geometry of the meteor path relative to the observation station. The figure also shows Fresnel oscillations in the amplitude of the radar echo as observed with a backscatter radar. Note that the point t_0 on the meteor path, is the center of the first Fresnel zone. Inset: The consecutive Fresnel zones are white if they are in phase with the first zone and black if they are out of phase (after McKinley, 1961 and inset from Kero, 2008).

The expression for the amplitude E_R is written as follows:

$$E_R = \frac{q}{2}\sqrt{(2Z_0\phi_e R_0\lambda)}e^{i(\omega t-2kR_0)}\int_{x_1}^{x} e^{i\left(-\pi\frac{x^2}{2}\right)}\ dx \tag{2.30}$$

and

$$E_R = \frac{q}{2}\sqrt{(2Z_0\phi_e R_0\lambda)}e^{i(\omega t-2kR_0)}(C - iS) \tag{2.31}$$

where C and S are Fresnel integrals in optical diffraction theory and are given below:

$$C = \int_{x_1}^{x} cos\frac{\pi x^2}{2}dx \tag{2.32}$$

and

$$S = \int_{x_1}^{x} sin\frac{\pi x^2}{2} dx \tag{2.33}$$

The normalized variable *x* in the Fresnel integral is a function of time and generally referred to as the Fresnel length. The maximum varying frequency of *C* and *S* with time is much less than the radar frequency (McKinley, 1961). The orthogonal plot of *S* and *C* results in the formation of Euler spiral or Cornu spiral of Fresnel diffraction theory (Figure 2.5) as it is known today (Levien, 2008). It should be observed that most of the contribution to the signal amplitude from the meteor trail comes from the first Fresnel zone whose length can be expressed in terms of R and wavelength dependence $F_1 = \sqrt{2\lambda R}$.

Typical scattering zone lengths for a meteor at a range of 140 km are 900 m at 50 MHz, 1200 m at 30 MHz and 2500 m at 6 MHz (Ceplecha et al., 1998). The full interpretation of the values of the normalized *x* parameter along the Cornu spiral in Figure 2.5 is given by Hecht and Zajac (1974), however a condensed summary is also given in the text below.

The origin of the meteor echo is positioned at $x = -\infty$ in the negative quadrant. From there, the electric field phasor follows the spiral toward the origin, and the amplitude of the returned signal increases continuously. At the same time, the phase angle decreases. The amplitude reaches the maximum value at the moment when a meteor crosses the first Fresnel zone past point t_0 and the value of *x* is 1.217 (Figure 2.4 and 2.5). When the point of the maximum amplitude is passed, there is a decrease in magnitude and increase in frequency as the value of *x* increases toward infinity. The time t_0 (Figure 2.4 and 2.5) occurs at when *x* is at the origin. The phase reaches the maximum value when the value of *x* is 0.6 and beyond this point, the oscillations of decreasing magnitude and increasing frequency take place. It should be noted that the phase and amplitude oscillations are in quadrature with the phase leading (Cervera, 1996). The Cornu spiral is a convenient way to graphically examine the behaviour of the power and phase of the returned echo. The

example of the effects of the diffusion on the echo power and the phase can be observed in (Figure 2.6). McKinley (1961) treats this subject significantly more in depth, and a discussion about Fresnel diffraction of radio signals can be found in most texts covering the subject of antennas and radars (e.g. see Balanis, 2005 for discussion).

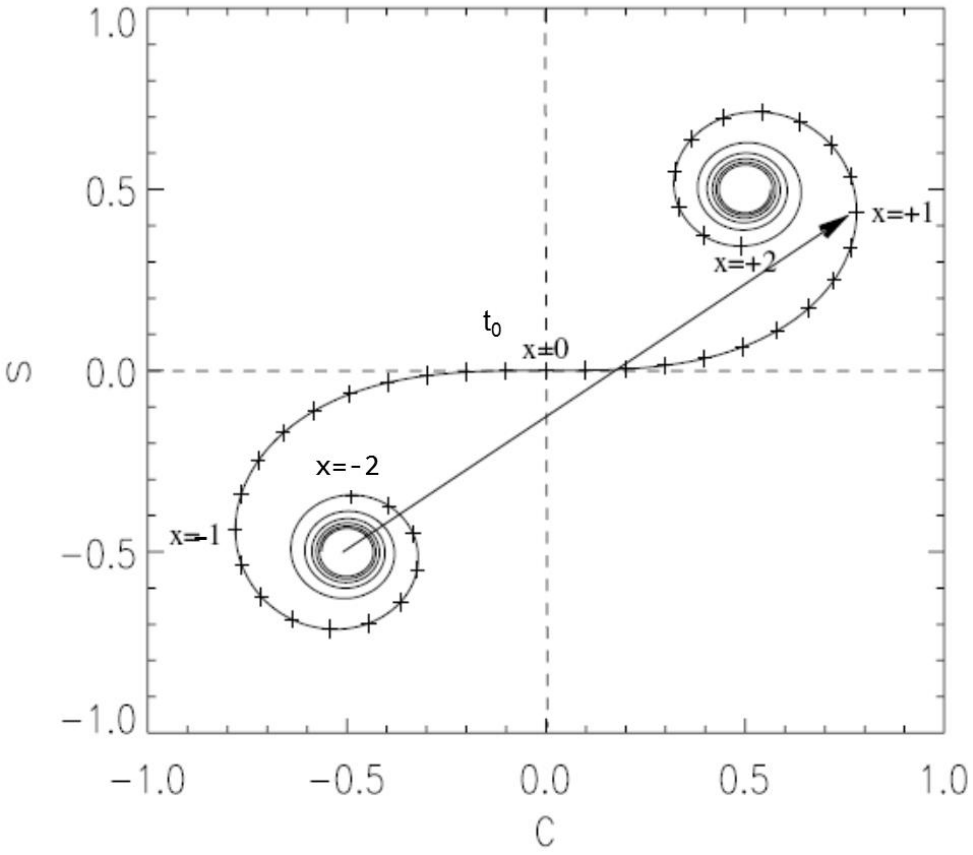

Figure 2.5: Modelled Cornu spiral with no diffusion. The amplitude vector at x = ±1 is shown (Baggaley and Grant, 2005).

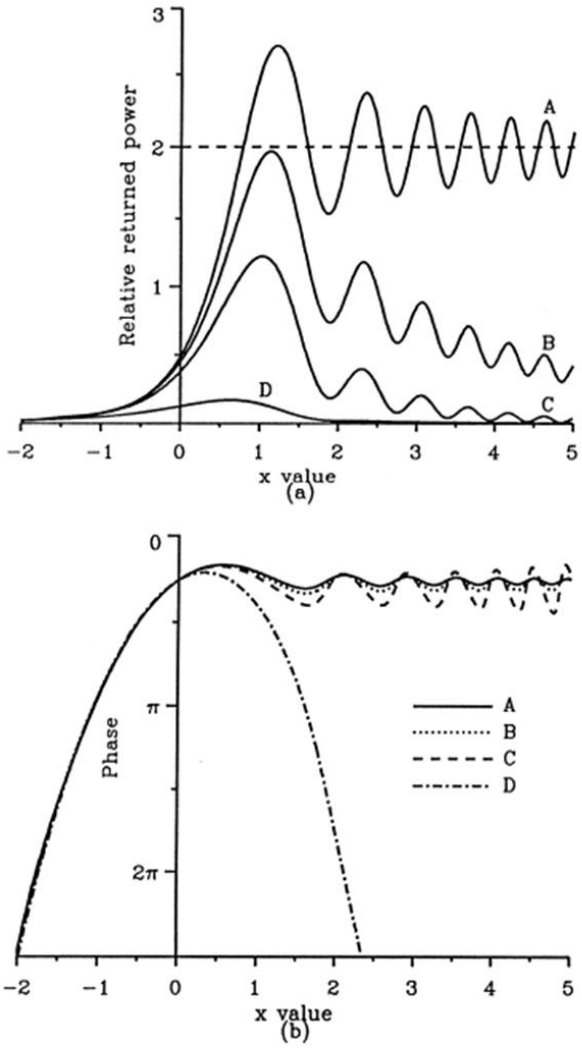

Figure 2.6: Predicted behavior of the power and phase of the radar echo from an underdense trail. Curve A is based on Equation (2.31) and shows the case for no diffusion. Curves B, C, and D show the effect of an increasing degree of diffusion of the trail (Ceplecha et al., 1998).

However, the application of the Fresnel diffraction in the radar meteor theory extend much farther, where for example it is possible to accurately determine meteor speeds using Fresnel techniques (e.g. see Hocking, 2000; Elford, 2004; Baggaley and Grant, 2005; Campbell-Brown and Elford, 2006). The magnitude of the oscillatory field for a particular value of *x* (Badger, 2002) is given by:

$$E_{R_0} = \frac{q}{2}\sqrt{2R_0\lambda\phi_e Z_0}\,(C^2 + S^2) \tag{2.34}$$

and the power flux can be written as:

$$\phi_R = \frac{\left(E_{R_0}\right)^2}{2Z_0} = q^2\frac{\phi_e R_0\lambda}{4}(C^2 + S^2) \tag{2.35}$$

Then the power delivered to the receiver from the scattering contributions of the entire trail is given by:

$$P_R = q^2\frac{\phi_e G_R R_0}{16\pi}(C^2 + S^2) = q^2\frac{\phi_i G_R\lambda^3 r_e^2}{16\pi R_0}(C^2 + S^2) \tag{2.36}$$

After the substitution for ϕ_i is made, then the final expression for the received power is:

$$P_R = P_T G_R\lambda^3 q^2 r_e^2\frac{(C^2 + S^2)}{64\pi^2 R_0^3} \tag{2.37}$$

The signal amplitude falls to *1/e* of its initial value when $r = \lambda/2\pi$. For underdense meteors, the returned radar echo from the trail will be attenuated due to the backscatter from the opposite side of the trail being delayed in phase relative to the front of the trail (relative to the observer). That attenuation will be the function of the trail radius and the wavelength and will become severe when $\lambda/4 \sim r$.

Expressing equation (2.26) in terms of the meteor trail cross-section σ_T (Sugar, 1964), and again assuming that antenna and receiver impedances are matched, gives:

$$P_R = \frac{G^2 P_T\lambda^2\sigma_T}{16\pi^2 R^4} \tag{2.38}$$

If however one writes the expression for the scattering cross section of the trail as a function of diffusion (discussed in upcoming section), then the equation becomes:

$$\sigma_T = \left(\sqrt{\frac{R\lambda}{2}}\,r_e q^2\right)^2 e^{-\left(\frac{32\pi^2 Dt}{\lambda^2}\right)} \tag{2.39}$$

where the scattering cross section of the trail is σ_T, R and λ are distance from the transmitter and the wavelength respectively and r_e is the classical radius of the electron. The diffusion coefficient is given by *D*, q is the electron line density and t is the time

measured from the formation of the trail (in seconds). Because the initial distribution of electrons in the trail mimics the Gaussian, then the expression for radius is written as:

$$r_{trail} = \sqrt{4Dt} \tag{2.40}$$

Using equations (2.38) and (2.39) and rewriting the expression for the P_R, assuming the existence of the initial radius r_0 that will be discussed later in the text, one obtains:

$$P_R = \frac{G^2 P_T \lambda^3 r_e^2 q^2}{32\pi^2 R^3} \exp\left(-\frac{8\pi^2 r_0^2}{\lambda^2}\right) \exp\left(-\frac{32\pi^2 Dt}{\lambda^2}\right) \tag{2.41}$$

This equation contains the attenuation terms which approximate the behaviour of the real signal from the meteor trail. The first attenuation factor $\exp\left(-\frac{8\pi^2 r_0^2}{\lambda^2}\right)$ arises because of the finite width of the trail, and the second represents the attenuation with time as the trail expands and a destructive interference begins. Here, the assumption is also made that the trail is of infinite length and that every trail has its first Fresnel zone, and exhibits the resulting signal reflection. Since the trails have a finite length in practice, this may not be the case, thus the returned signal may be weak or indistinguishable.

However, the case of underdense meteors is more complicated than the initial assumptions that were made during the theoretical treatment of the underdense meteor trail scattering used to illustrate the fundamentals of the radio theory. In general, there are several attenuation factors that are function of velocity and height, that affect the amplitude of the radio echo from underdense meteors and by extension, to the similar degree from overdense meteors. As clearly observed above, the first one is the initial radius factor which depends on atmospheric density, velocity of the meteoroid and radar wavelength. The second factor is the finite velocity of the meteor which affects the echo amplitude due to the differential diffusion and expansion of the trail at the beginning, middle and end of the observed trail segment. The third factor is the attenuation as a result of pulse repetition. This is relevant when the interpulse period of the meteor radar is comparable or longer than the decay time of the echo due to radial diffusion of the trail ionization, so it is possible that a trail formed after the passage of a transmitted pulse may not be detected (Ceplecha et al., 1998). Finally, ionospheric attenuation factors are relevant especially at heights when ionosphere below meteor trail behaves as a doubly

refracting medium for the passage of radio waves from the meteor radar. This applies to radar frequencies below 10 MHz. Another contribution of ionosphere to the echo amplitude attenuation is the Faraday rotation of the plane of polarization, especially above 15 MHz (Ceplecha et al., 1998).

2.3.2 Underdense Meteors – Properties and Characteristics

Thus far, the exact characteristics defining underdense meteors have still not been elaborated completely. The generalized assumptions made in the previous section are necessary to develop a foundation for interpretation of the experimental radar observation of the physical behaviour of underdense meteors. The additional factors that need to be considered in a study of underdense meteors range from environmental to dynamical. For instance, the contribution of turbulence and wind shear must be considered especially around and below the mesopause.

As noted earlier, the initial radius and ionic diffusion, and its variation with height and meteor velocity affects the radar echo interpretation and it must be accounted for. These parameters will be analyzed in more detail in the next several sections, but for now, more elaborate analysis of underdense meteors will be given.

The duration time of underdense meteor echoes was investigated early on by Herlofson, (1951) and Eshelman, (1995) and was reviewed by McKinley (1961). They considered the phase effects in the trail where the echoes are the strongest and immediately after trail formation. For the purpose of calculation, consider for example an annular ring which is located on the boundary of the meteor trail cross-section (Figure 2.7).

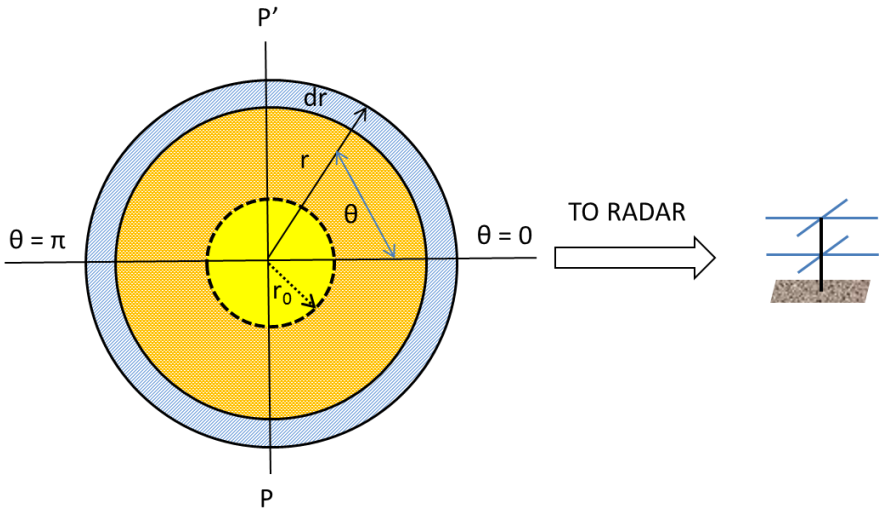

Figure 2.7: Cross section of ionized trail near t_0 point. Initial radius of the meteor trail is denoted by r_0, and the plane PP' is defined as plane of zero phase, which is drawn normal to the line of sight of the far distant radar station.

Then the amplitude of the echo signal from all electrons in that ring is:

$$dA = 2Nrdr \int_0^{\pi} sin\left(2\pi ft - \frac{4\pi r}{\lambda} cos\theta\right) d\theta \tag{2.42}$$

The phase angle of the electrons in the ring element is $(4\pi r/\lambda)cos\theta$ (McKinley, 1961). The total number of electrons in the ring N is obtained from the classic solution for the diffusion of the cylindrical meteor trail, with initial radial electron distribution assumed to be Gaussian.

Using the Bessel Function the integral above is expanded:

$$\int_0^{\pi} cos\left(\frac{4\pi r}{\lambda} cos\theta\right) d\theta = \pi J_0\left(\frac{4\pi r}{\lambda}\right) d\theta \tag{2.43}$$

Here, the corresponding integral of the sine function is zero thus the expression for amplitude can be written as:

$$dA = 2\pi N J_0\left(\frac{4\pi r}{\lambda}\right) rdr\, sin2\pi ft \tag{2.44}$$

Comparing the obtained amplitude with the one that would result if all electrons were localized in the cross-sectional center, it can be seen that the amplitude of the latter is greater.

Taking into consideration that the resultant phase angle is always zero for any ring, the ratio of the added up amplitude contributions from each ring and resulting amplitude of the electrons in the center can be expressed:

$$\frac{A}{A_0} = \frac{2\pi \int_0^\infty N J_0\left(\frac{4\pi r}{\lambda}\right) r\, dr}{2\pi \int_0^\infty N r\, dr} \tag{2.45}$$

While the analytic solution to the integral in the numerator is difficult because of the presence of the Bessel Function J_0, the solution can be easily obtained in the tables of integral solutions in books like "Handbook of integral equations" (Polyanin and Manzhirov, 2008).

The resulting integration becomes:

$$\frac{P_R(t)}{P_R(t)} = \left(\frac{A}{A_0}\right)^2 = \exp\left(-\frac{8\pi^2 r_0^2}{\lambda^2}\right) \exp\left(-\frac{32\pi^2 D t}{\lambda^2}\right) \tag{2.46}$$

The obtained result is the same as the attenuation factors obtained in equation (2.38) and echo power primarily decays as a result of diffusion. From the power-amplitude relation in the equation above, and by defining the echo-amplitude decay time t_u as the time when power falls over *1/e* by convention, the expression is easily written as:

$$t_u = \frac{\lambda^2}{16\pi^2 D} \tag{2.47}$$

Echo-amplitude decay time is a function of wavelength and diffusion and consequently height, and it remains the same for all underdense meteors, as long as the electron line densities lie below the boundary that separates underdense and overdense meteors. It should not however, be confused with the actual echo duration time of the underdense meteors (Figure 2.8) which is observed by the radar equipment. This theoretical relationship is very important as it can be exploited significantly in other areas of research (e.g. Hocking et al., 1997). If the sole mechanism for electron dissipation in the

underdense meteor trail is ionic diffusion (Kaiser, 1953), then the amplitude *A* of a radar echo can be written in simple notation using the t_u from (2.47) as:

$$A = A_0 \exp\left(-\frac{t}{t_u}\right) \tag{2.48}$$

As it will be seen later, this is not the case, and the topic will be revisited during the discussion about diffusion in the upcoming sections.

Finally, for backscatter meteor radar, typical decay times for underdense meteors vary between 0.015 s and 0.3 s for the frequencies in the range 30 MHz – 55 MHz (Singer et al., 2008).

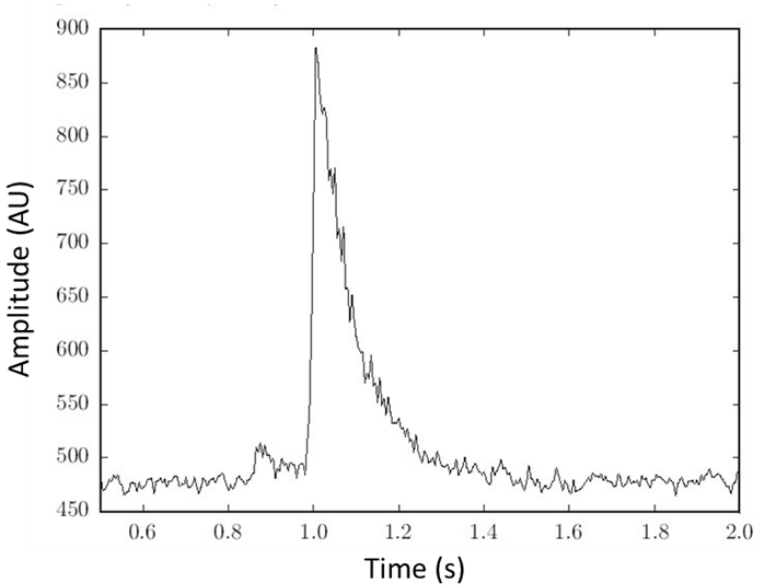

Figure 2.8: Typical underdense signal. Note that signal amplitude is in arbitrary units. (source: http://brams.aeronomie.be/pages/theory).

2.3.3 Transition Between Underdense and Overdense Meteors

The previous section inevitably leads to the question about the boundary between underdense and overdense meteors. That question was answered with slightly varying results by several authors beginning with Kaiser and Close (1952), Manning and Eshleman, (1959), and recently by Jones and Collins (1974) and Poulter and Baggaley

(1977; 1978). An easy way of deriving this transition via ratios of received and transmitted power is given by Sugar (1964).

However, in the spirit of historical developments and understanding of the derivation, the approach that uses the dielectric constant is discussed here. The meteor trail is essentially an ionized gas and as such it has a dielectric constant (this term is used in older texts; newer texts refer to it as relative permittivity) which can be defined by:

$$\kappa = 1 - \frac{N\lambda^2}{\pi} r_e \approx 1 - 81\frac{N}{f^2} \tag{2.49}$$

where N is the number of electrons per cubic meter, $r_e = \frac{\mu_0 e^2}{4\pi m_e} = \frac{\sigma_e}{4\pi} = 2.8178 * 10^{-15}\, m$ is the electron radius, and μ_0, e, m_e and σ_e are permeability of free space, electron charge, mass and cross section, respectively. The incident radiation wavelength is λ and f is the frequency. In general, the meteor trail is considered quasineutral, and underdense meteor trails do not exhibit the resonant oscillation under the incident radiation due to the large separation of electrons and ions, if the incident electric vector is parallel to the axis of the meteor trail (McKinley, 1961). In the case when the electric vector of the radiation is perpendicular to the axis of the meteor trail, resonant effects will occur because of the close ion-electron separation and resulting restoring force. As noted earlier, the density of electrons in the underdense trail is sufficiently low where consequently each electron acts as an independent scatterer. On the opposite end, in overdense trails the electron density is large enough such that the secondary scattering from electron to electron occurs and becomes relevant. The incident radio wave does not penetrate the column completely and the dielectric constant κ in equation (2.49) becomes negative. It is important to distinguish the discussion here between ionized gases and metals. In the wave equation the conductivity is real for metals while it is imaginary for ionized gases. In ionized gases, the phase velocity is greater than the group velocity of light. As a result, when an electromagnetic wave passes through the ionized region, the phase angle continues to increase. The phase angle increases proportionally with the increase in ionized gas density. The critical density of electrons can be found from equation (2.49) by setting $\kappa = 0$. The dialectic constant will change from negative values to zero at some critical value of the trail radius, r_c.

Equating the classical solution[1] to the radial diffusion (will be discussed in more detail further in the text) and the equation (2.49) when $\kappa = 0$, it is possible to find a solution for the critical value of electron density (N_c):

$$N_c = \frac{\pi}{\lambda^2 r_e} = \frac{q}{\pi(4Dt + r_0^2)} \exp\left[-\left(\frac{r_c^2}{4Dt + r_0^2}\right)\right] \tag{2.50}$$

where D is ambipolar (ionic) diffusion and r_0 and r_c are initial train radius (at $t=0$) and critical radius for the transition regime, respectively. The value of the transitional electron line density q_{tr} (Figure 2.9) is then obtained by setting

$r_c{}^2 = 4Dt + r_0^2 = \lambda^2/4\pi^2$, thus the expression for q_{tr} can be written as:

$$q_{tr} = \frac{e}{4r_e} \approx 2.4 * 10^{14}\ electrons/meter \tag{2.51}$$

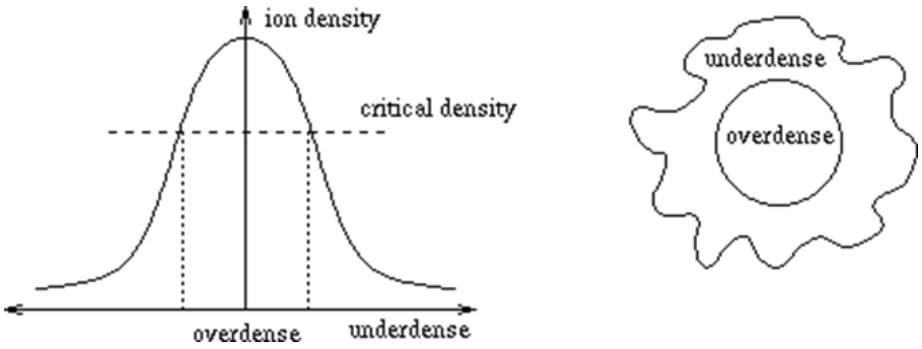

Figure 2.9: Graphical representation of the transition between underdense and overdense electron density distribution in the meteor trail.
(Source: http://brams.aeronomie.be/pages/theory)

This is the basis of the approach taken by Kaiser and Closs (1952) in their calculation. Further discussion can be explored either in their paper or in the review given by McKinley (1961). The transitional values of electron densities defined by other authors are reasonably similar to the above derived value (see Poulter and Baggaley, 1977, 1978). Finally by convention, the transition between underdense and overdense meteors occurs

[1] For instance see "*The mathematics of diffusion"*, Crank, J. (1979)

when the evanescent wave amplitude is reduced by 1/e at the trail axis. It must be noted however that Jones (1995) showed that the distribution of ionization in the meteor trail does not necessarily correspond to Gaussian. Moreover, the effects of geomagnetic field became significant above 95 km and the behaviour of the ionized trail must be treated differently. The main effect of the geomagnetic field is the elliptical shape of diffusion classical radial expansion (Figure 2.10).

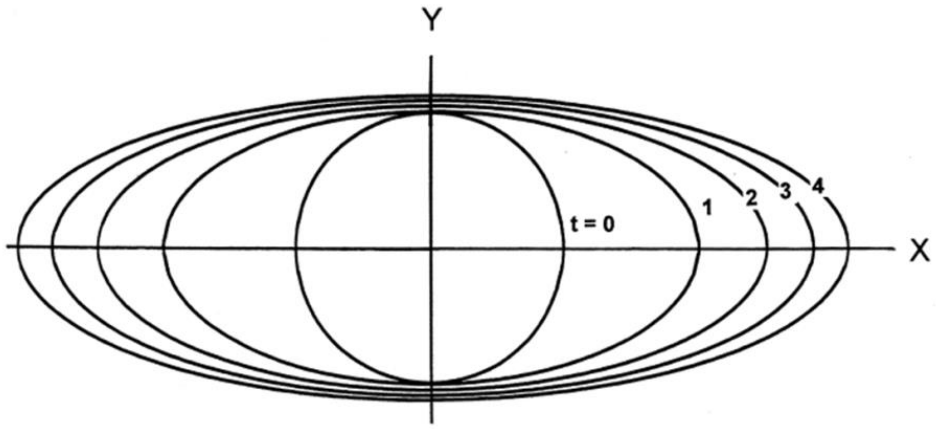

Figure 2.10: Section of a meteor trail at 105 km at four successive equal intervals of time after the trail has formed at $t = 0$. Contour plots are the curves of constant electron density. The Earth's magnetic field lies in the plane containing the axis of the trail and the major axis of the ellipse. Diffusion in the direction of the major axis is unaffected by the field; diffusion in the direction of the minor axis is severely inhibited. The angle between the field and the meteor trail axis is 50° (Ceplecha et al., 1998).

Before exploring the topic of overdense meteors, which is one of the focal points in this thesis, recent developments regarding the underdense meteors will be touched upon, followed by a brief review of remaining radar topics relevant to this work.

Poole and Kaiser (1967) investigated the distributions of height and maximum ionization for underdense meteors, and based on the work by Kaiser (1953), they obtained an expression for the maximum ionization in terms of atmospheric density and linear concentration of electrons per unit length. They obtained surprising results which indicate that ionization profiles are shorter than predicted by the simple evaporation theory. Their work confirms that the role of geomagnetic field on the ionized trains is considerable, and

that high elevation winds affect trail dynamics for echoes lasting more than one second. In the important work by Jones (1975), a study was conducted to determine the discrepancy between the theoretical and observational variations of radar observed diffusion in underdense meteor trail. The role of chemical removal of electrons was noted along with the wind contribution that requires modification of the equation (2.45) (for details see Jones, 1975). That and the contribution from other factors such as the secondary reflection point and finite velocity effect, are plotted in Figure 2.11 as a function of height.

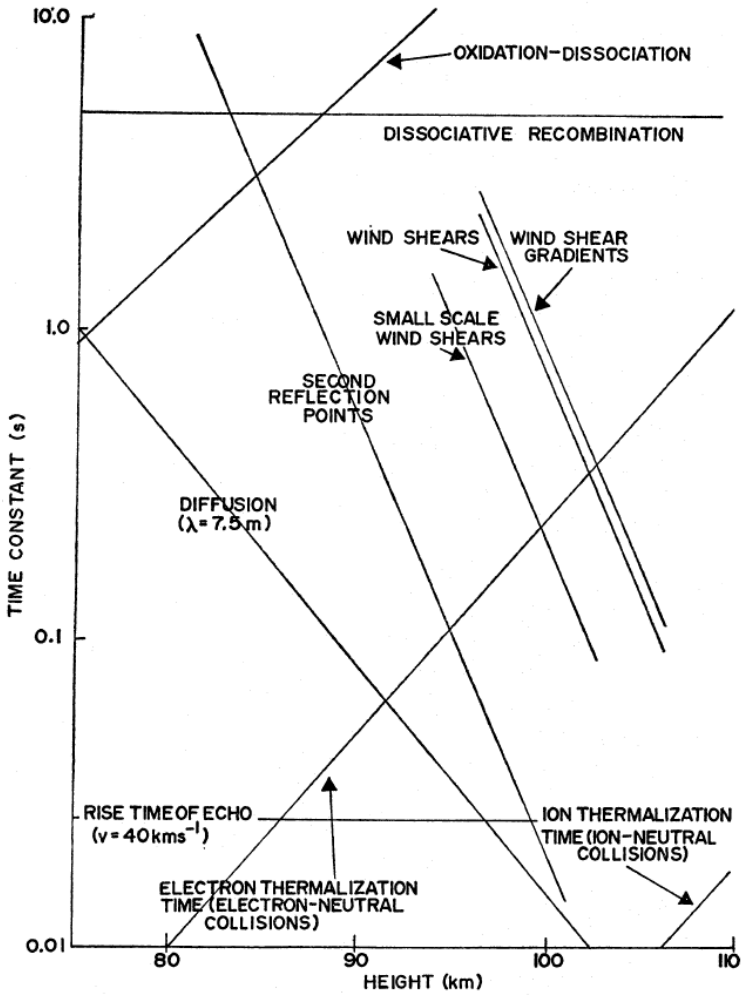

Figure 2.11: Relevant processes that affect underdense meteor trail, as a function of height (Jones, 1975).

Moreover, among less investigated aspects affecting the echo duration of underdense meteor trails, especially with lower electron densities, are the influences of the mesospheric metallic and ice dust layer, which may impact diffusion by up to ten percent (Havnes and Sigernes, 2005; Singer et al., 2008).

2.3.4 Additional Notes on Meteor Radar

2.3.4.1 Some Limitations of the Radar Technique for the Study of Meteors

Early on (Eshelman, 1959) it was realized that some small deviation from the simple scattering theory occur at very high frequencies. However, following the subsequent work of Greenhow and Hall, (1960a,b), it was realized that those departures are more serious, and as such may introduce serious uncertainties in obtained results (Greenhow, 1963). Primary uncertainties originate from the early absence of reliable data at the time of the initial meteor train formation and loss of electrons by chemical process. Another potential issue is the assumption that all electrons in the initial radius are in linear arrangement. A comprehensive review of some meteor radar limitations was given by Greenhow (1963); however, several decades of the continuous work since then seem to mitigate many of those issues (e.g. Baggaley and Cummack, 1974; Baggaley,1980a; Foschini, 1998; Campbell-Brown, 2003; Jones and Campbell-Brown, 2005).

More recently, some of the still outstanding issues regarding different frequencies in meteor radar work have been revisited and analysed by Mathews (2004). Nevertheless, this investigation pertains more to the systems such as Arecibo, ALTAIR and meteor head echo theory, rather than typical VHF meteor radar used in this thesis. Mathews (2004) however makes one peculiar observation, suggesting that a significant portion of the long duration overdense meteor echoes likely originate from Field-Aligned Irregularities. The validity of this observation should be indeed investigated in more detail, as it is not substantiated in other investigations.

2.3.4.2 Meteor Radar Interferometry

Traditional meteor radar in principle detects only specular reflections (perpendicular to the line of sight) from meteor events. Subsequently, it is very important to determine the direction and spatial coordinates from where the radar echo originates. That information

is critical in many aspects of the physical study of meteor orbital properties and cosmic sources. A number of authors have investigated the methods of determining echo direction in the past (Robertson et al., 1953; Eshelman and Mlodonsky, 1957; Kaiser, 1961; Weiss and Elford, 1963; Jones and Morton, 1977; Morton and Jones, 1982; Baggaley et al., 1994). However, the process of determining meteor radar echo direction has been made significantly easier by the implementation of portable computer systems and their evolution (Jones et al., 1998). On a basic level, the interferometric technique relies on the comparison of the phase of an echo signal at each receiving antenna which are strategically separated at about 0.5λ to also allow for unambiguous determination of echo direction and to avoid coupling effects. In essence, the performance of a radar interferometer depends primarily on the signal phase precision measurement. The design by Hocking et al. (1997) solved many problems and used a 5 antenna array with all sky coverage, while refining the precision of the echo determination to a remarkable range of 1.5%. The following year, Jones et al. (1998) calibrated the system further, and it is now an integral part in all SKiYMET meteor radars. More recently, Poole (2004) further discussed a simplified design of meteor radar antenna interferometer that uses only four receiving elements, where the fourth element is intended to resolve ambiguity. The relevance and practical application of the meteor radar interferometry has been shown by Hocking (2000) where he used the interferometric radar for determination of real-time meteor entry speeds.

2.3.4.3 Meteor Radar Response Function

In order to discriminate between different types of meteors, such as meteor showers and sporadics, especially over long periods of observations, it becomes necessary to develop a meteor radar response to specific events with a particular radiant and characteristics. The fundamentals of the radar response function depend primarily on the antenna pattern, the flux of meteors as a function of mass, zenithal electron density, ionization profile of meteors, the polarization of the radio waves with respect to meteor trail, the elevation of the meteor radiant, the minimum detectable electron line density of the specific radar system, attenuation factors due to the reflection properties of the trail and the detection criteria for a specific radar system (Cervera, 1996). Therefore, if the parameters of the

meteor radar system are well defined and known, the theoretical echo rate for a point source radiant of unit strength can be determined for all positions of the radiant in elevation and azimuth. One of the first aspects to consider in developing the response function is the fact derived from observational data, which indicates that all meteors trails scatter specularly and those events with the same velocities tend to ablate and produce ionized trails at the same height region and over a wide distribution of masses.

Subsequently, the result of such calculations describes the radar system's response to a radiant in any position in the sky and is appropriately defined as a "response function" of the radar (Ceplecha et al., 1998). With the reference to the Figure 2.12, the basic steps in the calculation can be briefly summarized as follows. First, the zenithal angle is used to calculate the meteor flux with some minimum electron line density. Second, the total echo rate can be found by integration over the echo plane strip which contains element *dS*. The detailed treatment and calculation of the response function can be found in (Cervera, 1996; Cervera and Elford, 2004) and a concise review was given by Ceplecha et al. (1998). The importance of meteor radar response function rests in the fact that it can help distinguish the distribution of sporadic meteors in the Earth's orbit and their fraction detectable by radar in much greater detail than it was possible during the early stages of meteor radar research, when computational resources were not available Elford (1964).

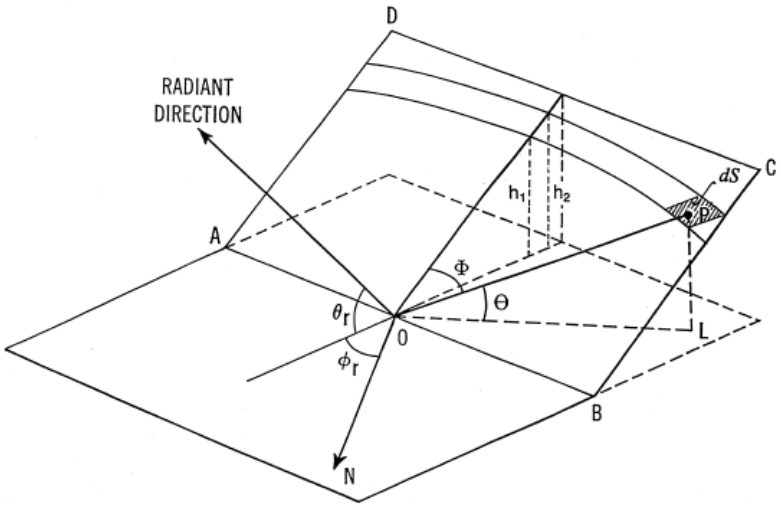

Figure 2.12: Geometry of the echo plane. The radiant direction is defined by the elevation angle θ_r and azimuth angle ϕ_r relative to the radar site at ***O***. The reflection point ***P*** on the meteor trail in the echo plane ***ABCD*** is at elevation Θ and echo-plane azimuth Φ.

Meteors of a given velocity have beginning and end heights h_2 and h_1, respectively (Ceplecha et al., 1998).

2.3.5. Overdense Meteors

While deceivingly simple in its interpretation, the treatment of overdense meteors is definitely not a trivial matter. Manning (1958), who treated forward scattering of overdense echoes, pointed out that no adequate theory existed during the late fifties to treat overdense echo duration. Herlofson (1951) was the first one to employ the wave treatment to the meteor trail scattering. He investigated the validity of the independent scatterer model and suggested the possibility of the resonant plasma oscillations due to charge separation when the incident wave has a polarization perpendicular to the ionizing column. The problem arises as the wave equations do not possess analytic solutions for the usual Gaussian radial distribution of ionization. That problem was successfully addressed by Poulter and Baggaley (1977) where their seminal work finally resolved several unanswered questions and defined overdense meteors in term of electron density and radar echo behaviour, and confirmed earlier results by Jones and Collins (1974) who showed that the transitional region between underdense and overdense meteor trains linear electron densities lays in the range between $>10^{13}$ and 10^{16} electrons m^{-1}. Further step forward in the investigation of the scattering form the overdense trains for the purpose of forward scattering calculations and geometry was made by Jones and Jones (1990a; 1990b; 1991) who investigated the application of Maxwell's equations (essentially almost the same method applied by Poulter and Baggaley (1977) using a numerical and analytical approach in order to derive the scattering properties and reflection coefficients.

However, before the additional aspects of overdense meteors are further discussed, some historical and quantitative aspects will be first reviewed now. As in the underdense case, a maximum in the backscattered power occurs when the trail is perpendicular to the incident wave and primarily originates from the first Fresnel zone. The backscattered radar echo from overdense meteor (Figure 2.13) may generally last up to several seconds, depending on the radar frequency (Valentic et al., 1996). This review will also try to shed some light on the rather ambiguous understanding of how overdense meteors are

observed with radar, and how they are classified in terms of their visual magnitude, mass, size and possibly composition.

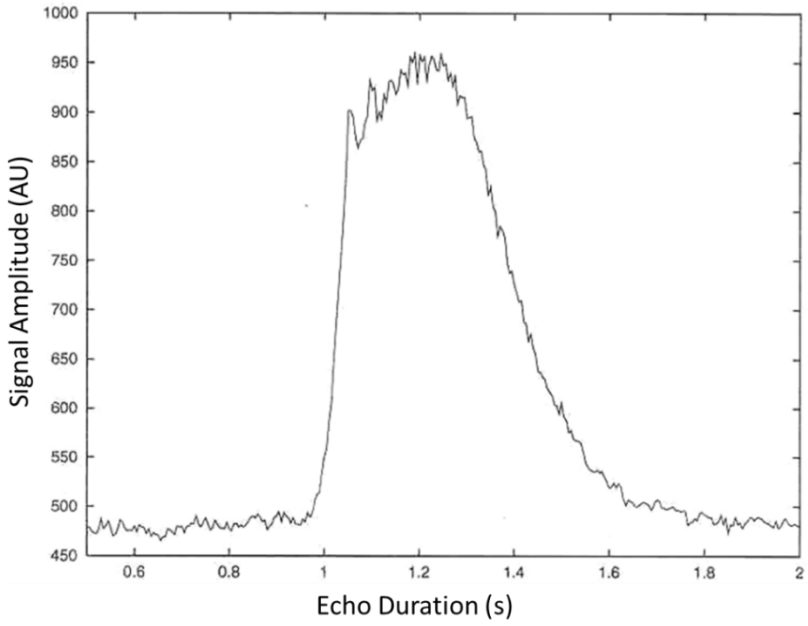

Figure 2.13: Illustrative example of a typical overdense meteor echo. Note that signal amplitude is in arbitrary units (Source: http://brams.aeronomie.be/pages/theory).

While generally accepted by earlier authors, the finding by Derbeneva (1968) that all overdense meteors are visual meteors is the first critical step in narrowing down the physical parameters that define radio overdense meteors, which are not explicitly specified in the principal literature. Depending on the radar frequency and observed height, the range of radio meteors extends broadly from lower underdense limit electron volume density of around 10^{11} m^{-3}, and on the far end of overdense spectrum, meteors with about 10^{20} electrons m^{-3} (Bronshten, 1983; Borovicka, 1993; Borovicka and Zamorano, 1995; Foschini, 1999). Ceplecha et al. (1998) stated that true overdense meteors have electron line densities $> 10^{16} m^{-1}$ with a transitional regime below that extending to the critical value derived in the previous section. To illustrate the problem at hand, one may observe different published values of overdense meteors in the literature, over the period of several decades. For instance, Derbeneva (1968) stated that a meteor

with electron line density of 10^{15} m^{-1}, has a visual magnitude of -2. On the other hand, Pallinen-Wannberg et al. (1998) gave the visual magnitude of +4 for a particle of 1.0 mm diameter, which definitely is capable of producing electron line densities in excess of 10^{-15} m^{-1} (Kharchenko, 2012). Cevolani and Gabucci, (1996) gave the range of masses for radar and visual meteors, where the two types intersect in the range of mass of about 10^{-6} kg, while Mann et al. (2011) gave the intersecting masses for radar and optical meteors in the range between 10^{-8} and 10^{-5} kg. In terms of visual magnitudes, some authors constrain overdense meteors from forward scatter radar observations, between -1 and +3 on the visual magnitude scale (Meisel and Richardson, 1998). Now, when a brief divergence of sometimes confusing values published in literature is presented, it is easy to see that more work is needed to define what truly constitutes the radio overdense meteor in terms of mass, size, composition and visual and radio magnitude. However, the values published by Manning and Eshleman (1959) and reviewed by Sugar (1964) (Table 2.1) will be taken as authoritative for the purpose of this work.

Table 2.1: Meteor electron densities as a function of mass, radius and visual magnitude (after Manning and Eshleman, 1959 and Sugar 1964).

APPROXIMATE BEHAVIOR OF METEORS OF VARIOUS SIZES

Line Density q Meters^{-1}	Average Flux $m^{-2}s^{-1}$	Average Interval Between Meteors	Maximum Reflection Coefficient	Radar Cross Section Meter^2	Theoretical Duration at 30 mc	Comments
10^{17}	1.6×10^{-15}	16 hours	4.2	13×10^{6}	4 hours	fireball
10^{16}	1.6×10^{-14}	100 minutes	2.4	4.2×10^{6}	25 seconds	0th magnitude
10^{15}	1.6×10^{-13}	10 minutes	1.3	1.3×10^{6}	2.5 second	visual losing effect
10^{14}	1.6×10^{-12}	60 seconds	~0.5	0.2×10^{6}	0.5 second	5th magnitude, visibility limited
10^{13}	1.6×10^{-11}	6 seconds	0.089	6×10^{3}	0.5 second	———
10^{12}	1.6×10^{-10}	0.6 second	0.0089	60	0.5 second	10th magnitude
10^{11}	1.6×10^{-9}	0.06 second	0.00089	0.6	0.5 second	———
10^{10}	1.6×10^{-8}	0.006 second	0.000089	0.006	0.5 second	15th magnitude
10^{9}	?	?	0.0000089	0.00006	0.5 second	beyond present radio limit

Note: The average interval between meteors is computed for an observed area of sky of 10^4 km^2; the reflection coefficient was computed for a range of 150 km at a frequency of 30 mc.

ORDER-OF-MAGNITUDE ESTIMATES OF THE PROPERTIES OF SPORADIC METEORS[1]

	Mass (grams)	Visual Magnitude	Radius	Number of this mass or greater swept up by the earth each day	Electron line density (electrons per meter of trail length)
Particles pass through the atmosphere and fall to the ground	10^{4}	−12.5	8 cm	10	—
Particles totally disintegrated in the upper atmosphere	10^{3}	−10.0	4 cm	10^{2}	—
	10^{2}	− 7.5	2 cm	10^{3}	—
	10	− 5.0	0.8 cm	10^{4}	10^{18}
	1	− 2.5	0.4 cm	10^{5}	10^{17}
	10^{-1}	0.0	0.2 cm	10^{6}	10^{16}
	10^{-2}	2.5	0.08 cm	10^{7}	10^{15}
	10^{-3}	5.0	0.04 cm	10^{8}	10^{14}
	10^{-4}	7.5	0.02 cm	10^{9}	10^{13}
	10^{-5}	10.0	80 microns	10^{10}	10^{12}
Approximate limit of radar measurements →	10^{-6}	12.5	40 microns	10^{11}	10^{11}
	10^{-7}	15.0	20 microns	10^{12}	10^{10}
	10^{-8}	17.5	8 microns	?	?
Micro-meteorites (Particles float down unchanged by atmospheric collisions)	10^{-9}	20.0	4 microns	Total for this group estimated as high as 10^{20}.	Practically none
	10^{-10}	22.5	2 microns		
	10^{-11}	25.0	0.8 micron		
	10^{-12}	27.5	0.4 micron		
Particles removed from the solar system by radiation pressure	10^{-13}	30	0.2 micron	—	—
	—	—	—	—	—

[1] Reproduced from L. A. Manning and U. R. Eshleman, "Meteors in the Ionosphere," PROC. IRE, vol. 47, p. 191: February, 1959, by permission of The Institute of Electrical and Electronics Engineers, Inc.

Similarly to derivation of the underdense echo duration time, using the expression for the transitional value of electron line density Manning (1958) defined the overdense echo duration time as:

$$T_{overdense} = \frac{q\lambda^2 r_e}{4\pi^2 D} = \frac{\lambda^2 q}{4\pi^2 D q_{tr}} \tag{2.52}$$

where q, λ and r_e are electron line density, radar wave length and electron radius respectively. At this point the sole mechanism of the trail expansion is assumed to be ambipolar diffusion denoted by D. In principle the value of T_{ov} must be greater of equal

to the trail expansion time defined as $r_0^2/4Dt$ where r_0 is the initial trail radius at t_0 and t is the time since t_0 (McKinley, 1961).

The electron line density in the overdense meteor trail can be defined in terms of wavelength λ (Figure 2.14) and the transitional value of linear electron concentration q_{tr}, which was derived earlier. Thus it can be stated:

$$q \geq \frac{\pi^2}{r_e}\left(\frac{r_0}{\lambda}\right)^2 = \pi^2\left(\frac{r_0}{\lambda}\right)^2 q_{tr} \tag{2.53}$$

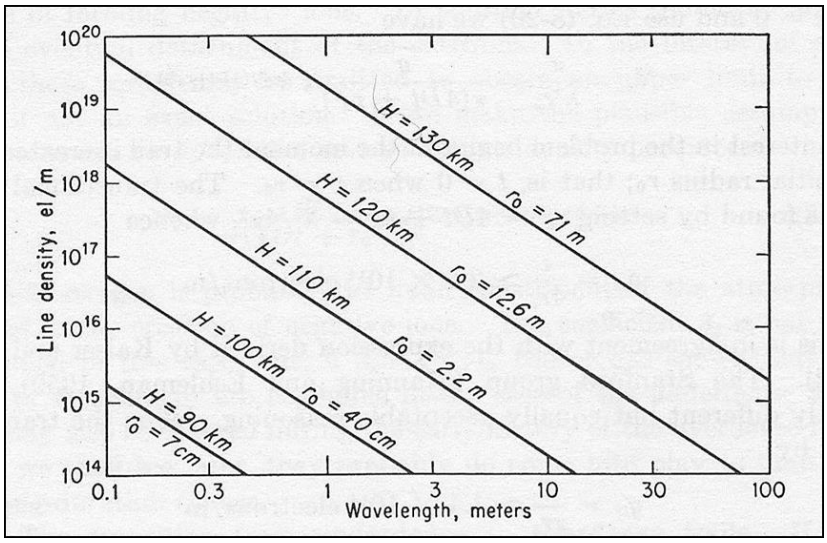

Figure 2.14: McKinley gave the minimum electron line density required to produce an overdense-type echo, which is plotted against the wavelength for selected values of atmospheric height (*H*) and initial radius (McKinley, 1961). Note however that the values for the initial radius appearing here have been significantly revised since in the last several decades and will be discussed in the next section.

Using equation (2.50) from the previous section, it is possible to write the expression for the critical radius for overdense meteors as:

$$r_c^2 = (4Dt + r_0^2)\, ln\left[\frac{q\lambda^2 r_e}{\pi^2(4Dt + r_0^2)^2}\right] \tag{2.54}$$

Again, the ambipolar diffusion is the only mechanism of expansion assumed here. The critical maximum radius can be then obtained by differentiation of the equation above with respect to time and setting it to zero (McKinley, 1961).

The obtained value of critical maximum radius $r_{c\,(max)}$ is expressed as:

$$r_{c(\max)}^2 = \frac{q}{\pi e N_c} = \frac{q\lambda^2 r_e}{\pi^2 e} \tag{2.55}$$

The expression is independent of initial radius, however if the $r_{c\ (max)}$ is less than the initial radius, then the observed meteor is no longer overdense, and classical underdense approach can be taken.

Consequently, the time at which overdense transitions into an underdense meteor trail can be expressed in terms of the initial radius and critical electron density N_c and can be written:

$$t_{(max)} = \frac{1}{4De}\left(\frac{q}{\pi N_c} - r_0^2\right) \tag{2.56}$$

Returning again to equation (2.50) and setting $r_c = 0$, it is possible to obtain the duration of overdense echo T_{ov}, before it transition to underdense, in similar fashion to that done in the underdense case. Then the equation can be stated as (Greenhow, 1952; Kaiser and Greenhow, 1953):

$$T_{ov} = \frac{q}{4\pi N_c} - \frac{r_0^2}{4D} \cong \frac{q}{4\pi N_c D} \cong \frac{q\lambda^2 r_e}{4\pi^2 D} \tag{2.57}$$

$$T_{ov} \cong 7 * 10^{-17}\frac{\lambda^2 q}{D} \tag{2.58}$$

Here $r_e \cong 2.8 * 10^{-15}\, m$ is the classical electron radius. The value published by Ceplecha et al. (1998) derived by using reflection coefficients closely matches the above value. Assuming again that $r_0 \gg \lambda$ and the approximation that an overdense meteor trail behaves like a metallic cylinder with specular reflection toward the observing location at distance R_0, and taking into consideration that the power flux incident upon the "cylinder" is $P_T G_T / 4\pi R_0^2$, the expression for the received power at the receiver, accounting for the distance attenuation factor $1/4\pi R_0^2$ and total collecting area of the receiving antenna $G\lambda^2/4\pi$, is written as:

$$P_R = \frac{P_T G^2}{64\pi^2 e^{0.5}} \left(\frac{\lambda}{R_0}\right)^3 \sqrt{r_c q} = 1.6 * 10^{-11} P_T G^2 \left(\frac{\lambda}{R_0}\right)^3 \sqrt{q} \quad (2.59)$$

where G is the matched gain of the transmitter and receiver. The unit of P_R is Watts. On the side note, the value for the P_R from Ceplecha et al. (1998) is relatively close, with the exception that P_R is approximately proportional to $q^{0.55}$ vs. $q^{0.50}$ derived by McKinley (1961). While $q^{0.55}$ is found to represent the behaviour of overdense meteors better, the $q^{0.50}$, which describes the metallic cylinder, is still the appropriate value used in many discussions covering the topic (Ceplecha et al., 1998).

Baggaley (1979) reaffirmed that, beside the diffusive process, a simple attachment theory discussed in some of the early work is not sufficient to explain the observed radar behaviour of overdense meteor trails. It was clearly shown (Baggaley and Cummack, 1974) that ozone is the main contributing factor, and that the process of oxidation reactions and subsequent dissociative recombination involving meteoric ions is responsible for electron removal from the train. This will be further discussed in the upcoming section of this thesis. Another relevant point observed by Baggaley (1979) indicates that for the slower meteors, because of their deeper atmospheric penetration, the radar echo duration will last much less because of higher density of the reacting atmospheric constituents and subsequent faster removal of electrons from the meteor train (Figure 2.15).

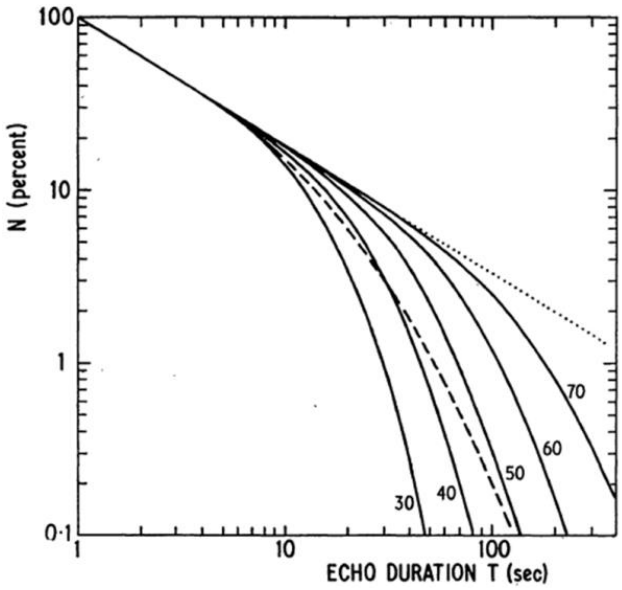

Figure 2.15: Cumulative occurrence frequency-duration distribution of overdense echoes for a 10 m radar wavelength. The velocities are indicated beside each curve in km/s and the dashed curve is for relative comparison with earlier results from McCorsky and Posen (1961) (after Baggaley, 1979).

Moreover, depending on the duration time that the overdense radar echo is observable, there are additional factors besides diffusion and chemical processes that act on the meteor train (Nicholson and Poole, 1974). Those factors might be due to the turbulence, wind shears and gravity waves; however their effect is negligible on the time scale of less than one second.

2.3.6 Overdense Meteors and Ionization Distribution

It was Whipple (1943) and Herlofson (1948) followed by Kaiser (1953) who developed the foundation for understanding of the meteor ionization process and its intensity in the atmosphere.

Production of ionization formed as a result of meteoric ablation, and its subsequent length, always depend on height, velocity, mass and zenith angle of the incident meteoroid and it will follow a very specific curve that is a function of those parameters (Whipple, 1954; Eshleman, 1956; Greenhow and Neufeld, 1957; Lindblad, 1963).

Theoretical ionization curve shown in (Figure 2.16) closely matches observed results that can be obtained by optical means.

Moreover the height of maximum ionization closely corresponds to the height of the maximum visual magnitude (McKinley, 1961), and thus it is possible to derive the electron density from the visual magnitude.

For instance, the visual magnitude M_v (McKinley, 1961; Verniani, 1965) of the observed meteor shown in equations (2.17) and (2.18) at the maximum height of ionization can be related to the luminous intensity I (in Watts) and is rewritten again for pedantic reasons as:

$$M_v = 6.8 - 2.5 log I \tag{2.60}$$

Luminous intensity, which is proportional to kinetic energy of the ablated atoms, can be written in terms of the mass m and velocity v of the meteor:

$$I = -\tau \frac{v^2}{2} \frac{dm}{dt} \tag{2.61}$$

This can be rewritten to account for deceleration:

$$I = -\tau \left(\frac{v^2}{2} \frac{dm}{dt} + mv \frac{dv}{dt} \right) \tag{2.62}$$

Where τ is luminous efficiency, $\frac{dm}{dt}$ is the rate of mass loss and the second term in the brackets accounts for the energy loss due to deceleration (Ceplecha et al., 1998).

For overdense meteors, the length of the path of the ionization will be in excess of 25 km. For the case of underdense meteor ionization, this curve length will be significantly narrower (Greenhow and Neufeld, 1957). Consequently, the electron line density will also be directly proportional to the mass, composition, velocity and zenith angle of the meteor. Furthermore, electron density in the meteor train depends also on the ionization coefficient (Jones, 1997) discussed earlier. It should be noted that when the electron density of the meteor trail is discussed, what is generally meant is the electron production at the maxima of the ionization curve. This is a very important fact, as it will be revisited in detail during the discussion about the methodology deployed in this work in Chapter 3.

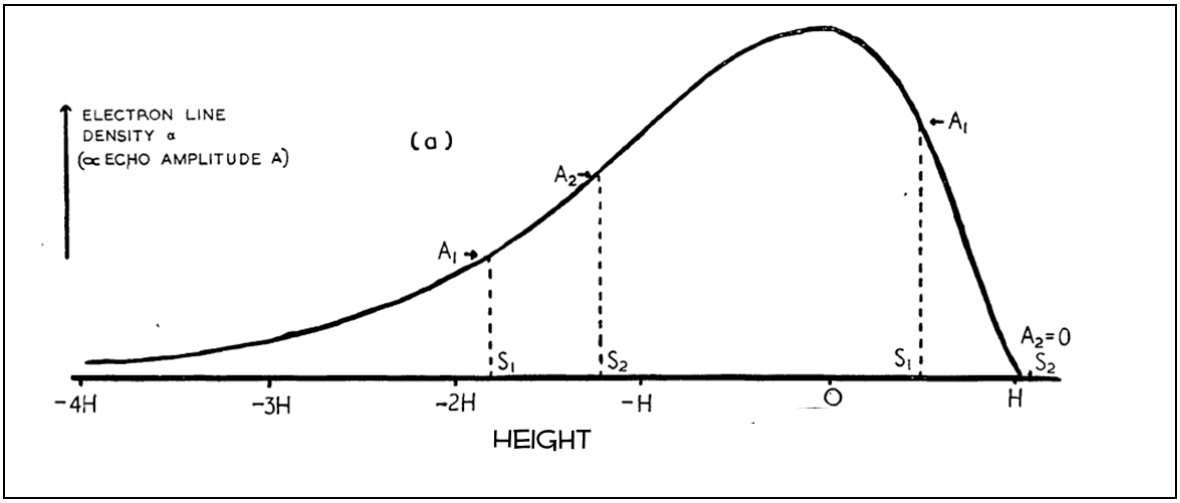

Figure 2.16: Theoretical ionization curve for overdense meteors which is calculated from the following expression: $\frac{\alpha}{\alpha_{max}} = \frac{9}{4}\frac{p}{p_{max}}\left(1 - \frac{1}{3}\frac{p}{p_{max}}\right)^2$, where p and p_{max} are atmospheric pressures at ionization height and at the height of the maximum ionization, respectively. Their ratio is expressed in terms of scale height *H* and atmospheric height *h* as: $\frac{p}{p_{max}} = exp\left[-\left(\frac{h-h_{max}}{H}\right)\right]$, where h_{max} is the height of the maximum ionization. The electron density and the maximum electron density are denoted by α and α_{max}, respectively. The principal equation above can be also expressed in terms of atmospheric density. The vertical axis on the plot above represents the electron line density which can be inferred from the echo amplitude (adapted from Greenhow and Neufeld (1957) and originally published by Herlofson (1948)).

As mentioned earlier, overdense meteor electron line densities, that are appropriately adjusted using ionization profiles and used for the purpose of this work, will be based on the published data by Sugar (1964). As an example, interpolating from his values, it is readily seen that a meteoroid 3 mm in diameter produces an electron line density of $5 \cdot 10^{15}$ m^{-1}. While technically this electron density is still in the transition regime (Poulter and Baggaley, 1977, 1978), at least it is possible to begin to reasonably constrain the sizes of radar-detected overdense meteors. This same value of electron density for the same mass is also obtained by Pellinen-Wannberg and Wannberg (1994). This is in line with the observation that all visible meteors have diameter of more than 2 mm (Murad and Williams, 2002).

Overdense meteors represent only small fraction of the total atmospheric influx, and by some estimates may consist up to 5% of the total meteoric flux (Figure 2.17)

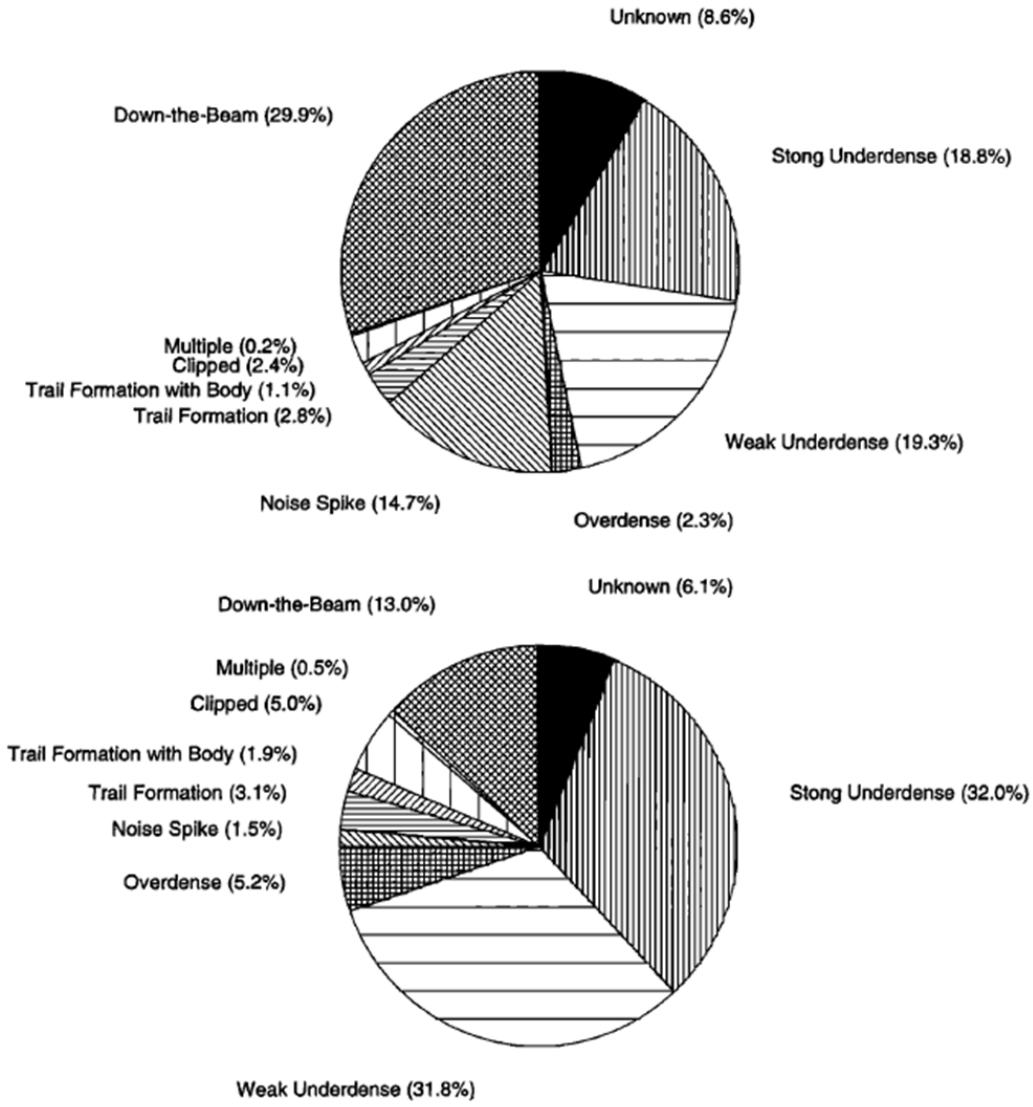

Figure 2.17: The distribution of the echo types observed by two separate VHF radar stations at Buckland Park, near Adelaide, Australia. One system was developed by the Atmospheric Physics Group at the University of Adelaide. The other radar belongs to the University of Colorado's Meteor Echo Detection and Collection (MEDAC) system. The top graph shows the distribution of echo classes within the MEDAC. The bottom graph shows the events seen simultaneously by both systems (Valentic et al., 1996).

In conclusion of this section it should be noted that the ionization process of the meteor in the atmosphere will not be possible if the meteoroid velocity is below 9 km/s as the

sufficient kinetic energy is not generated by the incident atmospheric molecules (Jones and Halliday, 2001).

2.4 Initial Radius of the Meteor Train

To date there is no complete satisfactory theory that comprehensively explains in physical terms the formation of the initial radius. Knowledge of the initial meteor radius is of critical importance to correctly interpret radio meteor data. Early theoretical work had been pioneered by Öpik (1958), Manning (1958) and Kashcheyev and Lebidenites (1963). Subsequently, many early and contemporary investigators have tried to model the formation of initial train with various degree of success (see for example Mitrov, 1960; Jones, 1995). Following the definition from the early literature, the term initial radius refers to the half-width of the initial Gaussian distribution of ions (or in the case of radio studies, electrons) that has "instantaneously" formed immediately after the passage of the meteor head. For the purpose of the radio studies it is assumed that the initial train radius is much smaller than the radar wavelength.

In principle, the incident atmospheric molecules will impact the meteoroid moving at hypervelocity, with energies of up to several hundreds of electron volts. Because of the high velocity factor, the path of the ablated meteoric atoms will not be a random three-dimensional walk (Manning, 1958). The total kinetic energy will depend on the meteoroid velocity. In the general case after the elastic rebound, the impacting atmospheric molecules may have velocities that are in excess of that of the meteoroid. The meteoric atoms that have left the surface of the meteoroid either as a result of sputtering or ablation, will have a wide range of velocities, ranging from slow "thermal" (Mirtov, 1960) to those that might be greater than that of the particle entering the Earth's atmosphere. The probability of inelastic collisions between the molecules in the energy range of tens of thousands of electron volts increases with energy of the colliding particles (Mirtov, 1960). Consequently, during the time that a meteoroid travels through the atmosphere, a great number of inelastic collisions will occur between the meteoric atoms initially leaving the surface of the meteor and incident atmospheric molecules.

Manning (1958) was originally of the opinion that the initial radius of the meteor trail will be in the order of 14 mean free paths in the atmosphere. While it had been shown

that the diameter of the initial meteor train is significantly greater than fourteen mean free paths, based on photographic and radio measurements (Sugar, 1964), it is indeed the atmospheric density that is controlling the factor on the size of the initial radius, but that dependence is again much less than previously thought (Baggaley, 1970, 1980, 1981). Manning (1958) did, however, point out correctly the importance of the mean free path of the atmosphere, ionic diffusion, temperature and meteor velocity in the formation and the size of the initial meteor radius. Moreover, he also realized that the initial radius of overdense meteors will be significantly different from that of underdense events as the temperature in the overdense trail is many times greater. Greenhow and Hall (1960) used experimental photographic and radio data to derive the values of initial radius as a function of height. Their results were significantly greater than those of Manning (1958) and they also observed a strong relationship between the meteor velocity, atmospheric height and the initial radius size (Figure 2.18). As a side-note, it is interesting to observe that the contribution of mass and meteoroid diameter had been rarely mentioned in those early investigations, as most of the events studied were taken as underdense.

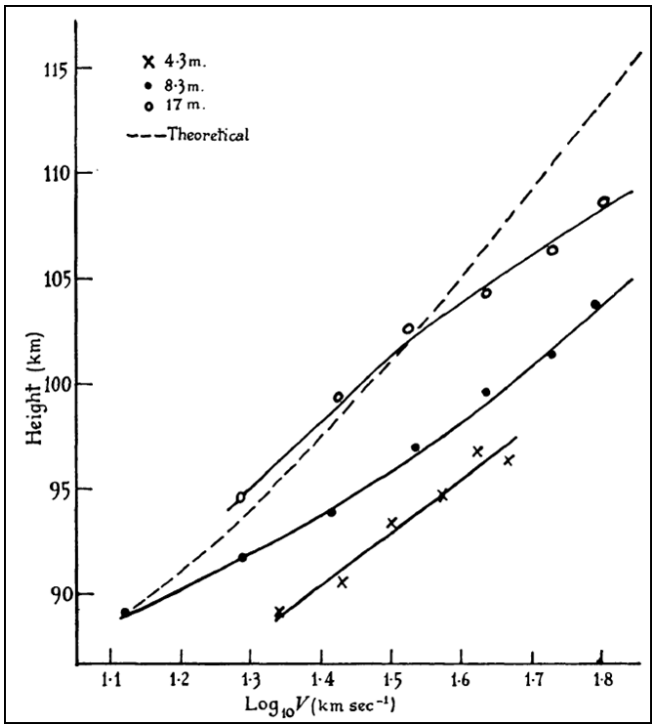

Figure 2.18: The height-velocity relationship for meteors observed by radio echo methods and compared with the theoretical curve (Greenhow and Hall, 1960).

Typical radar determinations of the initial underdense meteor radius are based on the known dependence of the radar echo amplitude on the wavelength and the initial radius diameter. Taking the value of the initial radius r_0 as finite, then the echo amplitude is attenuated by a factor of $exp\left(\frac{2\pi r_0}{\lambda}\right)^2$. If the $r_0 = \lambda/2\pi$, then the echo attenuation is 8.7 dB. However, when $r_0 > \lambda/2\pi$, the attenuation becomes severe, as discussed earlier. Then it is possible to use two different wavelengths and evaluate the echo amplitude ratio, which can be written as: $\left[(2\pi r_0)^2\left(\frac{1}{\lambda_1^2} - \frac{1}{\lambda_2^2}\right)\right]$, where $\lambda_1 \, and \, \lambda_2$ are different wavelengths. When this ratio is determined together with the radar echo height for meteor events, it is possible to estimate the value for initial radius as a function height and meteor velocity (Baggaley, 1970). It should be noted that the Faraday's rotation must be taken into account when measuring the initial radius with VHF radars, where the degree of rotation will depend on the radio wave frequency (Elford and Taylor, 1997).

Baggaley and Fisher (1980) investigated the diameter of the initial meteor radius as a function of electron density in the trail with particular focus on overdense meteors. They had used triple frequency radar setup as a way to improve accuracy of their measurements. For the overdense meteors, the principle of r_0 determination is the same, with the exception that their duration time will be different. Rewriting again equation (2.52) from the previous section, the duration time, in the absence of the chemical contribution or other factors, is:

$$T_{overdese} = \alpha \frac{r_e \lambda^2}{4\pi^2 D} - \frac{r_0^2}{4D} \tag{2.63}$$

here α is the linear electron density, r_e is the classical electron scattering radius and the expression $\frac{r_0^2}{4D}$ can be thought of as the time since the formation of the train. Note that the symbol α is used here for the electron line density, instead of q used earlier in the text. Both symbols are intermittently used in literature, however, for the purpose of clarity only alpha will be used in the remainder of this thesis. Thus, for the meteor entering the Earth's atmosphere, an upper limit to initial radius can be determined by simply recording the lowest wavelength at which an overdense echo can be observed. That can be written in concise form as:

$$r_0 < (\lambda_{lower}/\pi)\sqrt{(\alpha r_e)} \tag{2.64}$$

Correspondingly, the absence of an echo at a short wavelength defines the lower limit of the initial radius,

$$r_0 > (\lambda_{upper}/\pi)\sqrt{(\alpha r_e)} \tag{2.65}$$

Knowing the scattering radius of an electron, and with typical wavelength of meteor radar, the necessary wavelength to observe the initial radius of the overdense meteor trail, can be written as: $\lambda = 1.7r_0$ (Baggaley and Fisher, 1980). They were able to obtain values of the initial radius between 75 km and 105 km. For illustrative purpose, Table 2.2 with different values of the initial radius compiled from the literature by Ceplecha et al. (1998) is given below. The reported error in the results obtained by Baggaely and Fisher (1980) is about 50%. However, to date, their work is the most reliable estimate of the initial overdense meteor radius, and will be used primarily in the calculation in further chapters in this thesis. It is interesting to observe with respect to the work done in this thesis, that Baggaley and Fisher (1980) remarked that chemical removal of free electrons can contribute to the initial radius values. The relevance of this statement will become considerably clearer in later chapters.

Table 2.2: Values of initial radius in metres. The values in the outlined column are from Baggaley and Fisher (1980) and are used in this thesis (compiled by Ceplecha et al., 1998).

Height	Experimental				$v = 40$ km s^{-1}	
km	$v = 20$ km s^{-1}	40 km s^{-1}	60 km s^{-1}	Bright	Theory $(1/\rho)$	$r_{0(\text{eff})}$
75	0.22	0.33	0.42	0.35*	–	–
80	0.27	0.40	0.51	0.56*	–	–
85	0.33	0.49	0.63	0.93*	–	–
90	0.41	0.61	0.78	1.62*	0.72	0.72
95	0.51	0.77*	0.98	2.83*	1.53	1.38
100	0.63	0.96*	1.23*	5.00*	3.22	2.16
105	0.79	1.20*	1.53*	8.77	6.82	2.66
110	0.98	1.49*	1.90*	–	15.6	3.10
115	1.19	1.81*	2.30	–	30.6	3.63
120	1.41	2.13	2.72	–	64.4	4.30

A wide range of values of initial meteor trail radius obtained by different authors prior and including 1970, and their significant deviation is illustrated in the Figure 2.19.

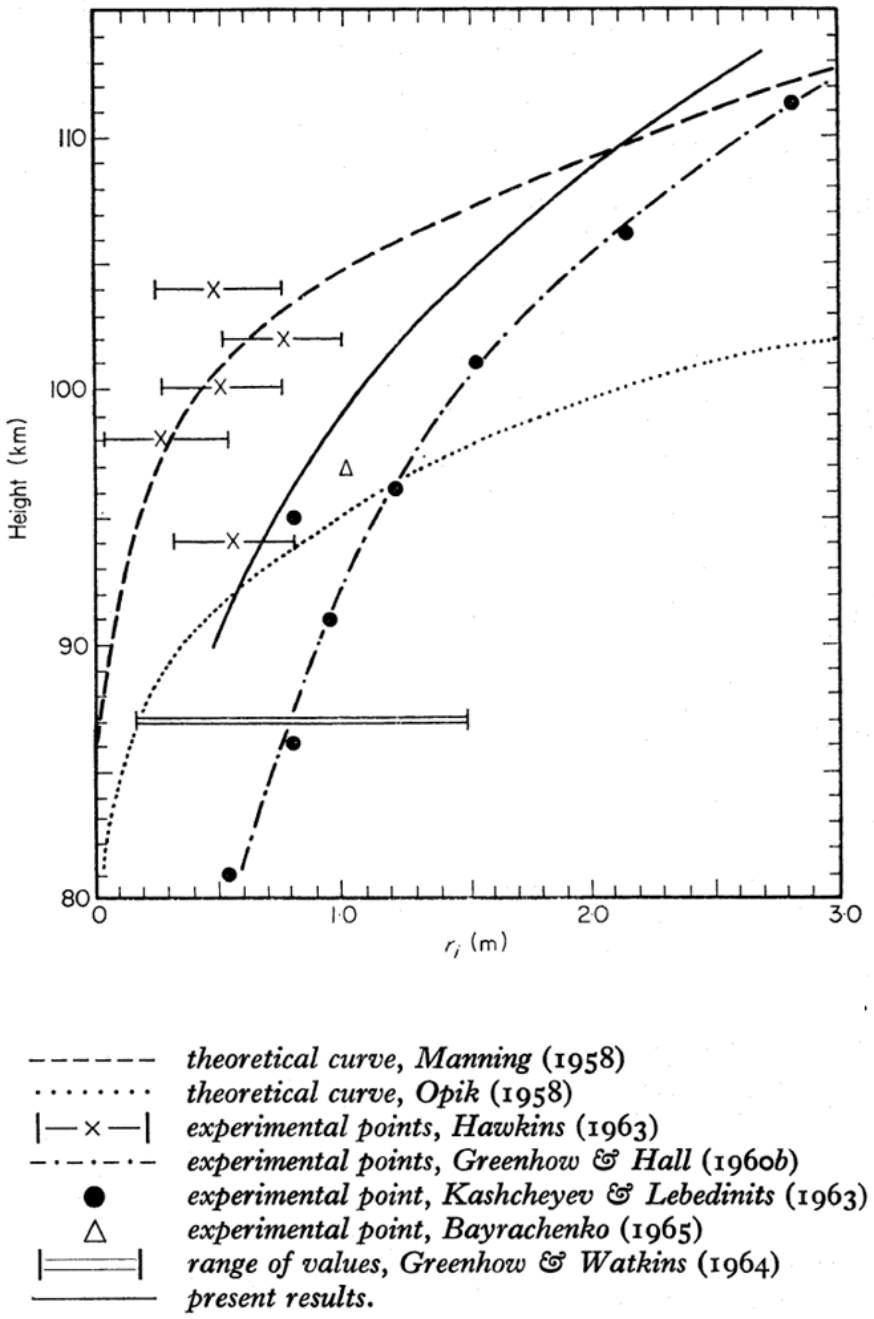

Figure 2.19: The summary of the estimates of meteor initial radius compiled up to 1970. The "present results" legend above refers to the experimental results obtained by Baggaley (Baggaley, 1970).

Ablated and ionized meteoric atoms will experience thermalization during the collisions with the surrounding atmosphere (Bronshten, 1983), where the atoms will lose about one third of their speed after each collision, or about half of their energy (Sugar, 1964). It takes about 1 x 10^{-3} seconds for the meteoric ions to thermalize while electrons will thermalize much slower (Baggaley and Webb, 1977; Ceplecha et al., 1998)(Table 2.3).

Table 2.3: Thermalization times of electrons (ms) (Ceplecha et al., 1998).

Height	Line density (m^{-1})		
(km)	$< 2.5 \times 10^{14}$	2.5×10^{15}	2.5×10^{16}
80	0.6	0.6	0.5
90	4.0	3.3	1.8
100	21	16	7.5
110	85	66	45
120	240	240	240

Between 75 km and 96 km, the effects of the geomagnetic field will not be significant and the initial trail cross section will have a circular shape. More recently, Jones and Campbell-Brown (2005) investigated the radius of sporadic underdense meteors using dual frequency radar observation, with the results being in close agreement to that of Greenhow and Hall (1960) and diverging slightly from those results obtained by Baggaley (1970) and Ceplecha et al. (1998).

A full theoretical treatment of the initial radius was done by Jones (1995). The importance of this seminal work rests in the fact that he had shown that the radial electron density within the trail is not fully Gaussian. Using computer simulations, Jones (1995) had shown that thermal equilibrium for ions is reached after about 15 – 20 collisions which is relatively close to the value of 14 derived by Manning (1958). An important note however must be made regarding Jones' (1995) derivation, which pertains to the fact that his calculations use the assumption of only elastic collisions. In reality, as indicated at the beginning of this section, in addition to elastic collisions there is a large number of

inelastic ones (Mirtov, 1960). At this point however, it is not clear if the inclusion of that fact would change the outcome of the final result. From the theoretical treatment in Bronshten (1983) and Jones (1995) it can be easily seen that the initial radius (in this case the solid particle with no fragmentation is assumed) can be expressed as $\rho^a v^b$ where $a \sim -1$ and $b \sim 0.8$.

At this point it might be appropriate to recall the derivation of the critical line density defining the transition to the overdense meteor regime (McKinley, 1961) discussed in the previous section. The initial radius will depend on electron density, as pointed by Jones (1995). If McKinley's treatment is followed, then at radar wavelength of 11.4 m the critical density is $8.67 \cdot 10^{14}$. Now using Bronshten's (1983) formula and its improved version (Jones, 1995)

$$r_0 = 2.845 \times 10^{18} v^{0.8} / n_a \tag{2.66}$$

It can be calculated that the initial radius is approximately 15 m at 110 km, for a non-Gaussian profile. If the profile is Gaussian, then the necessary electron linear density must be in excess of $6.3 \cdot 10^{15}$ m^{-1}. Here, the n_a is atmospheric density at specific height.

Accordingly, it can be reasonably concluded that the initial radius will also depend on an assumed type of cross-sectional electron density distribution. Consequently, the treatment of the initial radius cannot be the same for underdense, transitional and overdense meteors as pointed by Jones (1995), Baggaley and Fisher (1980) and inferred from the calculations of Poulter and Baggaley (1977; 1978).

2.5 Meteor Trail Diffusion

Following the formation of the initial radius in the region between the 80– 95 km, the meteor trail expands under the effect of ambipolar diffusion, which itself is a function of temperature and pressure, and can be expressed in terms of those parameters as $D = K\left(\frac{T^2}{P}\right)$ (Hocking et al., 1997), where *K* is the constant, and *T* and *P* are temperature and pressure, respectively.

Below 80 km, the presence of high density neutrals and complex oxidation-dissociation chemistry will increasingly affect the rate of ambipolar diffusion of the meteor trail

expansion. Above 95 km, the role of geomagnetic field starts to play a role in the diffusion of the meteor trail (Kaiser, 1968; Elford and Elford, 2001).

The concept of ambipolar diffusion, without diverging too much into the field of plasma physics, can be presented as follows. The newly formed ionized column with some initial radius left behind a fast moving meteor, is essentially a quasineutral plasma, containing positive metallic ions and electrons. The ions are affected by two primary forces; one is a thermodynamic force resulting from the density gradient within the trail and relative to the ambient atmosphere, and the other is the electric Coulomb force arising between the ions and electrons. The ablated metallic ions have in excess of 100 eV of energy, which is a function of meteor velocity (Baggaley, 1980). This translational energy, through the series of collisions, is converted to heating of the meteor trail and the atmosphere, which is the process that thermalizes both ions and electrons. The process of thermalization is generally over in several tens of milliseconds for ions and around 0.1 s for electrons (Delov, 1975; Baggaley and Fisher, 1977). Free electrons may possess energies in the range of up to 10 eV. However, the metallic ions which are many orders of magnitude heavier than electrons will consequently move much more slowly. The rapid dispersion of electrons is retarded by the electric field induced by separation of charged species, which simultaneously adjusts the ions' speeds and ensures the overall equal diffusion of both electrons and ions. Consequently, the ions and electrons will move together as a single gas under the influence of gravity, density and temperature gradients. In principle, ambipolar diffusion is greater than free molecular diffusion.

If the assumption is made again that the distribution of ionization within the meteor trail (and consequently electrons) is Gaussian, than it is possible to state the standard form of diffusion equation:

$$\frac{\partial n}{\partial t} = D \frac{\partial^2 n}{\partial x^2} \tag{2.67}$$

Here at the moment, *D* is considered just general diffusion coefficient. Then assuming radial symmetry, the equation (2.67) can be written in the cylindrical from:

$$\frac{\partial n}{\partial t} = \frac{D}{r}\frac{\partial}{\partial r}\left(r\frac{\partial n}{\partial t}\right) \tag{2.68}$$

Here, the *D* can be taken as ambipolar diffusion coefficient. Then the classical solution, for this type of equation, applied to meteor trail, can be expressed as:

$$n\,(r,t) = \frac{q}{\pi(4Dt + r_0^2)}\exp\left[-\left(\frac{r^2}{4Dt + r_0^2}\right)\right] \tag{2.69}$$

This is in fact the volume density where $n\,(r,t)$ represents the amount of the diffused electrons, and r_0 and r are the initial radius of the meteor train and the radial distance from the center, respectively. The equation (2.68) becomes nonlinear and consequently far more difficult to solve analytically when additional terms are added representing the effects of the geomagnetic field, chemistry, turbulence and wind shear.

Now, with the assumption that ambipolar diffusion is the only agent of the ionized trail disintegration, it has been shown that in the echo amplitude from an underdense meteors decays as (Herlofson, 1951; Kaiser, 1953):

$$A = A_0\exp\left(-\frac{t}{\tau}\right) \tag{2.70}$$

Where *t* is the elapsed time since formation of the train and $\tau = t_u$ from equation (2.47) and following the convention, it can be written again as:

$$\tau = \frac{\lambda^2}{16\pi^2 D} \tag{2.71}$$

The diffusion coefficient can be estimated by defining the decay time $\tau_{1/2}$, from equation (2.71) as the time it takes for the radio echo to decrease to half from its peak, and subsequently *D* can be expressed as:

$$D = \frac{\lambda^2 ln2}{16\pi^2\tau_{1/2}} \tag{2.72}$$

This is the approach that was taken in early research to evaluate ambipolar diffusion of the meteor trails. However, this is only a general discussion about ambipolar diffusion. A more elaborate discussion about the derivation of ambipolar diffusion can be seen in the work of Francey (1963), Pickering and Windle, (1970) and more recently in the

comprehensive treatment by Robson (2001). Additionally, the approach by Liu (1970) should be noted, as he used very rigorous mathematical procedures, starting with the Maxwell-Boltzmann equation to treat the expansion of the meteor trails more accurately.

However, for the purpose of completeness, a brief mathematical treatment of ambipolar diffusion based on the phenomenological transport equation will be presented. First, the ions are considered in a dilute system and their flux $\boldsymbol{\Phi}_i$ (or particle current density) can be written as:

$$\boldsymbol{\Phi}_i = n_i \mu_i \boldsymbol{E} - D_i \frac{\partial n_i}{\partial \boldsymbol{r}} \tag{2.73}$$

Here $D_i, n_i \, and \, \mu_i$ are the ionic diffusion coefficient, ion density and ion mobility, respectively. The vector quantities are in bold, where $\boldsymbol{E}$ is the electrostatic force and $\boldsymbol{r}$ is the radial distance (Jones and Jones, 1990). Now the equation above is written for electrons with corresponding parameters:

$$\boldsymbol{\Phi}_e = -n_e \mu_e \boldsymbol{E} - D_e \frac{\partial n_e}{\partial \boldsymbol{r}} \tag{2.74}$$

Dividing both sides of equation (2.73) and equation (2.74) by μ_i and μ_e respectively, the resulting expressions are given by:

$$\frac{\boldsymbol{\Phi}_i}{\mu_i} = n_i \boldsymbol{E} - \frac{D_i}{\mu_i} \frac{\partial n_i}{\partial \boldsymbol{r}} \tag{2.75}$$

and for electrons:

$$\frac{\boldsymbol{\Phi}_e}{\mu_e} = -n_e \boldsymbol{E} - \frac{D_e}{\mu_e} \frac{\partial n_e}{\partial \boldsymbol{r}} \tag{2.76}$$

Now, equations (2.75) and (2.76) can be added with assumption that $n_e = n_i$ and that $\boldsymbol{\Phi}_i = \boldsymbol{\Phi}_e$. Moreover, $\boldsymbol{E}$ can be eliminated, and above conditions allows for setting the expression:

$$\boldsymbol{\Phi}_{\boldsymbol{i,e}} = -D_{\boldsymbol{a}} \frac{\partial n_{i,e}}{\partial \boldsymbol{r}} \tag{2.77}$$

Then the general expression for the ambipolar diffusion coefficient can be written:

$$D_a = \frac{D_e \mu_i + D_i \mu_e}{\mu_e + \mu_i} \tag{2.78}$$

For a dilute system considered here, it is possible to apply the Einstein's relation:

$$D_i = \mu_i kT \tag{2.79}$$

Where D_i is the ion diffusion coefficient, k is Boltzmann's constant and T is the temperature. The expression (2.79) can also be written for electrons in the same manner.

Considering that $\mu_e \gg \mu_i$ and $D_e \gg D_i$ and using Einstein's relation to substitute for D_e in equation (2.78), it can be easily seen that for quasi-equilibrium, $D_a \approx 2D_i$.

The expression (2.67) can be easily derived by substituting the Einstein's relation in the expression for the total flux equation (2.77) and taking the divergence of it. The calculations are elegantly presented in Jones and Jones (1990).

The problem of the behaviour of the ionized meteor trail after formation has been considered by many authors in the past and present. At least one hundred peer reviewed papers have been published on the subject of the meteor trail diffusion alone, between 1949 and 1980.

Greenhow (1952) investigated the behaviour of electrons after formation of the meteor trail. Kaiser (1953) conducted a comprehensive study of the meteor trail diffusion by combining theoretical and experimental methods, established that the role of what was called chemical attachment at the time, contributes to the meteor trail diffusion. Further work was done by Weiss (1955), where he investigated the diffusion coefficients from the rate of decay of the meteor trail of 112 events. Even from a relatively small sample, he was able to observe large scattering, resonance effects and contribution of the magnetic field. The method of the split beam technique was deployed by Greenhow and Neufeld (1955) in order to study diffusion of low electron density meteor trails. Following the already proven method (Kaiser, 1953), they utilized the amplitude records of radio observations to evaluate the diffusion coefficients. The results that they obtained were the best at the time. Murray (1959) used the same methodology and investigated ambipolar diffusion of faint meteors, obtaining the similar results as earlier authors, confirming the existence of large and significant fluctuations in the data (Murray, 1959).

The use of two widely spaced antennas and a single receiver was adopted by Greenhow and Hall (1961). This approach enabled them to significantly improve the result obtained by Greenhow and Neufeld, (1955). The problem of large data scatter could not be avoided again as it can be seen from the Figure 2.20.

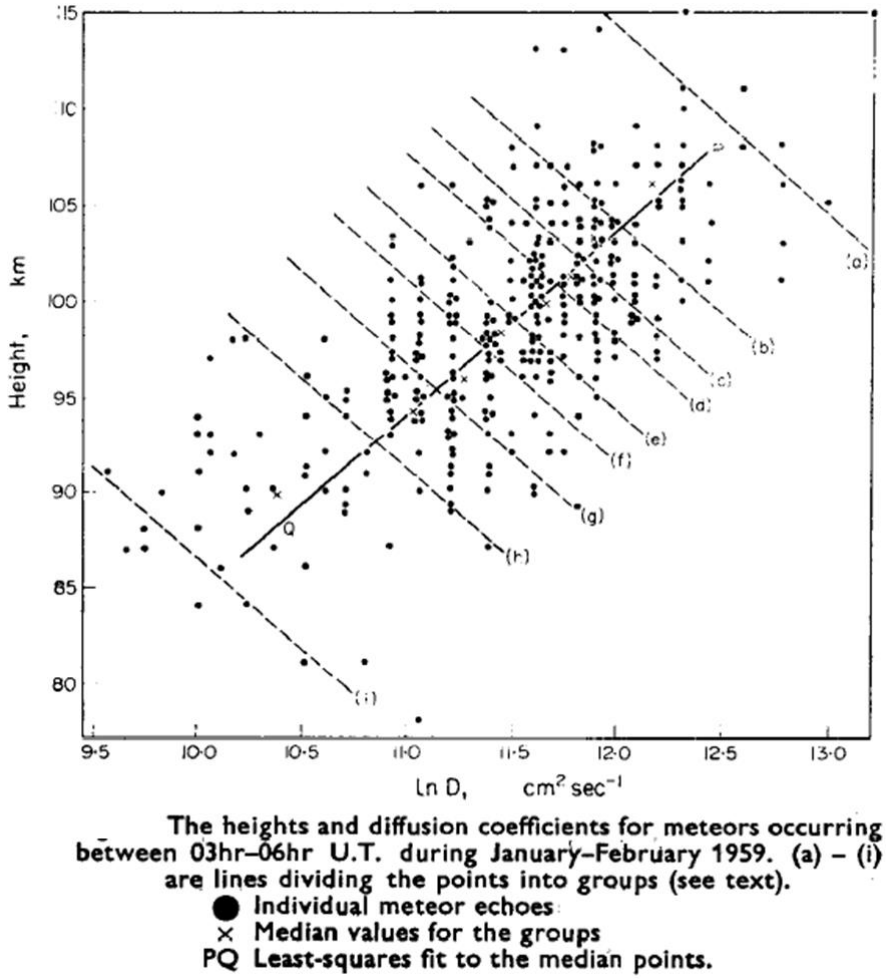

The heights and diffusion coefficients for meteors occurring between 03hr–06hr U.T. during January–February 1959. (a) – (i) are lines dividing the points into groups (see text).
● Individual meteor echoes
× Median values for the groups
PQ Least-squares fit to the median points.

Figure 2.20: Dispersion in obtained diffusion data and the result of fitting (Greenhow and Hall, 1961)

Despite a great uncertainty in obtained results, their results are amongst most reliable even when compared with the work of contemporary authors, prior to the 1990s. Another relevant aspect of their work was the observation that there is significant latitudinal and

seasonal variation in the ambipolar diffusion coefficient, which is also recognized to be susceptible to the effects of chemistry.

Jones (1975) concluded that even underdense meteor diffusion is affected by chemical processes. His results and comparison with the earlier work are shown in Figure 2.21 below.

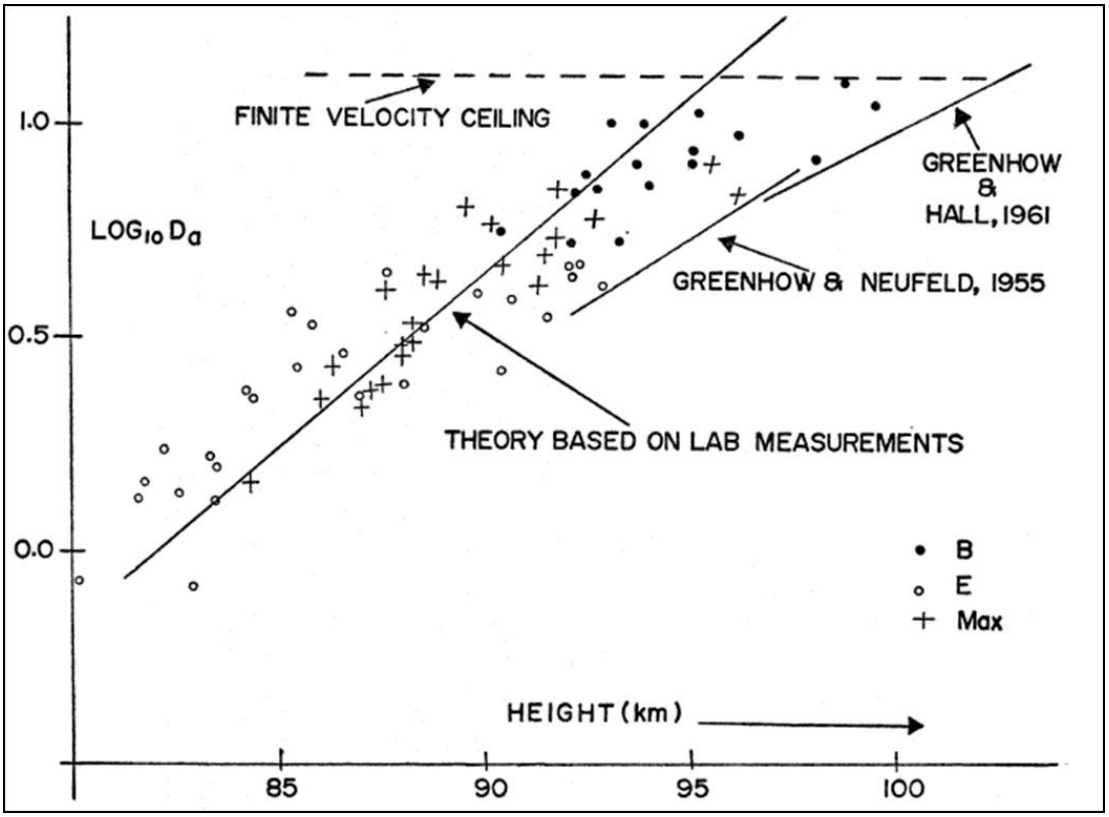

Figure 2.21: The comparison of values of ambipolar diffusion obtained by Jones (1975) and the earlier results.

Likely causes of the large scatter in data in the previously mentioned investigations were discussed by Novotny (1978). He has identified the rotation of meteor trail under the influence of the height gradient of the horizontal wind component, chemical processes, non-uniformity of the electron line density along the meteor trail, resonance effects and data recording methods as the main sources of dispersion in the data. Jones and Jones (1990) examined the relationship between the theoretical and observational diffusion

coefficients. Furthermore, they have theoretically estimated the ionic mobility and analyzed the case of the multiple ion species in the meteor trail. They acknowledged the role of ozone in chemical processes and two-body recombination, which removes electrons from the trail, especially in events with long lasting radio echoes, thus confirming the work of Poole and Nicholson (1975) and Baggaley (1979) which will be discussed in the next section. One of the critical remarks made by Jones and Jones (1990) is the fact that while it is relatively easy to treat the diffusion in the presence of the same ionic species, significant complications arise when there are several different ionic species, even in the case when they have the same molecular mass. The comparison of radar and lidar obtained diffusion coefficients showing significant deviation (Figure 2.22), with lidar data showing greater meteor diffusion rates (Chilson et al., 1996). The influence of the neutral turbulence has been investigated by Hall (2002). Considering that the time scale of signals obtained in this thesis is lower than one second and that Hall (1996) recognized that turbulence will act at time scale equal or greater than 1.6 seconds, it can be concluded that the turbulence will not have any appreciable effect on the data and results obtained here.

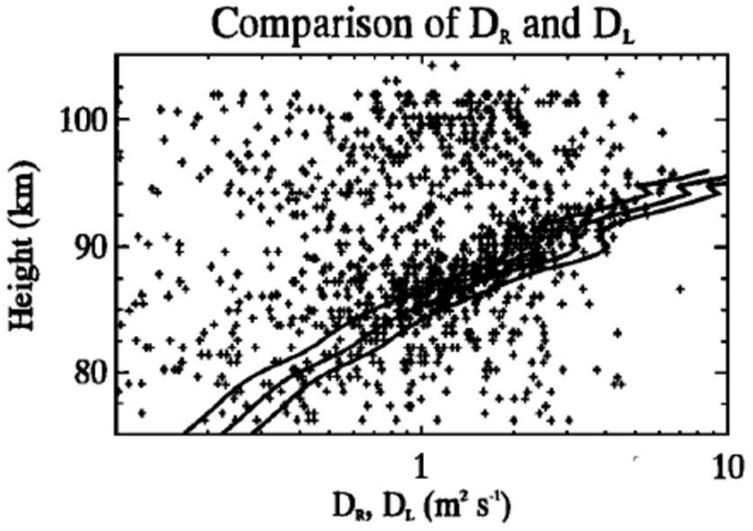

Figure 2.22: Scatter plot of the diffusion coefficients obtained from the radar data (D_R) as a function of height compared to the three line profiles of the height vs. diffusion coefficients calculated from the lidar data (D_L) for different values of K_0 (Chilson et al., 1996).

For maximum accuracy, Galligan et al. (2004) used a tristatic setup at the Advanced Meteor Orbit Radar (AMOR) to study ambipolar diffusion from a large set of meteor data, in the region between 70 km and 120 km. They considered the effects of geomagnetic field influence on the diffusion coefficient of meteor trails; however, they did not observe any serious fluctuations in ambipolar diffusion below 100 km, directly induced by the geomagnetic field.

Yee and Close (2011) conducted a meteor plasmas diffusion study using data from a non-specular trail detected by the Advanced Research Project Agency (ARPA) Long-range Tracking and Identification Radar (ALTAIR). The diffusion coefficients determined from non-specular events were compared to the results from specular studies. They concluded that the results from non-specular trails do not correspond to the results from specular trails, as there is an order of magnitude difference between diffusion coefficients.

Table 2.4 shows selected and compiled values of ambipolar diffusion for heights of 80 km and 100 km, illustrating the divergence in values obtained by various authors throughout years. However, the introduction of the SKiYMET meteor radar system (for example see Hocking et al., 1997; Hocking et al., 2001) has improved the measurement of meteor trail diffusion significantly. SKiYMET has achieved the level of accuracy that was not possible in the early days or by other contemporary meteor radar systems. This will be discussed in more detail in the next chapter.

Table 2.4: Compiled literature values of the observed and calculated ambipolar diffusion coefficients, for comparative purpose, obtained by different authors over the period of four decades

Year	Author	Title of the Paper	Method	Formula	D_a at 80 km (in m^2/s)	D_a at 100 km (in m^2/s)	Comments
1961	McKinley, D. W. R.	Meteor science and engineering	Theoretical and Experimental	$D \approx 10^{(0.067h-5.6)}$	0.575	12.589	As per Greenhow and Neufled, 1955
1961	Greenhow and Hall	The height variation of the ambipolar diffusion coefficient for meteor trails	Experimental fit	$D \approx 10^{(0.0543h-4.373)}$	0.935	11.402	Most reliable according to Verniani and Hawkins, 1964
1970	Jones, J.	On the variation of the ambipolar diffusion coefficient with height	Theoretical	$D \approx e^{((h-13)/7.4)}$	0.855	12.761	In original equation D is in cm^2/sec
1986	Thomas et al.	Frequency Dependance of Radar Meteor Echo Rates	Experimental	$D \approx 10^{(0.0758h-6.51)}$	0.358	11.749	
1990	Jones, W and Jones, J.	N/A	Republished (theoretical)	$D \approx e^{((h-79.3)/7.24)}$	1.101	17.446	Published by Gilligan et al. 2004 (data refitted)
1990	Jones, W and Jones, J.	An analysis of the physical parameters of 5759 faint radio meteors	Fit from Verniani experimental data	$D \approx 10^{(0.086h-7.23)}$	0.446	23.442	Fit
1990	Jones, W and Jones, J.	Ionic diffusion in meteor trains	Massey's formula based	$D \approx 10^{(0.06h-4.74)}$	1.148	18.197	Theoretical value fit (original)
1998	Thomas, G	Meteoric diffusion studies of the middle atmospheric dynamical structure	Experimental fit (AMOR)	$D \approx e^{((h-84.8)/4.83)}$	0.342	23.266	Thesis
2004	Galligan et al.	On the relationship between meteor height and ambipolar diffusion	Experimental fit	$D \approx e^{((h-87.9)/4.43)}$	0.168	15.354	

2.5.1 Diffusion of Meteor Trails in the Presence of Geomagnetic Field

Since the geomagnetic field plays a negligible role on the results in this study, an elaborate discussion about diffusion under the geomagnetic influence will be omitted, and the reader is pointed toward comprehensive studies conducted by several key authors in the field. However, the basic premise of the problem of the geomagnetic effect on diffusion is presented here along with a brief historical cross-section of this specific research.

The effect of the geomagnetic field on ambipolar diffusion can be characterized in a way that it increases the lifetime of meteor trails especially in the region above 100 km (Lowell, 1965; Elford and Elford, 2001). This is most applicable to meteors with low plasma density (underdense) as the distance between plasma collisions is relatively large, such that the influence of magnetic field on the ion/electron path is significant. Robson (2001) gave a basic expression for the effective diffusion coefficient as:

$$D_{eff} = D_{paralel} sin^2\mu \, sin^2\theta + D_{orthogonal}(1 - sin^2\mu \, sin^2\theta) \tag{2.80}$$

where $D_{paralel}$ and $D_{orthogonal}$ are the ambipolar diffusion coefficients parallel and orthogonal to the magnetic field, θ is the angle the field makes with the meteor trail, and μ is the angle between the wave vector and the normal to the plane of the trail and the field. The Figure 2.23 illustrates variation of diffusion coefficients with height.

Francey (1964) and Lowell (1965) conducted theoretical calculations of the meteor trail diffusion in the presence of the magnetic field. Additional comprehensive theoretical treatment of ambipolar diffusion in the magnetic field was presented by Kaiser (1968) which laid the foundation for subsequent studies. Phase coherent radar using the horizontally polarized Yagi antennas was deployed by Baggaley and Webb (1980) to investigate a theoretical application to the experiment. Due to a large scatter of diffusion values as a function of height, it was not possible to definitively discern the contribution of geomagnetic field using backscatter radar. They only remarked about a slight decrease of the diffusion coefficient for underdense meteors under the geomagnetic field. However, the effect on overdense meteors was observed to be negligible, at least in backscatter radar measurements.

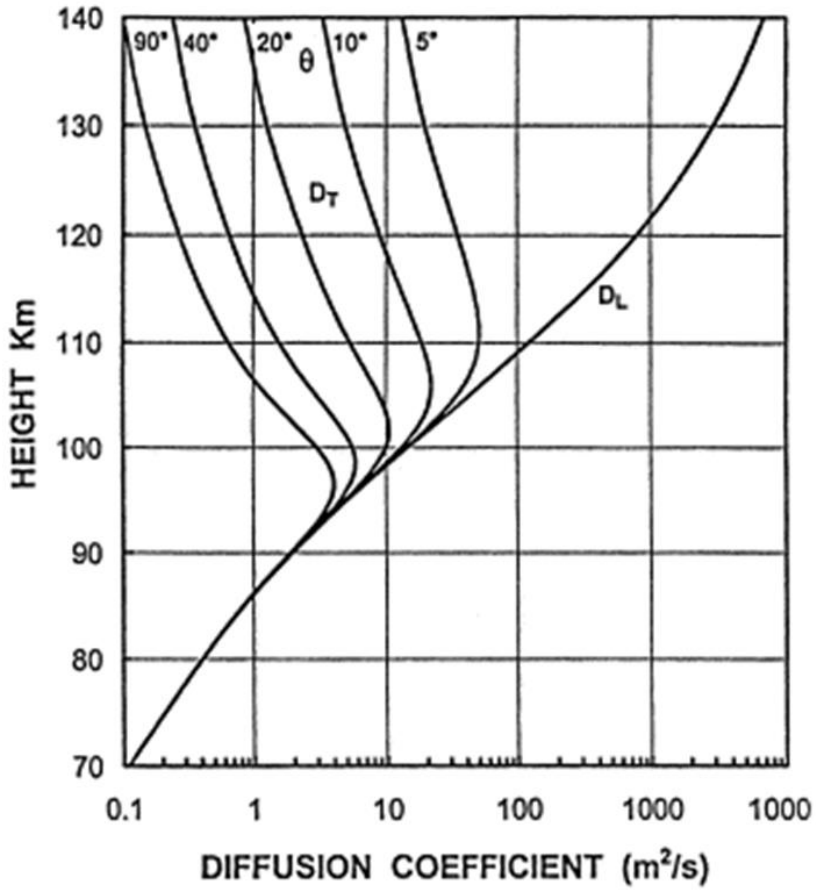

Figure 2.23: Height variation of the ambipolar diffusion coefficients parallel (D_L) and orthogonal (D_T) to the geomagnetic field. The angle θ is defined as the angle the axis of the trail makes with the direction of the magnetic field (Elford, 2001).

Another important theoretical work (Jones, 1991) resulted in the formulation of the analytic solution to the diffusion in "ionized cylindrical train" in the magnetic field. He had also shown that diffusion will be inhibited the most by the effect of the geomagnetic field when the angle between the meteor train axis and the magnetic field lines is close to zero.

A theoretical and modeling study was conducted by Robson (2001) from the perspective of a pure plasma physics approach. He criticized the approach and assumptions taken by Jones (1991) and general treatment of ambipolar diffusion in meteor literature. Robson's approach, while consistent with the conventional plasma physics treatment, diverges to an extent from the results obtained in mainstream meteor literature. Hocking (2005)

conducted an important study of anisotropic meteor trail diffusion under the influence of the geomagnetic field. The critical observation with a significant implication for future studies of anisotropic meteor trail diffusion, suggests the contribution of external electric field in addition to magnetic field effects.

Sophisticated modeling studies of the topic conducted by (Oppenheim et al., 2000; Dyrud et al., 2001; Oppenheim et al., 2003; Dimant et al., 2006) shine a new light on the behaviour of meteor trail plasma in the geomagnetic field and suggest considerable effects only above 105 km.

2.5.2 The Remaining Questions Regarding Ambipolar Diffusion

Among several critical investigations that motivated the work done in this thesis are four recent papers which have questioned the validity of ambipolar diffusion in the meteor region.

Younger et al. (2008) considered the role of the background dust, in the meteor region, in absorption of electrons from the underdense meteor trail which potentially affects the backscatter radar observed diffusion duration. Taking the dust concentration to be in the range of 5×10^{9} to 5×10^{10} m^{-3} and meteor train electron line densities between 10^{11} - 10^{14} m^{-1} at altitude of 85 km, they have observed that the echo duration times deviate up to 30% for the meteor trails with lower limit of electron line densities. Similar observations were made by Havnes and Sigernes (2005).

By now it has become obvious that ambipolar diffusion is not the only mechanism which contributes to the electron removal and dispersion from the expanding meteor trail, at least from the perspective of radio observations. While it is well established that chemistry plays an important role in long duration overdense echoes (Baggaley and Cummack, 1974), it is clear that even underdense meteor trails do not diffuse only under the influence of ambipolar diffusion. The question that remains to be answered is what are the other possible mechanisms which remove electrons from the meteor trail.

The same question was asked by Ballinger et al. (2008) as they investigated ambipolar diffusion using the VHF (All-Sky Interferometric Meteor Radar or SKiYMET) backscatter system. Furthermore, they have discussed the vertical decay time profile and

peculiar maxima at approximately 83 km, after which the decay time decreases (Figure 2.24), not predicted by the classical ambipolar theory. The possibility of electron-ion recombination as the probable cause for this peculiar behaviour has been proposed.

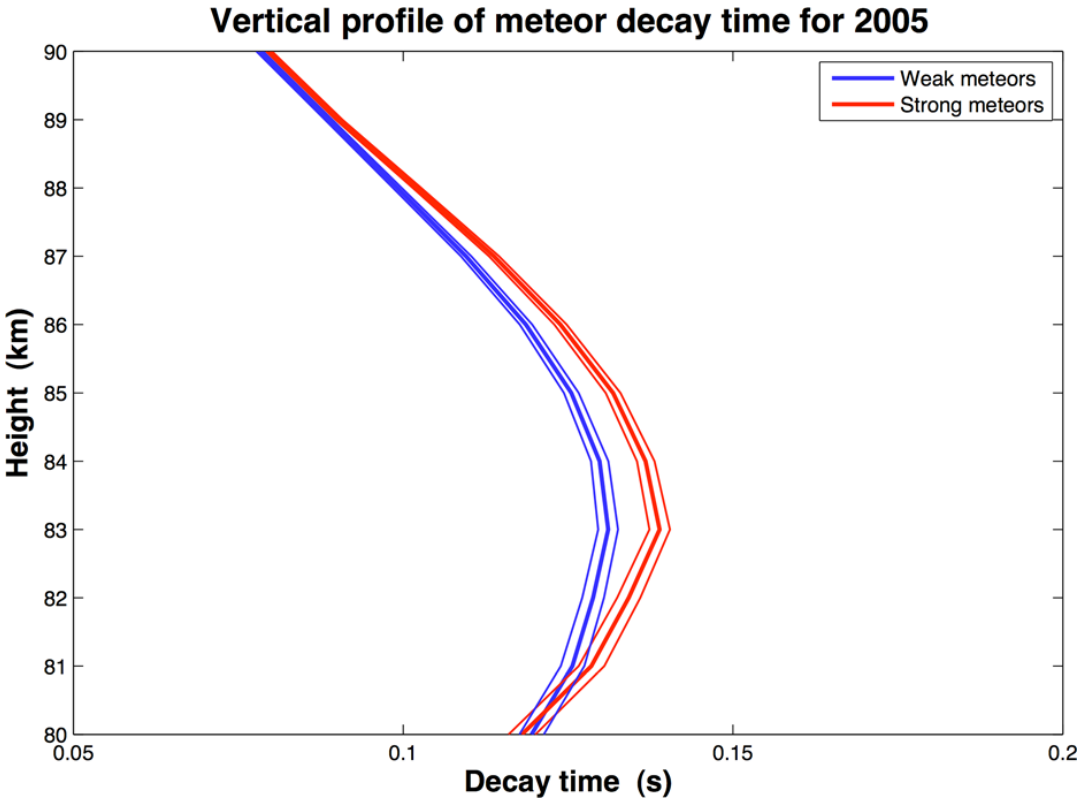

Figure 2.24: The vertical profiles of mean decay time for 2005 obtained by Ballinger et al. (2008). The profile of weak meteors (SNR<12 dB) is shown in blue; strong meteors (SNR12 dB) in red. The thin lines on either side of the mean profiles indicate the 99% confidence interval bounds.

A recent study by Kumar and Subrahmanyam (2012) employed the data from the Sounding of the Atmosphere using Broadband Emission Radiometry (SABER) instrument on-board the Thermosphere Ionosphere Mesosphere Energetics and Dynamics (TIMED) satellite, and they compared it with the radar data to further refine the values of the ambipolar diffusion coefficient in meteor trails. They selected meteors with the echo duration times ($\tau_{1/2}$) $\leq$ 0.3 seconds, and the highest observed meteor count around 90-92 km. The results of this study show a sharp deviation of meteor diffusion observed by

radar and diffusion derived from satellite data (Figure 2.25). The exponential decrease in decay time observed by SABER is in line with theoretical expectations. The large difference represented by the red bars in the figure on the right, especially in the region below 85 km, can only be explained with the contribution from chemistry that removes electrons from the trail, while the rest of the meteor trail constituents continue ambipolar and thermodynamic expansion. The comparison of the satellite and radar results suggests that the diffusion is fastest in the region of 80-88 km. Perhaps not surprisingly, the radar and satellite data match well in the region of 90-96 km as the role of chemistry is subsiding. However, the interesting result of the investigation by Kumar and Subrahmanyam (2012) points to the fact that above 96 km, the radar slightly overestimates the diffusion rates relative to the satellite. This is surprising as the influence of the geomagnetic field was supposed to somewhat inhibit the diffusion rates.

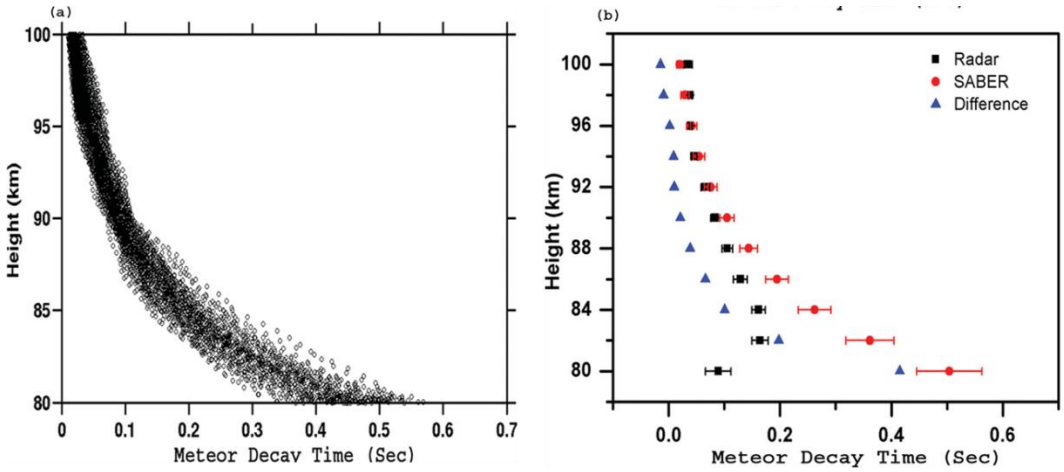

Figure 2.25: (a) Distribution of meteor trail decay time with respect to height measured using SABER observations during the winter season of 2007 and (b) height profiles of mean meteor trail decay time obtained using radar and SABER observations during the winter season of 2007. The blue triangle profile represents the difference between the SABER and radar measurements (Kumar and Subrahmanyam , 2012).

The authors point toward the dust and aerosols absorption of electrons as discussed in the earlier studies by Havnes and Sigernes (2005) and Younger et al. (2008) as the main contributor for the behaviour of the diffusion coefficient observed by radar. Considering

the low background dust concentration and the phenomena of the thermal and shock wave during the formation of the initial radius, it is not clear how the above mentioned mechanism can play a significant role in removing electrons from the meteor trail.

Then, if chemistry is indeed responsible for the behaviour of the radar observed meteor trail diffusion processes, the question must be posed as to what kind of chemistry is at play here. Considering the small time scales observed during diffusion, it becomes apparent that equilibrium chemistry, which takes place in long lasting overdense meteors, cannot be the culprit here. Indeed, the work of this thesis aims to answer the question posed above. Before that however, the meteor chemistry must be addressed first and will be discussed in detail in the next section.

2.6 Meteor Trail Chemistry, Spectra, Temporal and Thermal Evolution

A comprehensive understanding of meteor interactions with the Earth's atmosphere is still not available (Jenniskens, 2003), despite numerous investigations in the past (see Bronsheten, 1983; Ceplecha et al, 1998). Differential ablation and evaporation of the meteoroids (Vondrak et al., 2008) result in deposition of different meteoric species at a range of heights, and depending on the atmospheric density, composition, ambient temperature, rates of vertical transport and mixing and chemical reactions (Plane, 1991; Hughes, 1992; Helmer et al., 1998; Plane et al., 1999). These effects will impact chemical and physical dynamics in the upper mesosphere and lower thermosphere (MLT) and give rise to relatively narrow layers of metallic ions in the region centered around 90 km altitude (Figure 2.26), in addition to the phenomena of noctilucent clouds.

Correspondingly, spectral evidence of high temperatures in the meteor trail and the meteor head region (Borovicka, 1993,1994; Berezhnoy and Borovicka, 2010) suggests additional thermal and shock modification of the limited cylindrical atmospheric region along meteor trail axis (Zinn et al., 1999).

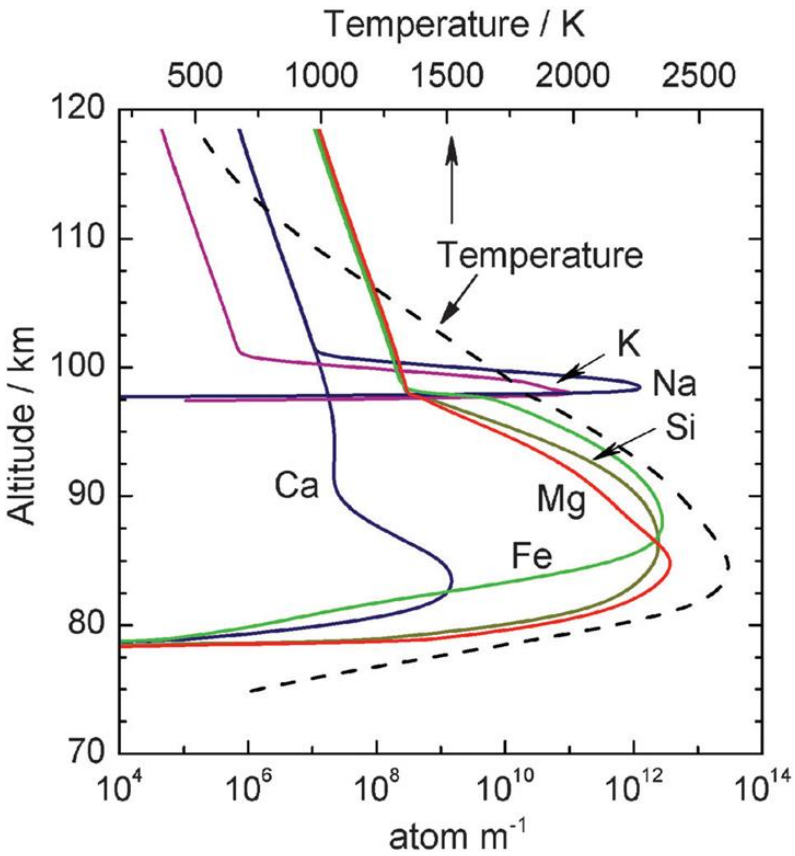

Figure 2.26: Elemental ablation profiles for a 5 mg meteoroid entering at 20 km s^{-1}, as predicted by the Chemical Ablation Model (CABMOD). The particle temperature is shown on the top abscissa (Plane, 2012).

Three major processes controlling the reduction of initial kinetic energies of ablated meteoric atoms to thermal level are elastic scattering, excitation and ionization. Elemental abundances from meteor spectra indicate compositional and chemical background of the original body, and can be used to understand the time scales required for the formation of thermodynamic equilibrium following the fast (~10^{-8} s) atomic collisional excitation and de-excitation processes (Berezhnoy and Borovicka, 2010). Additionally, the meteor spectra give an indication of the chemical processes in and around the meteor trail. For instance, it is known that O^+ is the most abundant positive ion in the meteor column (Sida, 1969) and can rapidly exchange charge with N_2 and O_2, where both of these processes are much faster than ion loss by radiative recombination with electrons. The charge exchange mentioned above initiates a sequence of reactions

that lead to the formation of oxygen molecules in the first excited state (Baggaley, 1977). A number of theoretical and experimental investigations, combined with spectral methods and other optical means as well as radar studies of the meteor trail have resolved most of the aspects of the meteor train chemistry (Plane, 2003), yet some unresolved questions still need to be addressed (Jenniskens, 2003).

Thus, before a discussion about contemporary scientific understanding of the physical and chemical dynamics and processes controlling the atmospheric evolution of a meteor trail, first a clear distinction must be made in terms of the equilibrium and non-equilibrium processes. While the former received a prominent attention in mainstream meteor publications (e.g. Baggaley and Cummack, 1974), non-equilibrium chemistry and dynamics of the meteor trail (e.g. Park and Menees, 1978) received little or no attention in the literature for the set of reasons elaborated by Dressler (2001). Therefore, the aim of this section is to present the state of knowledge of meteor chemistry with the reflection on the historical progress and evolution of the field, and attempt to subsequently explore the final frontier of hyperthermal chemistry and radiative processes in and around the meteor head and trail.

When discussing meteor chemistry, anomalous diffusion times observed by radar methods in the past must be recognized as the main indicator that ambipolar diffusion is not a singular mechanism governing the removal of electrons from the meteor trail. The main reason for such conclusion is the well understood behaviour of signal amplitude and duration which is taken to be proportional to the electron density in the meteor trail. However, overdense and underdense echoes must be separated as the signal amplitude in the case of the former is much less sensitive to the mass of the observed meteor (Baggaley, 1979). Overdense meteor echoes are predominantly considered based on the echo duration. This is one of many factors which make overdense meteors more suitable for study of chemistry effects in the MLT region.

As far back as 1953, Kaiser proposed a simple mechanism of electron attachment to explain the anomalous behaviour of the meteor radar echo. A similar explanation for overdense echoes was offered by Davis et al. (1959), Greenhow and Hall (1961), Manning (1964) and McIntosh (1966). However, the chemical processes of electron

removal from the meteor trail had been shown to be significantly more complicated than the simple electron attachment, especially in the case of overdense trains (Baggaley, 1972).

Baggaley (1972) had discussed a numerical model of temperature dependent attachment among potentially important mechanisms, where the three body mechanism results from a collision in which an electron and neutral molecule form an excited negative ion, where the reaction is stabilized in a third-body collision, followed by radiation emission. Numerical solutions were obtained for a possible role of detachment involving the negative oxygen molecule.

Additionally, Baggaley (1972) modelled the mechanism of the ion-electron recombination, suggesting that in dense plasmas, the collisional process will control the recombination, while in a tenuous region the radiative process will be dominant. He recognized the controlling role of ozone in dissociative recombination, pointing out that it will not occur unless an ion-atom interchange or charge transfer produces a significant number of diatomic ions. In 1974, Baggaley's perhaps most important contribution to meteor chemistry was the collaborative theoretical investigation and a model of meteor train ion chemistry (Baggaley and Cummack, 1974). In addition to other reactions discussed, the ozone was recognized as the MLT constituent that can react exothermically and sufficiently fast with the meteor metallic ions and through subsequent reactions remove an electron from the trail. Below 80 km however, the three body association involving O_2 and N_2 plays a significant role. Similarly, formation of water clusters at these same heights could have minor relevance, where meteoric ion reacts with H_2O and N_2. Baggaley and Cummack (1974) concluded that the time scale of electron attachment to atmospheric neutrals increases from 2.8 s at 70 km and reach 2×10^3 s during the day and 140 s during the night at 90 km. Table 2.5(a,b) shows a relatively small list of chemical reactions which occur in and outside of the meteor trail, as suggested by Baggaley and Cummack (1974). The list is small relative to the true extent of complex chemistry processes which take place between meteoric ions, molecules, and the surrounding ionosphere (e.g. Whalley et al., 2011).

Table 2.5: (a) Chemical reactions in and around meteor train (Baggaley and Cummack, 1974).

	Process	Rate employed*	Reference
Attachment			
R1	$e + O_2 + O_2 \rightarrow O_2^- + O_2$	$1{\cdot}6 \times 10^{-30}$	Chanin *et al.* (1959)
R2	$e + O_2 + N_2 \rightarrow O_2^- + N_2$	$1{\cdot}0 \times 10^{-30}$	Hirsh *et al.* (1966)
R3	$e + O_3 \rightarrow O^- + O_2$	$7{\cdot}0 \times 10^{-12}$	Fehsenfeld and Ferguson (1968)
Detachment			
R4	$O_2^- + O \rightarrow O_3 + e$	3×10^{-10}	Fehsenfeld *et al.* (1967)
R5	$O_2^- + O_2 (^1\Delta_g) \rightarrow 2O_2 + e$	2×10^{-10}	Fehsenfeld *et al.* (1969a)
R6	$O^- + O \rightarrow O_2 + e$	$1{\cdot}9 \times 10^{-10}$	Ferguson and Fehsenfeld (1969)
R7	$O^- + O_2 (^1\Delta_g) \rightarrow O_3 + e$	$3{\cdot}0 \times 10^{-10}$	Fehsenfeld *et al.* (1969a)
R8	$O_3^- + O \rightarrow 2O_2 + e$	$1{\cdot}0 \times 10^{-10}$	Adams and Megill (1967)
R9	$O_3^- + O_3 \rightarrow 3O_2 + e$	$1{\cdot}0 \times 10^{-10}$	Adams and Megill (1967)
R10	$O^- + h\nu \rightarrow O + e$	1·40	Branscombe (1964)
R11	$O_2^- + h\nu \rightarrow O_2 + e$	0·30	Woo *et al.* (1969)
R12	$O_3^- + h\nu \rightarrow O_3 + e$	0·06	Dasa (1967)
R13	$CO_3^- + h\nu \rightarrow CO_3 + e$	0·04	Kamiyama (1970)
R14	$NO_2^- + h\nu \rightarrow NO_2 + e$	0·04	Dasa (1967)
R15	$NO_3^- + h\nu \rightarrow NO_3 + e$	0·03	Kamiyama (1970)
Exchange reactions			
R16	$O^- + O_3 \rightarrow O_3^- + O$	$7{\cdot}0 \times 10^{-10}$	Fehsenfeld *et al.* (1967)
R17	$O^- + 2O_2 \rightarrow O_3 + O_2$	$2{\cdot}0 \times 10^{-30}$	Chanin *et al.* (1959)
R18	$O_2^- + O \rightarrow O^- + O_2$	$1{\cdot}0 \times 10^{-11}$	Dasa (1967)
R19	$O_2^- + O_3 \rightarrow O_3^- + O_2$	$3{\cdot}0 \times 10^{-10}$	Fehsenfeld *et al.* (1967)
R20	$O_2^- + O_2 + M \rightarrow O_4^- + M$	$3{\cdot}5 \times 10^{-31}$	Pack and Phelps (1971) McKnight and Sawina (1970) Parkes (1971)
R21	$O_3^- + O \rightarrow O_2^- + O_2$	$1{\cdot}4 \times 10^{-10}$	Lelevier and Branscombe (1968)
R22	$O_3^- + CO_2 \rightarrow CO_3^- + O_2$	$4{\cdot}0 \times 10^{-10}$	Fehsenfeld *et al.* (1967)
R23	$O_3^- + NO \rightarrow NO_2^- + O_2$	$1{\cdot}0 \times 10^{-11}$	Arnold and Krankowsky (1972)
R24	$O_4^- + O \rightarrow O_3^- + O_2$	$4{\cdot}0 \times 10^{-10}$	Fehsenfeld *et al.* (1969b)
R25	$O_4^- + O_2 \rightarrow O_2^- + 2O_2$	$2{\cdot}0 \times 10^{-14}$	Payzant and Kebarle (1972)
R26	$O_4^- + CO_2 \rightarrow CO_4^- + O_2$	$4{\cdot}3 \times 10^{-10}$	Fehsenfeld *et al.* (1969b)
R27	$O_4^- + NO \rightarrow NO_3^{-*} + O_2$	$2{\cdot}5 \times 10^{-10}$	Fehsenfeld *et al.* (1969b)
R28	$CO_4^- + O \rightarrow CO_3^- + O_2$	$1{\cdot}5 \times 10^{-10}$	Fehsenfeld *et al.* (1969b)
R29	$CO_4^- + O_3 \rightarrow O_3^- + CO_4$	$1{\cdot}0 \times 10^{-10}$	Arnold and Krankowsky (1971)
R30	$CO_4^- + NO \rightarrow NO_3^{-*} + CO_2$	$4{\cdot}8 \times 10^{-11}$	Fehsenfeld *et al.* (1969b)
R31	$CO_3^- + O \rightarrow O_2^- + CO_2$	$8{\cdot}0 \times 10^{-11}$	Fehsenfeld *et al.* (1967)
R32	$CO_3^- + NO \rightarrow NO_2^- + CO_2$	$9{\cdot}0 \times 10^{-12}$	Fehsenfeld *et al.* (1967)
R33	$NO_2^- + O_3 \rightarrow NO_3^- + O_2$	$1{\cdot}8 \times 10^{-11}$	Fehsenfeld and Ferguson (1968)
R34	$NO_2^- + NO_2 \rightarrow NO_3^- + NO$	$4{\cdot}0 \times 10^{-12}$	Ferguson (1972b)
R35	$NO_3^- + NO \rightarrow NO_2^- + NO_2$	$1{\cdot}5 \times 10^{-11}$	Ferguson (1972b)

* Two body reaction rate unit is $cm^3\ s^{-1}$; three body reaction rate unit is $cm^6\ s^{-1}$; photoprocesses have a rate unit of s^{-1}.

Table 2.5: (b) Chemical reactions in and around meteor train (Baggaley and Cummack, 1974).

	Process	Rate employed	Reference
Reactions for Fe^+			
R36	$Fe^+ + O_3 \rightarrow FeO^+ + O_2$	$1{\cdot}5 \times 10^{-10}$	Ferguson and Fehsenfeld (1968)
R37	$Fe^+ + O_2 + M \rightarrow FeO_2^+ + M$	$1{\cdot}0 \times 10^{-30}$	Ferguson and Fehsenfeld (1968)
R38	$Fe^+ + e \rightarrow Fe^+ h\nu$	$3{\cdot}0 \times 10^{-12}$	Bates (1962)
R39	$Fe^+ + e + M \rightarrow Fe + M$	$1{\cdot}0 \times 10^{-26}$	Danilov (1970)
R40	$FeO^+ + O \rightarrow Fe^+ + O_2$	$1{\cdot}0 \times 10^{-10}$	Estimate
R41	$FeO^+ + e \rightarrow Fe + O$	$5{\cdot}0 \times 10^{-7}$	Estimate
R42	$FeO_2^+ + O \rightarrow FeO^+ + O_2$	$1{\cdot}0 \times 10^{-10}$	Estimate
R43	$FeO_2^+ + e \rightarrow Fe + O_2$	$3{\cdot}0 \times 10^{-6}$	Swider (1969)
Reactions for Mg^+			
R44	$Mg^+ + O_3 \rightarrow MgO^+ + O_2$	$2{\cdot}3 \times 10^{-10}$	Ferguson and Fehsenfeld (1968)
R45	$Mg^+ + O_2 + M \rightarrow MgO_2^+ + M$	$2{\cdot}5 \times 10^{-30}$	Ferguson and Fehsenfeld (1968)
R46	$Mg^+ + e \rightarrow Mg + h\nu$	$3{\cdot}0 \times 10^{-12}$	Bates (1962)
R47	$Mg^+ + e + M \rightarrow Mg + M$	$1{\cdot}0 \times 10^{-26}$	Danilov (1970)
R48	$MgO^+ + O \rightarrow Mg^+ + O_2$	$1{\cdot}0 \times 10^{-10}$	Ferguson and Fehsenfeld (1968)
R49	$MgO^+ + e \rightarrow Mg + O$	$5{\cdot}0 \times 10^{-7}$	Estimate
R50	$MgO_2^+ + O \rightarrow Mg^+O + O_2$	$1{\cdot}0 \times 10^{-10}$	Estimate
R51	$MgO_2^+ + e \rightarrow Mg^+O_2$	$3{\cdot}0 \times 10^{-7}$	Swider (1969)
Reactions for Si^+			
R52	$Si^+ + O_3 \rightarrow SiO^+ + O_2$	$1{\cdot}0 \times 10^{-10}$	Estimate
R53	$Si^+ + O_2 + M \rightarrow SiO_2^+ + M$	$1{\cdot}0 \times 10^{-30}$	Estimate
R54	$Si^+ + e \rightarrow Si + h\nu$	$3{\cdot}0 \times 10^{-12}$	Bates (1962)
R55	$Si^+ + e + M \rightarrow Si + M$	$1{\cdot}0 \times 10^{-26}$	Danilov (1970)
R56	$SiO^+ + O \rightarrow Si^+ + O_2$	$2{\cdot}0 \times 10^{-10}$	Fehsenfeld (1969)
R57	$SiO^+ + e \rightarrow Si + O$	$5{\cdot}0 \times 10^{-7}$	Estimate
R58	$SiO_2^+ + e \rightarrow Si + O_2$	$3{\cdot}0 \times 10^{-7}$	Swider (1969)
Reactions for Na^+			
R59	$Na^+ + 2N_2 \rightarrow Na^+ . N_2 + N_2$	$1{\cdot}0 \times 10^{-31}$	Estimate
R60	$Na^+ . N_2 + N_2 \rightarrow Na^+ + 2N_2$	$1{\cdot}0 \times 10^{-13}$	Keller and Beyer (1971)
R61	$Na^+ . N_2 + e \rightarrow Na + N_2$	$5{\cdot}0 \times 10^{-6}$	Estimate
R62	$Na^+ + e \rightarrow Na + h\nu$	$3{\cdot}0 \times 10^{-12}$	Bates (1962)
R63	$Na^+ + e + M \rightarrow Na + M$	$1{\cdot}0 \times 10^{-26}$	Danilov (1970)
Ion–ion reactions			
R64	$X^+ + O^- \rightarrow X + O$	$1{\cdot}0 \times 10^{-12}$	Estimate
R65	$X^+ + AB^- \rightarrow X + AB$	$1{\cdot}0 \times 10^{-7}$	Estimate
R66	$XO^+ + O^- \rightarrow XO + O$	$1{\cdot}0 \times 10^{-7}$	Estimate
R67	$XO^+ + AB^- \rightarrow XO + AB$	$1{\cdot}0 \times 10^{-7}$	Estimate
R68	$XO_2^+ + O^- \rightarrow XO_2 + O$	$1{\cdot}0 \times 10^{-7}$	Estimate
R69	$XO_2^+ + AB^- \rightarrow XO_2 + AB$	$1{\cdot}0 \times 10^{-7}$	Estimate

The reactions discussed by Baggaley (1972) and Baggaley and Cummack (1974) are the equilibrium processes that take place on time scale of minutes. The mechanism of the fast electron removal reactions has not been completely addressed yet. The key points to recognize here are that the previous mechanisms suggested by earlier authors cannot account for the relatively short lifetime of such phenomena in the meteor trail (e.g. the meteor trail luminosity and red afterglow) compared to the proposed time scale of minutes. The likely mechanism that may cause such manifestations is the chemical production of excited species whose quenching is in the order of seconds.

In overdense meteors, a substantial portion of chemical processes occurs during the meteor trail adiabatic expansion into warm air plasma (~4400 K) (Jenniskens, 2004) which is a result of the shock wave expansion of the surrounding atmosphere following the hypervelocity collisions with a meteoroid. To illustrate the importance of chemistry in overdense meteors, one might for example consider applying the theory initially derived by Kaiser (1953) to the observed event. Taking an overdense meteor of visual magnitude -3 at 80 km, detected by a 30 MHz VHF system, the theory indicates that such radio echo should last in excess of 20 minutes (Baggaley, 1979). In practice, the received echo from such an event barely lasts 60 seconds in the case of forward scatter radar (Figure 2.27).

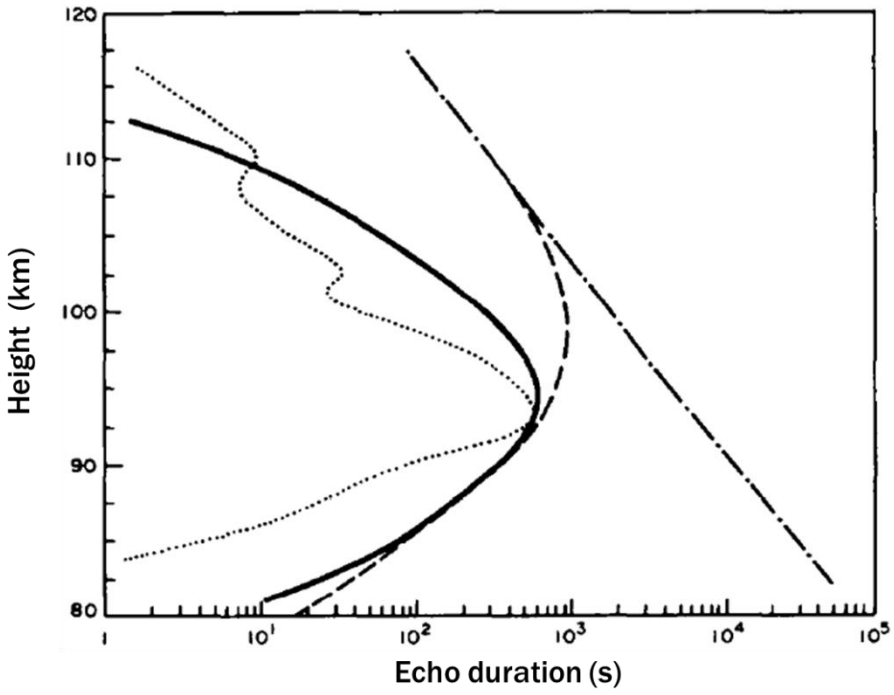

Figure 2.27: Meteor echo duration vs. reflection heights for radar wavelength λ=9 m. The solid line represents full theoretical profile for electron line density of $6 \cdot 10^{18}$ m^{-1} occurring at 88 km altitude and assumes a classical ionization curve. The dashed line is for the same electron density, for all heights. The dot-dash line represents the profile assuming the classical duration expression. The dotted line represents the experimental profile obtained by McKinley (1961) (Baggaley, 1978).

Clearly, the proposed mechanisms of simple electron attachment are not sufficient to accomplish this, as the rates of reaction for such a process is too large, and thus the reaction time scales are too long. This can be seen from looking at one of the proposed attachment reactions:

$e + O_3 \rightarrow O^- + O_2$ and

$e + O_2 + X \rightarrow O^-_2 + X$, where X is a third body

This mechanism is slow and proceeds at rates much less than the electron detachment, which is in essence restoring electrons at a much faster pace than they are consumed.

$O^- + O \rightarrow O_2 + e$ and

$O_2^- + O \rightarrow O_3 + e$

It is therefore apparent that the so called negative ion formation, as a mechanism for electron removal, is insignificant at meteor heights. Nicholson and Poole (1974) examined the problem of overdense meteor echoes behaviour in detail and suggested the contribution of ozone, which agrees with conclusions of Baggaley and Cumack (1974). That conclusion was confirmed when Baggaley (1978, 1979) defined the ozone reactions as primary mechanism responsible for the removal of electrons from the overdense meteor trail. The oxidation chemical reactions can be stated as follows:

$$M^+ + O_3 \rightarrow MO^+ + O_2 \tag{2.81}$$

Here, M^+ can represent any of the main meteoric ions (Fe, Mg, Si). The reaction that follows is *dissociative recombination*:

$$MO^+ + e \rightarrow M + O \tag{2.82}$$

In overdense trains, the first reaction (2.81) is the one that controls the echo duration, because it is much slower that the second reaction. To obtain the reaction life time, the classical kinetic theory (Upadhyay, 2006) needs to be consulted, where for some reaction:

$$A + B \rightarrow C + D$$

Then:

$$Rate\ of\ Reaction \approx -\frac{d[A]}{dt} = -\frac{d[B]}{dt} = \frac{d[C]}{dt} = \frac{d[D]}{dt} \tag{2.83}$$

where the bracketed terms are respective concentrations. Using the relation that the rate of reaction equals the inverse to the reaction lifetime τ, it is easy now to solve for the lifetime:

$$\tau^{-1} \approx \frac{d[A]}{dt} \approx k_A[A] \tag{2.84}$$

Taking the reaction coefficients (Baggaley, 1979) for the two reactions as $k_1 = 2 \cdot 10^{-10}$ and $k_2 = 5 \cdot 10^{-7}$ $cm^3 s^{-1}$, and taking in consideration the height dependent ozone density at 90 km to be approximately $2 \cdot 10^{14}$ m^{-3}, it is easy to see that at this altitude, the lifetime of the first reaction is approximately 25 seconds. For (2.82) the lifetime can be estimated at 10^{-3} seconds, assuming the overdense train with electron line density of 10^{16} m^{-1}. The reduction reaction, which can be written as:

$$MO^+ + O \rightarrow M^+ + O_2 \quad (2.85)$$

will proceed again much slower than (2.82) (Baggaley, 1979), thus it will not have appreciable impact on the evolution of meteor trail. For illustrative purpose, the reaction (2.85) lifetime is about 3 seconds at 80 km and about 200 seconds at 100 km.

Moreover, additional reactions such as the three-body charge transfer involving the metallic ion, oxygen and a third body and the subsequent dissociative recombination will become relevant in terms of meteor timescales only at lower altitudes. In addition, the reaction involving N_2 and M^+ will also proceed under the presence of the third body and will contribute to the electron removal from the meteor trail. Baggaley (1979) numerically modeled chemical mechanisms by solving a system of differential equations for each chemically reacting species, using a 10 point finite difference scheme. The results were in line with observed duration times. Figure 2.28 below shows the calculated results and the effects of chemical reactions on duration of meteor echoes from trails with large electron densities. The conclusions, comparing the experiment and models indicate that the effects of chemical processes in the meteor trail are nonlinear, which is opposite of what would be expected from a simple electron attachment process. Moreover, the results from the model show an echo duration diurnal variability which is proportional to the ozone diurnal cycle and corresponds well with the experimental observation (Nicholson and Poole, 1974).

Baggaley's (1979) conclusions confirmed the results obtained earlier by Poole and Nicholson (1975) showing that ozone is a dominant agent in meteor chemistry and that a dissociative recombination of meteoric oxide ions derived from the reaction with ozone in meteor trains is the primary mechanism of the electron removal from the meteor train.

It should be noted that the ionization potential of metal atoms (5-9 eV) from the meteor trail is appreciably less than those of O_2 and N_2, therefore metal ions are stable against charge exchange with major neutrals in the atmosphere (Baggaley, 1980).

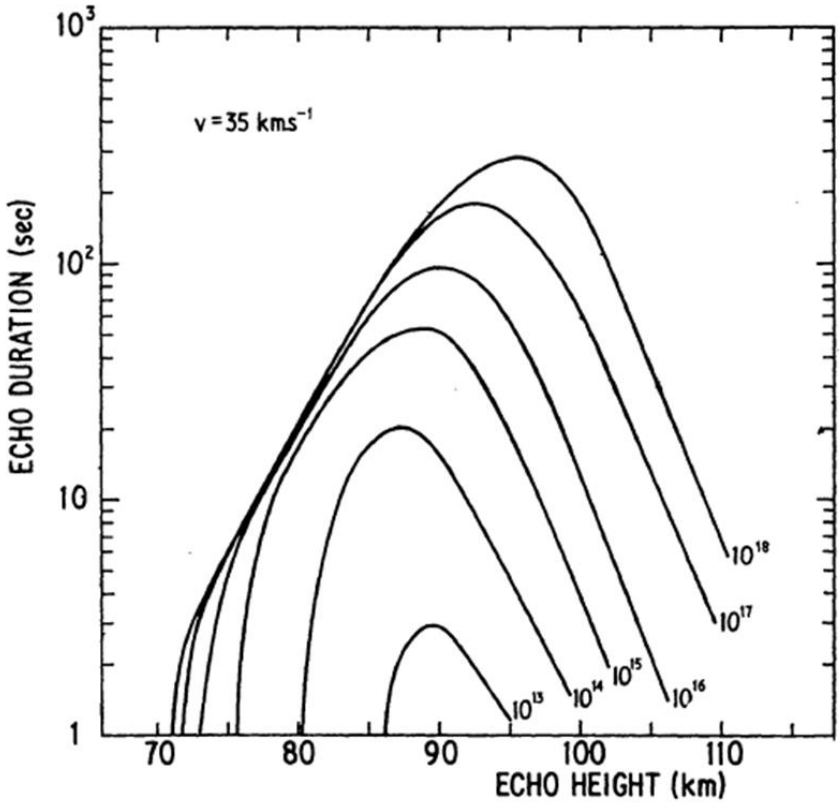

Figure 2.28: Echo duration vs. height profiles for different value of maximum line density. Note that in this figure line density is in electrons cm^{-1}, a norm in early literature. For large electron densities, the profiles are distorted at lower altitudes (top of the figure), while the smaller electron line density profiles behave according classical ionization theory (from Baggaley, 1979).

Out of all meteor metal ions detected in the meteor trail and consequently either in metallic layers or in trace quantities in the upper atmosphere, iron, magnesium, calcium, aluminum, potassium, silicon and sodium are the most abundant (Plane, 1991). A comprehensive review of detailed experimental studies that were conducted on the main meteoric ion species in the last several decades was presented by Plane (1991, 2003). Some of the commonly observed and meteor-metal-ion related atmospheric phenomena such as atmospheric glow occurs because the sodium reaction with ozone. This example is brought up, to illustrate dynamic and complex chemistry processes in the upper atmosphere, and can be useful in relating to the topic of luminosity and persistent meteor trains is discussed in the next section. Meteoric metals also play a role in the formation of

sporadic E layers, which can be described as thin layers of metallic ions, typically 1-3 km wide, occurring above 90 km altitude. These phenomena significantly impact radio communication and take place because neutral iron atom reacts with ionized O_2^+ where subsequently Fe will photo-ionize and lose electrons thus contributing to the formation of intermittent dense layers of electrons in the specific region of the atmosphere which have been defined as sporadic E layers in the text above. Taking an illustrative example of the Fe and Mg, which represent the dominant meteor metal ion concentration well, the schematic drawing of the chemical iron and magnesium cycle (Figure 2.29a,b), in and around the meteor trail, is shown below. Correspondingly Fe, Al, and Ca have similar chemical cycles and now it is possible to glance at the complex system of the meteoric metal chemistry. Whalley et al. (2011) studied kinetics of Mg+ and Mg containing reactions with O_3, O_2,N_2, CO_2, N_2O and H_2O. Of particular interest for this thesis are the reaction rates and energies involving O_3. An important observation had been made suggesting that the reaction between Mg^+ and O_3 occurs at the Langevin capture rate and are temperature independent, and the rate coefficient for the mesospheric region was determined to be k(190-340 K) = $(1.17 \pm 0.19)\cdot 10^{-9}$ $cm^3 molecule^{-1} s^{-1}$. Plane and Whalley (2012) treated Mg kinetics extensively in a comprehensive laboratory treatment of the full spectrum of magnesium chemistry, reproducing the conditions in the upper atmosphere. They have obtained a new set of rate coefficients relating to the reactions of magnesium oxide, magnesium dioxide and $MgCO_3$ with neutral atomic oxygen. Moreover, these results indicate a significantly more important role of O_2 in the mesosphere where it initiates holding cycles by recombining with radical species such as MgO_2. Finally, they had presented a new atmospheric model that can explain the Mg chemical cycle, which corresponds well to physical observations of Mg related atmospheric structures such as Mg layers and their seasonal variations.

The work by Whalley et al. (2011) and Plane and Whalley (2012) confirmed the previously established fact that ozone is the most efficient removal agent of meteoric metal ions. It should be noted at this point that all the above discussion was primarily about equilibrium processes. In addressing the non-equilibrium meteor train chemistry, one should be aware of temperatures in the meteor train and the energies of both electrons and ions discussed earlier in the text.

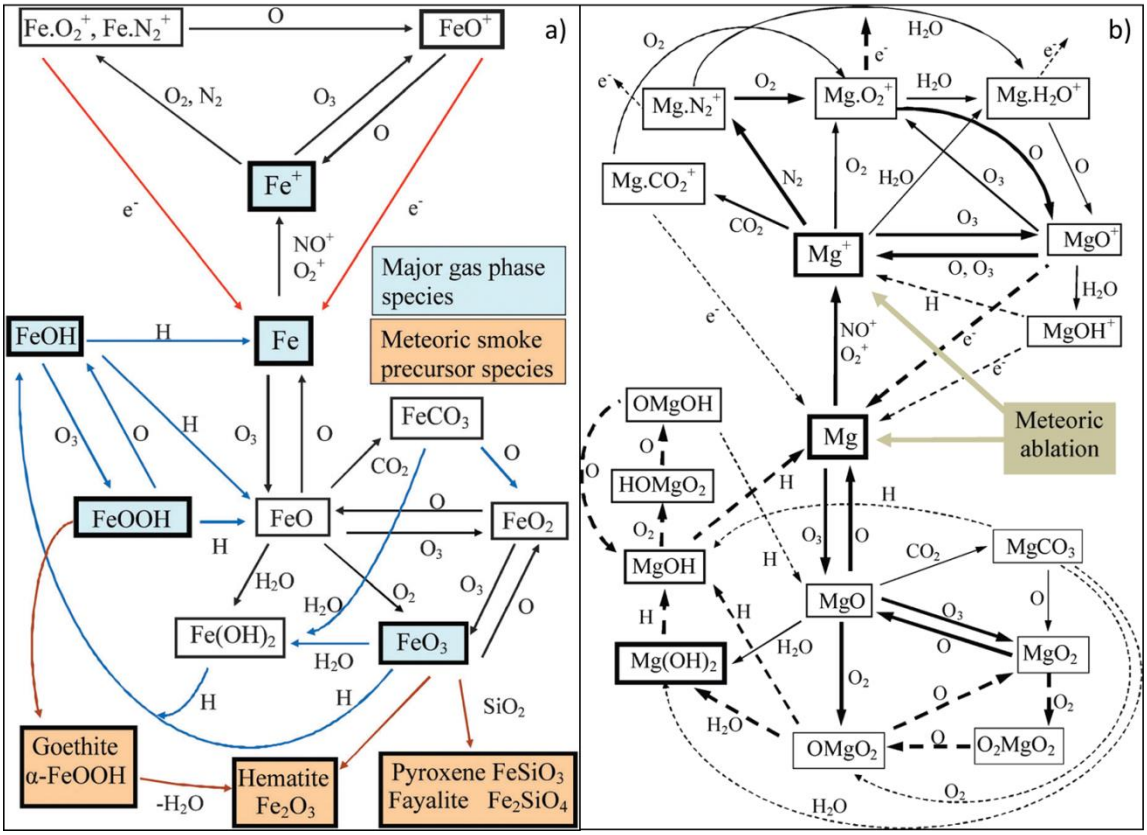

Figure 2.29: a) Fe chemistry in the MLT. Black arrows: reactions with measured rate coefficients; red, blue, brown arrows indicate reactions which need laboratory study. (Plane, 2012). b) Schematic diagram of magnesium chemistry in the upper mesosphere/lower thermosphere region. Major magnesium species are shown in boxes with bold outlines. Important reaction pathways are indicated with thicker arrows. Reactions with measured rate coefficients are indicated with solid arrows; broken arrows indicate pathways for which rate coefficients are estimated or fitted. Note the role of O_2 in the MgO_2−O_2MgO_2−$OMgO_2$ and MgOH−$HOMgO_2$−OMgOH holding cycles (Plane and Whalley, 2012).

2.7 Initial Temperature of the Meteor Wake and Trail – An Indication of Hyperthermal Chemistry

New studies are offering improved understanding of the dynamic evolution of small meteoroids in the Earth's atmosphere, with important chemical implications (Jenniskens et al., 1998). Remarkably, it was observed experimentally (using spectral techniques) (Borovicka, 1994) and modeled theoretically that a small meteoroid produces very high

temperatures in its immediate wake (Boyd, 2000; Popova et al., 2000; Jenniskens et al., 2000). While the observation indicates temperatures of up to 10000K (Borovicka and Jenniskens, 1998), it is reported that the new models predicts time dependent temperatures of about 6300 K at 10 m behind the main meteoroid mass, and 3400 K at the distance of about 40 m from the meteoroid (Jenniskens and Stenbaek-Nielsen, 2004). The new model (Boyd, 2000) shows that the ablation vapor cloud resulting from collisional sputtering travels along with the meteor, determines the size of the meteor wake, and dramatically increases the collision cross-section of the meteoroid (Jenniskens and Stenbaek-Nielsen, 2004). Photographic evidence from the meteor of visual magnitude M_V = -3 (Figure 2.30), studied by Jenniskens and Stenbaek-Nielsen (2004) using a high speed intensified CCD imager, showed the existence of much slower infrared cooling, in addition to the observation of the forbidden green line emission of OI at 5577Å with a short lifetime, discussed in the next section. This is contrary to the model of rapid cooling obtained by Boyd (2000). However, Jenniskens and Stenbaek-Nielsen (2004) observed much lower temperatures of 4300 K from the meteor spectra, which is significantly lower than either models or previous observations. Furthermore, they detected metallic ions such as Mg I having high energy states (5.11 eV in the case of Mg I). This is significant for the existence of hyperthermal chemistry, which is one of the topics of this thesis. Further implications of the Jenniskens and Stenbaek-Nielsen (2004) work was to document the peculiar phenomenon (Figure 2.31) of the vapour “shield” (shock like structure) of a significantly larger radius than the meteoroid, moving along through the atmosphere with it, and consequently not only affecting the size of the initial radius, but also the ablation coefficient and the behaviour of the shockwave and thermal envelope around the initial radius. This subject of the newly observed shock like structure had been further considered by Stenaek-Nielsen and Jenniskens (2004). They estimated dimensions of this peculiar phenomenon to be up to several hundred meters in diameter. It developed gradually with height (initial altitude of 110 km) and it was observed to be proportional to the meteor brightness. Comparison of the observation with high speed images other three meteors recorded with this camera system showed that the shock like structure does not manifest with faint events. They, however, had not identified the process that is responsible for the formation of this previously unobserved phenomenon.

Observations of the phenomena confirmed the results obtained by model (Boyd, 2000), which showed an ablation vapour cloud about ten times bigger than the meteoroid. Application of the Popova et al. (2000) model suggests that the wake should be 6 m in diameter if Boyd's initial radius of the shock structure is taken to be 19 cm.

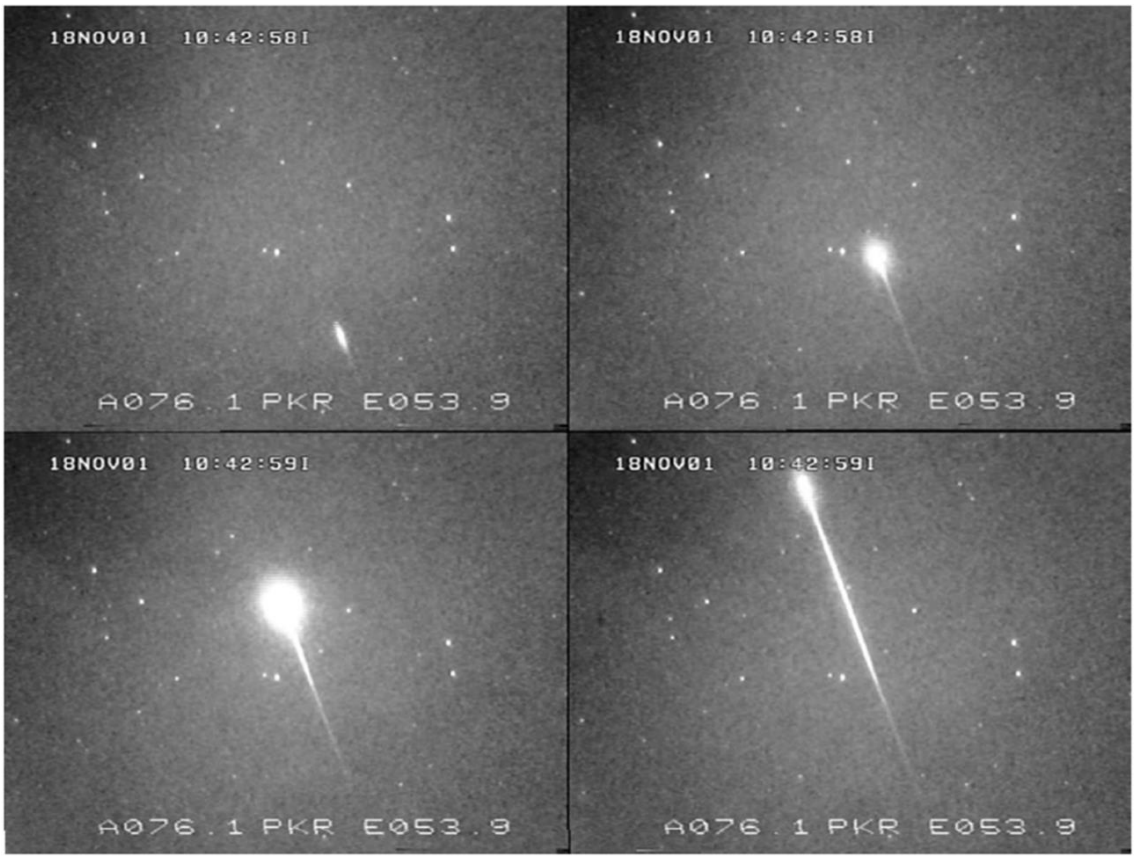

Figure 2.30: The intensified TV images of meteor of visual magnitude M_V= -3 studied by Jenniskens and Stenbaek-Nielsen (2004).

Figure 2.31: The images show meteor evolution and development of the meteor morphology at 1000 frames/s. The gas "shield" cap in front of meteor head has important implications regarding the ablation efficiency, initial radius and shock and thermal envelope around the meteor trail. The intensified TV images of meteor of visual magnitude M_V= -3 studied by Jenniskens and Stenbaek-Nielsen (2004).

Figure 2.32 shows the rendering of the different scales of the observed structure. A very interesting concluding comment by Stenbaek -Nielsen and Jenniskens (2004) suggests the role of UV ionization in formation of this phenomena.

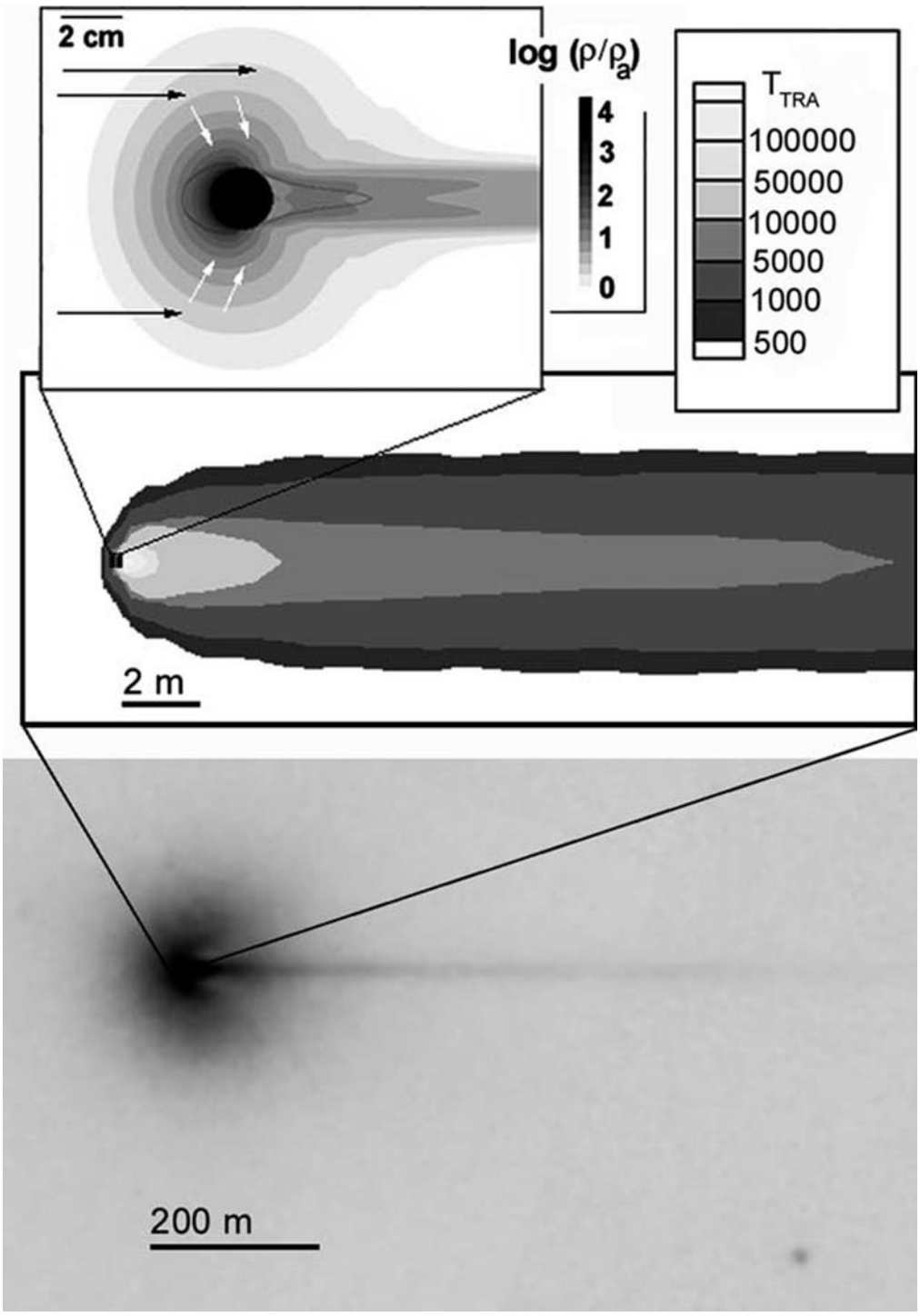

Figure 2.32: Three scale-sizes of physical phenomena in the Leonid meteor images. Top section of figure shows the meteor vapor cloud calculated by Popova et al., 2000. The center section shows the meteor wake calculated by Boyd, 2000. These models do not describe the UV-induced halo and shock-like structure seen in the high frame rate imager (bottom) (Stenaek-Nielsen and Jenniskens 2004).

Spectral measurements indicate that the values of the metal atom excitation temperature are in the range of 3000 K to 5500 K, and do not have a meteoroid mass or velocity dependence (Jenniskens et al., 2004). The highest temperature in the meteor wake has been deduced by Ceplecha (1971) from analysis of OI curve growth and from nitrogen lines. Borovicka (1994) had shown that based on the OI (7774 Å) spectra, that the temperatures in the range of 10000 K are most common in bright meteors, especially in the region of the meteor head and immediate wake. Jenniskens et al. (2004) found that for meteoroid masses above 10^{-5} g, which is the lower mass limit for "hot" meteors, temperature does not change dramatically with increasing mass. While it is well understood that meteoric plasma heating results from collisions with the ambient air, Jenniskens et al (2004) indicated that during the radiation emissions from the meteor trail, there is still translational velocity difference in excess of 5 km/s, between air plasma and the ambient air in the direction along the meteor path. Subsequently, the cooling process in the meteor trail is conducted primarily through the collisional energy transfer and through radiative processes. Jenniskens et al. (2004) showed indeed that even small underdense meteors will have temperature of about 4500 K in their wakes and around the head region. Moreover, this temperature range is favourable for hyperthermal chemical reactions, where the energy input is required for reaction to proceed.

One of the most important publications in the area of the meteor train chemistry (Berezhnoy and Borovicka, 2010) explored the formation of the molecules in bright meteors. From discussions of the meteor physics covered in previous sections, it can be recognized that immediately in the meteor wake and during and post initial meteor trail radius formation, the collisional rate is rapidly decreasing and the level population is not kept at equilibrium (Borovicka and Jenniskens, 2000). During the "bright meteor" phase, the hydrodynamic time scale, defined as the typical lifetime of ablated meteoroid atom/ion/matter in the emitted region which can also be recognized as the relaxation time scale, is also a function of height and meteor trail density (see Baggaley and Webb, 1977), and based on the work of Borovicka and Jenniskens (2000) it can be estimated for large overdense meteors in the mid-atmosphere at 0.05 s for the 4000 K and 0.1 s for the 2000 K temperature. The hydrodynamic time scale is proportional to the radius of the meteor (Berezhnoy and Borovicka, 2010). The chemical time scales for the temperature

of the bright meteor radiation (~5000 K) are 10^{-4} s. However, at heights above 80 km, in early stages of the meteor trail formation, "*chemical equilibrium"* (generally referred to as local thermodynamic equilibrium or LTE) cannot be reached when a hydrodynamic time scale is too short (~10^{-3} s) and the emitted region is still lower than 4000K. Therefore in the meteor region, the oxide formation is expected to occur in the cooling stages (Figure 2.33) of the initially "hot" trail around 2000-3000 K (Berezhnoy and Borovicka, 2010). The temperature at the point of the peak abundance of molecules and the relative abundance of metal oxides will decrease with decreasing pressure.

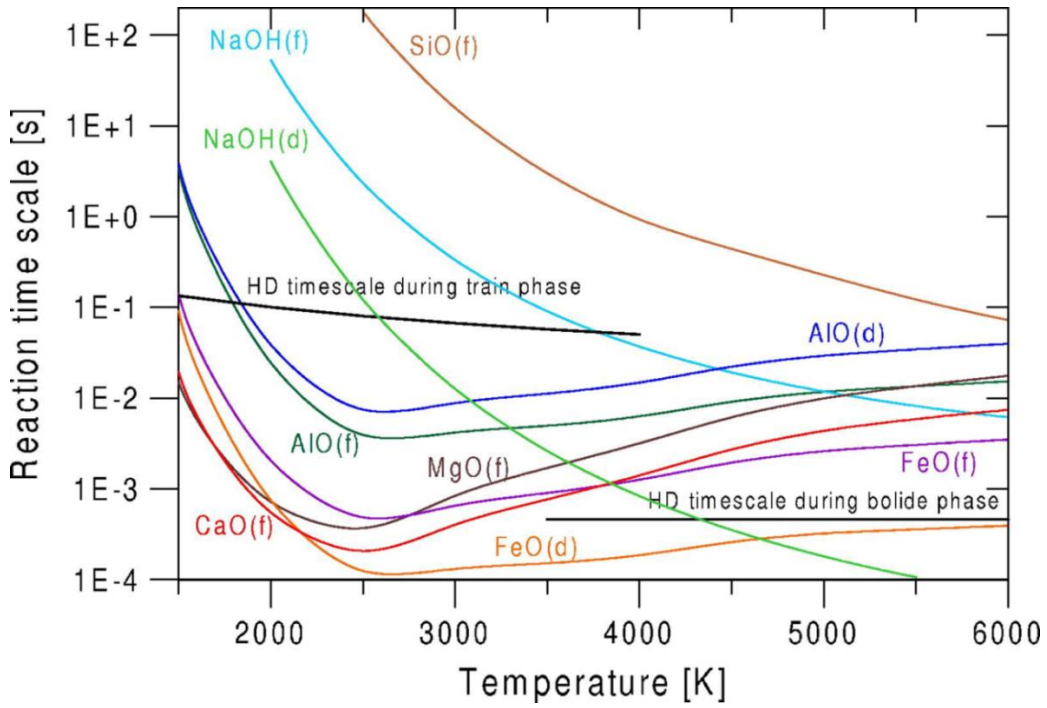

Figure 2.33: Time scales of chemical reactions involving metal-containing species for the case of cooling of a high-altitude Leonid meteoroid of CI elemental composition. Pressure is 4×10^{-5} bar, altitude is 80 km. Air-to-meteoroid vapor mass ratio is 30. Symbols CaO(f), AlO(d), AlO(f), MgO(f), FeO(f), FeO(d), and SiO(f) represent reactions $Ca + O_2 = CaO + O$, $AlO + O = Al + O_2$, $Al + O_2 = AlO + O$, $Mg + O_2 = MgO + O$, $Fe + O_2 = FeO + O$, $FeO + O = Fe + O_2$, $Si + O_2 = SiO + O$, respectively. Hydrodynamic time scales are also given (Berezhnoy and Borovicka, 2010).

In principle, there are no appreciable mutual reactions between ablated meteoric constituents, therefore the ratios of metal oxide to metal in the meteor train is

independent of the abundance of other metals in the meteor trail and meteoric composition (McNeil et al., 1998; Berezhnoy and Borovicka, 2010). A critical observation made by Berezhnoy and Borovicka (2010) indicates that at 80 km, the ratio of FeO and Fe is about 10^{-5} (Borovicka and Spurny, 1996). That makes sense for strong overdense meteors as the initial formation of FeO does not come from O_3; in fact it comes from reactions with the ground and excited O_2 that is formed by as a result of thermal and photo dissociation of ozone in the immediate vicinity of the meteor head and trail, as it will become evident in Chapters 4 and 5. One should consider that Borovicka and Spurny (1996) were observing strong bolides (electron line density $>10^{19}$ m^{-1}, according to Sugar (1964)). Consequently, the ratio they obtained corresponds to ozone density in that region ($\sim10^{14}$ m^{-3}). The importance of this observation will soon be clear. Berezhnoy and Borovicka (2010) concluded that the metal oxides are the most abundant in the temperature range of 2000 – 2500 K.

The rather indirect evidence from a wide spectrum of literature clearly proves the existence of a hyperthermal chemistry regime in the formation stages of the meteor trail. On such short time scale, there are only very limited number of endothermic chemical reaction that can occur that fast (Dressler, 2001). These hyperthermal chemical reaction(s) and their implications and applicability are the main topic of this work and will be discussed in the upcoming chapters.

2.8 Meteor Spectra

The study of meteor spectra is a fairly mature field of meteor study, with original observations starting in the 1860s by English astronomer Herschel (Millman, 1963). Spectral research of meteor phenomena was accelerated post World War II, reaching its peak in the 1960s and 1970s. For a historical reflection, the reader is referred to the review by Millman (1963) and Ceplecha (1968). Early on, an abundance of various spectral lines was observed, with a few surprising discoveries such as the forbidden OI green line. Accordingly, the discussion in this section is intentionally initiated by reviewing the problem of the oxygen forbidden green line emissions as it has a significant implication on the work in this thesis. However, the meteor spectra are a far broader area of study, and this review cannot do justice to the immense body of work done in the past

century or so. Nevertheless, the hope is to give the most relevant and important aspects of the research, through which the work and results in this thesis can be judged.

"Forbidden" atomic transitions simply imply that they are disallowed for electric dipole radiation, which is the most efficient mechanism. However, according to classical theory, forbidden transitions have small probabilities to occur spontaneously if the atom or molecule is raised to an excited state. This discussion is focused on the forbidden oxygen lines observed from the meteor column. Table 2.6 below gives the forbidden transitions for the natural oxygen atom.

Table 2.6: The forbidden transitions, wavelengths and lifetimes for natural oxygen (Baggaley, 1976c).

Forbidden transitions in OI		
Transition	Wavelength, Å	Lifetime, S
$2p^4\ {}^1D_2 \rightarrow 2p^4\ {}^3P_2$	6300·3	$1{\cdot}96 \times 10^2$
$\rightarrow\ {}^3P_1$	6363·9	$6{\cdot}10 \times 10^2$
$2p^4\ {}^1S_0 \rightarrow 2p^4\ {}^3P_1$	2972·3	14·9
$\rightarrow\ {}^3P_2$	2958·4	$2{\cdot}7 \times 10^3$
$2p^4\ {}^1S_0 \rightarrow 2p^4\ {}^1D_2$	5577·3	0·74
$2p^3\ 3s\ {}^5S_2^0 \rightarrow 2p^4\ {}^3P_2$	1355·6	$7{\cdot}7 \times 10^{-4}$
$\rightarrow\ {}^3P_1$	1358·5	$2{\cdot}5 \times 10^{-3}$

The origin of the 5577 Å spectral line [*O(1S) → O(1D)*], observed at meteor heights by Halliday (1960) and Millman (1960) in very bright meteors, and lasting only up to one second, is of the great importance to meteor studies. It was determined that the presence of the oxygen green line in meteor trains was strongly related to meteor velocity (Baggaley, 1977a). The observed lifetime is in line with theoretical radiative lifetime of the transition *O(1S) → O(1D)*. This observation was initially controversial as the 5577 Å green line is dominantly a feature of the middle thermosphere auroral phenomena. While Halliday (1960) did not offer any explanation for the observed phenomenon, several

authors, such as Baggaley (1976c) attempted to explain the detected spectra, suggesting high energy electron collisions with ground state atomic oxygen as the excitation agent.

$$e + O(3P) \rightarrow O(1S) \rightarrow e \tag{2.86}$$

Here the energy threshold of 4.18 eV is required for the reaction to proceed (Henry et al., 1969). It must be noted that the maximum cross section for this collision ($2\cdot 10^{-18}$ cm^2) is a function of energy in this case and is obtained around 9 eV. The other mechanism is a collision with molecular oxygen:

$$e + O_2 \rightarrow O + O(1S) + e \tag{2.87}$$

where in this case the energy threshold is 9.29 eV (Henry et al., 1969) with the maximum cross section obtained at around 25 eV (Baggaley, 1976c).

Baggaley (1976d) also offered the possibility of nitrogen collisions with oxygen, first suggested by Parkinson and Zipf (1970). Another proposed mechanism is energy transfer from excited molecular oxygen (Figure 2.34), chemical reactions such as a triple oxygen recombination, atom exchange in nitric oxide, neutralization and finally dissociation of molecular oxygen ions (Baggaley, 1976c). It is the last process that is of particular interest in this thesis.

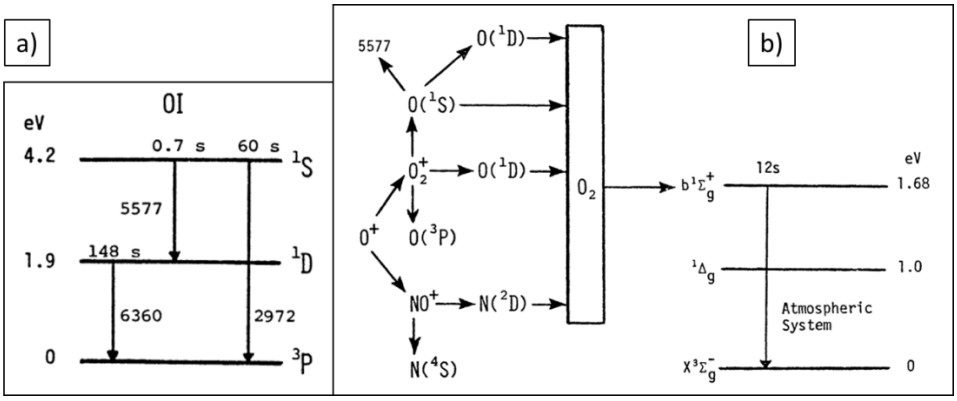

Figure 2.34: a) Excitation energies and states of the atomic oxygen, with transition wavelength and radiative life times outlined. b) Possible routes for the loss of atomic oxygen ionization energy (Baggaley, 1980).

One peculiar feature of the green line spectra, and the one with potentially significant implications, is the set of intermittent observations that show the delayed onset of the 5577 Å line, where the maximum intensity will occur at a fraction of a second after the meteor train formation (Baggaley and Cummack, 1977). This behaviour indicated the existence of some kind precursor mechanism prior to the production of *O(1S)*. A numerical model of production of O(1S) was performed by Baggaley and Cumack (1977) where they considered collisional processes with O^+ as highly reactive and abundant species in the meteor trail and ground state oxygen and nitrogen.

The reactions used in the model can be written as follows:

$$O^+(4S) + O_2\left(X^3\sum_g^-\right) \rightarrow O_2^+\left(\,^2\pi_g\right) + O(3P) + 1.55\ eV$$

$$O^+(4S) + N_2\left(X^1\sum_g^+\right) \rightarrow NO^+\left(\,^1\sum\right) + N(4S) + 1.10\ eV$$

where $O_2\left(X^3\sum_g^-\right)\ and\ N_2\left(X^1\sum_g^+\right)$ are ground states of oxygen and nitrogen respectively. The excited oxygen and nitrogen are given by $O_2^+\left(\,^2\pi_g\right)\ and\ NO^+\left(\,^1\sum\right)$.

Then the radiative recombination is written as:

$$O^+(4S) + e \rightarrow O + hv$$

While this theoretical treatment of the 5577 Å green line emission may not have illuminated the full complexity of the process behind it, the results of the simulation were in line with experimental observations and show for instance that the lifetime of the green line ranges from 0.03 s at 90 km and goes up to 0.6 s at 120 km, corresponding closely with experimental findings. Furthermore, the additional observational campaigns of the meteor green line emission indicate that a two-step charge exchange involving meteoric O^+ is the likely mechanism responsible for its formation (Baggaley, 1977b).

Moreover, the commonly observed range of orange-red emission 5900 – 6500 Å cannot be atomic in nature, in contrast to the regular meteor spectrum, since any long wavelength multiplets of meteoric atoms or ions would be dominated by stronger multiplets in the blue (Baggaley, 1975a). Baggaley (1977a) argued clearly for the chemical production of excited species. Additionally, the forbidden O(1D) line (6300-6364Å) is prominent in the middle and upper thermosphere where it has a lifetime of

~100s in auroras, and it should not exist below 100 km due to collisions with atomic nitrogen, but it has been continuously observed in meteor spectra. Poole (1979) had shown however that dissociative recombination of oxidized meteoric ion with free electrons is the main process responsible for the luminosity of meteor trains.

In principle, meteor spectra consist of individual emission lines of common chemical elements, including both neutral and singly ionized. The atomic lines identified in meteor spectra belong to H, Li, N, N^+, O, Na, Mg, Mg^+, Al, Si, Si^+, Ca, Ca^+, Ti, Ti^+, Cr, Cr^+, Mn, Fe, Fe^+, Co, Ni, and Sr (for the review of the elemental spectra see Bronshten, 1983; Ceplecha et al., 1998). The great contributions to the field in regard to meteor train spectra were made by Millman (1952), Öpik, (1958), Ceplecha (1968) and a great many others who cannot justifiably be listed here. A historical note and quantitative discussion of meteor spectra can be found in Bronshten (1983). While large atomic and molecular spectral lines had been observed from meteors (and discussed in detail by Bronshten, 1983) the meteor spectrum is dominated by Fe and Mg bands and FeO and MgO oxides, especially in the meteor "wakes" (Ceplecha, 1971). Meteor spectra can be classified in terms of their temporal and spatial origin, as the brightest spectral bands will be observed from the meteor head and the weakest from the meteor trail at some time following the extinction of luminous phenomenon (Borovicka, 1994). A More comprehensive classification scheme was devised by Millman (Millman and McKinley, 1963) according to which lines are the brightest. The four main types are:

Type Y – H and K lines of Ca II (3968 and 3934 Å) are the strongest.

Type X – the Na I or Mg I lines are the strongest.

Type Z – the Fe I or Cr I are the strongest.

Type W – none of the above.

The review by Ceplecha et al. (1998) discusses this in more detail. Another critical application of the meteor spectra is the ability to derive estimates of both electron and elemental densities as well as to measure temperatures of the meteor (Borovicka, 1993, 1994).

In a broad study of sporadic meteors, Borovicka et al. (2005) had shown that only a minority of meteorites show chondritic composition and surprisingly concluded that the iron meteoroids prevail among the millimeter sized particles impacting Earth's atmosphere. Reasonably strong ultraviolet radiation from the study of meteor spectra was detected by Abe et al. (2007) while a previous study by Abe et al. (2004) detected very strong UV emissions, in particular at 3534 Å, which corresponds to N_2^+ and a temperature of 10000 K. A spectral measurement of the relatively small masses ranging from 10^{-6} to 10^{-3} kg, equivalent to visual magnitudes ranging from +3 to -4 has yielded evidence of high temperatures ranging from the 4500 to 10000 K (Borovicka et al., 1999). Prior to that, Borovicka (1994) determined that the source of 10000 K temperature comes from the meteor head region (Ca II lines), and that it only corresponds to 0.02% of the total vapour volume in a small meteor and extends up to 5% in larger events. He had suggested that the high temperature region probably corresponds to the meteor shock wave. Detection of FeO in the in the persistent meteor trails showed clearly the classical mechanism of metal atom catalyzed recombination of ozone and oxygen atoms in the long lasting meteor trains (Jenniskens et al., 2000).

2.8.1 Sources of Long Lived Meteor Emission

Long lasting meteor trains in the MLT region are a window into upper atmosphere chemistry (Jenniskens et al., 2000). The persistent luminosity and red afterglow in the meteor trains, which may last for 1 s to 20 s between 80 – 90 km altitudes, following the initial trail formation, has not been completely understood. Luminous phenomena observed in the bright meteor wake for a relatively brief time, and determined to be a function of the initial electron density of the meteor, are generally explained in the early literature in terms of the collisional excitation. Observational evidence (Figure 2.35) and theoretical models clearly point out that most of the chemistry that causes luminous phenomena and long lived meteor trains occurs in the region of the outer boundary of the meteor train cross-section.

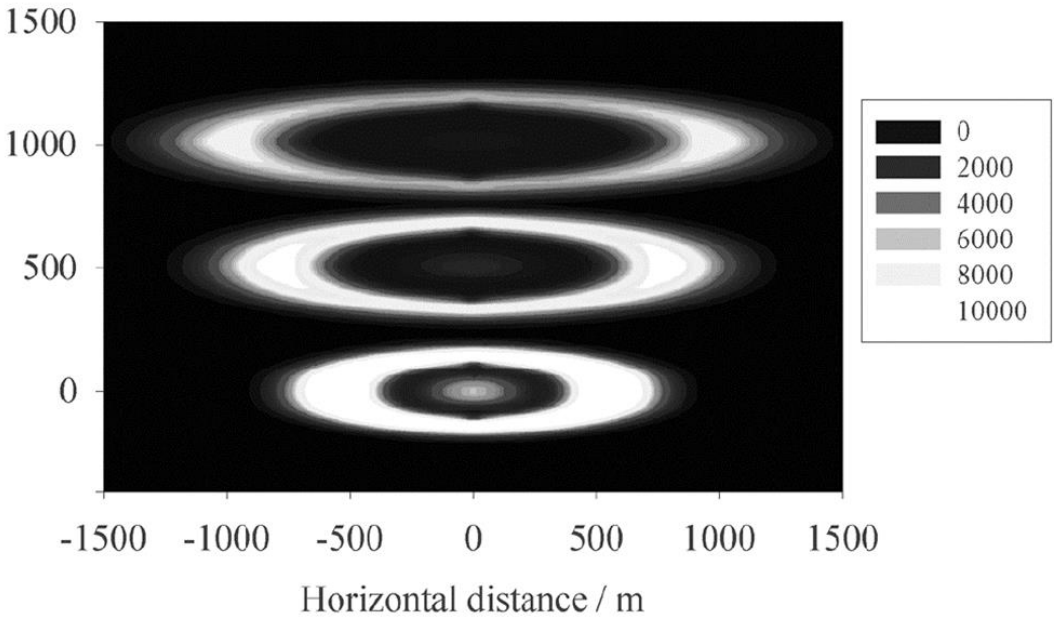

Figure 2.35: Three cross-sections through the persistent train at an altitude of 86 km, showing the modeled emission intensity at times 50s (bottom), 100s and 150s after the meteor. The 100 and 150 s sections have been displaced upward by 500 and 1000 m, respectively, for the purpose of presentation. The central emission patch visible at 50 s and 100 s is due to [OI] emission, the outer ring is due to chemiluminescence from metal atom reactions with ambient ozone (Jenniskens et al., 2000).

The immediate spectrum of the meteor trail is dominated primarily by Fe, Mg, O, Si and Na ions formed during initial high energy collisional processes, with average energy levels of 5 eV (Baggaley, 1975a). The main spectral contribution of the long lasting luminous phenomena is observed during early observations (Liller and Whipple, 1954) to be in the long wavelength range of orange and red (Figure 2.36). Baggaley (1975d) has treated the subject extensively, reviewing possible sources of the afterglow, and concluded that the emission from various chemiluminescent afterglow processes in atmospheric gases alone would be several orders of magnitude too low to account for the observation from luminous meteor trains. Furthermore, he suggested that the likely source of afterglow luminous phenomena in the meteor trail comes from the chemical reactions involving meteoric species.

In important studies, Baggaley (1976b) and Poole (1978) have concluded that reduction of meteoric oxides, formed in reaction with ozone, is the main source of the long lived

meteor train luminosity and radiation. Earlier investigation showed that the additional role of nitric oxide in chemiluminescent processes is not sufficient to count as a primary source of meteor train luminosity (Baggaley, 1975b). Subsequent work however suggests that sodium and ozone reactions are important for extremely long lived meteor emissions with initial visual magnitude $M_v < -10$ (Baggaley and Cummack, 1979).

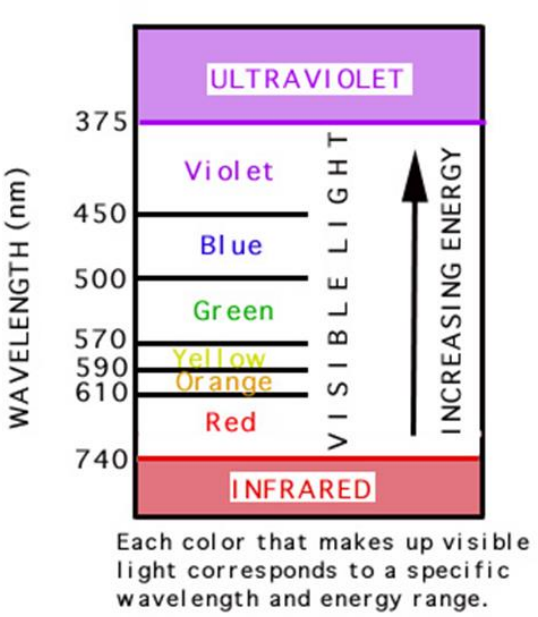

Figure 2.36: The infrared, visible and UV spectra and wavelengths. (Credit: nature.berkeley.edu)

2.9 Meteor Head

In simple terms, a spherical large cross-sectional area in front of the hypervelocity meteor that propagates with the same geocentric velocity along with it, and reflects radio signals, is defined as a head echo. The opening sentence and definition at the beginning of this section, is intentionally vague as it is intended to illustrate to the reader the illusiveness of the meteor head echo phenomena. While the meteor echo was first observed in 1947 by Hey et al. (1947) and definitely recognized and acknowledged by McKinley and Millman in 1949, a large body of research since then has not yielded many satisfactory answers regarding the formation, origins and overall behaviour of meteor head echoes. Moreover, the mechanism of the scattering of radio signals from the meteor head is not yet

completely understood. Early on it was recognized that the phenomenon is closely associated with bright meteors and that the radar cross-section of the target is very large (many hundreds of m^2 according to Cook and Hawkins (1960)) in comparison to the meteoroid size which may be only a few cm in diameter. Additionally, the meteor head echo peak occurs in the region of the ionization curve maxima (McIntosh, 1963). At this point one might be tempted to draw parallels to the high speed photographic image of meteor head captured by Jenniskens and Stenbaek-Nielsen (2004) shown in the previous section. However, that parallel will be explored in upcoming chapters. To explain this, McKinley and Millman (1949) had suggested a hypothesis to account for the ionization of the large area in front of the meteor. They proposed that fast moving and ablating meteoroid acts as the source of intense ultraviolet radiation which ionizes a significant region surrounding the meteoroid. The primary criticism of their hypothesis rested on the fact that at that time there was no known recombination process which would remove electrons rapidly enough to yield an effective "moving ball" target (McIntosh, 1962). Cook and Hawkins (1960) examined McKinley and Millman's (1949) hypothesis, and after mathematical and theoretical treatment, they concluded that photoionization from the region of meteor head can be responsible for the head echoes observed by radar. The new theory of meteor head echoes based on diffraction (Browne and Kaiser, 1953) suggested that the head echo is due to diffraction at the discontinuity in ionization at the end of the ionized column. In that case, the echo amplitude intensity is given by extending the Fresnel diffraction pattern for a considerable distance along the trail, where the echo is expected to fall very rapidly. That had been shown not to be the case (McKinley, 1955), thus Browne and Kaiser's (1953) theory had been proven not to be valid. Moreover, McKinley (1955) showed that ionization persists for only 10^{-3} to 10^{-4} seconds after the passage of the meteor. The further uncertainty in meteor head echo treatment was introduced when Greenhow (1961) suggested that meteor head echo may persist for many seconds after the meteor passage. He had also proposed that the explanation for the head echo can be understood on the basis of a rough or broken electron trail had been addressed by McIntosh (1962) who showed that Greenhow's interpretation did not correspond to true meteor head echoes. Jones and Jones (1997) observed meteor head echoes with visual magnitudes as low as $M_v = +4$. Their most

significant findings can be summarized as follows: a) ***every visual meteor produces a head echo***; b) *the scattering areas associated with the head echoes seem to be distributed approximately as a truncated power law such that the minimum or cut-off scattering area is of the order of less than 1 m^2*.

The study of the meteor head echo was to an extent reinvigorated during the 1990s (e.g. Pellinen-Wannberg and Wannberg, 1994; Pellinen-Wannberg et al., 1998) and the applications of the observations of meteor head echoes range from velocity determinations of a meteor to calculating meteor plasma density and meteoroid mass from the head echo scattering (Close et al., 2004).

For analytical treatment of the meteor head, it can be assumed that the head plasma density behaves as a Gaussian function and that the radius of the head plasma depends on altitude and scales with the atmospheric mean free path and meteoroid speed (Close et al., 2004). Moreover, it can be assumed that the reflecting component of the head plasma can be approximated as spherically symmetric (Figure 2.37). Experimental data obtained by Close at al. (2002) indicates that the meteor head scattering results from overdense plasma scattering. In addition, Close et al. (2002) showed that at lower altitudes, where the mean free path is small, the radar cross section (RSC) of the head echo will be proportionally smaller.

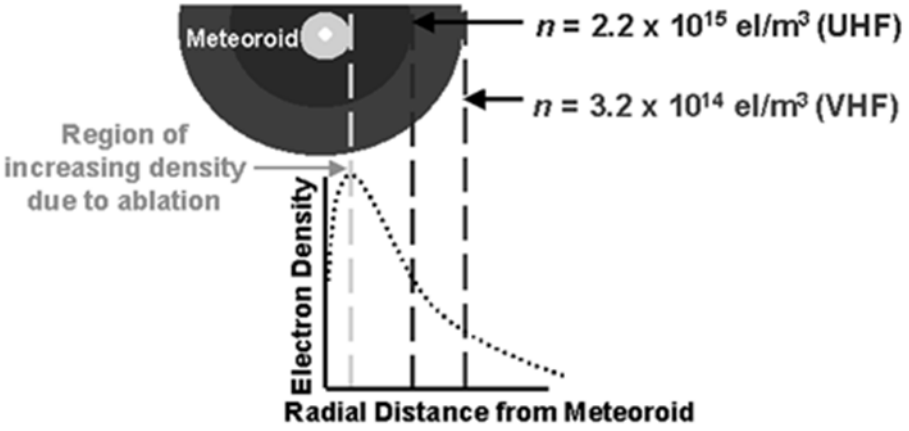

Figure 2.37: Illustration of how electron density theoretically varies as a function of distance from the meteoroid . The solid white center represents the meteoroid, the shaded portion denotes the region where the electron density increases, and the subsequent dark rings show how the electron density decreases with radius. By assuming overdense reflection, the ultra high frequency (UHF) wave (higher critical frequency) penetrates

further into the meteoroid than the very high frequency (VHF) reflection, thus explaining the lower UHF RCS (radius of head echo) (Close et al., 2002).

A comparison of very high frequency (VHF) meteor radars and ultra-high frequency (UHF) systems shows that head echo target is significantly larger for VHF, because waves with smaller wavelengths penetrate deeper into plasma. Experimental observations indicate that the number of electrons ahead of the meteoroid correspond to the number of electrons in the line density in the trail left behind the meteor (Pallinen-Wannberg, 2005).

2.10 Physical and Chemical Properties of Upper Mesosphere and Lower Thermosphere (MLT) Region

The atmosphere is both a dynamically and chemically complex system (Smith, 2012). The vertical layers are distinguished based on their physical properties such as temperature, pressure and consequently density. This picture gets exponentially more complicated when one considers dynamical aspects such as winds, turbulence and the range of wave phenomena on one side and complex chemistry and photochemical effects on the other. To fully understand the atmosphere, one needs to understand the "orderly chaos". For the purpose of this work the intricacies of the main part of atmosphere below 75 km will not be considered. Much work has been done in the past and much work remains to be done in the future. Rather than reference individual papers, the reader is pointed to several books that would introduce the complex subject of atmospheric physics and chemistry (Salby, 1996; ed. Hewitt and Jackson, 2008; Seinfeld and Pandis, 2012). In this work, the primary concern revolves around understanding the physics and chemistry of the upper mesosphere and lower thermosphere (MLT) which is commonly known as the meteor region.

As the name suggests, the ionosphere, which could be considered weakly ionized plasma, is characterized by the presence of ions and electrons, the latter ones in sufficient concentration that they affect the propagation of radio signals. The term was first used by Watson-Watt, one of the early radar developers, in 1926. In general, the ionized region extends from about 50 km to 1000 km altitude (Pavlov, 2012). The electron concentration is primarily a function of the height and radiation budget (Kelly, 2009), however, many other factors may contribute to variation in electron densities. For ground based sources

of radio waves, the ionosphere exhibits properties of a reflector, contributing significantly to the evolution of radio communications in the past. The term ionosphere encompasses the regions of the upper mesosphere and the lower thermosphere, a region between the heights of 75 – 110 km (Figure 2.38). It is considered the boundary between the atmosphere and space (Plane, 2003) and the region of energetic coupling between the neutral and ionic regions of the atmosphere (Plane, 1991).

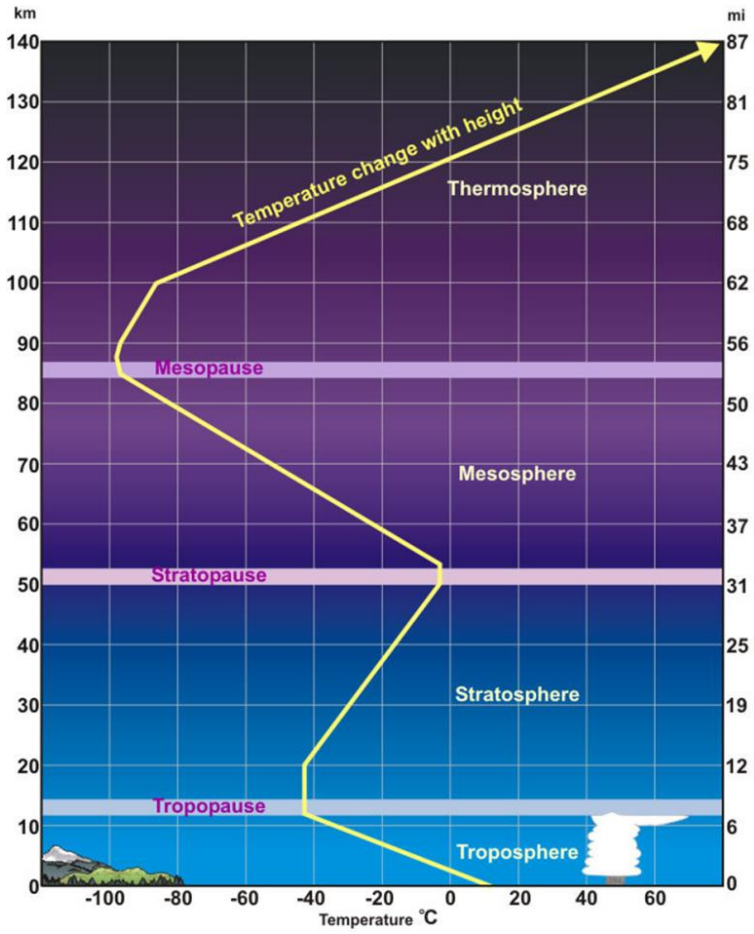

Figure 2.38: An average temperature profile through the lower layers of the atmosphere. Height (in miles and kilometers) is indicated along each side. Temperatures in the thermosphere continue to climb, reaching as high as 2000°C (Credit: National Weather Service).

This region is of particular interest in meteor research as most meteors are detected at these altitudes, where they exhibit highest ionization and ablation. It is also a very

dynamic and energetic region, as gravity and planetary waves and atmospheric tides deposit energy from the direction of the Earth's surface, while high energy input in the form of solar electromagnetic radiation and wind also comes from the space. MLT is also the coldest region in the Earth's atmosphere with temperatures average of 140 K during the summer season (Stickland, 1972; Plane, 1991). The main cause for such counterintuitive behaviour is the adiabatic expansion of the mesosphere. The anatomy of the underlying forces that cause such low temperature in the MLT region can be explained in terms of gravity waves propagating upward from the troposphere. As they travel upward, the wave amplitude increases with the exponentially decreasing pressure, and around 80-90 km in altitude, waves become unstable and break, depositing the energy and momentum in that region of MLT. This results in a drag effect on zonal winds, affecting a southward meridional flow. Consequently, the upwelling air at northern latitudes which feeds this meridional flow is cooled by adiabatic expansion.

Above 90 km, in the thermosphere, temperatures increase rapidly, reaching 1000 K. However, it must be remarked that this is the kinetic temperature where the vibrational and rotational modes of molecules are not in local thermodynamic equilibrium (LTE) as a result of very low pressure (Plane, 2003). Low pressures in the MLT will affect mean fee paths where for example at 110 km altitude, the mean free path is around one meter. Accordingly, molecular diffusion is the dominant dispersion mechanism. Moreover, the height of about 105 km is defined as the actual boundary between Earth and space, and is referred to as the turbopause. Above 75 km, atomic oxygen O has the highest mixing ratio (Jacob, 1999) (Figure 2.39), and therefore is the most dominant reactive species at these altitudes (Plane, 2003). It also exhibits a strong diurnal variation similar to O_3, as a result of the O_2 photolysis rate variation.

A high plasma concentration above 70 km is due to a strong influx of solar photons that have enough energy to ionize the regional constituents. The O^+_2 and NO^+, formed by photoionization, are dominant above 95 km, while below that, at altitudes 70-95 km negative ions are abundant. O1S and O1D are formed via photolysis of O_2, below and in the Schumann-Runge continuum (1300-1950 Å) and the Schumann-Runge bands (1750-1950 Å) (Figure 2.40).

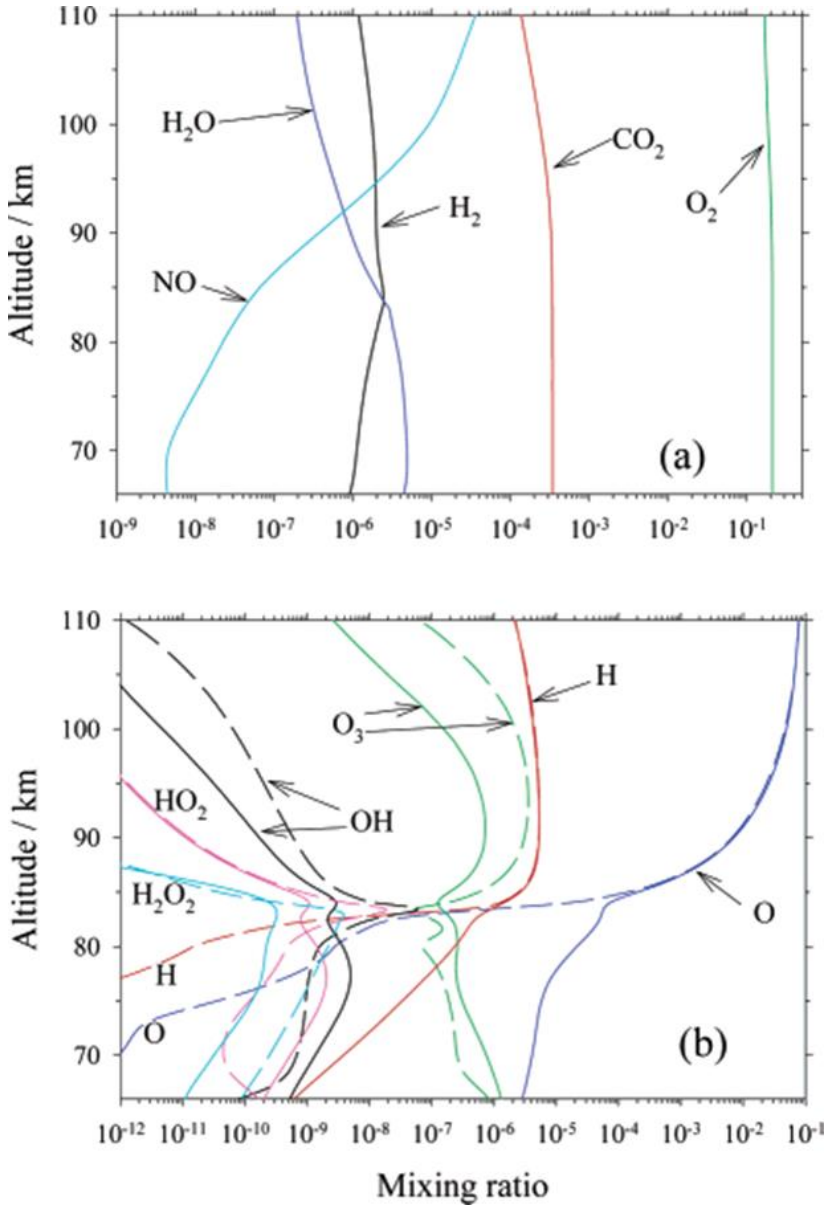

Figure 2.39: Vertical profiles of the mixing ratios of atmospheric constituents in the mesosphere and lower thermosphere: (a) species with no diurnal variation; (b) reactive species with significant diurnal variations, where broken lines indicate the nighttime profiles. Profiles calculated using the UEA 1-dimensional mesospheric model for 40°N in January (Plane, 2003).

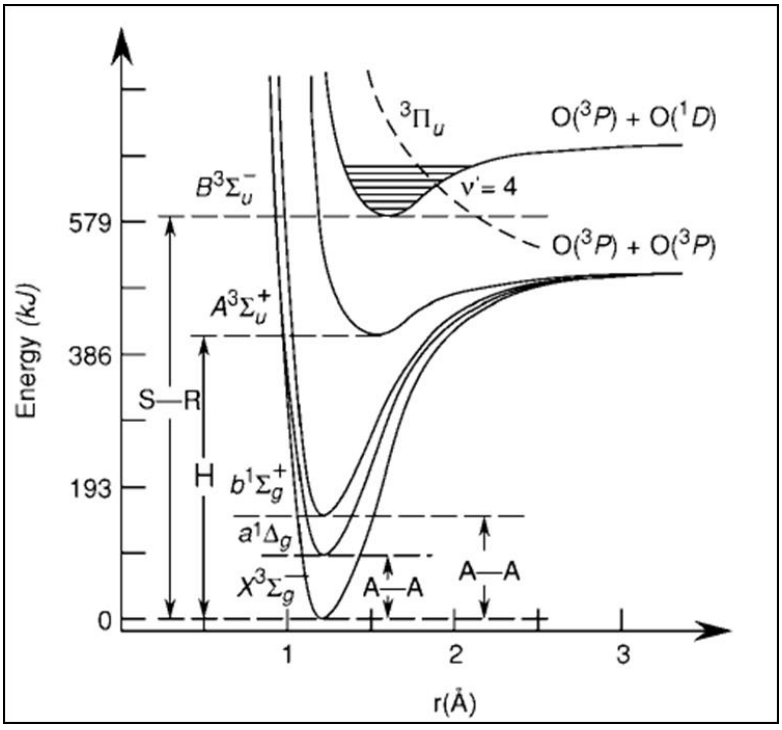

Figure 2.40: Potential energy curves for ground and first four excited states of O_2. S-R = Schumann-Runge system, H = Herzberg continuum, A-A = atmospheric bands (originally published by Gaydon, 1968 and adopted from Finlayson-Pitts and Pitts, 1999).

Moreover, above 100 km, in the lower E region, electrons also exhibit diurnal variation because at those altitudes, the primary source of ions and electrons are solar X-rays and extreme ultraviolet radiation with a wavelength less than 1030 Å. It should be noted that in the D region which stretches from 50 km to 95 km (Figure 2.41), due to increased atmospheric density relative to the MLT region, the overall chemistry including the ion chemistry is very complex, and it is beyond the scope of this review. The text by Finlayson-Pitts and Pitts (1999) and the articles by Plane (2003) and Smith (2004) give substantial reviews of the D region chemistry. As indicated in the previous section, the MLT region also hosts the metallic layer which further complicates things chemically. Thus, it is apparent at this stage that combining and understanding the meteor chemistry in the ionospheric setting is a formidable task.

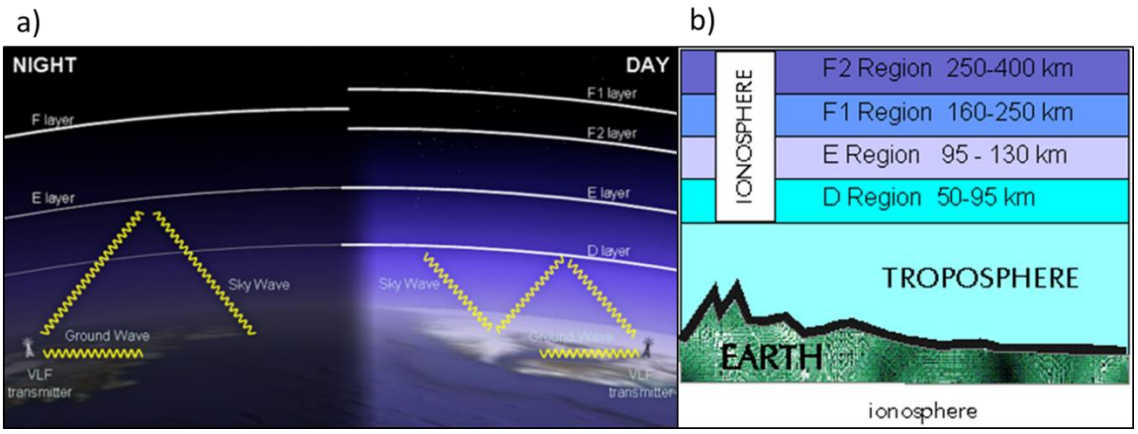

Figure 2.41: a) The ionosphere has layers called D, E, F1, and F2 with the D-layer being the lowest. Depending on whether it's night or day and on intensity of solar radiation - these layers can reflect (E, F1, and F2) or absorb (D and E) radio waves. b) The altitudes corresponding to the specific ionospheric layer (Images adopted from online sources: http://tymkrs.tumblr.com/post/4838083914/21-ionosphere-ham-lesson-o-de-day and www.faxswitch.com, respectively).

2.11 Ozone

Ozone is perhaps the most important minor constituent of the atmosphere. When at ground level in gaseous form, it is very toxic; impacting harmfully both flora and fauna. However, ozone plays a critical role in the middle and upper atmosphere as a shield against harmful UV radiation, thus protecting the terrestrial ecosystem (Blake and Carver, 1977). It is also a major contributor in atmospheric chemical processes, and because of its optical and chemical properties, ozone affects the thermal structure and dynamics of the atmosphere (London, 1980). Moreover, ozone is responsible for the chemical evolution of the whole atmosphere on a long term geologic scale (Hunten and Strobel, 1974), and probably a significant factor in the evolution of life on Earth in its present form. It consists of three atoms of oxygen bound together and is very reactive and unstable. Ozone is also pale blue in colour (gaseous from) and has a very distinctive odour hence its name is derived from the Greek word *ozein* (to smell). It exhibits the highest concentration in the stratosphere.

A sudden increase of ozone concentration in the region of the upper mesosphere and lower thermosphere, with maxima between 85 and 90 km, defies the theoretical

prediction of ozone decrease with increasing height and it is better known as the secondary ozone maximum. Its existence has been known since 1970 (Evans and Llewellyn, 1972; Hays and Roble, 1973 and Miller and Ryder, 1973). On an important note, ozone is the most dominant reactive species in the MLT (Smith et al., 2013).

However, a secondary ozone maximum in the MLT region is in a no man's land, at least in terms of attention of the scientific community. While the lower atmosphere has been extensively studied during the last century, and the exosphere is a domain of satellites, this particular "middle region" has received the least amount of attention in atmospheric literature. That is because the altitude is too high for effective use of stratospheric measurement techniques and too low for in situ satellite measurements (Allen et al., 1984). Mesospheric ozone exhibits strong diurnal (Vaughan, 1982; Green et al., 1986 and Verronen et al., 2005) (Figure 2.42) and seasonal variations (Rogers et al., 2009 and Thomas, 1990). It varies diurnally by almost an order of magnitude (Smith and Marsh, 2005).Vertical diffusive transport may also play a role in ozone diurnal variability.

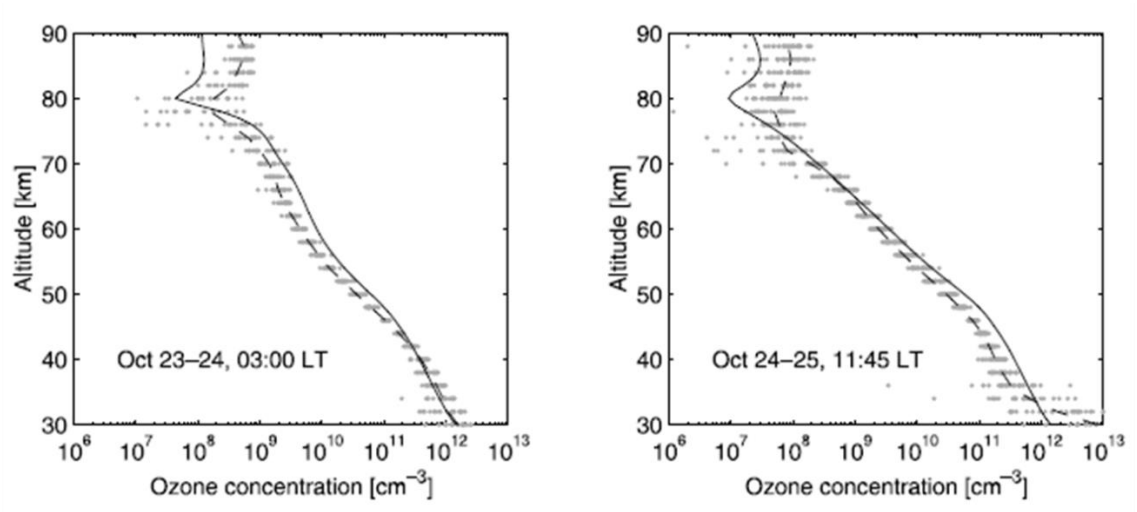

Figure 2.42: The diurnal variation (nighttime on the left and daytime on the right) in density of O_3 in the upper atmosphere as measured by Verronen et al. (2005).

In principle, the mechanism behind the diurnal variability of the secondary maximum is well understood. At night, ozone is much more abundant, because of the absence of

photolytic destruction which dominates during the day. Molecular oxygen photolysis by solar radiation in the Schuman-Runge bands and Herzberg continuum produces atomic oxygen (Figure 2.43).

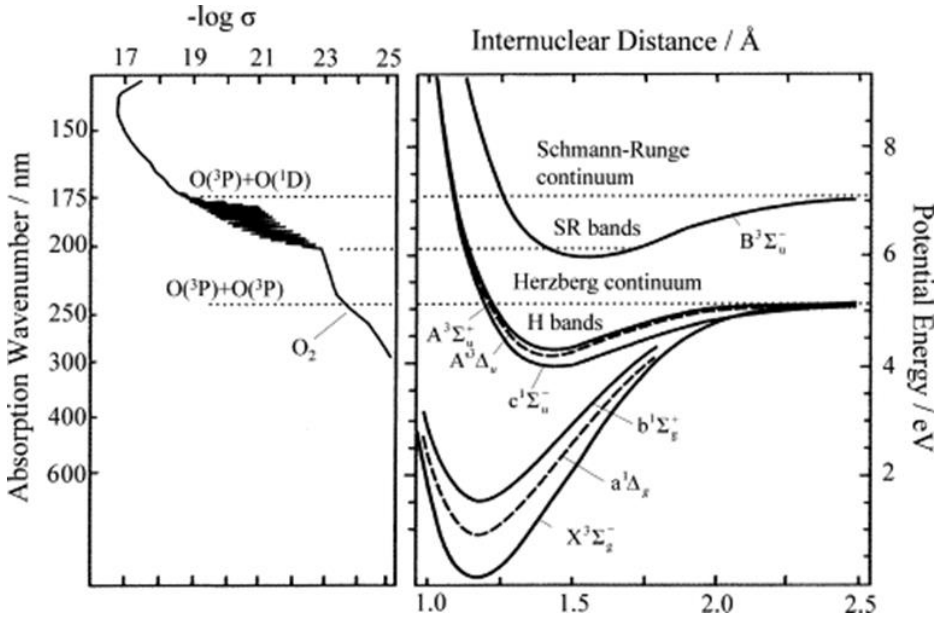

Figure 2.43: Absorption spectrum and potential energy curves for O_2. The first (O(3P) + O(3P) and second (O(3P) + O(1D)) dissociation limits are indicated at 2420 and 1760 Å, respectively. Reproduced from Koda and Sugimoto (2003).

Ozone is formed through the three body associative reaction of O and O_2 as expressed below. For the demonstrative purpose, rather than discussing the Chapman cycle which describes how sunlight converts various form of oxygen from one to another and upon which the ozone chemistry is based, a table with about 50 kinetic and photolytic reactions that in actuality control ozone in the mesosphere is given below (Table 2.7). However, for the illustrative purpose, the general Chapman mechanism for the formation of ozone can be written as follows:

$$O_2 + h\nu \rightarrow O + O \quad (495\ kJ;\ \lambda = \ 2410\text{Å}) \tag{2.88}$$

where O_2 absorbs ultraviolet light at 2410 Å and dissociates into two atomic oxygen. Consequently, another O_2 (because of high concentrations in atmosphere) will react with

a single O alone or in the presence of the third molecule which facilitates heat energy budget, so:

$$O_2 + O \rightarrow O_3 \tag{2.89}$$

and

$$O_2 + O + M \rightarrow O_3 \tag{2.90}$$

where M can be N_2 for example.

It should be remarked again that the above reactions are only for illustrative purpose as the ozone cycle and related chemistry are far more complex process.

Intricacies of the production and destruction cycle of ozone are discussed by several authors (Wayne and White, 1968; Crutzen, 1971; Prather, 1973; Allen et al., 1981; Snelling, 1981; Allen et al., 1984; Hippler et al., 1990) and will not be covered in detail here.

At the mesopause (~80km) there is a significant transformation of the active-O chemical cycle. In that region, active-O as a group becomes short lived and as a result cycles among the group constituents rapidly during the daylight hours, with the nature of the dominant species dependent on the exact altitude (Allen et al., 1984).

Smith and Marsh (2005), using a three-dimensional dynamical chemical model, investigated the reasons for the secondary ozone maximum. They showed that the nighttime ozone mixing ratios are the same or even larger than those at the stratospheric maximum. Moreover, they concluded that the low temperature in the MLT region is a relevant factor in the increased ozone density, as low temperatures accelerate the formation of ozone and inhibit the loss. Furthermore, eddy diffusion acts to decrease the night time ozone by bringing water up from lower altitudes as water contains hydrogen which destroys ozone. However, molecular diffusion acts to increase the nighttime ozone concentration by moving atomic hydrogen upward out of the MLT region (Smith and Marsh, 2005). Molecular diffusion also increases the concentration of atomic oxygen below 105 km which acts as the additional mechanism for the increase of ozone. Satellite measurements of the secondary ozone maximum show some disagreement, especially above 75 km (Smith et al., 2013) (Figure 2.44).

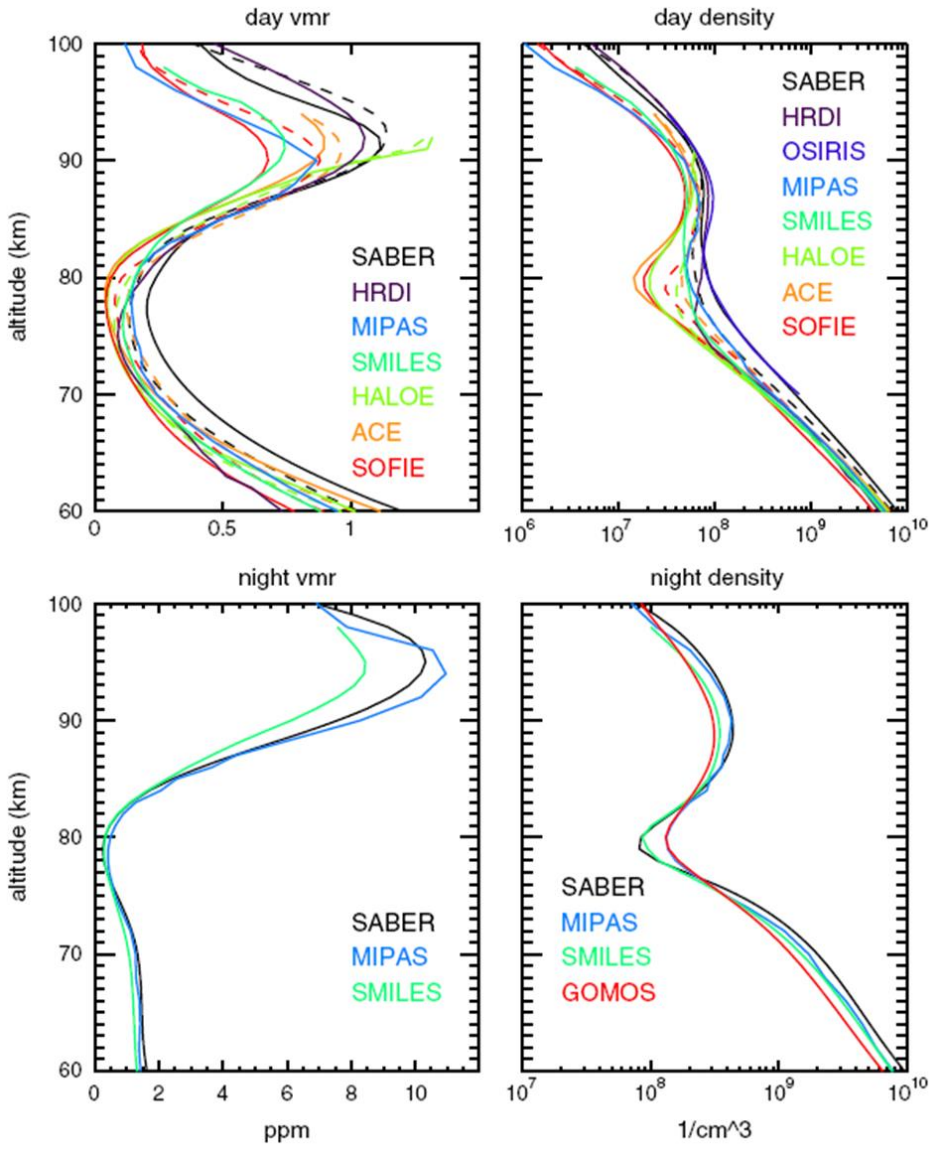

Figure 2.44: Left panels give the average of all ozone profiles for each of the instruments on board every satellite with volume mixing ratio information. The right panels give the ozone density of all instruments used. For SABER, the solid lines are for 9.6 µm ozone and the dashed line is for 1.27 µm. For the solar occultation cases (HALOE, ACEFTS, and SOFIE), solid lines are for sunrise and dashed lines are for sunset. Volume mixing ratio units are in ppmv; density units are cm^{-3} (after Smith et al., 2013).

A worrying trend in observed ozone decrease (Lemonie, 2004) warrants continuous monitoring and measurements of its atmospheric levels. Considering that satellite

measurements are thought to be most accurate, a new method to additionally constrain mesospheric ozone concentration may be needed. The VHF meteor radar and study of overdense meteor trail diffusion behaviour may offer just such possibility.

Table 2.7: List of main photochemical reactions that control ozone in the mesosphere. (after Prather, 1981).

	Reactions	Rate ($cm^3\ s^{-1}$ or $cm^6\ s^{-1}$)		Note*
(R1)	$O + O_2 + M = O_3 + M$	1.05E-34	exp (+510/T)	LPWM
(R2)	$O + O_3 = O_2 + O_2$	1.5E-11	exp (−2218/T)	NASA
(R3)	$O + O + M = O_2 + M$	9.6E-34	exp (+480/T)	LPWM
(R4)	$O + OH = H + O_2$	4.0E-11		NASA
(R5)	$O + HO_2 = OH + O_2$	3.5E-11		NASA
(R6)	$O + H_2 = OH + H$	5.3E-11	exp (−5100/T)	LPWM
(R7)	$O(^1D) + N_2 = O + N_2$	2.0E-11	exp (+107/T)	NASA
(R8)	$O(^1D) + O_2 = O + O_2$	2.9E-11	exp (+67/T)	NASA
(R9)	$O(^1D) + H_2O = OH + OH$	2.3E-10		NASA
(R10)	$O(^1D) + H_2 = OH + H$	0.99E-10		NASA
(R11)	$O_3 + H = OH + O_2$	1.4E-10	exp (−470/T)	NASA
(R12)	$O_3 + OH = HO_2 + O_2$	1.6E-12	exp (−940/T)	NASA
(R13)	$O_3 + HO_2 = OH + O_2 + O_2$	1.1E-14	exp (−580/T)	NASA
(R14)	$H + O_2 + M = HO_2 + M$	1.90E-32	exp (+350/T)	LPWM
(R15)	$H + HO_2 = H_2 + O_2$	4.2E-11	exp (−350/T)	LPWM
(R16)	$H + HO_2 = OH + OH$	4.2E-10	exp (−950/T)	LPWM
(R17)	$OH + HO_2 = H_2O + O_2$	4.0E-11		NASA
(R18)	$OH + H_2 = H_2O + H$	1.2E-11	exp(−2200/T)	NASA
(R19)	$OH + CO = CO_2 + H$	1.35E-13	[1 + p(atm)]	NASA
(R20)	$OH + OH = H_2O + O$	1.0E-11	exp (−500/T)	NASA
(R21)	$NO + O + M = NO_2 + M$	4.0E-33	exp (+940/T)	LPWM
(R22)	$NO + HO_2 = NO_2 + OH$	3.4E-12	exp (+250/T)	NASA
(R23)	$NO + O_3 = NO_2 + O_2$	2.3E-12	exp (−1450/T)	NASA
(R24)	$NO_2 + O = NO + O_2$	9.3E-12		NASA
(R25)	$NO_2 + H = NO + OH$	4.8E-10	exp (−405/T)	NASA
(R26)	$N + NO = N_2 + O$	3.4E-11		NASA
(R27)	$N + O_2 = NO + O$	4.4E-12	exp (−3220/T)	NASA
(R28)	$HCl + OH = Cl + H_2O$	2.8E-12	exp (−425/T)	NASA
(R29)	$HCl + H = Cl + H_2$	2.3E-11	exp (−1816/T)	LPWM
(R30)	$Cl + H_2 = HCl + H$	3.5E-11	exp (−2290/T)	NASA
(R31)	$Cl + CH_4 = HCl + CH_3$	9.9E-12	exp (−1359/T)	NASA
(R32)	$Cl + HO_2 = HCl + O_2$	4.5E-11		NASA
(R33)	$Cl + O_3 = ClO + O_2$	2.8E-11	exp (−257/T)	NASA
(R34)	$ClO + NO = Cl + NO_2$	7.8E-12	exp (+250/T)	NASA
(R35)	$ClO + O = Cl + O_2$	7.7E-11	exp (−130/T)	NASA
(R36)	$CH_4 + OH = H_2O + CH_3$	2.4E-12	exp (−1710/T)	NASA
(R37)	$CH_4 + O(^1D) = OH + CH_3$	1.4E-10		NASA
(R38)	$O_2 + h\nu = O + O$			
(R39)	$O_3 + h\nu = O_2(^1\Delta) + O(^1D)$			
(R40)	$O_3 + h\nu = O_2 + O$			
(R41)	$HO_2 + h\nu = OH + O$			
(R42)	$H_2O + h\nu = OH + H$			
(R43)	$NO_2 + h\nu = NO + O$			
(R44)	$NO + h\nu = N + O$			
(R45)	$HCl + h\nu = H + Cl$			
(R46)	$ClO + h\nu = Cl + O$			
(R47)	$CH_4 + h\nu = H_2 + CH_2$			

*NASA refers to *NASA-JPL* [1979]. LPWM refers to Logan *et al.* [1978].

2.11.1 Ozone Density Obtained from Radars

The relationship between overdense meteor echo durations and meteor ion-ozone chemistry was utilised during the end of the last century to measure ozone concentration in the MLT region (e.g. Jones et al., 1990; Jones and Simek, 1995). The basis for such an undertaking is a well-known relationship between the number of meteors and echo durations plotted on a log scale, where the change in slope indicates the transition from underdense to overdense regime (Figure 2.45). This relationship can be further treated and it is possible to derive the following expression:

$$N_T \propto T^{-\frac{3(s-1)}{4}} \tag{2.91}$$

where N_T is the cumulative number of radar echoes having duration greater or equal than chosen duration time T, and s is the value of the slope (Figure 2.45). This trend was observed and studied by early authors (e.g. Kasier, 1953; Weiss, 1961; McKinley, 1961; and McIntosh, 1966). It must be noted that relationship (2.91) only applies to the underdense echoes. However, early authors did not have sufficient knowledge of the meteor train chemistry and they assumed that electrons are removed by simple attachment process such as one stated below:

$$e + A \rightarrow A^- \tag{2.92}$$

where A is an atmospheric molecule.

It was realized that electron density (n_e) decreases according to: $n_e \propto e^{-T/T_C}$ where if diffusion is ignored, T_C depends on the chemical reaction rate R (see Jones et al., 1990).

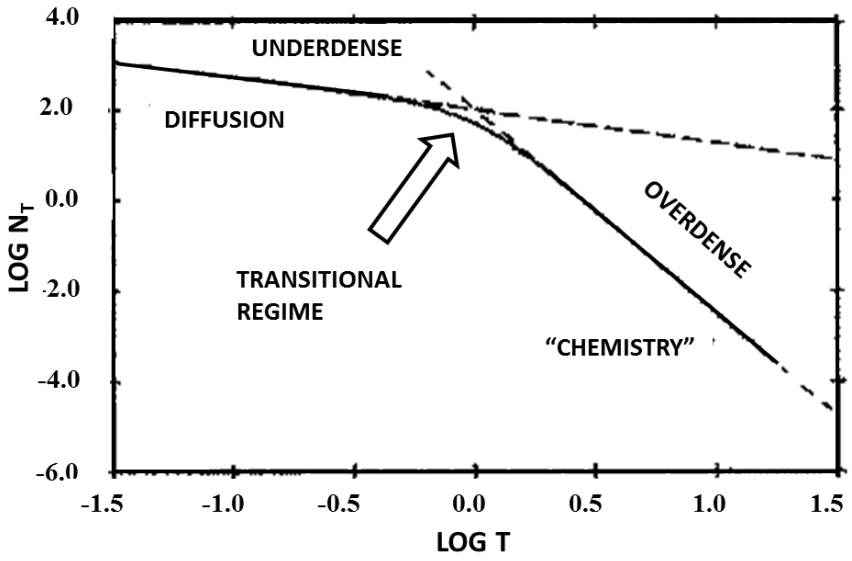

Figure 2.45: Log of cumulative number of events vs. log of radar echo duration (modified from Jones et al., 1990).

However, Weiss (1961) determined that the relation (81) can be restated for the case of intermediate (transitional overdense) echoes durations:

$$N_T \propto T^{-\frac{9(s-1)}{2}} \tag{2.93}$$

where *s* can be obtained experimentally directly by observing either showers or time cumulative events. Then T_C can be expressed in terms of a chemical reaction (R_A):

$$T_C = (R_A[A])^{-1} \tag{2.94}$$

This can be immediately recognized as a classic form of kinetic rate law. In the case when the chemical reaction, which is responsible for electron removal, can be defined, it then can be written:

$$e + A + B \rightarrow A^- + B \tag{2.95}$$

Thus,

$$T_C = (R_{AB}[A][B])^{-1} \tag{2.96}$$

Accordingly, the same chemical reactions identified by Baggaley and Cummack (1974) and Poole and Nicholson (1975) and discussed in the earlier sections can be used here. For the convenience of the reader, those chemical reactions will be restated, where meteor metallic ion reacts primarily with ozone as the most dominant reactant:

$$M^+ + O_3 \rightarrow MO^+ + O_2 \tag{2.97}$$

$$MO^+ + e \rightarrow M + O \tag{2.98}$$

Using the above methodology, researchers were able to obtain ozone concentration within reasonable accuracy, but the outstanding issue was uncertainty in height (Jones and Simek, 1995; Cevolani et al., 1999). That issue was resolved to a degree by Cevolani and Pupillo (2003). Moreover, those investigators were using the forward scatter systems, thus they were able to track the meteor for a number of seconds and even minutes. That would give plenty of time to observe equilibrium chemical reactions (e.g. reaction (86) is the controlling one as it is slow and reaction (87) cannot proceed unless (86) is completed). That, as explained in the previous sections, is not possible to accomplish with backscatter radar, and consequently equilibrium chemical reactions cannot be detected by a backscatter system.

In conclusion, Cevolani and Pupillo (2003) have reported observations of the downward trend in ozone concentration between 85 and 90 km. If confirmed, such a trend would be a very worrying development and further investigation and measurements on an ongoing basis are needed to assess the global mesospheric ozone trends.

Chapter 3

The most exciting phrase to hear in science,
the one that heralds new discoveries,
is not 'Eureka!' but 'That's funny...'

- Isaac Asimov

3. Methods

3.1 Radar – Instrument Fundamentals

All radar locations in this study host versions of Yagi-type "All-Sky Interferometric Meteor Radar" (SKiYMET) (Hocking et al., 2001; http://mardoc-inc.com), a commercially available and well tested, proven and reliable meteor radar system (Hocking et al., 2001). The design of the system was prioritised to provide not only all sky monitoring capability through the deployment of a wide beam, but also to enable interferometry, using optimal receiver spacings. The system was optimized to accommodate very high pulse repetition frequencies of more than 2 kHz and to operate in the range of 20-50 MHz. High pulse repetition frequencies (PRF) can cause problems in the sense that the aliasing range becomes relatively small, at least in terms of meteor observations. The system is described in detail by Hocking et al. (2001), therefore only the fundamentals of the operation and design will be discussed here.

The system is comprised of five antenna elements. The planar schematic of the antenna arrangement is given in the Figure 3.1. The location of the transmitting antenna is not critical as long as it is not too close to the receiving units. What is important is that the receiving antennas must all be in the horizontal plane. From the Figure 3.1, it can be seen that the optimal separation for the receiving antennas is 2 λ and 2.5 λ in the asymmetric cross arrangement (where λ is the radar wavelength). The receiving antennas are all connected to separate receivers with cables of equal phase length (generally that length is 70 m, as a longer cable will cause significant signal strength loss).

These receivers are part of the Radar Data Acquisition System (RDAS) and are interfaced with the digitization system. The reference frequencies are provided to both transmitter and receiver by the Frequency Synthesizer Unit (FSU). The transmitter unit is comprised

of solid state modules (1 kW each), and is modular in construction to allow for additional installations. It is connected to the transmitting antenna via a high power low-loss cable. Early SKiYMET used a transmitting power of 6 kW, and it is possible to manipulate the selection of the type of the pulsed signal, its duration and length as needed. The whole system is controlled by a UNIX based computer, aiding speed and efficiency in the treatment of data. The schematic of the complete system is shown in Figure 3.2. Details of the underlying software and detection algorithms can be found in Hocking at al. (2001a). It should be noted that the proper meteor event signature selection and discrimination is a rigorous and multistage process, enabling the elimination of false positives and is also sufficiently optimized to allow for high resolution data input.

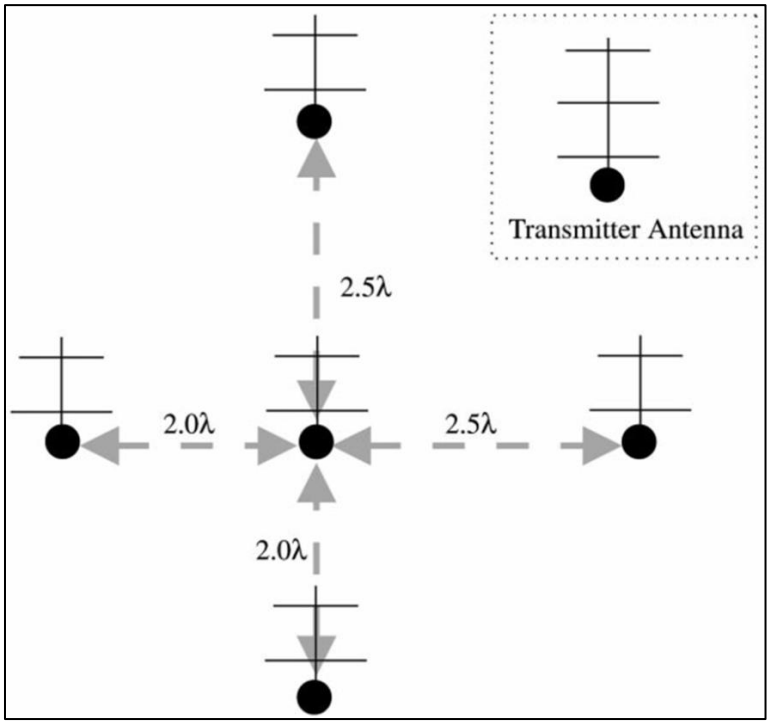

Figure 3.1: Planar view of the antenna arrangement for the radar system. The location of the transmitter antenna is not critical and can be placed in any convenient location. The receiving antennas all need to be in a horizontal plane. The symbol λ represents the radar wavelength (Hocking et al., 2001).

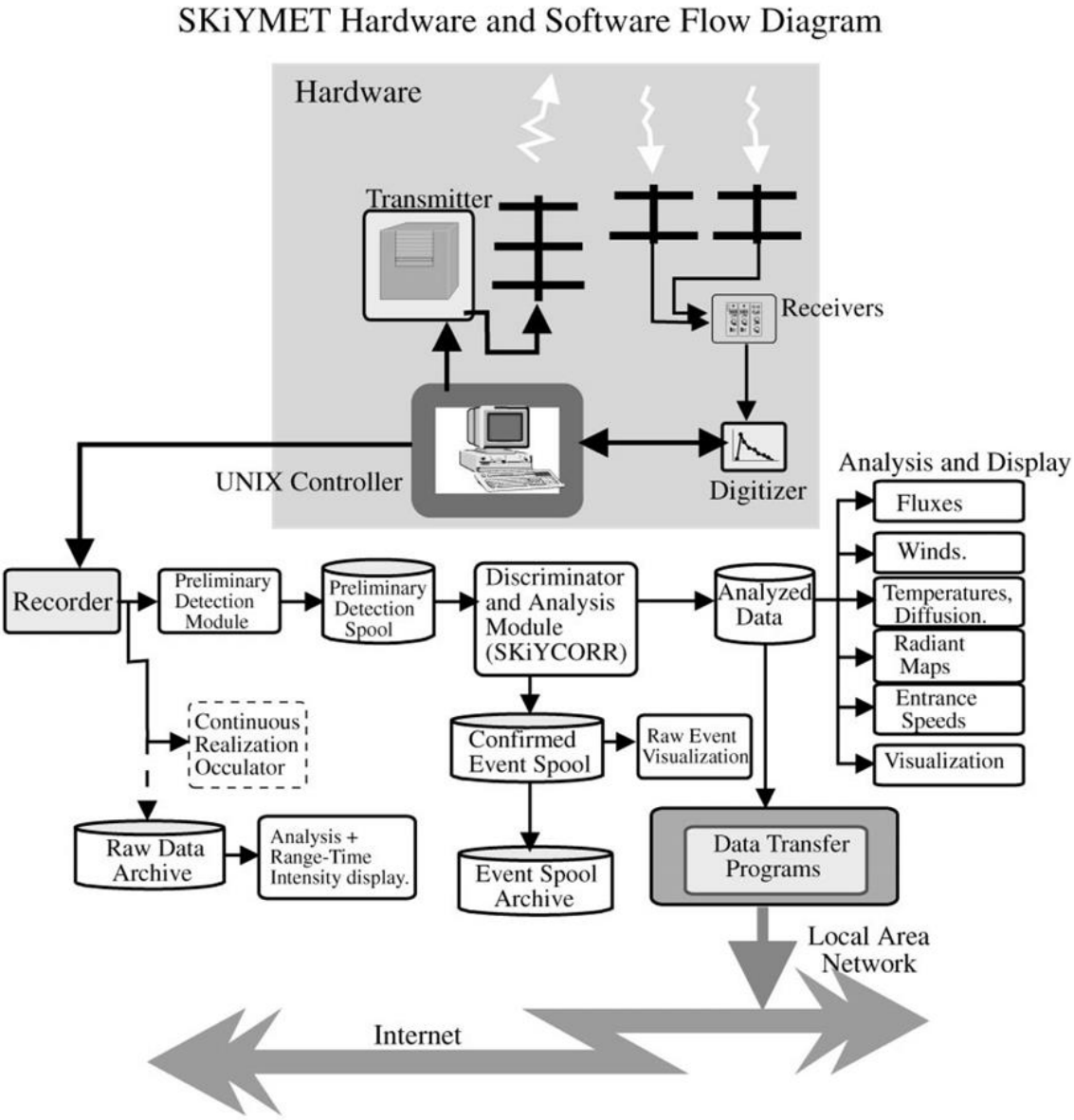

Figure 3.2: Schematics of the complete SKiYMET system showing the interaction between and within various software and hardware components (Hocking et al., 2001a).

The SKiYMET system is also an excellent tool for the study of the dynamics of the mesosphere and lower thermosphere and is capable, for example, of measuring mesospheric winds and mesospheric temperatures that can be derived from underdense meteor diffusion times (Hocking et al., 1997; Hocking 1999; Singer et al., 2003; Hocking et al., 2004; Singer et al., 2004; Hocking, 2004). Moreover, it can be easily

accommodated for the use in space research and space debris studies. The typical radiation pattern of the SKiYMET system is given in Figure 3.3.

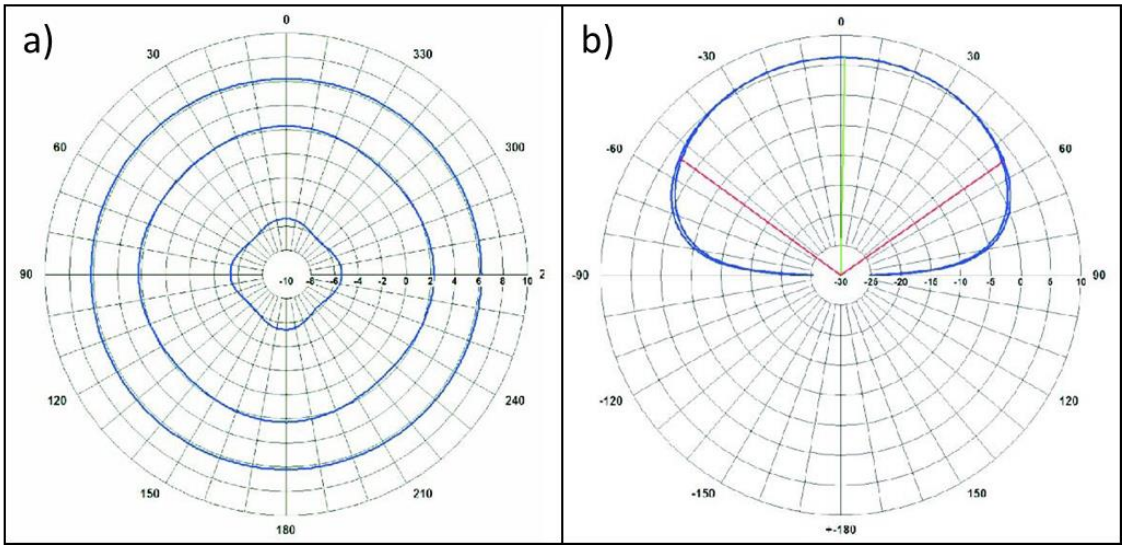

Figure 3.3: Typical radiation pattern of the Yagi-type SKiYMET antenna. **a)** Horizontal radiation pattern with azimuthal cuts at 10°, 60° and 80° zenith angle; **b)** Vertical radiation pattern with zenithal cuts at 0° and 45° azimuth and a 3-dB beam width of 109° (after Singer et al., 2004 and therein courtesy of Genesis Software).

3.2 Sites

The data were collected for a period of several years, defined more specifically later in the text in the data table, from five geographically distinct sites. They are listed according to their latitudinal locale starting from the most northern site (Resolute Bay) and progressing toward the equator.

3.2.1 Resolute Bay, Nunavut

The Resolute Bay radar site has the coordinates 74.7°N and 94.9°W (Figure 3.4). The system operates at 51.5 MHz. A typical live feed from the site is shown in the Figure 3.5 below, where it gives the real time information about the flux, decay time, and wind speed. The complete description of the Resolute Bay radar system and operational

parameters are given by Hocking et al. (2001b). It should be noted that this is the only site that operates at a frequency above 50 MHz.

Figure 3.4: Mars-like landscape at Resolute Bay, Nunavut (Credit: Sukara, R. (2012)).

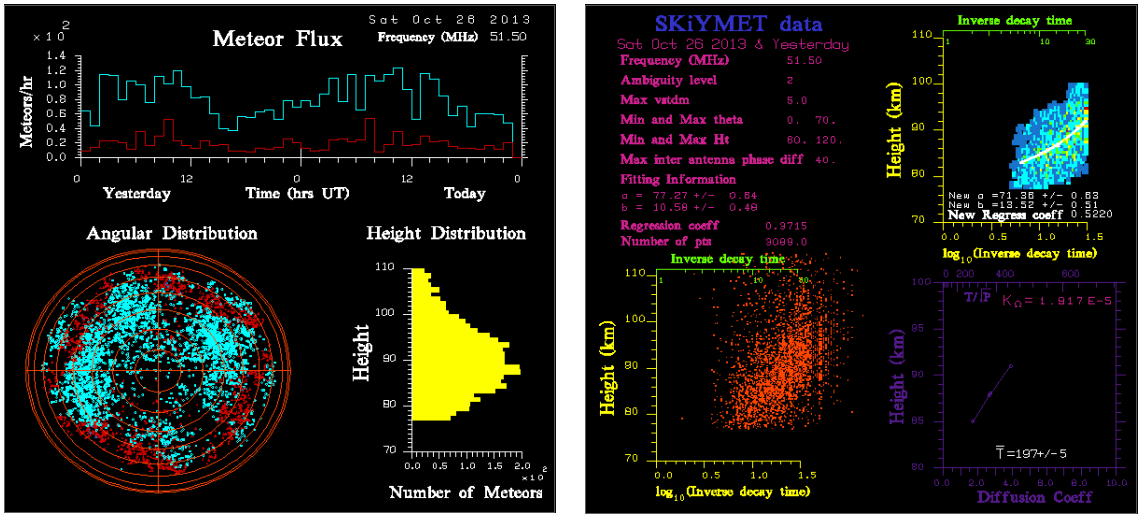

Figure 3.5: Typical real time output from all SKiYMET radar sites offering meteor fluxes, mesospheric temperatures and wind speed (www.physics.uwo.ca/~whocking/axonmet/radarsites).

3.2.2 Yellowknife, NWT

The Yellowknife installation is located at 62.5°N and 114.3°W. The radar operates at **35.6** MHz and is located on the property of the Yellowknife Geophysical Observatory, a facility of Natural Sciences Canada.

3.2.3 CLOVAR, London, ON

The CLOVAR site, located at 43°.07N, 81°.34W, is in the renovation stage at the moment. The data was obtained for the period while in operation in the past. However, when it comes to the meteor files, this site had the scarcest and most sporadic data, because of its intermittent operation in the past, where the system was in experimental mode, being switched between meteor radar and wind profiler (see Hocking, 1997). The details of CLOVAR technical and operational specification were described by Hocking (1997). The operational frequency of this radar is **40.68** MHz.

3.2.4 Socorro, New Mexico

This radar is owned by Mardoc Inc. and leased to the University of Western Ontario. It is located at 34.06°N and 106. 92°S, and it is situated on the property owned by The New Mexico Institute of Mining and Technology. The system operates at **35.24** MHz.

3.2.5 Costa Rica

This is the most southern radar site from which data was collected. It is located at the Santa Cruz campus of the University of Costa Rica. The radar operates at **35.65** MHz, and the latitude and longitude of the site location are 10.29°N 85.59°W.

All radar sites are marked, from north to south in the order discussed in the text, on the Google Earth to illustrate the geographical arrangement of noted locations (Figure 3.6).

Figure 3.6: The locations of the radar sites used in this work are marked on Google Earth in the same order as that described in the text.

3.3 The Hyperthermal Chemistry, the Mechanism and the Role of Ozone in Electron Removal from the Meteor Trail

The "new" model for the mechanism of hyperthermal chemistry and the role of ozone in the removal of electrons in the initial stage of the "hot" meteor trail formation will now be presented. It is the basis of this new and previously ignored mechanism which is subsequently used to calculate ozone density from overdense meteor trails in the MLT region.

However, some fundamentals need to be discussed first. It is important to note as a preamble, that this model is only applicable to overdense events and the physical

interpretation and reasoning for that will become clear shortly. Moreover, it only applies to the expansion of the "hot" meteor trail before the trail temperature decreases below the critical value for the hyperthermal reactions (T > 1500 K, based on the work by Berezhnoy and Borovicka, 2010; Dressler, 2001).

For an unbiased observer, the meteor field as a subset of astronomy has been to a certain extent insulated for the past five to six decades. This statement is not made lightly, but considering somewhat limited collaboration and knowledge exchange with other fields, it is justified. Consider, for example, the atmospheric interactions of the hypervelocity body entering the Earth's atmosphere. It has been known for the past several decades that the flow field of the hypervelocity body (velocity > 7 km s^{-1}) emits radiation resulting from the aerodynamically shock heated air with high intensity in UV spectrum (e.g. Kemp, 1959; Keck et al., 1959; Kivel, 1961; Camm et al., 1961; Strack, 1962; Nerm, 1965; Reis, 1967; Anderson, 1969; Levin et al., 1993; Erdman et al., 1993). However, only a handful of recent meteor research papers have acknowledged the phenomena and its subsequent manifestation during the meteor flight (e.g. Stenbaek-Nielsen and Jenniskens, 2004; Kasuga et al., 2005). It is not clear why the existence of aforementioned phenomena has not been exploited in meteor research, but it should be acknowledged that almost all literature dealing with the ultraviolet radiation from the hypervelocity bodies in the atmosphere was under a domain of defense and military sponsored research. Such circumstances could be reasonably justified to explain why such knowledge has not permeated the wider meteor research field.

The importance of the subject discussed above and its application to meteor research is best viewed through the lenses of meteor chemistry. General sizes of overdense meteors (> 10^{-3} m) and their average velocities (~30 km s^{-1}) are sufficient to form a hydrodynamic interaction layer (or a shock layer) in front of the meteoroid (Popova et al., 2003; Stenbaek-Nielsen and Jenniskens, 2004) which emits strong UV radiation and as a consequence, instantaneously photo dissociates the ambient atmosphere, with special emphasis here given to ozone.

Such a dichotomy between research disciplines is unfortunate when the missed opportunities are considered. For example in 1949, McKinley and Millman discussed UV

radiation from the meteor head but were subsequently ignored. This present knowledge however, can be consequently easily exploited and utilised now.

However, before a discussion of the possible meteor related scientific application of the existence of such phenomena proceeds, another mechanism of ozone destruction must be considered first. In Chapter 2, the high temperatures around a meteor head and wake have been explored (Figure 3.7).

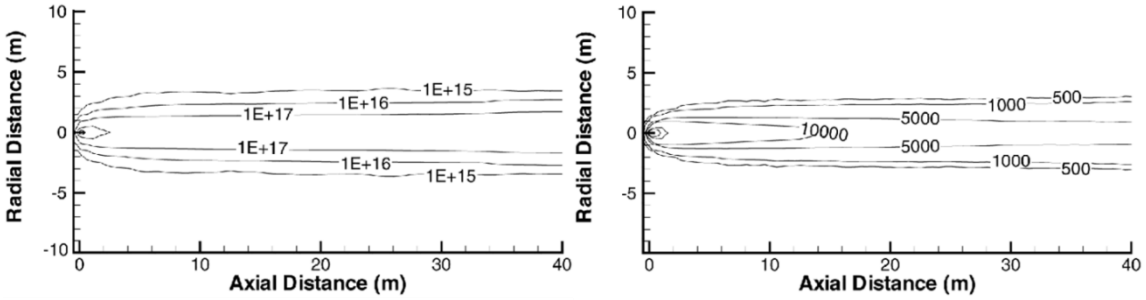

Figure 3.7: Left: Contours of the number density of ablated vapor; Right: Contours of the translational temperatures in the immediate wake of the small overdense Leonid meteor (after Boyd, 1998).

The relevance of the high temperature regime lies in the fact that the thermal shock wave and high temperatures of the meteor trail (up to 10000 K) are sufficient to cause wide thermal decomposition of ozone (Wulf and Tolman, 1927; Pshezhetskiy et al., 1959; Jones and Davidson, 1962; Michael, 1971; Peukert et al., 2013), a rate of which is inversely proportional to pressure. While ozone will easily decompose at temperatures as low as 373 K, at temperatures above 1373 K that process will be very rapid and will produce an excited oxygen singlet.

Thus it is apparent that at least in the case of overdense meteors, there are two primary physical mechanisms of ozone decomposition in a limited volume around the meteor train.

It is important to remark at this point, that underdense meteors in most cases do not develop a shock layer because of their small size and thus are not observed to emit ultraviolet radiation and consequently photo-dissociate ozone. However, it is very likely

that the thermal front propagating orthogonally from the initially formed underdense trail will decompose a small volume of ozone around the meteor trail.

Finally, the question of how the above discussed mechanisms can be exploited to determine ozone from radar observation of overdense meteor trail can be answered.

Consider a simple photo dissociation of ozone under ultraviolet radiation ($\lambda \leq 3100$ Å). The reaction will proceed as follows:

$$O_3 + h\nu \rightarrow O_2\left(a^1\Delta_g\right) + O(1D) \tag{3.1}$$

where $O_2\left(a^1\Delta_g\right)$ is the so called singlet oxygen, which is one energy level up from the ground state and it is highly reactive because of the electron shells arrangement. $O(1D)$ is the first excited state (singlet) of the single atomic oxygen (Fote et al., 1996), and is relatively unstable with a short lifetime. In the MLT region, the photolysis rate is $J_{O3} = 8.1 \cdot 10^{-3}$ and therefore it proceeds almost instantaneously (Khabibrakhmanov et al., 2002). Under the regular equilibrium chemistry regime, a meteoric metal ion (M^+) would react with ozone to form an oxide, which is responsible for the removal of electrons from the expanding meteor trail. However, that is not physically possible in the first stage of the expansion of the "hot" meteor trail, when ions and electrons have large translational energies and the trail temperature is in thousands of Kelvin. Moreover, a meteoric metal ion is unlikely to react with any constituents of the meteor trail as discussed in the previous chapter, and it cannot react collisionaly with ground state or excited atomic oxygen in equilibrium. However, an endothermic reaction between $M^+ \; and \; O_2\left(a^1\Delta_g\right)$ occurs in the initial post-adiabatic expansion of meteor train (time scale < 0.1 second) and depends on thermodynamic and mixing considerations (Dressler, 2001). This is indeed high energy hyperthermal chemistry which occurs very rapidly that was either not considered in the past or was just not known to exist. It is interesting to observe that at least to the best knowledge of the author here, and prior to this work, there are only two published papers (Menees and Park, 1976; Park and Menees, 1978) and one book chapter (Dressler, 2001) dealing with the problem of meteor train hyperthermal chemistry either directly or indirectly.

An important detail must be emphasized at this point. Meteoric metal ions have low ionization potentials and can be ionized more efficiently in high velocity collisions relative to the main atmospheric constituents such as N_2 and O_2. Moreover, another important aspect needs to be highlighted, which is that no neutrals (i.e. O) have been observed in the immediate wake of the meteor having more than 4 eV in excitation energies (Bronshten, 1983). This implies that neutrals such as O in the immediate meteor spectrum must have formed through the following reaction (dissociative recombination) that was already seen earlier in the text:

$$MO^+ + e \rightarrow M + O \tag{3.2}$$

Most reactive collisions in meteor trail occur below 20 eV (Dressler, 2001). The important hyperthermal chemical reaction according to Dressler (2001) in the initially formed meteor trail, which needs to take place before the reaction above can proceed, is given below:

$$M^+ + O_2 \rightarrow MO^+ + O \tag{3.3}$$

For the case when M = Fe^+ or Mg^+ in the last equation, observational evidence indicates that under hyperthermal conditions, subsequent reactions proceed at the collisional rate (Ferguson and Fehsenfeld, 1968). This agrees well with the observed trend in data in this thesis. However, there is a slight problem with this approach. A key point to observe is that for the case of overdense meteors, the temperature field and UV radiation in the vicinity of the trail are sufficiently strong to cause either decomposition or ionization of neutral oxygen in the narrow volume around meteor train. Consequently, the resulting products (O_2^+, O) cannot react with M+ in the immediate vicinity of the meteor train. The only available agent that can react more aggressively with a metal ion under hyperthermal conditions is $O_2(a^1\Delta_g)$ which results from either photo dissociation or thermal decomposition of ozone. Thus the full circle has been completed, and the fast and time limited hyperthermal chemistry regime responsible for the removal of electron from the meteor trail has been identified with confidence.

From the experimental observations it is known, in general, that metal ion species will undergo collision controlled reactions with oxygen forming an oxide, below 100 eV in

collisional energies (Rutherford and Vroom, 1976). The threshold collisional energy for Mg reaction with O_2 is 5.12 eV, where reaction cross section will depend on the collisional energy (Figure 3.8).

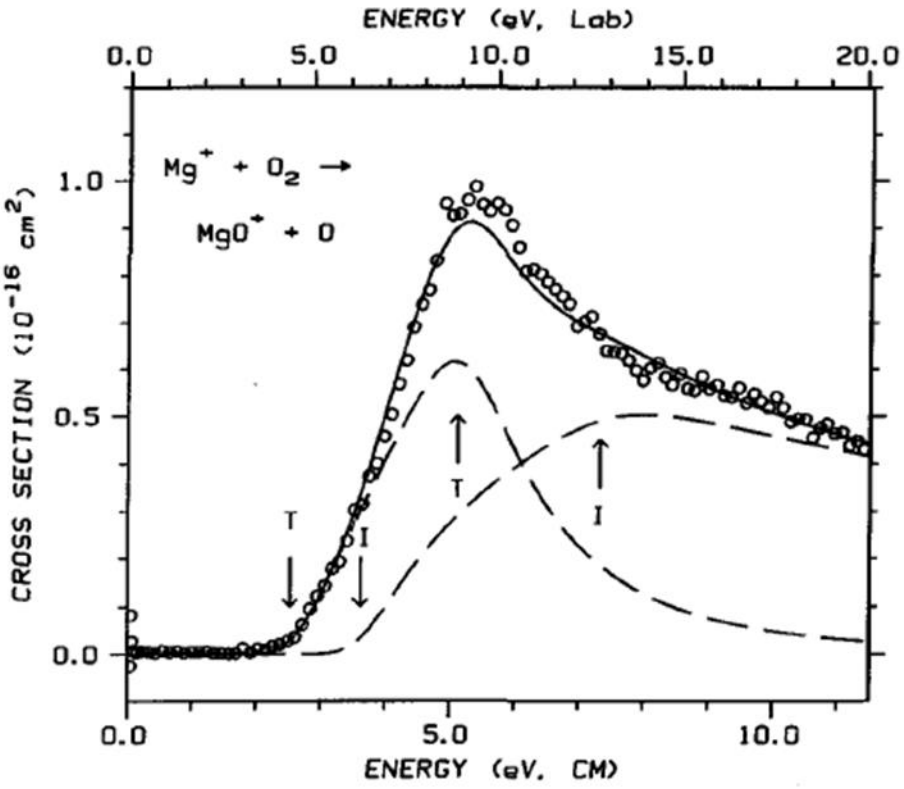

Figure 3.8: The collision energy dependence of the $Mg^+ + O_2 \rightarrow MgO^+ + O$ reaction cross section which is a function of kinetic energy in the center-of-mass frame (CM) (lower x axis) and laboratory frame (upper x axis). Note that a cross section σ (used to define the probability of interaction between particles) is a hypothetical area measure around the target atom and if another particle crosses that surface there will be some interaction. Arrows pointing down indicate the thresholds for thermodynamic and impulsive reactivity (labeled ”T” and ”I”, respectively), and arrows pointing up indicate the thermodynamic and impulsive onsets of reaction $M^+ + O_2 \rightarrow M^+ + O + O$:(- - -), models of the thermodynamic and impulsive reactivity, convoluted over the experimental kinetic energy distribution; (-), the sum of these models (Dressler, 2001 and reference therein).

Threshold energies for $Fe^+ + O_2 \rightarrow FeO^+ + O$ are slightly higher than for $Mg^+ + O_2 \rightarrow MgO^+ + O$ (Armentrout et al., 1982). Therefore, it is reasonable to expect the similar or

smaller threshold energies for $O_2(a^1\Delta_g)$ relative to its high reactivity. Considering that meteor metal ions possess up to several hundreds of eV in translational energy, which is a function of meteor velocity, the reaction will take place within the first several collisions. The time scale for the reactions of Mg^+ and Fe^+ may take up to 0.1 s relative to the meteor trail temperature (Berezhnoy and Borovicka, 2010). To further constrain time scales of the considered reactions, one must also consider electron thermalization time discussed in Chapter 2 that may take also up to about 0.1 s depending on the altitude (Baggaley and Webb, 1977). The reason for such electron thermalization dependency may be understood in terms those high energy electrons are not likely to participate in the reaction below:

$$MO^+ + e \rightarrow M + O \tag{3.4}$$

Therefore, the expected time scale at which hyperthermaly formed oxides engage in removal of ambipolarly diffusing electrons from the boundary of the meteor trail and the ambient atmosphere should be in the range of 0.1 second or less, which is in line with the observations obtained in this work. Moreover, the observational data indicates that meteor trail cools more slowly that it was theoretically expected (Jenniskens and Stenbaek-Nielsen, 2004).

What has been left out of the discussion so far in this section is the application to the ozone measurement using backscatter radar observations of overdense meteors. To address that, consider a meteor trail immediately after instantaneous adiabatic formation at t = 0 and r = r_0 (Figure 3.9).

The ozone in the ambient region of the atmosphere has been photo dissociated and thermally decomposed in some limited volume around trail (Figure 3.10), with the highest concentration of the $O_2(a^1\Delta_g)$ at the boundary of the initial radius, and decreasing likely at a rate slower than exponential.

Therefore, the main region of interest is the meteor trail boundary. As the ambipolar diffusion proceeds to expand the meteor trail, in some very small time increment Δt, the amount of ions will diffuse under ambipolar diffusion at the boundary and rapidly react with $O_2(a^1\Delta_g)$. The electrons which have assumed the Gaussian distribution within the

trail will also diffuse through the boundary under ambipolar diffusion and will be rapidly consumed on the other side by the maximum concentration of newly formed ionic metal oxide. Thus, if one can solve for the number of electrons removed from the boundary region by the ionic metal oxide, then by extension it is possible to determine ozone density. The validation of this theory will be tested in Chapters 4.

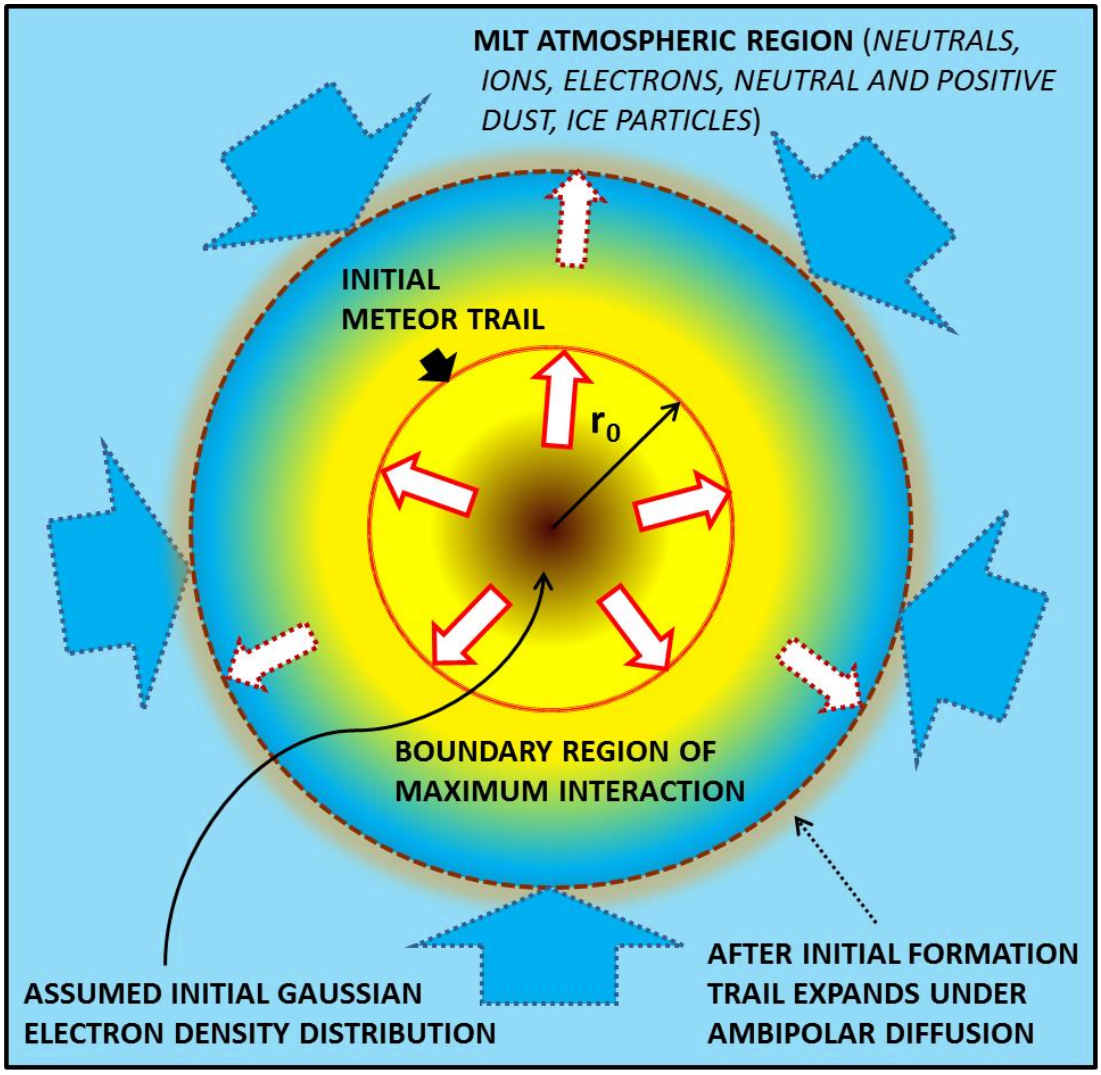

Figure 3.9: The cross-section of the meteor trail depicting the postadiabatic expansion trail with initial radius r_0 (inner circle), and outer circle depicts expansion driven under ambipolar diffusion. A point to note here is that the region of the maximum hyperthermal chemistry (formation of ionic metal oxides) surrounds the meteor trail boundary at or in

immediate vicinity of r_0 (depicted through the brightest yellow colour). Moreover, the assumed distribution of electron in the meteor train is Gaussian.

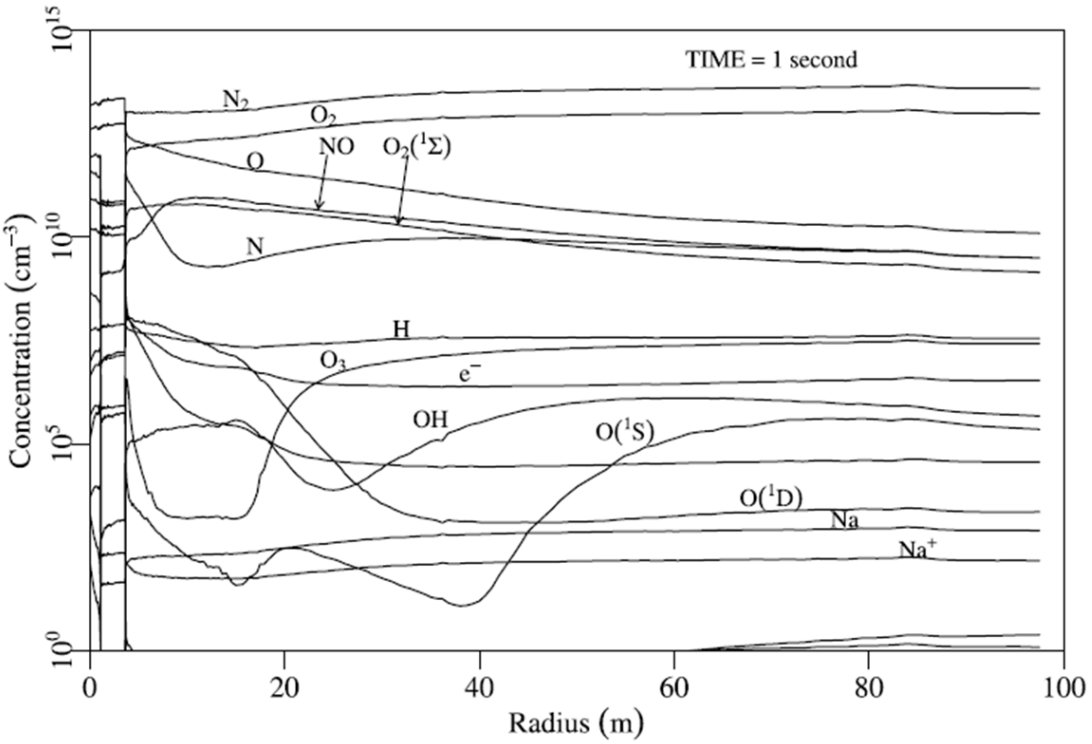

Figure 3.10: Computed radial profiles of 19 atmospheric constituents 1 second after ablation, for the 526 g Leonid object. Note that the large mass of this fire ball can be easily scaled down to average masses of overdense meteors. A particular attention should be directed at the concentration of O_3, O1D and $O_2(^1\sum)$. Note that $O_2(^1\sum)$ is the same as the notation for the $O_2(a^1\Delta_g)$ in this work. The inverse proportionality between O_3 and O(1D) for example is in line with what is proposed here (Zinn and Drummond, 2005).

3.4 The Modified Diffusion Equation, Solution, Parameters and Application to Ozone Density Calculation

Resolving the behaviour of meteor echoes duration, inconsistency in ambipolar diffusion and possible effects of hyperthermal chemistry, especially on overdense meteors (Figure 3.11) is not a trivial task. Since the early days, effects of chemical processes on echo duration had been known (Davies et al., 1959; Greenhow and Hall, 1962), albeit not completely understood. In addition, the peculiar statistical behaviour and trend in the logarithmic plot of the cumulative number of meteor echoes and echo duration times was

experimentally observed and understood in cases where echoes could be detected for a long period of time (i.e. forward scatter radar). That statistical trend showing the change in slope between underdense and overdense meteors had been related to meteoroid mass distribution (Weiss, 1961; McIntosh, 1966) and meteor electron line density (Manning, 1962, 1963). Moreover, Manning (1962) theoretically treated the subject extensively and showed that the slopes will change with changing heights and meteor electron densities.

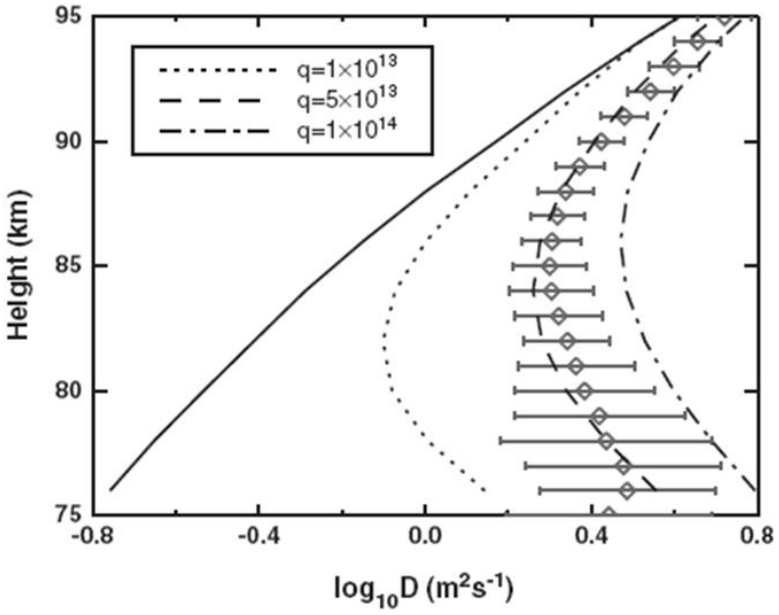

Figure 3.11: Observed daytime diffusion coefficient profile for January 2012 at King Sejong Station, Antarctica, taken from Aura EOS MLS satellite instrument (solid line) and the 33 MHz meteor radar (error bars). Numerical simulations for different initial electron line densities are shown for comparison (broken lines) (Lee at al. 2013).

More recent examples of logarithmic plots of cumulative number of detected meteors vs. meteor radar echo duration times obtained from the forward scatter radar can be seen in Ye et al. (2013) published by Dr. Peter Brown's Group at Western University.

When the logarithmic plots of the cumulative number of events vs. echo duration times were initially plotted for the backscatter radar data set used here, the obtained results were rather surprising. The well-known behaviour of the slopes (Figure 3.12) on the aforementioned plot was also observed in the past (e.g. Kaiser, 1953) and more recently practically applied by Jones et al. (1990). Jones et al. (1990) were able to calculate ozone

concentration from the duration time on a logarithmic plot using the transition from underdense to overdense regimes, as discussed in the previous chapter of this thesis. However, this type of behaviour was only thought to occur in data that were obtained from forward scatter radars, and where the effect of equilibrium chemistry had enough time to take place and is consequently observed (Baggaley, 1979). This type of thermal equilibrium chemistry, where ozone reacts with a metal ion to form oxide, which in turn consumes an electron, was discussed in detail by Poole and Nicholson (1975) and Baggaley (1979).

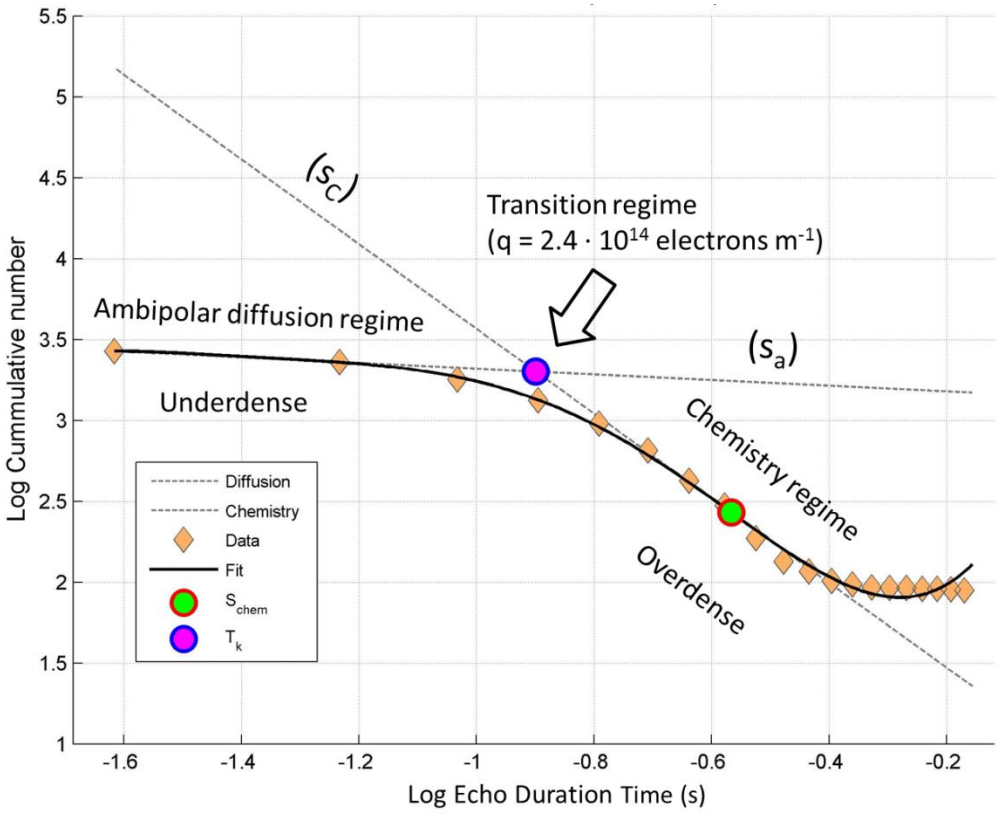

Figure 3.12: The log-log plot of the cumulative number of events versus echo duration times. The plot shows well know behaviour of slopes of ambipolar diffusion controlling underdense trails and chemistry regime, which in turn controls the removal of electrons from overdense meteor trails. Note, however, that the behaviour of the slope of chemistry was thought to apply only to the spontaneous and exothermic chemical reactions between ozone and meteor metallic ions, where ionic oxide (product) is responsible for the removal of electrons from the meteor trail. The transition region between underdense and overdense meteors marked by the arrow, corresponds to the electron line density of $2.4 \cdot 10^{14}$ electrons m^{-1}.

First, the treatment introduced by Jones et al. (1990) and discussed in Chapter 2 cannot be utilized in the case here as the time scale is too short to apply the rate coefficient for the reaction ($\boldsymbol{MO^+ + e}$) in calculation of ozone density. Also, in the case of hyperthermal chemistry, equilibrium rate reactions do not apply. The solution can be sought in earlier literature (e.g. Manning, 1962, 1963; McIntosh, 1966) that developed the theoretical treatment and interpretation of the behaviour change in slopes between what today can be called the diffusion and chemistry regimes. These authors preferred to use the term "attachment" instead of chemistry process.

Applying the complicated differentiations of logarithmic functions, as done by Manning (1962) to account for the observed slope changes, which would not be usable anyway at this stage of research, it is reasonable, based on the existing accumulated knowledge of ambipolar diffusion and the effects of chemistry, to simply relate experimentally obtained values of diffusion and chemistry regime slopes. This approach can be justified knowing that ambipolar diffusion is a function of temperature and pressure (Hocking, 1997), and chemistry is a function of atmospheric density, composition and meteor electron line density. Because the theoretical and experimental values of ambipolar diffusion are widely known, the goal is to relate the role of chemistry to already known parameters.

First however, the full diffusion equation for the total loss of electrons from the meteor train can be written as follows:

$$\frac{dn_e(r,t)}{dt} = D_a \frac{d^2 n_e}{dx^2} - f(C_{NE}) - f(C_E) - f(A_D) - f(E_D) + f(e_E) \tag{3.5}$$

On the right hand side, the first term represents the loss due to ambipolar diffusion, the second ($f(C_{NE})$) and third ($f(C_E)$) terms are due to the loss resulting from non-equilibrium and thermal equilibrium chemical processes, where the next two terms ($f(A_D)$ and $f(E_D)$) are the loss resulting from neutral and positive dust absorption and eddy and turbulent diffusion. The last term $f(e_E)$ describes the linear production of electrons in that region of the atmosphere. The loss due to neutral and positively charged dust was discussed by Havnes and Sigernes (2005) and Younger et al. (2008), while Hall (2002) treated effects of the eddy diffusion and turbulence. The last four terms on the right can be neglected, as they are time dependent and have slow reaction rates so they

will not take place immediately upon the formation of the initial radius. At this point, suppose that the initial electron loss from a non-equilibrium process is solely related to ozone. Now, the goal is to find the total number of electrons lost to non-equilibrium process with the assumption that it will correspond to the ozone density at a particular height. If the distribution of electrons in the meteor train is assumed to be initially Gaussian, then accordingly one should consider Figure 3.13 below. The figure schematically represents the expansion of the initially formed meteor trail with an assumed Gaussian electron density distribution and subsequent onset of hyperthermal chemical reactions. The temporal evolution of the electron density distribution is denoted by t_0, t_1 and t_2 respectively. The growth of the trail radius as a function of time is denoted by $r_0 + (4\pi D t_1)^{0.5}$ at t_1 and $r_0 + (4\pi D t_2)^{0.5}$ at time t_2. Consider now the total number of electrons that remains in the boundary region, just beyond the initial radius, due to ambipolar diffusion and removal as a result of hyperthermal chemistry. Then equation (3.5) can be rewritten without extra terms:

$$\frac{dn_e(r,t)}{dt} = D_a \frac{d^2 n_e}{dx^2} - f(C_{NE}) \tag{3.6}$$

Here, the goal is to solve for the total number of electrons consumed as a result of the hyperthermal chemistry. However, this equation is nonlinear and it is a classical form of reaction diffusion equation with no analytical solution (see for example Smoller, 1983; Fort and Mendez, 2002; Chen et al., 2006; Isern and Fort, 2009; Permikin and Zverev, 2013). Moreover, considering that the parameters of the hyperthermal chemistry are not known in this case, the new approach is needed to isolate the contribution of this regime. From looking at Figure 3.13, it is reasonable to assume that the number of diffused and chemically consumed electrons at the r_0 boundary is the same, at least in the initial post adiabatic, “hot” meteor trail expansion.

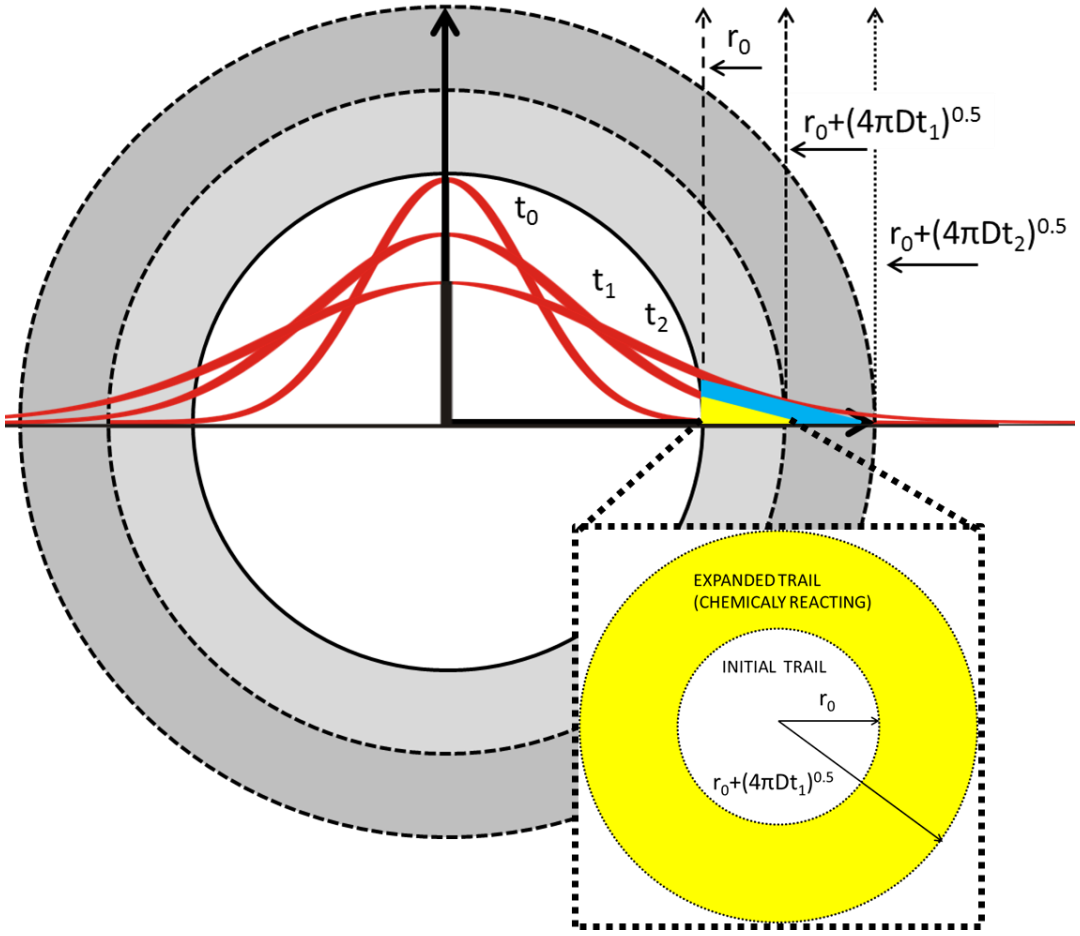

Figure 3.13: Schematics of a meteor train expansion with assumed initial Gaussian electron density distribution, under the effects of ambipolar diffusion and (inset) pictorial representation of the outlined boundary region where ambipolarly diffused electrons are affected by hyperthermal chemistry process that takes place in that area.

Therefore, expressed mathematically for the boundary region, the total number of electrons diffused through the boundary is the same as the number of electrons consumed by hyperthermal chemistry on the other side of the boundary, is written as:

$$\left[\frac{d^2 n_e}{dx^2}\right]_{\substack{ambipolar\ diffusion \\ throught\ the\ boundary}} = f(C_{NE}) = \left[\frac{d^2 n_e}{dx^2}\right]_{\substack{hyperthermaly\ removed\ just \\ outside\ of\ the\ boundary}} \tag{3.7}$$

This is a critical observation which allows treatment of the contribution of hyperthermal chemistry (in terms of calculations) to be considered in the same manner as the mechanism of physical diffusion (or in this case here, ambipolar diffusion).

It must be emphasized at this moment that the hyperthermal chemistry will consume the same number of electrons as removed by ambipolar diffusion, just at a much faster rate. Accordingly, during a very short time ($t < 1$ s), following the adiabatic formation of the meteor trail with initial radius r_0, that fast rate of the removal of meteor trail electrons by hyperthermal chemistry just outside of r_0, can be considered in terms of the hyperthermal chemistry diffusion coefficient, which can be now defined as D_C.

At this point, the impasse would be reached, at least in terms of further calculation, that cannot be overcome through any further simplification, were it not for the rather obscure theoretical treatment of the relationship between slope values of ambipolar and chemistry regime, derived by Manning (1962, 1963), and by extension used here in modified form. That relationship relates the ambipolar diffusion coefficient and the chemical removal of electrons to the exponential power of slopes of the ambipolar diffusion and chemistry regime shown in Figure 3.12, and can be simplified and expressed in the following way:

$$\frac{D_a}{D_C} = \left(\frac{s_a}{s_C}\right)^p \tag{3.8}$$

where s_a and s_C are the slopes of the ambipolar and chemistry regimes, respectively. For the purpose of the investigation here, the value of the exponent p is taken to be $p \approx 1$.

Now it is possible to define the coefficient of the "hyperthermal chemistry diffusion" D_C, in terms of the ambipolar diffusion coefficient and the slopes of the diffusion and chemistry regimes which are already known quantities:

$$D_C = \frac{D_a s_C}{s_a} \tag{3.9}$$

The advantage of the above approach is the elimination of the solutions in terms of chemical reaction rate constants, which are not known in the first place and the chemical removal of electrons is treated just like another form of diffusion calculation with the

known coefficient D_C, that has been shown in this study to vary with height. Therefore, the already familiar diffusion equation can be written as:

$$\frac{\partial n_{eC}(r,t)}{\partial t} = D_C \frac{\partial^2 n_{eC}}{\partial x^2} \tag{3.10}$$

This equation can now be rewritten in its proper cylindrical form that describes the meteor initial post-adiabatic train diffusion of electrons:

$$\frac{\partial n_{eC}(r,t)}{\partial t} = D_C \left[\frac{\partial^2 n_{eC}}{\partial r^2} + \frac{1}{r}\left(\frac{\partial n_{eC}}{\partial r}\right)\right] \tag{3.11}$$

The solution to this equation can be written in classical form (Crank, 1975; Baggaley in ch. 6 of Murad and Williams, 2002):

$$n(r,t) = \frac{\alpha}{\pi(r_0^2 + 4D_C t)} exp\left[\frac{-(r^2)}{r_0^2 + 4D_C t}\right] \tag{3.12}$$

where α is the electron line density and $r^2 = (r_0^2 + 4D_a t)$. The physical reason for defining r^2 in terms of ambipolar diffusion is rather simple. The goal is to define the number of hyperthermally removed electrons within the volume of the meteor train defined by the boundary of initial radius and the small incremental increase in meteor trail radius expanded under the influence of ambipolar diffusion. Therefore, the final expression for the number of removed electrons under the influence of hyperthermal chemistry in the initial post-adiabatic expanding meteor train is:

$$n(r,t) = \frac{\alpha}{\pi(r_0^2 + 4D_C t)} exp\left[\frac{-(r_0^2 + 4D_a t)}{r_0^2 + 4D_C t}\right] \tag{3.13}$$

It must be reiterated again that the hypothesis proposed here is that by solving for the number of electrons removed as a consequence of hyperthermal chemistry, it is possible to solve for the ozone density as the agent considered to be responsible for the initial chemical reactions with meteoric metal ion.

The laboratory value of ambipolar diffusion (Jones and Jones, 1990) is used in the calculations here, as the slope of the diffusion regime experimentally obtained in this work will appropriately correct the value of theoretical ambipolar diffusion for the temperature and pressure variations. If a direct measured value of ambipolar diffusion

determined from the meteor radar sites was used here, then it would be impossible to properly calculate the value of chemical diffusion coefficient as the values would be skewed (corrected for atmospheric temperature and pressure twice).

Furthermore, the analytical treatment for evaluation of number of electrons removed under hyperthermal chemistry is assumed not to have the same level of accuracy as the numerical approach in solving full reaction diffusion equation. Consequently that will be the focus of future studies.

However, as discussed in Chapter 2, the electron line density will not be constant, and will vary with the height of maximum ionization. To insure consistency and the quality of results, two approaches were taken to calculate the ionization and thus electron density as a function of height. The first one is based on work by Herlofson (1948) which was further developed by Kaiser (1953). The second approach is based on the empirical treatment by Kharchenko (2012).

Herlofson's (1948) and Kaser's (1953) treatment is given first, however as it will be seen later from the results, both approaches give almost the same numerical values of the adjusted electron line density. The equation for the electron line density along the ionization curve for the overdense meteors can be written as:

$$q(I) = \frac{9}{4} q_{max} \frac{\rho}{\rho_{max}} \left(1 - \frac{1}{3} \frac{\rho}{\rho_{max}}\right)^2 \tag{3.14}$$

where ρ and ρ_{max} are atmospheric densities at ionization height and at the height of the maximum ionization, respectively. Their ratio is expressed in terms of scale height *H* and atmospheric height *h* as:

$$\frac{\rho}{\rho_{max}} = exp\left[-\left(\frac{h - h_{max}}{H}\right)\right] \tag{3.15}$$

where h_{max} is the height of the maximum ionization. The electron density and the maximum electron density are denoted by q and q_{max} respectively.

Note that the form of the same equation, just with a different notation for electron line density was used in overdense meteors section in Chapter 2, for the preservation of historical accuracy. Here, however, the contemporary notation is deployed. Therefore,

equation (3.13) is modified to account for the variable electron line density as a function of ionization curve, and the expression is rewritten as:

$$n(r,t) = \frac{\alpha(I)}{\pi(r_0^2 + 4D_C t)} exp\left[\frac{-(r_0^2 + 4D_a t)}{r_0^2 + 4D_c t}\right] \tag{3.16}$$

where the determination of the maximum ionization is trivial, and will be discussed shortly with the choice of the numerical value for the electron line density.

Kharchenko's (2012) empirical approach is to some extent more exhaustive, and it allows for employment of different masses and velocities of the meteor. The variation of the electron line density is written as:

$$q(h) = 4.03 \cdot 10^{14} \frac{m(v - 8.15)^3}{H} cos\gamma \cdot z(t) \tag{3.17}$$

where m and v are the mass and velocity of the meteoroid during the entry into meteor region, respectively. The limiting function z(t) which in its initial appearance resembles Herlofson's formula, is aimed at constraining the ionization curve, and it is stated as:

$$z(t) = \frac{9}{4} e^{-t}\left(1 - \frac{1}{3} e^{-t}\right) \quad when - ln3 \leq t \leq 1.7 \tag{3.18}$$

else $z(t) = 0$, and *t* is defined as:

$$t = \frac{(h - h_{max})}{H} \tag{3.19}$$

Where h is the atmospheric height and h_{max} is the height with the maximum linear electron density. H is the reduced atmospheric height, defined as:

$$H = 6.4 + 0.09(h - 95) \tag{3.20}$$

The height of maximum ionization is given as:

$$h_{max} = 47.4 + 12.76\ lnv \tag{3.21}$$

Finally, the maximum electron line density can be written as follows:

$$q_{max} = 4.03 \cdot 10^{14} \frac{m(v - 8.15)^3}{H} \tag{3.22}$$

3.5 Determinations of the Experimental Height of the Maximum Ionization

The height of maximum ionization was chosen as the height of maximum number of meteors (Figure 3.14). This corresponds well to the one calculated from Kharchenko's (2012) equation. The height of the maximum ionization corresponds to the height with maximum electron line density which has been determined by selecting the electron line density of the most common overdense meteor echoes (Manning, 1962).

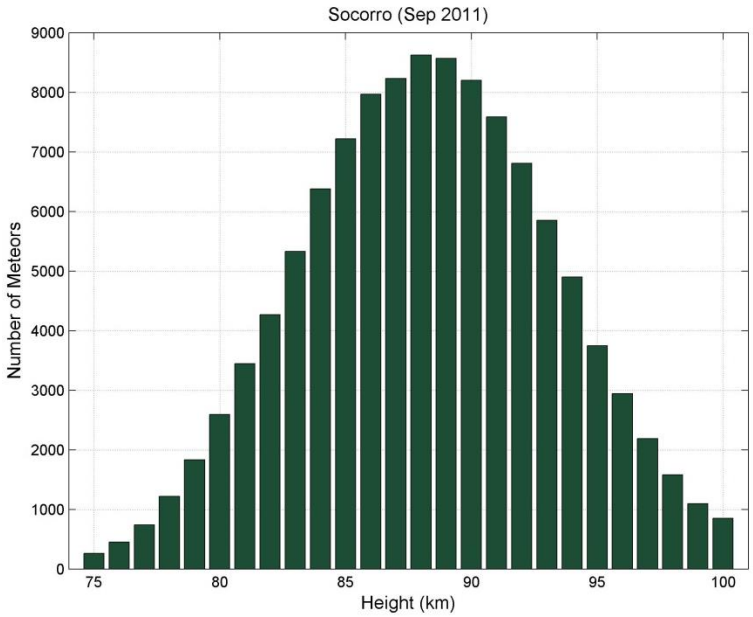

Figure 3.14: Number of observed meteor echoes as a function of altitude (September, 2011, Socorro).

If the transitional value for electron density is taken to be $2.4 \cdot 10^{14}$ electrons m^{-1} (McKinley, 1961) and a typical metal cylinder behaviour for overdense meteors starts at 10^{16} electrons m^{-1} (Poulter and Baggaley, 1977, 1978), then it is reasonable to take the most common value of electron density somewhere in the middle. Cervera and Elford (2000) state that the meteor does not become fully overdense unless the electron line density is at least 10^{15} electrons m^{-1}. In addition to the above, a careful consideration of published meteor masses, visual magnitudes and their interpretation in terms of electron line density (Sugar, 1964) led to the selected value used throughout this thesis of $5.5 \cdot 10^{15}$ electrons m^{-1}. This is the mean value between various estimates of the transitional

electron line density and the true overdense meteor behaviour and its electron line density. Moreover, this value agrees well with the inferred sizes and masses of overdense events and agrees well for instance with the value for overdense meteor electron line densities published by Pallinen-Wannberg and Wannberg (1994). However, the author acknowledges that this value can be further refined in statistical terms, by relying on additional careful observational radio and visual data from overdense meteors.

3.6 Initial Radius and Hyperthermal Chemistry Duration Time

The most comprehensive treatment of the initial radius of visual and overdense meteors had been performed by Baggaley and Fisher (1980). They had found that the initial radius of overdense meteors is proportional to the atmospheric density in the following way: $r_i \propto \rho^{-0.63}$ with the exponent uncertainty of 10%. Thus, the values of initial radius in this work are taken based on the results obtained by Baggaley and Fisher (1980) and also tabulated in Ceplecha et al. (1998).

The determination of the hyperthermal chemistry duration time is different from the previous treatment (Jones et al., 1990). Initial consideration was given to the separation of the chemistry regime duration times identified from the logarithmic plots of cumulative number of meteor echoes versus echo duration times. The observed trend in chemistry duration times can be summarized as follows: between 75 and 80 km, the hyperthermal chemistry time increases sharply, after which it gets tapered around 80 km and has almost an exponential decrease. That type of behaviour is contrary to the previously observed and expected height dependent chemistry duration times (e.g. Baggaley, 1979), as the time for the chemical processes is supposed to increase as a function of the reduced atmospheric pressure and density. To overcome that contradiction, the combined duration times obtained from the logarithmic plots of cumulative number of events vs. echo duration times were used for each specific height in calculations here. The Matlab code was appropriately modified to be able to run the calculations with total duration times as a function of height, and also to accommodate the runs with mean (constant) time durations, while at the same time accounting for uncertainties. That aspect will be discussed in the next two sections. It should be noted that the mean echo duration time between 75 and 100 km is ~0.2 seconds. However, for

the future work that might expand on what was learned here, it would be interesting to utilize chemistry duration times measured at the point of the chemistry slope determination and examine the implications for the calculated values.

3.7 Comments and Considerations on Matlab Processing Code

The summary of a rather cumbersome computation procedure, including the initial approaches and considerations, is presented here. The goal was to define and quantify the ambipolar diffusion and chemistry diffusion regimes, determine the slope of each diffusion regime, determine the ambipolar diffusion duration time, calculate the transition time (intercept between ambipolar and chemistry diffusion regimes), and finally determine the combined duration times and use all this information to find the concentration of ozone as a function of height between 75 km and 100 km. Three main Matlab programs were made to process data and perform the analysis discussed in this chapter. These programs were designed to execute specific computations for the following steps: (i) processing raw data, (ii) initial data analysis and preparation for O_3 concentration calculation, and (iii) determination of O_3 concentration and measurement error. Overall, more than 10^6 meteor events were individually processed for the five radar sites.

3.7.1 Processing raw data

Raw data are stored in text format. The quantities of interest in this study were the date, height, duration time (τ) and ambiguity, where the latter is a measure of certainty whether a given meteor echo is a properly located (ambiguity = 1 means the data are unambiguous and aliasing is eliminated). On a side note, it should be mentioned that aliasing arises from the use of the pulsed repetition frequency (PRF), however, it is generally easy to deal with (see Hocking et al., 1997). A Matlab program was written to import all raw files, select and save only meteors with unambiguous location for further processing and then separate events by month and year. In total, 345 months of data of were processed.

3.7.2 Initial Processing

All events confined to the region between 75 km and 100 km were selected and divided into height increments of 1 km. The total number of meteors per each height increment

was produced for statistical purposes. The echo duration time cutoff (τ_{cutoff}), which is mainly driven by the radar operational frequency, was set at 0.4 seconds for Resolute Bay and 0.7 seconds for all other sites (Figure 3.15).

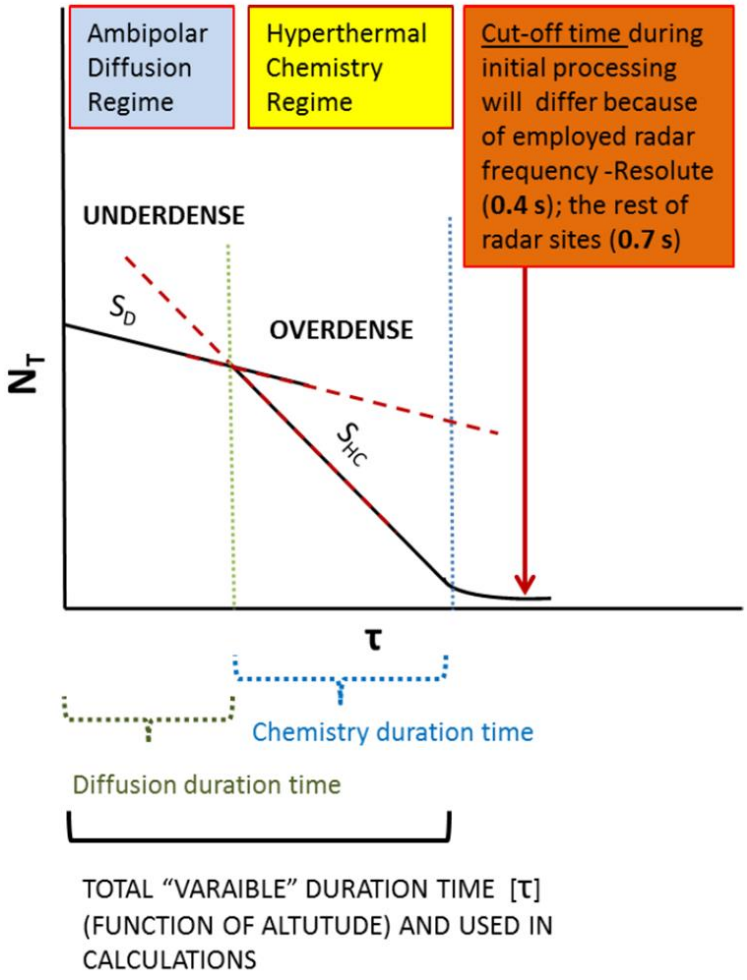

Figure 3.15: The schematic plot of the observed ambipolar and hyperthermal chemistry regimes outlining their duration times, slopes, and the cut-off time selection criteria for the Resolute Bay radar and the other radar sites.

This means that all events with the echo duration time $\tau < \tau_{cutoff}$ were included in further processing, while those events with echo durations $\geq \tau_{cutoff}$ were discarded. It is useful to remember at this point that the wavelength of the Resolute Bay system is about 6 meters where for all other sites is about 10 m. At this point, a meteor echo duration time

distribution histogram for each height increment was generated (Figure 3.16), along with the number of meteors per given height increment.

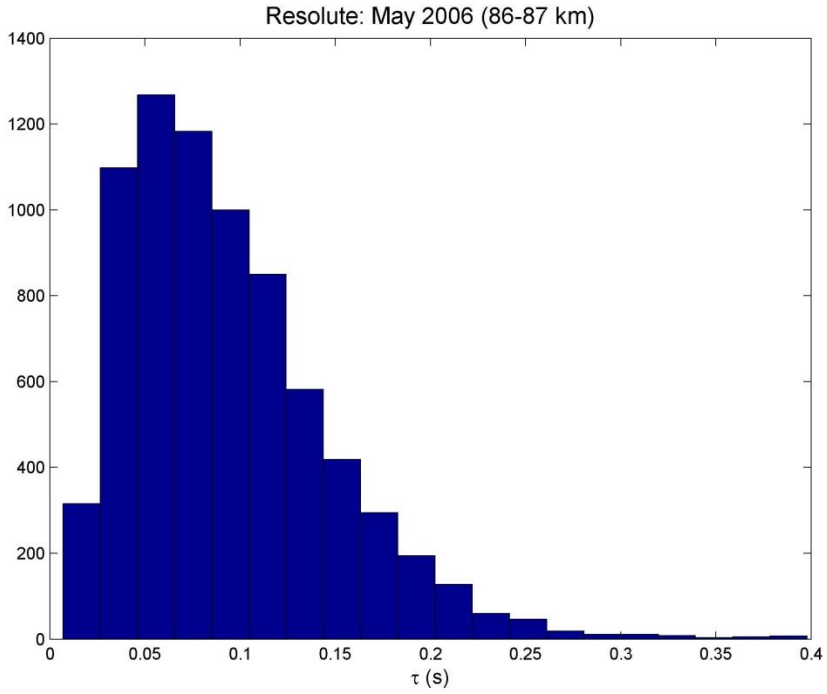

Figure 3.16: Histogram of the number of events corresponding to the specific duration times for the Resolute Bay, May, 2006, for height between 86 and 87 km.

The next step was to obtain the cumulative number of meteors for each height range, binned over a select number of bins in log-log space. Several bin numbers (10 – 50) were experimented with first, before making the final selection of 20 (Figure 3.17). A number of 10 bins was too small, while a large number of bins (> 20) was not suitable either. First, there was not enough data to spread it over 30 or more bins. This unnecessarily introduced a 'tail' effect when the data drops down to very small cumulative numbers. Second, spreading the data over a number of points that is too large 'smears' out the ambipolar diffusion slope and introduces bias. In this case a bias would be introduced since the predetermined number of points for determination of ambipolar diffusion slope would not produce consistent results in the case of higher resolution binning. While experimentally determined to work the best, it is not completely clear at the moment why 20 bins gives the best and most reliable performance across the board. That being said, it

is suspected that in the case when a higher density of data is available, higher binning might produce equally consistent result.

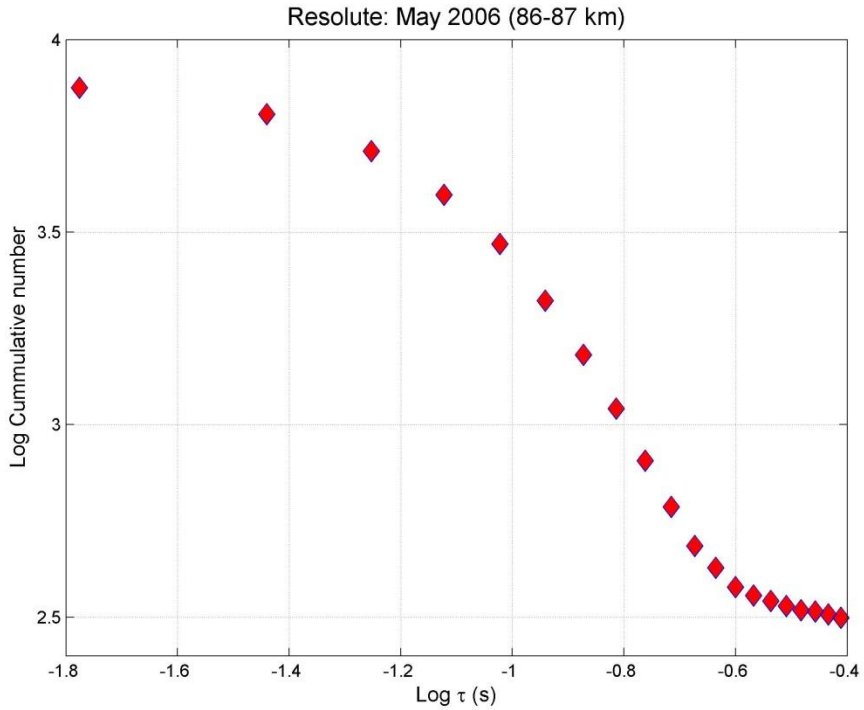

Figure 3.17: Log cumulative number of overdense meteors (in 20 bins) as a function of duration time for May 2006 at Resolute Bay. The data covers the height increment between 86 – 87 km.

Since there are a relatively small number of points along the cumulative number of meteors as a function of duration time, a fine increment interpolation was made to enable polynomial curve fitting in log-log space (Figure 3.17). After experimenting with various fits, it was determined that a 5^{th} degree polynomial provided the best fit and smallest residuals over the entire span of the data. The fitted curve, superimposed over the data is shown in Figure 3.18.

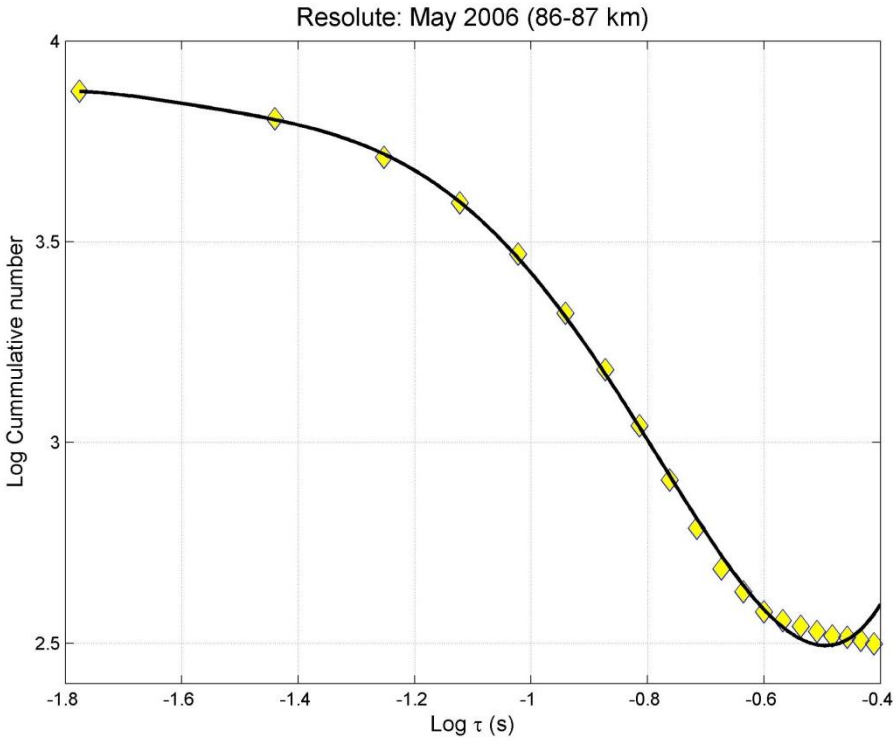

Figure 3.18: Log cumulative number of meteors (yellow diamonds) as a function of duration time for May 2006 at Resolute Bay. The black curve shown is the 5th order polynomial fit. The data include the overdense meteors between 86 – 87 km altitudes.

The ambipolar diffusion region is characterized by the flat appearance of the curve, just before it 'bends' into the chemistry diffusion region. To find the ambipolar diffusion slope in a consistent manner for the entire dataset, the first two points were selected and then used for the calculation. The next step was to find the chemistry slope. This was done through finding the minima of the first derivative of the fitting function in the chemistry diffusion region. The minimum corresponds to a specific set of coordinates on the fitting function curve (log-log cumulative number vs. τ). Thus, using this set of coordinates, it is straightforward to find the slope at this point along the fitting function curve (Figure 3.19).

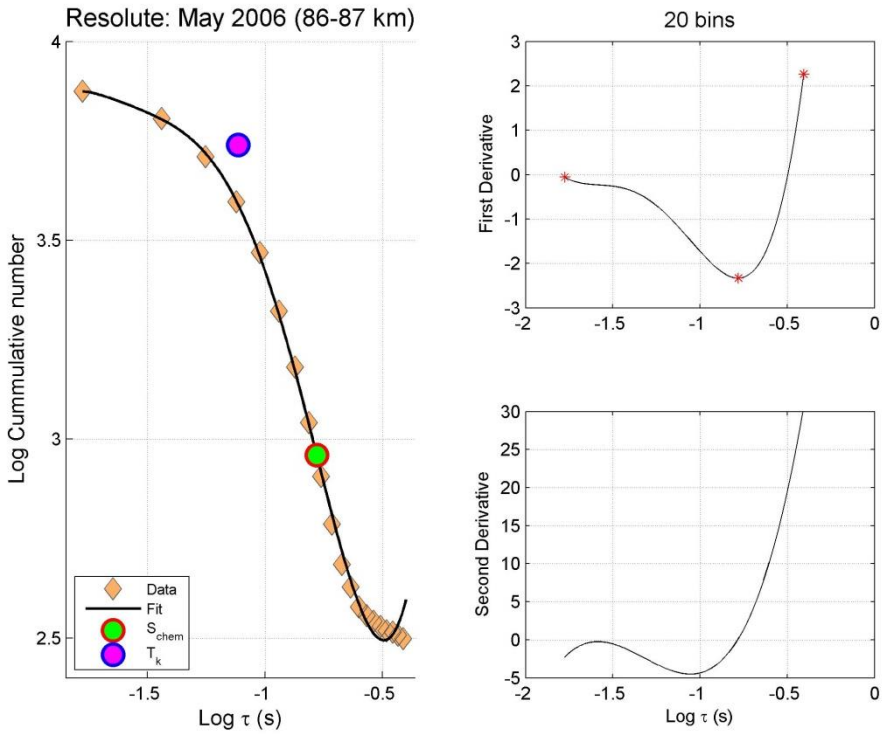

Figure 3.19: Left: plotted log-log curve of the number of cumulative events vs. duration, where the blue/magenta circle marks the intercept between the slopes of the diffusion and chemistry regimes. The red/green circle marks the point of the minima in the first derivative and the point where the slope of the chemistry regime is determined. Right: the upper figure is the first derivative of the fitting function and the lower figure is the second derivative of the same (used to confirm the minima in the first derivative).

The lines corresponding to the slope and intercept for both ambipolar diffusion and chemistry diffusion regimes are shown in Figure 3.20. The intercept of these lines represents the 'knee', which is a transition between the ambipolar and chemistry diffusion regimes. Therefore, the ambipolar diffusion time is the time measured from the left as seen in Figure 3.20 up to the 'knee'. Then the chemistry cut-off time is defined by the region from the 'knee' and to the right, up to the point where the chemistry slope line falls off into the 'tail' of the curve. However, due to the tail effects, a significant degree of uncertainty exists when the total duration time is determined (Figure 3.20). Consequently, the computation of the total duration time had to be manually and individually inspected and confirmed as precise. At this point, all parameters were saved and used for the next phase in data processing.

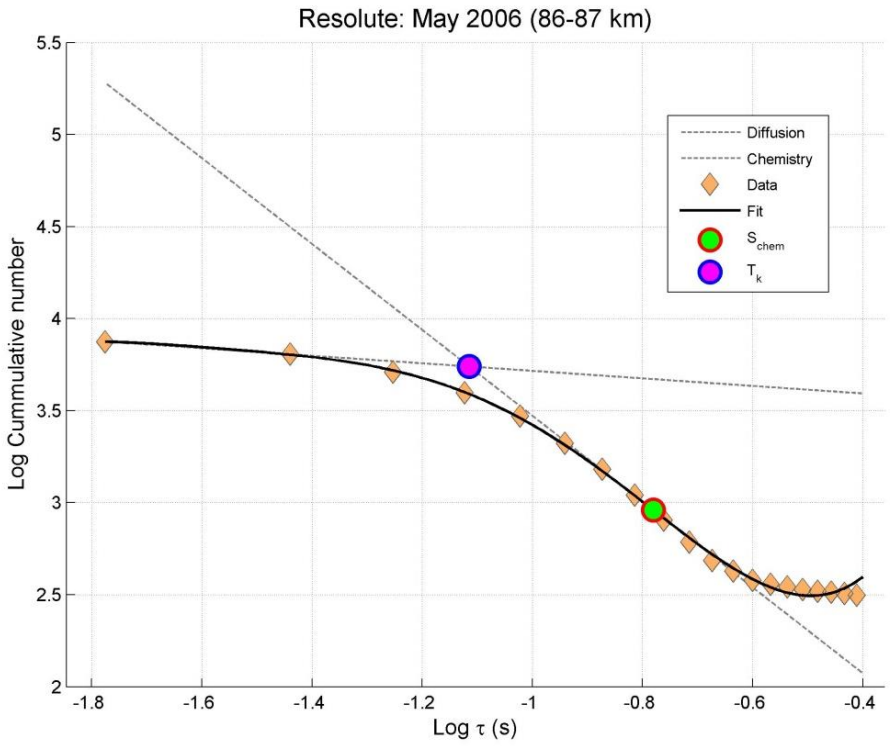

Figure 3.20: The slope intercept between the diffusion and hyperthermal chemistry regime (Resolute Bay, May, 2006, 86-87 km), with noticeable tail effect and tapering introduced by change in trend of experimentally obtained data.

All pertinent information listed below was stored in .mat format for further analysis:

- Site
- Month and year
- Height
- Number of meteors in each height increment
- Diffusion slope and intercept
- Chemistry slope and intercept
- Ambipolar diffusion duration
- Chemistry diffusion duration
- Knee time

3.7.3 Concentration Calculation

The electron line density function (α) was adopted from (Khacharenko, 2012) and (Herolfson, 1948; Kaiser, 1953). Since, by equations stated in both aforementioned references, α exhibits an abrupt and physically unrealistic jump at its minimum, a simple tapering cubic function was applied to smoothen out the transition (Figure 3.21).

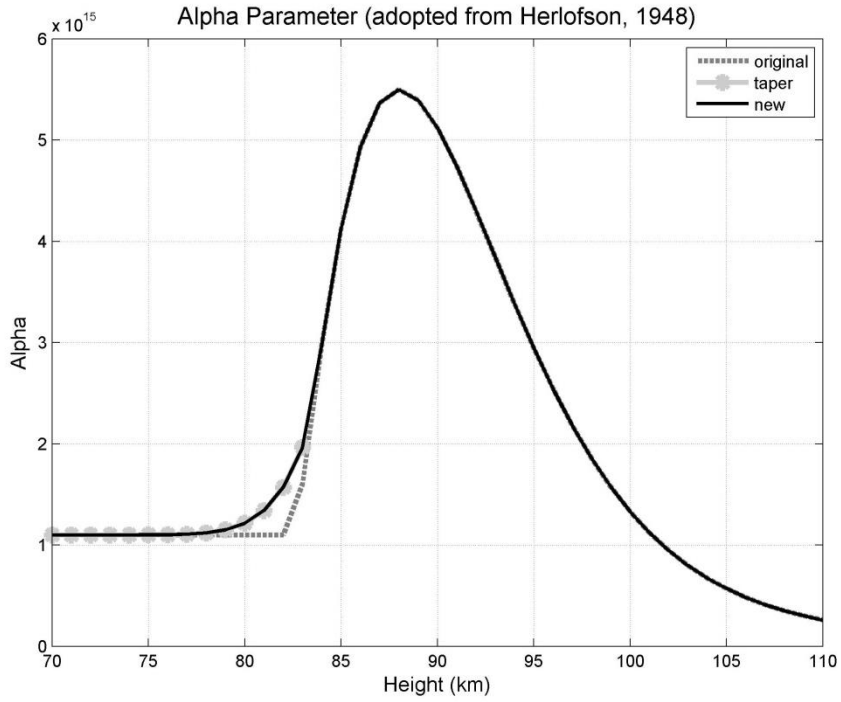

Figure 3.21: The pre and post tapering in the ionization curve using a simple 5th degree polynomial (i.e. the curve with maximum electron line density) is shown where the curve has been stabilized after tapering at 10^{15} electrons m^{-1} (e.g. definition of minimum electron line density in true overdense meteors (for the comment on overdense meteors see Cervera and Reid, 2000).

Moreover, the physical argument and reasoning behind the introduction of mild tapering in the ionization curve becomes apparent in consideration of Figure 3.22, where it is apparent that the overdense and visual meteor will not "completely burn up" immediately past the region of the maximum ionization.

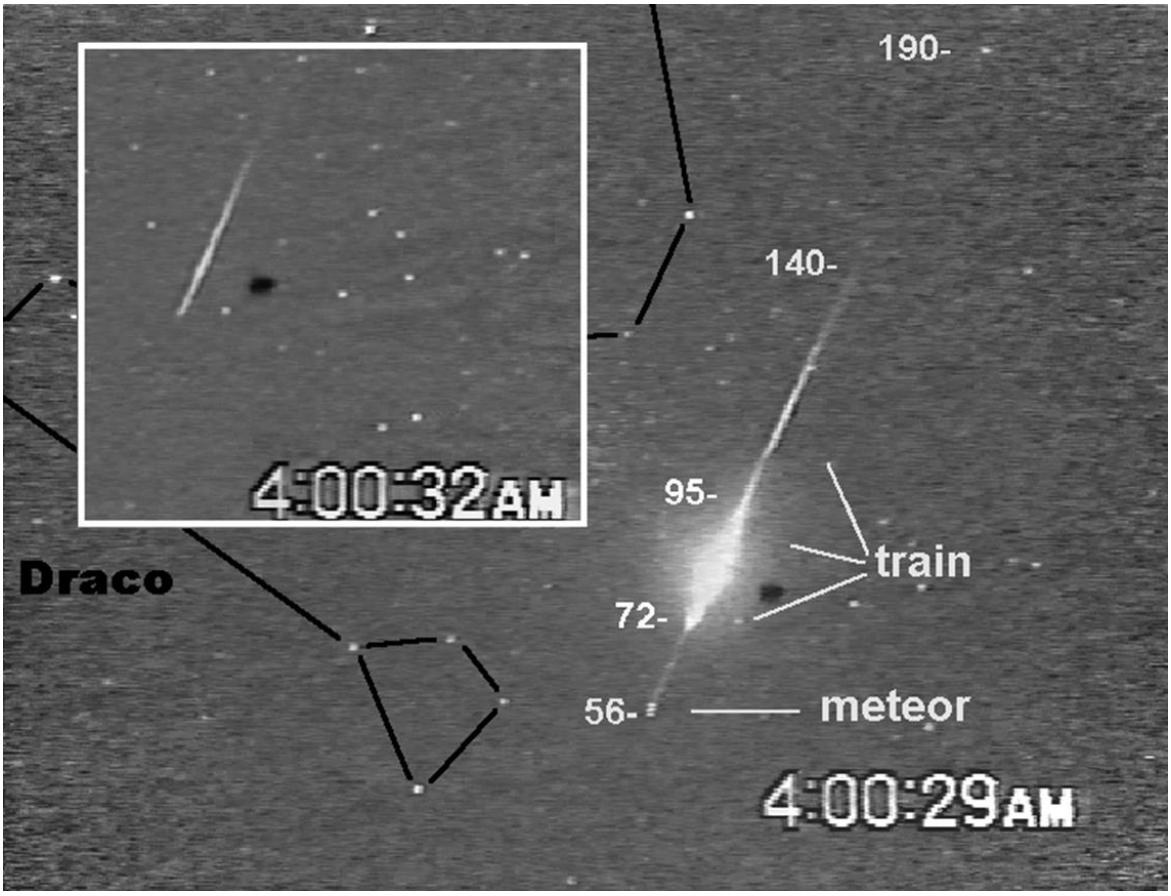

Figure 3.22: An image of a bright Leonid meteor taken by the direct image camera from the ARIA aircraft. The inset shows the meteor three seconds later (Borovicka and Jenniskens, 2000). It is apparent from the pictures that the meteor did not burn up completely and continued leaving an ionized trail.

It is important to note that the event observed by Borovicka and Jenniskens (2000) had the visual magnitude of -13 and estimated mass of 1 kg which is the upper limit for overdense meteors that can be observed by radar (electron line density of about 10^{20} electrons m^{-1}) (Sugar, 1964). Furthermore, the effects of the hydrodynamic cap that formed in front of the meteor head when the meteor dimensions exceeded the mean free path of the atmosphere must be considered, as the effect of such phenomena is to taper and impede the intensity of the ablation process due to the absence of the direct atmospheric impact on the meteoroid (Rajchl, 1969; Popova et al., 2003). As could be expected, such an effect becomes important for overdense meteors below 80 km.

The peak of the electron density function occurs in the region of maximum ionization, which in the context of this work was determined by evaluating the height corresponding to the highest number of meteors (Figure 3.23). Therefore, the electron density function for a range of possible maximum ionization heights (85 – 95 km) was calculated, so it could be used as input in later steps.

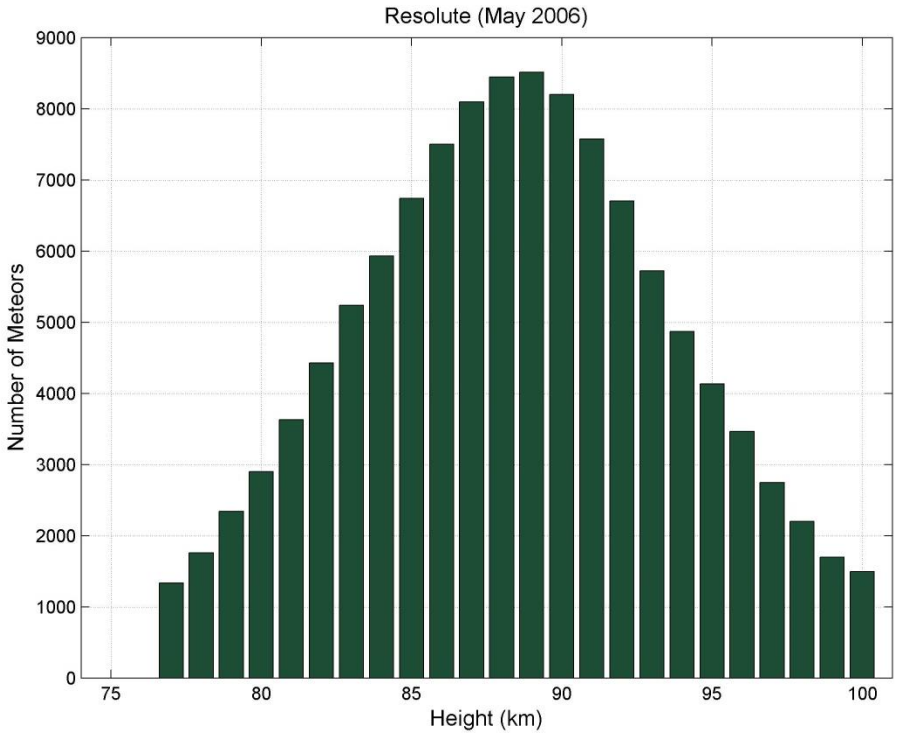

Figure 3.23: Maximum ionization height is determined from the plot of the maximum number of meteors as function of specific height, where the height with the highest number of events is taken as the maximum height of ionization. This particular figure displays the histogram for the May, 2006, Resolute Bay.

The maximum ionization height for each site and for each month of year was calculated by taking the average of the heights corresponding to the highest number of meteors across the same month for each given site. For example, the average height for all months of May for Resolute Bay is 88 ± 1 km. Table 3.1 shows the maximum ionization heights as a function of month for Resolute Bay.

Table 3.1: Maximum ionization heights for determined for each month (Resolute Bay).

Resolute Bay			
Month	Count #	Average Height (km)	Standard Deviation (km)
1	6	87	1
2	6	86	1
3	7	87	1
4	9	88	1
5	9	88	1
6	9	88	1
7	8	89	1
8	9	88	1
9	8	88	1
10	6	88	1
11	8	88	1
12	8	88	1

Having determined the electron line density, the maximum ionization height and total duration times, the finishing step was to calculate the O_3 concentration as a function of height, smooth the data and apply error bars. To validate the computation process, in addition to the electron line density from Khacharenko (2012) and Herlofson (1948), the constant value of α ($5.5 \cdot 10^{15}$) across all heights was also used during the initial early stage of calculations to explore the validity of the approach. The Matlab program written to execute the concentration calculation was customized to take either mean or directly measured variable total duration times. It must be noted that while the actual "total duration time" was well constrained for some heights and some months, it was poorly constrained for others. Hence, to avoid bias, and for comparison purposes, both the variable total duration times as determined from the logarithmic plot of the diffusion and chemistry regimes, and a set time of 0.20s ± 0.10s were used in the final calculations. The choice of 0.20s ± 0.10s for the duration time comes from a careful investigation and analysis of overall duration times for well constrained months and heights. A built in Matlab Butterworth filtering function, as a part of signal processing toolbox, was used to smooth out the concentration data (Figure 3.24). This is similar to applying a moving average filter.

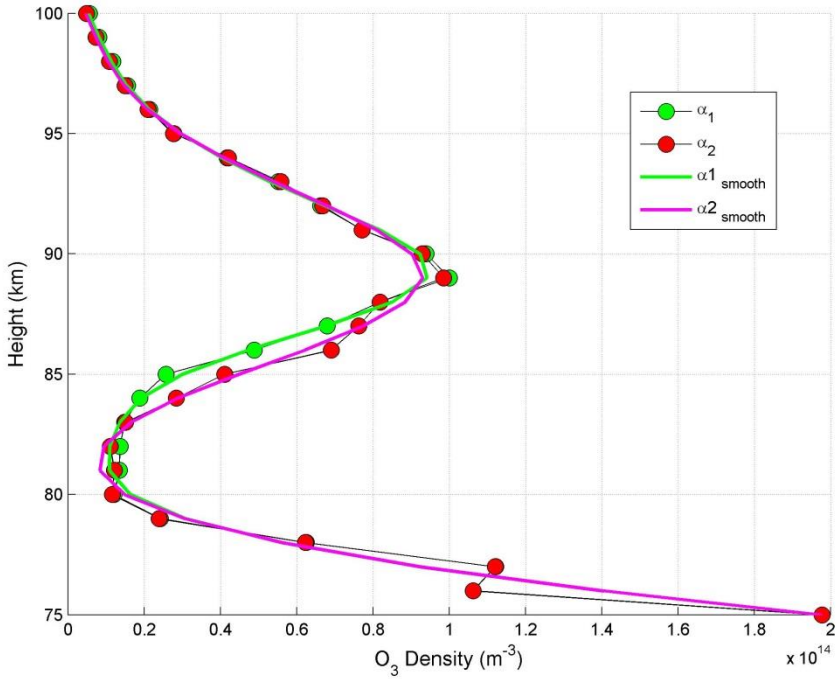

Figure 3.24: The example of calculated ozone profile data before and after smoothing using built-in filtering function in Matlab signal processing toolbox.

While the standard measurement in diffusion can be obtained from initial echo duration times plotted as a function of height, with the relatively small scatter obtained from the SKiYMET system relative to the earlier measurements, and error and height and the standard deviation of the scattered data can be resolved immediately, this work deals with cumulative statistical trends, that are based on the raw data. Therefore, the calculation of error and standard deviation in the results here must be approached differently. Moreover, the total number of processed and calculated iterations would not be practical if the error is propagated in a standard way (Bevington and Robinson, 1992) considering that the calculation would have to be made for 345 months individually with the use of exponential forms of solutions.

Finally, to determine the error as a function of height for each month in the data set, a numerical iterative method using the input variables (D_a, r_0 and total duration time) with an assorted range of initial values lying within their minimum and maximum boundaries

was implemented. The values of considered parameters were randomly generated within the determined maxima and minima bounds. These upper/lower bounds are as follows: D_a = ±10%, r_0 = ±25% and signal duration time = ±50%. This process produced as the output the O_3 concentration with the maximum range of possible values as a function of height (Figure 3.25). The error bars are given by the standard deviation of concentration values as a function of height. This process, but with the varying initial values applied to each individual monthly data set, was performed for each processed month to produce error bars unique to that particular month. The explanation for this particular choice of error treatment is discussed in the next section.

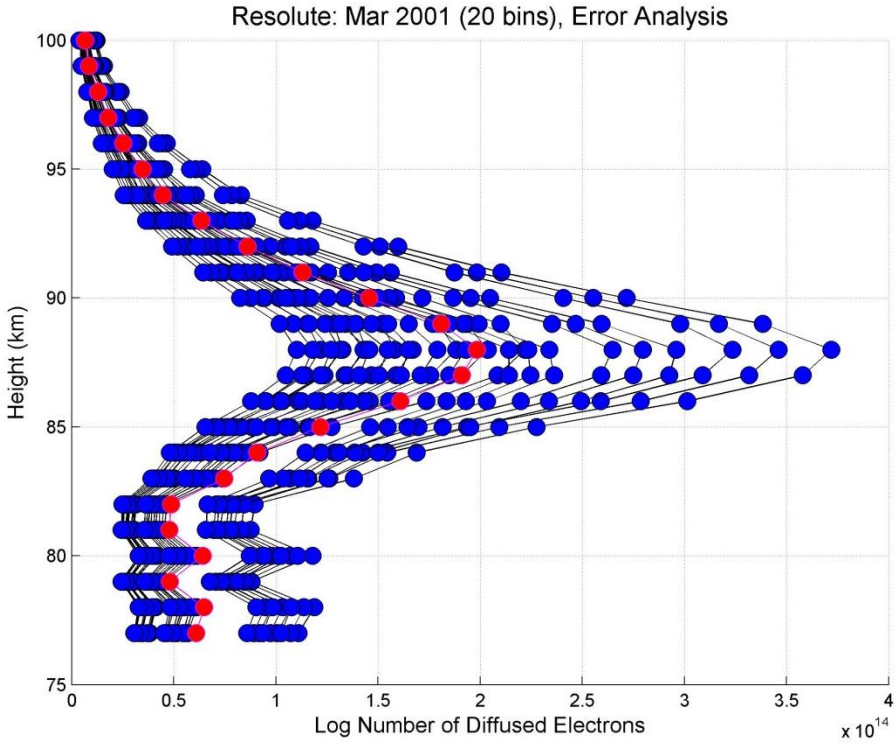

Figure 3.25: The spread in values as the result of the random variables calculations (the range of maximum and minimum values for the quantities with uncertainties) where red points represent the mean value of the calculated set.

3.8 Comment on the Error and Uncertainty Treatment

At this stage of investigation, only absolute and random errors are considered. While systematic errors are possible but very rare for the type of instrument and available data used in this work, they will not be considered in the calculation of the final results.

For the purpose of this work, the value of electron line density at the point of maximum ionization is taken as constant ($5.5 \cdot 10^{15}$ electrons m^{-1}) at the height of maximum ionization. The main physical argument for settling on this particular value of electron line density can be understood in terms of statistical meteor trends and the behaviour of the logarithmic plot of cumulative number of echoes versus the duration time, where the point of the chemistry regime slope (overdense meteors) measurement corresponds to the most stable region of the curve, which in turn, according to Manning (1962, 1963) corresponds to the most common overdense line density. From various sources discussed earlier, that the value of electron line density was determined to be $5.5 \cdot 10^{15}$ electrons m^{-1}. While this approach is taken in these preliminary stages of the investigation, continued future studies may consider refining this value further and varying the maximum electron line density to additionally constrain uncertainties in final calculations.

The total error estimate (Baggaley and Fisher, 1980) in initial radius of overdense meteors of 50% is taken as reasonably reliable and is adopted in the uncertainty calculations here, without further adjustments. However, with the availability of the new technologies, computational power and SKiYMET systems, in addition to a better processing software, it would be desirable to conduct an expanded investigation and narrow the uncertainties in the measurements of the initial radius of overdense meteors in the future.

The error in duration times may seem unreasonably large (100%), however a great caution must be exercised at this stage of investigation, as there are still significant uncertainties about the behaviour and time scales of hyperthermal chemistry processes with increasing altitude, noted earlier. For the normal local thermal equilibrium chemistry regime, time scales involving reactions between ozone and metal ion at lower altitudes (~80 km) are in the order of seconds, while at 100 km that time gets extended to about 200 seconds (see Baggaley, 1979). It is reasonable to expect a similar trend in

hyperthermal chemistry, especially considering that thermalization of both ions and electrons and consequently meteor trail takes longer at increasing altitudes (Baggaley and Webb, 1977; Baggaley, 1980). However, the hyperthermal chemistry regime duration is observed not to exhibit same behaviour with increasing height. When the denser data sets are available (numbers obtained by Kim et al., 2013 for example), a statistical treatment of the slope obtained duration times will help reduce this rather significant uncertainty. However, for now the above noted error will be applied to calculations in this work.

Last but not the least, the question of uncertainty in ambipolar diffusion and consequently in chemical diffusion is addressed in the light of recent advances and the availability of the SKiYMET system, which has improved overall measurements of meteor parameters with far greater accuracy (Hocking, 1999; Hocking et al., 2001; Hocking et al., 2004; Holdsworth et al., 2006; Kim et al., 2013) in comparison with any previous measurements in the past. The advantage of SKiYMET is the ability to accurately resolve temporal variation in ambipolar diffusion (Figure 3.26).

Prior to the introduction SKiYMET, the best estimate of typical error in meteor trail diffusion measurement was 30-40%, which was the width of the standard deviation and was considered reasonably acceptable (Tsutsumi et al., 1994). In general, the measurements of the ambipolar diffusion prior to the 1990s are not reliable due to the large scatter in data discussed in Chapter 2, which is induced by temperature and pressure variability, angular detection accuracy, pulse length, phase errors, plasma processes and variation in meteoroid metallic content. Those factors are discussed in detail by Hocking (2004). The main point to note here is that the observational error of meteor echo decay times from SKiYMET systems is generally smaller than the error of measured height (Kim et al., 2013) which can be directly applied to the value of ambipolar diffusion coefficient. If the value of height uncertainty is taken from Kim et al (2013) and Holdsworth et al. (2006) to be ~1 km, that translates into 15% error in ambipolar diffusion (Tsutsumi et al., 1994). Considering the very small error in subsequent MST temperature measurement using meteor radar decay times (Figure 3.27), which is much less than ±7 K (e.g. Hocking et al., 1997; Hocking et al., 2007; Meek et al., 2013), the estimate of the error in slope adjusted theoretical diffusion (Jones and Jones, 1990) of

20% used in this work and carried over in calculation of the "chemical diffusion coefficient" may seem like an overestimate.

However, it can be reasoned that at least for the purpose of the calculations of the ozone density, the determined error in both diffusion and chemistry coefficient is reasonable in consideration that the new technique is being employed here. Moreover, the slopes of diffusion regime (Figure 3.28) which are instrumental in calculation of the chemical diffusion coefficient, have the purpose of correcting theoretical diffusion for the effects of the temperature and pressure variation. Considering that the effects of those corrections are still not completely defined, the 20% error applied to resulting calculations is sufficient to account for uncertainties.

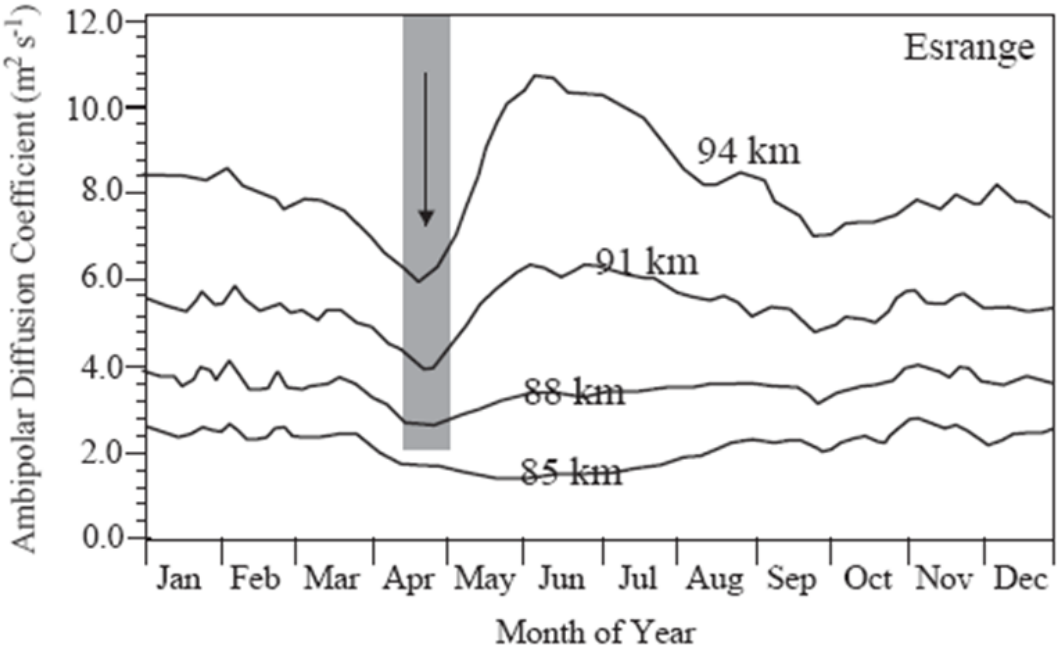

Figure 3.26: Plots of the ambipolar diffusion coefficient measured at Esrange, Sweden, as a function of time for heights of 85, 88, 91, and 94 km (Hocking et al., 2004). A particularly interesting feature of this plot of ambipolar diffusion coefficient obtained from underdense meteors is the local minima in April, which coincides with ozone maxima.

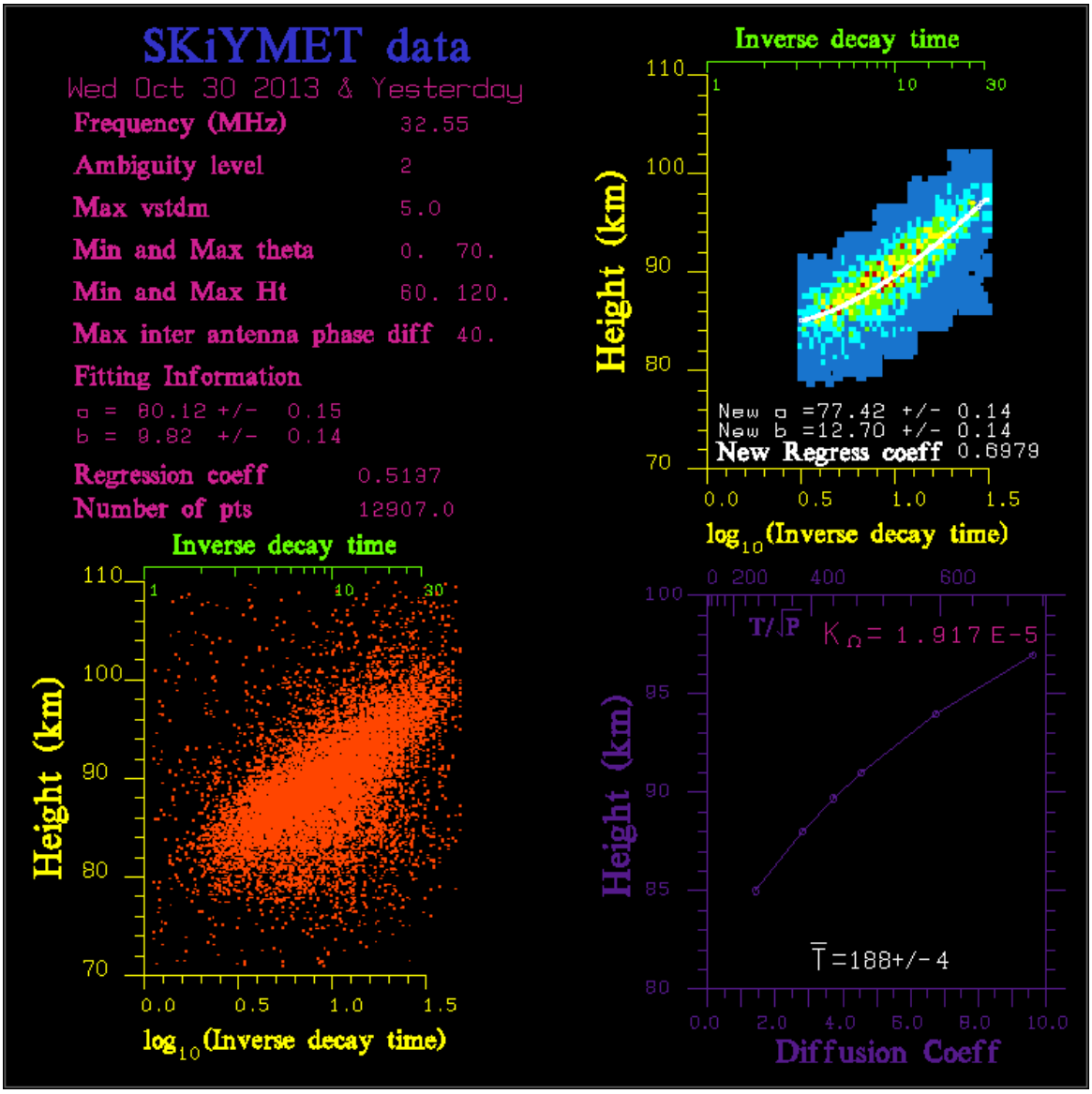

Figure 3.27: Screen shot of the live feed from the Tierra del Fuego, Argentina, which is a part of the SKiYMET network, given to illustrate accurate real time temperature determination from meteor radar diffusion times (http://www.physics.uwo.ca/~whocking/axonmet/radarsites/tierradelfuego/).

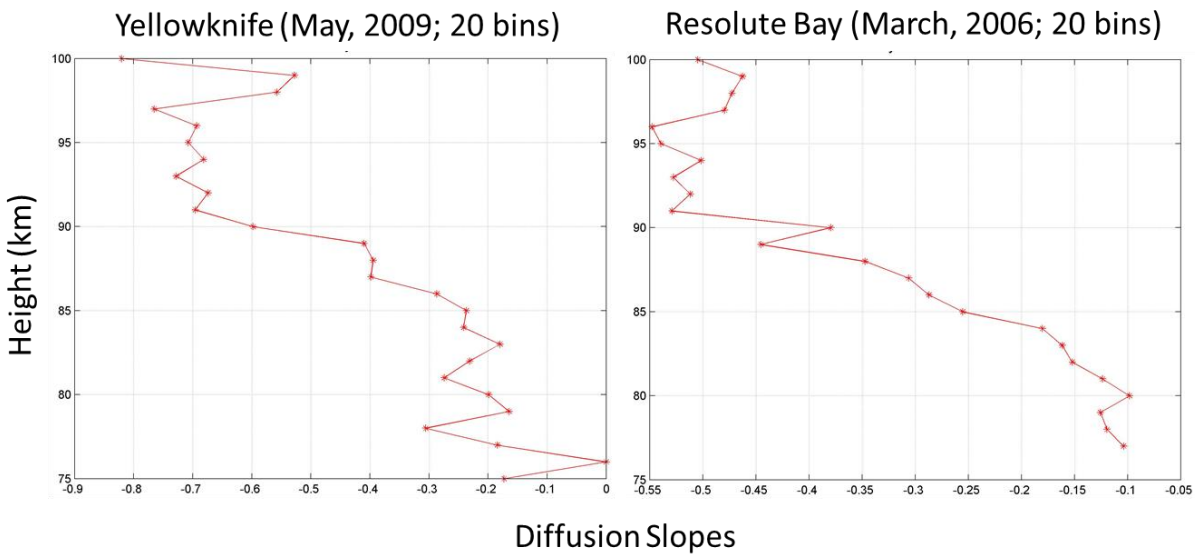

Figure 3.28: Slopes of the ambipolar diffusion shown here for illustrative purpose, for Yellowknife (May, 2009) and Resolute (March, 2006) and determined from the plot of the cumulative number of events versus the echo duration times, obtained from experimental meteor data. The ambipolar diffusion slopes are used to correct theoretical ambipolar diffusion coefficient for the effects of pressure and temperature.

3.9 Chapter Graphical Flowchart Summary

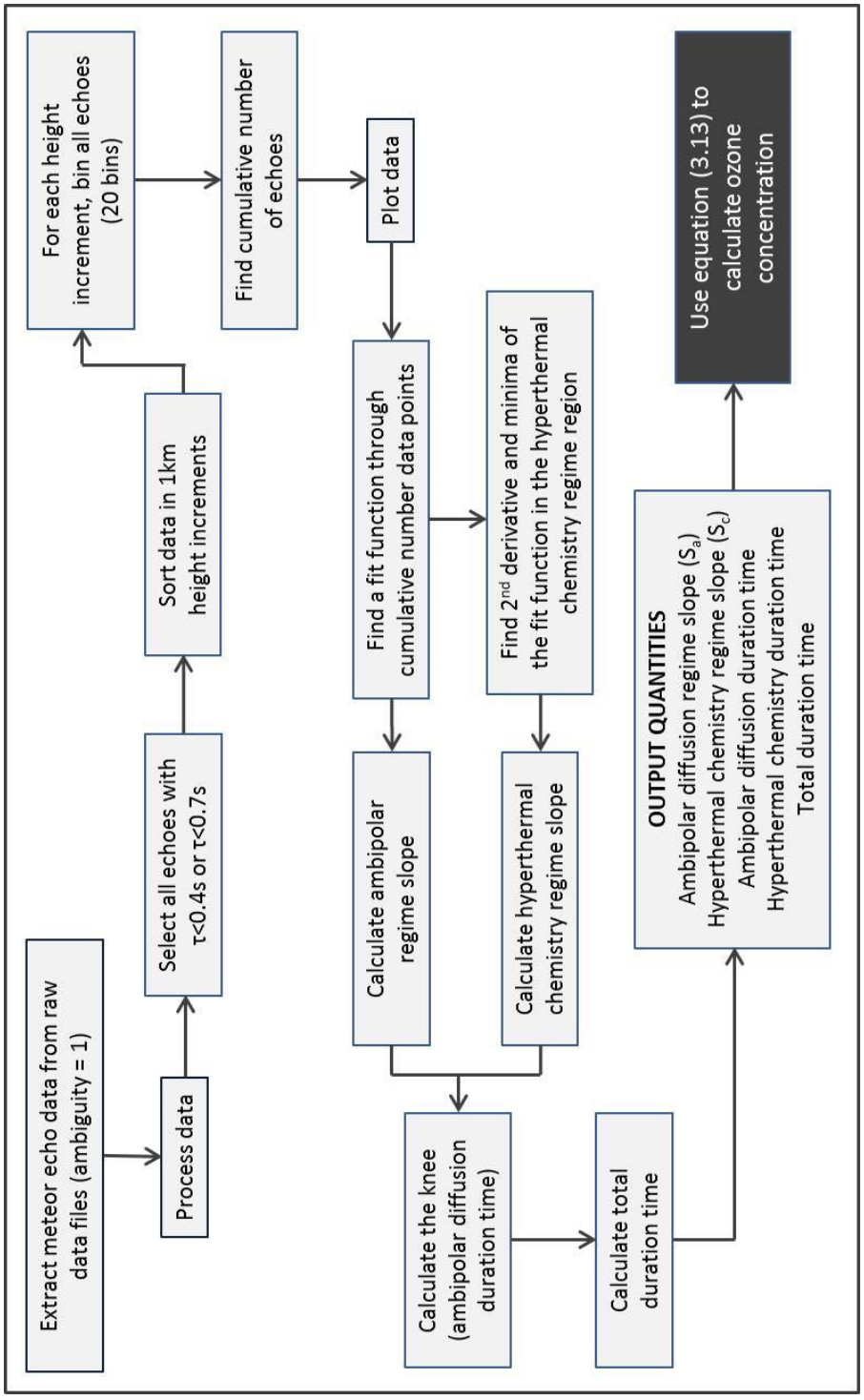

Figure 3.29: Flowchart

Chapter 4

It's not that I'm so smart, it's just that I stay with problems longer.

- Albert Einstein

4. Results

The initial hypothesis stating that it was possible to evaluate ozone density in the MLT region using the backscatter radar observation of overdense meteor diffusion, which motivated the work in this thesis, has been proven correct. By evaluating the number of electrons consumed by the "hyperthermal chemistry regime" at the boundary of the meteor train, in the initial expansion phase of the "hot" meteor trail, it was possible to evaluate ozone density in the MLT region with reasonable accuracy. That was achieved by calculating the number of removed electrons for each height increment, using the ionization curve corrected electron line densities and duration times obtained from the logarithmic plot of the cumulative number of events and echo duration times for each specific altitude.

It was demonstrated that the proposed mechanism of ozone participation in the hyperthermal chemistry regime, where singlet oxygen formed by the photo dissociation and thermal decomposition of O_3 by the meteor shock UV layer radiation and thermal shockwave, reacts with metallic ions at suitable temperatures and subsequently removes electron from the expanding meteor train. The results obtained for chemically removed electrons match the ozone vertical MLT density profile well, as it will be seen from the satellite measurements comparison, where the obtained results are within the margin of errors of satellite measurements. It should be noted here that the calculated profiles are mean monthly densities of ozone because there were not enough daily events for all locations to discriminate diurnal variations. For the purpose of this study, that presented a slight obstacle as diurnal variations which may be up to an order of magnitude, could not be investigated. However, a future study, with the availability of high density data will enable diurnal measurements and more refined seasonal trends. Despite the acknowledged difficulty in measuring ozone profile accurately above 70 km (Froidevaux et al., 2008) and inherent uncertainty in those measurements (Smith et al., 2013), the

initial results obtained here look very promising and confirm the supposition by Hajduk et al. (1999) that radar is a viable instrument to measure ozone density in the MLT region.

The problem, however, with the initial data was that only two sites (Resolute Bay and Socorro) had enough events to do calculations for more than one full year. At other sites, with the exception of Yellowknife, 2009, monthly data was either sparse, intermittent, or the number of meteors was too low for any meaningful data analysis. Correspondingly, it is important to note that if the number of meteors is below ~20000 per month in general, it is difficult to extract any usable results, because of an insufficient number of individual events for statistical logarithmic plotting.

The results of this study perform better in comparisons to previous mesospheric ozone determinations using forward scatter radar (Jones et al., 1990; Hajduk et al., 1999; Cevolani and Pupillo, 2003) on several different levels. First, in this study, the density as a result of altitude is obtained with vertical resolution of 1 km, which was not possible in the aforementioned investigations. Furthermore, the vertical profiles of ozone obtained in the MLT region, closely match the actual ozone density distribution as a function of height and are closely in line with satellite derived profiles. Additionally, no attempt was made here to identify specific meteor showers and their specific contribution as the initial data was considered on a cumulative basis.

The chapter is organized in the following way: First, the individual sites will be discussed and presented separately, with results presented and analysed in order to show how the data were obtained, concluding with brief statistical treatment and satellite comparisons. Because of the large amount of processed data and figures that resulted from this work, only one representative year or month for each site will be discussed in the main body of the thesis, while the part of the data tables and figures will be available in appendix, and the rest will be available upon request from Professor Wayne K. Hocking in the Department of Physics and Astronomy at Western University.

4.1. Resolute Bay

Table 4.1 summarizes the total number of meteors for each given month for Resolute Bay in the period between 2000 and 2012. The table cells were colour coded upon initial evaluation, to describe the quality and usability of data. It is apparent that only a limited continuity in meteor numbers as a function of season and year exists, therefore impeding the assessment of long term calculated trends in ozone. Moreover, the additional data from satellite ozone density measurements in the MLT region in very high latitudes such as for Resolute Bay are not readily available and that presents challenge in validation of the results obtained in this study.

Table 4.1: Number of total events for Resolute Bay, where colour coding indicating the quality of the data during the initial processing. The legend is below the table. While Resolute is the best performing in terms of data density and quality, it is still apparent that data does not exhibit required continuity to evaluate long term trends when ozone is calculated.

Resolute Bay	2000	2001	2002	2003	2004	2005	2006	2007	2008	2009	2010	2011	2012
Jan	n/a	22972	**76477**	n/a	n/a	**52244**	**32830**	62530	n/a	n/a	26364	7293	538
Feb	n/a	45654	**53839**	2174	n/a	***26812**	12846	37358	9670	n/a	*33930	n/a	2317
Mar	n/a	**47579**	**57863**	48809	n/a	**34482**	**52198**	*46756	12370	n/a	10329	n/a	2607
Apr	n/a	**56553**	**91697**	**84896**	n/a	*86268	*93575	*89884	61767	*28004	17017	n/a	2845
May	n/a	**72509**	**121080**	**124195**	n/a	**27516**	**137997**	**91081**	*48541	**42755**	*34864	n/a	6000
Jun	14475	*88102	**96853**	18856	n/a	n/a	**178371**	25727	30345	31845	*70637	n/a	1155
Jul	54997	**106783**	n/a	n/a	***18345**	41015	102955	n/a	**124519**	**74069**	33563	n/a	n/a
Aug	**101503**	**97785**	n/a	n/a	**97273**	**99541**	116431	**63494**	28658	*48195	*14633	n/a	n/a
Sep	**67785**	**82086**	n/a	n/a	**86018**	**73565**	**79699**	**50875**	36992	30168	n/a	n/a	n/a
Oct	18064	**73864**	n/a	n/a	n/a	**57969**	**65692**	8706	***34822**	***40722**	n/a	n/a	n/a
Nov	11834	**82664**	n/a	n/a	13325	**50262**	**63423**	n/a	**29247**	***31644**	6914	19576	n/a
Dec	**43716**	**91628**	n/a	n/a	**94959**	***45779**	***66391**	n/a	30954	***26093**	28759	5911	n/a

Colour/Symbol	Legend
	Very Good Performing Data and Plots
	Good Behaviour
	Potentially Usable
	Not Usable
Bolded	Best Behaving Data
*	Outlier(s) Present

Figures 4.1 - 4.2(a,b) show the calculated hyperthermal chemistry diffusion coefficient comparison with theoretical ambipolar diffusion coefficient (Jones and Jones, 1990) as a function of altitude. An interesting trend can be observed on all plots (e.g. Figure 4.2a,b) where the calculated hyperthermal chemical diffusion coefficient exhibits the highest magnitude in the region around 85 km in general and decreases at both below and above that height. This is closely in line with the known maxima in ozone density. At about 92-95 km, the hyperthermal chemistry diffusion coefficient attains the same value of the

ambipolar diffusion coefficient which corresponds to the decreasing role of chemistry with altitude in the meteor trail and it accordingly also corresponds to the ozone decrease with altitude. Similar observations were noted by Jones and Jones (1990) where they investigated direct chemical reactions of ozone with meteor ions seconds (minutes) after an initial meteor train formation. Moreover, merging of the hyperthermal chemistry diffusion coefficients (herein referred to as HCDC) and theoretical ambipolar diffusion coefficient coincides with the same trend in behaviour of measured and theoretical diffusion coefficients from the early studies. This was discussed in Chapter 2 to some extent, but one might recall that the deviation of the measured diffusion coefficients in the early investigations was attributed to the role of chemical "attachment".

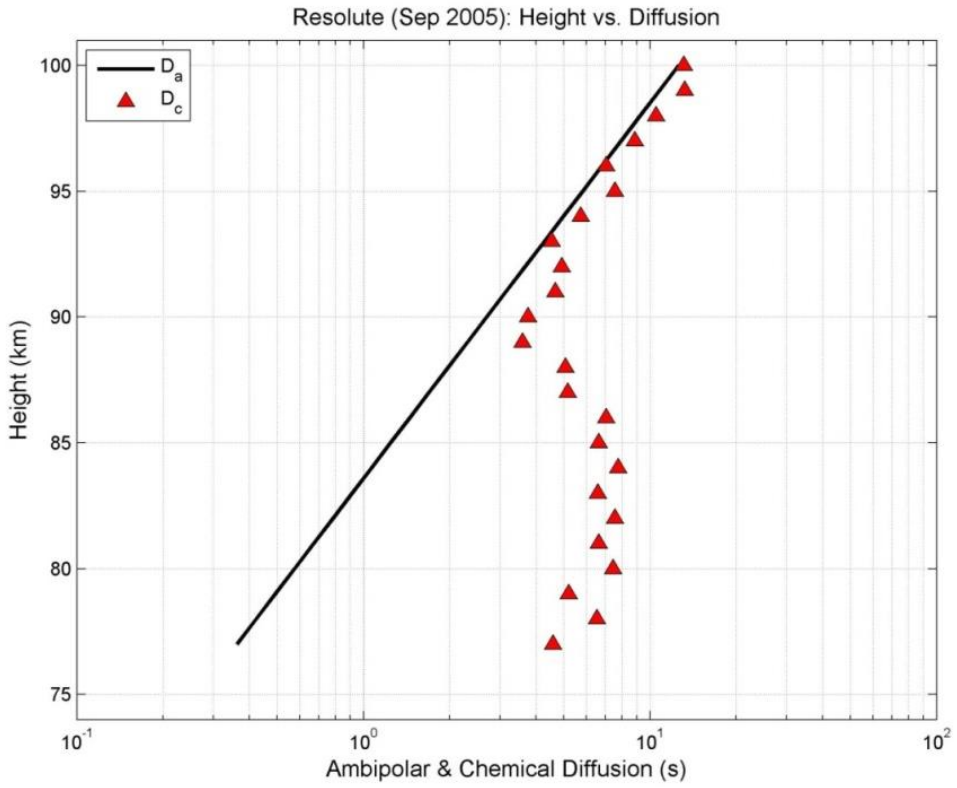

Figure 4.1: Typical profile of the calculated hyperthermal diffusion coefficient" compared with theoretical ambipolar diffusion coefficient as a function of height (September 2005, Resolute Bay).

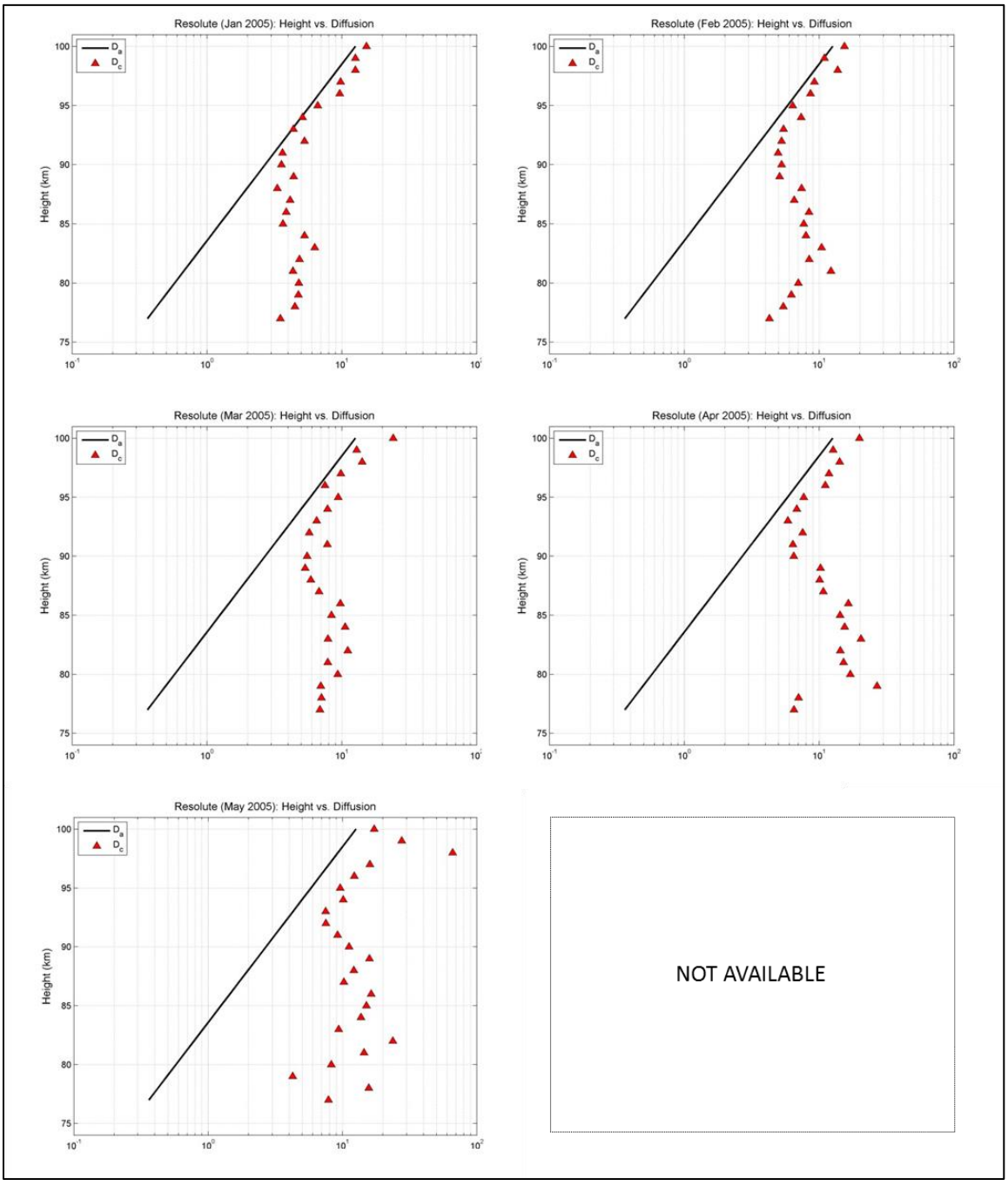

Figure 4.2: (a) The behaviour of the calculated hyperthermal diffusion coefficient compared with theoretical diffusion coefficient calculated from Jones and Jones (1990).

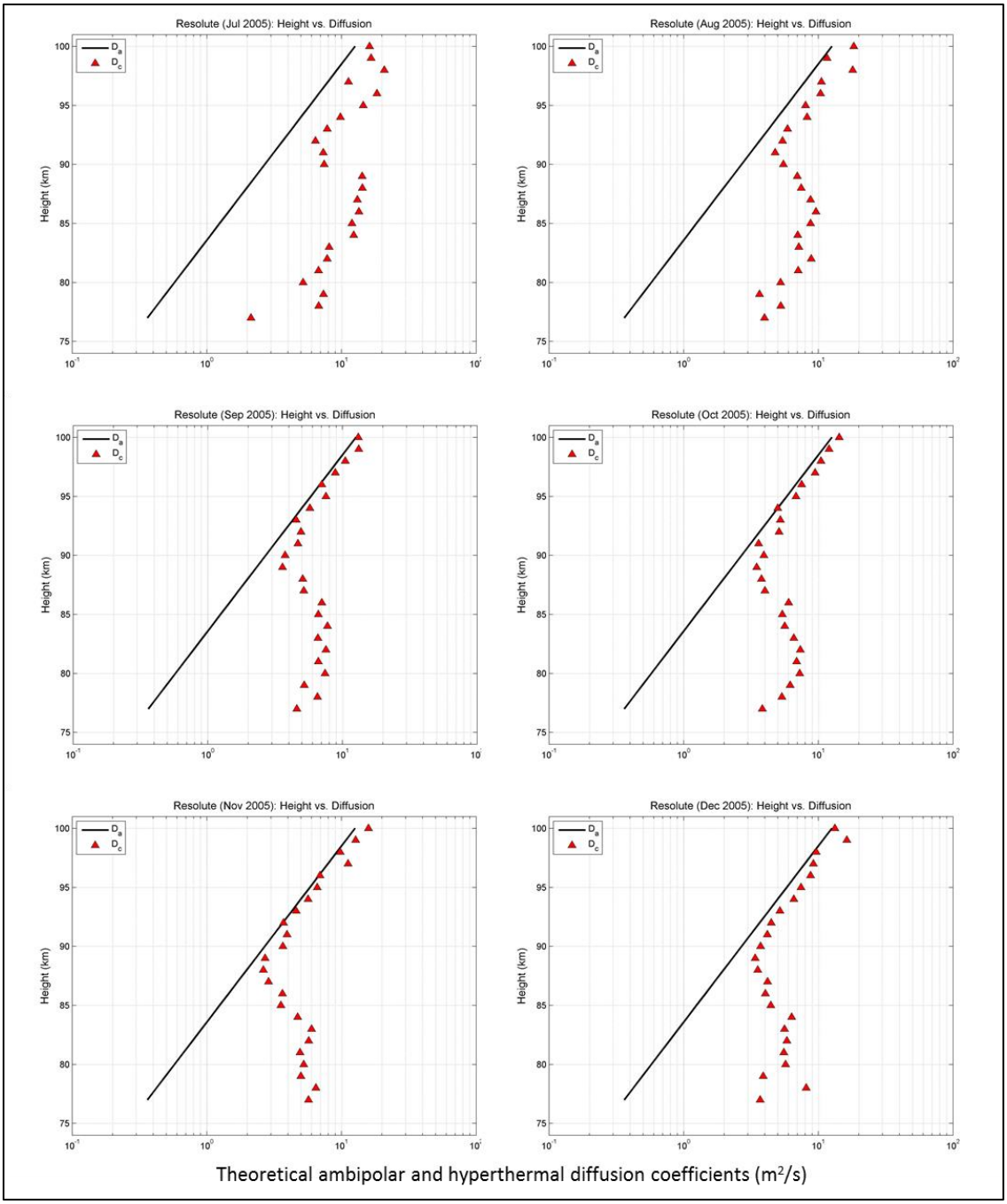

Figure 4.2: (b) The behaviour of the calculated hyperthermal diffusion coefficient compared with theoretical diffusion coefficient calculated from Jones and Jones (1990).

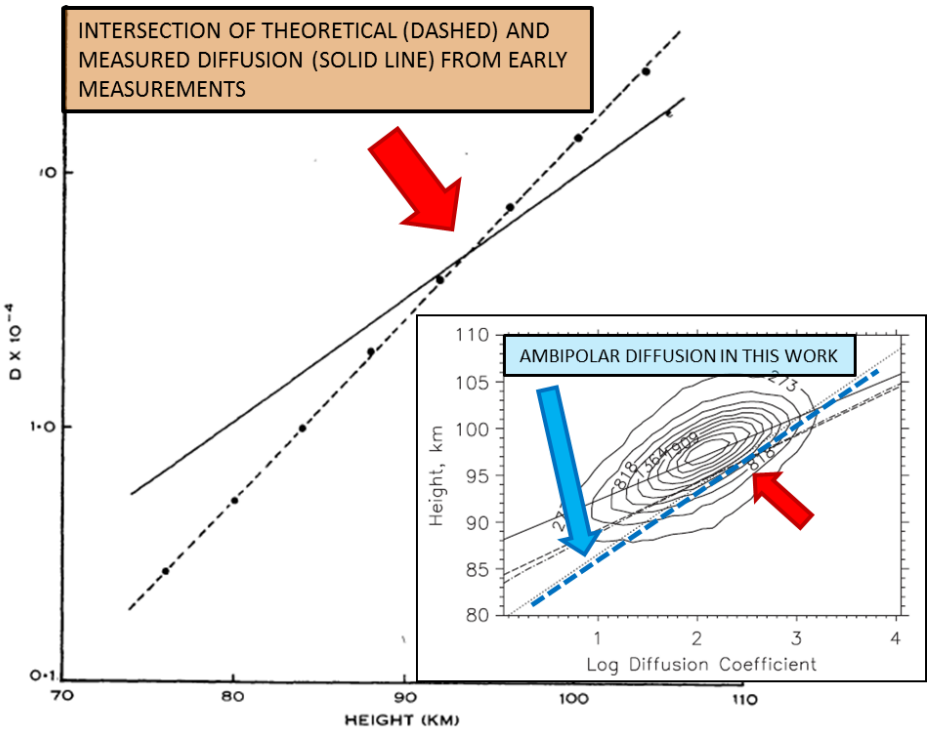

Figure 4.3: The main figure: The theoretical and measured diffusion as a function of height as measured by Weiss (1955). Note that the altitudes are on the abscissa in this case. Inset: Relationship between diffusion coefficient and height from the AMOR data set. The solid line is diffusion coefficient obtained by Galligan et al. (2004) and dotted, dashed and blue dashed line are from Jones and Jones (1990) where blue line corresponds to theoretical value of ambipolar diffusion used in this work. The dot-dashed line is derived using temperature and pressure based on USAA (1976). Note that in both figures, theoretical and measured diffusion coefficients merge at altitudes around 95 km, which is a similar trend to that observed in the convergence of hyperthermal diffusion coefficient and theoretical diffusion coefficient obtained in this work and plotted in figure above.

From Figure 4.2b, it can be also seen that there is a seasonal variation in shape and magnitude of HCDC which was expected based on already understood seasonal changes in ozone.

Furthermore, plotting the absolute slope values of ambipolar diffusion and HCD, the same trend can be observed where the “hyperthermal chemistry” dominates below 95 km (Figure 4.4a,b). Of importance is to note the behaviour of these slopes as a function of season, which implies they are sensitive to the changes in temperature and pressure and variations of ozone concentration.

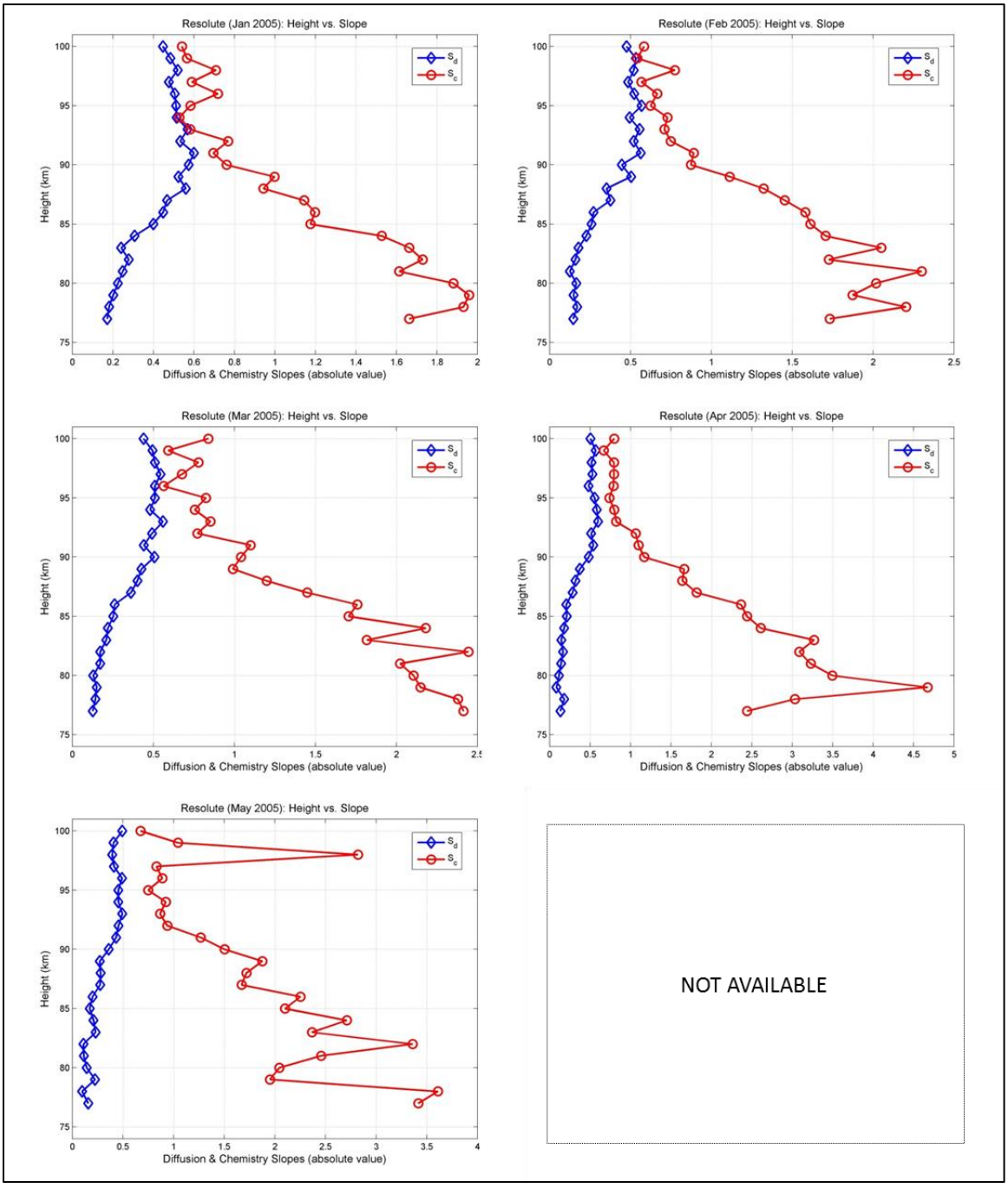

Figure 4.4: (a) Slopes of ambipolar diffusion regime compared with hyperthermal chemistry regime as a function of height, for 2005, Resolute Bay (the blue line represents the ambipolar diffusion slope and the red line is hyperthermal chemistry slope).

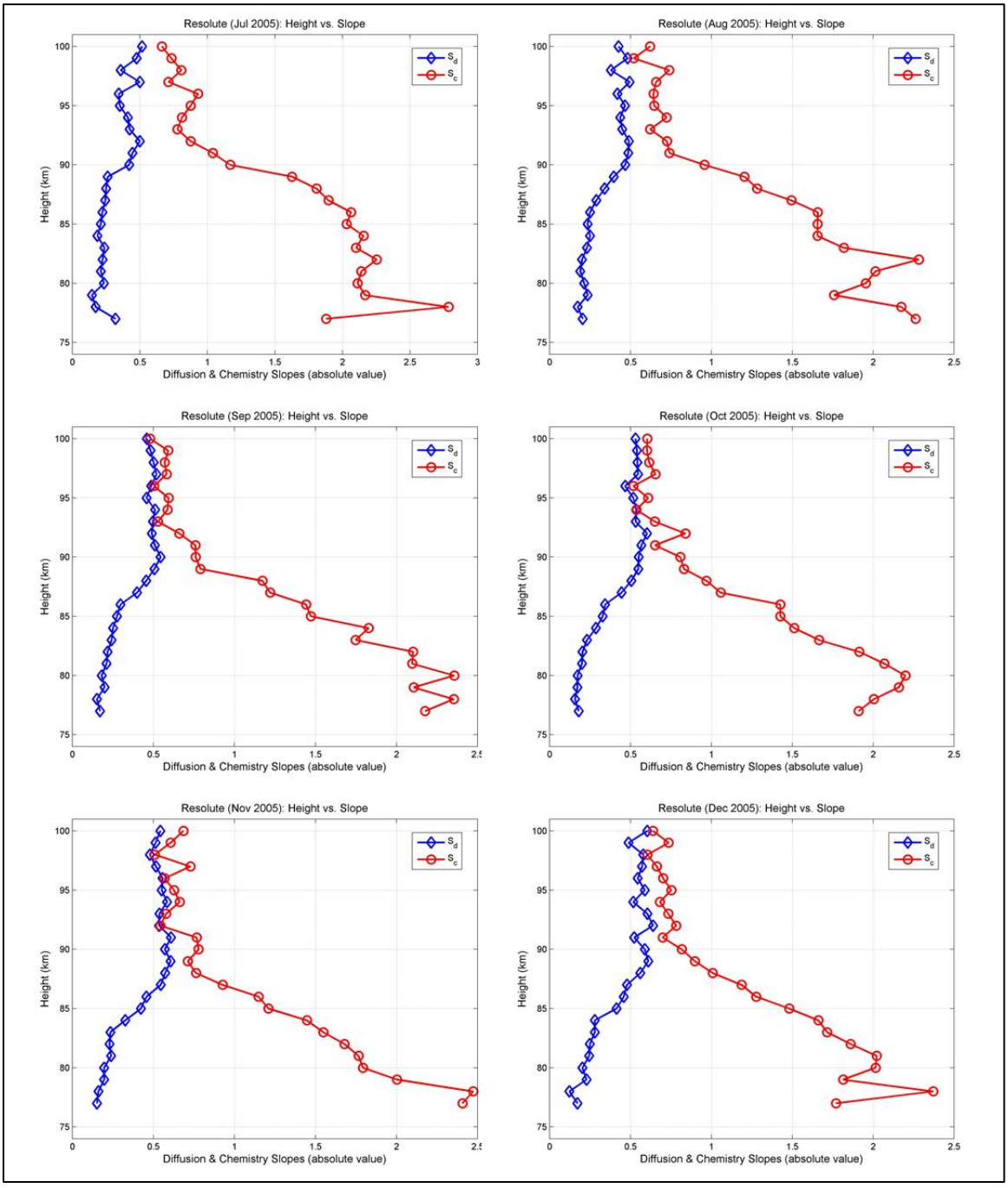

Figure 4.4: (b) Slopes of ambipolar diffusion regime compared with hyperthermal chemistry regime as a function of height, for 2005, Resolute Bay (the blue line represents the ambipolar diffusion slope and the red line is hyperthermal chemistry slope).

The observation of the ambipolar diffusion regime times compared to the total echo duration times as a function of altitude (Figure 4.5) and their difference, suggests the decrease in hyperthermal chemistry duration times with height, which is contrary to the previously observed "equilibrium" chemistry lifetime of the reaction of ozone and meteoric metal ion. There is no immediate explanation for this and future investigation should address this behaviour in more detail.

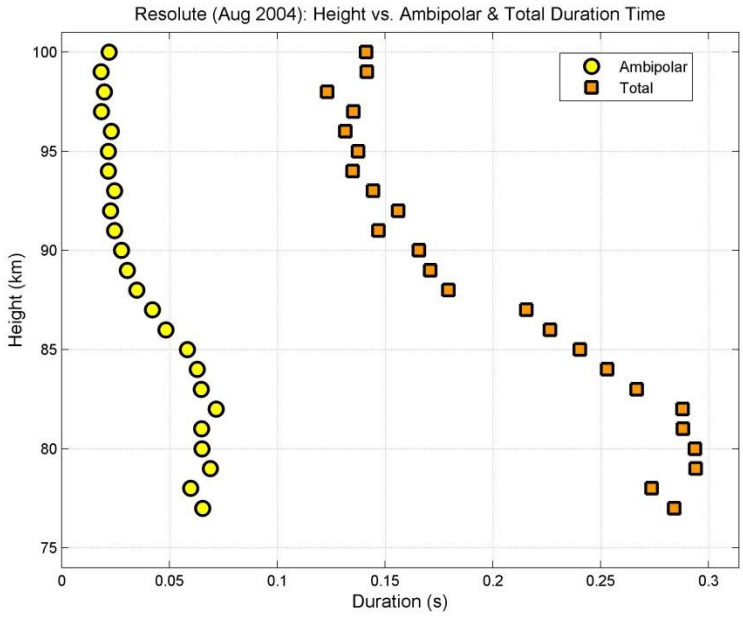

Figure 4.5: The altitude vs. ambipolar diffusion time and total diffusion time derived from the logarithmic plot of the total number of events vs echo duration times for August 2004, Resolute Bay. The difference between two regimes is taken to be hyperthermal regime duration.

To resolve the height of the maximum ionisation and to apply it to the calculation of the ozone density, the height with the maximum number of events (e.g. Figure 4.6) was taken to be the height of the maximum ionization and hence height of the maximum electron line density. The application of the Herlofson (1948) formula or adaptation of the treatment by Kharchenko (2012) in the standard solution to the diffusion equation produces almost identical results (Figure 4.7 and Figure 4.8). Furthermore, the representative examples of the calculated ozone density using either variable time derived from the logarithmic plot of the cumulative number of events vs. duration time with error

bars are shown in Figure 4.9 - Figure 4.11. The application of the mean time in calculation will produce only slightly different shape of the ozone density profile (which is still within the margin of error of the results derived by using variable statistical-plot-derived time). In Figure 4.12a below, it is only shown as an illustrative example. However, even as the calculated ozone density profiles here are only monthly means, using the mean time will still enable observation of significant seasonal variations, as it could have been expected.

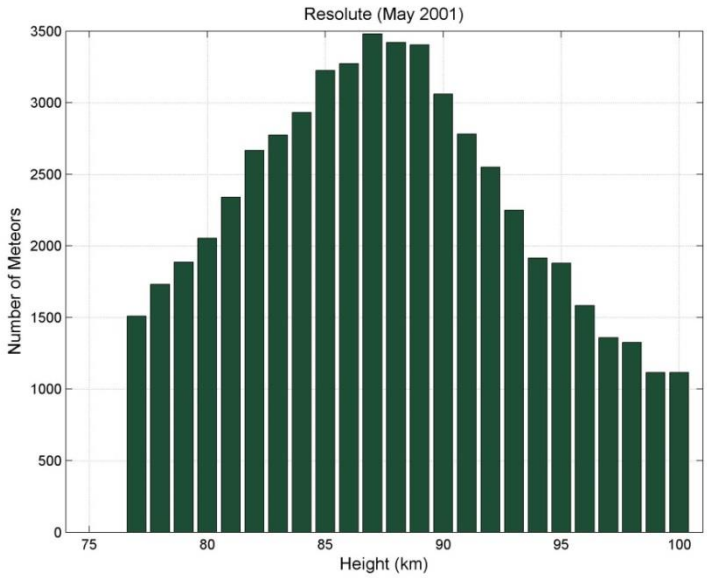

Figure 4.6: Example how the maximum number of meteor events vs. altitude was used to determine the height of the maximum ionization and consequently maximum electron line density.

The use of both Herlofson (1948) and Kharchenko (2012) treatments for the ionization curve correction in the electron line density has been shown to be viable (Figure 4.7 and Figure 4.8), where both approaches are possible based on the preference, type of calculation and subsequent complexity level. While it is possible to obtain mass and a velocity dependent form of Herlofson's (1948) ionization curve treatment, the empirical treatment by Kharchenko (2012) appears to be reliable and can be easily exploited to contributions and effects of different masses and velocities.

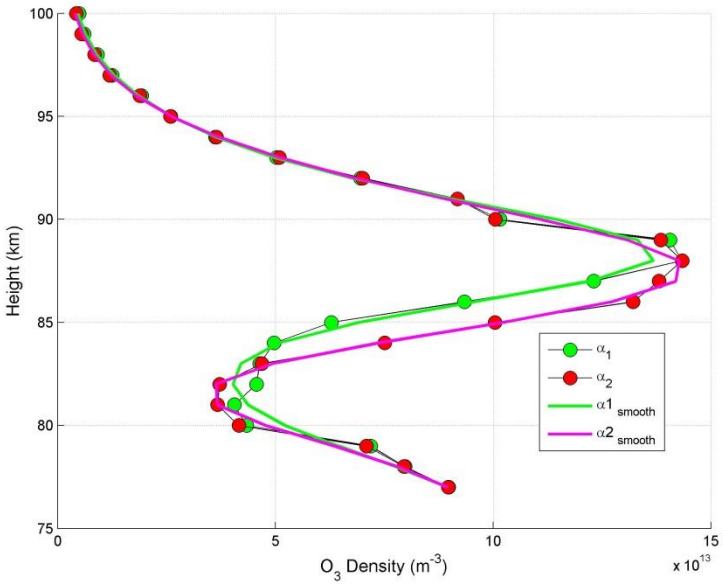

Figure 4.7: The application of Herlofson's (1948) [α_2]and Kharchenko (2012) [α_1] formula lead to closely matching results in ozne density calculaton.

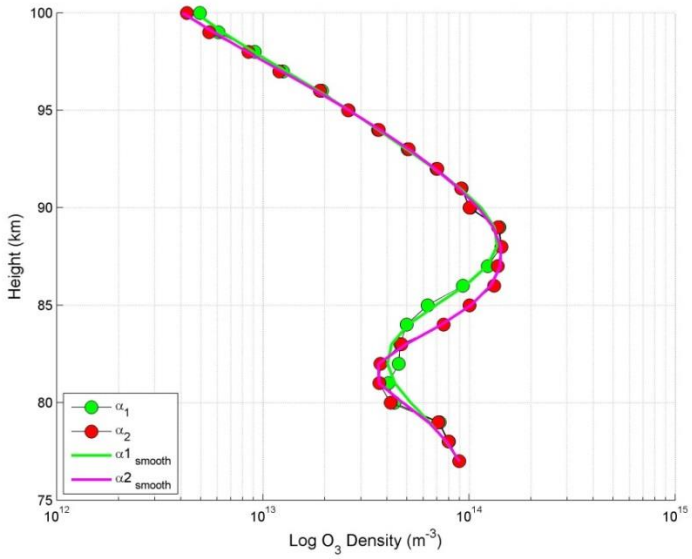

Figure 4.8: Height vs. log density of ozone for May, 2001, Resolute Bay.

The error bars reflect the initial uncertanites in primary data during the calculation. While the uncertanties are relatively large (Figures 4.9 – 4.11), a consideration must be given to the fact that the mean monthly profiles are obtained here. Moreover, in consideration of

the large uncertainties that exist in satellite measurements (see Smith et al., 2013 for discussion), the assumed error in the results in this work seems reasonable.

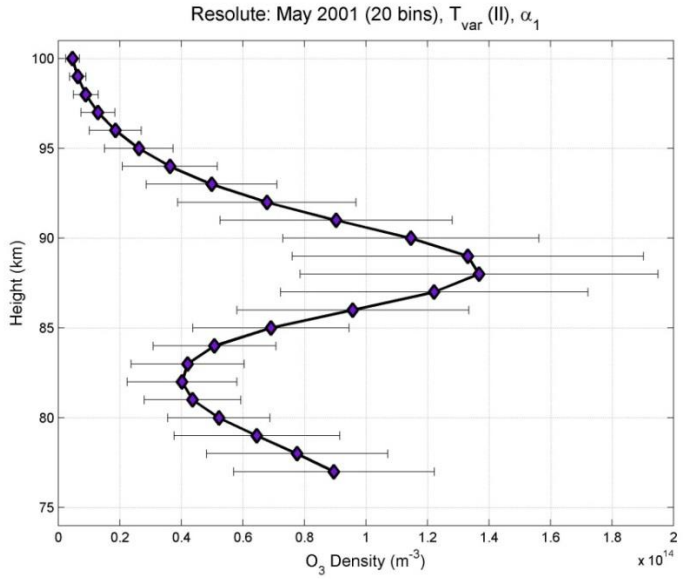

Figure 4.9: Height vs. ozone density with error bars applied using (α_1) and the height dependent variable durationt time, for May 2001, Resolute Bay.

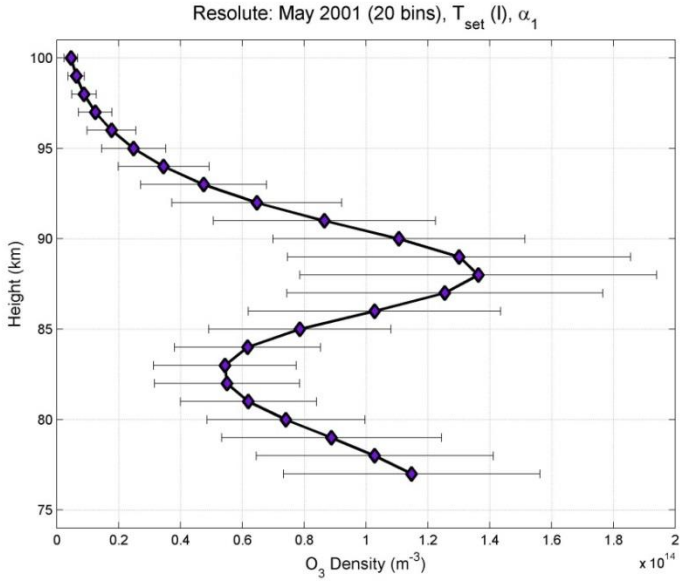

Figure 4.10: Height vs. ozone density with error bars applied using (α_1) and the mean duration time, for May 2001, Resolute Bay.

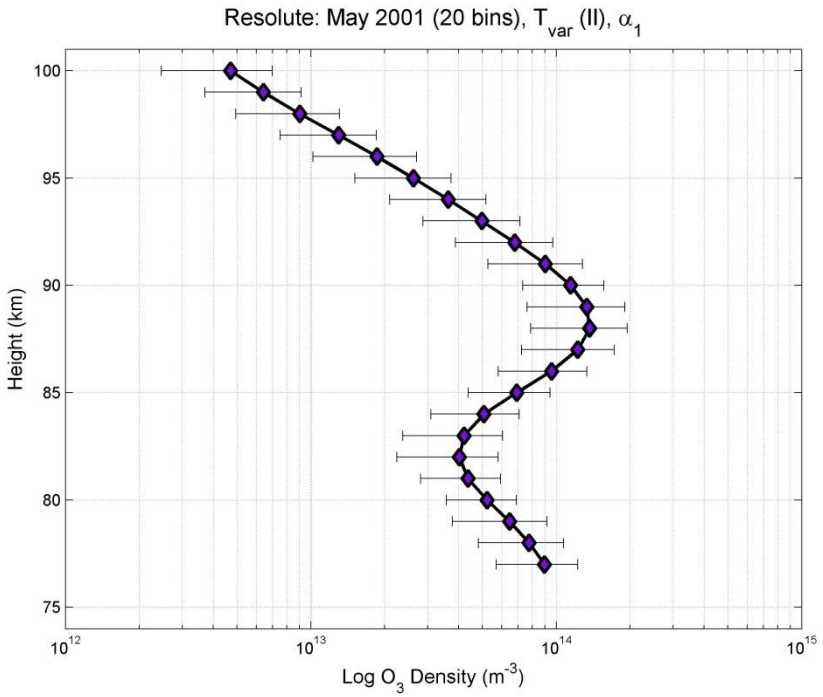

Figure 4.11: Log of ozone density as a function of height with error bars applied to resuts at incremental altitudes, for May, 2001, Resolute.

The full assessment of diurnal and to some extent seasonal variations of the ozone density in the MLT region has not been possible in this work, primarily due to insufficient density of data. The results reflect the mean monthly profiles of ozone in the MLT region between 78 and 100 km as it can be seen from the figures below (Figure 4.12a,b). Because of the diurnal averaging the high resolution in the vertical variation as well horizontal variations of the ozone profile as shown in Figure 4.13 is currently not accessible. However, that will be easily resolved when high density data is available on continuous basis from multiple sites in future studies. At the moment, this work can be considered just as a simple validation of the new successfully developed method that needs further refinement.

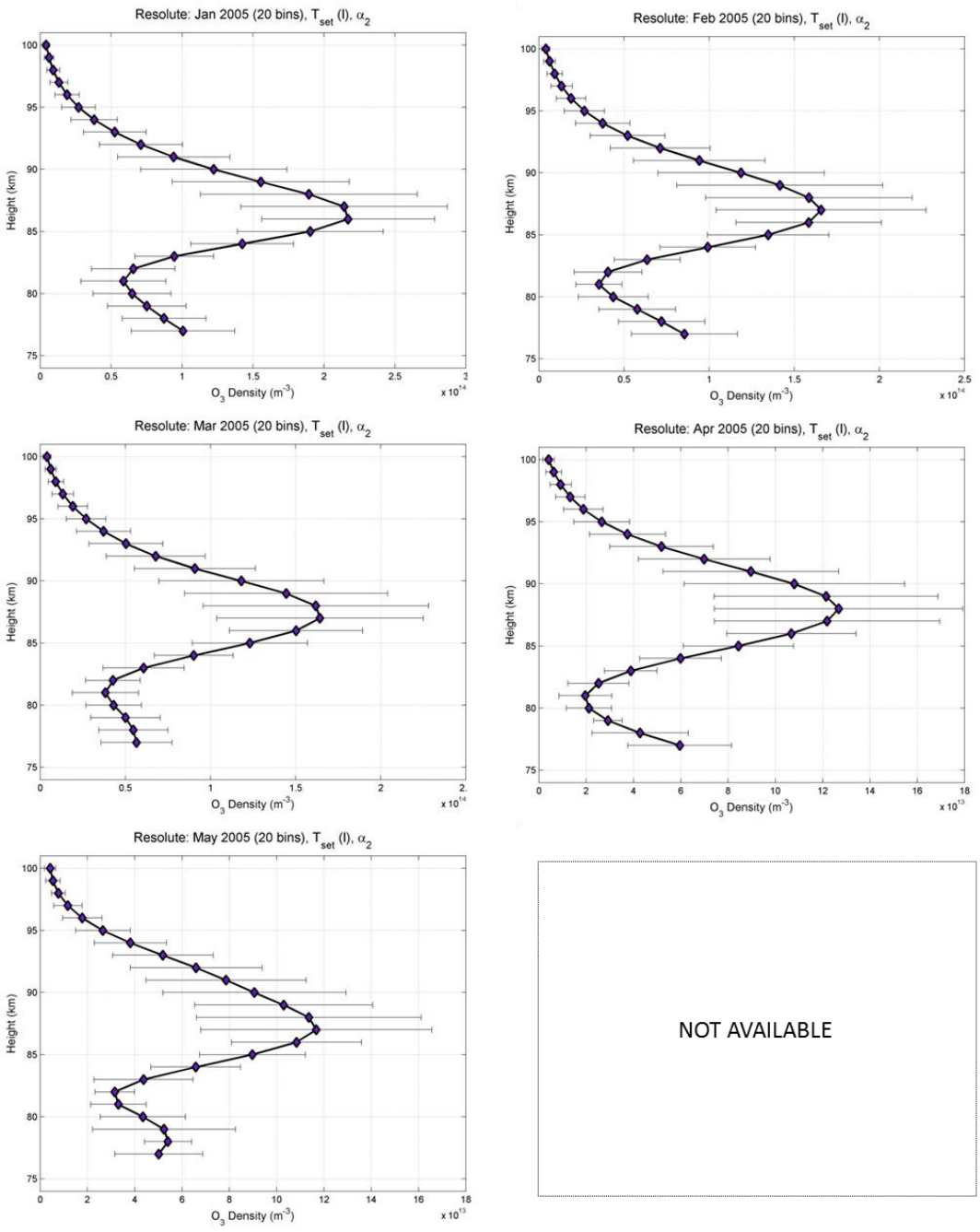

Figure 4.12: (a) The seasonal behaviour of the ozone density using mean time in calculations. Error bars are shown to illustrate uncertainty. Even with the use of the mean time in calculation results obtained for ozone density as a function of height and throughout year show considerable seasonal variations. The results are shown for 2005, Resolute Bay.

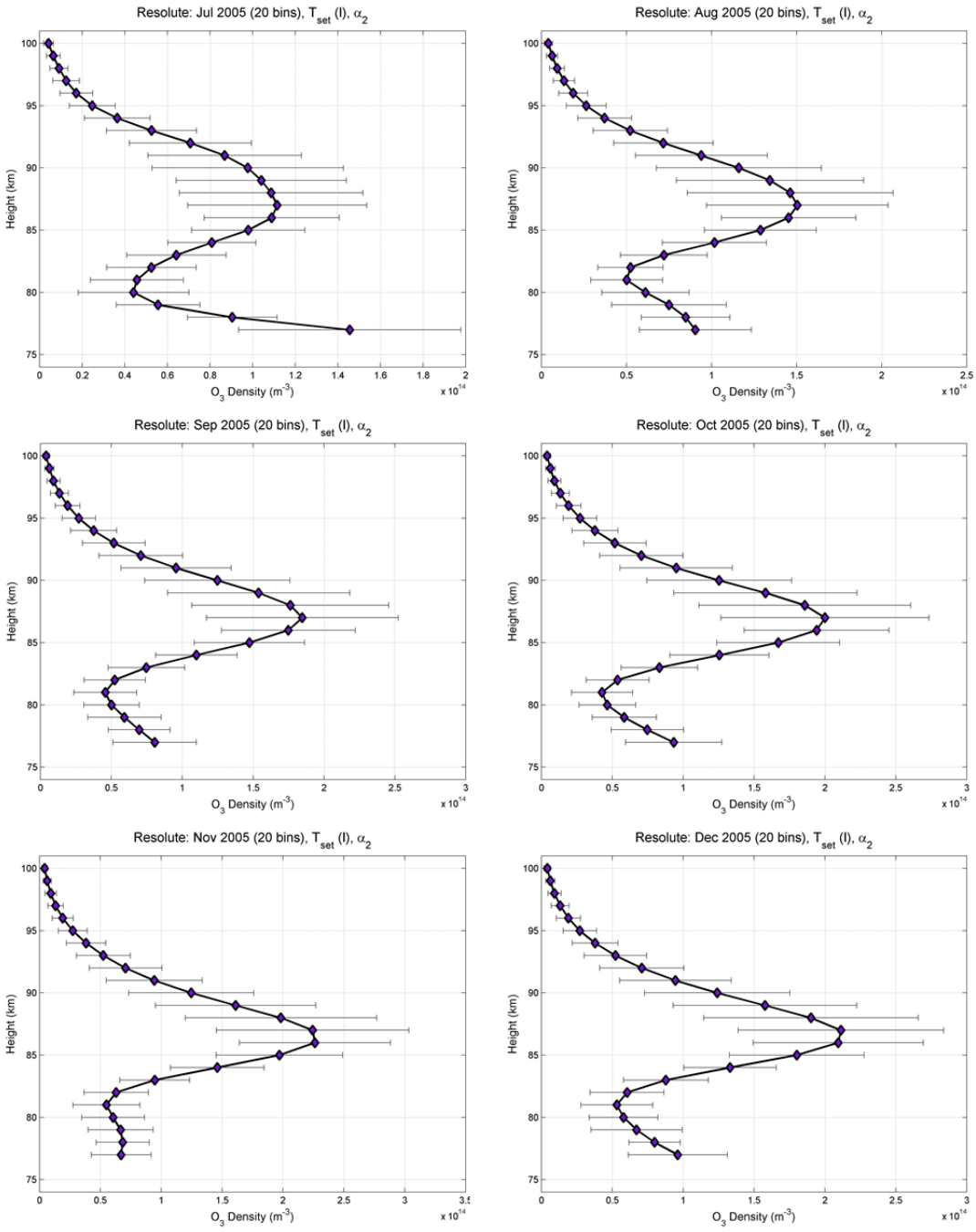

Figure 4.12: (b) The seasonal behaviour of the ozone density using mean time in calculations. Error bars are shown to illustrate uncertainty. Even with the use of the mean time in calculation results obtained for ozone density as a function of height and throughout year show considerable seasonal variations. The results are shown for 2005, Resolute Bay.

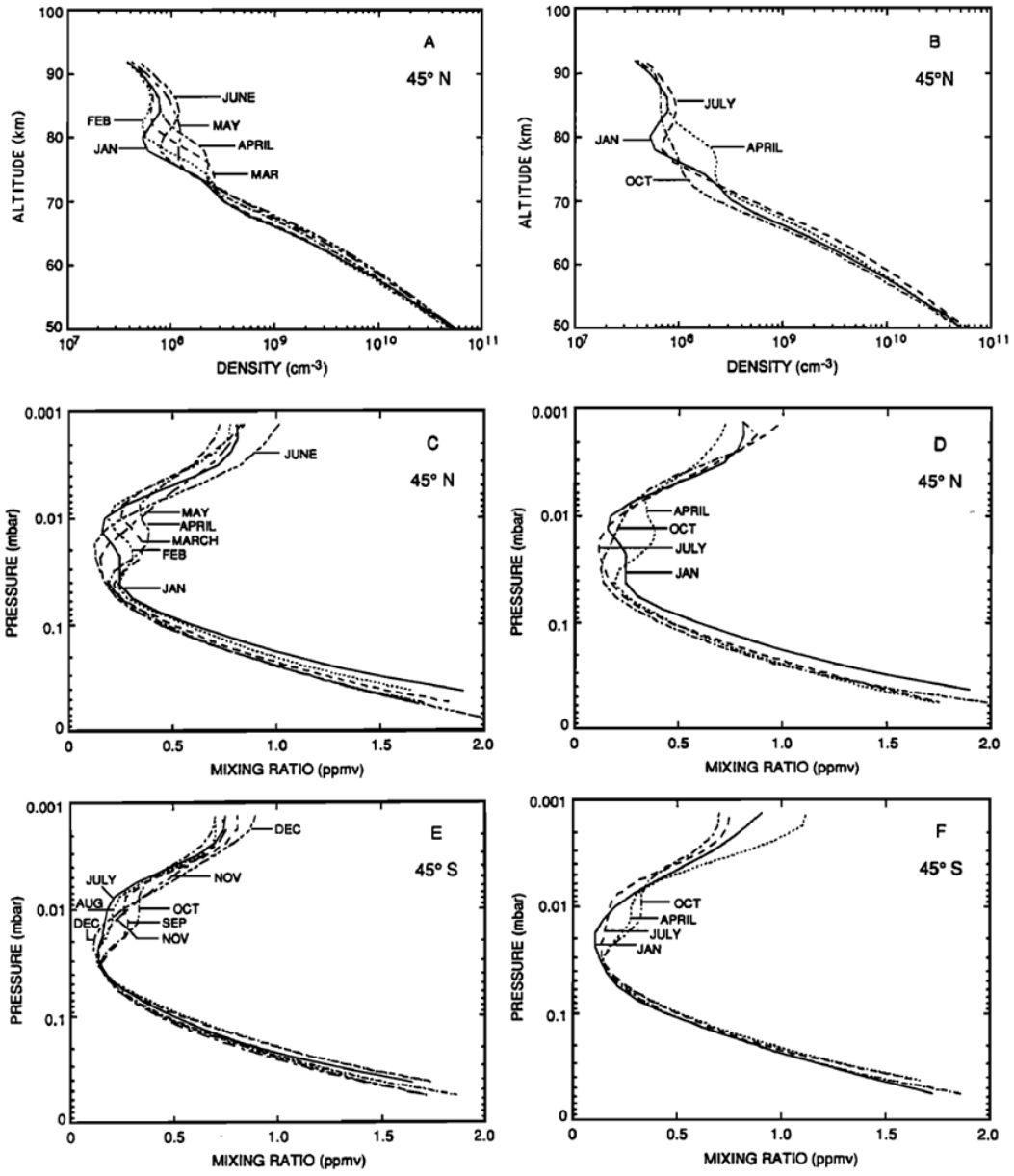

Figure 4.13: The seasonal variations in secondary ozone maxima in MLT region as a function of altitude as measured at 45° N. What can be immediately observed is vertical variation of the secondary ozone maxima as a function of season. The ozone density is plotted in Figures a) and b). In January and July the secondary maxima is near 85 km. The ozone mixing ratio is plotted against pressure in Figure c), d), e) and f). While data in Figure a) and c) are the same, the relationship between altitudes and pressure changes from month to month and does not correspond to a horizontal displacement of the combined Figures. The data in figure e) are from 45° S (displaced 6 months) so it can match to data from Figure c). The same relationship exists between Figure b), d) and f) (Thomas, 1990).

It should be acknowledged that it is difficult to get access to reliable satellite data for polar latitudes. Thus when the seasonal trend in ozone density was analyzed for Resolute Bay, there was significant doubt in the validity of the obtained results as the seasonal trend radically deviated from the know trends that exist in mid-latitudes (see Thomas, 1990; Rogers et al., 2012 for analysis). However, upon comparing the seasonal ozone trend observed in Resolute with the seasonal variations in echo duration times, observed by Singer et al. (2008) at 69° N, it was clear that calculated ozone densities above Resolute Bay are accurate as there is the well-known inverse relation between the echo duration time (Figure 4.14) and the ozone concentration (Figure 4.15).

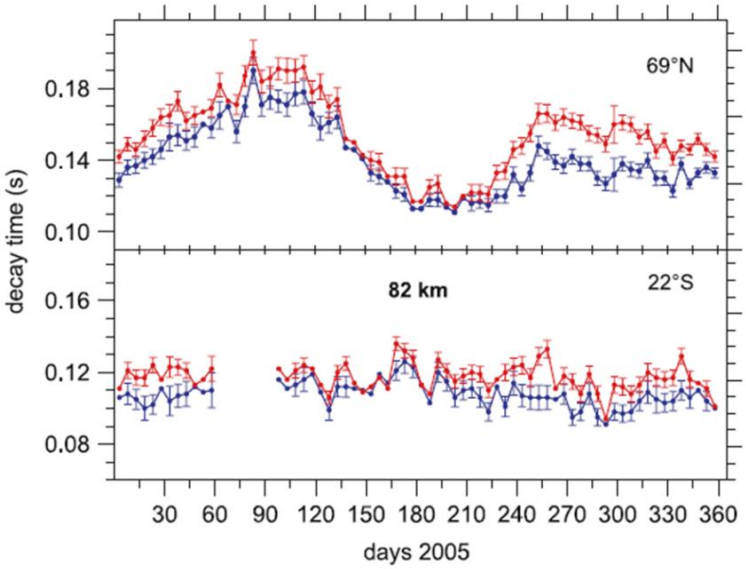

Figure 4.14: Seasonal variations of the meteor decay times at 82 km altitude observed by meteor radars at 69 N and 22 S. Decay times of strong meteors echoes are shown in red and decay times of weak echoes are in blue. An important thing to note is that while there are no measurements of seasonal variation of ozone in the far northern latitudes (i.e. Resolute Bay), this plot is interesting as it shows maximum duration times where seasonal ozone densities for Resolute Bay are the lowest, thus implying inverse relationship and indirectly confirming unusual seasonal mesospheric ozone trends observed at Resolute Bay (Singer et al., 2008).

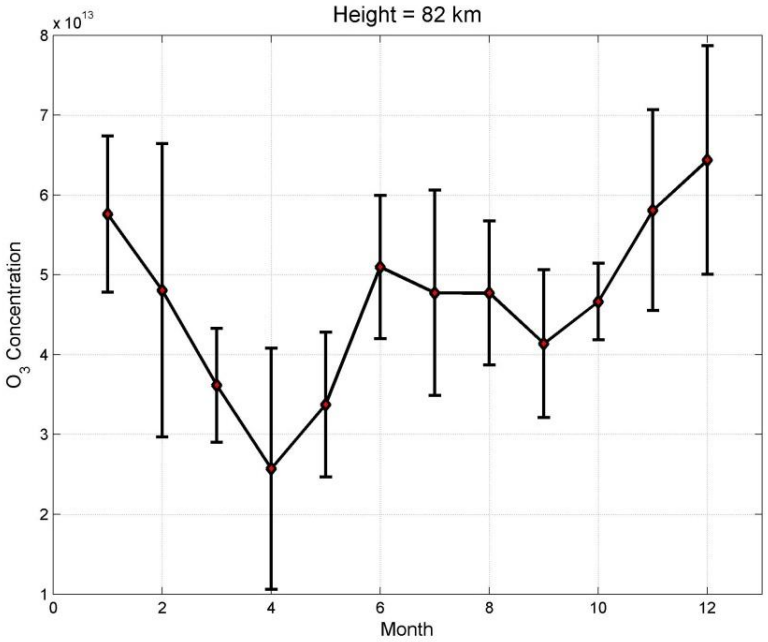

Figure 4.15: Seasonal variation of ozone density at altitude of 82 km, above Resolute Bay, obtained from the meteor radar observation of overdense meteor decay times. Error bars represent uncertainty in calculated results.

For the purpose of the assessment of annual trends, seasonal behaviour of ozone density is plotted as a function of altitude on the contour plot (Figure 4.16). The overall behaviour of ozone density observed from Resolute, above 84 km, starts to reasonably correspond to the trends observed at lower latitudes as observed by Thomas, (1990) and Rogers et al. (2012).

The comparison of ozone density with satellite measurements which show diurnal variation (Figure 4.17 and Figure 4.18) confirms the initial argument in this work, which suggested that only averaged monthly means of ozone density in the MLT region could be calculated with the available data resolution. This is indeed an additional validation of the work in this thesis and confirms again that with high data resolution, it will be possible to resolve diurnal ozone variations. The residuals plotted for comparison of nightly and daily variations of the satellite ozone data with the data obtained in this work (Figure 4.19(a-g)), show reasonably good behaviour considering that the extent of the diurnal variations can approach order of magnitude.

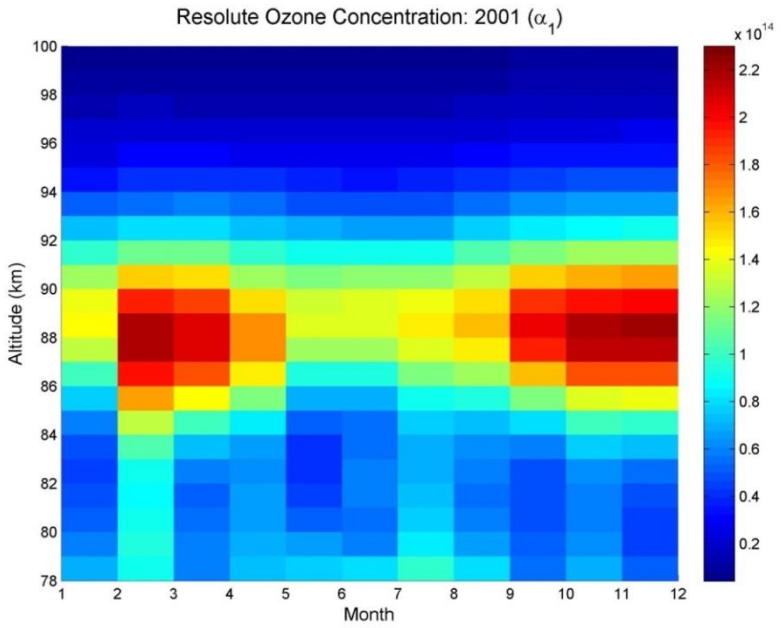

Figure 4.16: Seasonal density plot of ozone concentration as a function of altitude for 2001, Resolute Bay.

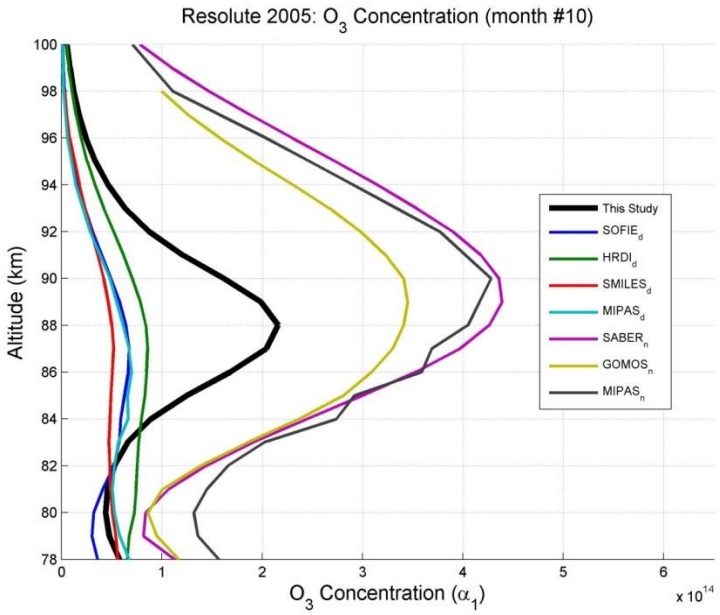

Figure 4.17: Ozone density profile measured in this work (black thick line) compared with satellite measurements for night density (lines on the far right) and daily densities (lines on the far left) as a function of height. The comparison agrees well with conclusion that this work was only able to evaluate monthly means in ozone density profile and could not account for diurnal variations. A note must be made at this point that diurnal satellite measurements are latitudinal averages, rather than region specific (for further details see Smith et al., 2013).

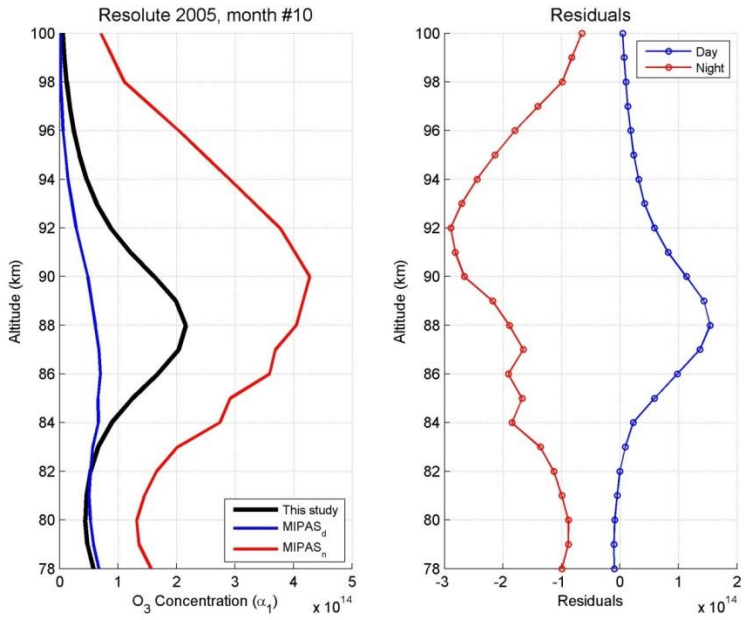

Figure 4.18: Left: Comparison of satellite and radar derived ozone profiles. Right: Residuals of the nightly and daily ozone values from satellite (MIPAS) compared to the values from this work for Resolute Bay.

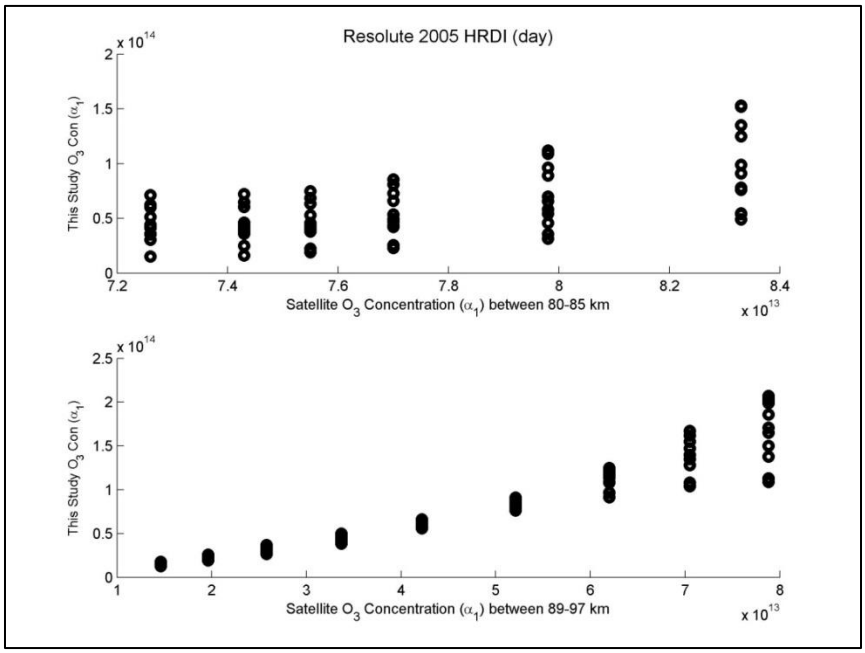

Figure 4.19: (a - g) For comparison and data validation, the regression plots of the data obtained in this work with daily and nightly variations from different satellites are presented above.

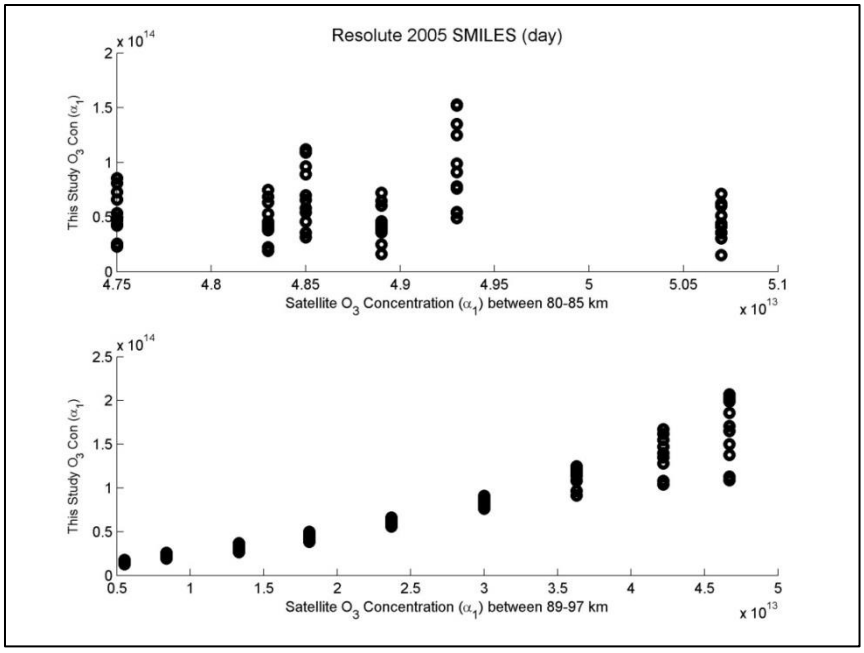

Figure 4.19: (b)

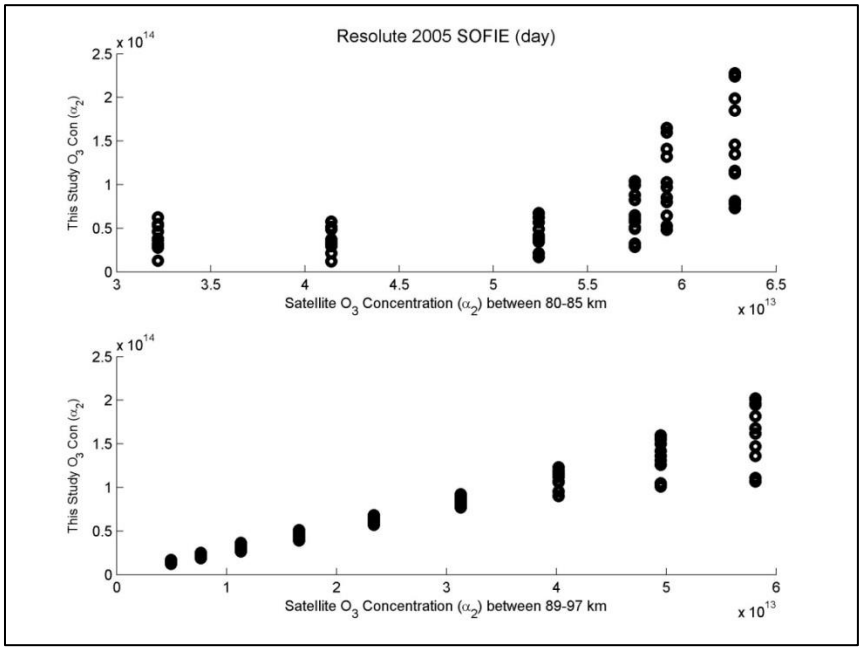

Figure 4.19: (c)

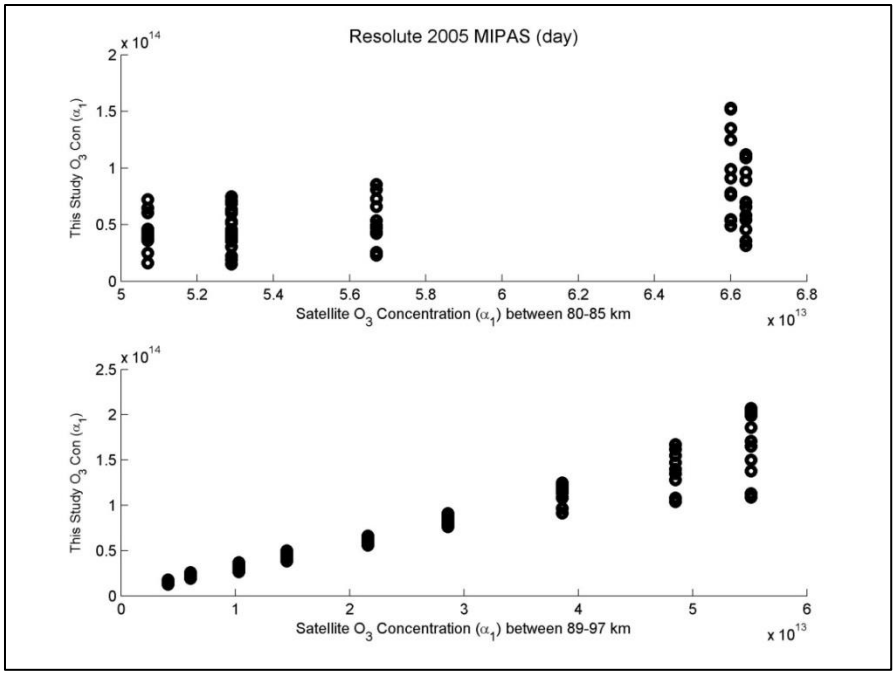

Figure 4.19: (d)

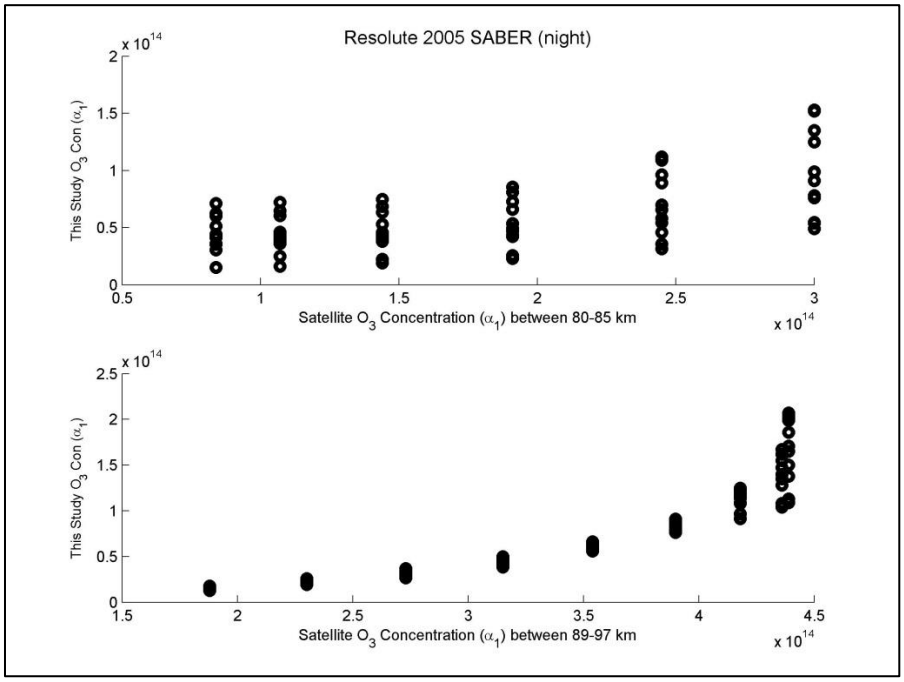

Figure 4.19: (e)

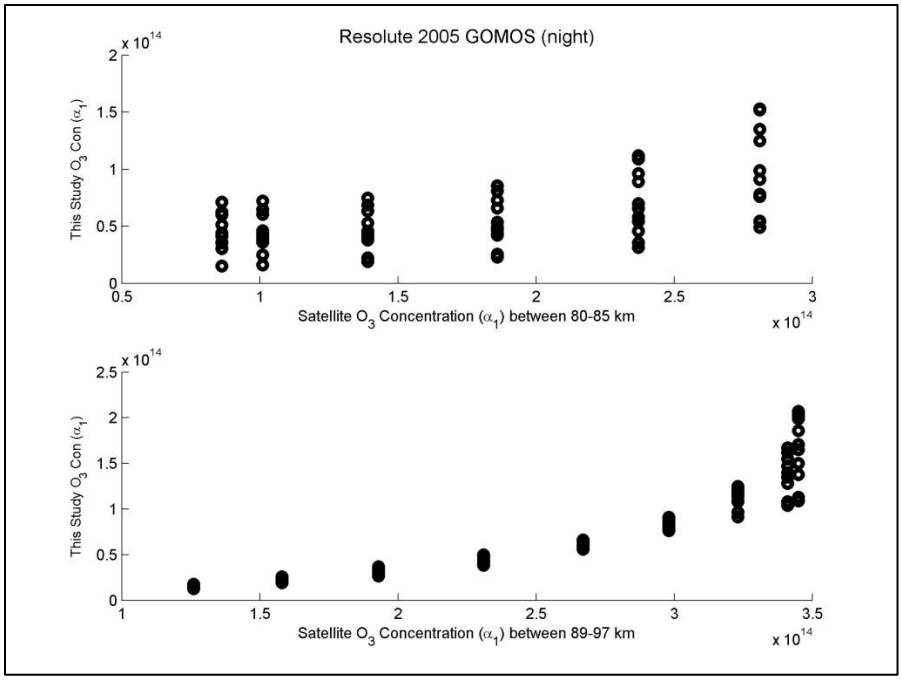

Figure 4.19: (f)

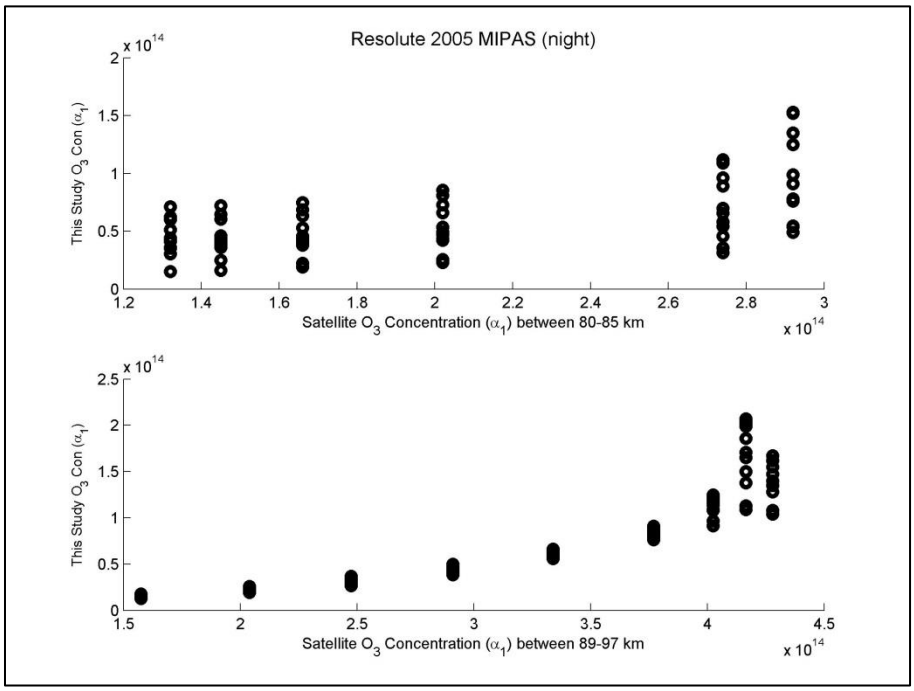

Figure 4.19: (g)

4.2 Yellowknife

Overall, the tabulated number of monthly events and subsequent initial assessment quality and usability of data for Yellowknife in Table 4.2 indicates poor performance. That is primarily due to the relatively low data resolution (i.e. low overall number of monthly meteor events). It is also conceivable that there is an inherent noise in the Yellowknife data; however that discussion is beyond the scope of this thesis. In principle however, while the overall Yellowknife meteor data cannot be used beyond reasonable doubt to evaluate ozone MLT concentration except several months in 2008 and 2009, it can be used as a relative benchmark for the poor quality data, to establish which data should not be used in calculations. Thus, this particular section will be focused on showcasing the contrast of the poorly constrained data and the results with well behaving examples.

Table 4.2: Table with number of total events for Yellowknife, where colour coding indicating the quality of the data during the initial processing. The legend is below the table. Yellowknife data, for the most part, is not of sufficient resolution and overall performance is not sufficient for meaningful calculation of ozone density.

Yellowknife	2002	2003	2004	2005	2006	2007	2008	2009
Jan	n/a	0	15338	16226	**17868**	5995	n/a	**30556**
Feb	n/a	1418	10156	11131	15745	2503	n/a	21702
Mar	n/a	3541	10344	10402	19833	n/a	n/a	**27948**
Apr	n/a	10200	**21274**	17343	27567	n/a	12478	34943
May	n/a	14087	**24219**	**29253**	40483	1500	38497	**37870**
Jun	**59141**	26909	35150	**59956**	50730	1009	**76669**	56179
Jul	**90675**	29249	6872	5151	**55336**	n/a	51112	**68497**
Aug	**69976**	23907	**21574**	**29597**	**35162**	n/a	**63289**	**85302**
Sep	n/a	17277	18667	**28850**	7590	n/a	**40762**	**55489**
Oct	n/a	19494	23013	***31968***	547	32	**34732**	44190
Nov	n/a	8659	18143	**27394**	2884	699	21920	**53122**
Dec	n/a	**20059**	18869	**38770**	6177	2721	**34721**	9913

Colour/Symbol	Legend
	Very Good Performing Data and Plots
	Good Behaviour
	Potentially Usable
	Not Usable
Bolded	Best Behaving Data
*	Outlier(s) Present

First, consider the well behaved duration time and noisy scattered time (Figure 4.20 and Figure 4.21) derived from the logarithmic plots of cumulative number of events versus echo duration times. The calculated ozone density from scattered time cannot be as reliable. While it is possible to statistically treat scattered time and apply a smoothing function of best fit, there will still be an unacceptable level of uncertainty in the derived results. In this work, a great effort was made to only calculate ozone from the well behaving profiles of duration times to ensure quality and repeatability of results.

For comparative purpose, the example of the initially calculated ozone profile, using a well behaved variable duration time compared with the noisy result derived from poorly constrained time is given below (Figure 4.22). The differences are apparent, especially when one considers that the well behaving ozone density results for the same months of different years exhibit virtually the same profile and densities (Figure 4.23). Such results, which clearly indicate that the number of removed electrons is seasonally matched in different years, further validate methods and results in this work.

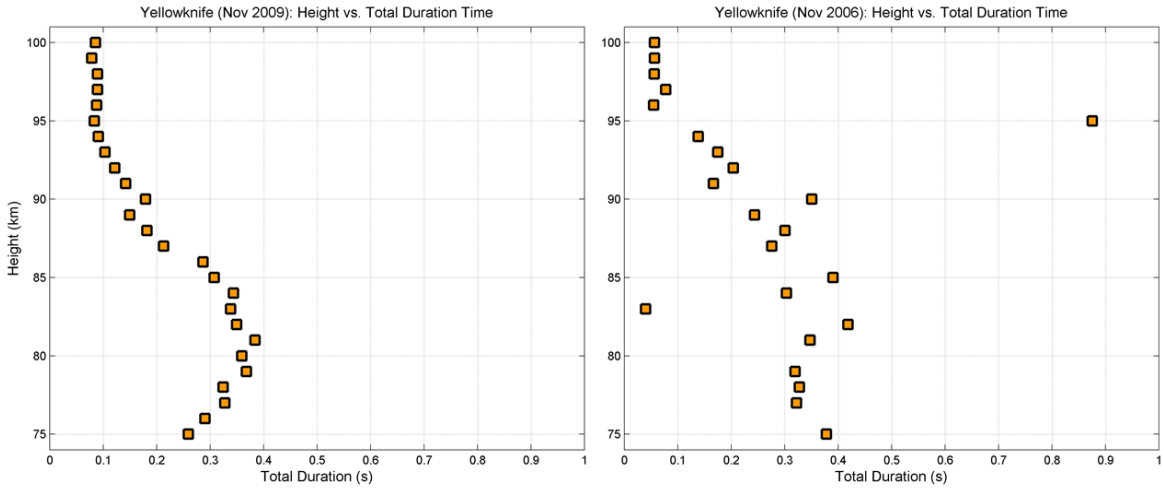

Figure 4.20: The example of well-behaved total duration times as a function of height, obtained from the logarithmic plot of the cumulative number of events vs. total echo durations, contrasted against the example of scattered and poorly behaved duration time for the month of November for 2009 and 2006.

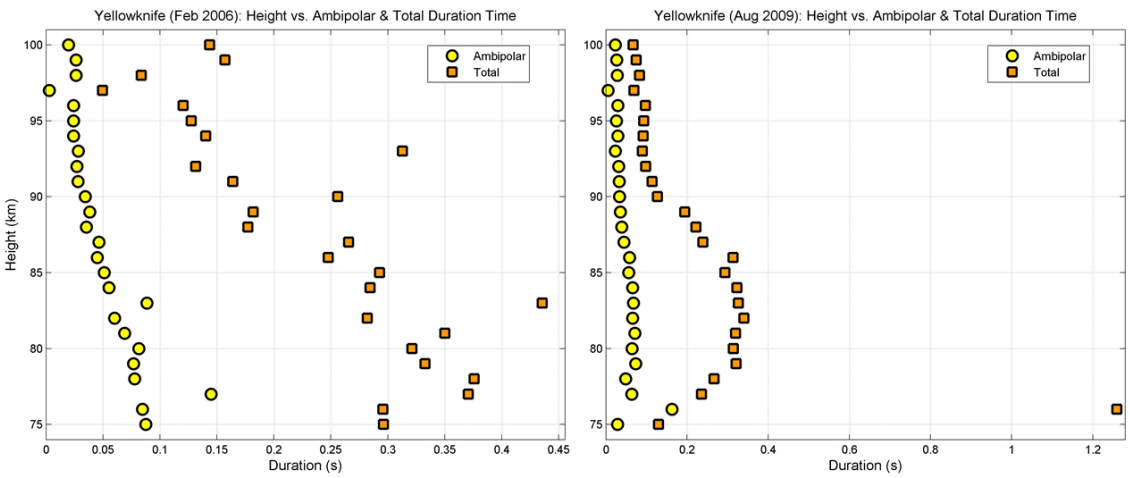

Figure 4.21: The scattered behaviour of the total duration plotted with reasonably behaved duration time for ambipolar diffusion regime as a function of height for February, 2006 (left) contrasted against the well behaved total and ambipolar diffusion duration times for August, 2009 (right).

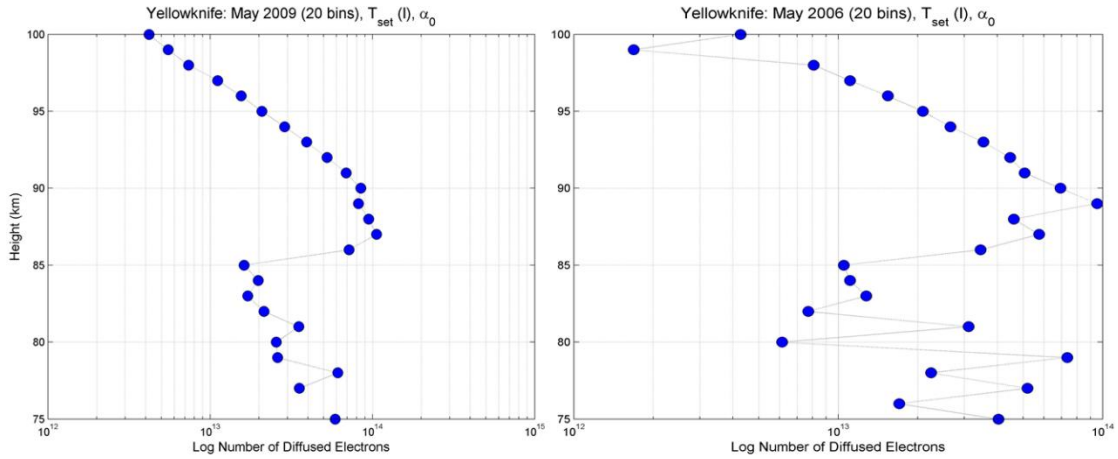

Figure 4.22: The example of the initially calculated number of removed electrons by hyperthermal chemistry regime, where on the left, the result was obtained from well behaved monthly meteor data (May, 2009) and on the right is the example of the poorly behaved result obtained from the month with problematic data (May, 2006).

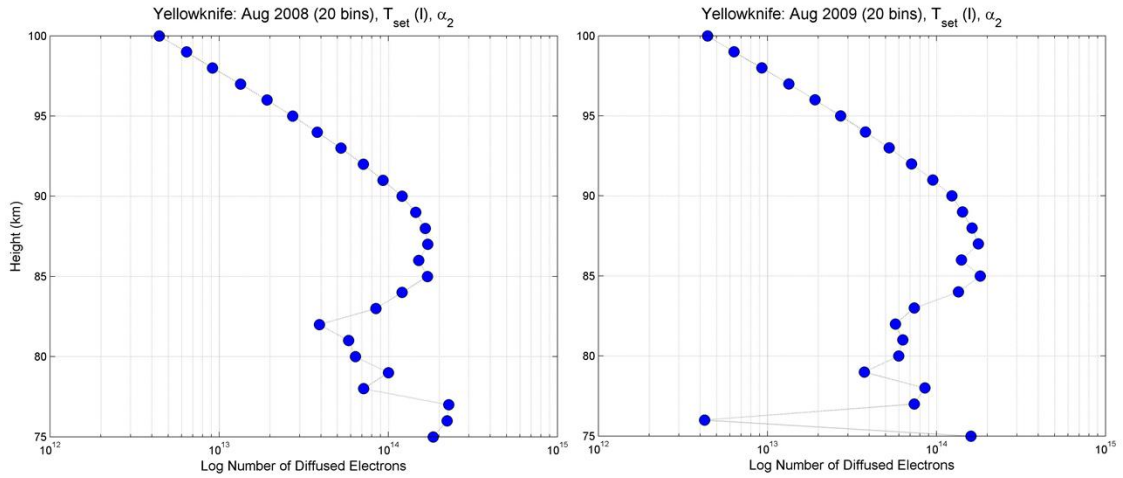

Figure 4. 23: The example of the matching quantitative and shape behaviour of the plots of the calculated hyperthermally removed electrons for the same moths of different years. (August, 2008 and 2009). Note that same behaviour is observed across all radar sites for the months which have well behaving data.

Furthermore, the primary reason for the rigorous use of only well constrained data, can be readily seen below (Figure 4.24), where the HCDC has been calculated from reasonably well behaving duration times and contrasted with the one calculated from scattered duration times profile.

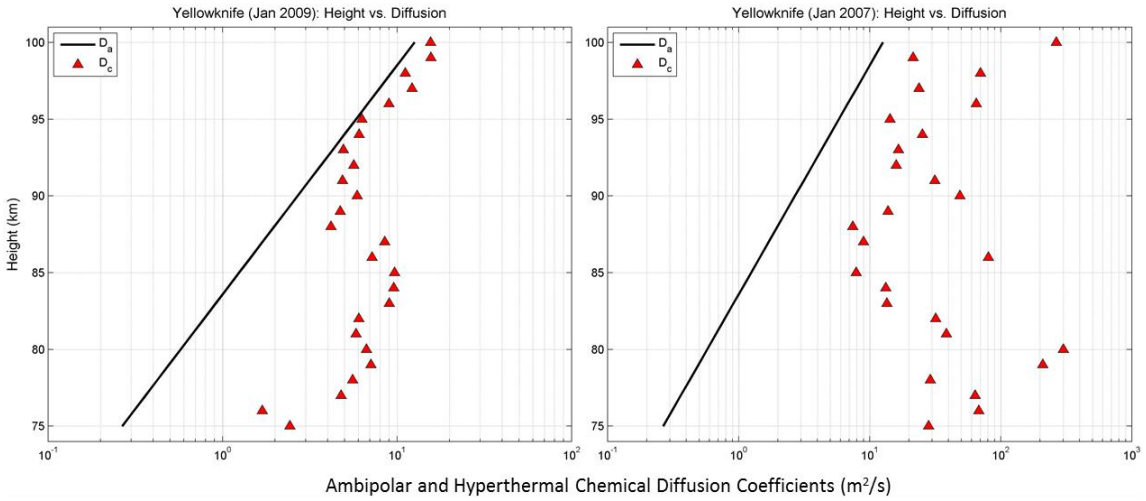

Figure 4.24: Contrasting behaviour of well constrained calculated hyperthermal chemistry diffusion coefficient plotted along theoretical ambipolar coefficient as a function of height, for January, 2009 (left) with poorly constrained and scattered one calculated for the January, 2007 (right).

In principle, well constrained meteor echo duration times will give well behaved profiles of ozone density as it can be seen in Figure 4.25.

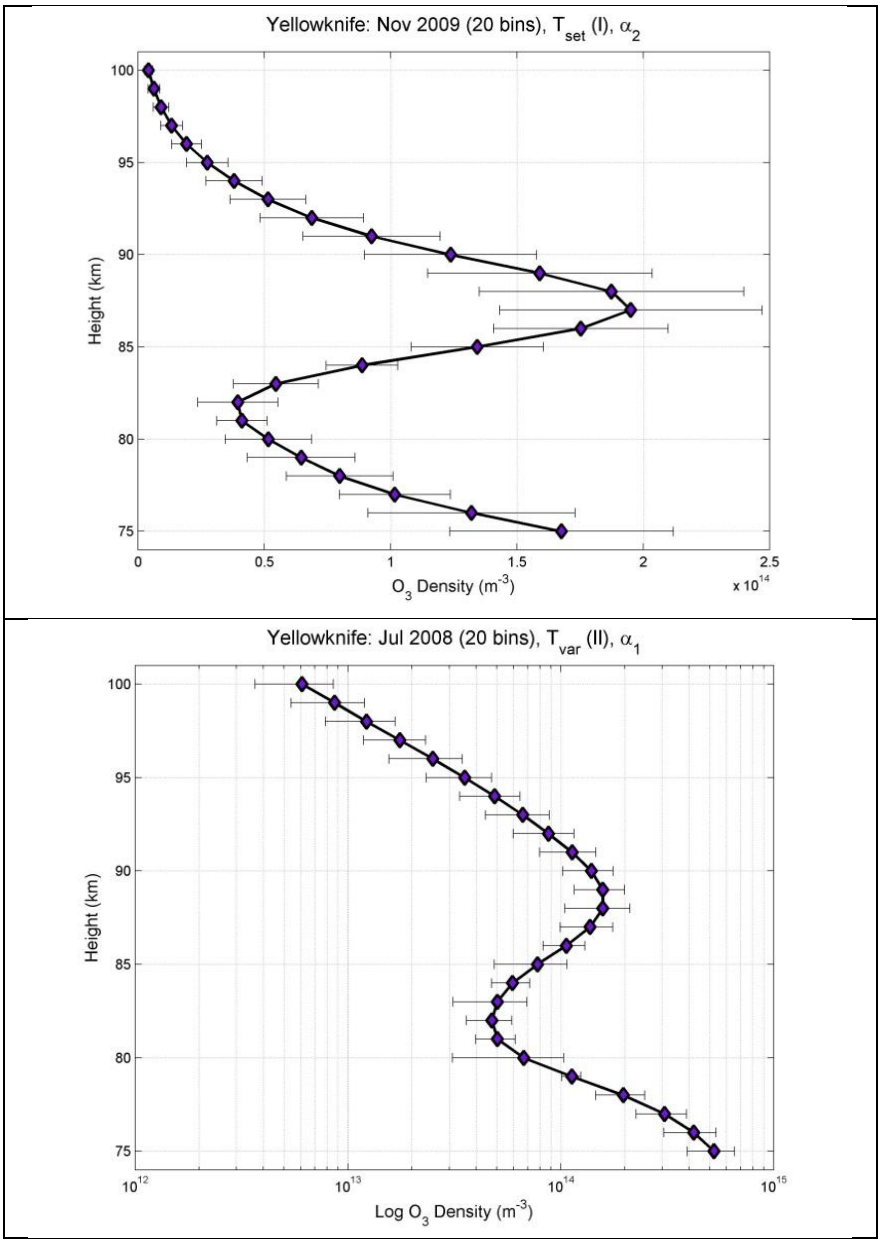

Figure 4.25: Representative examples of the obtained results calculated from the well behaved data. Upper figure: Ozone density calculated for November, 2009 using the mean time; Lower Figure: Log of calculated ozone density using variable time (from the log-log plot) for July, 2009 (Yellowknife).

Comparing the calculated results for Yellowknife in this study (for well behaving months) closely matches the seasonally and latitudinally averaged satellite ozone profiles (Figure 4.26). However, it must be noted that the obtained results of ozone density from Yellowknife are in general greater than the averaged satellite profiles, which is reasonable considering high latitude of the radar site.

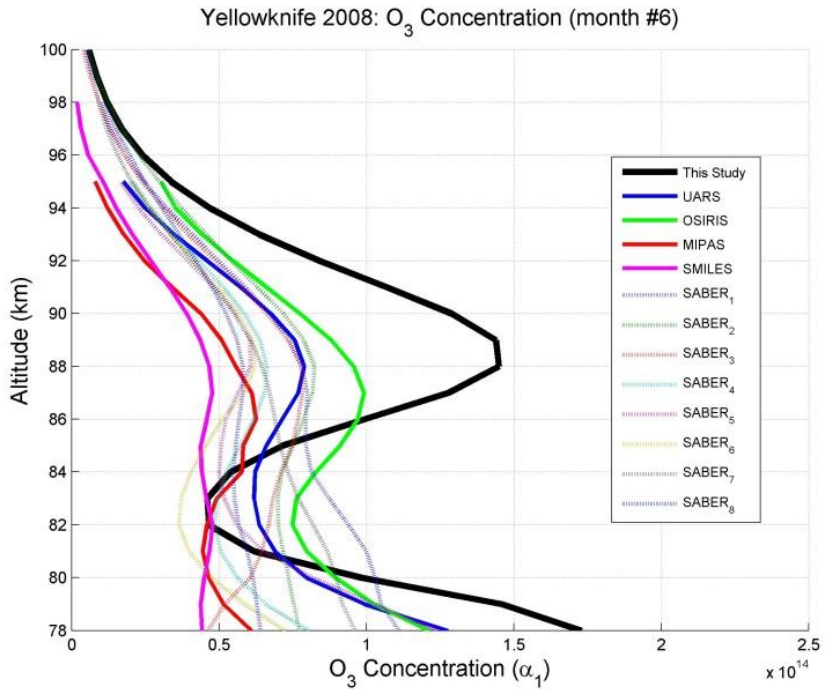

Figure 4.26: The calculated ozone density for the month of June, 2008, Yellowknife, compared with latitudinally and seasonally averaged data from different satellites. The immediate trend in all Yelloknife results suggests that calculated values for ozone density in the MLT region are higher than averaged satellite values.

The comparison of nightly and daily satellite ozone density profiles with ozone results obtained from the Yellowknife meteor radar shows reasonably good agreement, with notable observation that satellite nightly profiles are in general show much greater deviation from the mean monthly profiles obtained in this work, especially when compared with the daily satellite ozone values (Figure 4.27).

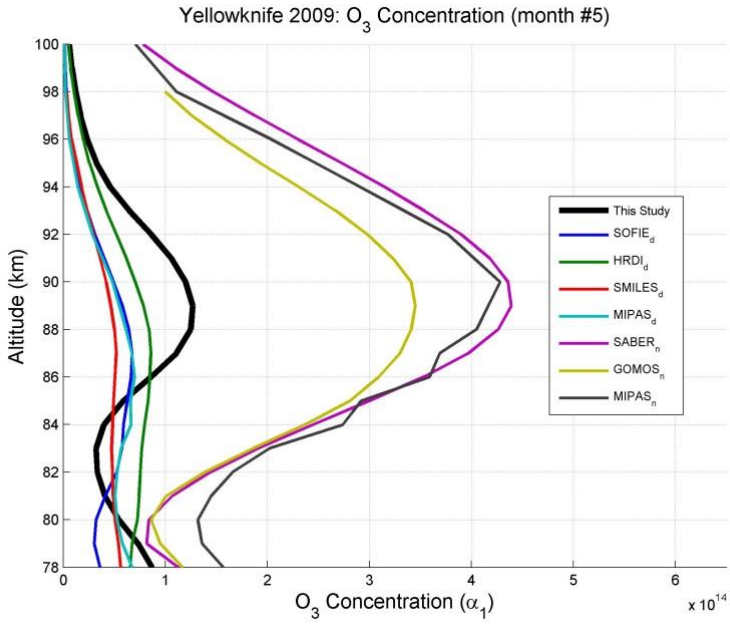

Figure 4.27: Daily and nightly ozone density profiles obtained from different satellites compares with the ozone density as a function of height, for May, 2009, Yellowknife.

The residual values between the satellites (SOFIE and MIPAS) daily and nightly profiles and the mean monthly profile calculated for January, 2009 and July, 2008, Yellowknife, are given below in (Figures 4.28 and Figure 4.29) for comparative purpose.

The regression plots comparing Yellowknife ozone density results with daily, nightly and averaged values obtained from different satellites generally exhibit reasonably good trend. The example can be seen in Figure 4.30a,b.

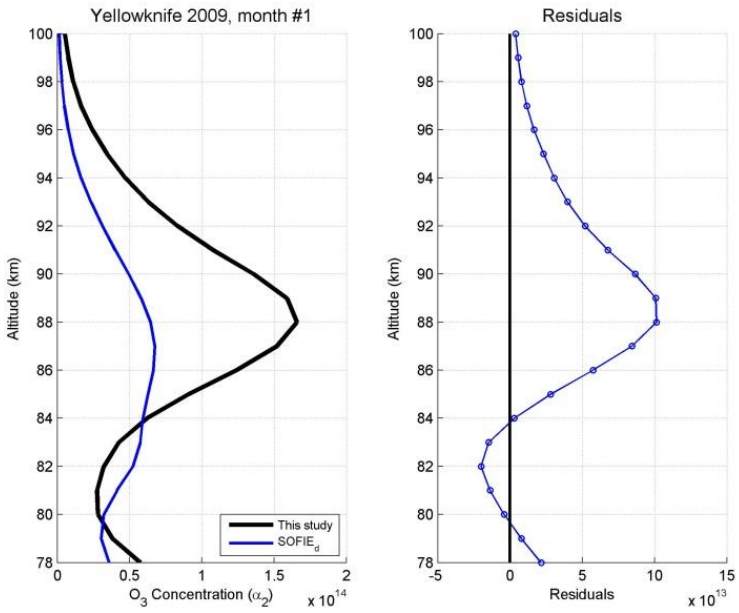

Figure 4.28: Left: Comparison of satellite and radar derived ozone profiles. Right: The residuals between SOFIE longitudinally and seasonally averaged ozone density values as a function of height and the ozone density profiles for January, 2009, Yellowknife.

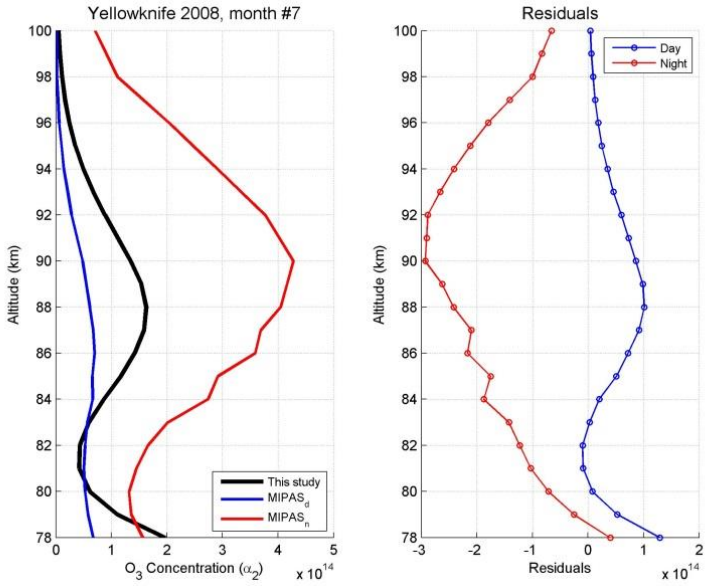

Figure 4.29: Left: Comparison of satellite and radar derived ozone profiles. Right: Daily and nightly residuals between MIPAS ozone profiles and results obtained for July, 2008, Yellowknife.

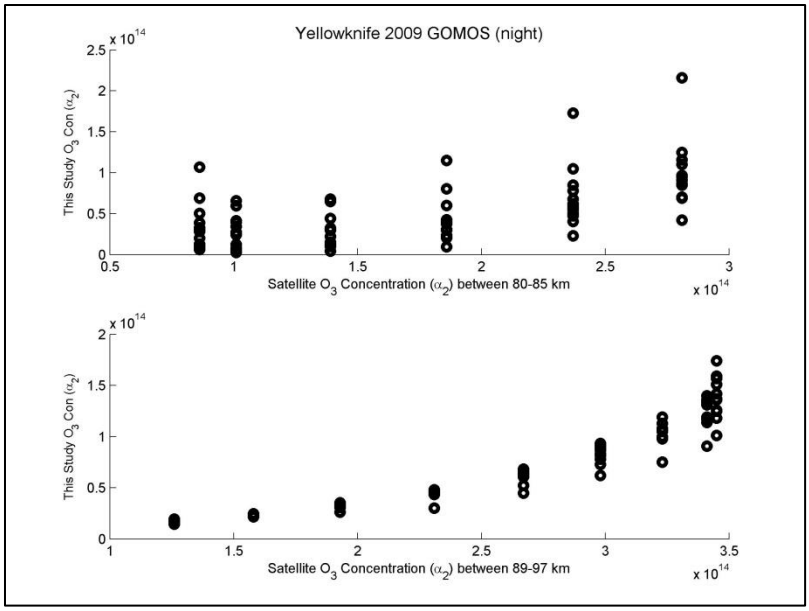

Figure 4.30: (a) Regression plots of GOMOS (nightly) ozone density comparison with 2003 and 2009 Yellowknife ozone data. Reasonably good trend can be seen in both.

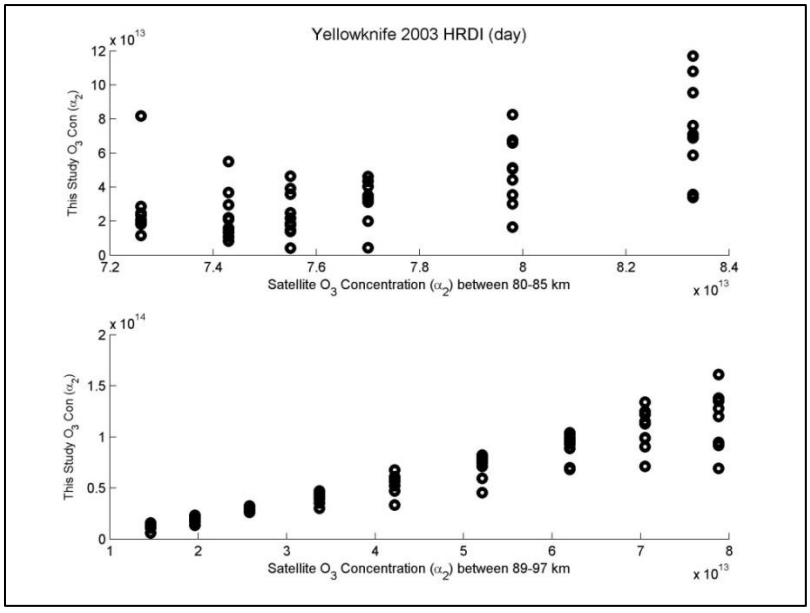

Figure 4.30: (b) Regression plots of HRDI (daily) ozone density comparison with 2003 and 2009 Yellowknife ozone data. Reasonably good trend can be seen in both.

4.3 CLOVAR

In terms of overall numbers, CLOVAR is the worst performing site in this study. However, considering CLOVAR's meteor radar intermittent operation over the period in which the data were collected for this study, it should be acknowledged that the overall performance of the "good" data, from the several selected well behaving months is very satisfactory. There is much less pronounced noise in obtained "good" data, relative to the Yellowknife radar, which strongly suggests that upon reconstruction, CLOVAR will be an excellent location for future meteor studies, at least in terms of reduced signal noise pollution.

From the plots of satellite daily and nightly ozone profiles compared with selected months for CLOVAR (Figure 4.31 and Figure 4.32), it can be seen that the overall results calculated here for well behaving months are satisfactory and in good agreement with satellite ozone values.

Table 4.3: Number of total events for CLOVAR, where colour coding indicating the quality of the data during the initial processing. The legend is below the table.

Clovar	2000	2001	2002	2003	2004	2005	2006	2007	2008
January	n/a	11848	12675	16651	n/a	n/a	n/a	n/a	2716
February	n/a	n/a	9763	10237	n/a	n/a	n/a	n/a	6346
March	n/a	n/a	8825	8060	n/a	n/a	n/a	n/a	10385
April	n/a	n/a	**13038**	12327	n/a	n/a	n/a	n/a	7036
May	n/a	n/a	14336	14406	n/a	n/a	n/a	n/a	706
June	n/a	n/a	**7966**	**22595**	n/a	n/a	n/a	n/a	11830
July	12693	n/a	12700	19985	n/a	n/a	n/a	n/a	5027
August	**25311**	n/a	**13262**	**24278**	n/a	n/a	n/a	n/a	6072
September	**20877**	n/a	6444	19538	n/a	n/a	n/a	n/a	9430
October	**16436**	n/a	6448	5585	n/a	n/a	n/a	n/a	**13582**
November	**16916**	10723	**14491**	n/a	n/a	n/a	n/a	n/a	n/a
December	13592	**15221**	17200	n/a	n/a	n/a	n/a	11008	n/a

Colour/Symbol	Legend
	Very Good Performing Data and Plots
	Good Behaviour
	Potentially Usable
	Not Usable
Bolded	Best Behaving Data
*	Outlier(s) Present

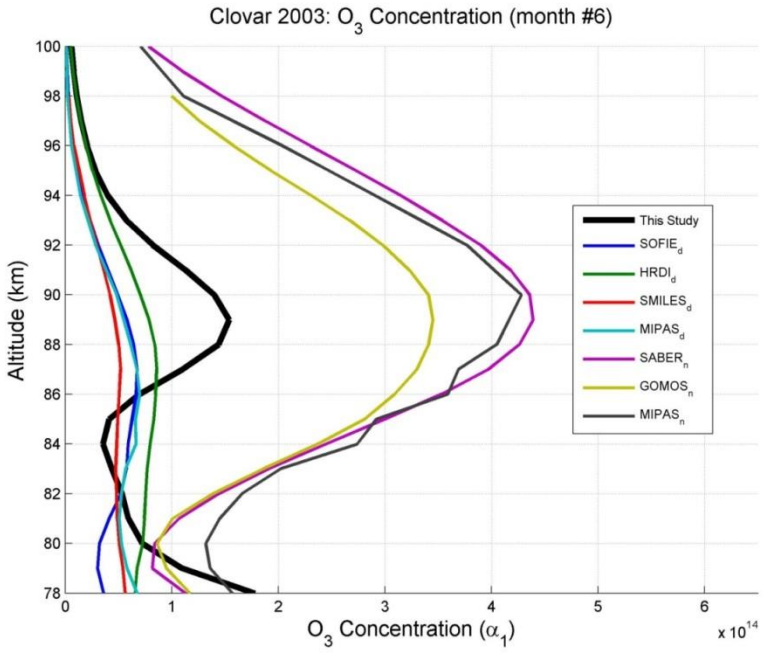

Figure 4.31: Daily and nightly ozone density profiles from different satellites compared with the calculated values for Jun 2003, CLOVAR.

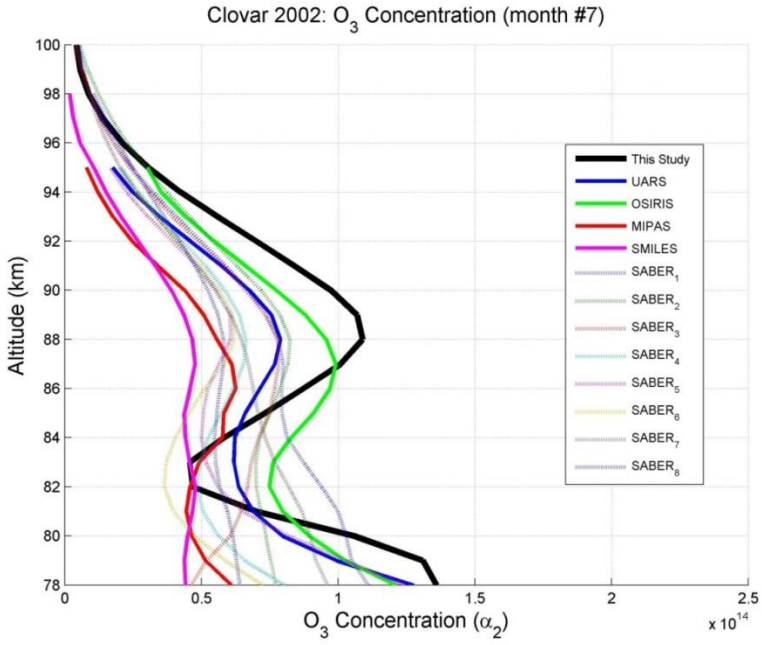

Figure 4. 32: Ozone density profile for July 2002, CLOVAR, compared with seasonally and latitudinally averaged satellite ozone density profiles.

4.4 Socorro

Socorro is the best performing radar site in this study in terms of number of monthly meteors and overall continuity of data (Table 4.4). Considering the number of meteor events recorded on a monthly basis, Socorro is among the best candidates, at least in terms of radar sites covered in this study, that can be utilized in the future for ongoing and continuous measurements of the MLT ozone density.

Table 4. 4: Number of total events for Socorro, where colour coding indicating the quality of the data during the initial processing. The legend is below the table.

Socorro	2002	2003	2004	2005	2006	2007	2008	2009	2010	2011	2012
January	n/a	n/a	n/a	*178226	n/a	n/a	n/a	***123628**	96484	***98773**	*87998
February	n/a	n/a	n/a	*165082	n/a	n/a	n/a	***90408**	***113728**	40060	***65393**
March	n/a	**28039**	n/a	***157749**	n/a	n/a	n/a	**97362**	141192	*67999	***74121**
April	14023	**39308**	n/a	**181758**	n/a	n/a	n/a	**60773**	142523	*81420	**79456**
May	***56287**	n/a	n/a	**199227**	n/a	***135817**	n/a	26692	**173761**	*40023	6417
June	39621	n/a	n/a	***156878**	n/a	**194117**	*95756	***77572**	**179169**	***49186**	n/a
July	24792	n/a	n/a	***137236**	n/a	***268842**	***201491**	**226099**	*221713	***80654**	n/a
August	***75971**	n/a	n/a	13314	n/a	1811	35037	**223481**	***206086**	***96388**	n/a
September	45049	n/a	n/a	n/a	n/a	n/a	n/a	**220553**	**195605**	***128871**	n/a
October	*54472	n/a	n/a	n/a	n/a	87	n/a	**212730**	**189781**	***157468**	n/a
November	7729	n/a	n/a	n/a	n/a	n/a	n/a	**160076**	**144696**	**110808**	n/a
December	n/a	n/a	n/a	n/a	n/a	n/a	*110706	112954	112653	***119223**	n/a

Colour/Symbol	Legend
	Very Good Performing Data and Plots
	Good Behaviour
	Potentially Usable
	Not Usable
Bolded	Best Behaving Data
*	Outlier(s) Present

For the most part, the obtained and calculated parameters from the Socorro meteor radar are well constrained and well behaved, without too much scatter or noise (Figure 4.33). That allows a high level of confidence in the final ozone density calculation.

Furthermore, the method of obtaining duration time from the logarithmic plot of cumulative number of events vs. echo duration times for the each specific height increment enables more straight forward determination of echo duration times and gives more constrained values relative to the statistical averaging based on the number density of observed meteor events and their duration times as shown in Figure 4.34.

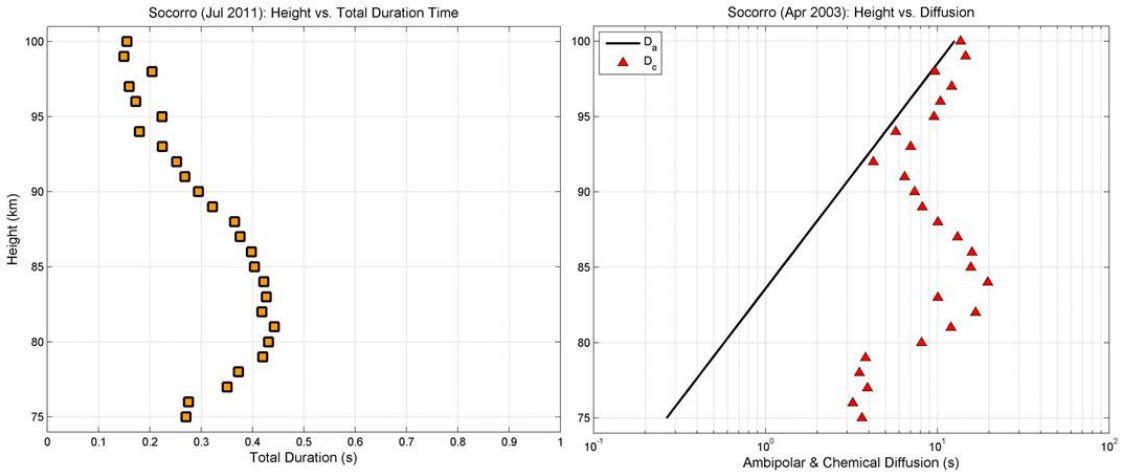

Figure 4.33: Right: The well behaved duration time for July, 2011, Socorro derived from the logarithmic plot of cumulative number of events versus echo duration times for specific height increments. Left: The ambipolar diffusion coefficient compared with calculated hyperthermal chemistry diffusion coefficient as a function of height for April 2003, Socorro.

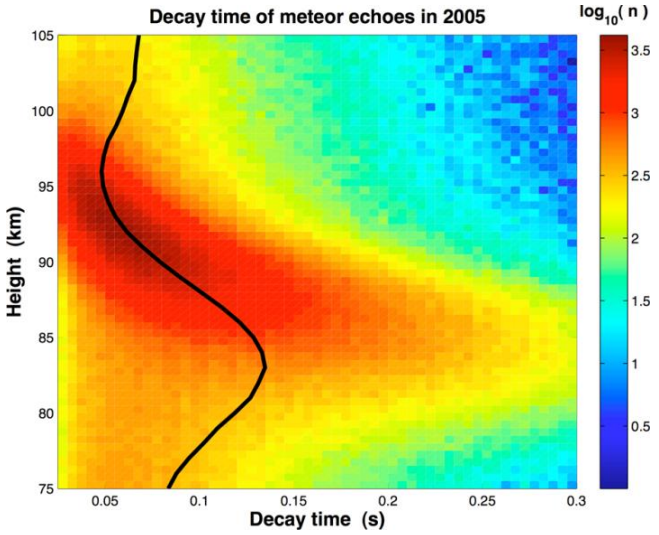

Figure 4.34: Decay time versus height of all meteors during 2005 from Ballinger et al. (2008). Color shading indicates the number of meteors, n (per 500m×5 ms window). The solid line indicates the mean decay time (Ballinger et al., 2008).

Further validation of the quality of the ozone density calculation comes from comparison of seasonal trends with the already known and proven values for similar geographical coordinates (Figures 4.35). The seasonal trend in ozone density obtained in this study by

using meteor radar and overdense echo durations closely matches the results obtained by Rogers et al. (2012) (Figure 4.36).

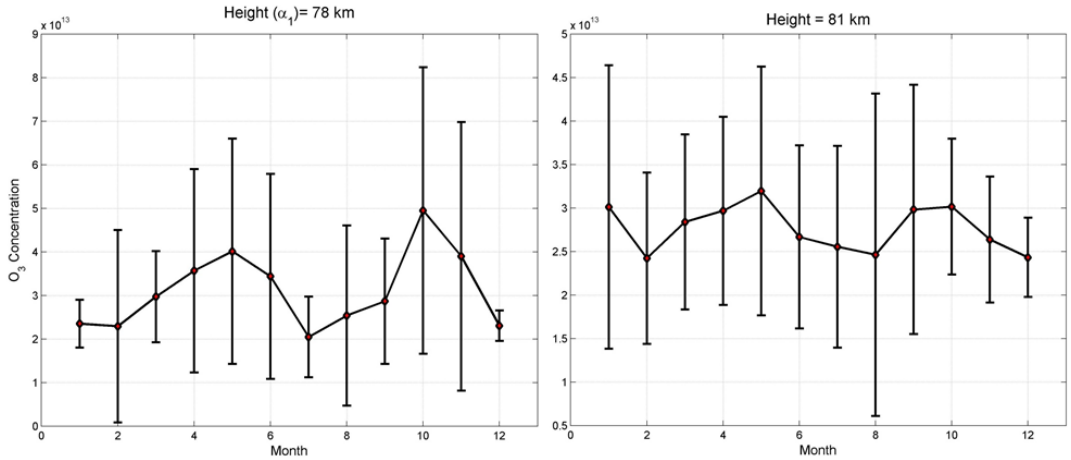

Figure 4.35: Ozone seasonal density profiles for 78 and 81 km altitude determined for Socorro.

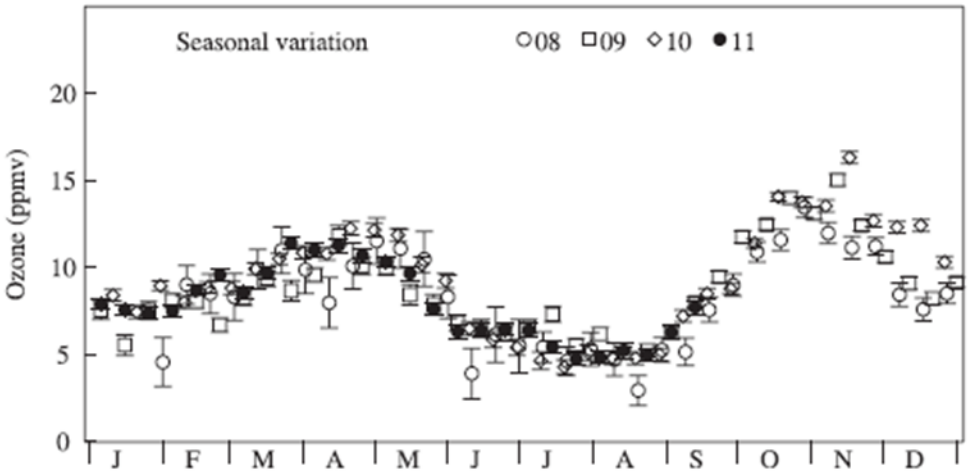

Figure 4.36: Seasonal variation of mesospheric ozone concentration above 80 km for a region centered at 38° N (Rogers et al., 2012).

Further comparison of the ozone density profiles obtained by backscatter meteor radar with the available satellite data for daily and nightly variations, along with comparison with seasonally and latitudinally averaged values, show excellent agreement (Figure 4.37 and Figure 4.38).

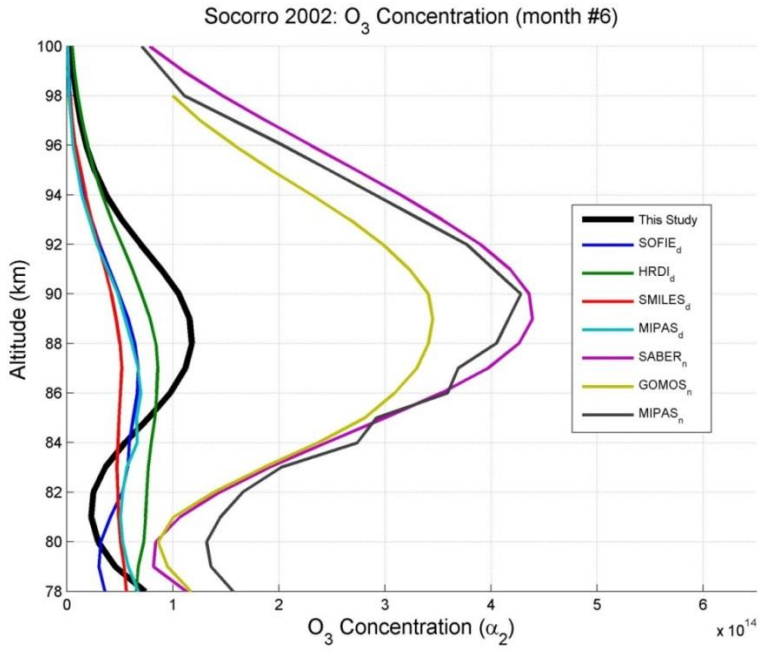

Figure 4.37: Daily and nightly ozone density profiles compared with the results obtained in this work for June, 2002, Socorro.

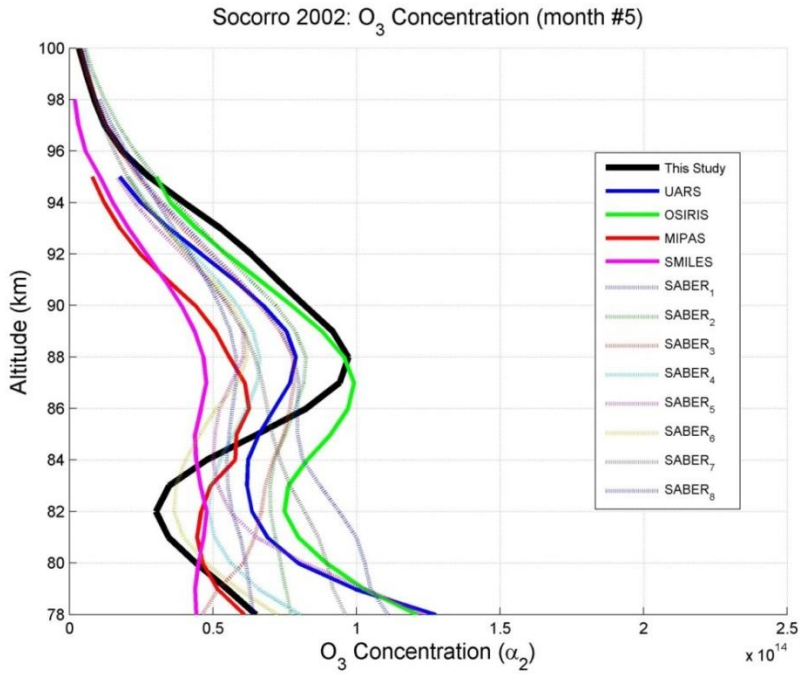

Figure 4.38: Seasonally and latitudinally averaged satellite ozone density profiles compared with calculated values for May, 2002, Socorro.

For illustrative purpose the residuals between ozone density profiles obtained for October, 2002, Socorro, and the daily and nightly values profiles from MIPAS are presented in Figure 4.39. The surface plot of the seasonal ozone density variation for Socorro (Figure 4.40) is in line with already known trends (Rogers et al., 2012).

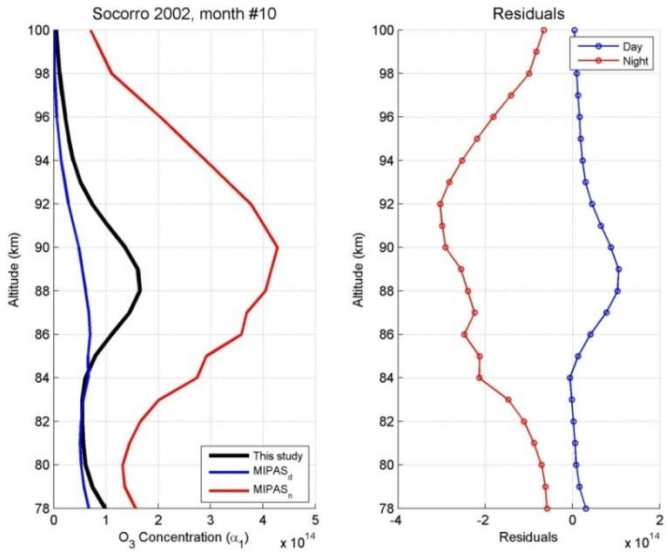

Figure 4.39: Left: Comparison of satellite and radar derived ozone profiles. Right: Residuals for MIPAS daily and nightly ozone profiles compared with the ozone values obtained in this work for October, 2002, Socorro.

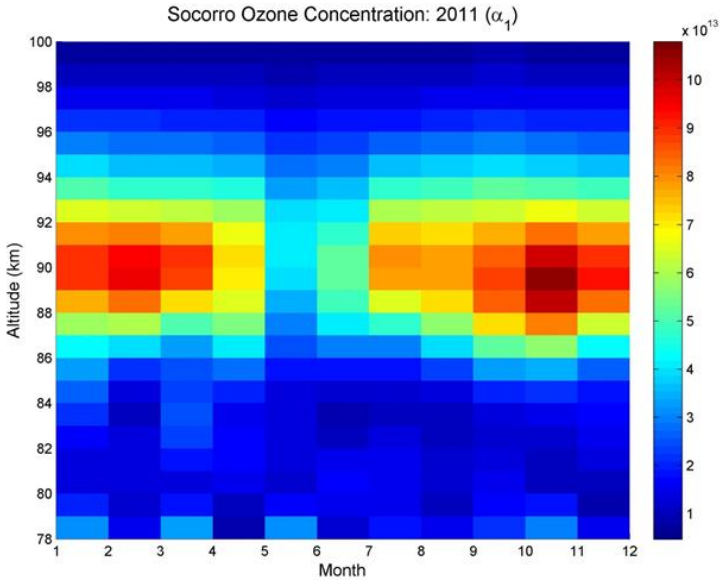

Figure 4.40: Seasonal density plot of ozone concentration as a function of altitude for for 2011 Socorro.

4.5 Costa Rica

In terms of overall data performance, Costa Rica can be considered satisfactory. While the monthly meteor data rate was sporadic for the most part, those months with a sufficient number of meteor events show reasonably good behaviour in terms of data quality (Table 4.5).

Table 4.5: Number of total events for Costa Rica, where colour coding indicating the quality of the data during the initial processing. The legend is below the table.

Costa Rica	2005	2006	2007	2008	2009	2010
Jan	n/a	**74354**	n/a	***77957**	n/a	1165
Feb	n/a	n/a	n/a	50555	n/a	8470
Mar	n/a	n/a	n/a	51677	9468	*32239
Apr	33444	n/a	34964	***47494**	28	23412
May	81261	n/a	***87644**	***75746**	52	1090
Jun	76981	n/a	***89015**	***69158**	n/a	***20495**
Jul	**93820**	n/a	**89271**	66958	38	10387
Aug	80685	n/a	70725	26254	3368	19616
Sep	**59694**	n/a	51515	*44488	7444	**24072**
Oct	**73872**	n/a	*58349	36351	***55201**	*25871
Nov	38731	n/a	33025	27848	430	8336
Dec	***52619**	n/a	***33024**	1371	n/a	1

Colour/Symbol	Legend
	.... Very Good Performing Data and Plots
	Good Behaviour
	Potentially Usable
	Not Usable
Bolded	Best Behaving Data
*	Outlier(s) Present

From looking at the Costa Rica meteor radar derived ozone data and its relative comparison to values obtained at the rest of radar locations in this study, it can be concluded that the overall ozone density is decreasing with decreasing latitude, and is lowest in the MLT above Costa Rica. That is an important observation and it agrees well with an already known ozone geographical trends where ozone density is lowest in the regions around the equator. Figure 4.41 and Figure 4.42 show ozone comparison between daily and nightly satellite derived values with ozone density from this study confirm that trend.

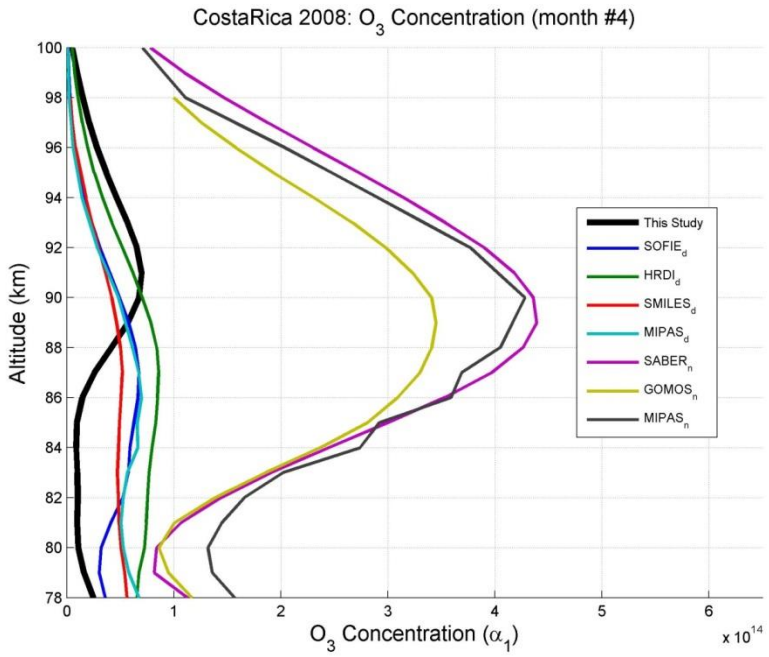

Figure 4.41: Satellite observed diurnal variation of ozone density compared with the ozone profile from this work for April 2008, Costa Rica.

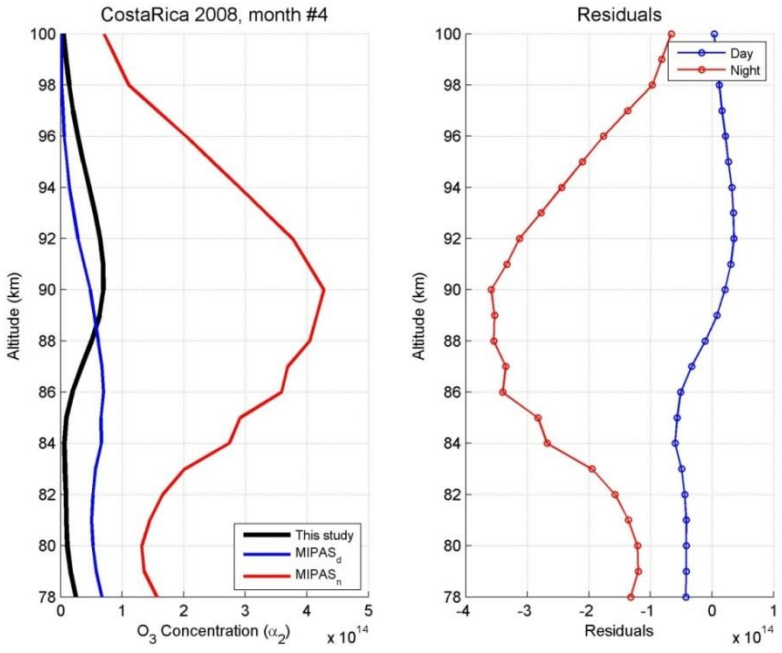

Figure 4.42: Left: Comparison of satellite and radar derived ozone profiles. Right: Residual values between daily and nightly satellite (MIPAS) profiles and calculated ozone density profile for April 2008, Costa Rica.

4.6 Chapter Summary and Concluding Remarks

The results of calculated ozone density profiles in the MLT region, using meteor radar observation of overdense meteors, for the five radar sites stretching from polar to equatorial region have been presented here. The results obtained in this study agree well with observations from different satellites. Additionally, the global trend of ozone decrease from maximum values in Polar Regions to minimum in the vicinity of the equator has been observed and is in line with known trends. Moreover, the seasonal variations in ozone density observed in this work (i.e. Socorro) match well with published seasonal ozone behaviour. In conclusion, the method proposed in this thesis has been validated where calculated results withstand scrutiny when compared with published literature.

Chapter 5

The pessimist complains about the wind;
the optimist expects it to change;
the realist adjusts the sails.

- William Arthur Ward

5. Discussion and Concluding Remarks

5.1 Summary and Discussion

Several significant milestones were accomplished as a result of the work in this thesis.

i) It has been shown that it is possible to measure ozone density in the MLT region using the SKiYMET backscatter meteor radar and observation of overdense meteor echo decay times as a function of height.

ii) It was demonstrated that the backscatter radar can "see" hyperthermal chemistry during the post-adiabatic initial meteor train expansion.

iii) The role of the UV radiation from the overdense meteor shock layer has been shown to be a significant factor in the hyperthermal chemistry regime, and knowledge of its effects enabled the ozone density determination.

iv) Identified the hyperthermal chemical reaction that involves indirect ozone contribution in the electron removal from the meteor train:

1) Ozone gets photo dissociated by the UV radiation from the meteor shock front.

$$O_3 + hv \rightarrow O_2\left(a^1\Delta_g\right) + O(1D)$$

2) Singlet oxygen reacts with meteoric metal ion:

$$M^+ + O_2\left(a^1\Delta_g\right) \rightarrow MO^+ + O$$

3) Ionic oxide removes an electron from the radially expanding "hot" meteor train:

$$MO^+ + e \rightarrow M + O$$

v) It was demonstrated that the use of slopes of ambipolar and hyperthermal chemistry regimes, derived from the logarithmic plot of cumulative number of events vs. echo duration times, which change with height, can be viably used in the calculation of the "hyperthermal chemistry diffusion coefficient". Subsequently, the value of the

"hyperthermal chemistry diffusion coefficient" is applied in the final ozone density determination.

vi) Modified diffusion equation to treat the chemical removal of electrons in terms of physical diffusion.

vii) Consequently, a comparison of the obtained values of ozone density profile is in line with the results obtained from different satellite observations.

viii) Finally, it was shown that there are two mechanisms of ozone dissociation resulting from the overdense meteor passage through the ambient atmosphere and those are:

1) Thermal dissociation stemming from the initial high temperature meteor train, and
2) Photo-dissociation as a result of meteor shock layer UV radiation.

Some important implications are discussed next.

In the past, due to the inherent challenges in interpretation and observation of overdense meteors by radar in terms of diffusion, electron density, echo duration times and (incompletely understood) effects of chemistry, overdense meteors have received much less scientific attention than underdense meteors. This is perhaps because of greater usability and applicability of the underdense meteor data in studies of ambipolar diffusion and temperature variations in the MLT region. The expectation here is that such a trend can be overturned, as the significance of overdense meteor echoes is clearly established in this work.

Consequently, it is evident that more research needs to be conducted with the specific focus on overdense radio meteors, to define, for example, their electron densities in terms of their masses, velocities and composition, since these are still poorly constrained. For instance, consider the ordinary chondritic overdense meteor with a visual magnitude $M_V = 0$ and corresponding electron density of ~10^{16} electron m^{-1} (Sugar, 1964). If the meteor velocity is 15 km s^{-1}, its diameter will be $2.0 \cdot 10^{-2}$ m, where if the velocity is 60 km s^{-1}, the size of the meteoroid is $0.5 \cdot 10^{-2}$ m (Ceplecha et al., 1998). Correspondingly, the visual magnitude for the same value of aforementioned electron line density, at least according to Baggaley (1972), deviates significantly and is given as $M_V \approx -5$.Thus, the knowledge of the distribution of visual magnitude ranges, masses, velocities and fluxes of overdense meteors is important in several ways. In this work, based on all the available and relevant published literature, it was determined that the most common electron line

density of overdense trains is $5.5 \cdot 10^{15}$ electron m^{-1}. It must be noted that such values of electron line density may need to be further refined. However, the diameter of meteoroids that produce overdense meteors, for the purpose of this study, was taken to be in the range of 200 mm $\geq$ d $\geq$ 2 mm with the particular emphasis that the overdense meteors which approach the fireball size are very infrequent. This is well in line with other observations (Dressler, 2001). Furthermore, theoretical work performed by Manning (1962, 1963) should be expanded and further experimentally explored beyond the application in this thesis.

In general, the physics of meteoric phenomena can be divided into three basic components (Dressler, 2001). The first one, which is the dynamics of the meteoroid motion in the atmosphere, had received a great deal of attention since early days and had been reinvigorated in recent decades by the availability of the computational power which permits computer modeling and validation of the theoretical and observational studies (e.g. Boyd, 2000). The second component, also well studied both in the past and recently (e.g. Plane, 2012) is concerned with the chemical and plasma kinetics induced by thermalized atoms and molecules deposited in the ambient atmosphere by meteor ablation. The third component, which has not received enough attention to date, is concerned with the small scale physical and chemical processes occurring in and on the boundary of the extreme environment of the "hot" meteor trail in the initial stages of the expansion, just after the adiabatic formation of initial radius. The goal of this thesis, at least in part, was to illuminate this often ignored aspect of meteor physics and chemistry, and furthermore illustrate its importance through the practical applicability. An example of such a pragmatic application is the measurement of ozone density in the MLT, as discussed in the previous chapter. This goal, which also encompassed the measurement of ozone density in the upper atmosphere using backscatter meteor radar, was successfully completed. However, it must be noted that this investigation only scratched the surface and presented the validity and the need for more extensive research.

The overdense meteor shock front production of the UV radiation and its full effect on the ambient atmosphere needs to be illuminated further, as it became obvious that the UV alteration of the atmospheric constituents will subsequently impact the local physical and

chemical processes even some time after thermal equilibration and diffusion of the meteor train. What was learned in this work however, is the importance of ablation processes and their contribution to the formation of the shock layer in the front of the overdense meteor trains and the subsequent UV emission (Figure 5.1 and 5.2).

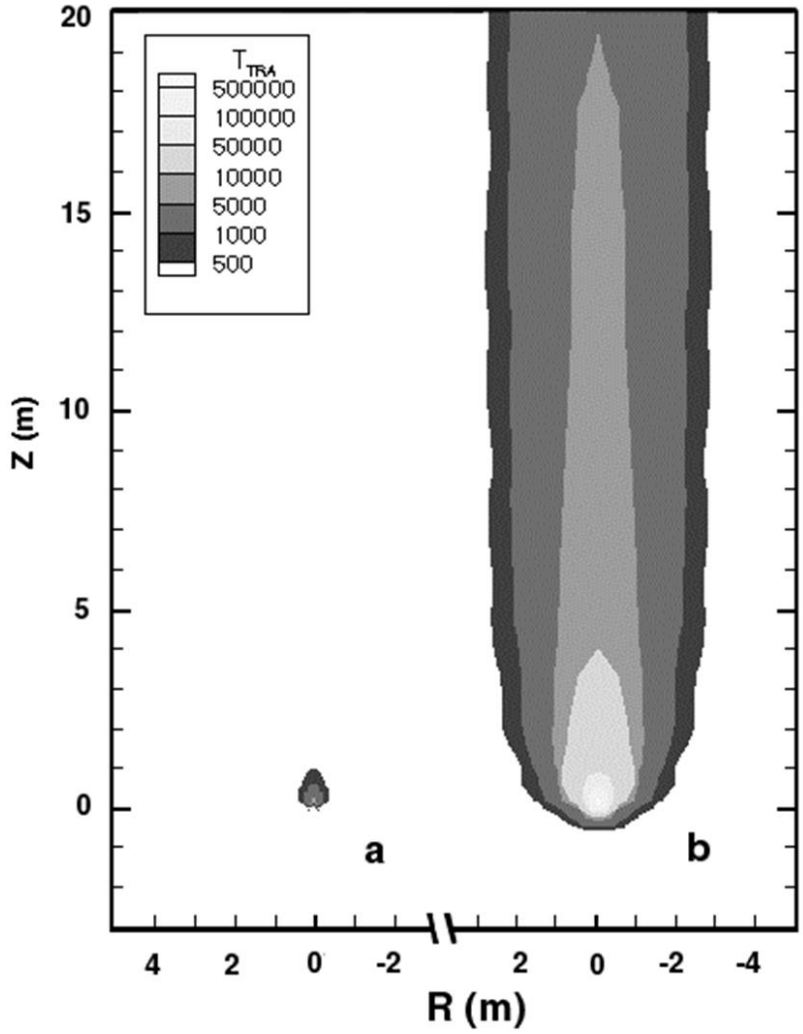

Figure 5.1: Translational temperature field from a rarefied flow model of a –1 magnitude Leonid meteor at 95 km altitude shown without ablation (a), and with ablation of Mg atoms (b) (Jenniskens et al., 1998b).

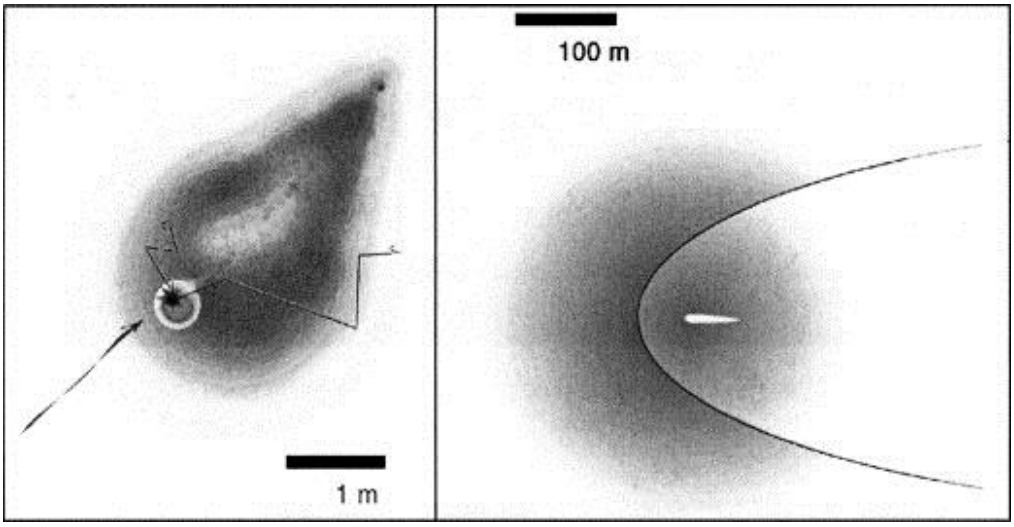

Figure 5.2: Popular depictions of the physical processes that lead to meteors. Left: air molecules hit vapor cloud products to expand into a 2 m diameter air plasma volume (1 cm Leonid at 95 km altitude). Right: UV light generated in this process is absorbed in the ambient atmosphere, causing an optical glow and "shock" (Jenniskens, 2004).

The final point that needs to be addressed is a comparison between forward and backscatter meteor radar and the difference in detection of the hyperthermal chemistry regime involving meteor ion and singlet oxygen and why this was not discovered in earlier investigations (Figure 5.3).

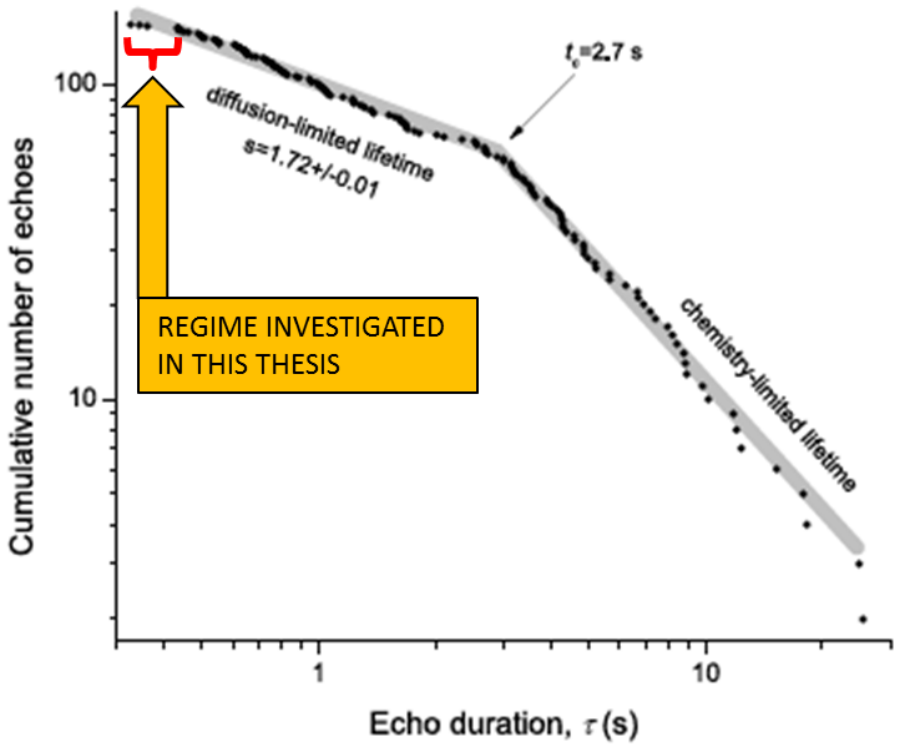

Figure 5.3: The mass index of the Draconids on October 8, 2011 determined with selected echoes in the overdense dataset. The turnover from diffusion-limited to chemistry-limited duration can be seen at t_c = 2.7 s. The mass distribution index determined by fitting the diffusion-limited portion is 1.72 ± 0.01 (Ye et al., 2013). Note that this plot shows the effects of the chemistry regime occurring in thermal equilibrium and not the hyperthermal chemistry. The arrow points at the hyperthermal regime investigated in the work performed in this thesis using the backscatter meteor radar system. Any anomaly observed in the logarithmic plot of cumulative number of events vs. echo duration times derived from the forward scatter data would be considered just a statistical noise which is primarily due to the low temporal resolution.

In that context, it should be noted that a significant percentage of the meteor studies in the past utilized forward scatter radar. While the use of forward scatter radar allows the observation of a diffusing meteor train on significantly longer time scales, it is not conducive to the observation of the meteor train dynamics on a small time scale. When the logarithmic plot of the cumulative number of events vs. echo duration times would have been plotted (see for example Ye et al., 2013), from the observed behaviour it would be unlikely to discriminate between the longer duration thermal equilibrium chemistry and the hyperthermal chemistry regime observed in this work using backscatter meteor

radar. In fact, a hyperthermal chemistry observed with backscatter meteor radar would be dismissed and considered as just a statistical artifact due to low temporal resolution if observed by forward scatter system.

5.2 Conclusions

The primary motivation behind this work was to explore the potential for measurement of ozone density in the region of the upper mesosphere and lower thermosphere (MLT) using backscatter meteor radar. In order to accomplish that, the anomalous behaviour of the ambipolar diffusion in overdense meteor trains has been studied with the SKiYMET meteor radar system at five latitudinally distinct geographical locations, beginning with Resolute Bay located within the arctic circle, and extending all the way to Costa Rica (10.29° N, 85.59° W).

The two primary mechanisms of the ozone destruction in the ambient atmosphere around the overdense meteor train as a consequence of meteor transit through the upper atmosphere have been identified. The first mechanism is the photo dissociation of ozone by the UV radiation from the overdense meteor shock front. The second mechanism involves the thermal decomposition of ozone by the thermal shock wave propagating orthogonally relative to the meteor train axis. Consequently, it is a singlet oxygen, which is the product of ozone photo-dissociation and thermal decomposition that reacts hyperthermally with the meteoric metal ions in the initial stages of post adiabatic “hot” meteor train expansion. The product, an ionic metal oxide, is what consumes electrons rapidly from the meteor trail. In this study, this indeed has been identified as the cause of the observed anomalous behaviour of ambipolar diffusion in the initial stages of the “hot” meteor trail expansion, and subsequently observed by meteor radar. Using this mechanism, it was demonstrated that the MLT ozone density profile can be measured using VHF meteor backscatter radar, thus confirming the initial hypothesis in this thesis. The ozone density profiles between 78–100 km are in good agreement with satellite measurements of ozone density. Furthermore, in consideration of the global network of SKiYMET meteor radars, this methodology has a great potential for commercial exploit and for global coverage of ozone density in the MLT region. It is expected that future

investigations will provide ozone density results with more accuracy and with reduced uncertainties, as a result of the availability of higher density data and more precisely constrained parameters such as height specific echo duration times and temperature and pressure dependent ambipolar diffusion. Additional reduction in uncertainties can be accomplished by deployment of numerical solutions to reaction-diffusion equation and utilized to calculate ozone MLT density. These results should be further validated by other investigators and in more comprehensive and encompassing studies. In conclusion, the observation of overdense meteors echo duration times with SKiYMET meteor radar has been demonstrated as a viable method for the determination of the ozone density in the MLT region with the significant potential for the development of the global meteor radar based secondary ozone maxima monitoring system.

5.3 Future Work

As a consequence of the newly identified hyperthermal chemistry reaction involving the singlet molecular oxygen and the meteoric metal ion, it is potentially possible to evaluate ozone density in the region of MLT by considering the metal oxide spectra from the overdense meteor train within the first 0.3 s following the formation of the initial meteor trail. That can be achieved by spectrally measuring the number of photons in the particular spectral range corresponding to the metal oxides. The number of neutral oxides will correspond to the number of removed electrons, which will in turn correspond to the ozone volume density in that region of the atmosphere. A potential collaborative project should be considered as a part of a broader investigation of overdense meteors and MLT ozone density.

It is important to note, that by using meteor radar, it is possible to determine ozone for the particular height from the ionization of single overdense meteor echo duration, and this might be an interesting project during the dense meteor showers such as the Leonids. The disadvantage of this approach is the ability to measure ozone density just for one specific height, and many individual measurements are needed to obtain the ozone profile compared to the method demonstrated in this thesis.

Moreover, now that it is understood that hyperthermal chemistry consumes a large number of electrons from the meteor train, corresponding to the ambient ozone density,

the new investigation of the ionization parameter β would be advisable, especially when it is known that it depends on the both velocity and meteor height (discussed in Chapter 2). This work has indirectly pointed out that the contribution of β to the overall meteor ionization and the consequent electron line density might be much less than previously considered.

This method for ozone density determination, demonstrated here, can be improved further by the availability of the high density data, and the numerical approach in further calculations. The analytical approach was employed here to simplify the actual reaction diffusion equation. However, the method used here lacks the level of refinement that can only be obtained if the full non-isothermal reaction diffusion equation is solved numerically. While not trivial, that can be accomplished fairly easy, as the reaction diffusion systems are familiar on many levels as they control the behaviour of many transport and rate processes in physical, chemical and biological systems. The primary reason for the numerical approach is the ability to model the hyperthermal chemistry dynamics of the meteor trail system and its interaction with UV and thermally perturbed ambient atmosphere.

Finally, this work might have potentially proven the hypothesis of McKinley and Millman (1949) which suggested that the meteor head phenomena is formed by the UV radiation, initiated by the overdense meteor collision with the upper atmosphere. Further discussion however, will have to await additional investigation. It should be noted that the presence of the O(1S) emissions from the meteor head region seems to confirm the aforementioned statement.

Concluding the future work prospects, it must be remarked that the determination of the actual rates of hyperthermal chemical reactions would be desirable, as it would allow further constraining of the time scales at which ionic metal oxides are formed and refinement of the timescales that it takes for subsequent electron removal from the meteor train. This should be hopefully a collaborative project with Dr. Plane as he had performed experimental work in the past involving neutral meteoric metals reactions with singlet

oxygen. The outcome of such study would be expected to further validate the results from this thesis.

Bibliography

Abe, S., Ebizuka, N., Yano, H., Watanabe, J. I., and Borovička, J. (2007) Search for OH (A–X) and detection of (B–X) in ultraviolet meteor spectrum. *Advances in Space Research*, *39*(4), 538-543.

Allen, M., Lunine, J. I., and Yung, Y. L. (1984) The vertical distribution of ozone in the mesosphere and lower thermosphere. *Journal of Geophysical Research: Atmospheres (1984–2012)*, *89*(D3), 4841-4872.

Allen, M., Yung, Y. L., and Waters, J. W. (1981) Vertical transport and photochemistry in the terrestrial mesosphere and lower thermosphere (50–120 km). *Journal of Geophysical Research*, *86*(A5), 3617-3627.

Andersen, H. H., and Bay, H. L. (1981) Sputtering yield measurements. In *Sputtering by particle bombardment I* (pp. 145-218). Springer Berlin Heidelberg.

Anderson, J. D. JR. (1969) An engineering survey of radiating shock layers. AIAA Journal, Vol. 7, No. 9, pp. 1665-1675.

Appleton, E., and Naismith, R. (1947) The radio detection of meteor trails and allied phenomena. *Proceedings of the Physical Society*, *59*(3), 461.

Armentrout, P. B., Halle, L. F., and Beauchamp, J. L. (1982) Reaction of Cr, Mn, Fe, Co, and Ni with O and NO. Examination of the translational energy dependence of the cross sections of endothermic reactions. *The Journal of Chemical Physics*, *76*, 2449.

Badger, D. (2002) Fine Structure in Radio Meteor Showers, PhD Thesis, Department of Physics and Mathematical Physics, The University of Adelaide, Adelaide, Austrialia.

Baggaley, W. J. (1970) The determination of the initial radii of meteor trains. *Monthly Notices of the Royal Astronomical Society*, *147*, 231

Baggaley, W. J. (1972) The effect of meteoric ion processes on radio studies of meteoroids. *Monthly Notices of the Royal Astronomical Society*, *159*, 203.

Baggaley, W. J. (1975a) Meteor trains and chemiluminescent processes. *Monthly Notices of the Royal Astronomical Society*, *173*, 497-512.

Baggaley, W. J. (1975b) Enduring meteor trains and chemiluminescence. *Bulletin of the Astronomical Institutes of Czechoslovakia*, *26*, 273-275.

Baggaley, W. J. (1975c) Sodium emission from long enduring meteor trains. *Nature*, *257*, 567.

Baggaley, W. J. (1975d) Meteor trains and chemiluminescent processes. *Monthly Notices of the Royal Astronomical Society*, *173*, 497-512.

Baggaley, W. J. (1976a) The chemical reduction of meteoric metal oxides as a source of meteor train emission. *Bulletin of the Astronomical Institutes of Czechoslovakia, 27*, 244-246.

Baggaley, W. J. (1976b) The role of the oxides of meteoric species as a source of meteor train luminosity. *Monthly Notices of the Royal Astronomical Society, 174*, 617-620.

Baggaley, W. J. (1976c) The excitation of the oxygen metastable OI/1S/state in meteors. *Bulletin of the Astronomical Institutes of Czechoslovakia, 27*, 173-181.

Baggaley, W. J. (1976d) The quenching of meteoric OI forbidden radiation. *Bulletin of the Astronomical Institutes of Czechoslovakia, 27*, 296-300.

Baggaley, W. J. (1977a) The red afterglow in meteor wakes. *Bulletin of the Astronomical Institutes of Czechoslovakia, 28*, 356-359.

Baggaley, W. J. (1977b) The velocity dependence of meteoric green line emission. *Bulletin of the Astronomical Institutes of Czechoslovakia, 28*, 277-280.

Baggaley, W. J. (1978) The de-ionization of dense meteor trains. *Planetary and Space Science, 26*(10), 979-981.

Baggaley, W. J. (1979) The interpretation of overdense radio meteor echo duration characteristics. *Bulletin of the Astronomical Institutes of Czechoslovakia, 30,* 184-189.

Baggaley, W. J. (1980) Measurements of the velocity dependence of the initial radii of meteor trains. *Bulletin of the Astronomical Institutes of Czechoslovakia, 31,* 308-311.

Baggaley, W. J. (1980b) Meteors and atmospheres. In *Solid Particles in the Solar System.*Vol. 90, pp. 85-100

Baggaley, W. J. (1981) Single wavelength measurements of the initial radii of radio meteor ionization columns. *Bulletin of the Astronomical Institutes of Czechoslovakia, 32*, 345-349

Baggaley, W. J. (2002) In Murad, E., and Williams, I. P. (Eds.) *Meteors in the Earth's Atmosphere: Meteoroids and Cosmic Dust and Their Interactions with the Earth's Upper Atmosphere*. Cambridge University Press. Ch.6.

Baggaley, W. J., and Cummack, C. H. (1974) Meteor train ion chemistry. *Journal of Atmospheric and Terrestrial Physics, 36*(11), 1759-1773

Baggaley, W. J., and Cummack, C. H. (1977) The behaviour of the meteoric OI 5577 Å emission. *Canadian Journal of Physics, 55*(15), 1379-1383.

Baggaley, W. J., and Cummack, C. H. (1979) The duration of long-lived meteor trains. *Bulletin of the Astronomical Institutes of Czechoslovakia, 30,* 180-183.

Baggaley, W. J., and Fisher, G. W. (1980) Measurements of the initial radii of the ionization columns of bright meteors. *Planetary and Space Science*, *28*(6), 575-580

Baggaley, W. J., and Grant, J. (2005) Techniques for measuring radar meteor speeds. In *Modern Meteor Science An Interdisciplinary View* (pp. 601-615) Springer Netherlands.

Baggaley, W. J., and Webb, T. H. (1977) The thermalization of meteoric ionization. *Journal of Atmospheric and Terrestrial Physics*, *39*(11), 1399-1403

Baggaley, W. J., and Webb, T. H. (1980) Measurements of the ionization heights of sporadic radio-meteors. *Monthly Notices of the Royal Astronomical Society*, *191*, 829-839

Baggaley, W. J., and C. H. Cummack. (1974) Meteor train ion chemistry, *Journal of Atmospheric and Terrestrial Physics* 36.11 (1974): 1759-1773.

Baggaley, W. J., Bennett, R. G. T., Steel, D. I., and Taylor, A. D. (1994) The advanced meteor orbit radar facility-AMOR. *Quarterly Journal of the Royal Astronomical Society*, *35*, 293.

Baggaley, W. J.: Radar observations, in: Murad, E., and Williams, I. P. (Eds.) (2002) *Meteors in the Earth's Atmosphere: Meteoroids and Cosmic Dust and Their Interactions with the Earth's Upper Atmosphere*. Cambridge University Press. 123–148.

Balanis, C. A. (2005) Antenna Theory, Hoboken. *New Jersey: John Wiley and Sons, Inc*, *8*, 21-31.

Ballinger, A. P., Chilson, P. B., Palmer, R. D., and Mitchell, N. J. (2008) On the validity of the ambipolar diffusion assumption in the polar mesopause region. In *Annales Geophysicae* (Vol. 26, No. 11, pp. 3439-3443) Copernicus GmbH

Bayrachenko, I. V. (1965) Measurements of the Initial Radii of Ionized Meteor Trails from Simultaneous Observations of Radio Meteors on two Wavelengths. *Geomagn. Aeron*, *5*, 353.

Berezhnoy, A. A., and Borovička, J. (2010) Formation of molecules in bright meteors. *Icarus*, *210*(1), 150-157.

Bevington, P. R., and Robinson, D. K. (1992) *Data reduction and error analysis for the physical sciences* (2^{nd} ed.) New York: McGraw-Hill.

Blake, A. J., and Carver, J. H. (1977) The evolutionary role of atmospheric ozone. *Journal of the Atmospheric Sciences*, *34*(5), 720-728.

Bohdansky, J. (1984) A universal relation for the sputtering yield of monatomic solids at normal ion incidence. Nuclear Instruments and Methods in Physics Research Section B: Beam Interactions with Materials and Atoms, 2(1), 587-591.

Borovicka, J. (1993) A fireball spectrum analysis. *Astronomy and Astrophysics*, *279*, 627-645.

Borovička, J. (1994) Two components in meteor spectra. *Planetary and Space Science*, *42*(2), 145-150.

Borovička, J., and Jenniskens, P. (1998) Time resolved spectroscopy of a Leonid fireball afterglow. *Earth, Moon, and Planets*, *82*, 399-428.

Borovička, J., and Spurný, P. (1996) Radiation study of two very bright terrestrial bolides and an application to the comet S–L 9 collision with Jupiter. *Icarus*, *121*(2), 484-510.

Borovička, J., and Zamorano, J. (1995) The spectrum of fireball light taken with a 2-m telescope. *Earth, Moon, and Planets*, *68*(1-3), 217-222.

Borovička, J., Koten, P., Spurný, P., Boček, J., and Štork, R. (2005) A survey of meteor spectra and orbits: evidence for three populations of Na-free meteoroids. *Icarus*, *174*(1), 15-30.

Borovicka, J., Stork, R., and Bocek, J. (1999) First results from video spectroscopy of 1998 Leonid meteors. *Meteoritics & Planetary Science*, *34*(6), 987-994.

Boyd, I. D. (1998) Computation of atmospheric entry flow about a Leonid meteoroid. *Earth, Moon, and Planets*, *82*, 93-108.
Bronshten, V. A. (1983) *Physics of meteoric phenomena*. D. Reidel Publishing Company

Brosch, N., Schijvarg, L. S., Podolak, M., and Rosenkrantz, M. R. (2001, November) Meteor observations from Israel. In *Meteoroids 2001 Conference* (Vol. 495, pp. 165-173)

Brown, P., Ceplecha, Z., Hawkes, R. L., Wetherill, G., Beech, M., and Mossman, K. (1994) The orbit and atmospheric trajectory of the Peekskill meteorite from video records. *Nature*, *367*(6464), 624-626.

Browne, I. C. and Kaiser, T. R. (1953) The radio echo from the head of meteor trails. *Journal of Atmospheric and Terrestrial Physics*, *4*(1), 1-4.

Brownlee, D. E. (1985) Cosmic dust: collection and research. *Annual Review of Earth and Planetary Physics*, 13:147–173

Buderi, R. (1996) *The invention that changed the world: how a small group of radar pioneers won the Second World War and launched a technological revolution*. Simon & Schuster.

Burke, J. G. (1991) Cosmic debris: meteorites in history. Univ of California Press.

Campbell, L., and Elford, W. G. (2006) Accuracy of meteoroid speeds determined using a Fresnel transform procedure. *Planetary and Space Science*, *54*(3), 317-323.

Campbell-Brown, M. D., and Koschny, D. (2004) Model of the ablation of faint meteors. *ASTRONOMY AND ASTROPHYSICS-BERLIN THEN LES ULIS*, *418*(2), 751-758.

Campbell-Brown, M., and Jones, J. (2003) Determining the initial radius of meteor trains: fragmentation. *Monthly Notices of the Royal Astronomical Society*, *343*(3), 775-780.

Ceplecha, Z. (1968) Meteor spectra (survey paper) In *Physics and Dynamics of Meteors* (Vol. 33, p. 73)

Ceplecha, Z. (1971) Spectral data on terminal flare and wake of double-station meteor No. 38421 (Ondrejov, April 21, 1963) *Bulletin of the Astronomical Institutes of Czechoslovakia*, *22*, 219.

Ceplecha, Z., Borovicka, J., and Spurný, P. (2000) Dynamical behavior of meteoroids in the atmosphere derived from very precise photographic records. *Astronomy and Astrophysics*, *357*, 1115-1122.

Ceplecha, Z., Borovička, J., Elford, W. G., ReVelle, D. O., Hawkes, R. L., Porubčan, V., and Šimek, M. (1998) Meteor phenomena and bodies. *Space Science Reviews*, *84*(3-4), 327-471.

Cervera, M. (1996) Meteor Observation With a Narrow Beam VHF Radar, Department of Physics and Mathematical Physics, The University of Adelaide, Adelaide, Austrialia.

Cervera, M. A., and Elford, W. G. (2004) The meteor radar response function: Theory and application to narrow beam MST radar. *Planetary and Space Science*, *52*(7), 591-602.

Cervera, M. A., and Reid, I. M. (2000) Comparison of atmospheric parameters derived from meteor observations with CIRA. *Radio Science*, *35*(3), 833-843.

Cevolani, G., and Gabucci, M. F. (1996) Mass distribution of meteoroids obtained by a meteor forward-scatter (MFS) radar method. *Il Nuovo Cimento C*, *19*(2), 271-282.

Cevolani, G., and Pupillo, G. (2003) Ground-based radio observations to probe the ozone content in the meteor region. *Annals of Geophysics*.

Cevolani, G., Hajduk, A., Hajdukova, M., Porubčan, V., and Trivellone, G. (1999) Ozone concentration at meteor heights determined from forward-scatter radar echoes. *Journal of atmospheric and solar-terrestrial physics*, *61*(7), 539-543.

Chen, X., Guo, J. S., and Ninomiya, H. (2006) Entire solutions of reaction-diffusion equations with balanced bistable nonlinearities. *Proc. Roy. Soc. Edinburgh Sect. A*, *136*(6), 1207-1237.

Chilson, P. B., Czechowsky, P., and Schmidt, G. (1996) A comparison of ambipolar diffusion coefficients in meteor trains using VHF radar and UV lidar. *Geophysical research letters*, *23*(20), 2745-2748

Chorley, R., and Barry, R. G. (1998) *Atmosphere, Weather and Climate*. Taylor & Francis.

Close, S., Oppenheim, M., Hunt, S., and Coster, A. (2004) A technique for calculating meteor plasma density and meteoroid mass from radar head echo scattering. *Icarus*, *168*(1), 43-52.

Close, S., Oppenheim, M., Hunt, S., and Dyrud, L. (2002) Scattering characteristics of high-resolution meteor head echoes detected at multiple frequencies. *Journal of Geophysical Research: Space Physics (1978–2012)*, *107*(A10), SIA-9.

Cook, A. F., and Hawkins, G. S. (1960) The meteoric head echo. *Smithsonian Contributions to Astrophysics*, *5*, 1.

Coulson, S. G., and Wickramasinghe, N. C. (2003) Frictional and radiation heating of micron-sized meteoroids in the Earth's upper atmosphere. *Monthly Notices of the Royal Astronomical Society*, *343*(4), 1123-1130.

Crank, J. (1975) *The Mathematics of Diffusion: 2d Ed*. Clarendon Press.

Crank, J. (1979) *The mathematics of diffusion*. Oxford university press.

Crutzen, P. J. (1971) Ozone production rates in an oxygen-hydrogen-nitrogen oxide atmosphere. *Journal of Geophysical Research*, *76*(30), 7311-7327.

Davis, J. A., Greenhow, J. S., and Hall, J. E. (1959) The effect of attachment on radio echo observations of meteors. *Proceedings of the Royal Society of London. Series A. Mathematical and Physical Sciences*, *253*(1272), 130-139.

Davis, J., and Hall, J. E. (1963) Meteor luminosity and ionization. *Proceedings of the Royal Society of London. Series A. Mathematical and Physical Sciences*, *271*(1344), 120-128.

Delov, I. A. (1975) On non-isothermicity of meteoric trails. *Astronomicheskii Vestnik*, *9*, 232-236

Derbeneva, A. D. (1968) The Luminous Flux and Ionizing Power of Meteor Trails. *Soviet Astronomy*, *11*, 688.

Dimant, Y. S., and Oppenheim, M. M. (2006) Meteor trail diffusion and fields: 1. Simulations. *Journal of Geophysical Research: Space Physics (1978–2012)*, *111*(A12)

Dressler, R. (Ed.) (2001) *Chemical dynamics in extreme environments* (Vol. 11). World Scientific.

Dyrud, L. P., Oppenheim, M. M., and vom Endt, A. F. (2001) The anomalous diffusion of meteor trails. *Geophysical Research Letters*, *28*(14), 2775-2778

Elford, W. G. (1964) *Calculation of the response function of the Harvard radio meteor project radar system*. Harvard College Observatory.

Elford, W. G. (2001) Novel applications of MST radars in meteor studies. *Journal of Atmospheric and Solar-Terrestrial Physics*, *63*(2), 143-153

Elford, W. G. (2004) Radar observations of meteor trails, and their interpretation using Fresnel holography: a new tool in meteor science. *Atmospheric Chemistry and Physics*, *4*(4), 911-921.

Elford, W. G., and Taylor, A. D. (1997) Measurement of Faraday rotation of radar meteor echoes for the modelling of electron densities in the lower ionosphere. *Journal of Atmospheric and Solar-Terrestrial Physics*, *59*(9), 1021-1024

Elford, W. G., and M. T. Elford. The effective diffusion coefficient of meteor trails above 100 km. *Meteoroids 2001 Conference*. Vol. 495. 2001

Erdman, P. W., Zipf, E. C., Espy, P., Howlett, C., Levin, D. A., Loda, R., et al. (1993) Flight measurements of low-velocity bow shock ultraviolet radiation. *Journal of Thermophysics and Heat Transfer*, *7*(1), 37-41.

Eshelman, V. R., (1959), Short Wave Length Radio Reflections From Meteoric Ionization. I. Theory for Low Density Trails. Stanford University, Contract no. AF 19(604)-1031, Rep. No.5.

Eshleman, V. R., and Mlodnosky, R. F. (1957) Directional characteristics of meteor propagation derived from radar measurements. *Proceedings of the IRE*, *45*(12), 1715-1723.

Eshleman,Von, R. (1957) The theoretical length distribution of ionized meteor trails. *Journal of Atmospheric and Terrestrial Physics*, *10*(2), 57-72.

Evans, W. F. J., and Llewellyn, E. J. (1972) Measurements of Mesospheric Ozone from Observations of the 1.27. μ Band. *Radio Science*, *7*(1), 45-50.

Ferguson, E. E., and Fehsenfeld, F. C. (1968) Some aspects of the metal ion chemistry of the earth's atmosphere. *Journal of Geophysical Research*, *73*(19), 6215-6223.

Fialko, E. I. (1959) An Approximate Estimation of the Probability of Meteoric Ionization. Soviet Astronomy, 3, 479.

Finlayson-Pitts, B. J., and Pitts Jr, J. N. (1999) *Chemistry of the upper and lower atmosphere: theory, experiments, and applications*. Elsevier.

Foote, C. S., Valentine, J. S., and Greenberg, A. (1995) Active oxygen in chemistry. *Structure energetics and reactivity in chemistry (SEARCH) series*, *2*.

Fort, J., and Méndez, V. (2002) Wavefronts in time-delayed reaction-diffusion systems. Theory and comparison to experiment. *Reports on Progress in Physics*, *65*(6), 895.

Foschini, L. (1997) On forward scatter of radio waves from meteor trails. *arXiv preprint astro-ph/9804279*.

Foschini, L. (1999) On the interaction of radio waves with meteoric plasma. *Astron. Astrophys, 341*, 634-639.

Francey, J. L. A. (1963) Ambipolar diffusion in meteor trails. *Australian Journal of Physics*, *16*(4), 500-506

Francey, J. L. A. (1964) Diffusion of meteor trails in the Earth's magnetic field. *Australian Journal of Physics*, *17*(3), 315-322

Froidevaux, L., Jiang, Y. B., Lambert, A., Livesey, N. J., Read, W. G., Waters, J. W., ... and Wagner, P. A. (2008) Validation of Aura microwave limb sounder HCl measurements. *Journal of geophysical research*, *113*(D15), D15S25.

Furman, A. M. (1961) A Theory of Ionization of Meteor Trails. II. The Role of Ionization Phenomena at the Surface of a Meteoroid in the Ionization of the Meteor Trail. *Soviet Astronomy* 4: 705.

Furman, A. M. (1960) The Theory of Ionization in Meteor Trails. I. Kinetics of the Variation of Ionization Parameters for Meteoroids Heated by Motion in the Earth's Atmosphere. *Soviet Astronomy, 4*, 489.

Furman, A. M. (1964) Notes on the Theory of Ionization of Meteor Trails. III. Ionization Due to Air Molecules and Atoms Reflected from a Meteoroid. *Soviet Astronomy, 7*, 559.

Furman, A. M. (1967) Meteor-Trail Ionization Theory. IV. Ionization Efficiency through Collision of Vaporized Meteoroid Particles with Air Molecules. *Soviet Astronomy, 10*, 844.

Galligan, D. P., Thomas, G. E., and Baggaley, W. J. (2004) On the relationship between meteor height and ambipolar diffusion. *Journal of atmospheric and solar-terrestrial physics, 66*(11), 899-906.

Gaydon, A. G. (1968) *Dissociation Energies: And Spectra of Diatomic Molecules*. Chapman and Hall.

Green, B. D., Rawlins, W. T., and Nadile, R. M. (1986) Diurnal variability of vibrationally excited mesospheric ozone as observed during the SPIRE mission. *Journal of Geophysical Research: Space Physics (1978–2012), 91*(A1), 311-320.

Greenhow, J. S. (1952) Characteristics of radio echoes from meteor trails: III The behaviour of the electron trails after formation. *Proceedings of the Physical Society. Section B*, *65*(3), 169

Greenhow, J. S. (1961) Head echoes from meteor trails. *Journal of Atmospheric and Terrestrial Physics*, *22*(1), 64-73

Greenhow, J. S. (1963) Limitations of radar techniques for the study of meteors. *Smithsonian contributions to astrophysics*, *7*, 5.

Greenhow, J. S., and Hall, J. E. (1960a) The importance of initial trail radius on the apparent height and number distributions of meteor echoes. *Monthly Notices of the Royal Astronomical Society*, *121*, 183.

Greenhow, J. S., and Hall, J. E. (1960b) The variation of meteor heights with velocity and magnitude. *Monthly Notices of the Royal Astronomical Society*, *121*, 174.

Greenhow, J. S., and Hall, J. E. (1961) Attachment processes in meteor trails. *Journal of Atmospheric and Terrestrial Physics*, *21*(4), 261-271.

Greenhow, J. S., and Hawkins, G. S. (1952) Ionizing and luminous efficiencies of meteors.

Greenhow, J. S., and Neufeld, E. L. (1957) The variation of ionization along a meteor trail. *Monthly Notices of the Royal Astronomical Society*, *117*, 359.

Greenhow, J. S., and Watkins, C. D. (1964) The characteristics of meteor trails observed at a frequency of 300 Mc/s. *Journal of Atmospheric and Terrestrial Physics*, *26*(5), 539-558

Hajduk, A., Hajduková, M., Porubcan, V., Cevolani, G., and Grassi, G. (1999). The ozone concentration in the meteor zone. In *Meteroids 1998* (Vol. 1, p. 91).

Halliday, I. (1960) Auroral Green Line in Meteor Wakes. *The Astrophysical Journal*, *131*, 25.

Havnes, O., and Sigernes, F. (2005) On the influence of background dust on radar scattering from meteor trails. *Journal of atmospheric and solar-terrestrial physics*, *67*(6), 659-664

Hawkes, R. L., and Jones, J. (1978) MNRAS, 185, 727

Hawkins, G. S. (1963) The initial diameter of meteor trails. *Smithsonian Contributions to Astrophysics*, *7*, 23

Hays, P. B., and Roble, R. G. (1973) Observation of mesospheric ozone at low latitudes. *Planetary and Space Science*, *21*(2), 273-279.

Hecht, E., and Zajac, A. (1974) *Optics*. San Francisco, CA: Addison Wesley.

Helmer, M., Plane, J., Qian, J., and Gardner, C. S. (1998) A model of meteoric iron in the upper atmosphere. *Journal of Geophysical Research: Atmospheres (1984–2012)*, *103*(D9), 10913-10925.

Henry, R. J., Burke, P. G., and Sinfailam, A. L. (1969) Scattering of Electrons by C, N, O, N^{+}, O^{+}, and O^{++}. *Physical Review*, *178*(1), 218.

Herlofson, N. (1951) Plasma resonance in ionospheric irregularities. *Ark. Fys*, *3*, 247-297.

Herlofson, N. (1951) *Radio Echoes from Meteor Trails and Ionospheric Scattering Centres* (Doctoral dissertation, University of Stockholm)

Herlofson, N.: (1948) The Theory of Meteor Ionization, *Rep. Prog. Phys.* 11, 444-454

Hewitt, C. N., and Jackson, A. V. (Eds.) (2008) *Handbook of atmospheric science: Principles and applications.*

Hey, J. S., and Stewart, G. S. (1947) Radar observations of meteors. *Proceedings of the Physical Society*, *59*(5), 858.

Hey, J.S., Parsons, S.J. Stewart, G.S.. (1947) Radar Observations of the Giacobinid Meteor Shower Mon. Not. R. Astron. Soc., 107, pp. 176–183.

Hill, K. A., Rogers, L. A., and Hawkes, R. L. (2004) Sputtering and high altitude meteors. *Earth, Moon, and Planets*, *95*(1-4), 403-412.

Hippler, H., Rahn, R., and Troe, J. (1990) Temperature and pressure dependence of ozone formation rates in the range 1–1000 bar and 90–370 K. *The Journal of chemical physics*, *93*, 6560.

Hocking, W. K. (1997) System design, signal-processing procedures, and preliminary results for the Canadian (London, Ontario) VHF atmospheric radar. *Radio Science*, *32*(2), 687-706.

Hocking, W. K. (1999) Temperatures using radar-meteor decay times. *Geophysical research letters*, *26*(21), 3297-3300.

Hocking, W. K. (2000) Real-time meteor entrance speed determinations made with interferometric meteor radars. *Radio Science*, *35*(5), 1205-1220.

Hocking, W. K. (2004) Radar meteor decay rate variability and atmospheric consequences. In *Annales Geophysicae* (Vol. 22, No. 11, pp. 3805-3814)

Hocking, W. K. (2005) Experimental radar studies of anisotropic diffusion of high altitude meteor trails. In *Modern Meteor Science An Interdisciplinary View*, pp. 671-679. Springer Netherlands.

Hocking, W. K. (2011) A review of Mesosphere–Stratosphere–Troposphere (MST) radar developments and studies, circa 1997–2008. *Journal of Atmospheric and Solar-Terrestrial Physics*, *73*(9), 848-882.

Hocking, W. K., Fuller, B., and Vandepeer, B. (2001a) Real-time determination of meteor-related parameters utilizing modern digital technology. *Journal of Atmospheric and Solar-Terrestrial Physics*, *63*(2), 155-169.

Hocking, W. K., Kelley, M., Rogers, R., Brown, W. O. J., Moorcroft, D., and St Maurice, J. P. (2001b) Resolute Bay VHF radar: A multipurpose tool for studies of tropospheric motions, middle atmosphere dynamics, meteor physics, and ionospheric physics. *Radio Science*, *36*(6), 1839-1857.

Hocking, W. K., Singer, W., Bremer, J., Mitchell, N. J., Batista, P., Clemesha, B., and Donner, M. (2004) Meteor radar temperatures at multiple sites derived with SKiYMET radars and compared to OH, rocket and lidar measurements. *Journal of atmospheric and solar-terrestrial physics*, *66*(6), 585-593.

Hocking, W. K., Thayaparan, T., and Jones, J. (1997) Meteor decay times and their use in determining a diagnostic mesospheric Temperature-pressure parameter: Methodology and one year of data. *Geophysical research letters*, *24*(23), 2977-2980

Holway Jr, L. H. (1965) Ambipolar diffusion in the geomagnetic field. *Journal of Geophysical Research*, *70*(15), 3635-3645

Hughes, D. W. (1978) Meteors. *Cosmic dust*, *1*, 123-185.

Hughes, D. W. (1992) The meteorite flux. *Space science reviews*, *61*(3-4), 275-299.

Hughes, D. W. (1997) Meteors and cosmic dust. *Endeavour*, *21*(1), 31-35.

Hunten, D. M., and Strobel, D. F. (1974) Production and Escape of Terrestrial Hydrogen. *Journal of Atmospheric Sciences*, *31*, 305-317.

Isern, N., and Fort, J. (2009) Time-delayed reaction-diffusion fronts. *Physical Review E*, *80*(5), 057103.

Jacob, D. (1999) *Introduction to atmospheric chemistry*. Princeton University Press.

Janches, D., Dyrud, L. P., Broadley, S. L., and Plane, J. M. C. (2009) First observation of micrometeoroid differential ablation in the atmosphere. *Geophysical Research Letters*, *36*(6), L06101.

Jenniskens, P. (2004) Meteor induced chemistry, ablation products, and dust in the middle and upper atmosphere from optical spectroscopy of meteors. *Advances in Space Research*, *33*(9), 1444-1454.

Jenniskens, P., and Stenbaek-Nielsen, H. C. (2004) Meteor wake in high frame-rate images-implications for the chemistry of ablated organic compounds. *Astrobiology*, *4*(1), 95-108.

Jenniskens, P., Lacey, M., Allan, B. J., Self, D. E., and Plane, J. M. (1998) FeO" Orange Arc" emission detected in optical spectrum of Leonid persistent train. *Earth, Moon, and Planets*, *82*, 429-438.

Jenniskens, P., Laux, C. O., Wilson, M. A., and Schaller, E. L. (2004) The mass and speed dependence of meteor air plasma temperatures. *Astrobiology*, *4*(1), 81-94.

Jenniskens, P., Nugent, D., and Plane, J. M. (1998) The dynamical evolution of a tubular Leonid persistent train. *Earth, Moon, and Planets*, *82*, 471-488.

Jenniskens, P., Wilson, M. A., Packan, D., Laux, C. O., Krüger, C. H., Boyd, I. D., et al. (1998b) Meteors: A delivery mechanism of organic matter to the early Earth. *Earth, Moon, and Planets*, *82*, 57-70.

Jones, J. (1975) On the decay of underdense radio meteor echoes. *Monthly Notices of the Royal Astronomical Society*, *173*, 637-648.

Jones, J., & Campbell-Brown, M. (2005) The initial train radius of sporadic meteors. *Monthly Notices of the Royal Astronomical Society*, *359*(3), 1131-1136.

Jones, J., and Collins, J. G. (1974) On the validity of certain approximations in radio meteor echo theory. *Monthly Notices of the Royal Astronomical Society*, *168*, 433.

Jones, J., and Jones, W. (1990b) Oblique-scatter of radio waves from meteor trains: Iong wavelength approximation. *Planetary and Space Science*, *38*(7), 925-932.

Jones, J., and Jones, W. (1991) Oblique-scatter of radio waves from meteor trains: Full-wave calculations. *Planetary and space science*, *39*(9), 1289-1296.

Jones, J., and Morton, J. D. (1977) The determination of meteor stream radiants from single station observations. *Bulletin of the Astronomical Institutes of Czechoslovakia*, *28*, 267-272.

Jones, J., and Simek, M. (1995) A note on the determination of ozone concentrations from radio-meteor duration distributions. *Earth, Moon, and Planets*, *68*(1-3), 329-338.

Jones, J., A. R. Webster, and W. K. Hocking (1998), An improved interferometer design for use with meteor radars, Radio Sci., 33, 55–65.

Jones, J., McIntosh, B. A., and Simek, M. (1990) Ozone and the duration of overdense radio meteors. *Journal of Atmospheric and Terrestrial Physics*, *52*(4), 253-258.

Jones, W. (1991) Theory of diffusion of meteor trains in the geomagnetic field. *Planetary and space science*, *39*(9), 1283-1288

Jones, W. (1995) Theory of the initial radius of meteor trains. *Monthly Notices of the Royal Astronomical Society*, *275*, 812-818

Jones, W. (1997) Theoretical and observational determinations of the ionization coefficient of meteors. *Monthly Notices of the Royal Astronomical Society*, *288*(4), 995-1003.

Jones, W. M., and Davidson, N. (1962) The thermal decomposition of ozone in a shock tube. *Journal of the American Chemical Society*, *84*(15), 2868-2878.

Jones, W., and Halliday, I. (2001) Effects of excitation and ionization in meteor trains. *Monthly Notices of the Royal Astronomical Society*, *320*(4), 417-423.

Jones, W., and Jones, J. (1990) Ionic diffusion in meteor trains. *Journal of Atmospheric and Terrestrial Physics*, *52*(3), 185-191

Jones, W., and Jones, J. (1990a) Oblique scattering of radio waves from meteor trains: theory. *Planetary and space science*, *38*(1), 55-66.

Kaiser, T. R. (1953) Radio echo studies of meteor ionization. *Advances in Physics*, *2*(8), 495-544

Kaiser, T. R. (1961) The determination of the incident flux of radio-meteors. *Monthly Notices of the Royal Astronomical Society*, *123*, 265.

Kaiser, T. R. (1968) Diffusion of meteor trains in the geomagnetic field. In *Physics and Dynamics of Meteors* (Vol. 33, p. 161)

Kaiser, T. R., and Closs, R. L. (1952) I. Theory of radio reflections from meteor trails: I. *Philosophical Magazine*, *43*(336), 1-32.

Kaiser, T. R., and Greenhow, J. S. (1953) On the decay of radio echoes from meteor trails. *Proceedings of the Physical Society. Section B*, *66*(2), 150.

Kalashnikova, O., Horanyi, M., Thomas, G. E., and Toon, O. B. (2000) Meteoric smoke production in the atmosphere. *Geophysical research letters*, *27*(20), 3293-3296.

Kashcheyev, B. L., and Lebedinets, V. N. (1963) The initial radius of ionized meteor trails. *Smithsonian Contributions to Astrophysics*, *7*, 19

Kasuga, T., Watanabe, J., and Ebizuka, N. (2005) A 2004 Geminid meteor spectrum in the visible-ultraviolet region. *Astronomy and Astrophysics-Les Ulis*, *438*(2), L17.

Keck, J. C., Camm, J. C., Kivel, B., and Wentink Jr, T. (1959) Radiation from hot air: Part II. Shock tube study of absolute intensities. *Annals of Physics*, *7*(1), 1-38.

Kelley, M. C. (2009) *The Earth's Ionosphere: Plasma Physics and Electrodynamics* (Vol. 96) Access Online via Elsevier.

Kemp N. H., (1959) Laminar Heat Transfer Around Blunt Bodies in Dissociated Air", Journal of the Aerospace Sciences, Vol. 26, No. 7, pp. 421-430.

Kero, J. (2008) *High-resolution meteor exploration with tristatic radar methods* (Doctoral dissertation, Umeå University).

Khabibrakhmanov, I. K., Degenstein, D. A., and Llewellyn, E. J. (2002) Mesospheric ozone: Determination from orbit with the OSIRIS instrument on Odin. *Canadian journal of physics*, *80*(4), 493-504.

Kharchenko, H. V. (2012) Calculation of the Areas Most Likely to Appear Suitable for Communication Meteor Trails. *International Journal of Electronics and Telecommunications*, *58*(2), 105-110.

Kim, J. H., Ha Kim, Y., Jee, G., and Lee, C. (2012) Mesospheric temperature estimation from meteor decay times of weak and strong meteor trails. *Journal of Atmospheric and Solar-Terrestrial Physics*.

Kivel, B. (1961) Radiation From Hot Air and Its Effect on Stagnation-Point Heating. Journal of the Aerospace Sciences, Vol. 28, No. 2, pp. 96-102.

Koda, S., and Sugimoto, K. (2003) Pressure effect on the absorption and photodissociation of O_2 near the dissociation threshold. *Journal of Photochemistry and Photobiology C: Photochemistry Reviews*, *4*(3), 215-226.

Krinov, E. L. (1960) Principles of meteoritics. Oxford, New York, Pergamon Press, 1960., 1.

Kumar, K. K., and Subrahmanyam, K. V. (2012) A discussion on the assumption of ambipolar diffusion of meteor trails in the Earth's upper atmosphere. *Monthly Notices of the Royal Astronomical Society: Letters*, *425*(1), L1-L5

Lebedinets, V.N., Shushkova, V.B., 1970. Micrometeorite sputtering in the Ionosphere. Planet.Space Sci. 18, 1653–1659.

Lee, C. S., Younger, J. P., Reid, I. M., Kim, Y. H., and Kim, J. H. (2013) The effect of recombination and attachment on meteor radar diffusion coefficient profiles. *Journal of Geophysical Research: Atmospheres*.

Levien, R. (2008) *The Euler spiral: a mathematical history*. Technical Report UCB/EECS-2008-111, EECS Department, University of California, Berkeley.

Levin, D. A., Loda, R. T., Candler, G. V., and Park, C. (1993) Theory of radiation from low velocity shock heated air. *Journal of thermophysics and heat transfer*, *7*(2), 269-276.

Liller, W., and Whipple, F. L. (1954) High-altitude winds by meteor-train photography. In *Rocket exploration of the upper atmosphere* (Vol. 1, p. 112)

Lindblad, B. A. (1963) The relations between visual magnitudes of meteors and the durations of radar echoes. *Smithsonian Contributions to Astrophysics*, *7*, 27.

Liu, V. C. (1970) Fluid mechanics of meteor trails. *Physics of Fluids, 13*, 62-65

Logan, J. A., Prather, M. J., Wofsy, S. C., and McElroy, M. B. (1978) Atmospheric chemistry: Response to human influence. *Philosophical Transactions of the Royal Society of London. Series A, Mathematical and Physical Sciences*, *290*(1367), 187-234.

London, J. (1980) Radiative energy sources and sinks in the stratosphere and mesosphere. In *Atmospheric Ozone and its Variation and Human Influences* (Vol. 1, p. 703)

Love, S. G., and Brownlee, D. E. (1993) A direct measurement of the terrestrial mass accretion rate of cosmic dust. *Science*, *262*(5133), 550-553.

Manning, L. A. (1958) The initial radius of meteoric ionization trails. *Journal of Geophysical Research*, *63*(1), 181-196

Manning, L. A. (1962) *The Theoretical Heights and Durations of Echoes from Large Meteors* DTIC Document (No. 62 137) STANFORD UNIVSITY, California, Stanford Electronics Labs.

Manning, L. A. (1963) *The Experimental Determination of Meteoric Line Densities and Attachment Rates* DTIC Document (No. 63 093) STANFORD UNIVSITY, California, Stanford Electronics Labs

Manning, L. A., and Eshleman, V. R. (1959) Meteors in the Ionosphere. *Proceedings of the IRE*, *47*(2), 186-199.

Markova, O. M., Yakovlev, O. I., Semenov, G. A., and Belov, A. N.: Evaporation of natural melts in a Knudsen chamber, Geokhimia, 11, 1559–1568, 1986.

Marsh, S. H., and Baggaley, W. J. (2001, November) Meteor trains as a probe for measuring the dynamics of the upper atmosphere. In *Meteoroids 2001 Conference* (Vol. 495, pp. 381-384).

Mathews, J. D. (2004) Radio science issues surrounding HF/VHF/UHF radar meteor studies. *Journal of atmospheric and solar-terrestrial physics*, *66*(3), 285-299.

Matsunami, N., Yamamura, Y., Itikawa, Y., Itoh, N., Kazumata, Y., Miyagawa, S., et al. (1981) A semiempirical formula for the energy dependence of the sputtering yield. *Radiation Effects*, *57*(1-2), 15-21.

McBride, N., Green, S. F., and McDonnell, J. A. M. (1999) Meteoroids and small sized debris in Low Earth Orbit and at 1 au: Results of recent modelling. *Advances in Space Research*, *23*(1), 73-82.

McCrosky, R. E., and Posen, A. (1961) Orbital elements of photographic meteors. *Smithsonian Contributions to Astrophysics*, *4*, 15-84.

McIntosh, B. A. (1962) The meteoric head echo. *Journal of Atmospheric and Terrestrial Physics*, *24*(4), 311-315.

McIntosh, B. A. (1963) Experimental study of the amplitude of radar meteor-head echoes. *Canadian Journal of Physics*, *41*(2), 355-371.

McIntosh, B. A. (1966) The determination of meteor mass distribution from radar echo counts. *Canadian Journal of Physics*, *44*(11), 2729-2748.

McKinley, D. W. (1955) The meteoric head echo, J. Atmos. Terr. Phys., 2, 65–73.

McKinley, D. W. R. (1961) Meteor science and engineering. *New York, McGraw-Hill*.

McKinley, D. W. R., and Millman, P. M. (1949) A phenomenological theory of radar echoes from meteors. *Proceedings of the IRE*, *37*(4), 364-375.

McNeil, W. J., Lai, S. T., and Murad, E. (1998) Differential ablation of cosmic dust and implications for the relative abundances of atmospheric metals. *Journal of Geophysical Research: Atmospheres (1984–2012)*, *103*(D9), 10899-10911.

Meek, C. E., Manson, A. H., Hocking, W. K., and Drummond, J. R. (2013, July) Eureka, 80° N, SKiYMET meteor radar temperatures compared with Aura MLS values. In *Annales Geophysicae* (Vol. 31, No. 7, pp. 1267-1277) Copernicus GmbH.

Meisel, D. D., and Richardson, J. E. (1998) Statistical properties of meteors from a simple, passive forward scatter system. *Planetary and space science*, *47*(1), 107-124.

Menees, G. P., and Park, C. (1976) Nitric oxide formation by meteoroids in the upper atmosphere. *Atmospheric Environment (1967)*, *10*(7), 535-545.

Michael, J. V. (1971) Thermal decomposition of ozone. *The Journal of Chemical Physics*, *54*, 4455.

Miller, D. E., and Ryder, P. (1973) Measurement of the ozone concentration from 55 to 95 km at sunset. *Planetary and Space Science*, *21*(6), 963-970.

Millman, P. M. (1952) Meteor News (Photographic Meteor Spectra), *Journal of the Royal Astronomical Society of Canada*, *46*, 121.

Millman, P. M. (1960) Meteor News (The Auroral Green Line in a Leonid Spectrum). *Journal of the Royal Astronomical Society of Canada*, *54*, 189.

Millman, P. M. (1963) A general survey of meteor spectra. *Smithsonian Contributions to Astrophysics*, *7*, 119.

Millman, P. M., and McKinley, D. W. R. (1956) Meteor echo durations and visual magnitudes. *Canadian Journal of Physics*, *34*(1), 50-61.

Mirtov, B. A. (1960) The mechanism of formation of a meteor trail. *Soviet Astronomy*, *4*, 485

Mitchner, M., and Kruger, C. H. (1973) *Partially ionized gases* (Vol. 8). New York: Wiley.

Morton, J. D., and Jones, J. (1982) A method for imaging radio meteor radiant distributions. *Monthly Notices of the Royal Astronomical Society*, *198*, 737-746.

Murad, E., and Williams, I. P. (Eds.) (2002) *Meteors in the Earth's Atmosphere: Meteoroids and Cosmic Dust and Their Interactions with the Earth's Upper Atmosphere*. Cambridge University Press.

Murray, E. L. (1959) Ambipolar diffusion of a meteor trail and its relation with height. *Planetary and Space Science*, *1*(2), 125-129

Nagaoka, H. (1929) Possibility of disturbance of radio transmissions by meteoric showers. *Proceedings of the Imperial Academy, Tokyo*, 5:233.

NASA-JPL, (1979) Chemical Kinetic and Photochemical Data for Use in Stratospheric Modelling, JPL Publications, 79-27, Jet Propulsion Laboratory, Pasedena, California.

Nerem, R. M., and Stickford, G. H. (1965) Shock-tube studies of equilibrium air radiation. *AIAA Journal*, *3*(6), 1011-1018.

Nicholson, T. F., and Poole, L. M. G. (1974) The observed characteristics of radio-echoes from overdense meteor trains. *Planetary and Space Science*, *22*(12), 1669-1689.

Novotny, V. (1978) The height dependence of the error in ambipolar diffusion coefficient measurement. *Bulletin of the Astronomical Institutes of Czechoslovakia*, *29*, 155-158

Öpik, E. J. (1958) Physics of meteor flight in the atmosphere. *New York, Interscience Publishers*.

Oppenheim, M. M., Dyrud, L. P., and Vom Endt, A. F. (2003) Plasma instabilities in meteor trails: 2-D simulation studies. *Journal of geophysical research*, *108*(A2), 1064

Oppenheim, M. M., vom Endt, A. F., and Dyrud, L. P. (2000) Electrodynamics of meteor trail evolution in the equatorial E-region ionosphere. *Geophysical research letters*, *27*(19), 3173-3176

Park, C., and Menees, G. P. (1978) Odd nitrogen production by meteoroids. *Journal of Geophysical Research: Oceans (1978–2012)*, *83*(C8), 4029-4035.

Parkinson, T. D., and Zipf, E. C. (1970) Energy transfer from N2 (A3Sigmau+) as a source of O (1S) in the aurora. *Planetary and Space Science*, *18*, 895.

Pavlov, A. V. (2012) Ion Chemistry of the Ionosphere at E-and F-Region Altitudes: A Review. *Surveys in geophysics*, *33*(5), 1133-1172.

Pecinová, D., and P. Pecina. "Radar meteors range distribution model. IV. Ionization coefficient." *Contributions of the Astronomical Observatory Skalnate Pleso* 38 (2008): 12-20.

Pellinen-Wannberg, A. (2005, January) Meteor head echoes-observations and models. In *Annales geophysicae* (Vol. 23, No. 1, pp. 201-205)

Pellinen-Wannberg, A., and Wannberg, G. (1994) Meteor observations with the European incoherent scatter UHF radar. *Journal of Geophysical Research: Space Physics (1978–2012)*, *99*(A6), 11379-11390.

Pellinen-Wannberg, A., Westman, A., Wannberg, G., and Kaila, K. (1998, November) Meteor fluxes and visual magnitudes from EISCAT radar event rates: a comparison with cross-section based magnitude estimates and optical data. In *Annales Geophysicae* (Vol. 16, No. 11, pp. 1475-1485) Springer-Verlag.

Permikin, D. V., and Zverev, V. S. (2013) Mathematical model on surface reaction diffusion in the presence of front chemical reaction. *International Journal of Heat and Mass Transfer*, *57*(1), 215-221.

Peukert, S. L., Sivaramakrishnan, R., and Michael, J. V. (2013) High Temperature Shock Tube Studies on the Thermal Decomposition of O3 and the Reaction of Dimethyl Carbonate with O-Atoms. *The Journal of Physical Chemistry A*, *117*(18), 3729-3738.

Pickering, W. M., and Windle, D. W. (1970) The diffusion of meteor trains. *Planetary and Space Science*, *18*(8), 1153-1161

Plane, J. M. (1991) The chemistry of meteoric metals in the Earth's upper atmosphere. *International Reviews in Physical Chemistry*, *10*(1), 55-106.

Plane, J. M. (2003) Atmospheric chemistry of meteoric metals. *Chemical reviews*, *103*(12), 4963-4984.

Plane, J. M. (2012) Cosmic dust in the earth's atmosphere. *Chemical Society Reviews*, *41*(19), 6507-6518.

Plane, J. M. C., Cox, R. M., and Rollason, R. J. (1999) Metallic layers in the mesopause and lower thermosphere region. *Advances in Space Research*, *24*(11), 1559-1570.

Plane, J. M., and Whalley, C. L. (2012) A new model for magnesium chemistry in the upper atmosphere. *The Journal of Physical Chemistry A*, *116*(24), 6240-6252.

Polyanin, A. D., and Manzhirov, A. V. (2008) *Handbook of integral equations*. CRC press.

Poole, L. M. G. (1978) The decay of luminosity in the trains of moderately bright meteors. *Planetary and Space Science*, *26*(7), 697-701.

Poole, L. M. G. (1979) The excitation of spectral lines in faint meteor trains. *Journal of Atmospheric and Terrestrial Physics*, *41*(1), 53-64.

Poole, L. M. G. (2004) A simplified interferometer design for use with meteor radars. *Radio Science*, *39*(2), RS2027.

Poole, L. M. G., and Kaiser, T. R. (1967) The duration distribution of radio-echoes obtained from underdense shower-meteor trains. *Planetary and Space Science*, *15*(7), 1131-1134.

Poole, L. M. G., and Nicholson, T. F. (1975) The effect of ionic processes on the characteristics of radio-echoes from meteor trains. *Planetary and Space Science*, *23*(9), 1261-1277.

Popova, O. (2004) Meteoroid ablation models. *Earth, Moon, and Planets*, *95*(1-4), 303-319.

Popova, O. P., Sidneva, S. N., Shuvalov, V. V., and Strelkov, A. S. (1998) Screening of meteoroids by ablation vapor in high-velocity meteors. *Earth, Moon, and Planets*, *82*, 109-128.

Popova, O. P., Sidneva, S. N., Strelkov, A. S., and Shuvalov, V. V. (2001) Formation of disturbed area around fast meteor body. In *Meteoroids 2001 Conference* . Meteor science and engineering. Vol. 495, pp. 237-245

Poulter, E. M., and Baggaley, W. I. (1978) The applications of radio-wave scattering theory to radio-meteor observations. *Planetary and Space Science*, *26*(10), 969-977.

Poulter, E. M., and Baggaley, W. J. (1977) Radiowave scattering from meteoric ionization. *Journal of Atmospheric and Terrestrial Physics*, *39*(7), 757-768.

Prather, M. J. (1981) Ozone in the upper stratosphere and mesosphere. *Journal of Geophysical Research: Oceans (1978–2012)*, *86*(C6), 5325-5338.

Pshezhetskiy, S. Y., Kamenetskaya, S. A., Gribova, Y. I., Pankratov, A. V., and Morozov, N. M. (1959) Kinetics of Ozone Decomposition and Explosion-USSR.

Rajchl, J. (1969) On the interaction layer in front of a meteor body. *Bulletin of the Astronomical Institutes of Czechoslovakia*, *20*, 363.

Reis, V. H. (1967) Chemiluminescent radiation from the far wake of hypersonic spheres. *AIAA Journal*, *5*(11), 1928-1933.

Robertson, D. S., Liddy, D. T., and Elford, W. G. (1953) Measurements of winds in the upper atmosphere by means of drifting meteor trails I. *Journal of Atmospheric and Terrestrial Physics*, *4*(4), 255-270.

Robson, R. E. (2001) Dispersion of meteor trails in the geomagnetic field. *Physical Review E*, *63*(2), 026404

Rogers, A. E. E., Lekberg, M., and Pratap, P. (2009) Seasonal and diurnal variations of ozone near the mesopause from observations of the 11.072-GHz line. *Journal of Atmospheric and Oceanic Technology*, *26*(10), 2192-2199.

Rogers, A. E., Erickson, P., Fish, V. L., Kittredge, J., Danford, S., Marr, J. M., et al. (2012) Repeatability of the Seasonal Variations of Ozone near the Mesopause from Observations of the 11.072-GHz Line. *Journal of Atmospheric and Oceanic Technology*, *29*(10), 1492-1504.

Rogers, L. A., Hill, K. A., and Hawkes, R. L. (2005) Mass loss due to sputtering and thermal processes in meteoroid ablation. *Planetary and Space Science*, *53*(13), 1341-1354.

Romig, M. (1964) The Physics of Meteor Entry. The RAND Corporation, Santa Monica, California (declassified)

Rumi, G. C. (1979) Detection of the height of maximum ionization in a meteor trail. *Il Nuovo Cimento C*, *2*(2), 235-245.

Rutherford, J. A., and Vroom, D. (1976) Ion–neutral reactions of Al with N, O, and NO. *The Journal of Chemical Physics*, *65*, 4445.

Salby, M. L. (1996) *Fundamentals of atmospheric physics* (Vol. 61) Access Online via Elsevier.

Seinfeld, J. H., and Pandis, S. N. (2012) *Atmospheric chemistry and physics: from air pollution to climate change*. John Wiley & Sons.

Sida, D. W. (1969) The production of ions and electrons by meteoritic processes. *Monthly Notices of the Royal Astronomical Society*, *143*, 37.

Singer, W., Bremer, J., Weiß, J., Hocking, W. K., Höffner, J., Donner, M., and Espy, P. (2004) Meteor radar observations at middle and Arctic latitudes Part 1: mean temperatures. *Journal of atmospheric and solar-terrestrial physics*, *66*(6), 607-616.

Singer, W., Latteck, R., Millan, L. F., Mitchell, N. J., and Fiedler, J. (2008) Radar backscatter from underdense meteors and diffusion rates. *Earth, Moon, and Planets*, *102*(1-4), 403-409.

Smith, A. K. (2004) Physics and chemistry of the mesopause region. *Journal of atmospheric and solar-terrestrial physics*, *66*(10), 839-857.

Smith, A. K. (2012) Interactions between the lower, middle and upper atmosphere. *Space science reviews*, *168*(1-4), 1-21.

Smith, A. K., and Marsh, D. R. (2005) Processes that account for the ozone maximum at the mesopause. *Journal of Geophysical Research: Atmospheres (1984–2012)*, *110*(D23)

Smith, A. K., Harvey, V. L., Mlynczak, M. G., Funke, B., García-Comas, M., Hervig, M., et al. (2013) Satellite observations of ozone in the upper mesosphere. *Journal of Geophysical Research: Atmospheres*.

Smoller, J. (1983) Shock waves and reaction-diffusion equations. In *Research supported by the US Air Force and National Science Foundation. New York and Heidelberg, Springer-Verlag (Grundlehren der Mathematischen Wissenschaften. Volume 258), 1983, 600 p.* (Vol. 258)

Snelling, D. R. (1974) The Ultraviolet Flash Photolysis of Ozone and the Reactions of O (1D) and O2 (1Σg+). *Canadian Journal of Chemistry*, *52*(2), 257-270.

Steel, D. I., and Elford, W. G. (1991) The height distribution of radio meteors: Comparison of observations at different frequencies on the basis of standard echo theory. *Journal of Atmospheric and Terrestrial Physics*, *53*(5), 409-417.

Stenbaek-Nielsen, H. C., and Jenniskens, P. (2004) A "shocking" Leonid meteor at 1000 fps. *Advances in Space Research*, *33*(9), 1459-1465.

Stickland, A. C. (1972) CIRA 1972: COSPAR international reference atmosphere 1972. *Berlin, East Germany, Akademie-Verlag GmbH, 1972. 460 p*.

Strack, S. L., (1962) Radiant heat transfer around re-entry bodies. *ARS Journal*, *32*(5), 744-748.

Sugar, G. R. (1964) Radio propagation by reflection from meteor trails. *Proceedings of the IEEE*, *52*(2), 116-136.

Swords, S. S. (1986) *Technical History of the Beginnings of RADAR*. P. Peregrinus.

Thomas, R. J. (1990) Seasonal ozone variations in the upper mesosphere. *Journal of Geophysical Research: Atmospheres (1984–2012)*, *95*(D6), 7395-7401.

Tielens, A. G. G. M., McKee, C. F., Seab, C. G., and Hollenbach, D. J. (1994) The physics of grain-grain collisions and gas-grain sputtering in interstellar shocks. *The Astrophysical Journal*, *431*, 321-340.

Tsutsumi, M., Tsuda, T., Nakamura, T., and Fukao, S. (1994) Temperature fluctuations near the mesopause inferred from meteor observations with the middle and upper atmosphere radar. *Radio science*, *29*(3), 599-610.

United States Committee on Extension to the Standard Atmosphere, (1976) U.S. Standard Atmosphere. NOAA, NASA, USAF, Washington, DC.

Upadhyay, S. K. (Ed.) (2006) *Chemical kinetics and reaction dynamics*. Springer.

Valentic, T. A., Avery, J. P., Avery, S. K., Cervera, M. A., Elford, W. G., Vincent, R. A., and Reid, I. M. (1996) A comparison of meteor radar systems at Buckland Park. *Radio Science*, *31*(6), 1313-1329.

Vaughan, G. (1982) Diurnal variation of mesospheric ozone. *Nature*, *296*(5853), 133-135.

Verniani, F. (1965) On the luminous efficiency of meteors. *Smithsonian Contributions to Astrophysics*, *8*, 141.

Verniani, F., and Hawkins, G. S. (1964) On the Ionizing Efficiency of Meteors. *The Astrophysical Journal*, *140*, 1590.

Verronen, P. T., Seppälä, A., Clilverd, M. A., Rodger, C. J., Kyrölä, E., Enell, C. F., et al. (2005) Diurnal variation of ozone depletion during the October–November 2003 solar proton events. *Journal of Geophysical Research: Space Physics (1978–2012)*, *110*(A9)

Vondrak, T., Plane, J. M. C., Broadley, S., and Janches, D. (2008) A chemical model of meteoric ablation. *Atmospheric Chemistry and Physics*, *8*(23), 7015-7031.

Wannberg, G., Westman, A., and Pellinen-Wannberg, A. (2011) Meteor head echo polarization at 930 mhz studied with the eiscat uhf hpla radar. In *Annales geophysicae* (Vol. 29, No. 6, pp. 1197-1208) Copernicus.

Watson, R. C. (2009) *Radar Origins Worldwide: History of Its Evolution in 13 Nations Through World War II*. Trafford Publishing.

Wayne, R. P., and White, I. F. (1968) Photolysis of Ozone at Low Pressures. *Berichte der Bunsengesellschaft für physikalische Chemie*, *72*(2), 131-134.

Weiss, A. A. (1955) Diffusion coefficients from the rate of decay of meteor trails. *Australian Journal of Physics*, *8*(2), 279-288

Weiss, A. A. (1961) The distribution of meteor masses for sporadic meteors and three showers. *Australian Journal of Physics*, *14*(1), 102-119.

Weiss, A. A., and Elford, W. G. (1963) An equipment for combined geophysical and astronomical measurements of meteors. *Proc. IRE Australia*, *24*, 197-203.

Weitzen, J. A., and Ralston, W. T. (1988) Meteor scatter: An overview. *Antennas and Propagation, IEEE Transactions on*, *36*(12), 1813-1819.

Weryk, R. J., and Brown, P. G. (2012a) Simultaneous radar and video meteors—I: Metric comparisons. *Planetary and Space Science*, *62*(1), 132-152.

Weryk, R. J., and Brown, P. G. (2013b) Simultaneous radar and video meteors-II: Photometry and ionisation. *Planetary and Space Science*.

Whalley, C. L., Martín, J. C. G., Wright, T. G., and Plane, J. M. (2011) A kinetic study of Mg+ and Mg-containing ions reacting with O3, O2, N2, CO2, N2O and H2O: implications for magnesium ion chemistry in the upper atmosphere. *Physical Chemistry Chemical Physics*, *13*(13), 6352-6364.

Whipple, F. L. (1943) Meteors and the Earth's upper atmosphere, Review of Modern Physics 15, 246-264.

Whipple, F. L. (1955) The Physical Theory of Meteors. VII. on Meteor Luminosity and Ionization. *The Astrophysical Journal*, *121*, 241.

William, J., and Murad, E. (2002) Models of meteoric metals in the atmosphere. *Meteors in the Earth's Atmosphere: Meteoroids and Cosmic Dust and Their Interactions with the Earth's Upper Atmosphere*, 265.

Wulf, O. R., and Tolman, R. C. (1927) The thermal decomposition of ozone. *Proceedings of the National Academy of Sciences of the United States of America*, *13*(5), 272.

Wyatt, S. P., and Whipple, F. L. (1950) The Poynting-Robertson effect on meteor orbits. *The Astrophysical Journal*, *111*, 134-141.

Yee, J., and Close, S. (2011) Diffusion of Plasmas from Ablating Meteoroids in the Ionosphere. 3rd AIAA Atmospheric Space Environments Conference, 27 - 30 June 2011, Honolulu, Hawaii

Younger, J. P., Reid, I. M., Vincent, R. A., and Holdsworth, D. A. (2008) Modeling and observing the effect of aerosols on meteor radar measurements of the atmosphere. *Geophysical Research Letters*, *35*(15)

Zinn, J., Judd, O. D. P., and ReVelle, D. O. (2004) Leonid meteor ablation, energy exchange, and trail morphology. *Advances in Space Research*, *33*(9), 1466-1474.

Zinn, J., Wren, J., Whitaker, R., Szymanski, J., ReVelle, D. O., Priedhorsky, W., et al. (1999) Coordinated observations of two large Leonid meteor fireballs over northern New Mexico, and computer model comparisons. *Meteoritics & Planetary Science*, *34*(6), 1007-1015.

Appendix 1

This appendix contains the results for most relevant quantities for all viable months and years from each sites.

Table A.1: CLOVAR number of meteors

CLOVAR: Number of meteors per height increment

Month	Year	75	76	77	78	79	80	81	82	83	84	85	86	87	88	89	90	91	92	93	94	95	96	97	98	99	100
		(km)	(km)	(km)	(km)	(km)	(km)	(km)	(km)	(km)	(km)	(km)	(km)	(km)	(km)	(km)	(km)	(km)	(km)	(km)	(km)	(km)	(km)	(km)	(km)	(km)	(km)
7	2000	38	45	74	91	117	185	252	361	529	560	645	765	853	799	786	733	715	607	480	450	338	322	230	165	124	139
8	2000	98	146	162	203	320	398	530	717	812	1039	1093	1223	1312	1335	1398	1346	1353	1239	1159	942	840	686	590	470	408	316
9	2000	119	146	176	207	311	317	439	530	631	739	782	897	977	1065	1108	1179	1047	998	947	887	757	632	533	411	376	282
10	2000	58	99	108	156	243	246	297	394	514	599	653	707	800	823	858	822	803	868	825	726	633	591	469	418	327	307
11	2000	59	79	104	159	216	245	291	382	480	507	571	656	708	787	824	836	871	871	831	742	665	590	521	374	358	306
12	2000	85	103	126	166	211	238	288	346	382	459	523	510	570	575	654	663	583	590	572	510	442	410	407	321	269	218
1	2001	75	86	114	145	171	213	270	318	363	431	421	519	508	556	549	580	533	524	479	458	410	346	357	235	233	176
11	2001	24	26	60	94	129	181	199	275	367	359	481	515	558	562	560	668	624	606	546	505	462	399	317	218	196	134
12	2001	62	59	100	111	175	246	280	346	495	554	701	734	854	858	873	875	858	777	740	698	606	498	374	311	269	194
1	2002	42	57	65	101	147	161	269	346	410	491	554	613	656	723	737	683	735	680	632	580	492	464	343	284	225	156
2	2002	33	42	57	83	119	147	192	265	338	379	444	544	579	605	610	597	515	502	433	422	332	262	230	215	160	108
3	2002	29	29	52	70	100	154	176	230	275	325	384	454	518	491	536	566	533	488	416	376	334	286	204	181	148	108
4	2002	21	57	57	79	128	186	266	336	468	567	643	709	776	818	790	790	779	730	617	522	435	380	273	241	163	152
5	2002	31	31	54	58	93	158	210	319	440	628	712	869	865	938	956	919	900	843	725	611	461	390	305	248	163	134
6	2002	22	27	23	38	49	71	128	204	236	356	465	508	576	537	549	512	483	383	327	297	249	196	178	164	84	97
7	2002	40	43	43	70	86	148	206	299	387	506	669	748	828	891	836	768	769	668	603	494	417	322	240	195	169	130
8	2002	37	52	61	80	122	168	190	308	431	523	632	708	776	743	831	794	774	732	686	565	487	435	313	228	202	146
9	2002	15	23	37	39	73	98	104	168	204	239	239	289	345	353	342	399	376	385	345	312	282	230	202	131	123	94
10	2002	9	14	25	31	60	91	114	166	215	268	304	317	334	331	391	391	386	328	324	308	284	217	216	165	116	81
11	2002	49	68	79	132	195	237	312	348	458	561	597	663	722	750	826	798	825	789	746	691	639	509	412	299	277	205
12	2002	51	76	111	152	205	305	393	487	558	691	743	867	937	981	1030	1021	948	906	854	796	620	569	465	322	275	228
1	2003	49	77	94	126	198	243	321	426	490	609	745	831	973	1027	965	991	948	964	817	713	667	526	442	336	252	183
2	2003	33	39	55	83	122	163	262	285	395	479	520	576	632	616	710	606	594	512	448	402	308	258	214	142	140	88
3	2003	26	21	42	73	94	152	217	252	342	372	456	494	532	498	520	479	471	431	360	330	225	182	158	99	93	54
4	2003	27	33	49	85	130	180	248	370	414	513	637	753	810	856	836	793	767	681	599	480	402	258	241	166	138	87
5	2003	30	38	42	74	108	138	240	326	483	682	740	930	984	1051	1060	991	889	752	648	542	460	282	256	202	139	114
6	2003	55	64	73	103	124	196	335	544	826	1051	1292	1611	1763	1745	1583	1552	1347	1207	934	789	604	481	347	269	189	135
7	2003	39	40	84	92	150	214	330	505	636	882	1148	1359	1383	1456	1423	1354	1234	1123	905	668	568	408	319	215	197	158
8	2003	62	103	124	164	248	340	448	634	758	1024	1117	1340	1458	1482	1417	1490	1451	1251	1197	1032	770	658	547	392	322	272
9	2003	60	89	108	156	211	319	416	500	617	786	834	984	999	1068	1155	1156	1161	1123	978	867	771	616	535	388	284	228
10	2003	13	22	26	36	58	86	114	173	202	229	245	286	301	363	359	319	327	347	305	274	214	181	127	110	72	59
12	2007	34	38	55	98	140	180	240	308	334	430	474	563	621	631	657	654	596	620	559	458	412	314	256	224	180	131
1	2008	14	14	15	22	35	33	57	66	104	102	101	118	148	172	149	164	136	138	142	108	109	88	75	48	47	40
2	2008	25	29	39	71	114	134	158	189	232	288	366	395	364	384	373	368	336	305	272	206	190	155	131	84	86	77
3	2008	36	52	59	95	139	184	260	323	390	449	506	542	636	660	663	634	590	523	462	389	312	277	210	167	119	92
4	2008	19	20	36	61	69	138	186	240	264	326	381	387	440	464	461	413	392	368	322	263	225	171	119	84	80	61
9	2008	23	32	53	75	69	144	203	251	304	347	396	459	530	571	553	602	573	483	498	434	344	307	267	164	140	105
10	2008	22	43	66	91	130	190	242	331	414	556	526	622	699	748	740	814	794	812	750	646	600	465	416	306	241	174

Table A. 2: Costa Rica number of meteors

Costa Rica: Number of meteors per height increment

Month	Year	75	76	77	78	79	80	81	82	83	84	85	86	87	88	89	90	91	92	93	94	95	96	97	98	99	100
		(km)	(km)	(km)	(km)	(km)	(km)	(km)	(km)	(km)	(km)	(km)	(km)	(km)	(km)	(km)	(km)	(km)	(km)	(km)	(km)	(km)	(km)	(km)	(km)	(km)	(km)
4	2005	155	204	273	379	513	698	822	1009	1196	1255	1565	1579	1803	1841	1930	1847	1817	1634	1485	1295	1059	835	671	533	397	331
5	2005	295	429	568	840	1105	1442	1870	2235	2652	3206	3728	4165	4425	4938	4959	5005	4640	4362	3779	3305	2659	2051	1475	1214	953	799
6	2005	294	355	528	642	839	1182	1463	1925	2327	2840	3340	3835	4256	4627	4877	4902	4930	4480	3940	3399	2771	2226	1648	1232	952	742
7	2005	483	518	689	958	1321	1797	2198	2458	3079	3593	4024	4552	4847	5280	5375	5439	5268	4925	4493	3836	3092	2520	1964	1479	1140	960
8	2005	502	541	710	846	1097	1420	1638	1965	2304	2674	3158	3377	3559	3909	4053	4257	4239	4058	3908	3318	2857	2290	1871	1463	1149	988
9	2005	436	516	610	696	921	1043	1247	1459	1734	1936	2243	2426	2722	2822	3013	3089	3031	2787	2683	2415	2031	1712	1337	1067	932	789
10	2005	489	534	722	877	1129	1379	1590	1890	2155	2429	2771	3017	3286	3538	3794	3863	3712	3686	3371	3093	2672	2205	1762	1445	1155	992
11	2005	254	290	363	458	550	692	840	937	1080	1400	1446	1718	1724	1863	2034	2071	2072	1856	1800	1621	1349	1165	919	741	600	516
12	2005	188	256	334	479	602	775	1002	1166	1435	1629	2062	2336	2546	2967	3175	3276	3204	3106	2919	2583	2091	1657	1302	1009	757	565
1	2006	410	318	459	644	824	1182	1469	1819	2197	2622	3188	3378	3805	3971	4345	4362	4302	4087	3840	3343	2688	2162	1680	1423	1094	839
4	2007	103	154	246	394	523	663	809	1020	1182	1291	1566	1704	1825	1884	2014	1978	2008	1753	1576	1343	1106	870	694	705	575	415
5	2007	311	429	683	923	1307	1701	2196	2580	3159	3703	4108	4693	4937	5199	5396	5391	5094	4550	4055	3355	2715	2144	1616	1309	973	847
6	2007	293	419	630	901	1258	1790	2408	2833	3608	4161	4583	5123	5461	5887	5803	5570	5025	4558	3830	3090	2482	1854	1429	1123	891	727
7	2007	262	421	606	928	1286	1831	2328	2952	3606	4240	4577	5052	5333	5500	5530	5422	5023	4484	3888	3232	2366	1775	1374	1084	923	755
8	2007	240	377	533	728	1027	1339	1616	2016	2375	2734	3106	3515	3749	3856	3946	4053	3990	3642	3143	2681	2267	1814	1479	1145	956	881
9	2007	269	370	510	705	875	1172	1446	1699	1986	2274	2581	2848	3095	3271	3305	3388	3267	2996	2705	2350	1998	1542	1257	957	777	691
10	2007	229	308	414	582	832	1108	1374	1678	1939	2259	2503	2743	3036	3157	3237	3157	3100	3053	2815	2436	2049	1698	1286	1108	869	762
11	2007	130	164	230	358	478	729	781	981	1151	1315	1565	1664	1814	1923	2022	1897	1888	1638	1571	1363	1245	923	707	541	424	350
12	2007	100	143	227	350	440	572	716	890	1099	1298	1496	1714	1877	1996	2088	2145	2087	1905	1643	1465	1148	918	740	575	393	304
1	2008	219	274	428	602	893	1334	1646	2144	2661	3098	3741	4012	4414	4830	5012	5055	4727	4354	3776	3149	2539	2048	1595	1198	931	712
2	2008	128	235	344	544	741	1091	1189	1548	1859	2154	2443	2679	2932	3182	3392	3303	3079	2835	2469	2123	1575	1255	963	723	542	422
3	2008	151	224	368	590	849	1063	1448	1650	1933	2354	2543	2924	3105	3369	3377	3399	3037	2743	2457	2026	1617	1179	826	626	487	346
4	2008	123	237	368	559	785	1082	1316	1609	1824	2085	2404	2655	2969	3016	3046	2987	2783	2356	1997	1789	1387	1076	783	579	482	357
5	2008	228	348	541	779	1178	1587	1936	2421	2934	3246	3784	4289	4477	4771	4746	4641	4324	3855	3355	2858	2260	1698	1334	1052	820	685
6	2008	200	314	473	665	904	1253	1661	2066	2599	3024	3538	3869	4314	4476	4577	4239	4083	3743	3171	2535	1918	1505	1220	876	671	577
7	2008	222	311	491	728	1018	1339	1792	2223	2662	3093	3400	3705	3982	4158	4206	4152	3766	3382	2803	2340	1851	1364	949	763	661	543
8	2008	107	137	173	244	408	534	698	815	952	1105	1292	1336	1432	1503	1522	1450	1440	1269	1119	954	756	547	464	356	330	296
9	2008	161	238	333	459	629	825	1042	1319	1484	1766	2008	2277	2423	2566	2546	2584	2409	2269	1980	1683	1434	1146	903	700	657	487
10	2008	167	211	285	406	567	666	833	1024	1230	1437	1645	1775	1843	2007	2030	2113	2011	1798	1647	1468	1180	970	798	638	516	455
11	2008	103	162	203	294	405	561	622	778	909	1031	1164	1287	1403	1430	1544	1512	1474	1376	1198	1125	958	813	616	510	419	349
3	2009	35	46	60	110	120	172	216	299	312	352	440	454	526	533	587	560	554	489	441	386	322	272	184	158	115	90
1	2010	5	4	8	2	15	6	15	41	21	37	32	44	61	62	71	66	62	64	61	54	53	57	45	35	25	22
2	2010	17	28	54	69	101	140	184	204	280	304	362	408	398	447	452	436	425	461	408	387	309	251	182	166	126	102
3	2010	129	116	177	292	383	493	664	806	913	1041	1264	1303	1420	1522	1537	1542	1550	1416	1342	1059	904	750	551	470	331	272
4	2010	165	104	145	168	218	323	332	440	523	561	633	684	750	723	795	827	778	725	679	588	500	451	345	292	279	221
6	2010	76	87	100	129	220	253	346	466	568	685	844	959	1113	1199	1236	1126	1185	1106	985	890	759	670	509	463	344	285
7	2010	42	57	80	89	119	130	184	222	280	338	394	431	496	515	555	617	568	576	511	462	391	332	253	212	193	142
8	2010	101	143	166	245	248	339	377	460	576	668	732	827	878	961	989	986	917	967	881	773	746	572	489	368	367	277
9	2010	134	152	187	220	337	373	472	571	659	812	909	1020	1021	1088	1210	1193	1258	1199	1093	1056	921	814	674	525	469	373
10	2010	106	132	209	223	317	395	483	578	698	802	973	1137	1193	1236	1348	1305	1298	1225	1165	1112	976	900	774	625	507	393
11	2010	38	41	58	74	122	130	169	223	285	319	346	397	435	399	421	458	433	419	366	378	286	276	209	176	146	140
10	2009	295	392	530	674	831	1107	1248	1504	1749	2035	2160	2400	2651	2761	2867	2916	2771	2653	2428	2183	1827	1460	1196	999	877	707

Table A.3: Resolute Bay number of meteors (part 1)

Resolute Bay: Number of meteors per height increment

Month	Year	75	76	77	78	79	80	81	82	83	84	85	86	87	88	89	90	91	92	93	94	95	96	97	98	99	100
		(km)	(km)	(km)	(km)	(km)	(km)	(km)	(km)	(km)	(km)	(km)	(km)	(km)	(km)	(km)	(km)	(km)	(km)	(km)	(km)	(km)	(km)	(km)	(km)	(km)	(km)
6	2000	--	--	138	182	230	252	306	348	490	538	627	687	756	855	956	928	905	810	672	573	454	391	319	280	217	172
7	2000	--	--	545	695	910	1200	1507	1932	2329	2563	2745	2911	3143	3270	3237	3055	2821	2621	2254	1945	1568	1378	1174	958	779	616
8	2000	--	--	1500	2019	2534	2982	3584	4241	4793	5431	5738	6059	6083	5990	5543	5220	4686	4037	3368	2952	2421	2029	1676	1337	1128	877
9	2000	--	--	1180	1492	1767	2044	2374	2668	3014	3296	3480	3687	3622	3713	3577	3312	3083	2780	2458	2133	1876	1566	1341	1060	901	745
10	2000	--	--	361	394	438	554	634	694	739	786	878	853	863	877	879	841	798	663	677	590	508	438	373	337	297	232
11	2000	--	--	321	293	329	392	436	449	471	501	512	543	519	538	463	480	449	420	366	350	320	268	268	215	206	174
12	2000	--	--	990	1191	1352	1640	1642	1854	2020	2201	2159	2271	2258	2163	2081	1936	1783	1594	1435	1318	1091	925	815	699	615	503
1	2001	75	86	409	466	553	647	681	773	860	941	925	1038	1041	1084	1027	1026	951	890	788	726	645	555	549	415	391	311
2	2001	--	--	1286	1439	1725	1758	1935	2041	2165	2227	2187	2186	2115	1953	1872	1680	1533	1291	1184	1086	940	877	778	700	593	562
3	2001	--	--	1302	1490	1616	1810	1906	2087	2235	2299	2417	2390	2251	2185	1991	1794	1621	1457	1234	1089	1002	887	741	726	582	558
4	2001	--	--	1313	1534	1664	1858	1935	2034	2153	2307	2469	2565	2499	2492	2407	2318	2137	1968	1725	1510	1394	1265	1118	965	958	865
5	2001	--	--	1508	1731	1886	2053	2339	2665	2774	2931	3225	3271	3479	3421	3404	3059	2780	2549	2248	1914	1880	1583	1359	1326	1116	1116
6	2001	--	--	1518	1814	2054	2327	2655	2944	3237	3675	3953	4081	4494	4369	4305	4033	3576	3274	2758	2445	2175	1973	1679	1570	1347	1165
7	2001	--	--	2264	2539	2831	3151	3411	3733	4003	4273	4477	4686	4599	4692	4586	4250	4023	3725	3284	2944	2756	2376	2194	1914	1728	1629
8	2001	--	--	1751	2052	2500	2826	3303	3731	4069	4517	4934	5151	5254	5194	5037	4712	4369	3942	3418	3020	2488	2224	1777	1592	1286	1110
9	2001	--	--	1512	1745	2089	2434	2763	3042	3328	3620	3856	4015	4032	4174	4055	3945	3601	3375	3112	2701	2384	2060	1785	1576	1325	1093
10	2001	--	--	1318	1563	1851	2209	2369	2684	2780	3041	3265	3365	3409	3587	3502	3441	3322	3102	2869	2599	2312	2099	1741	1594	1313	1130
11	2001	484	567	1658	1947	2225	2485	2763	3082	3332	3629	3688	3760	3901	3897	3768	3623	3428	3211	3002	2576	2445	2055	1793	1563	1351	1094
12	2001	1088	1407	1704	2042	2357	2720	3147	3332	3717	4038	4271	4414	4464	4646	4327	4286	4081	3690	3364	2880	2598	2289	1854	1499	1303	1051
1	2002	1155	1412	1685	1978	2342	2658	2896	3224	3474	3656	3824	4002	3864	3887	3752	3404	3173	2795	2446	2032	1762	1447	1222	953	760	663
2	2002	824	953	1213	1429	1596	1816	2073	2212	2443	2639	2694	2795	2771	2707	2602	2326	2255	1976	1640	1476	1255	983	864	729	605	519
3	2002	733	934	1145	1447	1681	2016	2233	2502	2836	3061	3320	3440	3688	3686	3622	3372	3241	2822	2487	2149	1794	1512	1197	1002	826	679
4	2002	719	909	1179	1537	1926	2268	2723	3074	3560	3904	4422	4611	5094	5244	5151	4932	4633	4432	3812	3227	2723	2298	1740	1464	1239	965
5	2002	655	904	1239	1647	2138	2721	3332	3934	4687	5290	5963	6768	7125	7478	7371	7200	6671	5991	5085	4383	3700	2965	2314	1801	1440	1138
6	2002	439	583	813	1141	1540	2021	2609	3085	3691	4391	5073	5686	6206	6513	6406	5923	5450	4740	3938	3297	2714	2239	1659	1311	997	786
3	2003	610	791	856	1111	1295	1476	1656	1913	2037	2221	2326	2568	2639	2506	2543	2292	2264	1896	1715	1456	1244	1004	853	691	548	524
4	2003	672	889	1145	1356	1684	2056	2455	2808	3309	3737	3943	4329	4682	4812	4778	4544	4348	3892	3472	2989	2435	2153	1736	1384	1125	857
5	2003	857	1217	1417	1944	2493	3109	3813	4507	5170	5945	6561	7209	7420	7589	7226	6878	6268	5320	4752	4043	3350	2672	2203	1710	1334	1093
6	2003	88	134	179	252	326	423	565	658	818	925	999	1134	1170	1239	1198	1056	1009	873	719	630	491	403	330	279	178	159
7	2004	--	--	161	205	313	380	495	572	761	869	922	1073	1078	1195	1242	1227	1048	958	749	567	473	361	305	237	171	123
8	2004	--	--	1098	1391	1806	2314	2791	3449	3902	4578	4958	5575	5956	6100	5786	5455	4857	4365	3609	3006	2556	2027	1681	1342	1113	923
9	2004	--	--	1184	1484	1789	2164	2489	2952	3205	3707	3919	4294	4541	4624	4431	4472	4119	3914	3523	3148	2692	2401	1972	1546	1313	1095
11	2004	--	--	268	333	347	403	447	482	524	564	573	612	609	649	631	574	553	558	492	456	387	362	285	273	204	176
12	2004	--	--	1694	2042	2366	2670	3182	3543	3733	4174	4457	4797	4864	4730	4746	4433	4217	3959	3362	3097	2774	2296	1953	1675	1461	1237
1	2005	--	--	836	1085	1230	1504	1672	1925	2088	2201	2430	2585	2732	2675	2583	2528	2290	2114	1955	1690	1460	1271	1081	877	774	726
2	2005	--	--	415	502	620	698	864	943	1035	1150	1210	1291	1386	1386	1382	1322	1213	1189	951	850	772	616	548	492	446	357
3	2005	--	--	558	622	786	912	1064	1181	1292	1396	1563	1682	1699	1732	1757	1653	1539	1471	1290	1167	968	875	751	617	584	505
4	2005	--	--	1040	1262	1609	2088	2409	2745	3318	3532	4051	4508	4725	4976	5060	4899	4643	4308	3664	3151	2646	2290	1897	1523	1187	973
5	2005	--	--	229	315	419	609	651	826	985	1141	1283	1435	1536	1627	1754	1698	1598	1399	1212	1054	879	774	626	478	361	316
7	2005	--	--	397	586	742	947	1133	1414	1600	1833	2066	2279	2470	2476	2511	2379	2179	1877	1570	1364	1032	844	738	567	441	384
8	2005	--	--	1196	1560	1942	2466	2876	3517	3982	4496	5054	5397	5902	5852	5773	5451	4844	4274	3668	3117	2510	2097	1775	1442	1185	995
9	2005	--	--	1198	1325	1645	2004	2274	2592	2898	3253	3365	3652	3887	3715	3657	3555	3357	3014	2761	2470	2120	1922	1580	1314	1171	973
10	2005	--	--	946	1174	1290	1543	1756	1951	2093	2323	2406	2622	2691	2701	2704	2617	2491	2432	2154	2141	1838	1679	1439	1278	1104	972
11	2005	--	--	975	1122	1246	1527	1631	1802	1923	2143	2266	2191	2360	2404	2283	2165	2179	2002	1844	1673	1527	1361	1178	992	913	772
12	2005	--	--	797	876	1108	1184	1438	1658	1768	1956	2080	2162	2206	2235	2301	2087	2103	2052	1697	1637	1455	1211	1051	933	760	626

Table A.4: Resolute Bay number of meteors (part 2)

Resolute Bay: Number of meteors per height increment

Month	Year	75	76	77	78	79	80	81	82	83	84	85	86	87	88	89	90	91	92	93	94	95	96	97	98	99	100
		(km)	(km)	(km)	(km)	(km)	(km)	(km)	(km)	(km)	(km)	(km)	(km)	(km)	(km)	(km)	(km)	(km)	(km)	(km)	(km)	(km)	(km)	(km)	(km)	(km)	(km)
1	2006	--	--	567	691	827	938	1040	1214	1332	1476	1509	1657	1697	1663	1591	1635	1476	1374	1176	1074	966	818	701	619	480	422
2	2006	--	--	317	418	448	485	553	576	614	581	661	692	603	594	569	519	479	443	421	347	284	241	233	175	180	141
3	2006	--	--	1029	1173	1364	1620	1876	2008	2251	2478	2617	2646	2790	2828	2694	2574	2283	2117	1871	1588	1360	1109	1053	754	698	586
4	2006	--	--	1278	1534	1894	2136	2678	3148	3430	3812	4365	4600	5037	5197	5216	5059	4842	4471	3932	3337	2894	2416	1951	1699	1424	1159
5	2006	--	--	1335	1756	2343	2899	3631	4427	5236	5930	6740	7499	8094	8442	8512	8197	7572	6701	5720	4869	4131	3465	2745	2200	1696	1493
6	2006	--	--	1516	2155	2895	3867	4859	5937	6995	8094	9381	10274	11155	11562	11744	10877	9860	8378	7027	5856	4740	3895	3115	2519	1931	1524
7	2006	--	--	1055	1432	1759	2427	2822	3461	4046	4733	5303	5922	6384	6488	6447	6096	5399	4634	3909	3062	2524	2080	1770	1366	1146	878
8	2006	--	--	1377	1791	2330	2846	3470	4152	4789	5445	6037	6530	6885	6893	6928	6537	5773	4964	4226	3552	2944	2350	1960	1635	1395	1078
9	2006	--	--	1133	1398	1755	2056	2399	2817	3100	3561	3854	4015	4257	4279	4307	4040	3937	3509	3186	2693	2434	1957	1640	1424	1207	967
10	2006	--	--	1016	1182	1403	1604	1996	2184	2378	2678	2806	2896	2999	3114	3004	2963	2930	2711	2538	2387	2042	1920	1653	1463	1288	1093
11	2006	--	--	1186	1424	1645	1811	2095	2303	2408	2648	2730	2848	2842	3001	2882	2814	2590	2530	2338	2151	1916	1698	1520	1338	1135	1006
12	2006	--	--	1391	1563	1885	2109	2278	2591	2804	2892	3084	3223	3205	3133	3103	2955	2791	2557	2369	2146	1777	1648	1433	1217	1058	842
1	2007	--	--	1418	1628	1894	2090	2451	2602	2777	3003	3125	3119	3082	2829	2785	2557	2214	1998	1817	1559	1248	1187	882	829	738
2	2007	--	--	661	742	980	1239	1271	1446	1598	1694	1851	1899	1922	1936	1916	1825	1596	1466	1318	1129	969	793	722	648	502	452
3	2007	--	--	730	931	1060	1278	1510	1756	1861	2031	2271	2351	2423	2501	2433	2359	2230	2003	1808	1545	1335	1138	933	783	704	563
4	2007	--	--	1170	1454	1891	2203	2675	3073	3600	3977	4337	4765	5048	5035	5138	5008	4665	4180	3631	3184	2731	2155	1847	1434	1181	1006
5	2007	--	--	1024	1273	1774	2113	2703	3074	3745	4105	4628	5140	5510	5461	5495	5213	4833	4237	3668	3120	2617	2156	1770	1327	1153	892
6	2007	--	--	193	285	378	547	650	883	995	1192	1311	1513	1659	1742	1698	1674	1441	1244	1027	871	671	526	462	335	272	234
7	2007	--	--	680	904	1170	1369	1766	2115	2455	2808	3208	3527	3669	3760	3718	3388	3093	2774	2253	1949	1657	1313	1162	942	849	706
8	2007	--	--	750	951	1155	1354	1563	1791	1980	2184	2384	2476	2669	2598	2612	2513	2365	2170	1901	1751	1450	1295	1062	884	776	649
9	2007	--	--	156	171	195	235	269	334	312	354	376	394	404	427	398	395	361	358	316	312	276	261	189	182	163	129
10	2007	--	--	146	187	236	261	297	327	363	435	456	502	511	518	585	520	483	448	374	312	287	231	193	153	126	108
2	2008	--	--	218	326	337	409	466	487	530	546	635	665	662	638	635	624	587	483	430	367	327	253	242	195	136	120
3	2008	--	--	774	954	1178	1410	1684	1990	2297	2550	2909	3111	3279	3384	3547	3460	3271	2924	2674	2263	1961	1602	1410	1137	934	767
4	2008	--	--	383	522	678	939	1163	1400	1625	1900	2148	2390	2605	2830	2989	3032	2925	2651	2313	2068	1695	1343	1070	876	763	603
5	2008	--	--	241	309	468	624	826	1007	1199	1344	1582	1785	1927	2032	1943	1926	1758	1543	1215	979	759	683	502	395	305	250
6	2008	--	--	1092	1472	1983	2646	3360	4012	4797	5734	6466	7238	7887	8346	8389	7938	6939	6017	4822	4000	3137	2557	2086	1716	1351	1093
7	2008	--	--	258	364	435	629	719	934	1112	1204	1416	1504	1694	1780	1766	1681	1530	1370	1093	926	787	636	561	447	371	307
8	2008	--	--	505	698	782	969	1128	1329	1451	1623	1744	1814	1903	1892	2000	1787	1783	1601	1493	1293	1117	939	801	739	552	506
9	2008	--	--	474	582	765	865	1010	1128	1317	1367	1441	1518	1678	1621	1520	1623	1517	1493	1441	1235	1164	1031	955	772	733	604
10	2008	--	--	522	597	654	833	859	964	1037	1181	1202	1260	1259	1382	1279	1279	1272	1205	1139	1025	963	794	711	629	559	481
11	2008	--	--	481	620	757	838	918	1090	1082	1263	1269	1372	1393	1409	1388	1390	1296	1265	1169	1070	922	857	762	689	557	478
12	2008	--	--	367	521	548	718	888	1021	1162	1222	1391	1453	1581	1665	1622	1569	1478	1298	1137	976	824	623	544	466	397	295
4	2009	--	--	611	818	1088	1312	1659	1828	2044	2330	2547	2751	2932	2955	2713	2505	2192	1688	1436	1074	878	638	454	384	294	238
5	2009	--	--	365	477	705	915	1126	1415	1603	1762	1924	2057	2212	2282	2261	1964	1672	1440	989	818	587	479	341	230	203	141
6	2009	--	--	663	908	1180	1560	2091	2558	2843	3346	3868	4402	4628	4798	4837	4733	4161	3458	2799	2300	1820	1607	1165	1039	730	648
7	2009	--	--	412	583	782	1022	1259	1575	1817	2177	2430	2691	2889	2974	3037	2963	2656	2331	1785	1557	1250	998	858	721	567	453
8	2009	--	--	398	513	607	729	908	976	1168	1251	1427	1401	1611	1546	1507	1521	1444	1304	1097	1028	866	686	649	562	482	383
9	2009	--	--	567	782	873	997	1135	1269	1393	1538	1672	1714	1965	1869	1932	1821	1857	1725	1585	1419	1398	1195	1065	957	801	672
10	2009	--	--	583	728	839	931	1058	1193	1238	1365	1434	1418	1474	1488	1478	1326	1362	1239	1152	985	927	770	720	653	561	443
11	2009	--	--	471	565	656	783	841	912	967	1156	1161	1182	1260	1277	1229	1081	1107	1095	896	893	760	635	595	467	445	379
12	2009	--	--	469	521	613	717	844	990	1064	1148	1243	1260	1315	1298	1301	1269	1103	1094	967	830	749	653	563	455	383	351
1	2010	--	--	657	776	956	1071	1204	1346	1461	1582	1705	1761	1767	1718	1615	1575	1511	1262	1184	986	898	713	619	536	427	388
2	2010	--	--	212	273	306	302	403	416	449	501	497	560	567	500	483	480	454	397	285	296	255	227	190	162	140	113
3	2010	--	--	217	230	285	349	434	499	623	637	770	824	918	845	935	888	853	780	752	657	562	533	423	344	296	260
4	2010	--	--	226	415	478	689	804	1028	1211	1478	1651	1880	2036	2163	2141	2119	1930	1816	1520	1246	1035	906	727	595	499	431
5	2010	--	--	421	632	937	1196	1638	2068	2531	3008	3615	3884	4449	4653	4880	4689	4230	3736	3002	2502	2035	1646	1316	1054	830	635
6	2010	--	--	278	385	511	694	842	1086	1351	1508	1744	1941	2125	2224	2193	2020	1817	1516	1251	1011	832	706	561	461	346	298
7	2010	--	--	137	209	256	319	381	483	545	664	739	817	874	976	896	826	735	664	521	432	377	329	276	230	172	140
8	2010	--	--	171	155	178	175	201	225	326	197	283	236	304	212	298	215	282	173	278	153	233	116	209	105	155	112
11	2010	--	--	633	655	721	824	873	869	1180	1043	1224	1050	1245	1101	1269	1085	1148	949	1065	812	882	628	780	515	614	433
12	2010	--	--																								

Table A.5: Socorro number of meteors (part 1)

Socorro: Number of meteors per height increment

Month	Year	75 (km)	76 (km)	77 (km)	78 (km)	79 (km)	80 (km)	81 (km)	82 (km)	83 (km)	84 (km)	85 (km)	86 (km)	87 (km)	88 (km)	89 (km)	90 (km)	91 (km)	92 (km)	93 (km)	94 (km)	95 (km)	96 (km)	97 (km)	98 (km)	99 (km)	100 (km)
4	2002	22	40	47	157	229	283	390	426	513	590	632	715	775	785	832	805	815	834	743	582	560	397	317	245	172	173
5	2002	106	154	234	782	1002	1256	1538	1838	2134	2350	2697	2793	3040	3135	3188	3072	2961	2690	2410	2016	1811	1402	1271	995	942	760
6	2002	65	115	134	498	696	884	1092	1303	1610	1772	1993	2216	2339	2444	2446	2291	2092	1891	1728	1459	1196	1000	844	665	546	428
7	2002	55	52	86	226	344	453	595	662	875	1076	1318	1438	1571	1565	1624	1550	1460	1301	1109	946	758	628	473	362	315	269
8	2002	142	222	276	851	1170	1484	1940	2317	2758	3263	3697	3971	4318	4531	4522	4450	4154	3875	3315	2853	2338	2027	1654	1433	1234	1071
9	2002	102	127	148	529	669	858	1092	1281	1649	1830	2058	2272	2469	2510	2706	2641	2548	2353	2086	1885	1576	1307	1086	901	751	650
10	2002	147	197	213	918	1080	1243	1451	1732	2042	2145	2676	2572	3092	2888	3021	2865	2300	2440	1894	1810	1482	1350	1401	1240	1244	1131
11	2002	32	35	51	171	176	181	200	247	281	287	366	318	456	379	393	401	330	333	243	262	181	197	198	201	159	153
3	2003	37	62	191	266	407	599	743	913	1119	1399	1531	1658	1860	1891	1826	1771	1633	1422	1169	980	724	567	429	321	256	194
4	2003	35	71	234	393	597	835	1090	1342	1605	1844	2177	2394	2552	2598	2635	2585	2486	2007	1809	1340	1060	739	499	413	291	237
1	2005	637	994	1523	2111	2933	4005	4859	5915	6958	8025	8851	9699	10262	10734	11167	10668	10289	9691	8645	7615	6256	4876	3614	2652	1786	1294
2	2005	616	976	1428	2123	2889	4064	4948	6023	7194	8232	9270	9915	10285	10420	10376	9988	9230	8159	7077	5986	4857	3671	2621	1903	1397	988
3	2005	566	932	1448	2198	3149	4218	5153	6178	7245	8341	9155	9882	10093	10194	9894	9384	8537	7466	6368	5080	4100	2999	2144	1519	1067	834
4	2005	486	870	1407	2150	3236	4460	5594	6998	8328	9727	10998	11747	12036	12275	11960	11130	10161	9020	7486	6109	4543	3298	2267	1667	1163	800
5	2005	486	811	1348	2126	3116	4444	5869	7247	8836	10514	11838	12588	13255	13551	13372	12708	11594	9812	8253	6418	4904	3768	2693	1924	1416	1085
6	2005	309	551	941	1499	2329	3415	4516	5783	7180	8567	9606	10582	11394	11268	10899	10283	8871	7627	6231	4799	3677	2682	1909	1279	933	649
7	2005	241	423	738	1200	1842	2867	3947	5049	6295	7402	8456	9299	9850	9975	9763	9111	8058	6702	5477	4130	3174	2294	1631	1171	837	679
8	2005	28	25	68	98	177	257	325	454	572	713	775	852	852	945	853	828	773	742	560	483	372	252	203	150	129	81
5	2007	222	456	760	1325	2135	3346	4304	5579	6819	7795	8551	9215	9318	9204	8912	8325	7376	6359	5300	4122	3066	2238	1545	1131	907	621
6	2007	349	664	1100	1791	2927	4301	6006	7673	9386	11046	12466	13129	13672	13162	12856	12112	10620	9147	7447	5800	4485	3366	2418	1767	1278	950
7	2007	448	757	1275	2091	3204	4888	6786	8948	11274	13837	15875	17777	18603	19359	18827	17819	16080	13857	11585	9245	7217	5397	4050	2879	2074	1566
6	2008	169	278	508	843	1375	2054	2803	3701	4512	5472	6417	6837	7193	7249	6933	6246	5432	4535	3570	2720	2045	1367	1007	673	468	348
7	2008	341	629	1106	1819	3012	4392	6014	7646	9691	11882	13557	14763	15628	15308	14766	13119	11062	9110	6902	5170	3926	2804	2003	1410	1047	809
8	2008	76	123	208	333	517	753	975	1257	1558	1786	2149	2354	2507	2581	2510	2228	1946	1642	1358	990	861	610	459	361	293	202
12	2008	336	562	822	1259	1832	2358	3025	3538	4316	4888	5451	6104	6418	6659	6800	6748	6370	6038	5456	4525	3783	2871	2240	1681	1220	957
1	2009	366	574	839	1358	1841	2673	3411	4084	5036	5661	6471	7013	7354	7789	7713	7754	7173	6622	5934	5027	4080	3186	2380	1755	1191	924
2	2009	262	421	671	1061	1455	1947	2385	2949	3312	4051	4661	5156	5289	5638	5630	5551	5254	4765	4294	3780	3051	2392	1783	1367	967	745
3	2009	259	403	721	1075	1685	2234	2894	3589	4208	4773	5332	5755	5913	5976	6003	5638	5366	4871	4389	3674	3126	2381	1834	1317	1007	673
4	2009	145	256	399	643	1042	1421	1812	2264	2727	3123	3421	3658	3656	3785	3751	3628	3305	3027	2588	2126	1726	1320	981	769	574	402
5	2009	72	130	182	308	398	574	683	848	997	1180	1271	1325	1365	1448	1518	1409	1472	1301	1135	1038	847	785	681	542	408	336
6	2009	196	321	524	851	1217	1932	2566	3173	3897	4649	5061	5410	5533	5632	5365	4679	4182	3409	2821	2045	1533	1117	802	565	349	284
7	2009	480	736	1266	2077	3327	4993	6911	9001	11230	13290	15108	16365	16856	16943	15999	14320	12488	10145	7736	5888	4252	3095	2171	1597	1185	950
8	2009	453	845	1403	2113	3164	4288	5707	7161	9042	10828	12661	13978	14727	15244	15399	14717	13187	11678	9647	7802	6219	4634	3396	2568	1996	1538
9	2009	456	825	1419	2301	3258	4658	5834	7338	8927	10556	12061	13443	14213	15039	15444	14654	13723	12013	10066	8240	6376	4656	3355	2391	1714	1186
10	2009	576	934	1670	2543	3741	5058	6233	7308	8937	9986	11156	12172	12752	13250	13554	13050	12467	11000	9581	7869	6371	4925	3619	2606	1989	1505
11	2009	634	974	1490	2069	2856	3627	4554	5402	6474	7462	8310	9023	9473	9687	9767	9671	9074	8153	7114	5932	4907	3865	2815	2087	1615	1170
12	2009	608	827	1143	1673	2196	2948	3477	4135	4647	5455	5890	6458	6686	6720	6699	6362	5836	5306	4555	3822	3242	2503	1954	1547	1151	900

Table A.6: Socorro number of meteors (part 2)

Socorro: Number of meteors per height increment

Month	Year	75	76	77	78	79	80	81	82	83	84	85	86	87	88	89	90	91	92	93	94	95	96	97	98	99	100
		(km)	(km)	(km)	(km)	(km)	(km)	(km)	(km)	(km)	(km)	(km)	(km)	(km)	(km)	(km)	(km)	(km)	(km)	(km)	(km)	(km)	(km)	(km)	(km)	(km)	(km)
1	2010	511	761	1119	1503	2020	2565	3176	3602	4273	4796	5313	5546	5726	5845	5861	5547	5109	4371	3779	3066	2437	1930	1478	1098	880	606
2	2010	405	613	992	1450	2017	2639	3411	4196	4892	5798	6174	6708	7068	7276	7438	7020	6629	5808	4940	4018	3180	2569	1822	1285	914	642
3	2010	404	646	1156	1784	2690	3578	4508	5468	6457	7491	8220	8776	9073	9099	9104	8601	7815	6901	5769	4756	3670	2771	2004	1512	1016	775
4	2010	330	589	1017	1572	2463	3421	4314	5426	6648	7486	8751	9217	9460	9401	9271	8758	8080	6993	5856	4523	3720	2845	1975	1386	934	676
5	2010	309	559	978	1811	2627	4027	5156	6353	7910	9176	10348	11258	11649	11881	11790	11030	10087	8683	7195	5614	4407	3158	2358	1726	1270	1007
6	2010	355	621	1074	1764	2678	3910	5217	6650	8268	9997	11254	12331	12863	12879	12695	11861	10504	8944	7153	5415	4100	2732	1910	1365	943	614
7	2010	422	709	1168	1937	2928	4397	6058	7657	9798	11765	13821	15183	15989	16190	16168	14996	13251	11377	9064	6937	5196	3734	2692	1824	1346	977
8	2010	363	606	1010	1757	2512	3629	4888	6037	7997	9561	11017	12615	13585	14266	14309	13679	12680	11129	9393	7846	5938	4568	3385	2505	1892	1510
9	2010	432	778	1336	2015	2960	4036	5164	6373	7834	9190	10577	11659	12496	12903	13200	12696	11862	10766	9095	7599	5992	4432	3327	2222	1589	1190
10	2010	461	826	1435	2187	3190	4227	5160	6375	7334	8578	9524	10305	11100	11677	11918	11676	11056	10141	9142	7694	6342	4996	3664	2825	2056	1408
11	2010	504	853	1185	1715	2436	3174	3899	4540	5649	6354	7254	8120	8501	8803	9013	8844	8311	7657	6858	5817	4835	3869	2835	2023	1512	1134
12	2010	552	796	1156	1607	2256	2807	3498	4189	4877	5530	6057	6671	6769	6889	6682	6093	5519	4933	4304	3741	3073	2385	1961	1528	1143	887
1	2011	427	634	901	1302	1729	2332	2841	3396	4096	4673	5194	5851	6026	6101	6057	5837	5270	4900	4275	3583	3042	2334	1714	1316	926	686
2	2011	135	218	404	576	826	1092	1413	1575	1927	2139	2300	2264	2362	2379	2344	2125	2039	1838	1628	1450	1100	875	677	507	398	272
3	2011	199	356	581	898	1265	1700	2143	2634	3062	3431	3674	4011	4176	4122	3980	3844	3530	3323	2836	2513	2110	1672	1253	921	651	474
4	2011	157	263	523	815	1287	1958	2526	3129	3821	4290	4600	4965	5117	5221	5083	4739	4584	4091	3529	2949	2415	1821	1341	937	731	481
5	2011	55	89	173	305	496	846	1158	1470	1833	2107	2206	2317	2463	2450	2339	2342	2200	1929	1654	1415	1107	972	778	589	473	388
6	2011	70	120	235	349	581	960	1394	1751	2302	2732	3163	3329	3442	3474	3386	3113	2790	2396	1982	1559	1200	911	669	452	303	262
7	2011	140	221	348	666	1016	1503	2195	2889	3753	4431	5190	5424	5584	5581	5505	5183	4570	3946	3174	2517	1955	1471	1113	883	655	471
8	2011	185	283	486	811	1225	1776	2386	3114	3806	4390	5134	5697	5898	6388	6348	6130	5639	5027	4424	3578	2993	2412	1831	1406	1089	828
9	2011	261	449	737	1217	1833	2595	3447	4268	5331	6375	7220	7967	8227	8622	8568	8199	7584	6804	5852	4896	3748	2943	2189	1580	1096	851
10	2011	358	629	1044	1761	2497	3494	4486	5324	6551	7272	8277	8986	9572	9760	9769	9756	9050	8199	7292	6061	4916	3815	2958	2164	1589	1144
11	2011	370	557	864	1329	1841	2357	2928	3632	4135	4762	5312	5976	6296	6598	6755	6592	6431	5864	5144	4437	3626	2940	2202	1707	1208	1002
12	2011	443	711	1147	1671	2217	3017	3595	4199	4964	5630	6035	6638	7042	6959	7186	6789	6416	5988	5213	4544	3655	2936	2312	1733	1407	953
1	2012	263	443	649	950	1289	1711	2193	2732	3285	3838	4357	4761	5165	5383	5618	5518	5312	4708	4240	3696	3103	2362	1814	1387	1021	748
2	2012	191	343	556	934	1213	1686	2098	2490	2934	3220	3489	3740	3920	4184	3929	3782	3638	3190	2763	2410	1921	1496	1125	931	611	452
3	2012	221	360	570	894	1268	1853	2226	2777	3157	3669	4051	4334	4558	4571	4550	4433	4093	3770	3247	2729	2118	1615	1288	950	683	490
4	2012	293	509	798	1176	1674	2200	2773	3097	3560	3999	4271	4613	4627	4607	4466	4295	3917	3581	3207	2725	2320	1838	1445	1150	866	660
5	2012	30	61	83	105	157	163	232	239	292	313	319	332	332	343	317	320	316	275	244	189	192	132	109	113	84	71

Table A.7: Yellowknife number of meteors (part 1)

Yellowknife: Number of meteors per height increment

Month	Year	75 (km)	76 (km)	77 (km)	78 (km)	79 (km)	80 (km)	81 (km)	82 (km)	83 (km)	84 (km)	85 (km)	86 (km)	87 (km)	88 (km)	89 (km)	90 (km)	91 (km)	92 (km)	93 (km)	94 (km)	95 (km)	96 (km)	97 (km)	98 (km)	99 (km)	100 (km)
6	2002	14	23	40	107	207	411	761	1214	1889	2871	3932	4869	5528	5777	5543	5026	4281	3267	2382	1600	1089	762	452	286	196	132
7	2002	29	50	85	198	385	780	1362	2214	3307	4485	5931	7146	8189	8289	8047	7305	6338	4907	3792	2593	1761	1083	761	543	382	291
8	2002	39	75	149	309	483	802	1187	1712	2374	3237	4014	4598	5202	5594	5546	5210	4845	3952	3205	2504	1743	1316	904	687	542	449
3	2003	24	27	41	56	66	93	97	129	147	197	202	223	216	223	209	206	179	139	132	118	86	57	55	41	32	30
4	2003	29	31	67	68	104	175	218	258	344	427	541	583	657	753	659	676	658	553	505	355	301	200	168	163	126	68
5	2003	18	29	38	54	102	179	264	406	530	719	934	1048	1071	1100	1005	957	837	703	515	445	296	232	184	135	103	86
6	2003	44	45	43	85	148	267	416	695	1097	1417	1886	2285	2432	2593	2387	1996	1560	1187	811	615	409	304	217	139	111	91
7	2003	21	32	36	89	162	292	514	744	1105	1542	1893	2406	2635	2746	2690	2337	1757	1335	867	652	474	327	262	188	161	160
8	2003	21	39	57	141	209	378	481	699	963	1224	1417	1677	1778	1788	1681	1547	1353	1103	940	647	502	445	378	288	234	226
9	2003	43	60	101	150	239	335	450	488	642	774	895	988	1054	1095	1154	1133	1076	906	757	701	520	401	339	255	188	135
10	2003	71	128	161	205	272	341	463	560	731	794	903	978	1114	1119	1131	1147	1075	978	912	812	652	565	406	344	280	209
11	2003	48	74	90	132	164	235	253	309	332	379	388	438	435	460	474	488	416	381	359	288	246	222	138	127	115	97
12	2003	101	190	235	320	432	571	717	774	811	959	1013	1038	1128	1075	1128	1050	1016	937	773	650	578	478	381	294	249	184
1	2004	99	144	220	254	386	463	564	652	773	845	811	847	876	914	848	740	694	641	466	445	375	310	242	191	154	123
2	2004	77	125	174	215	275	335	408	450	504	564	620	605	608	583	502	495	489	350	341	265	212	188	137	89	68	67
3	2004	44	87	108	144	199	273	343	397	476	506	575	657	659	588	617	542	518	455	407	322	261	239	167	135	100	101
4	2004	47	60	133	188	234	367	519	662	855	1053	1186	1301	1465	1460	1504	1473	1278	1137	914	800	586	454	347	249	184	153
5	2004	38	55	96	128	250	390	539	731	1009	1343	1602	1784	1949	1968	1786	1574	1366	1122	886	720	475	363	286	172	126	110
6	2004	42	56	93	143	232	475	748	1114	1595	2088	2611	2904	2987	3101	2868	2524	2001	1489	1094	878	587	391	262	219	162	88
7	2004	8	11	20	29	67	93	146	202	310	399	511	539	619	569	520	496	386	266	223	158	98	67	55	53	43	45
8	2004	49	78	93	129	209	321	417	569	851	982	1257	1376	1484	1494	1449	1381	1212	972	799	639	515	402	333	287	255	217
9	2004	56	73	126	160	223	271	386	460	634	768	830	1013	1021	1123	1183	1230	1232	1123	910	762	626	494	386	303	251	165
10	2004	90	132	149	254	311	375	488	632	741	852	1021	1109	1163	1262	1372	1353	1381	1291	1160	925	805	666	572	437	342	304
11	2004	100	109	184	232	330	414	480	591	733	779	864	907	985	1043	1065	1001	944	850	800	700	565	429	338	314	261	193
12	2004	71	127	176	218	320	384	477	602	722	950	980	1141	1220	1147	1189	1152	1022	837	804	598	522	402	369	264	204	153
1	2005	63	109	155	200	283	407	488	599	676	800	895	1037	1078	998	998	934	860	723	639	531	398	333	261	207	147	117
2	2005	62	78	99	128	218	248	320	371	457	458	600	662	718	737	704	733	593	519	436	386	276	227	198	147	97	81
3	2005	49	57	67	132	152	201	272	308	400	482	552	599	682	682	689	661	614	529	442	310	286	199	174	124	119	80
4	2005	50	90	110	163	219	292	357	495	631	763	924	992	1064	1111	1135	1105	1033	928	816	640	530	425	308	246	193	164
5	2005	56	72	119	146	248	397	570	833	1162	1529	1914	2150	2365	2355	2234	1980	1729	1343	1034	774	627	412	298	236	185	176
6	2005	61	68	132	202	329	619	1075	1695	2587	3579	4573	5252	5673	5762	5260	4506	3465	2532	1732	1202	788	505	369	249	187	163
7	2005	8	6	9	12	29	46	80	156	209	317	405	422	516	506	439	386	304	219	139	98	68	40	24	29	19	19
8	2005	36	62	96	159	272	442	645	982	1314	1641	1934	2270	2333	2328	2191	2033	1712	1304	1036	725	528	438	305	257	222	210
9	2005	79	113	190	286	481	608	781	997	1184	1424	1578	1703	1840	1891	1942	1870	1694	1480	1225	955	801	585	447	344	285	223
10	2005	112	173	266	340	459	548	736	883	1106	1292	1380	1515	1745	1821	1863	1991	1946	1815	1697	1424	1144	922	722	551	425	336
11	2005	99	156	227	326	406	539	645	791	967	1174	1324	1522	1523	1623	1610	1546	1514	1402	1258	1108	928	776	565	420	362	271
12	2005	145	225	271	415	565	737	885	1126	1355	1562	1779	2009	2247	2268	2453	2419	2333	2071	1921	1624	1347	1102	871	643	513	413

Table A.8: Yellowknife number of meteors (part 2)

Yellowknife: Number of meteors per height increment

Month	Year	75	76	77	78	79	80	81	82	83	84	85	86	87	88	89	90	91	92	93	94	95	96	97	98	99	100
		(km)	(km)	(km)	(km)	(km)	(km)	(km)	(km)	(km)	(km)	(km)	(km)	(km)	(km)	(km)	(km)	(km)	(km)	(km)	(km)	(km)	(km)	(km)	(km)	(km)	(km)
1	2006	83	100	147	225	272	394	454	550	705	771	894	933	982	1057	1052	1070	938	875	842	693	569	445	351	314	223	172
2	2006	111	154	199	286	352	452	597	649	751	810	856	861	951	912	937	866	726	653	537	463	368	285	226	171	129	96
3	2006	69	117	169	223	329	421	527	660	791	951	1132	1176	1256	1320	1311	1261	1137	1021	814	701	557	407	310	218	156	120
4	2006	56	108	138	220	310	444	558	734	970	1200	1340	1561	1752	1876	1986	1875	1749	1642	1306	1176	913	693	517	389	288	208
5	2006	29	51	80	131	210	406	628	913	1296	1752	2265	2706	3061	3391	3270	3301	2845	2422	1918	1559	1079	742	522	359	230	175
6	2006	41	47	70	113	196	384	634	1116	1695	2534	3364	4003	4674	4964	4760	4207	3611	2658	1949	1333	941	612	375	252	169	124
7	2006	35	61	61	110	199	335	615	1066	1656	2368	3298	4063	4920	5474	5627	5228	4310	3164	2263	1344	850	547	425	264	200	204
8	2006	22	23	61	85	174	325	487	745	1105	1550	2025	2383	2773	2863	3108	2835	2510	1935	1444	1008	768	523	412	344	267	249
9	2006	8	34	38	57	95	114	152	173	256	310	342	404	420	470	502	563	475	435	356	311	268	182	145	123	92	75
11	2006	15	19	14	35	42	60	70	106	118	137	161	167	148	159	176	168	145	136	123	102	108	75	59	37	33	27
12	2006	34	56	56	90	143	136	169	220	227	290	294	321	332	347	382	343	329	284	256	211	192	147	132	92	78	68
1	2007	40	60	79	133	150	196	256	261	324	321	360	310	317	339	264	250	247	213	193	160	132	117	96	88	59	51
2	2007	8	9	22	33	53	65	79	88	111	115	127	130	138	147	132	113	122	112	110	88	67	55	36	32	21	22
12	2007	11	29	37	65	83	100	123	122	122	149	151	165	141	131	140	124	115	105	108	66	70	57	41	38	22	19
4	2008	11	16	27	58	92	143	207	282	341	466	554	727	773	809	878	897	823	792	687	542	501	355	284	195	172	127
5	2008	16	33	66	110	196	315	505	821	1165	1678	2120	2631	2946	3212	3323	3148	2906	2331	1929	1458	986	725	464	349	221	169
6	2008	43	48	78	152	256	511	976	1628	2623	3781	5281	6385	7339	7681	7450	6489	5131	3876	2756	1832	1289	805	596	453	243	231
7	2008	38	48	70	122	250	397	774	1152	1720	2461	3288	4078	4543	4781	4897	4226	3434	2581	1889	1301	945	643	483	365	265	233
8	2008	44	62	106	186	365	604	902	1364	1985	2649	3426	4024	4618	4957	5019	4955	4500	3743	2878	2319	1714	1271	989	733	663	560
9	2008	49	90	140	221	356	479	645	860	1105	1454	1716	1991	2258	2560	2783	2900	2885	2687	2414	1974	1615	1336	942	744	577	408
10	2008	79	123	188	278	350	489	636	807	1009	1176	1416	1462	1795	1928	2139	2146	2180	2083	1888	1790	1427	1199	937	789	554	505
11	2008	62	114	159	194	256	339	486	506	694	780	928	1055	1232	1233	1372	1383	1331	1280	1149	1029	902	660	497	376	292	214
12	2008	111	172	251	344	474	685	774	1000	1187	1385	1606	1692	1869	1995	2106	2092	1978	1875	1790	1504	1348	1097	877	652	502	357
1	2009	94	126	208	291	423	538	684	863	1128	1404	1593	1735	1917	2027	2007	1910	1852	1580	1410	1215	982	761	620	484	385	254
2	2009	86	150	208	310	392	526	621	817	888	1014	1192	1272	1356	1344	1403	1264	1155	1085	873	788	551	455	367	310	196	177
3	2009	105	147	181	327	436	612	742	941	1081	1325	1458	1722	1866	1885	1829	1799	1638	1420	1320	997	763	636	464	327	248	209
4	2009	50	106	134	195	357	484	635	823	1011	1239	1637	1806	2047	2312	2435	2439	2404	2252	1947	1625	1261	1036	813	603	435	379
5	2009	41	40	79	125	191	354	518	798	1217	1678	2092	2536	2886	3084	3222	3156	2699	2327	1838	1408	996	675	533	371	245	177
6	2009	42	51	51	101	186	344	621	1068	1747	2624	3554	4357	5042	5465	5321	4804	3958	3107	2319	1628	1062	734	398	272	197	186
7	2009	44	47	65	133	253	491	785	1462	2183	3103	4126	5040	5903	6505	6417	5918	4957	3784	2825	1918	1318	927	645	451	386	312
8	2009	62	83	139	246	463	818	1252	1747	2549	3523	4449	5282	6158	6849	7190	6696	6055	5090	3917	2997	2160	1752	1338	973	834	751
9	2009	60	142	198	293	445	641	920	1140	1512	1881	2352	2789	3137	3571	3761	3970	3765	3705	3225	2830	2357	1757	1291	988	658	537
10	2009	87	135	198	284	390	555	769	907	1191	1419	1665	1923	2212	2421	2654	2785	2820	2722	2504	2251	2020	1614	1221	983	771	649
11	2009	181	267	393	591	692	970	1191	1526	1865	2156	2384	2667	2844	2983	3146	3090	3127	2849	2659	2384	1913	1585	1313	940	745	609
12	2009	36	63	75	100	138	163	269	260	345	416	466	524	521	530	607	575	596	551	459	421	358	284	234	190	157	118

Table A.9: CLOVAR ambipolar diffusion slope

CLOVAR: Ambipolar diffusion regime slope per height increment

Month	Year	75	76	77	78	79	80	81	82	83	84	85	86	87	88	89	90	91	92	93	94	95	96	97	98	99	100
		(km)	(km)	(km)	(km)	(km)	(km)	(km)	(km)	(km)	(km)	(km)	(km)	(km)	(km)	(km)	(km)	(km)	(km)	(km)	(km)	(km)	(km)	(km)	(km)	(km)	(km)
7	2000	-0.226	-0.069	-0.437	-0.230	-0.247	-0.273	-0.316	-0.224	-0.209	-0.190	-0.234	-0.341	-0.526	-0.464	-0.542	-0.525	-0.720	-0.687	-0.556	-0.517	-0.474	-0.405	-0.419	-0.462	-0.555	-0.257
8	2000	-0.561	-0.431	-0.217	-0.178	-0.277	-0.159	-0.120	-0.094	-0.215	-0.259	-0.279	-0.166	-0.450	-0.446	-0.474	-0.616	-0.516	-0.660	-0.584	-0.539	-0.539	-0.517	-0.480	-0.502	-0.473	-0.475
9	2000	-0.172	-0.493	-0.424	-0.205	-0.302	-0.208	-0.236	-0.245	-0.240	-0.138	-0.360	-0.323	-0.228	-0.303	-0.613	-0.542	-0.599	-0.722	-0.628	-0.520	-0.559	-0.568	-0.519	-0.381	-0.374	-0.428
10	2000	-0.576	-0.250	-0.235	-0.274	-0.185	-0.183	-0.192	-0.150	-0.212	-0.182	-0.326	-0.425	-0.305	-0.638	-0.476	-0.714	-0.671	-0.651	-0.559	-0.577	-0.563	-0.494	-0.540	-0.559	-0.352	-0.538
11	2000	-0.079	-0.452	-0.291	-0.296	-0.340	-0.208	-0.223	-0.125	-0.251	-0.399	-0.132	-0.361	-0.436	-0.527	-0.470	-0.626	-0.642	-0.629	-0.640	-0.585	-0.493	-0.533	-0.447	-0.567	-0.630	-0.479
12	2000	-0.297	-0.430	-0.542	-0.232	-0.249	-0.229	-0.282	-0.149	-0.241	-0.331	-0.417	-0.573	-0.174	-0.205	-0.225	-0.400	-0.402	-0.348	-0.703	-0.534	-0.570	-0.533	-0.475	-0.475	-0.383	-0.468
1	2001	-0.348	-0.183	-0.308	-0.407	-0.248	-0.349	-0.241	-0.198	-0.141	-0.117	-0.243	-0.138	-0.315	-0.258	-0.400	-0.724	-0.776	-0.571	-0.561	-0.522	-0.533	-0.514	-0.525	-0.510	-0.413	-0.419
11	2001	-0.232	-0.374	-0.361	-0.140	-0.052	-0.127	-0.163	-0.141	-0.121	-0.108	-0.094	-0.388	-0.394	-0.165	-0.229	-0.729	-0.409	-0.730	-0.599	-0.602	-0.602	-0.650	-0.586	-0.575	-0.576	-0.637
12	2001	-0.520	-0.363	-0.391	-0.330	-0.112	-0.161	-0.088	-0.218	-0.308	-0.115	-0.175	-0.111	-0.197	-0.551	-0.707	-0.506	-0.501	-0.658	-0.708	-0.677	-0.572	-0.593	-0.468	-0.597	-0.561	-0.306
1	2002	-0.353	-0.529	-0.237	-0.151	-0.068	-0.155	-0.149	-0.193	-0.185	-0.192	-0.180	-0.181	-0.287	-0.479	-0.481	-0.559	-0.680	-0.802	-0.713	-0.688	-0.426	-0.613	-0.763	-0.579	-0.595	-0.573
2	2002	-0.336	-0.438	-0.080	-0.055	-0.281	-0.070	-0.090	-0.087	-0.118	-0.156	-0.129	-0.156	-0.387	-0.311	-0.308	-0.350	-0.284	-0.705	-0.869	-0.458	-0.591	-0.554	-0.683	-0.480	-0.666	-0.673
3	2002	-0.572	-0.301	-0.253	-0.076	-0.362	-0.109	-0.281	-0.048	-0.129	-0.197	-0.162	-0.219	-0.334	-0.205	-0.382	-0.642	-0.351	-0.522	-0.632	-0.721	-0.696	-0.576	-0.801	-0.605	-0.475	-0.504
4	2002	-0.554	-0.619	-0.380	-0.249	-0.129	-0.274	-0.112	-0.090	-0.160	-0.116	-0.188	-0.132	-0.201	-0.474	-0.568	-0.590	-0.636	-0.668	-0.614	-0.571	-0.568	-0.570	-0.601	-0.471	-0.786	-0.478
5	2002	-0.360	0.000	-0.385	-0.591	-0.466	-0.248	-0.075	-0.109	-0.142	-0.149	-0.318	-0.371	-0.414	-0.499	-0.672	-0.254	-0.739	-0.577	-0.633	-0.407	-0.548	-0.529	-0.664	-0.572	-0.532	-0.451
6	2002	-0.356	-0.344	-0.872	-0.464	-0.402	-0.112	-0.266	-0.178	-0.281	-0.191	-0.148	-0.283	-0.184	-0.459	-0.417	-0.459	-0.468	-0.661	-0.660	-0.638	-0.525	-0.619	-0.908	-0.442	-0.584	-0.292
7	2002	-0.509	-0.328	-0.435	-0.420	-0.271	-0.387	-0.341	-0.260	-0.143	-0.253	-0.218	-0.150	-0.321	-0.455	-0.422	-0.408	-0.553	-0.705	-0.496	-0.556	-0.530	-0.544	-0.702	-0.577	-0.332	-0.390
8	2002	-0.501	-0.676	-0.237	-0.303	-0.240	-0.278	-0.116	-0.110	-0.142	-0.110	-0.227	-0.345	-0.211	-0.358	-0.403	-0.680	-0.586	-0.539	-0.529	-0.629	-0.600	-0.571	-0.431	-0.557	-0.494	-0.553
9	2002	-1.127	-0.343	-0.119	-0.688	-0.293	-0.234	-0.157	-0.081	-0.210	-0.137	-0.073	-0.127	-0.201	-0.471	-0.508	-0.258	-0.677	-0.474	-0.651	-0.556	-0.730	-0.543	-0.386	-0.682	-0.430	-0.516
10	2002	0.000	-0.156	-0.379	-0.138	-0.130	-0.229	-0.103	-0.070	-0.126	-0.070	-0.290	-0.118	-0.093	-0.158	-0.485	-0.592	-0.380	-0.688	-0.564	-0.597	-0.573	-0.490	-0.608	-0.470	-0.422	-0.583
11	2002	-0.308	-0.318	-0.120	-0.273	-0.142	-0.081	-0.139	-0.142	-0.173	-0.166	-0.177	-0.213	-0.371	-0.170	-0.298	-0.543	-0.652	-0.497	-0.684	-0.707	-0.558	-0.703	-0.626	-0.453	-0.570	-0.570
12	2002	-0.112	-0.148	-0.321	-0.278	-0.155	-0.107	-0.102	-0.112	-0.145	-0.112	-0.153	-0.094	-0.454	-0.300	-0.212	-0.751	-0.497	-0.754	-0.665	-0.592	-0.503	-0.543	-0.483	-0.592	-0.614	-0.558
1	2003	-0.388	-0.264	-0.360	-0.151	-0.211	-0.049	-0.268	-0.119	-0.116	-0.128	-0.168	-0.189	-0.178	-0.559	-0.468	-0.686	-0.349	-0.491	-0.762	-0.536	-0.648	-0.684	-0.735	-0.503	-0.473	-0.490
2	2003	-0.566	-0.434	-0.229	-0.277	-0.153	-0.102	-0.092	-0.136	-0.122	-0.099	-0.123	-0.177	-0.108	-0.345	-0.437	-0.283	-0.485	-0.580	-0.503	-0.490	-0.465	-0.602	-0.656	-0.576	-0.548	-0.910
3	2003	-0.154	-0.176	-0.266	-0.106	-0.352	-0.038	-0.068	-0.119	-0.076	-0.121	-0.043	-0.200	-0.149	-0.339	-0.338	-0.732	-0.650	-0.570	-0.673	-0.660	-0.474	-0.765	-0.612	-0.643	-0.676	-0.542
4	2003	-0.196	-0.289	-0.263	-0.427	-0.108	-0.265	-0.128	-0.077	-0.095	-0.110	-0.160	-0.116	-0.206	-0.116	-0.220	-0.674	-0.710	-0.568	-0.739	-0.529	-0.800	-0.735	-0.557	-0.559	-0.468	-0.333
5	2003	-0.102	-0.254	-0.439	-0.405	-0.135	-0.225	-0.223	-0.201	-0.173	-0.206	-0.239	-0.189	-0.190	-0.387	-0.517	-0.741	-0.679	-0.722	-0.583	-0.647	-0.489	-0.512	-0.481	-0.550	-0.520	-0.593
6	2003	-0.535	-0.505	-0.412	-0.538	-0.163	-0.410	-0.279	-0.383	-0.179	-0.254	-0.149	-0.185	-0.455	-0.446	-0.604	-0.688	-0.670	-0.682	-0.579	-0.594	-0.503	-0.482	-0.446	-0.422	-0.449	-0.482
7	2003	-0.245	-0.466	-0.384	-0.469	-0.348	-0.435	-0.416	-0.248	-0.213	-0.276	-0.235	-0.182	-0.430	-0.448	-0.322	-0.685	-0.666	-0.796	-0.594	-0.609	-0.568	-0.543	-0.477	-0.523	-0.395	-0.400
8	2003	-0.532	-0.372	-0.309	-0.202	-0.322	-0.156	-0.239	-0.096	-0.192	-0.246	-0.114	-0.276	-0.328	-0.252	-0.614	-0.631	-0.652	-0.653	-0.707	-0.642	-0.520	-0.536	-0.500	-0.602	-0.454	-0.449
9	2003	-0.532	-0.299	-0.339	-0.101	-0.185	-0.108	-0.109	-0.129	-0.157	-0.190	-0.139	-0.190	-0.350	-0.148	-0.627	-0.720	-0.562	-0.615	-0.619	-0.571	-0.677	-0.552	-0.618	-0.600	-0.624	-0.458
10	2003	0.000	-0.135	-0.414	-0.211	-0.224	-0.092	-0.082	-0.012	-0.080	-0.026	-0.109	-0.138	-0.220	-0.471	-0.310	-0.630	-0.521	-0.769	-0.685	-0.603	-0.525	-0.572	-0.605	-0.457	-0.831	-0.570
12	2007	-0.107	-0.148	-0.133	-0.608	-0.234	-0.120	-0.117	-0.064	-0.296	-0.125	-0.449	-0.401	-0.164	-0.224	-0.492	-0.597	-0.587	-0.593	-0.442	-0.530	-0.459	-0.648	-0.452	-0.496	-0.563	-0.546
1	2008	-0.405	0.000	0.000	0.000	-0.343	-0.282	-0.085	-0.343	-0.130	-0.092	-0.595	-0.792	-0.435	-0.138	-0.706	-0.574	-0.622	-0.466	-0.849	-0.395	-0.897	-0.715	-0.277	-0.562	-0.505	-0.361
2	2008	0.000	-0.196	-0.134	-0.122	-0.111	-0.185	-0.095	-0.122	-0.097	-0.216	-0.199	-0.411	-0.144	-0.392	-0.554	-0.231	-0.228	-0.497	-0.405	-0.464	-0.562	-0.601	-0.410	-0.574	-0.464	-0.811
3	2008	-0.552	-0.301	-0.366	-0.104	-0.085	-0.141	-0.170	-0.050	-0.032	-0.365	-0.077	-0.499	-0.295	-0.369	-0.316	-0.491	-0.527	-0.632	-0.634	-0.743	-0.600	-0.557	-0.429	-0.431	-0.247	-0.552
4	2008	-0.097	-0.335	-0.213	-0.296	-0.089	-0.076	-0.201	-0.102	-0.181	-0.048	-0.143	-0.077	-0.198	-0.545	-0.494	-0.706	-0.717	-0.530	-0.745	-0.594	-0.526	-0.502	-0.473	-0.360	-0.466	-0.750
9	2008	-0.232	-0.200	-0.637	-0.143	-0.369	-0.168	-0.132	-0.240	-0.163	-0.081	-0.262	-0.366	-0.196	-0.569	-0.460	-0.512	-0.712	-0.586	-0.488	-0.509	-0.472	-0.592	-0.437	-0.761	-0.629	-0.520
10	2008	-0.197	-0.283	-0.392	-0.451	-0.063	-0.162	-0.079	-0.191	-0.157	-0.096	-0.430	-0.189	-0.439	-0.352	-0.561	-0.786	-0.663	-0.703	-0.684	-0.607	-0.620	-0.603	-0.567	-0.548	-0.478	-0.471

Table A.10: Costa Rica ambipolar diffusion slope

Costa Rica: Ambipolar diffusion regime slope per height increment

Month	Year	75	76	77	78	79	80	81	82	83	84	85	86	87	88	89	90	91	92	93	94	95	96	97	98	99	100
		(km)	(km)	(km)	(km)	(km)	(km)	(km)	(km)	(km)	(km)	(km)	(km)	(km)	(km)	(km)	(km)	(km)	(km)	(km)	(km)	(km)	(km)	(km)	(km)	(km)	(km)
4	2005	-0.213	-0.120	-0.091	-0.196	-0.119	-0.079	-0.124	-0.136	-0.117	-0.125	-0.092	-0.105	-0.125	-0.204	-0.220	-0.274	-0.189	-0.587	-0.654	-0.625	-0.384	-0.625	-0.636	-0.476	-0.580	-0.588
5	2005	-0.118	-0.080	-0.077	-0.084	-0.166	-0.100	-0.095	-0.095	-0.073	-0.115	-0.120	-0.132	-0.139	-0.192	-0.249	-0.163	-0.399	-0.472	-0.601	-0.743	-0.752	-0.654	-0.689	-0.607	-0.586	-0.537
6	2005	-0.197	-0.104	-0.213	-0.107	-0.111	-0.065	-0.120	-0.093	-0.127	-0.096	-0.134	-0.140	-0.144	-0.150	-0.218	-0.277	-0.327	-0.353	-0.488	-0.646	-0.594	-0.672	-0.595	-0.288	-0.500	-0.444
7	2005	-0.258	-0.189	-0.190	-0.146	-0.160	-0.130	-0.185	-0.187	-0.201	-0.084	-0.148	-0.185	-0.186	-0.202	-0.208	-0.207	-0.369	-0.382	-0.455	-0.641	-0.777	-0.724	-0.775	-0.664	-0.522	-0.506
8	2005	-0.287	-0.153	-0.131	-0.295	-0.219	-0.184	-0.172	-0.168	-0.131	-0.144	-0.186	-0.174	-0.136	-0.226	-0.237	-0.242	-0.246	-0.482	-0.352	-0.835	-0.536	-0.762	-0.647	-0.600	-0.582	-0.534
9	2005	-0.485	-0.336	-0.164	-0.128	-0.304	-0.177	-0.198	-0.171	-0.156	-0.129	-0.171	-0.178	-0.186	-0.174	-0.210	-0.327	-0.383	-0.531	-0.347	-0.859	-0.745	-0.727	-0.636	-0.586	-0.313	-0.439
10	2005	-0.399	-0.259	-0.311	-0.169	-0.149	-0.142	-0.140	-0.124	-0.128	-0.121	-0.162	-0.147	-0.166	-0.216	-0.184	-0.330	-0.278	-0.440	-0.633	-0.776	-0.755	-0.741	-0.730	-0.638	-0.547	-0.376
11	2005	-0.214	-0.187	-0.172	-0.196	-0.107	-0.085	-0.062	-0.121	-0.228	-0.299	-0.154	-0.244	-0.177	-0.227	-0.125	-0.180	-0.272	-0.724	-0.299	-0.425	-0.497	-0.633	-0.690	-0.568	-0.403	-0.587
12	2005	-0.519	-0.102	-0.144	-0.240	-0.159	-0.069	-0.150	-0.215	-0.206	-0.135	-0.172	-0.150	-0.187	-0.215	-0.340	-0.283	-0.351	-0.501	-0.645	-0.553	-0.689	-0.856	-0.718	-0.746	-0.625	-0.676
1	2006	-0.271	-0.517	-0.351	-0.201	-0.315	-0.150	-0.230	-0.173	-0.186	-0.151	-0.122	-0.124	-0.181	-0.236	-0.316	-0.424	-0.399	-0.690	-0.725	-0.864	-0.815	-0.841	-0.707	-0.693	-0.679	-0.591
4	2007	-0.138	-0.163	-0.092	-0.063	-0.057	-0.095	-0.061	-0.043	-0.076	-0.077	-0.073	-0.132	-0.090	-0.112	-0.323	-0.218	-0.516	-0.201	-0.391	-0.615	-0.818	-0.579	-0.593	-0.505	-0.569	-0.628
5	2007	-0.118	-0.115	-0.108	-0.103	-0.125	-0.102	-0.118	-0.066	-0.093	-0.108	-0.083	-0.097	-0.116	-0.207	-0.178	-0.326	-0.460	-0.567	-0.707	-0.602	-0.748	-0.722	-0.635	-0.624	-0.562	-0.473
6	2007	-0.189	-0.153	-0.107	-0.126	-0.055	-0.058	-0.091	-0.099	-0.077	-0.111	-0.139	-0.107	-0.164	-0.181	-0.261	-0.279	-0.490	-0.524	-0.704	-0.519	-0.716	-0.685	-0.654	-0.520	-0.404	-0.488
7	2007	-0.055	-0.165	-0.135	-0.169	-0.100	-0.118	-0.121	-0.094	-0.120	-0.139	-0.143	-0.145	-0.130	-0.188	-0.304	-0.355	-0.473	-0.600	-0.691	-0.506	-0.711	-0.730	-0.627	-0.551	-0.522	-0.499
8	2007	-0.158	-0.049	-0.094	-0.099	-0.072	-0.073	-0.068	-0.067	-0.106	-0.065	-0.079	-0.155	-0.179	-0.216	-0.289	-0.308	-0.255	-0.595	-0.741	-0.379	-0.716	-0.341	-0.691	-0.519	-0.508	-0.461
9	2007	-0.186	-0.235	-0.075	-0.062	-0.110	-0.123	-0.092	-0.138	-0.074	-0.095	-0.119	-0.109	-0.144	-0.156	-0.254	-0.276	-0.427	-0.669	-0.533	-0.728	-0.531	-0.589	-0.712	-0.573	-0.388	-0.374
10	2007	-0.240	-0.047	-0.084	-0.099	-0.058	-0.103	-0.095	-0.125	-0.085	-0.079	-0.080	-0.117	-0.125	-0.156	-0.255	-0.389	-0.550	-0.679	-0.905	-0.808	-0.834	-0.640	-0.555	-0.610	-0.616	-0.500
11	2007	-0.311	-0.025	-0.050	-0.083	-0.077	-0.053	-0.129	-0.035	-0.136	-0.074	-0.082	-0.077	-0.101	-0.198	-0.179	-0.530	-0.238	-0.789	-0.896	-0.850	-0.785	-0.646	-0.665	-0.618	-0.612	-0.451
12	2007	-0.672	-0.371	-0.100	-0.163	-0.176	-0.124	-0.184	-0.121	-0.212	-0.128	-0.188	-0.254	-0.318	-0.417	-0.639	-0.475	-0.838	-0.995	-0.917	-0.951	-0.929	-0.754	-0.871	-0.570	-0.508	-0.565
1	2008	-0.176	-0.044	-0.203	-0.192	-0.192	-0.099	-0.171	-0.132	-0.174	-0.077	-0.115	-0.175	-0.198	-0.360	-0.355	-0.423	-0.695	-0.713	-0.857	-0.900	-0.847	-0.753	-0.750	-0.681	-0.550	-0.605
2	2008	-0.249	-0.289	-0.152	-0.071	-0.190	-0.201	-0.128	-0.179	-0.056	-0.151	-0.234	-0.182	-0.156	-0.217	-0.310	-0.333	-0.491	-0.693	-0.821	-0.617	-0.771	-0.741	-0.660	-0.725	-0.365	-0.558
3	2008	-0.062	-0.133	-0.043	-0.171	-0.075	-0.073	-0.065	-0.076	-0.130	-0.066	-0.109	-0.121	-0.092	-0.195	-0.258	-0.418	-0.492	-0.341	-0.486	-0.694	-0.689	-0.716	-0.752	-0.694	-0.638	-0.600
4	2008	-0.085	-0.122	-0.121	-0.080	-0.075	-0.092	-0.086	-0.097	-0.118	-0.102	-0.088	-0.099	-0.160	-0.221	-0.286	-0.324	-0.471	-0.446	-0.575	-0.633	-0.641	-0.659	-0.635	-0.625	-0.566	-0.323
5	2008	-0.133	-0.128	-0.172	-0.082	-0.053	-0.079	-0.068	-0.082	-0.143	-0.100	-0.126	-0.155	-0.169	-0.232	-0.279	-0.185	-0.526	-0.417	-0.651	-0.715	-0.704	-0.744	-0.507	-0.584	-0.401	-0.551
6	2008	-0.111	-0.082	-0.111	-0.096	-0.088	-0.101	-0.102	-0.111	-0.097	-0.091	-0.068	-0.104	-0.146	-0.198	-0.182	-0.364	-0.342	-0.548	-0.807	-0.657	-0.743	-0.593	-0.618	-0.664	-0.585	-0.487
7	2008	-0.173	-0.051	-0.088	-0.158	-0.091	-0.077	-0.108	-0.095	-0.102	-0.115	-0.085	-0.180	-0.201	-0.177	-0.273	-0.235	-0.385	-0.450	-0.544	-0.700	-0.721	-0.641	-0.594	-0.509	-0.466	-0.379
8	2008	-0.275	-0.089	-0.257	-0.067	-0.106	-0.143	-0.112	-0.114	-0.094	-0.104	-0.180	-0.129	-0.176	-0.151	-0.181	-0.672	-0.380	-0.568	-0.263	-0.558	-0.603	-0.410	-0.568	-0.607	-0.550	-0.501
9	2008	-0.469	-0.174	-0.144	-0.089	-0.130	-0.070	-0.090	-0.140	-0.074	-0.112	-0.083	-0.115	-0.125	-0.170	-0.174	-0.354	-0.489	-0.544	-0.606	-0.801	-0.712	-0.640	-0.598	-0.523	-0.579	-0.492
10	2008	-0.121	-0.211	-0.231	-0.082	-0.153	-0.182	-0.112	-0.096	-0.125	-0.097	-0.094	-0.131	-0.199	-0.151	-0.248	-0.289	-0.675	-0.279	-0.736	-0.776	-0.731	-0.514	-0.673	-0.481	-0.506	-0.587
11	2008	-0.461	-0.167	-0.152	-0.093	-0.074	-0.144	-0.176	-0.085	-0.199	-0.121	-0.179	-0.087	-0.093	-0.301	-0.116	-0.319	-0.525	-0.514	-0.487	-0.847	-0.640	-0.576	-0.535	-0.591	-0.553	-0.611
3	2009	-0.135	-0.315	-0.130	-0.161	-0.159	-0.181	-0.204	-0.044	-0.121	-0.162	-0.172	-0.141	-0.145	-0.216	-0.058	-0.188	-0.141	-0.167	-0.698	-0.719	-0.722	-0.601	-0.741	-0.399	-0.298	-0.371
10	2009	-0.179	-0.168	-0.223	-0.112	-0.140	-0.103	-0.078	-0.073	-0.137	-0.120	-0.124	-0.091	-0.101	-0.178	-0.344	-0.246	-0.424	-0.479	-0.647	-0.655	-0.737	-0.688	-0.599	-0.524	-0.491	-0.515
1	2010	--	--	--	--	-0.073	--	--	-0.082	-0.361	--	-0.033	-0.143	-0.052	-0.035	-0.074	-0.226	-0.139	-0.017	-0.194	-0.229	-0.226	-0.057	-0.050	-0.451	-0.229	--
2	2010	--	-0.063	-0.138	-0.204	-0.041	-0.095	-0.090	-0.047	-0.086	-0.060	-0.121	-0.087	-0.130	-0.093	-0.134	-0.135	-0.377	-0.317	-0.349	-0.389	-0.313	-0.209	-0.461	-0.390	-0.320	-0.246
3	2010	-0.228	-0.434	-0.156	-0.125	-0.213	-0.147	-0.085	-0.064	-0.092	-0.079	-0.061	-0.101	-0.125	-0.134	-0.175	-0.173	-0.262	-0.355	-0.471	-0.595	-0.624	-0.368	-0.611	-0.513	-0.797	-0.574
4	2010	-0.207	-0.074	-0.205	-0.184	-0.116	-0.134	-0.107	-0.098	-0.079	-0.081	-0.098	-0.109	-0.100	-0.097	-0.119	-0.147	-0.237	-0.224	-0.321	-0.401	-0.282	-0.495	-0.416	-0.467	-0.529	-0.218
6	2010	-0.270	-0.104	-0.090	-0.066	-0.177	-0.108	-0.093	-0.086	-0.150	-0.078	-0.096	-0.075	-0.119	-0.090	-0.127	-0.189	-0.239	-0.345	-0.352	-0.459	-0.448	-0.332	-0.420	-0.550	-0.465	-0.462
7	2010	-0.150	-0.093	-0.055	-0.188	-0.170	-0.218	-0.151	-0.070	-0.095	-0.112	-0.105	-0.089	-0.116	-0.090	-0.126	-0.151	-0.149	-0.121	-0.299	-0.179	-0.411	-0.336	-0.382	-0.354	-0.312	-0.516
8	2010	-0.147	-0.073	-0.104	-0.141	-0.138	-0.186	-0.132	-0.157	-0.123	-0.132	-0.103	-0.095	-0.138	-0.136	-0.119	-0.189	-0.276	-0.318	-0.411	-0.358	-0.405	-0.357	-0.575	-0.432	-0.380	-0.521
9	2010	-0.199	-0.104	-0.209	-0.134	-0.147	-0.138	-0.089	-0.118	-0.097	-0.115	-0.122	-0.131	-0.098	-0.126	-0.182	-0.149	-0.258	-0.293	-0.369	-0.459	-0.494	-0.574	-0.571	-0.479	-0.460	-0.411
10	2010	-0.116	-0.191	-0.277	-0.160	-0.120	-0.135	-0.055	-0.124	-0.091	-0.087	-0.107	-0.103	-0.088	-0.107	-0.168	-0.168	-0.142	-0.207	-0.402	-0.314	-0.377	-0.393	-0.402	-0.480	-0.420	-0.539
11	2010	-0.117	-0.062	-0.245	-0.059	-0.091	-0.106	-0.107	-0.038	-0.079	-0.080	-0.068	-0.094	-0.083	-0.135	-0.143	-0.115	-0.194	-0.320	-0.190	-0.447	-0.152	-0.701	-0.296	-0.695	-0.235	-0.336

Table A.11: Resolute Bay ambipolar diffusion slope (part 1)

Resolute Bay: Ambipolar diffusion regime slope per height increment

Month	Year	75	76	77	78	79	80	81	82	83	84	85	86	87	88	89	90	91	92	93	94	95	96	97	98	99	100
		(km)	(km)	(km)	(km)	(km)	(km)	(km)	(km)	(km)	(km)	(km)	(km)	(km)	(km)	(km)	(km)	(km)	(km)	(km)	(km)	(km)	(km)	(km)	(km)	(km)	(km)
6	2000	--	--	-0.139	-0.303	-0.116	-0.289	-0.250	-0.211	-0.216	-0.220	-0.221	-0.238	-0.277	-0.339	-0.323	-0.383	-0.315	-0.433	-0.457	-0.400	-0.339	-0.349	-0.493	-0.388	-0.503
7	2000	--	--	-0.182	-0.261	-0.225	-0.238	-0.216	-0.214	-0.187	-0.192	-0.207	-0.259	-0.279	-0.295	-0.314	-0.343	-0.343	-0.434	-0.434	-0.410	-0.355	-0.410	-0.394	-0.377	-0.397	-0.354
8	2000	--	--	-0.136	-0.172	-0.211	-0.161	-0.183	-0.235	-0.229	-0.222	-0.267	-0.304	-0.324	-0.376	-0.429	-0.445	-0.484	-0.434	-0.443	-0.458	-0.419	-0.470	-0.439	-0.461	-0.473	-0.460
9	2000	--	--	-0.150	-0.169	-0.192	-0.214	-0.221	-0.241	-0.275	-0.289	-0.311	-0.376	-0.389	-0.477	-0.552	-0.572	-0.588	-0.539	-0.534	-0.473	-0.449	-0.504	-0.484	-0.532	-0.504	-0.495
10	2000	--	--	-0.235	-0.223	-0.248	-0.267	-0.231	-0.248	-0.330	-0.379	-0.363	-0.468	-0.593	-0.522	-0.536	-0.636	-0.562	-0.638	-0.460	-0.565	-0.524	-0.556	-0.452	-0.597	-0.481	-0.430
11	2000	--	--	-0.282	-0.322	-0.229	-0.312	-0.326	-0.325	-0.481	-0.294	-0.546	-0.567	-0.534	-0.529	-0.542	-0.566	-0.499	-0.512	-0.500	-0.532	-0.580	-0.478	-0.459	-0.501	-0.397	-0.383
12	2000	--	--	-0.231	-0.211	-0.179	-0.205	-0.300	-0.315	-0.400	-0.388	-0.456	-0.546	-0.573	-0.638	-0.576	-0.597	-0.666	-0.534	-0.544	-0.587	-0.465	-0.479	-0.498	-0.488	-0.494	-0.430
1	2001	-0.348	-0.183	-0.300	-0.187	-0.223	-0.200	-0.190	-0.205	-0.245	-0.248	-0.242	-0.250	-0.284	-0.339	-0.355	-0.404	-0.459	-0.452	-0.369	-0.424	-0.451	-0.511	-0.424	-0.409	-0.483	-0.351
2	2001	--	--	-0.199	-0.240	-0.286	-0.351	-0.283	-0.289	-0.395	-0.433	-0.443	-0.518	-0.522	-0.544	-0.576	-0.529	-0.513	-0.568	-0.473	-0.461	-0.465	-0.407	-0.382	-0.403	-0.382	-0.395
3	2001	--	--	-0.170	-0.196	-0.185	-0.238	-0.193	-0.211	-0.281	-0.345	-0.385	-0.464	-0.477	-0.502	-0.575	-0.551	-0.543	-0.570	-0.508	-0.446	-0.510	-0.493	-0.400	-0.401	-0.381	-0.482
4	2001	--	--	-0.202	-0.232	-0.220	-0.202	-0.286	-0.263	-0.236	-0.269	-0.321	-0.365	-0.359	-0.375	-0.343	-0.457	-0.429	-0.468	-0.443	-0.436	-0.366	-0.442	-0.419	-0.438	-0.310	-0.411
5	2001	--	--	-0.226	-0.220	-0.245	-0.219	-0.203	-0.236	-0.220	-0.232	-0.231	-0.276	-0.280	-0.334	-0.370	-0.335	-0.395	-0.410	-0.399	-0.390	-0.365	-0.395	-0.318	-0.346	-0.269	-0.379
6	2001	--	--	-0.228	-0.187	-0.204	-0.230	-0.244	-0.290	-0.216	-0.232	-0.247	-0.259	-0.321	-0.306	-0.403	-0.411	-0.361	-0.419	-0.400	-0.351	-0.403	-0.413	-0.436	-0.357	-0.343	-0.338
7	2001	--	--	-0.250	-0.247	-0.249	-0.249	-0.278	-0.261	-0.267	-0.259	-0.263	-0.289	-0.299	-0.316	-0.352	-0.353	-0.350	-0.363	-0.363	-0.380	-0.393	-0.380	-0.393	-0.392	-0.360	-0.371
8	2001	--	--	-0.216	-0.216	-0.210	-0.229	-0.245	-0.272	-0.258	-0.241	-0.288	-0.307	-0.319	-0.342	-0.383	-0.414	-0.447	-0.446	-0.447	-0.418	-0.444	-0.459	-0.493	-0.457	-0.441	-0.440
9	2001	--	--	-0.170	-0.197	-0.189	-0.197	-0.194	-0.253	-0.230	-0.272	-0.302	-0.337	-0.410	-0.500	-0.533	-0.525	-0.517	-0.539	-0.488	-0.488	-0.492	-0.520	-0.516	-0.530	-0.513	-0.549
10	2001	--	--	-0.181	-0.207	-0.188	-0.193	-0.246	-0.250	-0.287	-0.271	-0.391	-0.435	-0.474	-0.536	-0.588	-0.574	-0.626	-0.561	-0.509	-0.524	-0.477	-0.510	-0.493	-0.530	-0.581	-0.452
11	2001	-0.150	-0.188	-0.149	-0.184	-0.201	-0.217	-0.217	-0.228	-0.330	-0.338	-0.349	-0.544	-0.531	-0.624	-0.644	-0.583	-0.562	-0.586	-0.551	-0.493	-0.473	-0.513	-0.522	-0.506	-0.503	-0.457
12	2001	-0.177	-0.157	-0.211	-0.175	-0.150	-0.230	-0.274	-0.310	-0.330	-0.407	-0.440	-0.523	-0.607	-0.606	-0.616	-0.656	-0.597	-0.612	-0.597	-0.573	-0.539	-0.527	-0.549	-0.570	-0.584	-0.468
1	2002	-0.181	-0.144	-0.148	-0.209	-0.211	-0.257	-0.315	-0.335	-0.406	-0.399	-0.515	-0.510	-0.639	-0.635	-0.590	-0.645	-0.545	-0.589	-0.552	-0.519	-0.452	-0.520	-0.534	-0.467	-0.576	-0.512
2	2002	-0.118	-0.122	-0.129	-0.160	-0.154	-0.197	-0.199	-0.214	-0.236	-0.268	-0.398	-0.379	-0.501	-0.467	-0.602	-0.595	-0.623	-0.565	-0.569	-0.554	-0.562	-0.513	-0.490	-0.527	-0.585	-0.496
3	2002	-0.132	-0.184	-0.113	-0.134	-0.107	-0.163	-0.112	-0.211	-0.201	-0.227	-0.258	-0.338	-0.420	-0.509	-0.499	-0.582	-0.639	-0.604	-0.594	-0.616	-0.549	-0.564	-0.521	-0.549	-0.560	-0.578
4	2002	-0.140	-0.085	-0.084	-0.112	-0.102	-0.107	-0.118	-0.132	-0.128	-0.174	-0.217	-0.209	-0.305	-0.405	-0.422	-0.450	-0.470	-0.566	-0.557	-0.535	-0.572	-0.552	-0.552	-0.563	-0.544	-0.504
5	2002	-0.161	-0.126	-0.147	-0.138	-0.111	-0.125	-0.128	-0.145	-0.145	-0.161	-0.183	-0.231	-0.245	-0.328	-0.364	-0.428	-0.455	-0.484	-0.475	-0.512	-0.509	-0.479	-0.556	-0.537	-0.494	-0.538
6	2002	-0.206	-0.150	-0.150	-0.138	-0.162	-0.196	-0.171	-0.187	-0.206	-0.201	-0.213	-0.232	-0.183	-0.306	-0.324	-0.409	-0.411	-0.452	-0.446	-0.447	-0.465	-0.486	-0.500	-0.566	-0.509	-0.487
3	2003	-0.175	-0.114	-0.136	-0.139	-0.163	-0.181	-0.181	-0.133	-0.269	-0.196	-0.326	-0.429	-0.469	-0.502	-0.577	-0.594	-0.547	-0.529	-0.511	-0.569	-0.501	-0.543	-0.524	-0.628	-0.636	-0.469
4	2003	-0.133	-0.116	-0.094	-0.159	-0.128	-0.127	-0.119	-0.137	-0.172	-0.167	-0.194	-0.276	-0.279	-0.334	-0.387	-0.458	-0.450	-0.497	-0.505	-0.489	-0.509	-0.458	-0.514	-0.542	-0.502	-0.569
5	2003	-0.157	-0.151	-0.118	-0.117	-0.137	-0.141	-0.140	-0.157	-0.169	-0.175	-0.197	-0.210	-0.232	-0.320	-0.354	-0.413	-0.463	-0.458	-0.474	-0.469	-0.470	-0.508	-0.445	-0.456	-0.589	-0.484
6	2003	-0.284	-0.267	-0.310	-0.162	-0.273	-0.235	-0.276	-0.180	-0.220	-0.207	-0.193	-0.257	-0.292	-0.370	-0.359	-0.432	-0.460	-0.376	-0.347	-0.412	-0.303	-0.444	-0.433	-0.429	-0.544	-0.316
7	2004	--	--	-0.111	-0.132	-0.141	-0.163	-0.175	-0.166	-0.186	-0.190	-0.214	-0.220	-0.215	-0.207	-0.339	-0.398	-0.349	-0.397	-0.407	-0.386	-0.386	-0.404	-0.414	-0.520	-0.497	-0.408
8	2004	--	--	-0.174	-0.172	-0.149	-0.192	-0.208	-0.202	-0.241	-0.231	-0.247	-0.251	-0.258	-0.365	-0.334	-0.422	-0.465	-0.468	-0.460	-0.436	-0.406	-0.491	-0.465	-0.449	-0.445	-0.458
9	2004	--	--	-0.143	-0.158	-0.145	-0.166	-0.173	-0.199	-0.221	-0.254	-0.294	-0.316	-0.376	-0.460	-0.523	-0.547	-0.608	-0.606	-0.542	-0.510	-0.520	-0.523	-0.549	-0.561	-0.588	-0.562
11	2004	--	--	-0.188	-0.185	-0.279	-0.274	-0.374	-0.351	-0.373	-0.400	-0.489	-0.653	-0.457	-0.505	-0.637	-0.640	-0.539	-0.669	-0.629	-0.423	-0.541	-0.483	-0.539	-0.591	-0.674	-0.465
12	2004	--	--	-0.162	-0.209	-0.212	-0.199	-0.236	-0.304	-0.314	-0.365	-0.438	-0.472	-0.480	-0.573	-0.610	-0.587	-0.581	-0.575	-0.518	-0.529	-0.497	-0.525	-0.576	-0.505	-0.502	-0.495
1	2005	--	--	-0.172	-0.182	-0.203	-0.225	-0.249	-0.279	-0.242	-0.308	-0.400	-0.449	-0.468	-0.561	-0.524	-0.574	-0.601	-0.533	-0.569	-0.516	-0.513	-0.506	-0.477	-0.521	-0.484	-0.447
2	2005	--	--	-0.147	-0.171	-0.149	-0.166	-0.126	-0.160	-0.180	-0.228	-0.261	-0.273	-0.377	-0.353	-0.505	-0.447	-0.564	-0.521	-0.557	-0.495	-0.570	-0.524	-0.486	-0.521	-0.534	-0.476
3	2005	--	--	-0.127	-0.143	-0.152	-0.130	-0.173	-0.173	-0.210	-0.220	-0.254	-0.262	-0.363	-0.403	-0.427	-0.507	-0.442	-0.492	-0.560	-0.481	-0.510	-0.511	-0.545	-0.510	-0.496	-0.440
4	2005	--	--	-0.136	-0.182	-0.086	-0.118	-0.143	-0.168	-0.147	-0.180	-0.213	-0.208	-0.287	-0.322	-0.375	-0.485	-0.541	-0.516	-0.602	-0.585	-0.559	-0.483	-0.532	-0.519	-0.570	-0.506
5	2005	--	--	-0.157	-0.097	-0.226	-0.142	-0.114	-0.111	-0.231	-0.210	-0.173	-0.200	-0.276	-0.280	-0.273	-0.361	-0.434	-0.457	-0.494	-0.455	-0.454	-0.492	-0.413	-0.395	-0.408	-0.493
7	2005	--	--	-0.320	-0.174	-0.145	-0.234	-0.213	-0.225	-0.237	-0.187	-0.211	-0.223	-0.245	-0.250	-0.263	-0.422	-0.446	-0.501	-0.425	-0.412	-0.352	-0.345	-0.500	-0.359	-0.477	-0.516
8	2005	--	--	-0.205	-0.175	-0.237	-0.214	-0.191	-0.202	-0.232	-0.251	-0.235	-0.251	-0.289	-0.340	-0.398	-0.468	-0.487	-0.491	-0.449	-0.437	-0.467	-0.420	-0.496	-0.379	-0.483	-0.426
9	2005	--	--	-0.172	-0.153	-0.199	-0.182	-0.212	-0.218	-0.243	-0.252	-0.276	-0.298	-0.400	-0.457	-0.507	-0.546	-0.509	-0.491	-0.498	-0.511	-0.458	-0.487	-0.520	-0.502	-0.483	-0.461
10	2005	--	--	-0.180	-0.158	-0.172	-0.174	-0.201	-0.204	-0.231	-0.287	-0.328	-0.344	-0.446	-0.506	-0.549	-0.552	-0.568	-0.602	-0.533	-0.536	-0.519	-0.468	-0.547	-0.543	-0.541	-0.532
11	2005	--	--	-0.153	-0.162	-0.197	-0.197	-0.240	-0.231	-0.236	-0.327	-0.424	-0.458	-0.546	-0.573	-0.607	-0.571	-0.610	-0.536	-0.538	-0.585	-0.552	-0.558	-0.517	-0.479	-0.514	-0.543
12	2005	--	--	-0.173	-0.123	-0.229	-0.203	-0.245	-0.250	-0.280	-0.280	-0.415	-0.459	-0.479	-0.561	-0.610	-0.589	-0.524	-0.640	-0.605	-0.518	-0.589	-0.545	-0.572	-0.580	-0.488	-0.605

Table A.12: Resolute Bay ambipolar diffusion slope (part 2)

Resolute Bay: Ambipolar diffusion regime slope per height increment

Month	Year	75 (km)	76 (km)	77 (km)	78 (km)	79 (km)	80 (km)	81 (km)	82 (km)	83 (km)	84 (km)	85 (km)	86 (km)	87 (km)	88 (km)	89 (km)	90 (km)	91 (km)	92 (km)	93 (km)	94 (km)	95 (km)	96 (km)	97 (km)	98 (km)	99 (km)	100 (km)
1	2006	--	--	-0.184	-0.128	-0.214	-0.198	-0.225	-0.226	-0.283	-0.274	-0.334	-0.440	-0.550	-0.654	-0.611	-0.645	-0.661	-0.531	-0.594	-0.553	-0.607	-0.569	-0.560	-0.636	-0.597	-0.503
2	2006	--	--	-0.263	-0.220	-0.315	-0.278	-0.283	-0.458	-0.467	-0.593	-0.654	-0.693	-0.602	-0.572	-0.696	-0.609	-0.670	-0.607	-0.645	-0.706	-0.525	-0.469	-0.613	-0.586	-0.624	-0.554
3	2006	--	--	-0.119	-0.133	-0.137	-0.160	-0.141	-0.189	-0.194	-0.226	-0.280	-0.345	-0.371	-0.485	-0.498	-0.518	-0.552	-0.573	-0.518	-0.573	-0.561	-0.566	-0.520	-0.473	-0.506	-0.500
4	2006	--	--	-0.047	-0.124	-0.195	-0.115	-0.117	-0.152	-0.192	-0.190	-0.191	-0.256	-0.293	-0.324	-0.390	-0.479	-0.386	-0.531	-0.555	-0.567	-0.506	-0.523	-0.463	-0.531	-0.450	-0.509
5	2006	--	--	-0.198	-0.114	-0.161	-0.149	-0.155	-0.169	-0.210	-0.177	-0.180	-0.205	-0.235	-0.263	-0.361	-0.352	-0.450	-0.400	-0.456	-0.458	-0.438	-0.477	-0.471	-0.466	-0.483	-0.451
6	2006	--	--	-0.157	-0.153	-0.153	-0.171	-0.240	-0.215	-0.228	-0.221	-0.249	-0.226	-0.250	-0.339	-0.337	-0.398	-0.446	-0.447	-0.424	-0.423	-0.436	-0.420	-0.474	-0.492	-0.489	-0.467
7	2006	--	--	-0.265	-0.201	-0.191	-0.181	-0.234	-0.209	-0.214	-0.244	-0.212	-0.238	-0.246	-0.312	-0.339	-0.461	-0.455	-0.438	-0.423	-0.404	-0.383	-0.401	-0.424	-0.438	-0.378	-0.426
8	2006	--	--	-0.185	-0.182	-0.147	-0.174	-0.194	-0.213	-0.256	-0.204	-0.250	-0.267	-0.284	-0.367	-0.437	-0.445	-0.497	-0.499	-0.430	-0.442	-0.434	-0.449	-0.475	-0.492	-0.440	-0.428
9	2006	--	--	-0.106	-0.207	-0.158	-0.198	-0.201	-0.227	-0.241	-0.232	-0.241	-0.300	-0.299	-0.492	-0.551	-0.560	-0.587	-0.572	-0.535	-0.452	-0.489	-0.504	-0.511	-0.511	-0.507	-0.511
10	2006	--	--	-0.206	-0.156	-0.171	-0.183	-0.202	-0.211	-0.252	-0.267	-0.314	-0.346	-0.351	-0.475	-0.539	-0.554	-0.554	-0.575	-0.559	-0.536	-0.535	-0.495	-0.427	-0.508	-0.557	-0.509
11	2006	--	--	-0.203	-0.180	-0.199	-0.263	-0.253	-0.288	-0.294	-0.351	-0.340	-0.506	-0.518	-0.561	-0.571	-0.560	-0.582	-0.565	-0.484	-0.492	-0.492	-0.523	-0.515	-0.568	-0.514	-0.531
12	2006	--	--	-0.185	-0.187	-0.214	-0.293	-0.299	-0.277	-0.353	-0.286	-0.446	-0.494	-0.476	-0.622	-0.625	-0.593	-0.576	-0.529	-0.588	-0.502	-0.502	-0.513	-0.483	-0.493	-0.549	-0.491
1	2007	--	--	-0.201	-0.224	-0.266	-0.259	-0.289	-0.331	-0.283	-0.430	-0.426	-0.593	-0.499	-0.616	-0.599	-0.654	-0.618	-0.641	-0.571	-0.516	-0.515	-0.533	-0.561	-0.500	-0.506	-0.584
2	2007	--	--	-0.148	-0.146	-0.191	-0.180	-0.122	-0.158	-0.293	-0.281	-0.320	-0.279	-0.458	-0.469	-0.598	-0.518	-0.499	-0.531	-0.549	-0.530	-0.572	-0.529	-0.552	-0.464	-0.458	-0.480
3	2007	--	--	-0.126	-0.133	-0.205	-0.146	-0.214	-0.160	-0.226	-0.224	-0.250	-0.297	-0.370	-0.449	-0.468	-0.472	-0.476	-0.528	-0.525	-0.546	-0.511	-0.483	-0.540	-0.549	-0.474	-0.533
4	2007	--	--	-0.081	-0.086	-0.076	-0.090	-0.104	-0.115	-0.138	-0.143	-0.155	-0.187	-0.235	-0.280	-0.310	-0.428	-0.511	-0.516	-0.543	-0.553	-0.447	-0.443	-0.539	-0.597	-0.499	-0.479
5	2007	--	--	-0.097	-0.162	-0.119	-0.172	-0.156	-0.161	-0.184	-0.169	-0.170	-0.206	-0.230	-0.304	-0.357	-0.415	-0.457	-0.498	-0.461	-0.460	-0.507	-0.493	-0.512	-0.526	-0.500	-0.515
6	2007	--	--	-0.376	-0.236	-0.201	-0.186	-0.237	-0.344	-0.278	-0.280	-0.233	-0.229	-0.317	-0.230	-0.363	-0.331	-0.522	-0.479	-0.465	-0.416	-0.413	-0.390	-0.401	-0.476	-0.477	-0.390
8	2007	--	--	-0.191	-0.205	-0.187	-0.173	-0.204	-0.207	-0.209	-0.203	-0.241	-0.254	-0.296	-0.361	-0.425	-0.497	-0.488	-0.497	-0.442	-0.461	-0.433	-0.436	-0.458	-0.504	-0.436	-0.470
9	2007	--	--	-0.185	-0.146	-0.274	-0.265	-0.201	-0.234	-0.222	-0.266	-0.317	-0.360	-0.461	-0.498	-0.510	-0.626	-0.552	-0.556	-0.520	-0.540	-0.494	-0.480	-0.466	-0.534	-0.452	-0.507
10	2007	--	--	-0.153	-0.078	-0.232	-0.262	-0.252	-0.216	-0.251	-0.266	-0.335	-0.378	-0.291	-0.479	-0.517	-0.537	-0.645	-0.610	-0.668	-0.554	-0.541	-0.545	-0.562	-0.614	-0.622	-0.694
2	2008	--	--	-0.038	-0.163	-0.076	-0.182	-0.280	-0.096	-0.142	-0.110	-0.245	-0.187	-0.263	-0.225	-0.329	-0.397	-0.423	-0.483	-0.458	-0.578	-0.454	-0.518	-0.409	-0.711	-0.614	-0.393
3	2008	--	--	-0.098	-0.134	-0.113	-0.131	-0.151	-0.192	-0.198	-0.322	-0.302	-0.274	-0.464	-0.434	-0.557	-0.564	-0.555	-0.680	-0.512	-0.558	-0.572	-0.557	-0.572	-0.555	-0.336	-0.607
4	2008	--	--	-0.145	-0.121	-0.137	-0.113	-0.131	-0.126	-0.199	-0.195	-0.213	-0.248	-0.293	-0.333	-0.408	-0.476	-0.442	-0.504	-0.571	-0.535	-0.596	-0.519	-0.501	-0.495	-0.519	-0.430
5	2008	--	--	-0.110	-0.152	-0.139	-0.100	-0.149	-0.132	-0.259	-0.202	-0.141	-0.189	-0.212	-0.242	-0.266	-0.398	-0.432	-0.450	-0.445	-0.480	-0.457	-0.467	-0.465	-0.383	-0.478	-0.489
6	2008	--	--	-0.174	-0.226	-0.182	-0.266	-0.228	-0.186	-0.248	-0.247	-0.182	-0.252	-0.291	-0.336	-0.323	-0.422	-0.447	-0.386	-0.408	-0.366	-0.451	-0.478	-0.473	-0.430	-0.468	-0.382
7	2008	--	--	-0.186	-0.155	-0.239	-0.192	-0.191	-0.204	-0.243	-0.240	-0.235	-0.226	-0.264	-0.298	-0.355	-0.401	-0.461	-0.482	-0.453	-0.406	-0.426	-0.403	-0.441	-0.488	-0.497	-0.454
8	2008	--	--	-0.189	-0.208	-0.185	-0.215	-0.224	-0.276	-0.291	-0.274	-0.256	-0.263	-0.302	-0.303	-0.377	-0.423	-0.454	-0.550	-0.432	-0.424	-0.438	-0.447	-0.473	-0.512	-0.478	-0.398
9	2008	--	--	-0.095	-0.185	-0.122	-0.116	-0.145	-0.108	-0.175	-0.139	-0.218	-0.289	-0.309	-0.291	-0.492	-0.568	-0.485	-0.535	-0.533	-0.535	-0.613	-0.481	-0.522	-0.499	-0.517	-0.545
10	2008	--	--	-0.079	-0.137	-0.096	-0.151	-0.145	-0.216	-0.179	-0.232	-0.233	-0.356	-0.409	-0.425	-0.528	-0.510	-0.537	-0.593	-0.543	-0.559	-0.458	-0.544	-0.542	-0.551	-0.498	-0.549
11	2008	--	--	-0.100	-0.166	-0.137	-0.150	-0.153	-0.214	-0.179	-0.242	-0.318	-0.369	-0.457	-0.513	-0.523	-0.542	-0.494	-0.493	-0.540	-0.546	-0.485	-0.492	-0.521	-0.463	-0.455	-0.465
12	2008	--	--	-0.129	-0.148	-0.164	-0.212	-0.281	-0.195	-0.285	-0.342	-0.439	-0.423	-0.500	-0.538	-0.571	-0.538	-0.568	-0.581	-0.544	-0.543	-0.570	-0.459	-0.604	-0.477	-0.520	-0.529
4	2009	--	--	-0.110	-0.111	-0.075	-0.093	-0.108	-0.115	-0.153	-0.117	-0.178	-0.172	-0.179	-0.265	-0.375	-0.345	-0.428	-0.531	-0.500	-0.520	-0.477	-0.522	-0.495	-0.484	-0.607	-0.435
5	2009	--	--	-0.153	-0.136	-0.181	-0.164	-0.155	-0.198	-0.173	-0.192	-0.207	-0.181	-0.223	-0.293	-0.295	-0.439	-0.498	-0.510	-0.488	-0.546	-0.489	-0.435	-0.450	-0.494	-0.393	-0.421
6	2009	--	--	-0.226	-0.175	-0.179	-0.130	-0.225	-0.261	-0.245	-0.283	-0.247	-0.265	-0.262	-0.256	-0.361	-0.283	-0.349	-0.540	-0.433	-0.525	-0.462	-0.442	-0.299	-0.459	-0.411	-0.430
7	2009	--	--	-0.274	-0.214	-0.183	-0.170	-0.161	-0.206	-0.240	-0.217	-0.226	-0.231	-0.244	-0.277	-0.335	-0.439	-0.471	-0.467	-0.481	-0.407	-0.431	-0.435	-0.468	-0.439	-0.442	-0.466
8	2009	--	--	-0.152	-0.175	-0.116	-0.116	-0.184	-0.195	-0.222	-0.240	-0.229	-0.227	-0.252	-0.315	-0.383	-0.443	-0.448	-0.514	-0.450	-0.472	-0.463	-0.467	-0.442	-0.523	-0.499	-0.460
9	2009	--	--	-0.147	-0.190	-0.164	-0.126	-0.262	-0.216	-0.200	-0.237	-0.223	-0.344	-0.359	-0.344	-0.477	-0.589	-0.451	-0.602	-0.552	-0.499	-0.552	-0.438	-0.510	-0.509	-0.510	-0.604
10	2009	--	--	-0.113	-0.181	-0.186	-0.165	-0.233	-0.205	-0.229	-0.320	-0.342	-0.385	-0.445	-0.530	-0.537	-0.573	-0.628	-0.603	-0.514	-0.535	-0.545	-0.560	-0.559	-0.547	-0.497	-0.510
11	2009	--	--	-0.171	-0.168	-0.261	-0.260	-0.324	-0.329	-0.260	-0.295	-0.198	-0.396	-0.482	-0.404	-0.541	-0.606	-0.543	-0.576	-0.549	-0.576	-0.515	-0.490	-0.455	-0.541	-0.543	-0.474
12	2009	--	--	-0.173	-0.319	-0.158	-0.238	-0.303	-0.262	-0.281	-0.295	-0.198	-0.360	-0.445	-0.416	-0.650	-0.658	-0.531	-0.625	-0.542	-0.600	-0.565	-0.520	-0.478	-0.550	-0.510	-0.406
1	2010	--	--	-0.246	-0.209	-0.229	-0.216	-0.248	-0.237	-0.314	-0.410	-0.416	-0.450	-0.504	-0.512	-0.587	-0.535	-0.587	-0.523	-0.525	-0.540	-0.481	-0.480	-0.480	-0.504	-0.463	-0.366
2	2010	--	--	-0.091	-0.133	-0.169	-0.195	-0.180	-0.190	-0.262	-0.216	-0.275	-0.342	-0.343	-0.566	-0.580	-0.625	-0.562	-0.599	-0.539	-0.537	-0.495	-0.596	-0.485	-0.452	-0.543	-0.527
3	2010	--	--	-0.211	-0.183	-0.288	-0.263	-0.129	-0.223	-0.200	-0.242	-0.247	-0.384	-0.468	-0.628	-0.550	-0.703	-0.457	-0.575	-0.523	-0.457	-0.619	-0.597	-0.507	-0.545	-0.703	-0.493
4	2010	--	--	-0.095	-0.137	-0.194	-0.083	-0.130	-0.226	-0.153	-0.185	-0.196	-0.146	-0.257	-0.346	-0.406	-0.313	-0.294	-0.604	-0.597	-0.452	-0.460	-0.496	-0.428	-0.472	-0.488	-0.485
5	2010	--	--	-0.098	-0.088	-0.184	-0.199	-0.285	-0.148	-0.172	-0.235	-0.255	-0.201	-0.282	-0.284	-0.295	-0.374	-0.444	-0.473	-0.499	-0.487	-0.519	-0.386	-0.462	-0.386	-0.491	-0.529
6	2010	--	--	-0.112	-0.181	-0.147	-0.128	-0.300	-0.222	-0.233	-0.247	-0.270	-0.262	-0.255	-0.323	-0.350	-0.411	-0.497	-0.488	-0.470	-0.432	-0.453	-0.469	-0.412	-0.512	-0.497	-0.489
7	2010	--	--	-0.174	-0.075	-0.239	-0.136	-0.154	-0.252	-0.185	-0.214	-0.250	-0.254	-0.265	-0.234	-0.376	-0.430	-0.419	-0.436	-0.432	-0.415	-0.381	-0.411	-0.447	-0.346	-0.457	-0.421
8	2010	--	--	-0.124	-0.186	-0.242	-0.222	-0.244	-0.176	-0.217	-0.198	-0.226	-0.208	-0.247	-0.312	-0.417	-0.449	-0.581	-0.439	-0.417	-0.412	-0.430	-0.470	-0.332	-0.434	-0.494	-0.380
11	2010	--	--	-0.069	-0.051	-0.008	-0.008	-0.047	-0.146	-0.030	-0.014	-0.024	-0.051	-0.009	-0.019	0.018	-0.141	-0.046	-0.180	-0.052	-0.214	-0.148	-0.139	-0.037	-0.111	-0.064	--
12	2010	--	--	-0.294	-0.087	-0.327	-0.336	-0.309	-0.323	-0.405	-0.260	-0.371	-0.321	-0.575	-0.516	-0.601	-0.493	-0.543	-0.539	-0.488	-0.544	-0.464	-0.518	-0.493	-0.273	-0.446	-0.507

Table A.13: Socorro ambipolar diffusion slope (part 1)

Socorro: Ambipolar diffusion regime slope per height increment

Month	Year	75	76	77	78	79	80	81	82	83	84	85	86	87	88	89	90	91	92	93	94	95	96	97	98	99	100
		(km)	(km)	(km)	(km)	(km)	(km)	(km)	(km)	(km)	(km)	(km)	(km)	(km)	(km)	(km)	(km)	(km)	(km)	(km)	(km)	(km)	(km)	(km)	(km)	(km)	(km)
4	2002	-0.245	-0.336	-0.103	-0.148	-0.170	-0.140	-0.085	-0.203	-0.182	-0.197	-0.276	-0.097	-0.141	-0.522	-0.610	-0.681	-0.659	-0.465	-0.573	-0.536	-0.574	-0.570	-0.606	-0.294	-0.581	-0.560
5	2002	-0.175	-0.300	-0.108	-0.281	-0.211	-0.243	-0.215	-0.232	-0.171	-0.198	-0.205	-0.219	-0.270	-0.355	-0.376	-0.313	-0.503	-0.588	-0.607	-0.560	-0.559	-0.566	-0.494	-0.533	-0.527	-0.344
6	2002	-0.252	-0.286	-0.338	-0.291	-0.154	-0.214	-0.172	-0.129	-0.223	-0.201	-0.204	-0.305	-0.276	-0.324	-0.503	-0.484	-0.553	-0.560	-0.537	-0.566	-0.561	-0.465	-0.502	-0.557	-0.551	-0.306
7	2002	-0.309	-0.204	-0.119	-0.099	-0.171	-0.247	-0.135	-0.155	-0.153	-0.121	-0.161	-0.244	-0.285	-0.208	-0.353	-0.568	-0.452	-0.385	-0.498	-0.573	-0.525	-0.549	-0.504	-0.481	-0.478	-0.529
8	2002	-0.283	-0.172	-0.184	-0.206	-0.185	-0.162	-0.181	-0.167	-0.174	-0.225	-0.192	-0.293	-0.253	-0.382	-0.488	-0.524	-0.625	-0.612	-0.646	-0.563	-0.608	-0.540	-0.521	-0.487	-0.526	-0.464
9	2002	-0.187	-0.158	-0.117	-0.159	-0.206	-0.146	-0.166	-0.137	-0.161	-0.193	-0.211	-0.241	-0.326	-0.366	-0.497	-0.548	-0.485	-0.616	-0.626	-0.581	-0.639	-0.634	-0.537	-0.543	-0.476	-0.469
10	2002	-0.044	-0.062	-0.122	-0.029	-0.054	-0.105	-0.045	-0.113	-0.107	-0.093	-0.091	-0.125	-0.198	-0.210	-0.345	-0.366	-0.514	-0.463	-0.512	-0.497	-0.542	-0.418	-0.336	-0.294	-0.239	-0.217
11	2002	-0.065	-0.091	–	-0.012	-0.012	-0.011	-0.031	-0.004	-0.026	-0.042	-0.095	-0.078	-0.050	-0.097	-0.096	-0.144	-0.193	-0.253	-0.169	-0.357	-0.396	-0.322	-0.125	-0.117	-0.235	-0.174
3	2003	-0.028	-0.340	-0.114	-0.088	-0.058	-0.059	-0.092	-0.086	-0.113	-0.100	-0.130	-0.135	-0.299	-0.263	-0.407	-0.465	-0.561	-0.602	-0.617	-0.616	-0.672	-0.548	-0.504	-0.526	-0.524	-0.540
4	2003	-0.120	-0.122	-0.139	-0.201	-0.221	-0.140	-0.115	-0.096	-0.163	-0.115	-0.137	-0.164	-0.200	-0.311	-0.425	-0.508	-0.614	-0.745	-0.667	-0.640	-0.589	-0.538	-0.635	-0.596	-0.610	-0.616
1	2005	-0.174	-0.094	-0.195	-0.064	-0.158	-0.148	-0.095	-0.200	-0.101	-0.114	-0.256	-0.322	-0.339	-0.381	-0.482	-0.508	-0.781	-0.773	-0.794	-0.833	-0.752	-0.699	-0.713	-0.626	-0.591	-0.582
2	2005	-0.232	-0.137	-0.214	-0.150	-0.085	-0.078	-0.115	-0.118	-0.126	-0.148	-0.152	-0.189	-0.223	-0.291	-0.415	-0.628	-0.558	-0.805	-0.774	-0.783	-0.748	-0.681	-0.677	-0.623	-0.647	-0.624
3	2005	-0.158	-0.107	-0.185	-0.106	-0.108	-0.176	-0.158	-0.187	-0.127	-0.136	-0.148	-0.259	-0.299	-0.345	-0.381	-0.602	-0.565	-0.781	-0.776	-0.739	-0.690	-0.843	-0.675	-0.594	-0.605	-0.615
4	2005	-0.152	-0.178	-0.074	-0.135	-0.115	-0.169	-0.172	-0.135	-0.122	-0.146	-0.162	-0.184	-0.250	-0.269	-0.413	-0.529	-0.579	-0.740	-0.737	-0.704	-0.667	-0.623	-0.670	-0.641	-0.665	-0.420
5	2005	-0.253	-0.165	-0.163	-0.095	-0.150	-0.140	-0.120	-0.129	-0.130	-0.137	-0.156	-0.202	-0.244	-0.311	-0.363	-0.542	-0.592	-0.697	-0.638	-0.634	-0.624	-0.600	-0.586	-0.538	-0.594	-0.579
6	2005	-0.098	-0.106	-0.166	-0.210	-0.123	-0.099	-0.087	-0.100	-0.104	-0.134	-0.128	-0.181	-0.241	-0.308	-0.378	-0.471	-0.556	-0.593	-0.586	-0.605	-0.586	-0.598	-0.593	-0.593	-0.619	-0.627
7	2005	-0.221	-0.126	-0.140	-0.106	-0.131	-0.074	-0.094	-0.086	-0.132	-0.118	-0.152	-0.171	-0.264	-0.324	-0.375	-0.509	-0.560	-0.612	-0.606	-0.616	-0.574	-0.626	-0.521	-0.538	-0.481	-0.617
8	2005	-0.233	-0.281	-0.234	-0.212	-0.080	-0.191	-0.051	-0.069	-0.066	-0.126	-0.112	-0.100	-0.078	-0.409	-0.285	-0.470	-0.425	-0.480	-0.599	-0.625	-0.605	-0.656	-0.535	-0.769	-0.533	-0.342
5	2007	-0.315	-0.066	-0.104	-0.149	-0.135	-0.094	-0.107	-0.124	-0.121	-0.145	-0.158	-0.201	-0.244	-0.341	-0.470	-0.599	-0.645	-0.769	-0.696	-0.633	-0.660	-0.649	-0.643	-0.612	-0.612	-0.599
6	2007	-0.429	-0.273	-0.346	-0.253	-0.156	-0.110	-0.129	-0.136	-0.134	-0.150	-0.167	-0.232	-0.267	-0.340	-0.474	-0.544	-0.572	-0.612	-0.648	-0.617	-0.583	-0.669	-0.636	-0.622	-0.670	-0.637
7	2007	-0.108	-0.134	-0.220	-0.167	-0.114	-0.080	-0.134	-0.160	-0.193	-0.160	-0.166	-0.215	-0.250	-0.281	-0.425	-0.478	-0.587	-0.623	-0.637	-0.628	-0.666	-0.667	-0.671	-0.689	-0.585	-0.614
6	2008	-0.321	-0.189	-0.090	-0.126	-0.118	-0.133	-0.150	-0.127	-0.164	-0.141	-0.147	-0.161	-0.185	-0.307	-0.394	-0.492	-0.565	-0.605	-0.642	-0.653	-0.624	-0.613	-0.668	-0.648	-0.564	-0.609
7	2008	-0.283	-0.111	-0.131	-0.137	-0.108	-0.121	-0.094	-0.092	-0.167	-0.137	-0.170	-0.225	-0.278	-0.331	-0.454	-0.566	-0.615	-0.650	-0.647	-0.585	-0.552	-0.583	-0.619	-0.621	-0.616	-0.591
8	2008	-0.128	-0.228	-0.058	-0.128	-0.058	-0.037	-0.076	-0.066	-0.085	-0.144	-0.275	-0.087	-0.287	-0.302	-0.478	-0.608	-0.381	-0.537	-0.593	-0.663	-0.687	-0.720	-0.653	-0.725	-0.589	-0.695
12	2008	-0.164	-0.120	-0.139	-0.199	-0.089	-0.218	-0.097	-0.119	-0.229	-0.129	-0.209	-0.249	-0.238	-0.391	-0.436	-0.501	-0.575	-0.678	-0.519	-0.668	-0.596	-0.626	-0.666	-0.628	-0.658	-0.645
1	2009	-0.148	-0.191	-0.088	-0.136	-0.108	-0.175	-0.146	-0.100	-0.194	-0.130	-0.183	-0.195	-0.333	-0.319	-0.506	-0.607	-0.573	-0.650	-0.671	-0.707	-0.681	-0.673	-0.653	-0.688	-0.693	-0.671
2	2009	-0.204	-0.096	-0.044	-0.172	-0.087	-0.059	-0.177	-0.079	-0.134	-0.121	-0.135	-0.178	-0.198	-0.226	-0.333	-0.435	-0.590	-0.590	-0.739	-0.756	-0.675	-0.716	-0.660	-0.539	-0.683	-0.790
3	2009	-0.114	-0.281	-0.120	-0.071	-0.224	-0.111	-0.117	-0.106	-0.135	-0.135	-0.173	-0.179	-0.182	-0.266	-0.364	-0.459	-0.632	-0.626	-0.531	-0.659	-0.624	-0.578	-0.637	-0.598	-0.714	-0.747
4	2009	-0.087	-0.295	-0.096	-0.083	-0.098	-0.073	-0.100	-0.104	-0.097	-0.126	-0.145	-0.166	-0.176	-0.265	-0.311	-0.353	-0.412	-0.357	-0.375	-0.506	-0.506	-0.555	-0.618	-0.589	-0.469	-0.628
5	2009	-0.359	-0.138	-0.280	-0.140	-0.191	-0.157	-0.177	-0.183	-0.064	-0.127	-0.080	-0.193	-0.207	-0.238	-0.264	-0.230	-0.563	-0.444	-0.417	-0.563	-0.605	-0.530	-0.610	-0.590	-0.382	-0.679
6	2009	-0.045	-0.139	-0.084	-0.163	-0.178	-0.150	-0.120	-0.111	-0.118	-0.159	-0.159	-0.202	-0.235	-0.429	-0.420	-0.577	-0.512	-0.647	-0.650	-0.609	-0.668	-0.614	-0.590	-0.723	-0.712	-0.423
7	2009	-0.335	-0.225	-0.124	-0.125	-0.125	-0.135	-0.126	-0.146	-0.130	-0.159	-0.158	-0.227	-0.305	-0.412	-0.506	-0.612	-0.666	-0.657	-0.662	-0.632	-0.619	-0.642	-0.646	-0.499	-0.636	-0.530
8	2009	-0.443	-0.294	-0.181	-0.098	-0.101	-0.097	-0.114	-0.094	-0.095	-0.142	-0.176	-0.227	-0.294	-0.307	-0.490	-0.612	-0.708	-0.690	-0.724	-0.687	-0.645	-0.688	-0.676	-0.678	-0.565	-0.592
9	2009	-0.159	-0.228	-0.194	-0.116	-0.124	-0.125	-0.116	-0.124	-0.130	-0.156	-0.199	-0.208	-0.326	-0.416	-0.515	-0.619	-0.650	-0.634	-0.717	-0.764	-0.707	-0.670	-0.689	-0.686	-0.684	-0.668
10	2009	-0.196	-0.241	-0.119	-0.196	-0.155	-0.115	-0.149	-0.102	-0.145	-0.178	-0.176	-0.235	-0.362	-0.429	-0.563	-0.610	-0.713	-0.706	-0.705	-0.675	-0.653	-0.667	-0.643	-0.646	-0.573	-0.658
11	2009	-0.170	-0.322	-0.201	-0.149	-0.138	-0.147	-0.136	-0.143	-0.147	-0.166	-0.196	-0.235	-0.312	-0.351	-0.550	-0.578	-0.662	-0.574	-0.703	-0.641	-0.689	-0.627	-0.620	-0.601	-0.600	-0.527
12	2009	-0.279	-0.196	-0.188	-0.081	-0.116	-0.144	-0.139	-0.159	-0.147	-0.169	-0.178	-0.183	-0.280	-0.408	-0.435	-0.498	-0.607	-0.577	-0.713	-0.602	-0.648	-0.659	-0.523	-0.586	-0.592	-0.559

Table A.14: Socorro ambipolar diffusion slope (part 2)

Socorro: Ambipolar diffusion regime slope per height increment

Month	Year	75 (km)	76 (km)	77 (km)	78 (km)	79 (km)	80 (km)	81 (km)	82 (km)	83 (km)	84 (km)	85 (km)	86 (km)	87 (km)	88 (km)	89 (km)	90 (km)	91 (km)	92 (km)	93 (km)	94 (km)	95 (km)	96 (km)	97 (km)	98 (km)	99 (km)	100 (km)
1	2010	-0.218	-0.157	-0.128	-0.117	-0.114	-0.174	-0.145	-0.132	-0.169	-0.250	-0.140	-0.237	-0.310	-0.417	-0.442	-0.474	-0.681	-0.601	-0.696	-0.701	-0.618	-0.702	-0.643	-0.614	-0.544	-0.612
2	2010	-0.250	-0.237	-0.085	-0.096	-0.093	-0.115	-0.102	-0.102	-0.117	-0.150	-0.121	-0.183	-0.204	-0.266	-0.340	-0.498	-0.571	-0.665	-0.690	-0.727	-0.706	-0.657	-0.591	-0.580	-0.654	-0.615
3	2010	-0.510	-0.315	-0.229	-0.138	-0.166	-0.109	-0.104	-0.086	-0.177	-0.143	-0.132	-0.228	-0.217	-0.320	-0.471	-0.511	-0.620	-0.643	-0.698	-0.686	-0.669	-0.642	-0.581	-0.597	-0.582	-0.660
4	2010	-0.143	-0.343	-0.382	-0.109	-0.152	-0.123	-0.200	-0.136	-0.189	-0.152	-0.221	-0.204	-0.262	-0.318	-0.383	-0.543	-0.700	-0.711	-0.699	-0.698	-0.685	-0.658	-0.644	-0.561	-0.457	-0.620
5	2010	-0.180	-0.352	-0.292	-0.205	-0.197	-0.197	-0.111	-0.130	-0.121	-0.149	-0.171	-0.193	-0.245	-0.318	-0.414	-0.531	-0.558	-0.612	-0.638	-0.563	-0.605	-0.652	-0.620	-0.675	-0.642	-0.563
6	2010	-0.166	-0.251	-0.137	-0.098	-0.120	-0.113	-0.102	-0.102	-0.118	-0.132	-0.163	-0.205	-0.244	-0.310	-0.429	-0.541	-0.593	-0.638	-0.604	-0.615	-0.577	-0.613	-0.571	-0.548	-0.574	-0.626
7	2010	-0.077	-0.121	-0.093	-0.111	-0.096	-0.123	-0.107	-0.119	-0.136	-0.154	-0.167	-0.217	-0.265	-0.364	-0.450	-0.575	-0.657	-0.696	-0.694	-0.663	-0.646	-0.668	-0.631	-0.627	-0.542	-0.633
8	2010	-0.229	-0.092	-0.212	-0.105	-0.117	-0.134	-0.120	-0.097	-0.134	-0.157	-0.180	-0.215	-0.274	-0.302	-0.444	-0.517	-0.586	-0.643	-0.677	-0.670	-0.677	-0.661	-0.628	-0.606	-0.639	-0.576
9	2010	-0.192	-0.128	-0.133	-0.096	-0.157	-0.107	-0.110	-0.123	-0.156	-0.170	-0.196	-0.215	-0.320	-0.388	-0.476	-0.533	-0.658	-0.685	-0.713	-0.645	-0.710	-0.666	-0.677	-0.691	-0.657	-0.634
10	2010	-0.130	-0.195	-0.210	-0.153	-0.152	-0.161	-0.128	-0.121	-0.143	-0.162	-0.220	-0.223	-0.330	-0.400	-0.515	-0.523	-0.644	-0.691	-0.697	-0.645	-0.638	-0.636	-0.631	-0.638	-0.641	-0.610
11	2010	-0.241	-0.115	-0.182	-0.135	-0.130	-0.098	-0.105	-0.113	-0.113	-0.149	-0.166	-0.201	-0.263	-0.342	-0.398	-0.487	-0.574	-0.706	-0.701	-0.688	-0.642	-0.658	-0.588	-0.604	-0.634	-0.644
12	2010	-0.341	-0.297	-0.183	-0.125	-0.088	-0.140	-0.133	-0.161	-0.168	-0.179	-0.194	-0.246	-0.247	-0.336	-0.369	-0.501	-0.552	-0.634	-0.630	-0.639	-0.588	-0.598	-0.557	-0.551	-0.543	-0.537
1	2011	-0.201	-0.202	-0.187	-0.187	-0.095	-0.136	-0.101	-0.182	-0.140	-0.193	-0.223	-0.164	-0.223	-0.281	-0.408	-0.508	-0.473	-0.631	-0.653	-0.705	-0.598	-0.598	-0.565	-0.600	-0.608	-0.586
2	2011	-0.234	-0.144	-0.176	-0.082	-0.109	-0.109	-0.158	-0.100	-0.090	-0.113	-0.147	-0.201	-0.196	-0.308	-0.378	-0.568	-0.558	-0.484	-0.679	-0.612	-0.626	-0.652	-0.658	-0.658	-0.346	-0.674
3	2011	-0.250	-0.220	-0.228	-0.176	-0.070	-0.103	-0.199	-0.161	-0.175	-0.168	-0.148	-0.166	-0.209	-0.230	-0.505	-0.443	-0.529	-0.538	-0.575	-0.634	-0.536	-0.630	-0.585	-0.657	-0.640	-0.590
4	2011	-0.290	-0.147	-0.137	-0.075	-0.120	-0.141	-0.106	-0.147	-0.133	-0.137	-0.150	-0.183	-0.215	-0.259	-0.285	-0.363	-0.447	-0.560	-0.544	-0.467	-0.636	-0.638	-0.661	-0.530	-0.493	-0.593
5	2011	-0.121	-0.225	-0.144	-0.088	-0.127	-0.109	-0.122	-0.109	-0.100	-0.112	-0.102	-0.112	-0.167	-0.123	-0.189	-0.258	-0.258	-0.329	-0.416	-0.408	-0.401	-0.499	-0.517	-0.467	-0.532	-0.560
6	2011	-0.155	-0.028	-0.072	-0.121	-0.097	-0.126	-0.103	-0.097	-0.092	-0.095	-0.124	-0.152	-0.164	-0.198	-0.237	-0.279	-0.307	-0.380	-0.415	-0.463	-0.485	-0.575	-0.586	-0.704	-0.674	-0.563
7	2011	-0.224	-0.116	-0.151	-0.104	-0.118	-0.113	-0.110	-0.117	-0.111	-0.112	-0.095	-0.153	-0.192	-0.234	-0.355	-0.399	-0.470	-0.508	-0.522	-0.555	-0.505	-0.561	-0.505	-0.453	-0.536	-0.492
8	2011	-0.193	-0.140	-0.085	-0.132	-0.093	-0.098	-0.098	-0.094	-0.095	-0.116	-0.133	-0.179	-0.220	-0.257	-0.336	-0.387	-0.474	-0.528	-0.547	-0.616	-0.570	-0.560	-0.592	-0.629	-0.598	-0.547
9	2011	-0.260	-0.272	-0.091	-0.092	-0.202	-0.105	-0.124	-0.112	-0.129	-0.157	-0.172	-0.230	-0.283	-0.323	-0.393	-0.422	-0.512	-0.601	-0.580	-0.603	-0.612	-0.678	-0.661	-0.682	-0.630	-0.599
10	2011	-0.099	-0.127	-0.213	-0.129	-0.073	-0.117	-0.123	-0.116	-0.146	-0.156	-0.190	-0.240	-0.309	-0.399	-0.443	-0.547	-0.573	-0.581	-0.633	-0.592	-0.590	-0.578	-0.612	-0.585	-0.572	-0.670
11	2011	-0.238	-0.246	-0.116	-0.113	-0.140	-0.078	-0.116	-0.183	-0.152	-0.133	-0.171	-0.206	-0.270	-0.332	-0.445	-0.492	-0.565	-0.616	-0.598	-0.607	-0.647	-0.598	-0.615	-0.715	-0.682	-0.711
12	2011	-0.097	-0.122	-0.172	-0.166	-0.075	-0.104	-0.141	-0.253	-0.135	-0.141	-0.195	-0.204	-0.318	-0.394	-0.554	-0.571	-0.552	-0.724	-0.656	-0.699	-0.610	-0.607	-0.628	-0.611	-0.572	-0.692
1	2012	-0.157	-0.164	-0.168	-0.075	-0.148	-0.082	-0.235	-0.102	-0.172	-0.118	-0.147	-0.139	-0.208	-0.377	-0.354	-0.371	-0.516	-0.587	-0.556	-0.521	-0.578	-0.617	-0.610	-0.699	-0.742	-0.716
2	2012	-0.074	-0.360	-0.349	-0.110	-0.122	-0.172	-0.077	-0.155	-0.109	-0.197	-0.106	-0.164	-0.389	-0.389	-0.314	-0.633	-0.446	-0.550	-0.612	-0.654	-0.623	-0.642	-0.598	-0.538	-0.520	-0.652
3	2012	-0.115	-0.312	-0.151	-0.247	-0.086	-0.143	-0.136	-0.096	-0.093	-0.101	-0.104	-0.167	-0.211	-0.273	-0.331	-0.412	-0.456	-0.487	-0.555	-0.545	-0.549	-0.582	-0.524	-0.614	-0.670	-0.699
4	2012	-0.215	-0.217	-0.245	-0.094	-0.177	-0.174	-0.163	-0.167	-0.123	-0.133	-0.168	-0.155	-0.246	-0.255	-0.470	-0.377	-0.463	-0.532	-0.528	-0.522	-0.558	-0.530	-0.501	-0.576	-0.473	-0.623
5	2012	-0.314	-0.320	-0.208	-0.278	-0.185	-0.087	-0.129	-0.228	-0.079	-0.134	-0.213	-0.159	-0.418	-0.355	-0.596	-0.531	-0.688	-0.617	-0.700	-0.638	-0.559	-0.406	-0.495	-0.488	-0.592	-0.491

Table A.15: Yellowknife ambipolar diffusion slope (part 1)

Yellowknife: Ambipolar diffusion regime slope per height increment

Month	Year	75	76	77	78	79	80	81	82	83	84	85	86	87	88	89	90	91	92	93	94	95	96	97	98	99	100
		(km)	(km)	(km)	(km)	(km)	(km)	(km)	(km)	(km)	(km)	(km)	(km)	(km)	(km)	(km)	(km)	(km)	(km)	(km)	(km)	(km)	(km)	(km)	(km)	(km)	(km)
6	2002	-0.289	-0.561	-0.164	-0.283	-0.263	-0.249	-0.221	-0.300	-0.313	-0.259	-0.221	-0.423	-0.514	-0.531	-0.642	-0.637	-0.688	-0.573	-0.629	-0.516	-0.599	-0.536	-0.511	-0.512	-0.582	-0.363
7	2002	-0.126	-0.119	-0.414	-0.637	-0.095	-0.137	-0.147	-0.268	-0.222	-0.225	-0.359	-0.467	-0.501	-0.475	-0.605	-0.613	-0.628	-0.604	-0.507	-0.424	-0.545	-0.589	-0.611	-0.420	-0.582	-0.403
8	2002	-0.180	-0.291	-0.137	-0.227	-0.187	-0.179	-0.229	-0.181	-0.266	-0.213	-0.319	-0.280	-0.323	-0.584	-0.616	-0.657	-0.613	-0.625	-0.501	-0.486	-0.551	-0.428	-0.524	-0.546	-0.462	-0.491
3	2003	--	--	-0.025	-0.095	-0.033	-0.080	-0.088	-0.490	-0.246	-0.064	-0.040	-0.156	-0.315	-0.338	-0.200	-0.428	-0.532	-0.629	-0.490	-0.523	-0.347	-0.800	-0.324	-0.355	-0.494	-0.557
4	2003	-0.226	-0.483	-0.121	-0.229	-0.139	-0.089	-0.079	-0.039	-0.047	-0.073	-0.109	-0.200	-0.226	-0.206	-0.170	-0.454	-0.355	-0.423	-0.445	-0.374	-0.522	-0.451	-0.496	-0.484	-0.272	-0.424
5	2003	-0.581	-0.428	-0.220	-0.117	-0.167	-0.104	-0.176	-0.087	-0.193	-0.134	-0.214	-0.337	-0.242	-0.195	-0.369	-0.529	-0.599	-0.635	-0.641	-0.584	-0.557	-0.357	-0.403	-0.674	-0.596	-0.443
6	2003	-0.590	-0.361	-0.817	-0.451	-0.213	-0.368	-0.340	-0.129	-0.154	-0.166	-0.252	-0.270	-0.331	-0.388	-0.565	-0.558	-0.622	-0.517	-0.538	-0.530	-0.464	-0.516	-0.377	-0.540	-0.577	-0.464
7	2003	-0.304	-0.510	-0.202	-0.186	-0.037	-0.286	-0.180	-0.243	-0.217	-0.201	-0.205	-0.256	-0.403	-0.414	-0.506	-0.493	-0.417	-0.629	-0.608	-0.533	-0.398	-0.530	-0.586	-0.474	-0.459	-0.466
8	2003	0.000	-0.705	-0.030	-0.062	-0.320	-0.204	-0.251	-0.070	-0.159	-0.234	-0.229	-0.255	-0.372	-0.403	-0.481	-0.471	-0.562	-0.518	-0.552	-0.484	-0.600	-0.455	-0.539	-0.519	-0.432	-0.446
9	2003	-0.436	-0.060	-0.451	-0.392	-0.127	-0.122	-0.151	-0.223	-0.202	-0.271	-0.420	-0.332	-0.377	-0.476	-0.376	-0.533	-0.602	-0.564	-0.686	-0.595	-0.579	-0.570	-0.447	-0.532	-0.694	-0.570
10	2003	-0.181	-0.082	-0.218	-0.120	-0.132	-0.143	-0.156	-0.131	-0.134	-0.212	-0.331	-0.203	-0.219	-0.521	-0.490	-0.649	-0.568	-0.423	-0.670	-0.674	-0.551	-0.653	-0.618	-0.358	-0.617	-0.691
11	2003	-0.049	-0.043	-0.091	-0.115	-0.069	-0.123	-0.055	-0.147	-0.134	-0.185	-0.323	-0.344	-0.195	-0.403	-0.404	-0.408	-0.324	-0.151	-0.374	-0.440	-0.578	-0.624	-0.092	-0.467	-0.448	-0.249
12	2003	-0.308	-0.305	-0.229	-0.233	-0.181	-0.079	-0.124	-0.146	-0.087	-0.274	-0.330	-0.339	-0.508	-0.567	-0.602	-0.587	-0.619	-0.545	-0.595	-0.552	-0.560	-0.591	-0.496	-0.405	-0.389	-0.396
1	2004	-0.100	-0.076	-0.148	-0.074	-0.062	-0.156	-0.200	-0.183	-0.281	-0.173	-0.369	-0.433	-0.545	-0.587	-0.488	-0.387	-0.521	-0.541	-0.492	-0.549	-0.645	-0.544	-0.683	-0.390	-0.332	-0.827
2	2004	-0.067	-0.236	-0.074	-0.112	-0.047	-0.115	-0.203	-0.165	-0.154	-0.235	-0.229	-0.265	-0.386	-0.402	-0.361	-0.473	-0.551	-0.227	-0.540	-0.455	-0.312	-0.637	-0.396	-0.124	-0.735	-0.480
3	2004	--	-0.392	-0.108	-0.052	-0.165	-0.250	-0.027	-0.137	-0.174	-0.121	-0.143	-0.125	-0.384	-0.423	-0.523	-0.462	-0.609	-0.699	-0.461	-0.585	-0.626	-0.507	-0.470	-0.293	-0.438	-0.718
4	2004	-0.260	-0.140	-0.376	-0.247	-0.139	-0.234	-0.261	-0.164	-0.172	-0.095	-0.206	-0.296	-0.296	-0.255	-0.510	-0.655	-0.537	-0.775	-0.736	-0.792	-0.650	-0.585	-0.660	-0.635	-0.377	-0.665
5	2004	-0.204	-0.207	-0.226	-0.144	-0.449	-0.384	-0.245	-0.276	-0.212	-0.147	-0.202	-0.312	-0.199	-0.310	-0.483	-0.646	-0.530	-0.676	-0.616	-0.333	-0.566	-0.577	-0.572	-0.520	-0.459	-0.717
6	2004	-0.164	-0.543	-0.141	-0.197	-0.332	-0.186	-0.200	-0.167	-0.187	-0.324	-0.334	-0.285	-0.292	-0.592	-0.558	-0.630	-0.564	-0.617	-0.593	-0.558	-0.569	-0.181	-0.523	-0.428	-0.405	-0.507
7	2004	--	--	--	-0.138	-0.139	-0.111	-0.235	-0.062	-0.151	-0.117	-0.113	-0.401	-0.264	-0.186	-0.200	-0.617	-0.251	-0.346	-0.418	-0.368	-0.390	-0.617	-0.355	-0.695	-0.132	-0.186
8	2004	-0.148	-0.238	-0.144	-0.295	-0.174	-0.275	-0.195	-0.147	-0.168	-0.223	-0.349	-0.255	-0.462	-0.507	-0.593	-0.633	-0.649	-0.607	-0.556	-0.604	-0.589	-0.571	-0.478	-0.496	-0.547	-0.378
9	2004	-0.581	-0.441	-0.133	-0.197	-0.281	-0.108	-0.127	-0.183	-0.211	-0.145	-0.269	-0.292	-0.332	-0.511	-0.681	-0.534	-0.533	-0.621	-0.462	-0.601	-0.593	-0.421	-0.692	-0.597	-0.629	-0.685
10	2004	-0.245	-0.193	-0.196	-0.156	-0.167	-0.186	-0.175	-0.249	-0.199	-0.245	-0.220	-0.390	-0.643	-0.608	-0.624	-0.648	-0.652	-0.603	-0.626	-0.585	-0.674	-0.551	-0.674	-0.640	-0.602	-0.641
11	2004	-0.075	-0.046	-0.117	-0.103	-0.148	-0.133	-0.077	-0.046	-0.165	-0.242	-0.496	-0.273	-0.486	-0.505	-0.669	-0.666	-0.598	-0.619	-0.589	-0.565	-0.667	-0.497	-0.562	-0.505	-0.505	-0.687
12	2004	-0.079	-0.129	-0.104	-0.168	-0.188	-0.091	-0.182	-0.249	-0.239	-0.206	-0.355	-0.362	-0.384	-0.390	-0.567	-0.458	-0.564	-0.542	-0.529	-0.485	-0.520	-0.393	-0.520	-0.593	-0.250	-0.539
1	2005	-0.228	-0.204	-0.068	-0.151	-0.111	-0.142	-0.046	-0.177	-0.191	-0.168	-0.358	-0.420	-0.494	-0.420	-0.708	-0.615	-0.646	-0.573	-0.603	-0.475	-0.665	-0.534	-0.432	-0.407	-0.726	-0.598
2	2005	-0.199	-0.286	-0.038	-0.051	-0.052	-0.162	-0.132	-0.092	-0.161	-0.027	-0.156	-0.291	-0.321	-0.416	-0.607	-0.361	-0.373	-0.309	-0.501	-0.593	-0.652	-0.179	-0.724	-0.390	-0.545	-0.431
3	2005	-0.427	-0.304	-0.237	-0.131	-0.132	-0.172	-0.065	-0.199	-0.252	-0.251	-0.313	-0.316	-0.482	-0.495	-0.285	-0.315	-0.584	-0.648	-0.685	-0.570	-0.357	-0.535	-0.398	-0.865	-0.822	-0.505
4	2005	-0.273	-0.132	-0.199	-0.030	-0.169	-0.029	-0.104	-0.186	-0.066	-0.047	-0.233	-0.226	-0.235	-0.441	-0.628	-0.532	-0.627	-0.379	-0.652	-0.567	-0.691	-0.518	-0.540	-0.631	-0.397	-0.314
5	2005	-0.146	-0.069	-0.075	-0.085	-0.158	-0.114	-0.069	-0.252	-0.155	-0.218	-0.191	-0.340	-0.284	-0.292	-0.354	-0.451	-0.495	-0.669	-0.561	-0.428	-0.444	-0.462	-0.436	-0.594	-0.379	-0.429
6	2005	-0.099	-0.391	-0.619	-0.212	-0.141	-0.285	-0.224	-0.237	-0.152	-0.288	-0.307	-0.356	-0.342	-0.462	-0.559	-0.483	-0.629	-0.621	-0.586	-0.539	-0.514	-0.396	-0.634	-0.489	-0.374	-0.187
7	2005	-1.405	-0.776	-0.654	-0.702	-0.214	-0.082	-0.068	-0.247	-0.153	-0.243	-0.221	-0.334	-0.298	-0.331	-0.444	-0.624	-0.808	-0.634	-0.906	-0.702	-0.602	-0.286	-0.699	-0.419	-0.950	-0.223
8	2005	-0.510	-0.110	-0.296	-0.126	-0.413	-0.141	-0.101	-0.185	-0.259	-0.332	-0.261	-0.450	-0.498	-0.567	-0.533	-0.721	-0.665	-0.638	-0.609	-0.664	-0.534	-0.469	-0.495	-0.463	-0.501	-0.447
9	2005	-0.242	-0.169	-0.278	-0.066	-0.097	-0.133	-0.179	-0.126	-0.139	-0.180	-0.255	-0.308	-0.338	-0.334	-0.517	-0.631	-0.541	-0.645	-0.636	-0.578	-0.531	-0.654	-0.580	-0.458	-0.605	-0.682
10	2005	-0.703	-0.313	-0.133	-0.158	-0.140	-0.085	-0.059	-0.121	-0.134	-0.324	-0.396	-0.561	-0.540	-0.588	-0.573	-0.638	-0.643	-0.537	-0.642	-0.655	-0.590	-0.639	-0.620	-0.712	-0.610	-0.609
11	2005	-0.222	-0.165	-0.113	-0.111	-0.221	-0.234	-0.131	-0.198	-0.290	-0.181	-0.386	-0.163	-0.154	-0.385	-0.687	-0.427	-0.734	-0.696	-0.667	-0.678	-0.615	-0.621	-0.573	-0.624	-0.643	-0.646
12	2005	-0.103	-0.168	-0.280	-0.131	-0.092	-0.187	-0.204	-0.240	-0.238	-0.192	-0.286	-0.268	-0.274	-0.522	-0.579	-0.672	-0.637	-0.673	-0.693	-0.647	-0.653	-0.632	-0.655	-0.387	-0.724	-0.496

Table A. 16: Yellowknife ambipolar diffusion slope (part 2)

Yellowknife: Ambipolar diffusion regime slope per height increment

Month	Year	75	76	77	78	79	80	81	82	83	84	85	86	87	88	89	90	91	92	93	94	95	96	97	98	99	100
		(km)	(km)	(km)	(km)	(km)	(km)	(km)	(km)	(km)	(km)	(km)	(km)	(km)	(km)	(km)	(km)	(km)	(km)	(km)	(km)	(km)	(km)	(km)	(km)	(km)	(km)
1	2006	-0.350	-0.578	-0.295	-0.187	-0.267	-0.097	-0.151	-0.123	-0.280	-0.205	-0.439	-0.381	-0.164	-0.601	-0.533	-0.522	-0.734	-0.655	-0.622	-0.626	-0.585	-0.629	-0.618	-0.686	-0.602	-0.596
2	2006	-0.318	-0.196	-0.043	-0.169	-0.204	-0.268	-0.209	-0.297	-0.088	-0.324	-0.212	-0.337	-0.216	-0.616	-0.518	-0.361	-0.617	-0.727	-0.210	-0.745	-0.744	-0.640	-0.828	-0.690	-0.240	-0.529
3	2006	-0.171	-0.294	-0.220	-0.125	-0.163	-0.151	-0.184	-0.180	-0.041	-0.152	-0.250	-0.291	-0.324	-0.436	-0.530	-0.508	-0.666	-0.612	-0.722	-0.661	-0.614	-0.427	-0.425	-0.692	-0.603	-0.632
4	2006	-0.524	-0.180	-0.364	-0.161	-0.079	-0.094	-0.056	-0.066	-0.128	-0.108	-0.179	-0.195	-0.147	-0.254	-0.370	-0.613	-0.503	-0.665	-0.597	-0.757	-0.394	-0.627	-0.605	-0.540	-0.616	-0.564
5	2006	-0.211	-0.085	-0.175	-0.115	-0.456	-0.059	-0.277	-0.105	-0.161	-0.151	-0.168	-0.157	-0.227	-0.202	-0.535	-0.453	-0.423	-0.537	-0.577	-0.604	-0.661	-0.639	-0.708	-0.638	-0.182	-0.605
6	2006	-0.306	-0.227	-0.708	-0.396	-0.316	-0.162	-0.468	-0.200	-0.308	-0.287	-0.246	-0.344	-0.362	-0.357	-0.545	-0.503	-0.575	-0.635	-0.616	-0.604	-0.606	-0.529	-0.573	-0.540	-0.498	-0.969
7	2006	-0.129	-0.120	-0.384	-0.155	-0.163	-0.199	-0.456	-0.301	-0.346	-0.326	-0.233	-0.200	-0.345	-0.467	-0.427	-0.533	-0.651	-0.710	-0.658	-0.619	-0.632	-0.509	-0.501	-0.533	-0.649	-0.438
8	2006	-0.082	-0.103	-0.167	-0.093	-0.136	-0.126	-0.283	-0.184	-0.129	-0.203	-0.132	-0.398	-0.202	-0.378	-0.543	-0.672	-0.747	-0.651	-0.679	-0.536	-0.563	-0.611	-0.619	-0.568	-0.461	-0.490
9	2006	-1.557	--	-0.027	-0.036	-0.034	-0.036	-0.034	-0.012	-0.051	-0.093	-0.158	-0.203	-0.190	-0.396	-0.169	-0.489	-0.207	-0.232	-0.208	-0.543	-0.431	-0.137	-0.106	-0.064	-0.062	-0.091
11	2006	-0.068	--	0.000	-0.091	--	--	-0.076	--	-0.060	-0.022	-0.026	-0.006	-0.128	-0.007	-0.085	-0.045	-0.356	-0.517	-0.413	-0.306	-0.071	-0.032	-0.020	0.000	-0.322	-0.049
12	2006	-0.031	-0.057	-0.133	-0.046	-0.022	-0.084	-0.085	-0.104	-0.128	-0.074	-0.147	-0.187	-0.207	-0.226	-0.224	-0.363	-0.453	-0.401	-0.094	-0.401	-0.426	-0.053	-0.198	-0.307	-0.220	-0.199
1	2007	-0.026	-0.018	-0.013	-0.031	-0.007	-0.005	-0.040	-0.043	-0.119	-0.131	-0.238	-0.034	-0.294	-0.352	-0.267	-0.105	-0.147	-0.463	-0.294	-0.290	-0.401	-0.152	-0.325	-0.167	-0.360	-0.044
2	2007	-0.391	--	--	-0.229	--	-0.163	-0.026	-0.046	-0.019	-0.044	-0.024	--	-0.045	-0.050	-0.057	-0.064	-0.087	-0.221	-0.203	-0.088	-0.149	--	-0.223	-0.033	--	--
12	2007	-0.401	--	-0.111	-0.183	-0.068	-0.040	-0.081	-0.096	-0.112	-0.165	-0.193	-0.106	-0.040	-0.096	-0.085	-0.097	-0.132	-0.075	-0.172	-0.133	-0.200	-0.098	-0.231	-0.326	-0.391	--
4	2008	-0.546	--	-0.137	-0.100	-0.130	-0.054	-0.109	-0.100	-0.096	-0.099	-0.075	-0.178	-0.151	-0.278	-0.317	-0.312	-0.469	-0.495	-0.732	-0.421	-0.583	-0.201	-0.223	-0.337	-0.718	-0.318
5	2008	-0.447	-0.276	-0.531	-0.223	-0.162	-0.049	-0.132	-0.209	-0.243	-0.205	-0.226	-0.330	-0.364	-0.277	-0.506	-0.563	-0.597	-0.605	-0.618	-0.591	-0.631	-0.511	-0.528	-0.440	-0.614	-0.453
6	2008	-0.068	-0.507	-0.389	-0.523	-0.194	-0.358	-0.219	-0.243	-0.264	-0.248	-0.253	-0.299	-0.432	-0.446	-0.489	-0.614	-0.603	-0.618	-0.551	-0.551	-0.453	-0.459	-0.478	-0.537	-0.414	-0.296
7	2008	-0.252	-0.645	-0.486	-0.357	-0.119	-0.447	-0.182	-0.218	-0.296	-0.203	-0.370	-0.303	-0.383	-0.567	-0.508	-0.551	-0.665	-0.617	-0.531	-0.569	-0.590	-0.544	-0.454	-0.513	-0.436	-0.584
8	2008	-0.207	-0.324	-0.452	-0.130	-0.313	-0.218	-0.222	-0.192	-0.288	-0.264	-0.323	-0.296	-0.381	-0.476	-0.555	-0.630	-0.639	-0.650	-0.558	-0.560	-0.510	-0.610	-0.505	-0.569	-0.556	-0.547
9	2008	-0.217	-0.016	-0.197	-0.188	-0.160	-0.082	-0.189	-0.134	-0.110	-0.208	-0.252	-0.335	-0.306	-0.494	-0.585	-0.719	-0.719	-0.704	-0.620	-0.695	-0.614	-0.575	-0.612	-0.729	-0.681	-0.762
10	2008	-0.348	-0.331	-0.201	-0.123	-0.110	-0.109	-0.111	-0.155	-0.095	-0.215	-0.205	-0.359	-0.441	-0.550	-0.677	-0.684	-0.613	-0.704	-0.689	-0.620	-0.655	-0.545	-0.690	-0.616	-0.577	-0.480
11	2008	-0.160	-0.119	-0.099	-0.169	-0.116	-0.065	-0.193	-0.183	-0.190	-0.245	-0.360	-0.452	-0.489	-0.462	-0.752	-0.584	-0.511	-0.732	-0.713	-0.652	-0.556	-0.686	-0.667	-0.589	-0.836	-0.612
12	2008	-0.241	-0.237	-0.354	-0.110	-0.026	-0.277	-0.226	-0.180	-0.156	-0.269	-0.289	-0.410	-0.532	-0.504	-0.529	-0.618	-0.630	-0.635	-0.666	-0.627	-0.647	-0.538	-0.558	-0.613	-0.537	-0.649
1	2009	-0.402	-0.349	-0.192	-0.191	-0.202	-0.184	-0.280	-0.232	-0.217	-0.254	-0.259	-0.340	-0.337	-0.599	-0.581	-0.564	-0.694	-0.697	-0.607	-0.720	-0.627	-0.627	-0.646	-0.692	-0.601	-0.745
2	2009	-0.096	-0.386	-0.204	-0.076	-0.206	-0.118	-0.091	-0.122	-0.211	-0.150	-0.195	-0.307	-0.358	-0.653	-0.591	-0.519	-0.730	-0.742	-0.677	-0.567	-0.705	-0.749	-0.639	-0.466	-0.653	-0.554
3	2009	-0.092	-0.194	-0.129	-0.115	-0.195	-0.174	-0.099	-0.096	-0.248	-0.145	-0.251	-0.408	-0.401	-0.392	-0.411	-0.611	-0.680	-0.685	-0.653	-0.603	-0.615	-0.599	-0.586	-0.610	-0.643	-0.634
4	2009	--	-0.140	-0.019	-0.066	-0.129	-0.122	-0.079	-0.078	-0.084	-0.085	-0.230	-0.232	-0.191	-0.406	-0.444	-0.428	-0.379	-0.463	-0.714	-0.716	-0.680	-0.718	-0.674	-0.582	-0.606	-0.608
5	2009	-0.173	--	-0.184	-0.305	-0.164	-0.199	-0.274	-0.231	-0.180	-0.241	-0.237	-0.287	-0.398	-0.394	-0.410	-0.598	-0.696	-0.674	-0.728	-0.681	-0.708	-0.693	-0.765	-0.557	-0.528	-0.820
6	2009	-0.445	-0.403	-0.621	-0.280	-0.320	-0.276	-0.192	-0.248	-0.309	-0.353	-0.300	-0.293	-0.363	-0.518	-0.520	-0.550	-0.554	-0.609	-0.628	-0.564	-0.492	-0.552	-0.627	-0.496	-0.460	-0.409
7	2009	-0.165	-0.254	-0.397	-0.552	-0.474	-0.122	-0.287	-0.200	-0.289	-0.180	-0.344	-0.386	-0.317	-0.447	-0.587	-0.620	-0.644	-0.638	-0.607	-0.597	-0.525	-0.606	-0.564	-0.484	-0.522	-0.562
8	2009	-0.180	-0.047	-0.179	-0.194	-0.112	-0.198	-0.230	-0.238	-0.253	-0.300	-0.355	-0.272	-0.416	-0.486	-0.543	-0.704	-0.670	-0.628	-0.538	-0.561	-0.516	-0.520	-0.495	-0.444	-0.459	-0.496
9	2009	-0.224	-0.316	-0.440	-0.132	-0.136	-0.135	-0.121	-0.095	-0.150	-0.210	-0.237	-0.306	-0.239	-0.419	-0.589	-0.729	-0.717	-0.677	-0.637	-0.620	-0.665	-0.596	-0.567	-0.601	-0.508	-0.618
10	2009	-0.081	-0.158	-0.242	-0.127	-0.068	-0.157	-0.120	-0.200	-0.163	-0.214	-0.374	-0.296	-0.340	-0.387	-0.430	-0.644	-0.659	-0.637	-0.621	-0.626	-0.595	-0.626	-0.623	-0.629	-0.636	-0.526
11	2009	-0.232	-0.230	-0.176	-0.191	-0.190	-0.216	-0.144	-0.207	-0.205	-0.169	-0.293	-0.358	-0.549	-0.623	-0.667	-0.603	-0.676	-0.649	-0.609	-0.571	-0.518	-0.526	-0.561	-0.603	-0.603	-0.508
12	2009	-0.430	-0.338	-0.499	-0.013	-0.257	-0.106	-0.456	-0.281	-0.397	-0.588	-0.635	-0.654	-0.488	-0.781	-0.457	-0.789	-0.797	-0.662	-0.349	-0.672	-0.575	-0.592	-0.501	-0.248	-0.507	-0.407

Table A.17: CLOVAR hyperthermal chemistry slope

CLOVAR: Hyperthermal chemistry regime slope per height increment

Month	Year	75 (km)	76 (km)	77 (km)	78 (km)	79 (km)	80 (km)	81 (km)	82 (km)	83 (km)	84 (km)	85 (km)	86 (km)	87 (km)	88 (km)	89 (km)	90 (km)	91 (km)	92 (km)	93 (km)	94 (km)	95 (km)	96 (km)	97 (km)	98 (km)	99 (km)	100 (km)
7	2000	-2.822	-7.020	-1.140	-2.542	-2.264	-1.890	-1.724	-1.853	-1.921	-1.827	-2.036	-1.953	-1.520	-1.583	-1.251	-1.406	-0.908	-1.122	-0.574	-0.557	-0.588	-0.796	-0.583	-0.747	-1.131	-0.964
8	2000	-0.833	-0.815	-1.047	-2.156	-1.298	-2.147	-2.553	-3.128	-1.917	-1.842	-1.843	-2.646	-1.624	-1.495	-1.463	-1.330	-1.294	-0.787	-1.086	-0.612	-0.941	-0.587	-0.983	-0.606	-0.593	-0.528
9	2000	-1.842	-0.948	-1.134	-1.517	-1.464	-2.712	-1.748	-1.749	-2.233	-2.629	-1.982	-1.826	-2.006	-1.986	-1.307	-1.381	-1.061	-0.920	-0.798	-0.703	-0.811	-0.976	-0.672	-1.102	-1.148	-0.791
10	2000	-4.119	-1.399	-1.146	-1.360	-1.772	-2.317	-2.934	-2.563	-2.148	-2.174	-1.849	-1.875	-2.124	-1.101	-1.434	-0.943	-1.059	-1.092	-0.591	-0.783	-0.717	-0.631	-0.618	-0.571	-0.874	-0.643
11	2000	-1.594	-1.234	-1.544	-1.334	-1.823	-1.812	-1.717	-2.170	-1.765	-1.903	-2.580	-1.786	-1.640	-1.570	-1.615	-1.308	-0.871	-1.163	-0.921	-0.860	-0.547	-0.704	-0.546	-0.676	-0.947	-0.549
12	2000	-1.626	-1.084	-0.885	-2.494	-1.674	-2.071	-1.611	-2.762	-1.999	-1.661	-1.421	-1.398	-2.609	-2.235	-2.656	-1.640	-1.413	-1.496	-0.722	-0.801	-0.759	-1.281	-0.874	-0.749	-0.867	-0.730
1	2001	-1.432	-2.046	-1.631	-1.333	-2.538	-1.305	-2.210	-2.119	-2.744	-4.764	-2.343	-2.746	-1.871	-1.881	-1.704	-0.962	-0.801	-1.180	-0.978	-0.852	-1.313	-0.847	-0.682	-1.078	-1.005	-0.833
11	2001	-1.699	-1.209	-1.872	-2.246	-4.522	-2.482	-2.939	-2.520	-2.476	-3.648	-2.747	-2.219	-1.580	-2.541	-2.119	-1.034	-2.025	-1.011	-1.092	-0.920	-1.120	-0.670	-1.075	-1.110	-1.047	-0.979
12	2001	-0.905	-1.306	-1.253	-1.437	-2.413	-2.378	-2.682	-2.376	-2.320	-2.853	-2.278	-2.689	-2.366	-1.757	-1.364	-1.277	-1.303	-0.897	-0.783	-0.802	-0.830	-0.810	-0.597	-0.779	-0.925	-1.818
1	2002	-1.526	-2.174	-1.427	-2.765	-4.851	-2.957	-3.044	-2.674	-2.457	-2.044	-2.885	-3.619	-2.071	-1.478	-1.617	-1.367	-0.970	-1.020	-1.067	-0.903	-1.416	-1.120	-0.878	-0.710	-1.153	-0.801
2	2002	-1.807	-1.075	-3.532	-3.774	-1.858	-2.650	-2.550	-3.071	-5.718	-2.660	-2.938	-3.495	-1.833	-1.655	-1.931	-1.980	-2.091	-1.022	-1.138	-1.208	-1.055	-1.799	-0.748	-1.100	-0.912	-0.932
3	2002	-2.262	-2.480	-1.976	-4.329	-2.760	-3.447	-2.190	-4.150	-3.707	-3.120	-3.076	-2.520	-2.556	-2.499	-2.090	-1.448	-2.391	-1.552	-1.025	-0.732	-1.291	-0.956	-0.925	-0.633	-0.946	-0.681
4	2002	-9.461	-1.656	-1.694	-1.213	-3.670	-2.221	-3.182	-3.178	-2.945	-3.149	-3.291	-3.295	-2.890	-1.954	-1.534	-1.611	-1.083	-1.161	-0.790	-1.154	-1.012	-1.338	-0.615	-0.651	-1.032	-1.064
5	2002	-1.033	-10.307	-1.146	-1.213	-1.112	-1.355	-5.630	-3.293	-2.757	-2.699	-2.086	-1.799	-1.781	-1.694	-1.307	-2.434	-0.949	-1.285	-0.891	-1.430	-1.113	-0.958	-0.828	-0.704	-1.994	-0.516
6	2002	-0.849	-1.598	-1.894	-1.207	-1.939	-1.869	-2.070	-1.990	-1.350	-3.000	-2.181	-2.176	-2.645	-2.036	-1.840	-1.923	-1.486	-0.751	-1.257	-1.248	-0.750	-0.803	-0.929	-0.679	-0.944	-2.865
7	2002	-0.823	-2.961	-2.455	-1.614	-2.139	-1.764	-1.578	-1.804	-2.311	-1.624	-1.809	-2.551	-1.973	-1.840	-2.032	-1.792	-1.190	-0.770	-1.462	-0.636	-1.032	-0.702	-0.868	-0.916	-1.701	-0.772
8	2002	-3.209	-1.068	-1.248	-3.644	-1.782	-2.234	-2.563	-2.499	-2.732	-2.988	-2.004	-2.176	-3.016	-1.777	-1.621	-1.321	-1.331	-1.412	-1.080	-0.893	-0.847	-0.992	-1.068	-0.956	-1.048	-1.119
9	2002	-2.242	-2.431	-11.418	-1.785	-1.812	-1.925	-3.196	-3.932	-2.150	-3.885	-3.039	-3.326	-3.551	-1.659	-1.753	-2.038	-1.133	-1.560	-1.099	-1.057	-0.971	-1.054	-1.109	-1.027	-0.932	-0.817
10	2002	-18.171	-2.123	-1.053	-1.068	-2.250	-4.154	-3.334	-2.859	-3.987	-14.253	-2.654	-2.664	-3.203	-2.673	-1.783	-1.582	-1.719	-0.946	-1.138	-1.207	-0.954	-0.564	-0.667	-2.052	-0.701	-1.307
11	2002	-1.078	-1.321	-3.681	-1.395	-2.600	-5.718	-2.701	-2.752	-2.435	-2.392	-2.162	-2.287	-1.914	-2.539	-2.216	-1.604	-1.224	-1.407	-1.028	-0.774	-0.586	-0.771	-0.659	-1.109	-0.965	-0.776
12	2002	-3.994	-7.797	-1.651	-1.762	-2.384	-2.764	-3.103	-3.159	-2.862	-3.392	-2.822	-2.971	-1.683	-1.894	-2.052	-1.140	-1.414	-1.062	-1.085	-1.167	-1.236	-0.753	-0.969	-0.637	-1.045	-1.069
1	2003	-1.787	-1.326	-6.159	-2.272	-2.464	-3.641	-2.704	-2.540	-2.702	-3.234	-3.061	-2.873	-2.280	-1.590	-1.798	-1.406	-1.809	-1.675	-1.089	-1.594	-0.965	-1.087	-0.879	-0.529	-0.540	-1.139
2	2003	-1.432	-2.282	-1.976	-1.737	-3.857	-2.838	-3.732	-3.009	-2.757	-2.379	-3.125	-2.562	-3.279	-2.138	-1.811	-2.338	-1.772	-1.432	-1.453	-1.565	-1.294	-0.710	-1.051	-1.539	-5.448	-4.078
3	2003	-2.454	-2.870	-1.298	-3.037	-3.201	-3.673	-7.430	-7.379	-3.150	-3.344	-3.912	-2.221	-3.187	-2.039	-2.152	-1.527	-1.353	-1.530	-1.235	-0.864	-1.180	-0.888	-0.729	-1.330	-0.813	-0.652
4	2003	-2.278	-2.700	-1.625	-0.905	-2.340	-2.369	-3.323	-4.349	-3.845	-2.997	-3.074	-2.800	-2.712	-2.978	-2.422	-1.508	-1.228	-1.419	-0.863	-1.361	-1.127	-1.025	-1.261	-0.761	-0.884	-0.559
5	2003	-1.744	-2.235	-1.171	-0.901	-1.462	-2.066	-2.240	-2.519	-2.320	-2.474	-1.999	-2.488	-2.270	-2.239	-1.505	-1.065	-1.008	-0.781	-1.275	-0.990	-1.177	-0.925	-0.852	-0.882	-0.817	-0.942
6	2003	-0.663	-1.127	-1.291	-0.914	-2.330	-1.323	-2.027	-1.545	-2.386	-1.821	-2.458	-2.526	-1.713	-1.684	-1.321	-1.106	-0.840	-1.017	-0.630	-0.823	-0.744	-0.820	-0.505	-0.426	-0.653	-0.610
7	2003	-1.913	-1.545	-1.131	-0.855	-2.094	-1.302	-1.555	-1.795	-2.504	-1.871	-2.288	-2.545	-1.526	-1.701	-1.991	-1.230	-0.964	-0.833	-0.723	-0.766	-0.736	-0.870	-0.498	-0.618	-0.622	-0.634
8	2003	-0.766	-0.914	-1.676	-1.775	-1.316	-2.258	-1.652	-2.808	-2.166	-2.142	-2.555	-1.774	-1.825	-1.947	-1.342	-1.321	-0.811	-0.786	-0.963	-0.789	-0.541	-0.923	-0.577	-0.707	-0.597	-1.120
9	2003	-4.092	-0.810	-1.531	-3.236	-2.414	-3.076	-2.925	-3.333	-2.820	-2.483	-2.996	-2.682	-1.928	-2.659	-1.496	-1.392	-1.490	-1.363	-0.809	-1.139	-0.894	-0.989	-0.845	-0.643	-0.706	-1.952
10	2003	-2.852	-6.242	-4.090	-1.483	-1.682	-9.713	-7.784	-5.326	-2.985	-4.388	-3.795	-2.731	-3.608	-1.729	-2.672	-1.217	-1.235	-1.006	-1.226	-1.155	-0.869	-0.806	-0.903	-1.264	-0.914	-0.858
12	2007	-1.804	-1.854	-3.328	-1.498	-2.376	-4.194	-2.755	-3.582	-1.831	-3.280	-1.825	-1.766	-2.520	-2.078	-1.537	-1.403	-1.195	-1.134	-1.419	-1.094	-1.052	-0.684	-1.076	-11.123	-0.860	-1.717
1	2008	-0.933	n/a	-3.067	-2.715	-2.806	-1.979	-3.119	-1.475	-2.985	-2.114	-1.329	-2.103	-3.456	-4.010	-1.007	-1.076	-1.092	-14.020	-1.206	-1.647	-1.799	-1.193	-6.667	-0.866	-1.042	-3.766
2	2008	-6.299	-1.311	-2.545	-2.449	-4.837	-2.711	-3.130	-4.087	-2.980	-2.022	-2.884	-1.740	-3.801	-1.952	-1.433	-2.297	-3.617	-1.283	-1.522	-1.070	-1.270	-1.187	-2.725	-0.700	-1.017	-1.042
3	2008	-9.041	-1.060	-1.670	-2.514	-2.398	-3.429	-3.282	-5.222	-5.146	-2.390	-4.296	-1.941	-2.068	-2.017	-2.102	-2.171	-1.288	-1.266	-1.160	-0.847	-1.122	-0.840	-1.156	-1.240	-1.166	-0.617
4	2008	-2.015	-6.257	-1.845	-3.212	-4.385	-2.086	-2.206	-3.375	-2.397	-4.961	-3.617	-3.285	-2.298	-1.630	-1.623	-1.310	-1.030	-1.325	-1.060	-1.204	-1.654	-0.568	-1.216	-1.463	-0.786	-0.995
9	2008	-0.410	-1.499	-1.564	-4.781	-1.501	-2.045	-2.545	-2.297	-3.413	-3.756	-2.237	-2.182	-2.105	-1.678	-1.518	-1.358	-1.383	-1.298	-1.178	-1.298	-1.316	-0.806	-1.042	-0.818	-0.788	-0.882
10	2008	-1.970	-0.795	-1.354	-1.648	-4.742	-2.067	-2.734	-2.696	-2.708	-2.821	-2.013	-2.306	-1.850	-2.030	-1.296	-0.946	-0.995	-1.144	-0.778	-0.880	-0.667	-0.651	-0.889	-0.584	-1.366	-1.084

Table A.18: Costa Rica hyperthermal chemistry slope

Costa Rica: Hyperthermal chemistry regime slope per height increment

Month	Year	75	76	77	78	79	80	81	82	83	84	85	86	87	88	89	90	91	92	93	94	95	96	97	98	99	100
		(km)	(km)	(km)	(km)	(km)	(km)	(km)	(km)	(km)	(km)	(km)	(km)	(km)	(km)	(km)	(km)	(km)	(km)	(km)	(km)	(km)	(km)	(km)	(km)	(km)	(km)
4	2005	-1.606	-2.531	-3.412	-2.275	-2.717	-2.526	-2.589	-2.387	-3.199	-2.668	-2.718	-2.728	-2.579	-2.168	-2.164	-1.959	-2.061	-1.503	-1.598	-1.432	-1.700	-0.739	-0.979	-1.363	-1.024	-0.906
5	2005	-2.398	-3.372	-2.879	-2.311	-2.275	-2.670	-3.046	-2.964	-3.668	-3.383	-2.932	-2.769	-2.371	-2.373	-2.254	-2.318	-1.887	-1.724	-1.494	-1.358	-1.120	-1.238	-0.992	-0.739	-1.054	-0.794
6	2005	-2.132	-2.348	-1.634	-2.535	-2.473	-3.267	-3.002	-3.291	-2.850	-3.249	-2.879	-2.742	-2.731	-2.454	-2.296	-2.117	-1.867	-1.750	-1.537	-1.369	-1.420	-1.019	-1.174	-2.330	-0.994	-1.147
7	2005	-1.612	-2.065	-2.188	-2.041	-2.297	-2.415	-2.062	-2.372	-2.079	-3.182	-2.721	-2.270	-2.431	-2.326	-2.410	-2.379	-2.037	-1.972	-1.848	-1.644	-1.307	-1.337	-0.995	-0.996	-1.302	-1.033
8	2005	-1.661	-2.107	-1.984	-1.565	-1.741	-2.114	-1.924	-2.509	-2.876	-2.528	-2.301	-2.411	-2.650	-2.094	-2.116	-2.185	-2.165	-1.845	-2.011	-1.214	-1.783	-0.990	-1.046	-0.919	-0.768	-0.661
9	2005	-1.285	-1.828	-2.213	-2.808	-1.542	-2.598	-2.299	-2.868	-2.560	-2.771	-2.580	-2.587	-2.293	-2.354	-2.210	-2.122	-1.934	-1.707	-1.921	-1.145	-1.258	-1.046	-0.903	-0.846	-1.861	-0.686
10	2005	-1.147	-1.991	-1.579	-2.366	-2.634	-2.495	-2.828	-2.961	-2.998	-3.262	-2.676	-2.728	-2.592	-2.362	-2.404	-2.060	-2.096	-1.911	-1.650	-1.394	-1.186	-1.057	-0.972	-0.790	-0.759	-1.788
11	2005	-2.667	-1.756	-2.397	-3.059	-3.772	-3.175	-4.439	-3.427	-2.125	-2.065	-3.122	-2.179	-2.889	-2.457	-3.068	-2.402	-2.244	-1.646	-2.020	-1.731	-1.582	-1.346	-0.880	-1.293	-2.090	-0.711
12	2005	-0.994	-4.636	-3.260	-2.024	-2.696	-4.344	-3.010	-2.909	-2.605	-3.017	-2.946	-3.187	-2.409	-2.292	-2.022	-2.200	-1.969	-1.784	-1.655	-1.715	-1.427	-1.405	-0.814	-0.889	-0.778	-0.953
1	2006	-1.331	-1.566	-1.738	-2.198	-1.688	-2.247	-2.075	-2.609	-2.526	-2.896	-3.406	-3.012	-2.447	-2.265	-2.077	-1.857	-1.948	-1.463	-1.541	-1.168	-1.075	-0.956	-0.755	-0.708	-0.718	-0.836
4	2007	-1.536	-2.008	-2.191	-2.520	-3.445	-2.668	-3.274	-3.557	-2.979	-2.845	-3.208	-2.356	-2.520	-2.298	-1.957	-2.043	-1.799	-2.115	-1.804	-1.499	-0.980	-1.440	-1.334	-1.104	-1.006	-0.784
5	2007	-2.370	-1.800	-1.962	-2.161	-1.865	-2.849	-2.535	-3.211	-2.991	-3.262	-3.014	-2.777	-2.559	-2.237	-2.218	-2.116	-1.806	-1.650	-1.410	-1.567	-1.132	-0.815	-1.149	-0.773	-1.041	-1.262
6	2007	-1.649	-1.990	-2.178	-2.742	-3.237	-3.583	-3.194	-3.241	-3.472	-3.181	-2.850	-2.999	-2.465	-2.335	-2.156	-2.094	-1.749	-1.708	-1.401	-1.554	-0.929	-0.991	-1.008	-1.253	-1.169	-0.780
7	2007	-2.481	-1.549	-1.971	-2.068	-2.725	-2.386	-2.548	-2.991	-2.961	-2.573	-2.554	-2.520	-2.756	-2.394	-2.183	-2.093	-1.984	-1.743	-1.625	-1.659	-1.392	-1.188	-0.890	-0.894	-1.036	-1.058
8	2007	-3.380	-4.909	-2.282	-2.604	-3.074	-2.847	-3.162	-3.430	-3.033	-3.469	-3.343	-2.443	-2.430	-2.247	-2.206	-2.188	-2.220	-1.803	-1.580	-1.850	-1.278	-1.697	-0.970	-1.296	-1.249	-1.198
9	2007	-2.019	-1.690	-2.755	-3.678	-2.861	-2.886	-3.551	-2.847	-3.521	-3.086	-3.053	-2.797	-2.504	-2.769	-2.263	-2.106	-2.159	-1.775	-1.750	-1.472	-1.611	-1.391	-0.836	-1.124	-1.622	-1.498
10	2007	-1.895	-5.030	-2.944	-2.682	-3.208	-3.342	-3.112	-3.229	-3.649	-4.170	-3.530	-3.007	-2.644	-2.629	-2.290	-2.059	-1.732	-1.741	-1.438	-1.207	-0.937	-0.675	-1.496	-1.180	-0.762	-1.202
11	2007	-2.560	-4.296	-3.255	-2.964	-2.748	-3.782	-2.824	-5.035	-2.913	-3.605	-3.700	-3.929	-3.125	-2.325	-2.365	-1.553	-2.236	-1.455	-0.940	-1.026	-1.248	-1.357	-0.892	-1.133	-0.850	-1.710
12	2007	-1.347	-3.793	-3.708	-3.155	-3.047	-3.121	-2.715	-3.770	-2.856	-4.032	-2.802	-2.597	-2.417	-1.979	-1.740	-1.852	-1.471	-1.207	-0.948	-0.986	-0.982	-0.818	-0.953	-0.609	-0.575	-0.630
1	2008	-2.173	-6.366	-2.227	-2.134	-2.614	-3.414	-2.889	-2.852	-2.864	-3.790	-3.086	-2.559	-2.431	-2.062	-2.034	-2.031	-1.485	-1.599	-1.307	-1.033	-0.989	-0.795	-0.967	-0.700	-0.689	-0.673
2	2008	-1.594	-1.612	-2.988	-3.556	-2.873	-2.631	-2.736	-2.671	-3.981	-2.588	-2.301	-2.376	-2.634	-2.221	-2.110	-2.014	-1.649	-1.589	-1.346	-1.538	-0.949	-0.762	-0.697	-0.931	-1.673	-0.866
3	2008	-2.968	-2.644	-3.195	-2.483	-3.799	-3.757	-3.363	-3.589	-2.993	-3.312	-2.462	-2.577	-2.736	-2.110	-2.059	-1.861	-1.734	-1.819	-1.588	-1.266	-1.277	-0.987	-1.144	-0.937	-1.026	-1.240
4	2008	-2.891	-2.140	-1.983	-2.347	-2.561	-2.522	-2.559	-2.697	-2.695	-2.563	-2.686	-2.513	-2.108	-1.988	-1.952	-1.843	-1.639	-1.601	-1.383	-1.193	-1.319	-0.997	-0.825	-1.089	-1.036	-1.486
5	2008	-2.134	-1.839	-2.157	-2.860	-3.306	-3.054	-3.650	-3.206	-2.791	-2.877	-2.909	-2.495	-2.393	-2.230	-2.056	-2.355	-1.710	-1.696	-1.392	-1.344	-1.273	-1.095	-1.581	-1.099	-1.473	-1.580
6	2008	-4.249	-2.600	-2.097	-2.295	-3.090	-2.880	-2.802	-3.179	-2.891	-3.268	-3.539	-3.025	-2.529	-2.411	-2.388	-1.952	-1.933	-1.584	-1.262	-1.413	-1.020	-1.357	-0.907	-0.844	-0.825	-1.367
7	2008	-4.010	-2.155	-2.889	-2.178	-3.266	-3.059	-2.802	-3.008	-3.113	-3.029	-3.134	-2.496	-2.387	-2.405	-2.131	-2.140	-1.904	-1.815	-1.736	-1.470	-0.998	-1.003	-1.087	-0.925	-1.340	-1.224
8	2008	-1.148	-2.341	-1.672	-2.543	-2.761	-2.301	-2.963	-2.995	-2.885	-2.929	-2.312	-2.657	-2.135	-2.490	-2.258	-1.642	-2.015	-1.651	-2.199	-1.653	-1.260	-1.687	-1.065	-0.946	-0.884	-1.054
9	2008	-1.503	-1.713	-2.473	-3.018	-2.767	-3.293	-3.046	-3.028	-3.075	-2.671	-3.252	-2.867	-2.418	-2.542	-2.290	-2.093	-1.896	-1.640	-1.583	-1.209	-1.220	-1.340	-0.663	-0.902	-0.778	-0.784
10	2008	-2.424	-2.151	-2.122	-3.429	-2.587	-2.043	-3.072	-3.723	-2.909	-3.345	-3.004	-2.762	-2.469	-2.598	-2.213	-2.168	-1.492	-1.949	-1.444	-1.279	-0.968	-1.452	-0.776	-1.316	-1.084	-0.800
11	2008	-2.223	-6.469	-2.296	-2.909	-3.286	-1.940	-2.871	-3.335	-2.251	-2.487	-2.390	-3.117	-2.552	-1.908	-2.330	-1.875	-1.528	-1.685	-1.586	-0.969	-1.272	-1.072	-1.241	-0.954	-1.013	-1.114
3	2009	-1.518	-2.751	-2.051	-2.351	-2.806	-2.319	-2.103	-3.910	-2.488	-2.168	-2.212	-2.402	-2.486	-2.184	-2.952	-2.000	-2.082	-1.936	-1.414	-1.153	-1.116	-1.002	-0.881	-2.221	-2.038	-0.926
10	2009	-1.606	-2.291	-1.571	-2.461	-3.170	-3.146	-3.136	-3.416	-2.996	-2.981	-2.805	-3.093	-2.767	-2.227	-1.958	-2.042	-1.754	-1.597	-1.420	-1.318	-1.178	-1.154	-0.853	-1.325	-0.870	-0.829
1	2010	-1.379	n/a	-4.537	n/a	-2.327	-1.097	-3.278	-3.813	-1.435	-5.946	-2.236	-2.382	-2.725	-2.354	-1.848	-1.900	-1.801	-3.238	-1.158	-1.359	-3.021	-2.767	-2.461	-1.662	-3.119	-1.635
2	2010	-1.322	-1.516	-1.183	-1.453	-3.002	-2.609	-2.757	-3.488	-2.797	-2.454	-2.191	-2.093	-2.418	-1.717	-2.075	-1.739	-1.480	-1.587	-1.761	-1.606	-1.415	-1.642	-1.097	-1.151	-1.355	-1.125
3	2010	-1.174	-1.184	-2.228	-2.186	-2.140	-2.457	-2.903	-3.376	-3.022	-3.090	-3.072	-2.671	-2.148	-2.097	-1.891	-1.829	-1.721	-1.464	-1.324	-1.299	-1.054	-1.342	-1.060	-1.196	-1.040	-0.697
4	2010	-0.794	-1.422	-1.022	-1.292	-1.564	-1.669	-2.014	-2.430	-2.220	-2.081	-2.595	-2.309	-2.077	-1.884	-1.762	-1.743	-1.444	-1.656	-1.511	-1.353	-1.276	-1.028	-1.269	-0.820	-1.051	-1.663
6	2010	-1.559	-1.425	-1.757	-2.443	-1.674	-2.182	-2.777	-2.572	-2.166	-2.686	-2.281	-2.404	-1.931	-1.937	-1.640	-1.615	-1.378	-1.426	-1.362	-1.218	-1.138	-1.208	-1.175	-0.931	-0.834	-1.159
7	2010	-1.695	-1.850	-3.330	-1.122	-1.377	-1.245	-2.197	-2.511	-1.633	-2.364	-1.671	-1.725	-1.706	-1.681	-1.627	-1.567	-1.485	-1.319	-1.121	-1.436	-1.180	-1.048	-0.975	-1.058	-0.915	-0.763
8	2010	-1.666	-3.165	-2.110	-1.377	-1.771	-1.565	-2.078	-2.198	-1.963	-2.165	-1.869	-2.411	-1.648	-2.019	-1.699	-1.717	-1.472	-1.370	-1.221	-1.277	-1.208	-1.320	-0.803	-1.042	-0.909	-0.891
9	2010	-1.431	-1.527	-0.927	-1.931	-1.828	-1.918	-1.977	-2.232	-2.727	-2.021	-2.188	-2.033	-2.119	-1.919	-1.597	-1.726	-1.474	-1.392	-1.387	-1.189	-1.240	-0.901	-0.969	-0.891	-0.819	-0.978
10	2010	-2.545	-1.888	-1.330	-1.761	-1.964	-2.205	-2.300	-2.266	-2.416	-2.621	-2.222	-2.220	-2.505	-2.187	-1.791	-1.665	-1.713	-1.626	-1.425	-1.339	-1.230	-1.094	-0.964	-0.871	-1.096	-1.044
11	2010	-6.568	-8.192	-1.117	-2.394	-2.168	-1.938	-2.522	-2.467	-2.481	-2.520	-2.614	-2.629	-2.072	-1.978	-1.802	-1.728	-1.589	-1.318	-1.478	-1.277	-2.942	-0.924	-1.480	-0.774	-1.455	-1.405

Table A.19: Resolute Bay hyperthermal chemistry slope (part 1)

Resolute Bay: Hyperthermal chemistry regime slope per height increment

Month	Year	75	76	77	78	79	80	81	82	83	84	85	86	87	88	89	90	91	92	93	94	95	96	97	98	99	100
		(km)	(km)	(km)	(km)	(km)	(km)	(km)	(km)	(km)	(km)	(km)	(km)	(km)	(km)	(km)	(km)	(km)	(km)	(km)	(km)	(km)	(km)	(km)	(km)	(km)	(km)
6	2000	--	--	-2.296	-1.489	-3.605	-1.944	-1.783	-1.998	-1.873	-2.302	-1.826	-1.880	-2.224	-1.416	-1.777	-1.197	-1.223	-1.348	-0.866	-0.758	-0.925	-1.074	-0.944	-0.828	-1.022	-0.875
7	2000	--	--	-2.587	-1.985	-2.046	-1.753	-1.944	-1.805	-2.066	-1.963	-1.730	-1.503	-1.434	-1.295	-1.235	-1.202	-1.080	-0.912	-0.849	-0.840	-0.989	-0.823	-0.833	-0.892	-0.834	-0.951
8	2000	--	--	-2.810	-2.203	-2.148	-2.364	-2.255	-1.851	-1.684	-2.001	-1.641	-1.409	-1.220	-1.108	-0.895	-0.752	-0.881	-0.635	-0.638	-0.641	-0.737	-0.590	-0.565	-0.574	-0.560	-0.537
9	2000	--	--	-2.427	-2.531	-2.510	-2.049	-2.495	-1.824	-1.742	-1.595	-1.371	-1.261	-1.267	-0.930	-0.795	-0.770	-0.721	-0.596	-0.578	-0.547	-0.505	-0.604	-0.523	-0.663	-0.576	-0.604
10	2000	--	--	-2.299	-2.191	-2.585	-2.261	-2.026	-2.190	-1.440	-1.522	-1.268	-1.289	-1.004	-1.074	-1.043	-0.706	-0.874	-0.714	-0.593	-0.628	-0.651	-0.894	-0.569	-0.713	-0.542	-0.674
11	2000	--	--	-2.209	-1.204	-2.336	-1.778	-1.619	-1.864	-1.400	-1.427	-1.069	-1.095	-0.932	-1.135	-0.948	-0.849	-0.807	-0.692	-0.539	-0.737	-0.739	-0.583	-0.749	-0.525	-0.682	-2.853
12	2000	--	--	-2.115	-2.890	-2.668	-2.094	-1.783	-1.681	-1.358	-1.427	-1.262	-1.035	-1.036	-0.839	-0.765	-0.732	-0.717	-0.580	-0.690	-0.645	-0.587	-0.551	-0.589	-0.494	-0.658	-0.651
1	2001	-1.432	-2.046	-1.825	-2.228	-1.900	-2.075	-1.996	-1.915	-1.620	-1.889	-1.549	-1.931	-1.212	-1.209	-1.189	-1.211	-0.983	-0.971	-1.243	-0.909	-1.079	-0.917	-0.799	-0.903	-0.795	-0.923
2	2001	--	--	-1.973	-2.031	-1.649	-1.945	-1.689	-1.676	-1.471	-1.323	-1.317	-1.125	-1.028	-0.992	-0.763	-0.855	-0.730	-0.683	-0.556	-0.585	-0.603	-0.705	-0.819	-0.788	-0.724	-0.776
3	2001	--	--	-2.293	-2.087	-2.404	-1.902	-1.998	-2.032	-1.576	-1.597	-1.313	-1.189	-1.187	-1.049	-0.851	-0.743	-0.672	-0.630	-0.669	-0.841	-0.632	-0.632	-0.707	-0.715	-1.102	-1.056
4	2001	--	--	-1.702	-1.644	-1.819	-1.795	-1.417	-1.506	-1.952	-1.547	-1.384	-1.271	-1.294	-1.207	-1.125	-0.912	-0.817	-0.819	-0.749	-0.789	-0.829	-0.796	-0.792	-0.939	-1.047	-0.914
5	2001	--	--	-1.844	-1.651	-1.689	-2.021	-2.037	-2.038	-1.984	-2.228	-1.910	-1.726	-1.568	-1.402	-1.098	-1.227	-0.933	-0.910	-0.893	-0.962	-1.033	-0.971	-0.985	-1.047	-1.111	-0.900
6	2001	--	--	-1.450	-1.908	-1.798	-1.733	-1.604	-1.547	-1.786	-1.932	-1.728	-1.849	-1.508	-1.433	-1.307	-1.073	-1.144	-1.009	-1.019	-1.082	-0.934	-0.909	-0.921	-1.113	-1.130	-1.099
7	2001	--	--	-1.497	-1.598	-1.470	-1.479	-1.462	-1.390	-1.413	-1.513	-1.462	-1.316	-1.325	-1.216	-1.086	-1.026	-0.991	-0.972	-0.949	-0.935	-0.861	-0.893	-1.023	-0.906	-1.065	-1.062
8	2001	--	--	-1.739	-1.594	-1.807	-1.838	-1.880	-1.616	-1.630	-1.643	-1.500	-1.391	-1.266	-1.279	-1.096	-0.868	-0.808	-0.694	-0.689	-0.705	-0.710	-0.642	-0.699	-0.670	-0.629	-0.828
9	2001	--	--	-2.212	-2.112	-2.116	-2.054	-2.058	-1.890	-1.903	-1.545	-1.355	-1.266	-1.125	-0.977	-0.948	-0.753	-0.678	-0.644	-0.640	-0.552	-0.575	-0.595	-0.755	-0.657	-0.581	-0.684
10	2001	--	--	-1.949	-1.981	-1.772	-2.170	-1.811	-1.737	-1.603	-1.636	-1.324	-1.191	-1.091	-0.864	-0.892	-0.743	-0.637	-0.697	-0.577	-0.549	-0.503	-0.534	-0.505	-0.554	-0.617	-0.461
11	2001	-2.295	-2.303	-2.616	-2.491	-2.771	-2.560	-2.256	-2.017	-1.775	-1.589	-1.551	-1.040	-1.125	-0.819	-0.760	-0.687	-0.643	-0.601	-0.573	-0.522	-0.513	-0.550	-0.555	-0.618	-0.531	-0.533
12	2001	-2.000	-2.556	-2.313	-2.678	-2.873	-2.063	-1.822	-1.705	-1.609	-1.385	-1.295	-1.179	-0.989	-0.899	-0.846	-0.767	-0.741	-0.660	-0.639	-0.704	-0.539	-0.609	-0.608	-0.646	-0.681	-0.503
1	2002	-2.522	-2.819	-2.801	-2.451	-2.110	-2.024	-1.697	-1.577	-1.434	-1.512	-1.172	-1.217	-1.025	-0.932	-0.741	-0.760	-0.656	-0.679	-0.642	-0.598	-0.491	-0.553	-0.666	-0.552	-0.670	-0.552
2	2002	-2.614	-2.731	-2.851	-2.362	-2.482	-2.281	-2.568	-1.986	-1.868	-1.655	-1.416	-1.444	-1.172	-1.123	-0.895	-0.742	-0.766	-0.736	-0.617	-0.679	-0.588	-0.546	-0.736	-0.685	-0.777	-0.598
3	2002	-2.897	-2.569	-3.122	-3.036	-3.115	-3.262	-3.367	-2.228	-2.348	-2.189	-1.816	-1.621	-1.444	-1.284	-1.197	-1.023	-0.833	-0.860	-0.754	-0.709	-0.801	-0.715	-0.616	-0.684	-0.649	-0.600
4	2002	-2.899	-3.354	-4.559	-3.662	-3.145	-3.904	-3.219	-3.651	-3.107	-2.779	-2.356	-2.112	-1.765	-1.366	-1.440	-1.248	-1.090	-0.956	-0.859	-0.789	-0.780	-0.818	-0.755	-0.782	-0.613	-0.794
5	2002	-1.991	-2.281	-2.486	-2.310	-2.852	-2.815	-2.759	-2.924	-2.848	-2.621	-2.546	-2.109	-1.953	-1.678	-1.474	-1.261	-1.140	-0.962	-0.879	-0.836	-0.782	-0.835	-0.829	-0.862	-0.848	-0.796
6	2002	-1.781	-2.545	-2.167	-2.318	-2.243	-2.359	-2.225	-2.360	-2.124	-2.098	-2.227	-2.010	-2.068	-1.653	-1.471	-1.146	-1.040	-0.860	-0.856	-0.803	-0.790	-0.818	-0.825	-0.740	-0.737	-0.592
3	2003	-2.047	-2.669	-2.811	-2.576	-2.648	-2.515	-2.436	-2.679	-1.938	-2.127	-1.642	-1.454	-1.202	-1.084	-0.922	-0.841	-0.837	-0.698	-0.814	-0.698	-0.685	-0.811	-0.596	-0.932	-0.654	-0.580
4	2003	-2.268	-2.493	-3.487	-2.495	-2.763	-2.873	-3.125	-2.836	-2.780	-2.631	-2.337	-1.757	-1.765	-1.516	-1.258	-1.108	-1.068	-0.858	-0.914	-0.864	-0.711	-0.801	-0.714	-0.677	-0.732	-0.751
5	2003	-2.445	-2.313	-2.548	-2.585	-2.668	-2.843	-2.604	-2.608	-2.443	-2.443	-2.284	-2.048	-2.024	-1.621	-1.336	-1.171	-0.936	-0.868	-0.903	-0.763	-0.733	-0.728	-0.846	-0.824	-0.739	-0.672
6	2003	-1.613	-2.141	-2.112	-2.970	-1.624	-1.904	-1.886	-2.250	-2.264	-2.082	-1.893	-1.831	-1.614	-1.344	-1.137	-0.979	-0.882	-0.920	-0.782	-0.952	-0.853	-0.727	-0.749	-0.931	-3.758	-0.746
7	2004	--	--	-2.585	-2.063	-2.423	-2.073	-1.849	-2.215	-1.721	-1.700	-1.650	-1.889	-1.764	-2.100	-1.344	-1.022	-0.989	-0.724	-0.770	-0.966	-0.818	-0.767	-0.844	-1.121	-0.680	-1.025
8	2004	--	--	-2.247	-2.061	-2.351	-2.142	-2.148	-2.364	-1.810	-1.881	-1.869	-1.628	-1.664	-1.272	-1.339	-0.998	-0.776	-0.771	-0.637	-0.601	-0.721	-0.603	-0.682	-0.577	-0.629	-0.590
9	2004	--	--	-2.339	-2.547	-2.803	-2.386	-2.623	-2.358	-2.301	-1.871	-1.673	-1.555	-1.354	-1.253	-1.061	-0.905	-0.716	-0.673	-0.581	-0.584	-0.578	-0.562	-0.598	-0.666	-0.601	-0.650
11	2004	--	--	-2.178	-3.278	-1.843	-1.618	-1.506	-1.839	-1.626	-1.452	-1.372	-0.898	-1.142	-0.728	-0.771	-0.806	-0.715	-1.299	-0.751	-0.546	-0.598	-0.535	-0.818	-1.534	-0.918	-0.692
12	2004	--	--	-2.456	-2.485	-2.240	-2.418	-2.026	-1.669	-1.695	-1.555	-1.352	-1.103	-1.251	-1.001	-0.880	-0.686	-0.847	-0.677	-0.616	-0.563	-0.521	-0.545	-0.700	-0.595	-0.526	-0.542
1	2005	--	--	-1.663	-1.931	-1.958	-1.881	-1.614	-1.729	-1.663	-1.528	-1.176	-1.198	-1.144	-0.944	-0.999	-0.761	-0.696	-0.770	-0.582	-0.528	-0.583	-0.719	-0.590	-0.709	-0.566	-0.542
2	2005	--	--	-1.732	-2.204	-1.874	-2.019	-2.300	-1.726	-2.050	-1.706	-1.613	-1.582	-1.454	-1.323	-1.114	-0.874	-0.891	-0.750	-0.710	-0.730	-0.624	-0.686	-0.567	-0.775	-0.543	-0.584
3	2005	--	--	-2.413	-2.379	-2.148	-2.106	-2.022	-2.444	-1.817	-2.181	-1.705	-1.758	-1.450	-1.199	-0.991	-1.041	-1.101	-0.772	-0.853	-0.756	-0.825	-0.564	-0.677	-0.779	-0.592	-0.839
4	2005	--	--	-2.443	-3.034	-4.674	-3.497	-3.230	-3.086	-3.271	-2.613	-2.442	-2.366	-1.819	-1.642	-1.664	-1.169	-1.100	-1.065	-0.825	-0.800	-0.740	-0.791	-0.796	-0.797	-0.670	-0.801
5	2005	--	--	-3.416	-3.610	-1.951	-2.044	-2.458	-3.360	-2.366	-2.711	-2.100	-2.253	-1.672	-1.719	-1.876	-1.504	-1.269	-0.938	-0.867	-0.923	-0.750	-0.888	-0.832	-2.821	-1.044	-0.674
7	2005	--	--	-1.880	-2.786	-2.168	-2.112	-2.140	-2.255	-2.102	-2.158	-2.031	-2.064	-1.897	-1.808	-1.627	-1.169	-1.041	-0.876	-0.779	-0.813	-0.877	-0.931	-0.712	-0.808	-0.734	-0.664
8	2005	--	--	-2.263	-2.174	-1.758	-1.955	-2.014	-2.282	-1.819	-1.656	-1.656	-1.658	-1.495	-1.284	-1.205	-0.957	-0.741	-0.727	-0.622	-0.724	-0.647	-0.643	-0.659	-0.740	-0.520	-0.622
9	2005	--	--	-2.177	-2.355	-2.106	-2.357	-2.097	-2.103	-1.748	-1.829	-1.472	-1.443	-1.221	-1.174	-0.791	-0.761	-0.760	-0.661	-0.529	-0.588	-0.595	-0.505	-0.582	-0.571	-0.593	-0.480
10	2005	--	--	-1.911	-2.005	-2.159	-2.199	-2.069	-1.915	-1.665	-1.513	-1.427	-1.426	-1.058	-0.970	-0.831	-0.809	-0.652	-0.840	-0.651	-0.537	-0.610	-0.518	-0.655	-0.616	-0.603	-0.604
11	2005	--	--	-2.408	-2.473	-2.004	-1.793	-1.766	-1.680	-1.550	-1.448	-1.210	-1.151	-0.928	-0.764	-0.714	-0.780	-0.768	-0.544	-0.579	-0.663	-0.628	-0.569	-0.729	-0.508	-0.608	-0.686
12	2005	--	--	-1.770	-2.372	-1.815	-2.015	-2.023	-1.861	-1.716	-1.662	-1.482	-1.277	-1.187	-1.009	-0.898	-0.817	-0.699	-0.783	-0.734	-0.682	-0.753	-0.703	-0.663	-0.605	-0.736	-0.639

Table A.20: Resolute Bay hyperthermal chemistry slope (part 2)

Resolute Bay: Hyperthermal chemistry regime slope per height increment

Month	Year	75	76	77	78	79	80	81	82	83	84	85	86	87	88	89	90	91	92	93	94	95	96	97	98	99	100
		(km)	(km)	(km)	(km)	(km)	(km)	(km)	(km)	(km)	(km)	(km)	(km)	(km)	(km)	(km)	(km)	(km)	(km)	(km)	(km)	(km)	(km)	(km)	(km)	(km)	(km)
1	2006	--	--	-1.937	-2.753	-2.189	-2.032	-2.181	-2.014	-1.672	-1.801	-1.655	-1.312	-1.014	-0.930	-0.954	-0.757	-0.761	-0.602	-0.729	-0.575	-0.733	-0.601	-0.590	-0.731	-0.645	-0.522
2	2006	--	--	-2.398	-2.518	-1.705	-1.807	-1.837	-1.600	-1.323	-1.191	-0.947	-1.235	-0.934	-1.107	-0.860	-0.679	-0.796	-0.885	-1.156	-0.958	-1.452	-0.638	-0.997	-1.216	-0.894	-0.670
3	2006	--	--	-2.485	-2.634	-2.687	-2.841	-3.034	-2.473	-2.310	-2.152	-1.955	-1.701	-1.617	-1.378	-1.282	-1.111	-0.890	-0.859	-0.856	-0.715	-0.747	-0.693	-0.650	-1.014	-0.780	-0.785
4	2006	--	--	-5.154	-2.919	-2.749	-2.874	-3.371	-3.101	-2.798	-2.859	-2.375	-1.972	-1.778	-1.698	-1.460	-1.251	-1.318	-1.004	-0.959	-0.819	-0.835	-0.812	-0.952	-0.793	-0.790	-0.699
5	2006	--	--	-2.251	-2.990	-2.598	-2.989	-2.757	-2.719	-2.392	-2.465	-2.554	-2.332	-2.033	-1.817	-1.460	-1.503	-1.215	-1.201	-0.958	-0.850	-0.808	-0.790	-0.843	-0.848	-0.774	-0.815
6	2006	--	--	-2.466	-2.596	-2.559	-2.556	-2.104	-2.221	-2.095	-2.121	-1.810	-2.045	-1.885	-1.578	-1.487	-1.185	-1.080	-0.849	-0.843	-0.864	-0.854	-0.922	-0.864	-0.814	-0.787	-0.814
7	2006	--	--	-1.876	-2.134	-2.350	-2.466	-2.054	-2.296	-2.189	-2.068	-1.958	-2.111	-1.922	-1.536	-1.577	-1.121	-0.938	-0.925	-0.859	-0.895	-0.939	-0.835	-0.885	-0.856	-0.903	-0.852
8	2006	--	--	-2.104	-2.425	-2.494	-2.588	-2.250	-2.259	-1.887	-2.148	-1.764	-1.596	-1.658	-1.317	-1.173	-0.974	-0.835	-0.788	-0.730	-0.597	-0.704	-0.688	-0.643	-0.590	-0.538	-0.693
9	2006	--	--	-3.218	-2.340	-2.475	-2.548	-2.510	-2.173	-2.254	-2.109	-1.775	-1.667	-1.594	-1.205	-0.977	-0.887	-0.763	-0.780	-0.580	-0.543	-0.525	-0.552	-0.562	-0.547	-0.620	-0.615
10	2006	--	--	-2.142	-2.461	-2.500	-2.815	-1.942	-1.851	-1.801	-1.643	-1.511	-1.411	-1.328	-1.024	-0.890	-0.714	-0.858	-0.636	-0.666	-0.648	-0.717	-0.600	-0.449	-0.682	-0.567	-0.556
11	2006	--	--	-2.083	-2.330	-2.225	-2.097	-2.049	-1.786	-1.437	-1.528	-1.427	-1.069	-0.945	-0.920	-0.766	-0.638	-0.630	-0.652	-0.525	-0.512	-0.563	-0.651	-0.587	-0.639	-0.631	-0.578
12	2006	--	--	-2.663	-2.239	-2.246	-1.772	-1.748	-1.753	-1.693	-1.715	-1.225	-1.235	-1.153	-0.905	-0.784	-0.841	-0.677	-0.680	-0.799	-0.528	-0.555	-0.615	-0.522	-0.698	-0.642	-0.568
1	2007	--	--	-2.206	-2.839	-2.165	-1.815	-1.788	-1.732	-1.809	-1.517	-1.370	-1.118	-1.153	-0.898	-0.783	-0.722	-0.684	-0.672	-0.616	-0.539	-0.527	-0.658	-0.618	-0.535	-0.539	-0.784
2	2007	--	--	-2.671	-2.589	-2.569	-2.563	-3.112	-2.793	-1.782	-1.986	-2.024	-1.772	-1.349	-1.421	-1.177	-1.083	-1.231	-1.020	-0.687	-0.849	-0.630	-0.735	-0.662	-0.829	-0.743	-0.807
3	2007	--	--	-3.034	-2.391	-2.474	-2.653	-2.285	-3.133	-2.155	-2.259	-1.903	-1.893	-1.564	-1.348	-1.353	-1.276	-1.149	-0.885	-0.871	-0.758	-0.709	-0.634	-0.676	-0.784	-0.843	-0.650
4	2007	--	--	-2.812	-4.262	-3.382	-3.399	-3.444	-3.405	-3.049	-3.061	-2.695	-2.328	-2.066	-1.793	-1.678	-1.338	-1.089	-1.013	-0.915	-0.897	-0.961	-0.794	-0.685	-0.731	-0.722	-0.737
5	2007	--	--	-2.987	-2.756	-3.235	-2.545	-2.431	-2.552	-2.632	-2.728	-2.460	-2.199	-2.122	-1.830	-1.467	-1.358	-1.131	-1.010	-0.970	-0.820	-0.796	-0.855	-0.773	-0.820	-0.804	-0.731
6	2007	--	--	-1.856	-1.675	-2.612	-2.570	-2.089	-1.482	-2.037	-1.640	-2.027	-1.865	-1.920	-2.089	-1.516	-1.656	-0.996	-1.054	-0.931	-0.991	-0.844	-1.250	-1.066	-0.898	-0.955	-0.879
8	2007	--	--	-2.293	-2.317	-1.900	-2.288	-2.365	-2.457	-2.120	-2.275	-1.852	-1.707	-1.712	-1.371	-1.202	-1.005	-0.844	-0.726	-0.726	-0.678	-0.789	-0.737	-0.616	-0.675	-0.665	-0.766
9	2007	--	--	-2.386	-2.630	-2.392	-2.126	-2.426	-2.229	-2.103	-1.808	-1.581	-1.417	-1.179	-1.109	-1.086	-0.816	-0.676	-0.624	-0.570	-0.583	-0.693	-0.537	-0.753	-0.621	-0.692	-0.852
10	2007	--	--	-2.162	-6.948	-2.888	-2.635	-2.396	-2.344	-2.469	-1.849	-1.691	-1.260	-1.521	-1.223	-1.071	-1.029	-0.892	-0.773	-1.077	-0.612	-0.900	-1.063	-0.751	-0.928	-2.040	-1.068
2	2008	--	--	n/a	-2.862	-3.547	-2.521	-2.194	-2.932	-2.595	-2.728	-1.939	-1.982	-2.230	-2.316	-1.407	-1.299	-0.937	-0.996	-0.974	-0.793	-0.745	-0.719	-0.594	-1.013	-0.747	-0.664
3	2008	--	--	-2.203	-2.415	-1.953	-2.470	-2.213	-2.020	-2.033	-1.775	-1.750	-1.666	-1.204	-1.196	-0.927	-0.990	-0.634	-0.797	-0.913	-0.628	-0.899	-0.725	-0.784	-0.726	-1.399	-1.022
4	2008	--	--	-2.987	-3.413	-2.939	-3.573	-3.419	-3.259	-2.895	-2.711	-2.059	-1.970	-1.863	-1.697	-1.448	-1.262	-1.275	-1.089	-0.943	-0.758	-0.843	-0.762	-0.837	-0.771	-0.739	-0.856
5	2008	--	--	-5.958	-2.845	-3.169	-4.417	-3.185	-3.164	-2.539	-2.549	-2.922	-2.421	-2.303	-2.056	-1.908	-1.439	-1.370	-1.208	-1.114	-1.037	-0.983	-0.816	-0.775	-0.971	-0.866	-0.839
6	2008	--	--	-2.462	-2.539	-2.272	-2.275	-2.223	-2.116	-1.702	-2.081	-2.078	-1.749	-1.646	-1.681	-1.456	-1.113	-1.179	-0.920	-0.939	-0.907	-0.967	-0.805	-0.938	-1.130	-1.244	-0.961
7	2008	--	--	-2.212	-2.422	-1.987	-2.390	-2.323	-2.313	-2.004	-2.030	-1.874	-2.046	-1.721	-1.641	-1.402	-1.248	-1.071	-0.846	-0.800	-0.942	-0.954	-0.957	-0.932	-0.896	-0.795	-0.677
8	2008	--	--	-1.919	-2.399	-2.083	-1.916	-1.732	-1.713	-1.714	-1.516	-1.739	-1.837	-1.728	-1.556	-1.285	-1.180	-0.976	-0.842	-0.938	-0.815	-0.891	-0.826	-0.759	-0.881	-0.943	-0.935
9	2008	--	--	-2.579	-2.637	-2.671	-3.279	-2.726	-2.999	-2.439	-2.400	-1.877	-1.669	-1.512	-1.708	-1.085	-0.919	-0.880	-0.653	-0.758	-0.557	-0.746	-0.843	-0.967	-0.628	-0.852	-0.674
10	2008	--	--	-1.889	-1.725	-2.088	-1.611	-1.987	-1.468	-1.528	-1.358	-1.358	-1.227	-1.010	-0.906	-0.793	-0.741	-0.744	-0.637	-0.596	-0.722	-0.667	-0.563	-0.601	-0.587	-0.619	-0.574
11	2008	--	--	-1.385	-1.621	-1.682	-1.722	-1.897	-1.494	-1.603	-1.274	-1.223	-1.028	-0.906	-0.921	-0.805	-0.729	-0.831	-0.560	-0.826	-0.692	-0.544	-0.489	-0.666	-0.548	-0.608	-0.518
12	2008	--	--	-1.766	-1.448	-1.680	-1.572	-1.686	-1.576	-1.401	-1.249	-1.146	-1.272	-1.042	-0.849	-0.788	-0.805	-0.734	-0.679	-0.670	-0.592	-0.739	-0.665	-0.659	-0.831	-0.602	-0.546
4	2009	--	--	-2.632	-2.450	-4.392	-3.391	-2.585	-3.404	-3.222	-3.010	-2.457	-2.813	-2.364	-1.869	-1.631	-1.844	-1.389	-1.163	-1.127	-0.848	-0.887	-0.934	-0.943	-0.808	-0.785	-0.902
5	2009	--	--	-2.156	-2.586	-2.641	-2.707	-3.261	-2.526	-2.523	-2.422	-2.494	-2.393	-2.219	-1.913	-1.844	-1.345	-1.044	-0.956	-1.026	-0.935	-0.781	-0.771	-0.955	-0.797	-0.909	-1.588
6	2009	--	--	-2.400	-2.400	-2.375	-2.928	-2.387	-2.362	-1.999	-1.747	-1.962	-1.832	-2.022	-2.040	-1.584	-1.852	-1.403	-0.788	-1.040	-0.833	-0.863	-1.119	-1.429	-0.854	-1.008	-1.386
7	2009	--	--	-1.873	-2.016	-2.452	-2.654	-2.582	-1.975	-2.137	-2.364	-1.994	-2.046	-1.795	-1.777	-1.410	-1.130	-0.952	-0.819	-0.832	-0.882	-0.785	-0.801	-0.862	-0.783	-0.696	-0.731
8	2009	--	--	-2.453	-1.974	-3.508	-2.616	-2.250	-2.185	-2.183	-1.876	-1.731	-2.251	-1.792	-1.614	-1.493	-1.203	-1.000	-0.784	-0.726	-0.822	-0.829	-0.745	-0.745	-0.795	-0.682	-0.765
9	2009	--	--	-2.270	-2.434	-2.537	-3.053	-2.014	-2.441	-2.392	-2.277	-1.860	-1.491	-1.498	-1.450	-0.956	-0.922	-0.928	-0.674	-1.021	-0.552	-0.747	-0.651	-0.681	-0.769	-0.612	-0.792
10	2009	--	--	-2.690	-2.783	-2.356	-2.371	-2.038	-2.128	-1.770	-1.694	-1.722	-1.418	-1.292	-1.046	-0.907	-0.791	-0.792	-0.697	-0.555	-0.663	-0.646	-0.625	-0.581	-0.671	-0.531	-0.635
11	2009	--	--	-3.046	-2.475	-2.950	-1.901	-1.962	-1.913	-1.594	-1.715	-1.409	-1.113	-1.183	-0.929	-0.838	-0.884	-0.702	-0.564	-0.617	-0.532	-0.524	-0.469	-0.703	-0.629	-0.753	-0.560
12	2009	--	--	-2.434	-2.195	-2.855	-1.982	-1.957	-1.954	-1.843	-1.949	-2.442	-1.714	-1.339	-1.483	-0.982	-0.718	-0.964	-0.695	-0.712	-0.664	-0.764	-0.715	-0.782	-0.666	-0.838	-0.616
1	2010	--	--	-1.911	-2.529	-1.890	-2.418	-2.169	-2.073	-2.096	-1.672	-1.710	-1.549	-1.249	-1.395	-1.036	-1.058	-1.045	-0.912	-0.659	-0.815	-0.762	-0.846	-0.610	-0.730	-0.783	-0.801
2	2010	--	--	-3.190	-2.920	-2.981	-2.321	-2.507	-2.249	-2.056	-2.158	-1.884	-1.580	-1.563	-1.091	-1.133	-0.881	-0.912	-0.743	-0.663	-0.813	-0.633	-0.766	-0.790	-0.654	-0.639	-0.850
3	2010	--	--	-2.928	-2.299	-2.585	-2.125	-4.041	-2.150	-2.295	-1.821	-1.743	-1.596	-1.186	-1.030	-1.106	-0.950	-0.963	-1.016	-0.656	-0.746	-0.769	-0.651	-1.173	-0.840	-1.462	-0.688
4	2010	--	--	-2.626	-2.203	-3.493	-3.984	-6.050	-1.939	-2.987	-2.429	-2.736	-2.801	-1.995	-1.901	-1.593	-1.581	-1.765	-0.920	-0.975	-0.988	-1.008	-0.932	-0.885	-0.839	-0.945	-1.103
5	2010	--	--	-2.527	-3.083	-2.054	-2.742	-2.517	-2.542	-2.623	-2.086	-2.116	-2.829	-2.109	-1.940	-1.745	-1.496	-1.184	-1.013	-0.892	-0.942	-0.868	-0.963	-0.891	-0.898	-0.710	-0.706
6	2010	--	--	-2.536	-2.026	-2.401	-2.590	-1.855	-2.381	-2.477	-1.988	-1.867	-1.867	-2.252	-1.715	-1.677	-1.325	-1.038	-0.871	-0.968	-0.877	-0.893	-1.011	-1.068	-0.982	-0.812	-0.847
7	2010	--	--	-2.386	-2.563	-1.943	-2.600	-2.609	-1.942	-2.255	-1.983	-1.877	-1.971	-2.020	-2.016	-1.293	-1.177	-1.096	-0.906	-0.822	-0.800	-0.912	-0.902	-1.027	-1.043	-0.730	-0.799
8	2010	--	--	-1.995	-2.462	-3.102	-2.109	-1.522	-3.911	-1.707	-2.000	-1.816	-2.306	-1.786	-1.395	-1.376	-0.944	-1.080	-0.577	-0.570	-0.604	-0.683	-0.569	-0.549	-0.622	-0.531	-0.612
11	2010	--	--	-0.209	-0.137	-0.322	-0.365	-0.176	-0.545	-0.347	-0.338	-0.232	-0.147	-0.325	-0.180	-0.277	-0.491	-1.332	-0.547	-0.313	-0.581	-0.458	-0.257	-0.347	-5.403	-0.284	-0.242
12	2010	--	--	-1.048	-1.277	-1.155	-1.173	-1.195	-1.005	-0.915	-1.025	-0.912	-1.052	-0.738	-1.080	-0.736	-0.826	-0.971	-1.029	-0.835	-0.666	-0.518	-0.845	-1.111	-0.892	-0.867	-0.955

Table A. 21: Socorro hyperthermal chemistry slope (part 1)

Socorro: Hyperthermal chemistry regime slope per height increment

Month	Year	75	76	77	78	79	80	81	82	83	84	85	86	87	88	89	90	91	92	93	94	95	96	97	98	99	100
		(km)	(km)	(km)	(km)	(km)	(km)	(km)	(km)	(km)	(km)	(km)	(km)	(km)	(km)	(km)	(km)	(km)	(km)	(km)	(km)	(km)	(km)	(km)	(km)	(km)	(km)
4	2002	-1.569	-1.701	-1.430	-1.970	-2.083	-2.088	-2.799	-2.117	-2.583	-1.978	-1.543	-3.115	-2.079	-1.382	-1.375	-1.290	-1.294	-1.537	-1.293	-1.124	-1.015	-1.237	-0.980	-2.207	-0.660	-0.732
5	2002	-1.608	-1.211	-2.236	-1.309	-1.953	-1.602	-1.754	-1.840	-1.821	-1.849	-1.766	-1.792	-1.681	-1.577	-1.499	-1.620	-1.231	-1.004	-0.758	-0.925	-0.895	-0.971	-0.895	-0.789	-0.809	-1.403
6	2002	-1.008	-1.588	-1.512	-1.557	-2.353	-1.732	-1.906	-2.551	-1.613	-1.794	-1.771	-1.611	-1.504	-1.584	-1.279	-1.286	-1.121	-1.061	-0.988	-0.938	-1.020	-1.161	-0.930	-0.937	-0.720	-1.320
7	2002	-0.790	-0.970	-1.756	-1.741	-1.390	-1.115	-1.391	-1.356	-1.500	-1.641	-1.667	-1.468	-1.425	-1.668	-1.351	-1.112	-1.249	-1.238	-1.140	-0.743	-0.650	-0.633	-0.641	-0.663	-0.529	-0.675
8	2002	-1.068	-1.277	-1.021	-1.439	-1.448	-1.532	-1.474	-1.743	-1.694	-1.569	-1.807	-1.561	-1.696	-1.493	-1.347	-1.232	-1.115	-1.070	-1.027	-0.978	-0.875	-0.779	-0.842	-0.735	-0.760	-0.839
9	2002	-0.835	-1.041	-1.782	-1.481	-1.480	-1.554	-1.696	-1.877	-1.661	-1.670	-1.769	-1.785	-1.593	-1.573	-1.439	-1.296	-1.495	-1.151	-1.153	-1.188	-1.031	-0.812	-0.923	-0.736	-0.930	-0.764
10	2002	-0.363	-0.346	-0.323	-0.309	-0.429	-0.439	-0.620	-0.603	-0.595	-0.765	-0.659	-0.865	-0.677	-0.886	-0.786	-0.921	-1.115	-0.841	-1.330	-0.783	-0.757	-0.819	-0.529	-0.363	-0.296	-0.251
11	2002	-0.162	-1.661	-0.737	-0.313	-0.452	-0.461	-0.501	-0.670	-0.649	-0.666	-0.552	-0.727	-0.568	-0.747	-0.728	-0.875	-1.106	-0.776	-1.962	-0.862	-0.961	-0.500	-0.373	-0.312	-0.327	-0.370
3	2003	-1.685	-0.857	-1.706	-1.836	-1.691	-2.245	-1.890	-2.070	-2.225	-2.141	-1.840	-1.783	-1.535	-1.527	-1.451	-1.369	-1.242	-1.220	-1.113	-0.885	-0.833	-0.810	-1.018	-0.981	-0.912	-1.111
4	2003	-1.644	-1.269	-1.500	-1.681	-1.718	-1.968	-2.052	-2.047	-1.800	-2.112	-1.731	-1.802	-1.549	-1.586	-1.510	-1.393	-1.264	-0.865	-1.095	-0.737	-0.968	-0.826	-0.976	-0.624	-0.829	-0.669
1	2005	-2.376	-2.803	-2.004	-3.762	-2.775	-3.161	-3.840	-2.397	-3.450	-3.108	-2.343	-2.287	-2.091	-2.048	-1.836	-1.822	-1.311	-1.361	-1.291	-1.153	-0.879	-0.910	-0.783	-1.034	-0.639	-0.648
2	2005	-1.995	-2.829	-2.129	-2.656	-3.527	-3.768	-3.500	-3.282	-3.090	-2.911	-2.606	-2.506	-2.299	-2.091	-1.895	-1.590	-1.721	-1.406	-1.329	-1.091	-0.887	-1.185	-0.929	-1.298	-0.797	-1.094
3	2005	-2.617	-2.810	-2.284	-3.371	-3.222	-2.709	-3.039	-2.680	-3.046	-3.021	-2.955	-2.350	-2.193	-2.102	-1.914	-1.614	-1.604	-1.284	-1.026	-1.069	-0.892	-0.755	-0.844	-0.762	-0.813	-0.912
4	2005	-2.171	-2.122	-3.290	-2.785	-2.711	-2.616	-2.660	-2.898	-3.112	-2.758	-2.636	-2.413	-2.192	-2.149	-1.880	-1.744	-1.674	-1.416	-1.334	-1.074	-1.058	-1.274	-0.820	-0.670	-0.950	-1.461
5	2005	-1.458	-2.182	-2.551	-2.814	-2.530	-2.647	-3.071	-2.884	-2.934	-2.920	-2.623	-2.233	-2.174	-2.071	-1.924	-1.653	-1.456	-1.220	-1.126	-1.093	-0.963	-0.885	-0.796	-0.868	-0.722	-0.793
6	2005	-4.650	-3.391	-2.014	-2.105	-3.038	-3.190	-3.183	-3.230	-3.111	-2.828	-2.825	-2.354	-2.150	-1.942	-1.720	-1.537	-1.274	-1.058	-1.020	-0.826	-0.836	-0.745	-0.781	-0.813	-0.815	-0.928
7	2005	-1.617	-2.514	-2.161	-2.606	-2.844	-3.640	-3.252	-3.190	-3.057	-2.823	-2.465	-2.257	-2.006	-1.878	-1.704	-1.442	-1.309	-1.116	-1.045	-1.010	-0.984	-0.852	-1.150	-1.141	-1.120	-0.821
8	2005	n/a	n/a	-4.758	-3.318	-5.127	-2.658	-3.624	-3.107	-3.269	-2.426	-2.432	-2.513	-2.592	-1.444	-1.692	-1.232	-1.620	-1.382	-0.995	-0.800	-1.045	-0.824	-1.205	-1.004	-1.046	-1.043
5	2007	-1.571	-2.827	-3.452	-2.726	-2.840	-3.181	-3.177	-2.676	-2.889	-2.522	-2.490	-2.231	-2.214	-1.958	-1.657	-1.451	-1.297	-0.913	-0.918	-1.103	-1.171	-0.827	-0.840	-0.773	-0.696	-0.651
6	2007	-1.246	-1.692	-1.751	-1.907	-2.625	-3.166	-3.007	-2.910	-2.811	-2.608	-2.422	-2.111	-1.981	-1.866	-1.597	-1.405	-1.338	-1.168	-0.983	-0.926	-1.023	-0.979	-0.791	-0.680	-0.739	-0.959
7	2007	-2.760	-2.146	-1.859	-2.520	-3.084	-3.581	-3.122	-2.703	-2.375	-2.678	-2.553	-2.377	-2.176	-2.083	-1.745	-1.601	-1.368	-1.217	-1.163	-1.185	-0.968	-0.972	-0.869	-0.935	-0.676	-0.635
6	2008	-1.507	-1.941	-3.784	-2.333	-3.024	-2.792	-2.656	-2.842	-2.544	-2.553	-2.612	-2.343	-2.184	-1.912	-1.689	-1.494	-1.290	-1.179	-0.882	-0.860	-0.838	-0.804	-0.743	-0.910	-1.175	-1.044
7	2008	-1.704	-2.515	-2.578	-2.844	-3.013	-3.121	-3.373	-3.625	-2.961	-3.049	-2.617	-2.309	-2.061	-1.966	-1.676	-1.488	-1.255	-1.137	-1.047	-1.117	-1.183	-0.893	-0.928	-0.875	-0.836	-0.937
8	2008	-3.314	-2.599	-7.219	-3.142	-4.404	-4.826	-3.593	-3.674	-3.565	-2.690	-2.171	-2.821	-1.938	-1.855	-1.574	-1.271	-1.541	-1.451	-1.164	-0.798	-0.833	-0.940	-0.951	-1.049	-1.273	-1.145
12	2008	-1.952	-2.648	-2.666	-2.289	-3.593	-2.310	-3.392	-3.365	-2.163	-2.777	-2.139	-2.112	-2.113	-1.892	-1.714	-1.596	-1.508	-1.325	-1.537	-1.115	-1.229	-0.907	-0.961	-0.830	-0.813	-0.927
1	2009	-2.823	-2.679	-2.807	-2.531	-3.188	-2.618	-2.850	-3.671	-2.396	-2.712	-2.295	-2.219	-1.881	-1.911	-1.515	-1.500	-1.465	-1.346	-1.195	-0.799	-1.118	-0.970	-1.017	-1.070	-1.144	-1.309
2	2009	-1.570	-3.824	-3.293	-2.992	-3.613	-3.813	-2.764	-3.654	-2.819	-2.969	-2.679	-2.309	-2.169	-2.089	-1.812	-1.606	-1.395	-1.471	-1.152	-1.179	-0.982	-1.001	-0.752	-1.443	-0.881	-0.991
3	2009	-2.303	-2.104	-2.749	-3.589	-2.480	-3.570	-3.240	-3.024	-2.749	-2.689	-2.487	-2.328	-2.311	-1.939	-1.690	-1.636	-1.369	-1.329	-1.493	-0.950	-0.919	-0.973	-0.731	-0.699	-0.927	-1.132
4	2009	-2.249	-1.570	-2.618	-2.914	-2.504	-3.102	-3.011	-2.767	-2.708	-2.439	-2.524	-2.101	-2.249	-1.834	-1.695	-1.527	-1.483	-1.580	-1.551	-1.152	-1.107	-1.036	-0.955	-1.053	-1.373	-1.015
5	2009	-1.078	-1.284	-1.691	-1.928	-1.745	-2.410	-2.434	-2.449	-3.017	-2.489	-3.193	-2.007	-1.878	-1.785	-1.994	-1.841	-1.330	-1.467	-1.417	-0.965	-0.985	-1.056	-0.911	-0.877	-1.374	-1.044
6	2009	-4.464	-2.338	-3.312	-2.616	-2.598	-2.887	-2.972	-3.359	-3.230	-2.578	-2.427	-2.215	-2.140	-1.823	-1.745	-1.449	-1.469	-1.071	-1.063	-0.615	-0.978	-1.111	-0.690	-0.763	-1.359	-1.055
7	2009	-1.431	-1.706	-2.319	-2.638	-2.814	-2.843	-2.923	-2.756	-2.980	-2.514	-2.484	-2.150	-1.960	-1.798	-1.624	-1.409	-1.302	-1.204	-1.018	-1.115	-1.049	-0.978	-1.018	-1.155	-0.875	-1.100
8	2009	-1.239	-2.159	-3.016	-2.831	-3.160	-3.129	-3.016	-3.477	-3.214	-2.775	-2.400	-2.207	-2.069	-1.937	-1.665	-1.432	-1.263	-1.273	-0.999	-0.831	-0.932	-0.883	-0.807	-0.943	-0.649	-0.613
9	2009	-2.397	-1.945	-2.312	-2.595	-2.938	-2.769	-2.988	-2.979	-2.794	-2.618	-2.216	-2.303	-2.022	-1.910	-1.723	-1.552	-1.500	-1.523	-1.326	-1.129	-1.060	-0.898	-0.943	-1.113	-0.886	-0.894
10	2009	-2.296	-1.977	-2.482	-2.138	-2.539	-3.126	-2.629	-3.094	-2.497	-2.441	-2.386	-2.268	-1.932	-1.771	-1.625	-1.532	-1.265	-1.150	-1.107	-1.077	-0.977	-1.015	-0.776	-0.859	-0.642	-0.778
11	2009	-1.629	-1.709	-1.948	-2.741	-2.716	-2.726	-2.684	-2.976	-2.876	-2.466	-2.415	-2.207	-1.957	-1.942	-1.577	-1.555	-1.396	-1.552	-1.256	-1.156	-0.905	-0.920	-1.100	-0.787	-0.975	-0.740
12	2009	-1.934	-2.315	-2.243	-3.825	-3.117	-2.897	-3.059	-2.708	-2.756	-2.289	-2.403	-2.441	-1.966	-1.693	-1.619	-1.564	-1.333	-0.926	-1.110	-0.832	-0.966	-1.205	-0.677	-0.799	-0.923

Table A.22: Socorro hyperthermal chemistry slope (part 2)

Socorro: Hyperthermal chemistry regime slope per height increment

Month	Year	75	76	77	78	79	80	81	82	83	84	85	86	87	88	89	90	91	92	93	94	95	96	97	98	99	100
		(km)	(km)	(km)	(km)	(km)	(km)	(km)	(km)	(km)	(km)	(km)	(km)	(km)	(km)	(km)	(km)	(km)	(km)	(km)	(km)	(km)	(km)	(km)	(km)	(km)	(km)
1	2010	-2.336	-2.625	-2.882	-2.742	-2.886	-2.697	-2.832	-2.910	-2.413	-2.029	-2.946	-2.251	-1.994	-1.715	-1.644	-1.676	-1.267	-1.308	-1.095	-1.029	-1.036	-0.846	-0.767	-1.060	-0.983	-0.877
2	2010	-2.039	-2.277	-3.168	-3.029	-3.103	-3.107	-3.375	-3.301	-2.992	-2.600	-2.695	-2.318	-2.246	-2.053	-1.904	-1.617	-1.484	-1.296	-1.132	-0.947	-1.098	-0.926	-1.036	-0.832	-0.978	-0.670
3	2010	-1.523	-1.755	-2.797	-3.051	-3.064	-3.618	-3.582	-3.691	-2.784	-2.941	-2.739	-2.345	-2.172	-1.993	-1.723	-1.604	-1.403	-1.323	-1.158	-0.801	-0.965	-0.868	-1.065	-0.811	-0.800	-0.799
4	2010	-2.936	-1.989	-1.943	-3.341	-2.750	-2.966	-2.238	-2.888	-2.192	-2.547	-2.161	-2.189	-2.060	-2.007	-1.924	-1.619	-1.412	-1.254	-1.142	-0.742	-1.012	-0.772	-0.798	-1.091	-1.334	-1.316
5	2010	-2.077	-1.672	-1.864	-2.131	-2.296	-2.224	-3.074	-2.910	-2.863	-2.589	-2.369	-2.202	-2.105	-1.923	-1.707	-1.493	-1.406	-1.190	-1.055	-1.160	-0.940	-0.962	-0.936	-1.039	-0.896	-0.608
6	2010	-1.723	-1.589	-2.221	-2.900	-2.748	-3.146	-3.117	-3.444	-3.023	-2.681	-2.385	-2.195	-2.037	-1.817	-1.597	-1.462	-1.257	-1.105	-0.967	-0.890	-0.993	-0.826	-0.792	-0.984	-0.849	-0.773
7	2010	-3.031	-2.499	-3.173	-2.814	-3.117	-2.872	-3.305	-3.202	-2.849	-2.661	-2.340	-2.226	-2.088	-1.958	-1.814	-1.526	-1.342	-1.165	-1.048	-1.051	-0.927	-0.888	-0.802	-0.921	-1.191	-0.843
8	2010	-1.585	-2.511	-1.948	-2.467	-2.681	-2.739	-3.098	-3.485	-2.762	-2.383	-2.228	-2.102	-1.902	-1.899	-1.611	-1.498	-1.352	-1.227	-1.108	-1.028	-0.966	-0.852	-0.712	-0.785	-0.675	-0.678
9	2010	-1.880	-2.626	-2.722	-2.829	-2.471	-2.807	-3.281	-2.774	-2.579	-2.362	-2.174	-2.111	-1.896	-1.786	-1.720	-1.539	-1.307	-1.216	-1.069	-1.166	-1.081	-0.913	-0.890	-1.016	-0.888	-0.668
10	2010	-1.878	-2.285	-2.095	-2.447	-2.479	-2.604	-3.111	-2.901	-2.615	-2.440	-2.111	-2.090	-1.826	-1.796	-1.564	-1.519	-1.295	-1.237	-0.993	-1.064	-0.881	-0.992	-0.860	-0.964	-0.780	-1.053
11	2010	-1.953	-3.153	-2.473	-2.912	-2.907	-2.963	-3.080	-2.969	-2.973	-2.407	-2.329	-2.181	-2.043	-1.814	-1.725	-1.571	-1.411	-1.205	-1.132	-1.124	-1.125	-0.892	-1.049	-0.793	-0.755	-0.818
12	2010	-1.600	-1.620	-2.038	-3.009	-2.974	-2.580	-2.978	-2.470	-2.600	-2.411	-2.119	-1.967	-1.948	-1.680	-1.727	-1.424	-1.350	-1.145	-1.101	-1.007	-1.051	-0.938	-0.897	-0.933	-0.832	-0.934
1	2011	-2.415	-2.197	-2.448	-2.573	-2.954	-2.754	-3.163	-2.538	-2.907	-2.278	-2.082	-2.320	-2.059	-2.037	-1.706	-1.564	-1.638	-1.351	-1.297	-1.037	-1.156	-0.843	-1.060	-0.663	-0.787	-1.205
2	2011	-1.956	-3.031	-2.101	-3.210	-3.161	-2.992	-2.700	-2.600	-3.362	-2.717	-2.350	-1.946	-1.938	-1.682	-1.588	-1.254	-1.240	-1.326	-0.901	-0.880	-1.081	-0.838	-0.725	-0.802	-1.917	-1.035
3	2011	-2.930	-1.996	-2.224	-2.471	-3.201	-2.920	-2.266	-2.391	-2.295	-2.196	-2.396	-2.103	-2.048	-2.060	-1.439	-1.601	-1.340	-1.290	-1.184	-0.776	-1.260	-0.899	-1.017	-0.871	-1.116	-1.193
4	2011	-1.543	-3.195	-2.050	-2.782	-2.926	-2.481	-3.282	-2.500	-2.349	-2.233	-2.188	-1.977	-1.836	-1.864	-1.704	-1.529	-1.427	-1.218	-1.153	-1.290	-0.877	-0.926	-0.665	-1.179	-1.409	-0.712
5	2011	-1.698	-1.458	-2.236	-2.358	-2.631	-2.542	-2.353	-2.302	-2.637	-2.354	-2.441	-2.191	-1.974	-2.151	-1.916	-1.610	-1.457	-1.449	-1.228	-1.298	-1.210	-1.053	-0.946	-1.200	-1.075	-1.136
6	2011	-1.775	-4.290	-2.073	-2.460	-2.230	-2.537	-2.931	-2.899	-2.526	-2.695	-2.373	-2.054	-1.971	-1.638	-1.566	-1.389	-1.419	-1.331	-1.225	-1.056	-0.953	-1.053	-1.051	-1.015	-0.886	-1.070
7	2011	-1.440	-1.996	-2.080	-2.325	-2.334	-2.511	-2.813	-2.759	-2.802	-2.531	-2.785	-2.040	-1.915	-1.756	-1.521	-1.341	-1.261	-1.122	-1.112	-1.042	-1.119	-0.997	-1.043	-1.385	-1.070	-1.048
8	2011	-1.466	-1.575	-2.567	-2.351	-2.991	-2.784	-3.045	-2.769	-2.976	-2.581	-2.351	-2.091	-1.833	-1.733	-1.578	-1.477	-1.351	-1.248	-1.176	-1.030	-1.034	-1.040	-0.811	-0.881	-0.926	-0.881
9	2011	-1.839	-2.006	-2.932	-3.070	-2.500	-3.194	-2.926	-3.161	-2.766	-2.449	-2.282	-1.956	-1.931	-1.938	-1.712	-1.711	-1.440	-1.195	-1.206	-1.135	-1.066	-0.976	-1.048	-0.962	-1.209	-1.391
10	2011	-2.604	-2.596	-1.937	-2.722	-3.622	-2.747	-3.061	-3.288	-2.672	-2.378	-2.312	-2.058	-1.986	-1.774	-1.698	-1.483	-1.380	-1.212	-1.095	-1.048	-0.898	-1.141	-1.073	-1.374	-1.167	-0.811
11	2011	-1.735	-2.042	-3.303	-2.992	-3.594	-3.857	-3.404	-2.431	-3.000	-2.667	-2.321	-2.120	-1.993	-1.839	-1.623	-1.547	-1.378	-1.283	-1.166	-1.086	-0.906	-0.952	-0.960	-0.895	-0.738	-0.835
12	2011	-3.122	-2.536	-2.518	-2.765	-3.862	-3.420	-3.059	-2.236	-2.846	-2.618	-2.232	-2.281	-1.965	-1.778	-1.441	-1.467	-1.451	-0.883	-1.073	-0.896	-1.002	-0.963	-0.694	-0.727	-0.836	-0.795
1	2012	-2.865	-2.787	-2.050	-3.045	-2.458	-3.462	-2.090	-3.702	-2.364	-3.103	-2.485	-2.429	-2.063	-1.716	-1.708	-1.675	-1.423	-1.285	-1.263	-1.344	-1.097	-0.965	-1.106	-0.731	-0.782	-1.134
2	2012	-2.783	-1.471	-1.856	-3.471	-2.610	-2.705	-3.500	-2.649	-3.213	-2.155	-2.862	-2.364	-1.770	-1.622	-1.715	-1.512	-1.442	-1.337	-1.146	-0.823	-0.979	-0.992	-1.052	-1.287	-1.151	-0.708
3	2012	-2.650	-2.037	-3.478	-2.195	-3.389	-2.960	-3.058	-3.408	-3.500	-2.931	-2.827	-2.169	-2.118	-1.939	-1.837	-1.624	-1.442	-1.337	-1.109	-1.264	-1.041	-0.980	-1.039	-1.184	-0.814	-1.205
4	2012	-1.884	-2.141	-2.140	-3.443	-2.545	-2.585	-2.711	-2.689	-2.869	-2.874	-2.422	-2.590	-2.047	-2.046	-1.479	-1.671	-1.528	-1.238	-1.210	-1.050	-0.991	-1.041	-1.078	-0.940	-1.179	-0.797
5	2012	n/a	-2.658	-2.375	-2.669	-2.547	-2.187	-2.692	-2.284	-3.295	-2.615	-1.791	-2.710	-1.643	-1.883	-1.084	-1.322	-1.045	-1.012	-0.926	-0.980	-0.669	-0.954	-1.647	-1.610	-1.420	-1.108

Table A.23: Yellowknife hyperthermal chemistry slope (part 1)

Yellowknife: Hyperthermal chemistry regime slope per height increment

Month	Year	75	76	77	78	79	80	81	82	83	84	85	86	87	88	89	90	91	92	93	94	95	96	97	98	99	100
		(km)	(km)	(km)	(km)	(km)	(km)	(km)	(km)	(km)	(km)	(km)	(km)	(km)	(km)	(km)	(km)	(km)	(km)	(km)	(km)	(km)	(km)	(km)	(km)	(km)	(km)
6	2002	n/a	-1.817	-8.150	-2.425	-2.494	-1.985	-1.954	-1.579	-1.578	-1.611	-1.920	-1.238	-1.211	-1.329	-1.106	-1.096	-0.846	-0.636	-0.710	-0.556	-0.778	-1.029	-1.150	-4.617	-0.830	-1.662
7	2002	-2.277	-2.239	-1.451	-1.066	-3.240	-2.375	-2.618	-1.760	-1.897	-1.892	-1.593	-1.444	-1.435	-1.476	-1.233	-1.052	-0.668	-0.707	-0.546	-0.448	-0.754	-0.991	-1.008	-0.462	-1.074	-1.761
8	2002	-2.323	-2.268	-3.210	-1.728	-2.157	-1.914	-1.781	-2.489	-1.672	-2.232	-1.760	-1.916	-1.814	-1.245	-1.097	-0.791	-0.693	-0.698	-0.550	-0.537	-0.613	-0.483	-0.698	-0.610	-1.401	-0.544
3	2003	-4.416	-5.406	-2.816	-5.571	-3.094	-3.649	-3.084	-2.965	-2.577	-4.184	-2.876	-1.791	-1.685	-1.317	-2.275	-1.268	-1.469	-0.815	-1.531	-0.961	-0.421	-1.157	-1.082	-12.191	-7.106	n/a
4	2003	-1.201	-1.546	-3.081	-1.932	-3.265	-2.451	-2.825	-3.559	-3.166	-2.806	-2.029	-2.191	-1.974	-2.027	-2.034	-1.486	-1.708	-1.445	-1.319	-1.343	-1.018	-1.091	-0.587	-0.932	-4.727	-2.121
5	2003	-1.390	-0.993	-2.908	-2.174	-2.393	-2.253	-2.435	-3.368	-2.718	-3.141	-2.137	-1.921	-1.884	-2.101	-1.601	-1.209	-0.976	-0.892	-0.713	-1.147	-1.037	-1.203	-1.173	-0.903	-0.790	-1.111
6	2003	-2.335	-0.823	-0.834	-1.146	-2.372	-1.511	-1.330	-2.570	-2.191	-2.205	-1.716	-1.745	-1.714	-1.416	-1.102	-1.032	-0.891	-1.133	-0.776	-1.135	-0.912	-1.064	-1.286	-1.102	-0.826	-0.799
7	2003	-0.745	-0.765	-0.987	-1.468	-4.031	-1.629	-1.707	-1.685	-1.912	-1.895	-2.118	-1.691	-1.443	-1.440	-1.286	-1.237	-1.397	-0.848	-0.732	-0.654	-1.359	-0.891	-0.723	-0.808	-0.644	-0.510
8	2003	-1.777	-1.559	-2.814	-2.196	-1.603	-1.946	-1.619	-3.296	-2.383	-1.732	-1.743	-1.783	-1.489	-1.491	-1.137	-1.152	-0.932	-0.979	-0.631	-1.074	-0.843	-0.868	-0.667	-0.885	-0.449	-0.470
9	2003	-0.960	-3.890	-1.228	-1.772	-3.401	-2.485	-2.776	-2.225	-2.002	-1.871	-1.464	-1.788	-1.720	-1.271	-1.622	-1.251	-1.111	-1.169	-0.890	-0.737	-0.944	-0.708	-1.346	-1.042	-0.984	-0.771
10	2003	-1.438	-3.199	-2.440	-2.867	-2.789	-2.034	-2.526	-2.743	-2.437	-1.994	-1.657	-2.083	-2.058	-1.228	-1.389	-0.966	-1.044	-1.478	-0.805	-0.937	-1.235	-1.109	-0.791	-1.349	-1.071	-0.806
11	2003	-2.414	-2.948	-2.716	-2.089	-2.865	-2.123	-2.988	-2.078	-1.821	-1.894	-1.496	-1.599	-1.993	-1.053	-1.269	-1.122	-1.326	-2.071	-1.339	-1.186	-0.908	-1.111	-16.806	-1.187	-0.793	-1.947
12	2003	-1.835	-1.819	-2.654	-2.105	-2.166	-3.354	-2.252	-2.260	-2.524	-1.783	-1.690	-1.689	-1.337	-1.086	-1.089	-1.054	-0.834	-1.186	-0.793	-0.893	-0.604	-0.718	-1.118	-1.379	-1.205	-6.073
1	2004	-3.266	-2.263	-2.901	-3.698	-2.815	-2.641	-2.048	-2.355	-2.056	-1.927	-1.605	-1.563	-1.219	-1.021	-1.268	-1.480	-0.780	-1.054	-0.864	-0.950	-0.688	-1.012	-0.942	-1.685	-1.422	-1.641
2	2004	-3.483	-2.060	-3.554	-2.495	-3.517	-2.241	-2.191	-2.211	-2.278	-1.849	-1.739	-1.671	-1.294	-1.466	-1.711	-1.540	-1.164	-1.604	-1.427	-1.125	-1.596	-1.088	-1.470	-20.170	-1.130	n/a
3	2004	-4.839	-1.443	-2.240	-2.824	-1.939	-1.872	-3.333	-2.477	-2.352	-2.350	-2.021	-2.564	-1.466	-1.265	-1.223	-1.305	-0.840	-0.779	-1.234	-0.632	-1.140	-1.060	-1.033	-1.780	-0.996	-0.910
4	2004	-1.603	-3.584	-2.170	-2.804	-2.456	-2.257	-2.221	-2.411	-2.161	-2.589	-2.077	-1.993	-2.053	-1.947	-1.479	-1.298	-1.387	-0.857	-0.797	-1.012	-1.103	-0.778	-0.857	-0.884	-1.484	-1.035
5	2004	-1.661	-1.503	-1.754	-5.159	-1.707	-1.821	-1.962	-1.845	-2.117	-2.441	-2.165	-1.988	-2.101	-1.846	-1.506	-1.053	-1.234	-0.731	-0.913	-1.805	-0.609	-0.683	-0.910	-0.745	-0.536	-1.109
6	2004	-1.480	-11.577	-1.581	-1.579	-1.651	-2.146	-1.965	-1.921	-2.204	-1.499	-1.631	-1.860	-1.874	-1.161	-1.174	-1.004	-1.097	-0.926	-1.147	-0.876	-0.935	-6.093	-0.623	-1.077	-0.939	-1.148
7	2004	-1.532	n/a	-1.978	-2.127	-2.161	-2.040	-1.881	-2.531	-2.048	-2.426	-2.109	-1.478	-1.995	-2.424	-3.004	-0.997	-1.915	-1.159	-1.432	-1.150	-1.227	-0.762	-1.156	-1.943	-2.687	-1.725
8	2004	n/a	-1.264	-1.973	-1.282	-1.575	-1.446	-1.837	-2.299	-2.216	-1.753	-1.573	-1.984	-1.430	-1.382	-1.169	-1.087	-0.876	-0.757	-0.724	-0.661	-0.868	-1.076	-0.489	-0.952	-0.813	-2.710
9	2004	n/a	n/a	-2.314	-2.551	-2.522	-2.410	-3.037	-2.780	-2.348	-2.302	-1.924	-1.827	-1.835	-1.406	-1.154	-1.471	-1.384	-0.805	-1.554	-0.814	-0.782	-1.205	-0.792	-1.356	-1.065	-0.825
10	2004	-1.225	-1.711	-1.511	-1.997	-2.526	-2.275	-2.283	-2.005	-2.036	-2.286	-2.216	-1.620	-1.305	-1.251	-1.207	-1.052	-0.936	-0.845	-0.906	-0.699	-0.918	-1.170	-0.813	-0.872	-0.695	-0.724
11	2004	-3.623	-2.364	-3.023	-5.050	-1.961	-2.404	-2.909	-3.389	-2.783	-2.322	-1.626	-2.240	-1.478	-1.274	-0.954	-1.036	-1.247	-0.966	-0.655	-0.672	-1.001	-1.392	-1.013	-1.518	-1.058	-0.835
12	2004	-2.935	-1.968	-1.973	-2.186	-2.480	-3.417	-2.194	-1.795	-1.768	-2.117	-1.767	-1.583	-1.451	-1.429	-1.040	-1.314	-0.830	-1.134	-0.661	-0.841	-0.859	-1.147	-0.765	-0.738	-1.805	-1.025
1	2005	-3.015	-2.954	-1.987	-4.623	-2.509	-2.896	-3.839	-2.195	-2.273	-2.361	-1.733	-1.551	-1.440	-1.527	-1.214	-1.265	-1.103	-1.181	-0.861	-1.192	-0.749	-1.196	-1.378	-1.320	-0.780	-2.515
2	2005	-1.989	-2.700	-3.787	-2.831	-3.462	-2.170	-2.913	-2.452	-2.373	-3.447	-2.666	-1.946	-2.001	-1.768	-1.306	-1.759	-1.798	-1.690	-1.228	-0.881	-0.708	-1.979	-0.828	-1.293	-1.229	-1.123
3	2005	-1.148	-2.590	-1.182	-2.142	-3.353	-2.286	-2.818	-1.970	-2.508	-2.209	-1.843	-1.939	-1.499	-1.446	-1.887	-1.914	-1.282	-0.865	-0.742	-0.648	-2.038	-1.187	-1.543	-1.147	-1.174	-1.325
4	2005	-4.368	-2.585	-5.771	-6.755	-2.334	-4.195	-3.198	-2.909	-3.998	-4.007	-2.493	-2.181	-2.258	-1.856	-1.308	-1.248	-1.309	-1.806	-1.087	-1.099	-0.804	-0.669	-0.808	-1.341	-2.056	-1.362
5	2005	-1.366	-7.208	-5.797	-3.075	-2.557	-2.628	-3.489	-1.876	-2.746	-2.006	-2.063	-1.624	-1.911	-1.754	-1.793	-1.379	-1.265	-0.988	-1.030	-1.128	-1.136	-1.007	-0.836	-0.905	-0.935	-0.706
6	2005	-1.924	-1.700	-0.953	-2.985	-2.820	-1.753	-2.427	-1.674	-2.309	-1.566	-1.639	-1.476	-1.580	-1.312	-1.122	-1.230	-0.909	-0.742	-0.753	-0.698	-0.792	-0.912	-0.723	-0.851	-0.927	-1.425
7	2005	n/a	n/a	-2.206	-16.353	-1.283	-1.625	-12.389	-1.597	-1.837	-1.900	-1.844	-1.616	-1.497	-1.838	-1.557	-0.791	-0.829	-1.048	-1.548	-0.769	-0.877	-16.975	-1.108	-0.848	-1.204	-0.988
8	2005	-3.050	-3.115	-1.692	-2.125	-1.321	-2.552	-3.042	-2.015	-1.675	-1.689	-1.846	-1.527	-1.620	-1.345	-1.361	-1.084	-0.925	-0.903	-0.710	-1.093	-0.621	-1.047	-1.382	-0.944	-0.816	-0.472
9	2005	-2.254	-2.166	-1.876	-3.654	-2.937	-3.015	-2.248	-2.988	-2.672	-2.037	-2.083	-1.862	-1.809	-1.774	-1.330	-1.188	-1.354	-0.904	-0.975	-0.774	-0.614	-0.718	-1.180	-1.293	-1.163	-0.730
10	2005	-1.439	-2.196	-1.947	-2.404	-2.546	-3.150	-3.236	-3.191	-2.784	-2.068	-1.869	-1.492	-1.586	-1.431	-1.411	-1.258	-1.124	-1.295	-0.744	-0.720	-0.803	-0.822	-0.835	-0.747	-0.652	-0.642
11	2005	-1.016	-1.714	-2.897	-3.153	-2.250	-2.707	-2.757	-2.338	-2.158	-2.314	-1.844	-2.770	-2.857	-1.912	-1.176	-1.677	-1.118	-0.806	-0.794	-0.808	-0.651	-0.905	-0.621	-1.131	-1.085	-1.115
12	2005	-2.303	-2.671	-2.269	-3.365	-3.023	-2.019	-2.382	-2.276	-2.456	-2.517	-2.125	-2.142	-2.109	-1.555	-1.424	-1.142	-1.164	-1.035	-0.984	-0.816	-0.947	-0.731	-0.726	-1.551	-0.898	-1.351

Table A. 24: Yellowknife hyperthermal chemistry slope (part 2)

Yellowknife: Ambipolar diffusion regime slope per height increment

Month	Year	75	76	77	78	79	80	81	82	83	84	85	86	87	88	89	90	91	92	93	94	95	96	97	98	99	100
		(km)	(km)	(km)	(km)	(km)	(km)	(km)	(km)	(km)	(km)	(km)	(km)	(km)	(km)	(km)	(km)	(km)	(km)	(km)	(km)	(km)	(km)	(km)	(km)	(km)	(km)
1	2006	-1.920	-2.785	-2.021	-2.503	-1.905	-3.174	-2.756	-3.090	-2.308	-2.461	-1.616	-1.895	-2.177	-1.298	-1.442	-1.594	-0.842	-0.874	-1.250	-0.957	-1.317	-1.029	-1.024	-1.048	-0.749	-0.994
2	2006	-2.177	-2.897	-4.389	-2.075	-2.020	-2.176	-2.109	-1.987	-3.210	-2.030	-2.044	-1.873	-2.101	-1.520	-1.671	-1.732	-1.198	-0.971	-2.176	-0.939	-0.920	-1.177	-1.191	-0.786	-1.648	-0.915
3	2006	-7.233	-1.835	-2.126	-2.252	-2.347	-2.550	-2.677	-3.284	-4.894	-3.033	-2.469	-2.281	-2.127	-1.710	-1.546	-1.575	-1.435	-1.358	-0.976	-1.278	-1.429	-1.725	-1.452	-0.772	-1.441	-0.995
4	2006	-1.709	-8.486	-1.708	-3.000	-4.021	-2.820	-3.715	-3.451	-2.842	-3.606	-2.614	-2.296	-2.629	-2.283	-1.891	-1.498	-1.583	-1.423	-1.355	-1.027	-1.887	-0.804	-0.710	-1.135	-0.838	-1.040
5	2006	-3.045	-2.687	-1.359	-2.000	-1.432	-3.022	-2.003	-3.183	-2.403	-2.246	-2.256	-2.247	-2.086	-2.222	-1.450	-1.519	-1.602	-1.447	-1.302	-1.293	-0.973	-0.820	-1.006	-0.773	-3.663	-0.687
6	2006	-0.850	-1.958	-1.186	-2.041	-1.817	-2.633	-1.460	-1.859	-1.676	-1.714	-1.710	-1.599	-1.633	-1.642	-1.233	-1.404	-1.274	-1.038	-0.988	-0.929	-0.676	-0.773	-0.583	-1.102	-0.663	-1.151
7	2006	n/a	-1.710	-1.718	-1.874	-3.021	-1.823	-1.525	-1.899	-1.480	-1.519	-1.773	-2.098	-1.658	-1.421	-1.641	-1.483	-1.268	-1.035	-0.723	-1.112	-0.798	-0.566	-0.531	-0.667	-0.670	-0.742
8	2006	-1.047	-1.541	-1.570	-2.245	-2.123	-2.246	-1.620	-2.351	-2.471	-2.029	-2.845	-1.535	-2.449	-1.725	-1.519	-1.167	-1.019	-1.143	-0.713	-0.553	-0.636	-0.738	-0.822	-0.815	-1.057	-0.825
9	2006	n/a	-1.153	-0.825	-0.896	-1.142	-0.964	-1.363	-1.465	-1.637	-1.583	-1.734	-1.430	-1.671	-1.409	-1.691	-1.258	-1.420	-1.490	-1.406	-0.985	-0.921	-0.873	-1.421	-0.909	-0.728	-0.601
11	2006	-1.127	-10.733	-1.450	-1.477	-2.186	-8.505	-2.155	-2.066	-2.029	-2.051	-2.369	-5.721	-1.762	-1.920	-1.877	-1.923	-1.347	-1.214	-1.252	-1.228	-1.234	-1.962	-1.835	-1.532	-1.101	-1.177
12	2006	-1.185	-1.219	-1.048	-1.987	-2.847	-2.046	-2.125	-1.858	-2.041	-1.986	-1.966	-1.956	-1.767	-1.927	-1.747	-1.558	-1.363	-1.443	-1.615	-1.123	-1.275	-1.846	-1.566	-1.387	-1.968	-1.142
1	2007	-2.776	-3.876	-2.280	-2.101	-2.849	-2.678	-2.309	-1.742	-1.759	-1.637	-1.514	-1.858	-1.562	-1.326	-1.603	-1.909	-1.468	-2.014	-1.146	-1.468	-0.988	-1.453	-0.981	-1.273	-0.719	-0.923
2	2007	-1.621	-3.080	-2.622	-1.573	-8.428	-2.587	-1.954	-2.215	-2.226	-2.316	-2.493	-1.874	-2.808	-1.435	-1.949	-2.027	-1.438	-1.771	-1.235	-1.673	-1.446	-1.818	-1.075	-0.975	-6.553	-1.423
12	2007	-6.176	-3.643	-6.713	-4.620	-3.286	-2.370	-2.489	-2.778	-2.297	-2.730	-2.244	-3.131	-2.464	-2.249	-2.700	-2.137	-2.238	-2.348	-1.845	-1.958	-1.500	-1.761	-2.461	-1.195	n/a	-8.778
4	2008	-6.349	-1.901	-9.461	-2.173	-2.257	-3.227	-3.932	-3.367	-3.018	-2.737	-2.857	-2.464	-2.327	-1.786	-1.674	-1.597	-1.384	-1.208	-0.807	-1.428	-1.074	-2.034	-1.663	-1.270	-1.090	n/a
5	2008	-1.621	-2.062	-1.100	-1.938	-3.309	-2.713	-2.595	-2.002	-1.670	-1.890	-1.546	-1.508	-1.454	-1.621	-1.221	-1.149	-1.100	-1.066	-0.899	-0.942	-0.639	-1.189	-1.199	-1.411	-0.675	-1.293
6	2008	n/a	-1.239	-1.419	-1.136	-3.372	-1.292	-1.650	-1.632	-1.420	-1.476	-1.638	-1.619	-1.285	-1.410	-1.287	-1.031	-0.914	-0.757	-0.822	-0.582	-0.495	-0.488	-0.558	-0.621	-0.439	-0.318
7	2008	-0.670	-0.994	-2.328	-1.590	-1.880	-1.250	-1.914	-1.955	-1.466	-1.727	-1.281	-1.674	-1.455	-1.238	-1.290	-1.312	-1.036	-0.697	-0.574	-0.747	-0.726	-0.633	-0.571	-0.533	-0.684	-0.729
8	2008	-1.365	-1.251	-1.189	-1.581	-1.981	-2.049	-1.911	-2.236	-1.555	-1.669	-1.502	-1.707	-1.492	-1.400	-1.267	-1.115	-1.069	-0.863	-0.665	-0.588	-0.536	-0.675	-0.614	-0.943	-0.595	-0.713
9	2008	-2.475	-2.046	-1.947	-2.211	-3.384	-2.867	-2.755	-2.689	-2.920	-2.242	-1.929	-1.757	-1.789	-1.402	-1.349	-1.051	-0.929	-1.011	-0.696	-0.843	-0.977	-0.646	-1.141	-0.859	-0.747	-1.143
10	2008	-2.649	-2.354	-2.269	-2.188	-3.698	-2.934	-2.873	-3.309	-2.619	-2.435	-2.264	-1.849	-1.483	-1.355	-1.025	-1.262	-1.130	-0.971	-0.739	-0.686	-0.787	-0.652	-0.881	-0.860	-0.674	-1.477
11	2008	-1.606	-1.084	-2.144	-1.828	-2.669	-2.716	-1.928	-2.081	-2.056	-2.089	-1.624	-1.455	-1.390	-1.523	-1.012	-1.277	-1.412	-0.925	-1.016	-0.796	-0.578	-1.023	-0.907	-1.200	-0.852	-0.675
12	2008	-1.867	-2.311	-1.812	-3.620	-4.091	-2.185	-2.320	-2.487	-2.356	-1.855	-1.849	-1.705	-1.343	-1.364	-1.260	-1.040	-1.096	-1.098	-0.894	-0.809	-0.764	-0.944	-0.659	-1.048	-0.666	-1.380
1	2009	-3.679	-1.905	-2.531	-2.524	-2.909	-2.140	-2.433	-1.791	-2.144	-2.275	-2.021	-1.687	-1.688	-1.267	-1.194	-1.240	-1.077	-1.077	-0.700	-0.877	-0.678	-0.830	-0.997	-0.836	-0.870	-0.923
2	2009	-2.641	-1.645	-1.867	-2.911	-2.834	-4.354	-3.289	-2.473	-1.811	-2.857	-2.409	-2.004	-1.891	-1.330	-1.296	-1.500	-1.136	-0.856	-0.941	-1.407	-0.786	-1.009	-1.418	-0.653	-1.289	-0.853
3	2009	-3.401	-2.928	-3.251	-2.818	-2.317	-2.360	-3.574	-3.287	-2.254	-2.580	-2.208	-1.914	-1.622	-1.588	-1.413	-1.228	-1.192	-1.094	-0.847	-0.838	-0.894	-0.831	-0.807	-1.034	-0.953	-0.709
4	2009	n/a	-3.237	-9.316	-3.004	-2.290	-3.204	-4.476	-3.493	-3.283	-3.541	-2.222	-2.164	-2.385	-1.636	-1.628	-1.632	-1.558	-1.457	-0.940	-0.995	-0.986	-0.844	-0.964	-1.256	-0.822	-1.034
5	2009	-1.622	-5.102	-2.256	-1.594	-2.070	-2.179	-1.694	-2.222	-1.920	-1.789	-1.886	-1.626	-1.502	-1.557	-1.530	-1.165	-1.007	-0.865	-0.796	-0.892	-1.066	-0.718	-1.007	-1.377	-1.168	-1.311
6	2009	-1.013	-20.100	-3.952	-1.621	-1.845	-1.542	-1.546	-1.462	-1.447	-1.174	-1.352	-1.576	-1.427	-1.152	-1.208	-1.249	-1.116	-0.617	-0.886	-0.893	-0.518	-0.558	-0.852	-0.995	-1.072	-0.441
7	2009	-2.002	-2.312	-1.896	-1.381	-1.073	-2.253	-1.714	-1.688	-1.538	-1.870	-1.429	-1.333	-1.568	-1.444	-1.193	-1.119	-0.924	-0.771	-0.751	-0.831	-0.601	-0.906	-0.854	-0.861	-0.547	-0.638
8	2009	-1.440	-15.526	-2.520	-1.888	-2.378	-2.030	-1.774	-1.690	-1.678	-1.584	-1.461	-1.767	-1.515	-1.491	-1.340	-1.012	-0.870	-0.786	-0.583	-0.659	-0.615	-0.667	-0.535	-0.520	-0.694	-0.591
9	2009	-3.282	-1.782	-1.497	-2.528	-3.260	-2.501	-2.294	-3.046	-1.966	-2.179	-2.109	-1.762	-2.035	-1.653	-1.437	-1.207	-0.992	-1.100	-0.792	-0.943	-0.789	-1.038	-0.762	-0.859	-1.485	-0.861
10	2009	-1.947	-2.139	-1.564	-3.126	-2.483	-3.144	-3.074	-2.431	-2.177	-1.931	-1.849	-1.859	-1.792	-1.636	-1.659	-1.119	-0.994	-1.027	-0.961	-0.740	-0.847	-1.113	-0.894	-1.152	-0.706	-0.666
11	2009	-1.737	-1.563	-2.242	-2.141	-1.764	-2.291	-2.668	-2.038	-1.893	-2.156	-1.799	-1.693	-1.285	-1.171	-1.103	-1.189	-0.982	-0.883	-0.895	-0.677	-0.592	-0.648	-0.714	-0.657	-0.635	-0.533
12	2009	-1.284	-1.624	-1.118	-6.601	-1.768	-2.475	-1.221	-2.373	-1.825	-1.151	-1.373	-1.498	-1.608	-1.062	-1.564	-0.967	-0.810	-1.130	-2.068	-0.903	-0.703	-0.725	-0.781	-1.843	-0.846	n/a

Table A.25: CLOVAR hyperthermal chemistry diffusion coefficient

CLOVAR: Hyperthermal chemistry diffusion coefficient per height increment

Month	Year	75	76	77	78	79	80	81	82	83	84	85	86	87	88	89	90	91	92	93	94	95	96	97	98	99	100
		(km)	(km)	(km)	(km)	(km)	(km)	(km)	(km)	(km)	(km)	(km)	(km)	(km)	(km)	(km)	(km)	(km)	(km)	(km)	(km)	(km)	(km)	(km)	(km)	(km)	(km)
7	2000	3.324	31.806	0.944	4.663	4.519	3.981	3.665	6.481	8.389	10.247	10.842	8.326	4.898	6.745	5.326	7.200	3.960	5.987	4.411	5.376	7.228	13.334	11.033	14.954	21.992	47.155
8	2000	0.396	0.587	1.750	5.115	2.310	7.750	14.245	26.062	8.155	7.597	8.225	23.185	6.117	6.621	7.113	5.807	7.877	4.371	7.946	5.660	10.157	7.725	16.241	11.167	13.539	13.995
9	2000	2.851	0.597	0.968	3.125	2.389	7.521	4.974	5.589	8.517	20.331	6.850	8.209	14.880	12.975	4.919	6.865	5.566	4.673	5.434	6.741	8.436	11.679	10.256	26.783	33.171	23.250
10	2000	1.904	1.735	1.765	2.102	4.730	7.295	10.252	13.409	9.270	12.778	7.060	6.416	11.780	3.415	6.953	3.552	4.958	6.146	4.514	6.775	7.410	8.671	9.076	9.454	26.753	15.052
11	2000	5.389	0.848	1.922	1.903	2.647	5.014	5.173	13.653	6.439	5.081	24.393	7.178	6.366	5.887	7.929	5.622	4.257	6.774	6.149	7.324	6.455	8.974	9.680	11.019	16.225	14.432
12	2000	1.459	0.782	0.591	4.542	3.319	5.215	3.840	14.526	7.585	5.360	4.240	3.547	25.463	21.590	27.261	11.021	11.041	15.770	4.392	7.485	7.755	16.324	14.594	14.571	24.396	19.667
1	2001	1.096	3.476	1.915	1.385	5.046	2.152	6.159	8.364	17.775	43.349	11.983	28.858	10.051	14.426	9.821	3.576	3.241	7.572	7.450	8.142	14.328	11.187	10.302	19.540	26.295	25.054
11	2001	1.949	1.004	1.877	6.768	42.534	11.248	12.095	13.972	18.776	36.073	36.354	8.313	6.796	30.406	21.349	3.818	15.535	5.072	7.795	7.627	10.834	6.998	14.554	17.838	19.621	19.357
12	2001	0.463	1.119	1.162	1.840	10.596	8.530	20.572	8.559	6.889	26.362	16.165	35.328	20.346	6.309	4.452	6.790	8.167	4.994	4.733	5.906	8.440	9.274	10.107	12.069	17.778	74.830
1	2002	1.149	1.277	2.186	7.761	35.116	10.960	13.733	10.834	12.137	11.334	19.933	29.063	12.243	6.101	7.753	6.576	4.480	4.660	6.405	6.550	19.343	12.414	9.115	11.340	20.914	17.594
2	2002	1.432	0.761	16.060	29.238	3.263	21.896	18.942	27.713	44.313	18.214	28.386	32.519	8.028	10.537	14.444	15.227	23.118	5.312	5.600	13.171	10.397	22.058	8.687	21.174	14.765	17.428
3	2002	1.052	2.560	2.826	24.011	3.760	18.268	5.229	68.520	26.365	16.927	23.636	16.711	12.985	24.150	12.605	6.069	21.413	10.895	6.934	5.063	10.805	11.272	9.157	9.673	21.482	16.998
4	2002	4.545	0.830	1.615	2.063	14.013	4.669	19.136	27.772	16.861	29.072	21.806	36.181	24.322	8.146	6.226	7.348	5.348	6.372	5.507	10.087	10.364	15.943	8.110	12.760	14.166	28.007
5	2002	0.764	–	1.078	0.867	1.176	3.144	50.434	23.786	17.698	19.333	8.158	7.045	7.283	6.715	4.490	25.810	4.035	8.164	6.024	17.512	11.821	12.289	9.893	11.385	40.416	14.398
6	2002	0.634	1.442	0.787	1.100	2.382	9.580	5.224	8.765	4.384	16.798	18.306	11.178	24.406	8.766	10.170	11.273	9.976	4.161	8.140	9.761	8.311	8.814	8.111	14.216	17.435	123.495
7	2002	0.430	2.801	2.045	1.625	3.897	2.621	3.106	5.427	14.767	6.845	10.316	24.669	10.405	7.993	11.099	11.832	6.758	4.005	12.599	5.706	11.327	8.762	9.798	14.689	55.309	24.904
8	2002	1.705	0.490	1.909	5.086	3.663	4.620	14.837	17.881	17.544	28.972	10.986	9.160	24.206	9.815	9.275	5.229	7.141	9.592	8.737	7.088	8.218	11.791	19.645	15.870	22.918	25.458
9	2002	0.530	2.202	34.851	1.097	3.053	4.729	13.653	38.170	9.372	30.327	52.053	37.975	29.987	6.962	7.962	21.262	5.256	12.075	7.220	9.488	7.746	13.170	22.756	13.919	23.380	19.926
10	2002	–	4.240	1.006	3.266	8.514	10.421	21.809	31.874	28.870	215.831	11.377	32.924	58.519	33.491	8.483	7.195	14.218	5.038	8.635	10.087	9.685	7.812	8.704	40.338	17.948	28.200
11	2002	0.930	1.289	11.125	2.163	9.064	40.609	13.058	15.201	12.865	15.361	15.221	15.601	8.755	29.478	17.170	7.955	5.894	10.383	6.420	5.458	6.115	7.452	8.334	22.611	18.279	17.142
12	2002	9.469	16.362	1.863	2.681	7.600	14.914	20.463	22.029	18.060	32.246	22.911	46.027	6.281	12.498	22.365	4.089	8.931	5.160	6.977	9.834	14.291	9.421	15.899	9.960	18.365	24.105
1	2003	1.224	1.560	6.196	6.347	5.768	42.439	6.783	16.715	21.297	26.929	22.747	22.114	21.667	5.624	8.874	5.516	16.287	12.493	6.114	14.825	8.660	10.788	9.478	9.731	12.316	29.244
2	2003	0.673	1.632	3.130	2.650	12.473	15.987	27.299	17.362	20.616	25.573	31.724	21.085	51.257	12.272	9.573	22.248	11.475	9.054	12.347	15.926	16.216	8.006	12.702	24.726	107.288	56.413
3	2003	4.237	5.078	1.765	12.127	4.490	55.181	73.355	48.733	38.004	29.524	114.392	16.144	36.175	11.878	14.701	5.618	6.536	9.832	7.841	6.530	14.489	7.877	9.438	19.131	12.993	15.140
4	2003	3.089	2.904	2.236	0.896	10.682	5.150	17.428	44.422	36.957	28.953	23.929	35.123	22.347	50.757	25.374	6.025	5.429	9.153	4.993	12.834	8.202	9.469	17.958	12.576	20.395	21.160
5	2003	4.530	2.730	0.966	0.941	5.350	5.294	6.751	9.832	12.275	12.797	10.391	19.152	20.242	11.442	6.712	3.870	4.660	3.968	9.344	7.639	14.022	12.275	14.032	14.839	16.961	20.011
6	2003	0.330	0.693	1.135	0.718	7.053	1.858	4.887	3.161	12.158	7.637	20.574	19.846	6.379	7.465	5.043	4.325	3.940	5.464	4.647	6.914	8.612	11.554	8.973	9.343	15.675	15.938
7	2003	2.074	1.029	1.066	0.770	2.968	1.721	2.510	5.670	10.770	7.220	12.116	20.359	6.017	7.510	14.284	4.832	4.546	3.838	5.205	6.271	7.541	10.885	8.275	10.925	16.990	19.963
8	2003	0.383	0.762	1.966	3.712	2.015	8.306	4.632	23.012	10.306	9.295	28.011	9.322	9.442	15.296	5.040	5.637	3.906	4.414	5.830	6.135	6.051	11.695	9.155	10.864	14.196	31.403
9	2003	2.046	0.843	1.638	13.578	6.429	16.442	18.038	20.229	16.420	13.954	26.907	20.557	9.327	35.437	5.503	5.202	8.327	8.120	5.587	9.956	7.689	12.176	10.835	9.909	12.207	53.694
10	2003	–	14.317	3.582	2.974	3.696	60.733	63.845	340.998	34.135	181.186	43.328	28.729	27.855	7.264	19.901	5.200	7.453	4.796	7.645	9.550	9.641	9.568	11.825	25.572	11.875	18.958
12	2007	4.508	3.889	9.093	1.041	5.005	20.075	15.754	44.195	5.664	27.956	5.054	6.400	26.099	18.353	7.202	6.331	6.397	7.001	13.712	10.295	13.348	7.175	18.855	207.505	16.470	39.605
1	2008	0.613	–	–	–	4.033	4.039	24.729	3.373	21.075	24.545	2.780	3.858	13.449	57.262	3.289	5.047	5.509	110.227	6.076	20.811	11.672	11.337	190.876	14.250	22.262	131.349
2	2008	–	2.076	6.899	8.486	21.567	8.432	22.182	26.295	27.994	9.976	18.086	6.153	44.806	9.840	5.861	26.723	49.902	9.454	16.088	11.520	13.161	13.410	52.703	11.278	23.671	16.182
3	2008	4.359	1.094	1.652	10.205	13.963	14.027	12.976	81.401	145.190	6.980	69.661	5.651	11.891	10.796	15.334	11.906	7.670	7.339	7.823	5.688	10.881	10.239	21.338	26.610	51.026	14.082
4	2008	5.512	5.798	3.144	4.591	24.442	15.764	7.358	25.862	12.109	109.782	31.376	62.306	19.620	5.917	7.580	4.998	4.514	9.156	6.083	10.116	18.295	7.675	20.403	37.612	18.218	16.689
9	2008	0.469	2.329	0.890	14.088	2.008	7.007	12.933	7.510	19.123	49.230	10.646	8.654	18.192	5.828	7.610	7.135	6.105	8.114	10.322	12.713	16.222	9.246	18.873	9.941	13.513	21.368
10	2008	2.656	0.873	1.253	1.543	36.908	7.366	23.106	11.049	15.747	31.201	5.831	17.711	7.147	11.419	5.333	3.241	4.716	5.958	4.863	7.236	6.264	7.325	12.415	9.856	30.809	28.990

Table A.26: Costa Rica hyperthermal chemistry diffusion coefficient

Costa Rica: Hyperthermal chemistry diffusion coefficient per height increment

Month	Year	75	76	77	78	79	80	81	82	83	84	85	86	87	88	89	90	91	92	93	94	95	96	97	98	99	100
		(km)	(km)	(km)	(km)	(km)	(km)	(km)	(km)	(km)	(km)	(km)	(km)	(km)	(km)	(km)	(km)	(km)	(km)	(km)	(km)	(km)	(km)	(km)	(km)	(km)	(km)
4	2005	2.008	6.530	13.591	4.912	11.265	18.396	13.999	13.799	25.020	22.835	36.897	37.790	35.051	21.055	22.690	19.257	34.326	9.376	10.441	11.434	25.769	8.031	12.214	26.500	19.061	19.394
5	2005	5.417	13.137	13.609	11.615	6.770	15.308	21.478	24.459	46.110	31.475	30.505	30.438	28.839	24.495	20.881	38.236	14.863	13.393	10.622	9.121	8.667	12.855	11.406	11.266	19.406	18.614
6	2005	2.879	7.007	2.774	10.022	11.002	29.050	16.740	27.773	20.512	36.122	26.782	28.431	32.165	32.465	24.264	20.558	17.936	18.168	13.470	10.572	13.907	10.303	15.635	74.907	21.435	32.525
7	2005	1.664	3.395	4.172	5.909	7.092	10.699	7.503	9.965	9.454	40.259	22.873	17.781	22.124	22.815	26.771	30.905	17.338	18.938	17.353	12.798	9.798	12.546	10.173	13.868	26.928	25.730
8	2005	1.540	4.276	5.493	2.245	3.930	6.615	7.495	11.727	20.115	18.754	15.391	20.113	33.007	18.331	20.566	24.340	27.648	14.014	24.433	7.254	19.366	8.819	12.818	14.170	14.248	15.561
9	2005	0.705	1.690	4.879	9.309	2.499	8.455	7.791	13.151	14.983	23.009	18.782	21.148	20.862	26.780	24.259	17.457	15.871	11.790	23.663	6.651	9.836	9.778	11.248	13.338	64.218	19.709
10	2005	0.764	2.383	1.839	5.922	8.743	10.151	13.528	18.711	21.448	28.752	20.624	26.966	26.450	21.628	30.153	16.812	23.661	15.900	11.152	8.960	9.140	9.697	10.554	11.455	14.956	59.845
11	2005	3.320	2.912	5.053	6.587	17.419	21.399	48.232	22.251	8.505	7.362	25.308	12.975	27.640	21.402	56.706	35.965	25.889	8.332	28.883	20.300	18.540	14.445	10.107	21.055	55.983	15.241
12	2005	0.509	14.116	8.205	3.561	8.350	36.397	13.464	10.626	11.545	23.889	21.363	30.884	21.774	21.093	13.741	20.922	17.627	13.057	10.978	15.477	12.054	11.140	8.984	11.020	13.429	17.755
1	2006	1.305	0.941	1.792	4.615	2.644	8.611	6.067	11.816	12.390	20.464	34.852	35.363	22.936	18.974	15.167	11.791	15.321	7.769	9.097	6.742	7.676	7.722	8.466	9.445	11.420	17.823
4	2007	2.968	3.832	8.676	16.842	29.927	16.215	36.078	64.689	35.987	39.456	55.074	25.913	47.227	40.593	13.962	25.246	10.946	38.650	19.711	12.149	6.975	16.886	17.819	20.211	19.066	15.735
5	2007	5.347	4.880	6.585	8.839	7.372	16.137	14.494	37.918	29.333	28.497	45.109	41.626	37.417	21.372	28.823	17.496	12.340	10.668	8.529	12.983	8.805	7.664	14.342	11.455	19.981	33.594
6	2007	2.327	4.033	7.407	9.235	29.280	35.493	23.463	25.736	40.990	30.707	25.612	40.669	25.495	25.445	19.078	20.192	11.206	11.951	8.512	14.943	7.549	9.821	12.218	22.276	31.202	20.128
7	2007	11.974	2.916	5.295	5.186	13.507	11.665	14.148	25.055	22.560	19.736	22.261	25.320	35.943	25.195	16.557	15.864	13.190	10.656	10.053	16.356	11.403	11.046	11.248	15.008	21.405	26.689
8	2007	5.711	31.334	8.815	11.123	21.141	22.585	31.266	40.170	26.192	56.887	52.489	22.907	22.992	20.595	17.597	19.154	27.346	11.104	9.120	24.334	10.389	33.774	11.117	23.085	26.538	32.740
9	2007	2.883	2.235	13.304	25.270	12.847	13.526	25.805	16.126	43.720	34.573	32.016	37.208	29.571	35.079	20.584	20.509	15.880	9.717	14.044	10.082	17.680	16.051	9.312	18.145	45.145	50.461
10	2007	2.105	33.593	12.778	11.406	27.193	18.643	22.112	20.274	39.395	56.242	55.243	37.298	35.873	33.317	20.756	14.261	9.898	9.392	6.791	7.450	6.536	7.168	21.349	17.899	13.182	30.288
11	2007	2.192	53.268	23.751	15.140	17.627	41.140	14.734	111.643	19.624	51.652	56.496	74.622	52.357	23.277	30.564	7.893	29.469	6.763	4.489	6.021	9.252	14.270	10.625	16.945	14.990	47.755
12	2007	0.533	3.171	13.399	8.192	8.562	14.472	9.903	24.438	12.335	33.486	18.554	14.867	12.888	9.381	6.278	10.483	5.513	4.443	4.418	5.172	6.154	7.370	8.668	9.890	12.210	14.047
1	2008	3.280	44.528	3.968	4.693	6.733	19.872	11.366	16.962	15.076	52.197	33.476	21.195	20.761	11.316	13.204	12.911	6.713	8.218	6.521	5.723	6.795	7.171	10.219	9.497	13.516	14.006
2	2008	1.703	1.732	7.115	21.092	7.453	7.519	14.360	11.692	64.551	18.340	12.230	18.986	28.636	20.273	15.680	16.277	10.552	8.409	7.009	12.432	7.163	6.979	8.367	11.863	49.434	19.564
3	2008	12.703	6.182	27.098	6.154	24.925	29.692	34.737	37.102	21.103	53.787	28.163	31.071	50.255	21.418	18.406	11.976	11.068	19.569	13.968	9.102	10.795	9.362	12.067	12.483	17.339	26.039
4	2008	9.010	5.432	5.919	12.362	16.904	15.720	19.935	21.737	20.891	26.943	37.887	36.760	22.351	17.791	16.941	15.308	10.935	13.155	10.274	9.405	11.976	10.273	10.290	16.115	19.759	57.947
5	2008	4.282	4.473	4.541	14.680	31.078	22.363	35.859	30.621	17.879	30.554	28.631	23.348	24.054	19.025	17.003	34.218	10.208	14.895	9.149	9.374	10.529	9.999	24.729	17.409	39.587	36.068
6	2008	10.162	9.864	6.831	10.130	17.273	16.380	18.385	22.398	27.350	38.341	64.484	42.354	29.411	24.037	30.197	14.435	17.771	10.585	6.689	10.737	7.988	15.546	11.629	11.751	15.225	35.370
7	2008	6.166	13.032	11.846	5.832	17.765	22.769	17.390	24.768	27.872	28.141	45.753	20.164	20.132	26.805	17.999	24.557	15.535	14.770	13.638	10.469	8.057	10.631	14.513	16.813	31.007	40.628
8	2008	1.111	8.175	2.354	16.136	12.794	9.266	17.710	20.624	27.930	30.047	15.999	29.922	20.541	32.568	28.819	6.575	16.649	10.652	35.705	14.788	12.151	27.927	14.853	14.405	17.338	26.506
9	2008	0.853	3.064	6.230	14.290	10.506	27.065	22.674	16.989	38.043	25.457	48.878	36.246	32.724	29.607	30.307	15.910	12.173	11.045	11.180	7.528	9.980	14.207	8.788	15.949	14.495	20.054
10	2008	5.353	3.168	3.327	17.744	8.340	6.446	18.400	30.364	21.360	36.818	39.918	30.723	21.060	34.066	20.591	20.165	6.944	25.638	8.391	8.219	7.700	19.191	9.145	25.293	23.108	17.150
11	2008	1.284	12.032	5.459	13.178	21.779	7.775	10.958	30.717	10.333	21.940	16.574	52.324	46.405	12.524	46.251	15.826	9.147	12.023	13.924	5.703	11.569	12.641	18.386	14.909	19.788	22.943
3	2009	3.005	2.716	5.722	6.169	8.728	7.393	6.915	70.304	18.822	14.319	15.963	24.756	29.026	19.969	117.389	28.639	46.526	42.461	8.655	8.003	8.999	11.316	9.429	51.471	73.803	31.399
10	2009	2.384	4.239	2.555	9.307	11.142	17.562	26.947	36.474	20.067	26.403	28.057	49.579	46.346	24.693	13.125	22.324	12.990	12.220	9.390	10.048	9.305	11.403	11.282	23.388	19.120	20.264
1	2010	–	–	–	–	15.785	–	–	36.650	3.634	–	83.937	24.135	88.217	134.111	57.527	22.606	40.754	700.740	25.539	29.553	77.924	330.888	391.862	34.087	147.052	–
2	2010	–	7.450	3.097	3.014	36.284	15.749	20.534	57.951	29.670	43.644	22.526	34.788	31.418	36.522	35.783	34.713	12.317	18.370	21.579	20.585	26.338	53.446	18.855	27.283	45.646	57.640
3	2010	1.369	0.846	5.177	7.392	4.946	9.608	23.057	41.610	30.082	41.700	63.145	38.531	29.187	30.873	24.894	28.423	20.661	15.095	12.027	10.900	9.827	24.760	13.763	21.585	14.088	15.306
4	2010	1.023	5.959	1.808	2.972	6.623	7.164	12.681	19.489	25.747	27.404	33.071	30.674	35.201	38.372	34.119	31.841	19.157	27.153	20.142	16.840	26.380	14.102	24.177	16.232	21.448	95.888
6	2010	1.536	4.260	7.058	15.576	4.673	11.684	20.079	23.307	13.214	36.555	29.645	46.279	27.556	42.565	29.693	23.044	18.092	15.168	16.557	13.255	14.780	24.709	22.186	15.666	19.357	31.607
7	2010	3.006	6.207	22.140	2.528	3.993	3.286	9.746	28.020	15.675	22.498	19.821	28.271	24.858	36.842	29.874	27.900	31.267	39.860	16.047	40.070	16.711	21.220	20.224	27.629	31.639	18.619
8	2010	3.014	13.511	7.362	4.142	6.350	4.830	10.604	10.964	14.594	17.502	22.595	36.882	20.222	29.261	33.022	24.420	16.779	15.806	12.708	17.811	17.347	25.072	11.078	22.316	25.819	21.523
9	2010	1.916	4.581	1.609	6.081	6.153	8.016	14.925	14.872	25.830	18.785	22.261	22.573	36.748	30.083	20.298	31.148	17.970	17.426	16.055	12.915	14.598	10.668	13.454	17.211	19.196	29.957
10	2010	5.844	3.061	1.739	4.643	8.080	9.411	28.218	14.332	24.401	32.075	25.834	31.294	48.510	40.439	24.646	26.724	37.937	28.820	15.165	21.279	18.999	18.917	19.022	16.766	28.151	24.383
11	2010	14.953	40.971	1.655	17.295	11.696	10.483	15.904	51.032	28.807	33.507	47.694	40.531	42.247	29.010	29.155	40.447	25.744	15.075	33.190	14.250	112.623	8.957	39.623	10.293	66.879	52.600

Table A.27: Resolute Bay hyperthermal chemistry diffusion coefficient (part 1)

Resolute Bay: Hyperthermal chemistry diffusion coefficient per height increment

Year	75	76	77	78	79	80	81	82	83	84	85	86	87	88	89	90	91	92	93	94	95	96	97	98	99	100
	(km)	(km)	(km)	(km)	(km)	(km)	(km)	(km)	(km)	(km)	(km)	(km)	(km)	(km)	(km)	(km)	(km)	(km)	(km)	(km)	(km)	(km)	(km)	(km)	(km)	(km)
2000	--	--	5.968	2.078	15.397	3.679	4.794	7.426	7.922	11.172	10.306	11.485	17.144	10.122	12.088	9.989	10.032	15.689	8.562	8.274	13.454	21.544	21.443	15.531	28.416	21.924
2000	--	--	5.152	3.212	4.482	4.237	6.039	6.597	10.079	10.908	10.411	8.424	8.702	8.678	9.069	9.438	9.897	7.693	8.038	10.212	16.199	13.625	17.539	20.902	22.696	33.846
2000	--	--	7.477	5.414	5.012	8.469	8.275	6.167	6.726	9.604	7.646	6.728	6.377	5.831	4.809	4.548	5.711	5.361	6.168	6.982	10.241	8.532	9.727	12.084	12.753	14.704
2000	--	--	5.846	6.332	6.433	5.504	7.579	5.921	5.800	5.887	5.487	4.868	5.524	3.856	3.321	3.625	3.851	4.053	4.626	5.761	6.541	8.149	8.550	11.524	12.314	15.358
2000	--	--	3.549	4.155	5.133	4.876	5.892	6.924	3.984	4.284	4.349	4.001	2.871	4.072	4.488	2.989	4.885	4.098	5.507	5.541	7.234	10.908	9.983	11.039	12.146	19.753
2000	--	--	2.837	1.578	5.037	3.281	3.331	4.491	2.663	5.179	2.435	2.804	2.956	4.240	4.030	4.035	5.086	4.950	4.616	6.916	7.417	8.281	12.935	9.679	18.549	93.705
2000	--	--	3.319	5.798	7.337	5.878	3.993	4.182	3.100	3.926	3.446	2.751	3.061	2.600	3.063	3.297	3.381	3.978	5.420	5.479	7.354	7.802	9.377	9.369	14.359	19.047
2001	1.096	3.476	2.203	5.030	4.194	5.957	7.059	7.307	6.051	8.127	7.965	11.239	7.234	7.052	7.717	8.072	6.732	7.861	14.390	10.690	13.939	12.201	14.943	20.384	17.774	33.100
2001	--	--	3.589	3.580	2.847	3.185	4.006	4.536	3.408	3.257	3.698	3.156	3.340	3.610	3.056	4.351	4.470	4.403	5.018	6.324	7.546	11.766	17.011	18.084	20.427	24.728
2001	--	--	4.886	4.506	6.402	4.600	6.953	5.118	4.934	4.241	3.725	4.216	4.132	3.413	3.631	3.886	4.047	5.626	9.406	7.205	8.696	14.016	16.479	31.247	27.580	
2001	--	--	3.054	3.000	4.082	5.102	3.329	4.482	7.559	6.147	5.370	5.055	6.111	6.365	7.565	5.377	5.983	6.414	7.238	9.022	13.182	12.231	14.968	19.816	36.414	28.026
2001	--	--	2.957	3.172	3.395	5.307	6.726	6.771	8.245	10.254	10.308	9.091	9.493	8.308	6.835	9.856	7.422	8.140	9.572	12.309	16.491	16.684	24.547	27.948	44.553	29.914
2001	--	--	2.307	4.321	4.343	4.328	4.416	4.186	7.565	8.899	8.695	10.381	7.961	9.245	7.481	7.018	9.944	8.821	10.895	15.394	13.502	14.938	16.728	28.814	35.586	40.944
2001	--	--	2.168	2.732	2.910	3.421	3.532	4.170	4.841	6.227	6.926	6.620	7.520	7.617	7.121	7.827	8.901	9.799	11.173	12.271	12.745	15.963	20.620	21.383	31.948	36.016
2001	--	--	2.922	3.121	4.236	4.624	5.161	4.650	5.776	7.282	6.478	6.587	6.723	7.397	6.596	5.646	5.680	5.695	6.588	8.409	9.315	9.497	11.236	13.575	15.390	23.677
2001	--	--	4.721	4.520	5.513	5.993	7.109	5.847	7.562	6.067	5.588	5.459	4.655	3.865	4.102	3.860	4.118	4.379	5.605	5.645	6.796	7.771	11.609	11.456	12.230	15.678
2001	--	--	3.910	4.053	4.644	6.463	4.948	5.443	5.106	6.449	4.211	3.982	3.901	3.188	3.498	3.487	3.197	4.557	4.852	5.221	6.134	7.115	8.115	9.652	11.448	12.842
2001	4.064	3.808	6.343	5.727	6.789	6.791	6.984	6.929	4.914	5.017	5.532	2.777	3.593	2.593	2.722	3.172	3.593	3.756	4.443	5.288	6.320	7.285	8.429	11.305	11.398	14.674
2001	3.001	5.062	3.979	6.478	9.424	5.166	4.462	4.307	4.453	3.626	3.668	3.274	2.762	2.932	3.170	3.144	3.901	3.952	4.581	6.129	5.824	7.857	8.782	10.495	12.577	13.532
2002	3.708	6.095	6.870	4.960	4.945	4.531	3.613	3.686	3.232	4.038	2.833	3.463	2.718	2.903	2.899	3.171	3.778	4.222	4.976	5.749	6.316	7.221	9.889	10.940	12.547	13.561
2002	5.915	6.982	8.013	6.240	7.970	6.680	8.668	7.264	7.230	6.579	4.422	5.528	3.967	4.750	3.427	3.357	3.861	4.770	4.638	6.118	6.092	7.233	11.892	12.022	14.337	15.181
2002	5.829	4.333	10.044	9.577	14.318	11.513	20.132	8.279	10.707	10.269	8.751	6.973	5.826	4.992	5.534	4.729	4.094	5.214	5.424	5.748	8.486	8.611	9.378	11.535	12.492	13.064
2002	5.513	12.267	19.675	13.773	15.205	21.062	18.366	15.775	18.007	17.415	17.317	13.236	13.514	10.113	9.335	7.935	7.872	7.292	7.906	8.146	8.947	11.823	11.812	14.845	18.530	18.604
2002	3.294	5.600	6.132	7.060	12.711	13.009	14.465	21.692	22.252	17.032	13.495	14.706	9.819	6.672	7.868	7.461	7.286	6.188	6.593	7.363	7.944	10.072	10.836	12.853	12.148	19.853
2002	2.305	5.280	5.223	7.108	6.820	8.677	8.754	9.907	9.445	11.110	13.038	12.585	19.181	10.676	10.485	7.536	7.951	6.970	8.203	8.955	9.898	11.440	13.091	12.099	15.610	15.297
2003	3.113	7.265	7.505	7.835	8.028	7.990	9.061	15.741	6.588	11.582	6.267	4.927	4.346	4.271	3.689	3.809	4.802	4.837	6.814	6.116	7.950	10.156	9.004	13.735	11.082	15.569
2003	4.553	6.677	13.474	6.654	10.681	13.031	17.642	16.275	14.766	16.803	15.002	9.261	10.716	8.975	7.493	6.507	7.448	6.331	7.735	8.821	8.142	11.879	11.003	11.548	15.740	16.627
2003	4.157	4.764	7.821	9.344	9.599	11.596	12.455	12.991	13.188	14.897	14.445	14.183	14.806	10.013	8.707	7.627	6.358	6.949	8.153	8.125	9.083	9.719	15.050	16.720	13.546	17.485
2003	1.511	2.485	2.470	7.772	2.939	4.669	4.585	9.776	9.426	10.739	12.212	10.347	9.374	7.186	7.309	6.095	6.018	8.971	9.640	11.533	16.355	11.128	13.710	20.076	74.568	29.704
2004	--	--	8.428	6.623	8.476	7.313	7.096	10.463	8.465	9.551	9.608	12.468	13.931	20.086	9.149	6.915	8.891	6.679	8.087	12.479	12.345	12.895	16.178	19.931	14.772	31.638
2004	--	--	4.677	5.067	7.809	6.431	6.928	9.176	6.853	8.671	9.414	9.412	10.938	6.900	9.237	6.360	5.245	6.034	5.918	6.887	10.339	8.345	11.635	11.893	15.258	16.202
2004	--	--	5.926	6.817	9.541	8.254	10.171	9.302	9.533	7.850	7.093	7.146	6.096	5.382	4.680	4.455	3.698	4.072	4.580	5.718	6.470	7.288	8.640	10.962	11.036	14.579
2004	--	--	4.200	7.506	3.262	3.399	2.705	4.105	3.990	3.874	3.494	1.996	4.236	2.851	2.793	3.389	4.163	7.119	5.106	6.443	6.433	7.524	12.035	23.994	14.701	18.757
2004	--	--	5.510	5.018	5.212	6.987	5.759	4.300	4.935	4.552	3.842	3.397	4.416	3.454	3.329	3.143	4.578	4.316	5.083	5.309	6.099	7.047	9.623	10.908	11.297	13.799
2005	--	--	3.501	4.487	4.767	4.801	4.352	4.853	6.292	5.289	3.658	3.874	4.141	3.327	4.397	3.569	3.638	5.293	4.373	5.107	6.623	9.652	9.797	12.600	12.602	15.236
2005	--	--	4.278	5.434	6.219	7.007	12.263	8.447	10.421	7.985	7.705	8.429	6.532	7.416	5.092	5.271	4.963	5.271	5.453	7.350	6.376	8.629	9.249	13.742	10.968	15.441
2005	--	--	6.889	7.056	6.980	9.352	7.860	11.095	7.898	10.575	8.368	9.754	6.776	5.889	5.352	5.526	7.822	5.749	6.514	7.834	9.414	7.506	9.851	14.134	12.894	24.041
2005	--	--	6.501	7.031	26.932	17.053	15.202	14.388	20.409	15.453	14.289	16.504	10.742	10.084	10.240	6.486	6.387	7.561	5.863	6.826	7.707	11.127	11.860	14.190	12.689	19.939
2005	--	--	7.875	15.683	4.266	8.259	14.455	23.680	9.376	13.749	15.102	16.355	10.253	12.151	15.852	11.204	9.187	7.523	7.499	10.120	9.611	12.264	15.978	66.045	27.603	17.219
2005	--	--	2.130	6.783	7.353	5.195	6.764	7.848	8.098	12.313	11.957	13.463	13.142	14.297	14.276	7.455	7.334	6.411	7.830	9.832	14.504	18.346	11.284	20.832	16.620	16.192
2005	--	--	3.991	5.264	3.666	5.258	7.100	8.874	7.164	7.045	8.756	9.608	8.764	7.460	6.990	5.505	4.778	5.424	5.918	8.267	8.055	10.388	10.541	18.047	11.630	18.364
2005	--	--	4.586	6.526	5.216	7.456	6.644	7.561	6.576	7.756	6.627	7.035	5.174	5.078	3.597	3.757	4.687	4.934	4.544	5.743	7.551	7.030	8.869	10.517	13.243	13.130
2005	--	--	3.841	5.372	6.177	7.291	6.920	7.348	6.581	5.632	5.409	6.022	4.025	3.793	3.493	3.948	3.605	5.112	5.228	5.000	6.846	7.520	9.487	10.483	12.026	14.305
2005	--	--	5.692	6.474	5.011	5.252	4.935	5.711	6.006	4.727	3.553	3.646	2.878	2.633	2.712	3.672	3.951	3.716	4.604	5.653	6.620	6.936	11.186	9.809	12.742	15.883
2005	--	--	3.704	8.123	3.906	5.709	5.549	5.837	5.605	6.336	4.448	4.042	4.197	3.555	3.396	3.737	4.191	4.483	5.184	6.576	7.440	8.753	9.182	9.643	16.267	13.310

Table A.28: Resolute Bay hyperthermal chemistry diffusion coefficient (part 2)

Resolute Bay: Hyperthermal chemistry regime slope per height increment

Year	75	76	77	78	79	80	81	82	83	84	85	86	87	88	89	90	91	92	93	94	95	96	97	98	99	100
	(km)	(km)	(km)	(km)	(km)	(km)	(km)	(km)	(km)	(km)	(km)	(km)	(km)	(km)	(km)	(km)	(km)	(km)	(km)	(km)	(km)	(km)	(km)	(km)	(km)	(km)
2006	--	--	3.810	9.089	5.043	5.919	6.511	7.000	5.406	7.009	6.166	4.328	3.126	2.813	3.601	3.158	3.614	4.149	5.246	5.186	7.035	7.168	8.357	10.620	11.655	13.065
2006	--	--	3.308	4.829	2.667	3.734	4.355	2.737	2.593	2.141	1.801	2.589	2.631	3.827	2.851	3.002	3.735	5.340	7.664	6.768	16.089	9.250	12.892	19.205	15.458	15.235
2006	--	--	7.574	8.389	9.666	10.197	14.451	10.234	10.881	10.140	8.699	7.169	7.393	5.619	5.937	5.775	5.065	5.489	7.065	6.223	7.760	8.314	9.900	19.850	16.634	19.768
2006	--	--	40.113	9.915	6.954	14.385	19.341	15.964	13.323	16.022	15.460	11.199	10.283	10.358	8.642	7.027	10.717	6.930	7.391	7.214	9.613	10.546	16.285	13.821	18.920	17.289
2006	--	--	4.117	11.117	7.957	11.583	11.968	12.633	10.394	14.838	17.670	16.527	14.675	13.657	9.344	11.499	8.483	11.004	8.977	9.252	10.737	11.256	14.191	16.844	17.308	22.753
2006	--	--	5.693	7.184	8.275	8.606	5.889	8.096	8.394	10.249	9.033	13.132	12.763	9.199	10.189	8.012	7.607	6.953	8.515	10.184	11.396	14.925	14.447	15.283	17.374	21.924
2006	--	--	2.564	4.485	6.055	7.844	5.908	8.595	9.375	9.058	11.498	12.859	13.260	9.744	10.740	6.547	6.476	7.745	8.678	11.044	14.271	14.151	16.543	18.064	25.741	25.162
2006	--	--	4.113	5.638	8.363	8.555	7.803	8.293	6.738	11.212	8.790	8.668	9.891	7.101	6.187	5.888	5.269	5.792	7.252	6.736	9.443	10.105	10.732	11.076	13.194	20.385
2006	--	--	11.011	4.783	7.716	7.411	8.373	7.506	8.554	9.685	9.180	8.065	9.042	4.846	4.092	4.260	4.082	4.992	4.631	5.994	6.029	6.251	7.438	8.707	9.895	13.186	15.135
2006	--	--	3.760	6.665	7.225	8.865	6.456	6.867	6.543	6.561	5.984	5.919	6.416	4.260	3.810	3.465	4.865	4.052	5.091	6.029	7.810	8.224	8.331	12.422	10.990	13.751
2006	--	--	3.722	5.460	5.510	4.594	5.427	4.851	4.463	4.643	5.223	3.067	3.087	3.242	3.095	3.067	3.401	4.225	4.640	5.188	6.661	8.454	9.037	10.414	13.245	13.719
2006	--	--	5.227	5.065	5.176	3.483	3.924	4.952	4.384	6.408	3.422	3.627	4.106	2.877	2.896	3.814	3.692	4.711	5.812	5.246	6.425	8.139	8.578	13.092	12.622	14.570
2007	--	--	3.968	5.347	4.008	4.038	4.147	4.104	5.852	3.763	4.003	2.735	3.918	2.882	3.016	2.972	3.474	3.840	4.619	5.214	5.951	8.383	8.738	9.890	11.504	16.888
2007	--	--	6.543	7.489	6.638	8.178	17.173	13.821	5.553	7.551	7.869	9.215	4.995	5.995	4.539	5.634	7.746	7.035	5.348	7.993	6.413	9.448	9.511	16.525	17.490	21.183
2007	--	--	8.722	7.609	5.946	10.482	7.186	15.317	8.721	10.772	9.468	9.267	7.163	5.942	6.674	7.280	7.581	6.148	7.089	6.930	8.069	8.915	9.933	13.191	19.181	15.374
2007	--	--	12.509	20.963	21.964	21.801	22.282	23.158	20.199	22.841	21.708	18.077	14.922	12.681	12.474	8.426	6.690	7.190	7.201	8.096	12.527	12.171	10.071	11.310	15.633	19.361
2007	--	--	11.146	7.192	13.437	8.507	10.442	12.385	13.082	17.208	18.039	15.504	15.643	11.895	9.488	8.809	7.772	7.435	9.005	8.887	9.139	11.770	11.962	14.406	17.346	17.866
2007	--	--	1.789	3.001	6.407	7.946	5.910	3.379	6.707	6.246	10.809	11.829	10.263	17.931	9.640	13.488	5.991	8.069	8.564	11.892	11.898	21.753	21.041	17.439	21.601	28.410
2007	--	--	4.346	4.776	5.017	7.604	7.787	9.291	9.287	11.924	9.558	9.767	9.797	7.506	6.524	5.450	5.436	5.357	7.031	7.333	10.595	11.481	10.677	12.380	16.445	20.530
2007	--	--	4.664	7.637	4.301	4.624	8.103	7.472	8.652	7.247	6.199	5.714	4.331	4.399	4.916	3.510	3.848	4.112	4.689	5.385	8.157	7.596	12.794	10.757	16.520	21.144
2007	--	--	5.118	37.452	6.131	5.794	6.377	8.496	8.985	7.408	6.282	4.836	8.861	5.054	4.777	5.161	4.343	4.644	6.892	5.513	9.685	13.254	10.579	13.977	35.362	19.378
2008	--	--	123.797	7.439	23.000	7.967	5.269	23.920	16.676	26.519	9.843	15.393	14.358	20.358	9.859	8.815	6.955	7.557	9.101	6.844	9.546	9.430	11.526	13.183	13.126	21.288
2008	--	--	8.129	7.641	8.530	10.835	9.863	8.236	9.405	5.874	7.213	8.834	4.393	5.449	3.843	4.724	3.585	4.299	7.627	5.611	9.147	8.853	10.860	12.098	44.947	21.185
2008	--	--	7.471	11.955	10.598	18.155	17.527	20.352	13.283	14.811	12.046	11.516	10.762	10.078	8.186	7.138	9.052	7.921	7.062	7.062	8.230	9.976	13.243	14.416	15.366	25.026
2008	--	--	19.624	7.932	11.279	25.469	14.318	18.802	8.969	13.466	25.839	18.584	18.436	16.811	16.519	9.727	9.963	9.842	10.705	10.768	12.531	11.868	13.223	23.457	19.570	21.630
2008	--	--	5.136	4.746	6.164	4.923	6.547	8.913	6.273	9.005	14.248	10.079	9.597	9.899	10.389	7.094	8.286	8.737	9.836	12.356	12.482	11.439	15.715	24.280	28.658	31.677
2008	--	--	4.303	6.621	4.103	7.157	8.151	8.889	7.526	9.016	9.919	13.167	11.033	10.883	9.114	8.368	7.299	6.440	7.551	11.578	13.022	16.130	16.768	16.984	17.253	18.767
2008	--	--	3.669	4.868	5.544	5.121	5.187	4.870	5.379	5.891	8.461	10.140	9.696	10.154	7.859	7.503	6.753	5.610	9.280	9.583	11.835	12.546	12.704	15.924	21.291	29.579
2008	--	--	9.803	6.023	10.778	16.254	12.623	21.696	12.728	18.404	10.700	8.398	8.292	11.615	5.084	4.355	5.696	4.468	6.076	5.190	7.086	11.895	14.687	11.635	17.795	15.588
2008	--	--	8.705	5.337	10.764	6.161	9.204	5.332	7.792	6.252	7.250	5.007	4.185	4.219	3.464	3.908	4.355	3.941	4.690	6.442	8.485	7.026	8.791	9.845	13.423	13.148
2008	--	--	5.015	4.128	6.038	6.626	8.310	5.474	8.203	5.620	4.779	4.050	3.362	3.545	3.547	3.622	5.286	4.165	6.543	6.327	6.533	6.748	10.119	10.932	14.435	14.036
2008	--	--	4.945	4.151	5.056	4.266	4.034	6.339	4.492	3.900	3.252	4.369	3.528	3.122	3.185	4.025	4.056	4.282	5.263	5.442	7.545	9.837	8.644	12.225	12.477	13.000
2009	--	--	8.704	9.317	28.847	20.995	16.042	23.146	19.298	27.504	17.181	23.797	22.431	13.959	10.034	13.838	10.200	8.021	9.639	8.133	10.825	12.155	15.093	15.458	13.961	26.104
2009	--	--	5.097	8.049	7.199	9.473	14.163	9.983	13.332	13.482	15.010	19.168	16.903	12.914	14.419	8.249	6.578	6.877	8.996	8.543	9.297	12.040	16.812	14.926	24.966	47.486
2009	--	--	3.847	5.784	6.537	13.004	7.120	7.095	7.463	6.580	9.902	10.056	13.102	15.778	10.130	17.644	12.609	5.352	10.271	7.924	10.881	17.215	37.807	17.214	26.441	40.541
2009	--	--	2.480	3.988	6.623	8.976	10.802	7.498	8.126	11.632	11.004	12.850	12.473	12.671	9.705	6.926	6.353	6.429	7.401	10.817	10.590	12.517	14.584	16.515	16.987	19.737
2009	--	--	5.829	4.767	14.892	13.031	8.192	8.780	9.005	8.349	9.408	14.378	12.038	10.148	8.989	7.315	7.011	5.593	6.902	8.681	10.426	10.823	13.355	14.051	14.742	20.936
2009	--	--	5.579	5.403	7.615	13.896	5.167	8.852	10.948	10.250	10.360	6.295	7.063	8.326	4.627	4.209	6.457	4.107	7.906	5.518	7.882	10.092	10.577	13.988	12.945	16.504
2009	--	--	8.602	6.515	6.252	8.263	5.874	8.132	7.069	5.643	6.261	5.349	4.918	3.906	3.898	3.715	3.956	4.232	4.616	6.182	6.896	7.585	8.236	11.342	11.514	15.695
2009	--	--	6.446	6.209	8.662	4.189	5.070	4.626	4.436	7.044	4.426	3.351	4.964	3.395	3.187	4.381	3.824	3.767	4.578	5.153	6.226	6.998	10.289	12.504	14.949	14.894
2009	--	--	5.086	2.910	8.911	4.791	4.334	5.850	5.989	7.056	15.389	6.917	5.103	7.057	3.486	2.939	5.699	4.080	5.621	5.522	7.883	9.335	12.951	11.213	17.723	19.106
2010	--	--	2.815	5.105	4.072	6.453	5.869	6.843	6.112	4.348	5.120	4.992	4.199	5.386	4.068	5.328	5.592	6.383	5.364	7.526	9.223	11.974	10.072	13.401	18.232	27.584
2010	--	--	12.699	9.286	8.704	6.838	9.338	9.273	7.184	10.654	8.514	6.704	7.713	3.808	4.502	3.790	5.099	4.545	5.259	7.548	7.441	8.730	12.918	13.373	12.692	20.285
2010	--	--	5.034	5.302	4.421	4.658	20.989	7.544	10.511	8.034	8.767	6.032	4.290	3.244	4.640	3.639	6.626	6.480	5.361	8.145	7.230	7.413	18.347	10.862	22.449	17.571
2010	--	--	10.058	6.793	8.879	27.532	31.364	6.716	17.864	13.977	17.339	27.920	13.181	10.854	9.042	13.589	18.865	5.577	6.976	10.906	12.746	12.763	16.397	16.448	20.887	28.619
2010	--	--	9.354	14.859	5.517	7.937	5.934	13.473	13.966	9.453	10.316	20.467	12.651	13.483	13.659	10.769	8.379	7.847	7.641	8.624	9.737	16.961	15.278	21.529	15.610	16.797
2010	--	--	8.200	4.745	8.055	11.685	4.148	8.400	9.723	8.573	8.604	10.350	14.974	10.508	11.062	8.671	6.553	6.536	8.801	10.121	11.466	14.645	20.545	17.757	17.623	21.805
2010	--	--	4.958	14.506	4.008	11.006	11.380	6.032	11.145	9.899	9.354	11.267	12.939	17.038	7.937	7.368	8.220	7.613	8.144	9.611	13.953	14.897	14.672	27.864	17.226	23.891
2010	--	--	5.844	5.589	6.314	5.473	4.192	17.461	7.185	10.776	9.992	16.090	12.276	8.846	7.613	5.662	5.840	4.811	5.837	7.319	8.216	13.106	13.277	11.608	20.287	n/a
2010	--	--	1.092	1.146	21.244	28.024	2.529	2.913	10.570	26.621	11.861	4.228	62.525	19.072	36.085	9.395	90.126	11.110	25.628	13.571	17.968	12.570	75.123	449.425	47.687	n/a
2010	--	--	1.292	6.227	1.740	2.010	2.599	2.436	2.065	4.204	3.058	4.760	2.176	4.143	2.827	4.507	5.617	6.995	7.318	6.110	6.508	11.091	17.871	23.403	20.956	23.694

Table A.29: Socorro hyperthermal chemistry diffusion coefficient (part 1)

Socorro: Hyperthermal chemistry diffusion coefficient per height increment

Month	Year	75	76	77	78	79	80	81	82	83	84	85	86	87	88	89	90	91	92	93	94	95	96	97	98	99	100
		(km)	(km)	(km)	(km)	(km)	(km)	(km)	(km)	(km)	(km)	(km)	(km)	(km)	(km)	(km)	(km)	(km)	(km)	(km)	(km)	(km)	(km)	(km)	(km)	(km)	(km)
4	2002	1.703	1.571	5.010	5.625	6.056	8.565	22.033	8.162	12.972	10.694	6.948	46.634	25.034	5.234	5.201	5.102	6.167	12.118	9.648	10.454	10.300	14.745	12.827	69.377	12.258	16.458
5	2002	2.452	1.253	7.471	1.973	4.556	3.797	5.482	6.209	9.742	9.970	10.717	11.906	10.540	8.775	9.195	13.940	7.690	6.262	5.344	8.247	9.322	11.653	14.366	13.678	16.572	51.357
6	2002	1.065	1.722	1.622	2.265	7.543	4.647	7.444	15.485	6.604	9.536	10.793	7.683	9.223	9.656	5.871	7.152	6.370	6.944	7.859	8.262	10.588	16.944	14.676	15.554	14.116	54.391
7	2002	0.680	1.473	5.334	7.453	4.008	2.597	6.930	6.872	8.955	14.483	12.891	8.736	8.482	15.859	8.832	5.267	8.681	11.792	9.794	6.471	7.213	7.824	10.069	12.756	11.961	16.088
8	2002	1.004	2.307	2.005	2.961	3.865	5.440	5.463	8.205	8.885	7.430	11.714	7.750	11.369	7.724	6.366	6.329	5.605	6.409	6.797	8.665	8.384	9.803	12.824	13.966	15.578	22.755
9	2002	1.187	2.045	5.502	3.928	3.550	6.123	6.843	10.747	9.423	9.207	10.424	10.765	8.287	8.487	6.678	6.367	9.688	6.841	7.880	10.207	9.390	8.703	13.620	12.527	21.098	20.504
10	2002	2.197	1.732	0.959	4.453	3.915	2.406	9.177	4.197	5.101	8.750	8.987	10.043	5.811	8.330	5.262	6.775	6.809	6.659	11.107	7.863	8.140	13.300	12.488	11.417	13.330	14.541
11	2002	0.666	5.676	n/a	10.922	19.226	23.354	10.760	127.806	22.917	16.913	7.203	13.619	19.404	15.190	17.482	16.360	17.972	11.225	49.748	12.037	14.136	10.559	23.629	24.609	15.045	26.686
3	2003	16.237	0.783	5.420	8.778	14.455	21.954	13.773	18.886	17.996	22.931	17.690	19.133	8.707	11.466	8.228	7.928	6.958	7.424	7.707	7.169	7.215	10.042	16.006	17.247	18.764	25.936
4	2003	3.650	3.226	3.924	3.528	3.827	8.105	12.020	16.727	10.104	19.666	15.693	15.938	13.138	10.089	8.204	7.381	6.466	4.255	7.022	5.740	9.570	10.431	12.167	9.687	14.657	13.684
1	2005	3.642	9.226	3.730	24.756	8.655	12.259	27.245	9.383	31.094	29.038	11.387	10.307	10.451	10.624	8.784	9.651	5.276	6.452	6.949	6.903	6.805	8.842	8.706	15.288	11.668	14.001
2	2005	2.285	6.430	3.596	7.490	20.497	27.894	20.397	21.862	22.443	20.975	21.313	19.240	17.497	14.220	10.526	6.822	9.688	6.398	7.341	6.951	6.909	11.813	10.878	19.282	13.278	22.085
3	2005	4.400	8.128	4.477	13.502	14.763	8.879	12.889	11.241	21.862	23.774	24.825	13.169	12.426	12.042	11.579	7.221	8.922	6.023	5.658	7.216	7.526	7.965	9.919	11.866	14.495	18.672
4	2005	3.800	3.707	16.126	8.735	11.615	8.900	10.392	16.862	23.295	20.156	20.252	19.017	14.850	15.815	10.497	8.867	9.077	7.008	7.744	7.605	9.227	13.894	9.695	9.656	15.419	43.810
5	2005	1.533	4.095	5.661	12.509	8.302	10.910	17.192	17.558	20.558	22.665	20.908	16.062	15.082	13.184	12.220	8.216	7.723	6.413	7.548	8.605	8.974	10.021	10.760	14.909	13.101	17.249
6	2005	12.638	9.943	4.394	4.237	12.179	18.603	24.480	25.426	27.468	22.573	27.568	18.915	15.127	12.456	10.489	8.793	7.198	6.532	7.443	6.813	8.302	8.470	10.439	12.685	14.199	18.637
7	2005	1.949	6.190	5.574	10.388	10.729	28.189	23.205	29.010	21.222	25.562	20.209	19.218	12.881	11.452	10.484	7.625	7.341	6.682	7.367	8.181	9.986	9.239	17.509	19.627	25.118	16.741
8	2005	15.673	63.546	7.372	6.602	31.815	8.014	47.995	35.177	45.584	20.491	26.987	36.475	56.222	6.982	13.684	7.062	11.976	10.559	7.103	6.385	10.052	8.527	17.850	12.068	21.169	38.439
5	2007	1.325	13.354	12.005	7.712	10.359	19.442	20.024	16.932	21.754	19.134	19.598	16.083	15.381	11.344	8.125	6.523	6.310	4.349	5.638	8.688	10.334	8.656	10.357	11.686	12.270	13.685
6	2007	0.773	1.922	1.834	3.182	8.276	16.612	15.715	16.765	19.134	18.540	18.096	13.242	12.569	10.866	7.776	6.951	7.345	6.992	6.490	7.483	10.202	9.946	9.858	10.252	11.913	18.956
7	2007	6.797	4.963	3.062	6.375	13.323	25.824	15.667	13.271	11.240	17.815	19.107	16.067	14.756	14.684	9.468	9.017	7.320	7.159	7.806	9.418	8.459	9.895	10.264	12.544	12.477	13.015
6	2008	1.248	3.186	15.182	7.799	12.638	12.104	11.908	17.552	14.183	19.320	22.178	21.123	20.040	12.327	9.899	8.175	7.177	7.137	5.870	6.572	7.818	8.901	8.821	12.985	22.462	21.596
7	2008	1.601	7.064	7.128	8.754	13.747	14.789	24.142	30.830	16.170	23.776	19.217	14.940	12.568	11.761	8.518	7.079	6.414	6.414	6.920	9.523	12.471	10.413	11.883	13.024	14.654	19.978
8	2008	6.914	3.545	44.839	10.357	37.791	75.808	31.676	43.845	38.159	19.993	9.839	47.289	11.441	12.135	7.602	5.629	12.699	9.896	8.394	6.006	7.053	8.874	11.541	13.376	23.329	20.748
12	2008	3.173	6.826	6.935	4.862	19.816	6.092	23.422	22.190	8.634	23.006	12.724	12.314	15.050	9.574	9.063	8.580	8.244	7.161	12.670	8.332	11.991	9.844	11.438	12.220	13.327	18.099
1	2009	5.084	4.356	11.566	7.867	14.605	8.613	13.090	28.848	11.322	22.280	15.621	16.543	9.574	11.836	6.910	6.648	8.039	7.592	7.620	5.639	9.564	9.790	12.349	14.389	17.802	24.558
2	2009	2.051	12.424	27.115	7.338	20.535	37.368	10.480	36.192	19.173	26.165	24.715	18.849	18.575	18.244	12.565	9.930	7.429	9.137	6.666	7.782	8.473	9.490	9.029	24.773	13.922	15.802
3	2009	5.399	2.323	8.291	21.319	5.472	18.525	18.600	22.352	18.642	21.261	17.928	18.879	21.532	14.439	10.702	9.587	6.804	7.777	12.026	7.190	8.565	11.431	9.093	10.810	13.994	19.073
4	2009	6.906	1.651	9.850	14.931	12.559	24.428	20.127	20.805	25.451	20.606	21.727	18.337	21.708	13.685	12.557	11.661	11.312	16.238	17.706	11.352	12.724	12.667	12.232	16.546	31.600	20.354
5	2009	0.798	2.893	2.191	5.823	4.506	8.819	9.210	10.480	42.820	20.954	49.626	15.098	15.339	14.844	17.419	21.525	7.423	12.117	14.536	8.544	9.475	13.540	11.827	13.758	38.856	19.346
6	2009	26.257	5.231	14.284	6.794	7.216	11.107	16.606	23.705	25.021	17.260	19.016	15.896	15.425	8.407	9.575	6.761	9.007	6.066	6.994	5.039	8.518	12.292	9.256	9.758	20.583	31.388
7	2009	1.137	2.355	6.770	8.932	11.109	12.101	15.525	14.772	20.943	16.859	19.600	13.752	10.892	8.625	7.399	6.198	6.142	6.712	6.577	8.802	9.868	10.337	12.487	21.412	14.852	26.165
8	2009	0.744	2.283	6.033	12.231	15.472	18.593	17.695	29.079	30.907	20.922	17.002	14.124	11.913	12.494	7.845	6.300	5.608	6.754	5.904	6.028	8.413	8.717	9.468	12.858	12.392	13.034
9	2009	4.001	2.646	4.316	9.493	11.714	12.726	17.348	18.903	19.629	17.910	13.832	16.055	10.509	9.069	7.712	6.747	7.243	8.804	7.909	7.365	8.732	9.100	10.841	15.007	13.973	16.850
10	2009	3.113	2.549	7.527	4.618	8.065	15.717	11.870	23.702	15.729	14.626	16.832	13.992	9.039	8.156	6.662	6.759	5.571	5.968	6.715	7.959	8.711	10.345	9.564	12.297	12.082	14.886
11	2009	2.550	1.649	3.503	7.777	9.687	10.704	13.226	16.363	17.919	15.876	15.298	13.669	10.627	10.935	6.617	7.237	6.622	9.916	7.644	8.998	7.649	9.962	14.058	12.108	17.545	17.678
12	2009	1.844	3.666	4.320	20.084	13.268	11.592	14.744	13.382	17.146	14.431	16.801	19.381	11.889	8.216	8.577	8.450	6.900	8.882	5.556	9.200	7.477	9.955	18.282	10.686	14.578	20.773

Table A.30: Socorro hyperthermal chemistry diffusion coefficient (part 2)

Socorro: Hyperthermal chemistry diffusion coefficient per height increment																															
Month	Year	75	76	77	78	79	80	81	82	83	84	85	86	87	88	89	90	91	92	93	94	95	96	97	98	99	100
		(km)	(km)	(km)	(km)	(km)	(km)	(km)	(km)	(km)	(km)	(km)	(km)	(km)	(km)	(km)	(km)	(km)	(km)	(km)	(km)	(km)	(km)	(km)	(km)	(km)	(km)
1	2010	2.856	5.192	8.133	9.874	12.512	8.940	13.106	17.228	13.041	8.654	26.108	13.797	10.914	8.133	8.585	9.510	5.847	7.972	6.733	7.318	9.762	8.193	9.455	15.973	19.487	18.034
2	2010	2.169	2.979	13.500	13.358	16.442	15.536	22.121	25.491	23.374	18.555	27.795	18.362	18.621	15.271	12.915	8.745	8.165	7.139	7.017	6.497	9.054	9.567	13.903	13.273	16.143	13.715
3	2010	0.795	1.731	4.416	9.334	9.100	19.093	23.223	33.653	14.354	21.928	25.770	14.956	16.995	12.296	8.431	8.452	7.111	7.546	7.100	5.827	8.403	9.183	14.529	12.546	14.817	15.250
4	2010	5.469	1.803	1.841	13.000	8.931	13.935	7.522	16.635	10.604	17.903	12.180	15.561	13.300	12.496	11.582	8.018	6.336	6.460	6.984	5.302	8.597	7.966	9.818	17.968	31.495	26.714
5	2010	3.071	1.475	2.311	4.402	5.756	6.494	18.525	17.600	21.651	18.575	17.245	16.538	14.583	11.965	9.511	7.569	7.921	7.122	7.066	10.274	9.050	10.031	11.963	14.218	15.066	13.593
6	2010	2.756	1.968	5.856	12.535	11.275	15.962	20.575	26.508	23.416	21.631	18.181	15.533	14.168	11.573	8.585	7.278	6.654	6.349	6.848	7.215	10.021	9.144	10.997	16.616	15.956	15.540
7	2010	10.520	6.392	12.402	10.726	16.014	13.428	20.830	21.045	19.097	18.413	17.463	14.876	13.336	10.648	9.308	7.145	6.420	6.141	6.460	7.912	8.349	9.022	10.062	13.578	23.702	16.751
8	2010	1.843	8.445	3.333	9.953	11.350	11.750	17.319	28.090	18.906	16.154	15.439	14.227	11.769	12.418	8.374	7.799	7.248	6.999	6.992	7.654	8.306	8.750	8.986	11.979	11.387	14.825
9	2010	2.604	6.391	7.424	12.496	7.785	15.126	20.065	17.723	15.100	14.830	13.827	14.274	10.051	9.104	8.334	7.775	6.239	6.501	6.410	9.016	8.855	9.317	10.424	13.598	14.582	13.273
10	2010	3.838	3.647	3.621	6.743	8.021	9.295	16.386	18.733	16.770	16.042	11.925	13.590	9.390	8.884	6.999	7.821	6.314	6.565	6.090	8.226	8.036	10.591	10.793	13.970	13.127	21.753
11	2010	2.154	8.494	4.911	9.098	11.046	17.331	19.664	20.514	24.124	17.186	17.432	15.733	13.180	10.494	10.000	8.685	7.727	6.255	6.904	8.150	10.200	9.211	14.145	12.138	12.833	16.003
12	2010	1.250	1.694	4.033	10.190	16.604	10.574	15.017	12.002	14.147	14.374	13.624	11.624	13.367	9.872	10.810	7.644	7.676	6.617	7.476	7.869	10.399	10.660	12.765	15.672	16.532	21.880
1	2011	3.203	3.381	4.754	5.808	15.396	11.645	21.003	10.917	18.929	12.585	11.618	20.520	15.638	14.312	9.640	8.292	10.874	7.850	8.492	7.336	11.264	9.577	14.865	10.225	13.985	25.879
2	2011	2.223	6.529	4.336	16.480	14.251	15.806	11.460	20.312	34.169	25.693	19.931	14.091	16.749	10.810	9.697	5.943	6.984	10.052	5.670	7.170	10.053	8.731	8.738	11.278	59.851	19.319
3	2011	3.116	2.813	3.526	5.941	22.733	16.397	7.660	11.632	11.972	13.917	20.196	18.406	16.619	17.719	6.573	9.737	7.959	8.785	8.806	6.108	13.679	9.698	13.772	12.255	18.826	25.461
4	2011	1.416	6.745	5.441	15.736	12.033	10.094	20.819	13.290	16.113	17.394	17.920	15.736	14.493	14.253	13.788	11.330	10.037	7.964	9.064	13.796	8.036	9.857	7.974	20.558	30.830	15.113
5	2011	3.739	2.012	5.623	11.383	10.222	13.438	12.941	16.542	24.124	22.414	29.673	28.487	20.011	34.659	23.342	16.826	17.735	16.131	12.623	15.889	17.585	14.347	14.500	23.763	21.810	25.531
6	2011	3.056	46.991	10.390	8.589	11.299	11.570	19.036	23.477	25.237	30.361	23.877	19.678	20.410	16.401	15.243	13.412	14.514	12.848	12.614	11.385	11.430	12.433	14.213	13.333	14.172	23.927
7	2011	1.715	5.352	4.993	9.417	9.793	12.837	17.157	18.537	22.985	24.068	36.637	19.395	16.868	14.834	9.875	9.054	8.428	8.090	9.110	9.367	12.908	12.061	16.376	28.288	21.523	26.824
8	2011	2.024	3.494	10.970	7.516	15.926	16.437	20.902	22.982	28.390	23.709	21.970	17.000	14.100	13.348	10.827	10.261	8.949	8.663	9.187	8.343	10.555	12.611	10.865	12.954	16.706	20.258
9	2011	1.882	2.293	11.660	14.077	6.099	17.586	15.790	22.200	19.636	16.668	16.502	12.343	11.545	11.846	10.045	10.928	8.837	7.289	8.886	9.393	10.145	9.786	12.567	13.046	20.712	29.214
10	2011	6.989	6.328	3.300	8.927	24.438	13.494	16.721	22.100	16.768	16.215	15.132	12.464	10.902	8.801	8.833	7.299	7.567	7.640	7.397	8.839	8.862	13.403	13.896	21.736	22.032	15.227
11	2011	1.943	2.576	10.316	11.165	12.651	28.293	19.764	10.418	18.098	21.359	16.887	14.943	12.504	10.964	8.415	8.468	7.666	7.633	8.336	8.921	8.146	10.809	12.374	11.570	11.682	14.780
12	2011	8.535	6.445	5.300	7.059	25.321	18.929	14.598	6.937	19.283	19.740	14.236	16.234	10.484	8.926	6.001	6.912	8.260	4.470	6.990	6.399	9.556	10.782	8.764	10.996	15.768	14.464
1	2012	4.861	5.270	4.433	17.100	8.210	24.449	5.962	28.511	12.533	28.111	21.063	25.376	16.831	9.011	11.134	12.168	8.662	8.024	9.706	12.856	11.037	10.627	14.371	9.663	11.372	19.950
2	2012	9.992	1.268	1.928	13.327	10.540	9.061	30.608	13.435	26.942	11.677	33.543	20.964	7.712	8.240	12.609	5.009	10.637	7.901	8.011	6.278	9.146	10.505	13.935	22.114	23.894	13.682
3	2012	6.126	2.025	8.358	3.749	19.526	11.918	15.071	27.914	34.580	30.944	33.764	18.837	17.039	14.057	12.819	10.601	9.933	10.063	8.546	11.561	11.042	11.429	15.715	17.843	13.118	21.711
4	2012	2.328	3.058	3.167	15.462	7.092	8.534	11.180	12.645	21.373	23.021	17.939	24.339	14.106	15.846	7.264	11.921	10.375	8.528	9.808	10.031	10.348	13.345	17.042	15.093	26.916	16.112
5	2012	13.328	2.581	4.131	4.054	6.803	14.463	13.996	7.851	38.072	20.757	10.461	24.752	6.668	10.495	4.196	6.694	4.770	6.010	5.659	7.657	6.967	15.950	26.370	30.533	25.905	28.427

Table A.31: Yellowknife hyperthermal chemistry diffusion coefficient (part 1)

Yellowknife: Hyperthermal chemistry diffusion coefficient per height increment

Month	Year	75	76	77	78	79	80	81	82	83	84	85	86	87	88	89	90	91	92	93	94	95	96	97	98	99	100
		(km)	(km)	(km)	(km)	(km)	(km)	(km)	(km)	(km)	(km)	(km)	(km)	(km)	(km)	(km)	(km)	(km)	(km)	(km)	(km)	(km)	(km)	(km)	(km)	(km)	(km)
6	2002	151.422	1.006	18.007	3.624	4.680	4.593	5.951	4.127	4.608	6.648	10.815	4.250	3.994	4.944	3.973	4.629	3.860	4.067	4.830	5.376	7.562	13.033	17.825	83.313	15.383	57.635
7	2002	4.804	5.836	1.270	0.708	16.816	9.998	11.927	5.142	7.802	8.972	5.525	4.486	4.853	6.144	4.701	4.617	3.341	4.291	4.604	5.266	8.054	11.426	13.084	10.162	19.902	54.958
8	2002	3.439	2.418	8.484	3.223	5.704	6.150	5.220	10.766	5.751	11.164	6.873	9.945	9.505	4.217	4.107	3.242	3.547	4.089	4.701	5.517	6.481	7.671	10.564	10.322	32.733	13.948
3	2003	n/a	n/a	40.870	24.813	46.928	26.410	23.454	4.746	9.574	69.938	89.621	16.633	9.059	7.700	26.232	7.963	8.678	4.744	13.361	9.174	7.066	9.824	26.457	317.163	155.201	n/a
4	2003	1.411	0.994	9.222	3.571	11.567	15.905	24.046	72.234	61.135	41.080	23.171	15.883	14.810	19.428	27.640	8.808	15.123	12.535	12.688	17.915	11.339	16.424	9.391	17.820	187.449	62.937
5	2003	0.636	0.721	4.779	7.835	7.077	12.452	9.289	30.437	12.875	24.948	12.453	8.269	13.177	21.291	10.006	6.157	5.117	5.148	4.756	9.792	10.833	22.881	23.101	12.385	14.295	31.577
6	2003	1.052	0.708	0.370	1.076	5.484	2.363	2.625	15.665	13.022	14.155	8.475	9.395	8.783	7.215	4.501	4.977	4.502	8.027	6.173	10.689	11.455	14.016	27.034	18.869	15.454	21.692
7	2003	0.653	0.466	1.773	3.338	53.128	3.281	6.353	5.429	8.039	10.072	12.857	9.594	6.075	6.880	5.870	6.750	10.524	4.939	5.149	6.116	19.866	11.412	9.785	15.772	15.142	13.796
8	2003	n/a	0.686	33.917	14.939	2.469	5.490	4.331	36.825	13.685	7.907	9.458	10.163	6.778	7.311	5.452	6.580	5.210	6.927	4.893	11.061	8.180	12.947	9.814	15.767	11.217	13.290
9	2003	0.586	20.068	0.986	1.912	13.237	11.683	12.359	7.827	9.083	7.367	4.339	7.816	7.736	5.287	9.965	6.312	5.801	7.593	5.544	6.178	9.482	8.437	23.867	18.104	15.289	17.035
10	2003	2.118	12.140	4.060	10.082	10.450	8.214	10.853	16.375	16.689	10.039	6.233	14.913	15.895	4.664	6.532	4.007	5.776	12.806	5.139	6.932	13.039	11.540	10.150	34.830	18.719	14.678
11	2003	13.117	21.187	10.833	7.682	20.632	9.971	36.440	11.117	12.438	10.936	5.761	6.744	17.336	5.164	7.242	7.413	12.845	50.221	15.327	13.453	9.153	12.102	n/a	23.527	19.091	98.509
12	2003	1.586	1.852	4.199	3.824	5.912	24.349	12.175	12.109	26.482	6.929	6.371	7.236	4.463	3.786	4.172	4.831	4.232	7.971	5.700	8.080	6.280	8.256	17.881	31.476	33.458	192.947
1	2004	8.666	9.198	7.123	21.264	22.529	9.763	6.873	10.098	6.688	11.866	5.412	5.242	3.791	3.439	5.989	10.303	4.700	7.139	7.516	8.637	6.207	12.638	10.942	39.964	46.283	24.996
2	2004	13.935	2.714	17.424	9.380	37.186	11.255	7.242	10.496	13.551	8.387	9.463	9.147	5.679	7.211	10.935	8.753	6.632	25.942	11.292	12.341	29.759	11.607	29.453	n/a	16.596	276.155
3	2004	n/a	1.142	7.501	23.041	5.795	4.308	84.289	14.207	12.363	20.651	17.593	29.869	6.468	5.912	5.394	7.602	4.335	4.085	11.442	5.390	10.594	14.200	17.399	56.152	24.554	15.968
4	2004	1.641	7.976	2.091	4.790	8.719	5.558	5.726	11.519	11.510	28.949	12.583	9.772	11.766	15.122	6.693	5.330	8.119	4.049	4.634	6.375	9.877	9.037	10.293	12.887	42.454	19.592
5	2004	2.172	2.254	2.806	15.118	1.877	2.732	5.387	5.235	9.127	17.692	13.333	9.254	17.864	11.771	7.186	4.384	7.314	3.961	6.343	27.073	6.260	8.051	12.602	13.246	12.576	19.479
6	2004	2.397	6.622	4.065	3.393	2.452	6.657	6.598	8.993	10.778	4.936	6.079	9.478	10.863	3.876	4.851	4.287	6.112	5.500	8.272	7.839	9.570	228.579	9.435	23.292	25.031	28.508
7	2004	n/a	n/a	n/a	6.515	7.696	10.581	5.367	31.858	12.380	22.203	23.335	5.349	12.829	25.837	34.646	4.353	24.007	12.280	14.670	15.576	18.289	8.382	25.809	25.832	219.717	116.851
8	2004	53.968	1.652	4.982	1.834	4.453	3.029	6.318	12.227	12.054	8.371	5.605	11.288	5.247	5.385	4.546	4.622	4.239	4.570	5.567	5.465	8.576	12.802	8.110	17.747	16.027	90.161
9	2004	7.986	13.137	6.282	5.473	4.431	12.789	16.037	11.930	10.178	16.961	8.916	9.085	9.372	5.441	3.909	7.414	8.158	4.753	14.385	6.755	7.671	19.461	9.073	20.994	18.264	15.146
10	2004	1.331	2.760	2.801	5.413	7.451	7.033	8.757	6.318	9.349	9.970	12.554	6.034	3.440	4.064	4.464	4.367	4.511	5.141	6.189	5.958	7.935	14.421	9.552	12.595	12.450	14.230
11	2004	12.846	16.102	9.326	20.797	6.536	10.426	25.365	57.465	15.379	10.256	4.081	11.935	5.153	4.984	3.287	4.189	6.547	5.720	4.758	5.931	8.738	19.029	14.289	27.773	22.589	15.315
12	2004	9.875	4.752	6.855	5.513	6.519	21.524	8.089	5.648	6.761	10.981	6.186	6.342	6.400	7.241	4.230	7.726	4.626	7.668	5.346	8.653	9.626	19.818	11.646	11.507	77.801	23.945
1	2005	3.512	4.491	10.585	12.981	11.148	11.772	55.789	9.711	10.870	15.007	6.026	5.364	4.941	7.189	3.959	5.538	5.362	7.549	6.105	12.525	6.547	15.216	25.275	29.969	11.595	52.992
2	2005	2.663	2.929	36.366	23.286	32.951	7.688	14.810	20.829	13.517	135.401	21.264	9.727	10.548	8.409	4.964	13.133	15.140	20.075	10.486	7.403	6.320	75.281	9.064	30.687	24.343	32.805
3	2005	0.716	2.649	1.809	6.918	12.488	7.659	28.923	7.743	9.110	9.374	7.333	8.916	5.265	5.775	15.281	16.373	6.893	4.893	4.636	5.668	33.246	15.079	30.712	12.262	15.410	33.013
4	2005	4.264	6.063	10.505	96.906	6.819	82.156	20.651	12.260	55.104	90.442	13.340	14.008	16.278	8.318	4.805	6.317	6.553	17.465	7.125	9.662	6.777	8.772	11.854	19.635	55.875	54.565
5	2005	2.488	32.407	28.176	15.295	7.963	13.262	34.206	5.844	16.197	9.813	13.410	6.944	11.401	11.886	11.678	8.236	8.019	5.415	7.846	13.160	14.898	14.796	15.194	14.076	26.621	20.703
6	2005	5.186	1.351	0.558	5.961	9.871	3.540	7.266	5.532	13.870	5.797	6.639	6.025	7.835	5.612	4.631	6.854	4.537	4.379	5.492	6.454	8.962	15.652	9.034	16.091	26.721	95.742
7	2005	17.954	13.231	1.222	9.845	2.956	11.458	122.220	5.070	10.967	8.329	10.388	7.028	8.510	10.995	8.091	3.414	3.224	6.061	7.308	5.461	8.478	403.273	12.566	18.718	13.667	55.840
8	2005	1.592	8.833	2.070	7.116	1.578	10.387	20.181	8.538	5.912	5.430	8.807	4.930	5.512	4.694	5.897	4.049	4.364	5.185	4.989	8.207	6.768	15.164	22.103	18.833	17.591	13.286
9	2005	2.474	3.983	2.449	23.470	14.916	13.034	8.422	18.530	17.545	12.092	10.168	8.784	9.078	10.489	5.938	5.067	7.855	5.133	6.555	6.676	6.729	7.458	16.133	26.097	20.739	13.481
10	2005	0.544	2.175	5.297	6.440	8.942	21.432	36.985	20.741	19.020	6.817	5.871	3.861	4.975	4.816	5.683	5.303	5.492	8.845	4.956	5.486	7.923	8.729	10.679	9.703	11.531	13.278
11	2005	1.219	3.232	9.279	12.018	5.026	6.670	14.094	9.268	6.794	13.645	5.954	24.640	31.506	9.825	3.952	10.576	4.783	4.239	5.091	5.946	6.162	9.894	8.591	16.764	18.217	21.726
12	2005	5.938	4.934	2.935	10.889	16.203	6.225	7.856	7.424	9.451	13.962	9.246	11.619	13.064	5.894	5.668	4.572	5.741	5.635	6.071	6.290	8.443	7.859	8.784	37.111	13.373	34.272

Table A.32: Yellowknife hyperthermal chemistry diffusion coefficient (part 2)

Yellowknife: Hyperthermal chemistry diffusion coefficient per height increment

Month	Year	75	76	77	78	79	80	81	82	83	84	85	86	87	88	89	90	91	92	93	94	95	96	97	98	99	100
		(km)	(km)	(km)	(km)	(km)	(km)	(km)	(km)	(km)	(km)	(km)	(km)	(km)	(km)	(km)	(km)	(km)	(km)	(km)	(km)	(km)	(km)	(km)	(km)	(km)	(km)
1	2006	1.459	1.495	2.482	5.670	3.526	18.867	12.282	19.733	7.547	12.800	4.585	7.224	22.440	4.272	6.238	8.229	3.604	4.891	8.599	7.625	13.115	11.118	13.122	14.130	13.412	21.011
2	2006	1.819	4.590	36.857	5.196	4.896	4.676	6.785	5.243	33.352	6.687	11.996	8.078	16.450	4.875	7.437	12.913	6.097	4.899	44.221	6.294	7.195	12.479	11.396	10.536	74.008	21.772
3	2006	11.251	1.937	3.507	7.621	7.089	9.727	9.792	14.317	109.747	21.241	12.276	11.363	11.119	7.762	6.728	8.338	6.770	8.131	5.779	9.652	13.559	27.463	27.074	10.315	25.770	19.816
4	2006	0.869	14.651	1.699	7.891	24.998	17.214	44.202	41.295	20.269	35.737	18.130	17.088	30.279	17.788	11.794	6.579	9.878	7.842	9.705	6.768	27.868	8.701	9.303	19.415	14.670	23.195
5	2006	3.846	9.807	2.813	7.348	1.548	29.459	4.861	23.653	13.633	15.875	16.755	20.757	15.557	21.767	6.257	9.028	11.897	9.867	9.643	10.687	8.568	8.714	11.261	11.195	217.445	14.290
6	2006	0.739	2.685	0.607	2.180	2.833	9.370	2.097	7.299	4.972	6.375	8.664	6.748	7.644	9.104	5.225	7.519	6.955	5.987	6.858	7.677	6.493	9.920	8.060	18.856	14.358	14.965
7	2006	20.730	4.434	1.623	5.123	9.146	5.272	2.246	4.944	3.912	4.970	9.465	15.250	8.150	6.013	8.858	7.484	6.118	5.342	4.699	8.964	7.354	7.549	8.413	11.575	11.144	21.310
8	2006	3.388	4.666	3.400	10.156	7.693	10.300	3.840	10.024	17.515	10.643	26.883	5.598	20.589	9.022	6.452	4.671	4.285	6.439	4.489	5.152	6.571	8.202	10.524	13.270	24.750	21.217
9	2006	8.042	n/a	11.043	10.570	16.537	15.245	27.008	100.152	29.284	18.156	13.687	10.214	14.886	7.034	23.134	6.921	21.539	23.531	28.942	9.056	12.436	43.327	106.606	131.409	126.121	83.475
11	2006	4.414	n/a	n/a	6.871	n/a	n/a	19.044	n/a	30.774	98.117	115.537	n/a	23.404	570.009	51.098	116.284	11.881	8.615	12.972	20.007	101.837	423.439	746.777	n/a	36.858	302.680
12	2006	10.165	6.684	2.858	18.357	64.585	14.023	16.864	14.030	14.550	28.657	16.657	15.198	14.494	16.876	18.010	11.565	9.449	13.192	73.737	13.974	17.402	238.382	62.791	41.835	96.535	72.416
1	2007	28.225	68.240	63.978	29.083	210.007	301.363	38.495	31.864	13.562	13.297	7.914	80.475	9.001	7.442	13.827	48.890	31.445	15.935	16.639	25.281	14.334	65.145	23.900	70.332	21.530	265.669
2	2007	1.103	n/a	n/a	2.901	n/a	9.138	50.997	38.081	109.579	55.774	129.212	n/a	106.149	56.938	79.365	84.685	51.634	29.391	26.079	95.036	56.689	n/a	38.237	269.872	n/a	n/a
12	2007	4.102	n/a	21.849	10.689	23.828	33.996	20.534	22.739	18.816	17.618	14.468	42.819	103.477	46.537	73.211	59.347	53.117	115.396	45.792	73.659	43.719	121.995	84.308	33.872	n/a	n/a
4	2008	3.094	n/a	24.965	9.226	8.541	34.356	24.160	26.305	28.623	29.595	47.162	20.085	26.153	12.710	12.195	13.780	9.265	8.949	4.709	16.934	10.724	68.734	59.097	34.849	16.368	633.764
5	2008	0.965	2.317	0.751	3.675	10.055	31.610	13.204	7.493	6.279	9.850	8.517	6.629	6.765	11.559	5.573	5.496	5.786	6.463	6.223	7.952	5.893	15.815	17.981	29.655	11.847	35.944
6	2008	99.676	0.759	1.322	0.918	8.594	2.077	5.067	5.256	4.922	6.345	8.076	7.862	5.038	6.254	6.070	4.525	4.757	4.494	6.375	5.262	6.358	7.233	9.245	10.682	11.451	13.513
7	2008	0.707	0.478	1.736	1.882	7.776	1.611	7.082	7.033	4.535	9.058	4.303	8.036	6.440	4.320	5.852	6.416	4.892	4.140	4.622	6.548	7.161	7.914	9.960	9.596	16.935	15.719
8	2008	1.751	1.199	0.954	5.132	3.126	5.400	5.774	9.141	4.937	6.751	5.790	8.367	6.644	5.809	5.264	4.762	5.256	4.867	5.098	5.236	6.124	7.516	9.642	15.338	11.555	16.436
9	2008	3.032	39.174	3.583	4.971	10.457	20.188	9.810	15.782	24.339	11.517	9.514	7.619	9.909	5.605	5.318	3.933	4.059	5.258	4.801	6.054	9.266	7.627	14.774	10.900	11.828	18.875
10	2008	2.028	2.208	4.095	7.503	16.565	15.493	17.360	16.676	25.090	12.064	13.713	7.473	5.702	4.871	3.489	4.962	5.792	5.049	4.592	5.514	6.991	8.126	10.110	12.915	12.603	38.781
11	2008	2.673	2.839	7.853	4.584	11.322	24.110	6.708	8.898	9.888	9.089	5.611	4.669	4.815	6.515	3.106	5.880	8.676	4.628	6.093	6.089	6.045	10.134	10.776	18.850	10.986	13.889
12	2008	2.065	3.032	1.855	13.968	79.142	4.541	6.898	10.849	13.781	7.351	7.961	6.044	4.276	5.349	5.493	4.531	5.459	6.336	5.739	6.437	6.876	11.921	9.354	15.814	13.381	26.778
1	2009	2.436	1.694	4.783	5.577	7.090	6.688	5.825	6.039	9.034	9.565	9.693	7.196	8.497	4.180	4.738	5.917	4.873	5.664	4.932	6.078	6.302	9.003	12.220	11.167	15.617	15.597
2	2009	7.314	1.322	3.321	16.298	6.802	21.316	24.172	15.915	7.852	20.371	15.414	9.480	8.954	4.029	5.059	7.774	4.885	4.225	5.945	12.386	6.489	9.153	17.604	12.959	21.295	19.379
3	2009	9.879	4.697	9.101	10.325	5.852	7.818	24.335	26.720	8.310	19.025	10.971	6.809	6.862	8.005	7.934	5.405	5.503	5.854	5.552	6.931	8.465	9.423	10.917	15.693	15.977	14.071
4	2009	n/a	7.164	173.867	19.359	8.763	15.067	37.840	35.124	35.652	44.342	12.009	13.557	21.143	7.972	8.452	10.262	12.914	11.540	5.633	6.931	8.448	7.983	11.328	19.979	14.630	21.418
5	2009	2.497	n/a	4.438	2.206	6.214	6.309	4.150	7.532	9.771	7.906	9.916	8.242	6.388	7.802	8.612	5.244	4.545	4.702	4.671	6.528	8.768	7.037	10.429	22.855	23.882	20.126
6	2009	0.606	15.485	2.305	2.442	2.843	3.214	5.406	4.616	4.279	3.543	5.608	7.815	6.668	4.399	5.363	6.119	6.322	3.708	6.035	7.902	6.130	6.872	10.775	18.549	25.157	13.571
7	2009	3.232	2.832	1.729	1.058	1.115	10.666	4.003	6.614	4.872	11.061	5.162	5.009	8.389	6.386	4.689	4.858	4.509	4.433	5.292	6.949	6.665	10.151	11.987	16.456	11.314	14.283
8	2009	2.126	102.428	5.098	4.114	10.500	5.888	5.168	5.555	6.054	5.639	5.129	9.417	6.171	6.069	5.697	3.866	4.081	4.581	4.630	5.859	6.940	8.717	8.575	10.817	16.291	15.008
9	2009	3.898	1.750	1.232	8.118	11.830	10.682	12.734	25.008	11.981	11.045	11.089	8.361	14.435	7.806	5.631	4.456	4.341	5.959	5.313	7.589	6.909	11.835	10.658	13.214	31.543	17.545
10	2009	6.369	4.212	2.343	10.409	18.095	11.523	17.251	9.533	12.225	9.643	6.161	9.135	8.918	8.365	8.893	4.673	4.735	5.906	6.618	5.893	8.290	12.076	11.359	16.945	11.982	15.929
11	2009	1.991	2.108	4.627	4.751	4.581	6.115	12.478	7.705	8.461	13.603	7.633	6.860	3.964	3.717	3.813	5.308	4.558	4.984	6.283	5.911	6.654	8.376	10.088	10.079	11.367	13.220
12	2009	0.795	1.494	0.812	214.080	3.395	13.433	1.799	6.615	4.201	2.087	2.694	3.325	5.581	2.687	7.885	3.299	3.191	6.258	25.359	6.705	7.125	8.324	12.342	68.634	17.994	440.098

Table A.33: CLOVAR ozone concentration (m^{-3})

CLOVAR: Ozone concentration per height increment

Year	75	76	77	78	79	80	81	82	83	84	85	86	87	88	89	90	91	92	93	94	95	96	97	98	99	100
	(km)	(km)	(km)	(km)	(km)	(km)	(km)	(km)	(km)	(km)	(km)	(km)	(km)	(km)	(km)	(km)	(km)	(km)	(km)	(km)	(km)	(km)	(km)	(km)	(km)	(km)
2000	1.94E+12	7.13E+13	1.05E+14	9.62E+13	6.85E+13	4.77E+13	3.98E+13	3.87E+13	4.29E+13	5.82E+13	8.74E+13	1.22E+14	1.48E+14	1.55E+14	1.45E+14	1.27E+14	1.07E+14	8.54E+13	6.41E+13	4.47E+13	2.99E+13	2.00E+13	1.39E+13	9.80E+12	6.54E+12	3.75E+12
2000	3.83E+14	2.69E+14	1.70E+14	9.80E+13	5.44E+13	3.11E+13	2.14E+13	2.48E+13	3.97E+13	6.01E+13	8.23E+13	1.07E+14	1.30E+14	1.43E+14	1.38E+14	1.18E+14	9.33E+13	7.10E+13	5.35E+13	3.99E+13	2.89E+13	2.03E+13	1.40E+13	9.76E+12	6.84E+12	4.69E+12
2000	9.23E+13	2.07E+14	2.33E+14	1.69E+14	8.37E+13	3.17E+13	1.92E+13	2.85E+13	4.67E+13	6.91E+13	8.96E+13	1.01E+14	1.06E+14	1.11E+14	1.16E+14	1.14E+14	1.00E+14	8.02E+13	5.98E+13	4.31E+13	3.05E+13	2.10E+13	1.40E+13	9.06E+12	5.96E+12	4.13E+12
2000	2.23E+13	9.74E+13	1.28E+14	1.08E+14	6.34E+13	2.64E+13	1.03E+13	1.50E+13	3.68E+13	7.09E+13	1.08E+14	1.37E+14	1.54E+14	1.57E+14	1.49E+14	1.31E+14	1.06E+14	8.15E+13	6.04E+13	4.43E+13	3.21E+13	2.25E+13	1.52E+13	9.99E+12	6.74E+12	4.85E+12
2000	8.81E+13	2.42E+14	2.95E+14	2.39E+14	1.41E+14	6.34E+13	2.85E+13	2.96E+13	4.96E+13	7.50E+13	1.01E+14	1.26E+14	1.45E+14	1.49E+14	1.41E+14	1.24E+14	1.03E+14	8.13E+13	6.11E+13	4.46E+13	3.22E+13	2.29E+13	1.60E+13	1.08E+13	7.18E+12	4.63E+12
2000	2.00E+14	2.08E+14	1.82E+14	1.26E+14	6.90E+13	3.23E+13	2.01E+13	3.30E+13	7.24E+13	1.25E+14	1.61E+14	1.54E+14	1.13E+14	7.18E+13	5.46E+13	5.78E+13	6.40E+13	6.26E+13	5.38E+13	4.19E+13	3.01E+13	2.04E+13	1.33E+13	8.89E+12	6.33E+12	4.81E+12
2001	5.39E+13	9.09E+13	1.12E+14	1.11E+14	9.33E+13	6.86E+13	4.51E+13	2.83E+13	2.36E+13	3.30E+13	5.23E+13	7.33E+13	9.00E+13	1.02E+14	1.12E+14	1.15E+14	1.05E+14	8.23E+13	5.50E+13	3.25E+13	1.97E+13	1.49E+13	1.34E+13	1.13E+13	7.81E+12	3.98E+12
2001	3.82E+14	2.87E+14	1.81E+14	8.16E+13	1.99E+13	2.25E+12	7.46E+12	1.38E+13	1.94E+13	3.55E+13	6.53E+13	9.32E+13	1.02E+14	9.28E+13	8.43E+13	8.41E+13	8.42E+13	7.50E+13	5.70E+13	3.73E+13	2.30E+13	1.60E+13	1.32E+13	1.05E+13	6.18E+12	9.53E+11
2001	3.10E+14	2.21E+14	1.45E+14	8.60E+13	4.52E+13	2.44E+13	2.24E+13	3.08E+13	3.79E+13	3.87E+13	4.03E+13	5.55E+13	8.73E+13	1.21E+14	1.35E+14	1.24E+14	9.81E+13	7.30E+13	5.46E+13	4.14E+13	3.09E+13	2.23E+13	1.57E+13	1.05E+13	5.63E+12	7.08E+11
2002	2.47E+14	1.90E+14	1.26E+14	6.46E+13	2.25E+13	8.57E+12	1.51E+13	2.82E+13	3.80E+13	4.32E+13	5.04E+13	6.82E+13	9.62E+13	1.22E+14	1.34E+14	1.29E+14	1.12E+14	8.93E+13	6.46E+13	4.29E+13	2.76E+13	1.85E+13	1.31E+13	9.22E+12	6.51E+12	5.00E+12
2002	2.62E+14	1.83E+14	1.05E+14	4.67E+13	1.88E+13	1.30E+13	1.32E+13	1.29E+13	1.46E+13	2.40E+13	4.44E+13	7.25E+13	9.60E+13	1.02E+14	8.90E+13	7.13E+13	6.09E+13	5.80E+13	5.35E+13	4.17E+13	2.58E+13	1.30E+13	6.85E+12	5.42E+12	5.21E+12	4.52E+12
2002	5.64E+11	5.51E+13	7.60E+13	6.59E+13	5.10E+13	4.56E+13	4.29E+13	3.56E+13	2.89E+13	3.23E+13	4.66E+13	6.49E+13	8.03E+13	9.02E+13	9.33E+13	8.80E+13	7.58E+13	6.08E+13	4.62E+13	3.23E+13	2.06E+13	1.34E+13	1.03E+13	8.77E+12	7.12E+12	5.36E+12
2002	2.76E+12	1.40E+14	1.88E+14	1.43E+14	6.73E+13	1.79E+13	4.80E+12	1.11E+13	1.96E+13	2.46E+13	3.10E+13	4.75E+13	7.66E+13	1.07E+14	1.23E+14	1.16E+14	9.50E+13	7.12E+13	5.14E+13	3.67E+13	2.61E+13	1.86E+13	1.38E+13	1.04E+13	7.30E+12	4.17E+12
2002	3.20E+14	2.74E+14	2.54E+14	2.33E+14	1.76E+14	9.14E+13	2.09E+13	-5.93E+12	1.08E+13	5.40E+13	1.03E+14	1.40E+14	1.55E+14	1.47E+14	1.25E+14	9.94E+13	8.02E+13	6.50E+13	4.93E+13	3.38E+13	2.27E+13	1.66E+13	1.29E+13	9.43E+12	6.54E+12	4.75E+12
2002	4.30E+14	3.74E+14	3.31E+14	2.78E+14	1.93E+14	9.92E+13	3.90E+13	2.65E+13	4.15E+13	5.84E+13	6.80E+13	7.36E+13	8.03E+13	8.79E+13	9.30E+13	9.25E+13	8.59E+13	7.35E+13	5.68E+13	3.99E+13	2.74E+13	2.00E+13	1.54E+13	1.11E+13	5.96E+12	1.79E+11
2002	4.90E+14	2.79E+14	1.62E+14	1.36E+14	1.31E+14	1.06E+14	7.00E+13	4.69E+13	4.58E+13	5.84E+13	7.33E+13	8.73E+13	1.01E+14	1.09E+14	1.07E+14	9.75E+13	8.40E+13	7.01E+13	5.60E+13	4.24E+13	3.06E+13	2.12E+13	1.40E+13	8.77E+12	5.69E+12	4.35E+12
2002	3.03E+13	1.41E+14	1.75E+14	1.30E+14	6.56E+13	2.32E+13	8.34E+12	1.05E+13	2.38E+13	4.58E+13	6.95E+13	8.63E+13	9.53E+13	1.02E+14	1.09E+14	1.08E+14	9.53E+13	7.48E+13	5.43E+13	3.87E+13	2.82E+13	2.09E+13	1.53E+13	1.03E+13	5.34E+12	8.93E+10
2002	8.61E+14	3.36E+14	2.95E+13	-2.86E+13	2.89E+13	7.11E+13	6.28E+13	3.37E+13	1.41E+13	1.06E+13	1.99E+13	4.08E+13	6.91E+13	9.28E+13	1.00E+14	9.11E+13	7.55E+13	6.15E+13	5.06E+13	4.09E+13	3.02E+13	1.88E+13	8.98E+12	3.41E+12	2.67E+12	4.94E+12
2002	n/a	1.03E+14	1.46E+14	1.19E+14	6.09E+13	1.40E+13	-3.84E+12	1.23E+12	1.64E+13	3.13E+13	3.92E+13	4.09E+13	4.65E+13	6.42E+13	8.71E+13	9.87E+13	9.11E+13	7.13E+13	5.08E+13	3.62E+13	2.69E+13	1.98E+13	1.29E+13	7.39E+12	4.96E+12	5.38E+12
2002	2.65E+14	2.37E+14	1.75E+14	9.24E+13	3.00E+13	4.35E+12	4.97E+12	1.61E+13	3.09E+13	4.93E+13	6.92E+13	8.34E+13	8.68E+13	8.40E+13	8.43E+13	8.86E+13	8.82E+13	7.73E+13	6.02E+13	4.40E+13	3.21E+13	2.34E+13	1.65E+13	1.11E+13	7.53E+12	5.46E+12
2002	3.89E+12	5.27E+13	8.29E+13	8.29E+13	5.81E+13	2.82E+13	9.91E+12	6.50E+12	1.29E+13	2.63E+13	4.77E+13	7.35E+13	9.29E+13	9.94E+13	9.78E+13	9.51E+13	9.00E+13	7.78E+13	5.95E+13	4.08E+13	2.70E+13	1.87E+13	1.41E+13	1.06E+13	7.10E+12	3.51E+12
2003	2.22E+14	1.31E+14	6.33E+13	2.99E+13	2.22E+13	2.42E+13	2.50E+13	2.24E+13	1.95E+13	2.11E+13	3.27E+13	5.81E+13	9.37E+13	1.24E+14	1.30E+14	1.08E+14	7.25E+13	4.29E+13	2.96E+13	2.75E+13	2.74E+13	2.40E+13	1.80E+13	1.20E+13	7.49E+12	4.42E+12
2003	3.21E+14	2.10E+14	1.19E+14	5.89E+13	2.67E+13	1.36E+13	1.18E+13	1.52E+13	2.01E+13	2.49E+13	3.16E+13	4.41E+13	6.38E+13	8.43E+13	9.44E+13	8.90E+13	7.19E+13	5.08E+13	3.30E+13	2.35E+13	2.14E+13	2.08E+13	1.74E+13	1.12E+13	4.99E+12	1.90E+11
2003	1.91E+14	1.28E+14	8.04E+13	5.00E+13	2.97E+13	1.46E+13	5.04E+12	2.46E+12	6.24E+12	1.51E+13	2.89E+13	4.77E+13	6.95E+13	9.01E+13	1.03E+14	1.05E+14	9.32E+13	7.36E+13	5.25E+13	3.49E+13	2.32E+13	1.73E+13	1.47E+13	1.24E+13	9.13E+12	5.12E+12
2003	1.17E+14	1.23E+14	1.25E+14	1.12E+14	8.10E+13	4.24E+13	1.43E+13	5.06E+12	1.12E+13	2.31E+13	3.20E+13	3.53E+13	3.86E+13	5.05E+13	7.26E+13	9.35E+13	9.88E+13	8.57E+13	6.38E+13	4.38E+13	2.98E+13	2.03E+13	1.32E+13	8.40E+12	5.83E+12	4.84E+12
2003	1.08E+14	1.59E+14	1.79E+14	1.56E+14	1.05E+14	5.47E+13	2.61E+13	2.32E+13	3.65E+13	5.27E+13	6.32E+13	7.03E+13	8.31E+13	1.05E+14	1.26E+14	1.32E+14	1.16E+14	8.79E+13	5.91E+13	3.86E+13	2.69E+13	2.03E+13	1.54E+13	1.09E+13	6.98E+12	3.94E+12
2003	4.06E+14	3.40E+14	2.62E+14	1.78E+14	1.08E+14	6.66E+13	5.12E+13	4.86E+13	4.85E+13	5.06E+13	6.22E+13	8.84E+13	1.22E+14	1.48E+14	1.53E+14	1.38E+14	1.11E+14	8.28E+13	5.85E+13	4.06E+13	2.84E+13	2.01E+13	1.44E+13	1.02E+13	7.25E+12	5.06E+12
2003	1.38E+14	2.98E+14	3.54E+14	2.90E+14	1.74E+14	8.42E+13	4.61E+13	4.20E+13	4.96E+13	6.04E+13	7.62E+13	9.87E+13	1.21E+14	1.31E+14	1.29E+14	1.18E+14	1.04E+14	8.64E+13	6.70E+13	4.81E+13	3.25E+13	2.16E+13	1.47E+13	1.05E+13	7.61E+12	5.28E+12
2003	5.29E+14	3.14E+14	1.57E+14	7.80E+13	5.27E+13	4.56E+13	3.78E+13	3.06E+13	3.20E+13	4.50E+13	6.62E+13	8.91E+13	1.08E+14	1.22E+14	1.28E+14	1.24E+14	1.09E+14	8.58E+13	6.26E+13	4.43E+13	3.16E+13	2.30E+13	1.65E+13	1.14E+13	7.42E+12	4.36E+12
2003	2.32E+12	1.00E+14	1.30E+14	9.16E+13	3.62E+13	4.99E+12	2.20E+12	1.34E+13	2.68E+13	3.91E+13	5.15E+13	6.54E+13	8.10E+13	9.74E+13	1.10E+14	1.11E+14	9.74E+13	7.62E+13	5.59E+13	4.06E+13	2.99E+13	2.22E+13	1.62E+13	1.10E+13	5.61E+12	7.91E+10
2003	n/a	1.72E+13	3.76E+13	5.21E+13	4.84E+13	2.83E+13	7.28E+12	-2.51E+12	-3.93E+11	9.23E+12	2.46E+13	4.58E+13	6.97E+13	8.90E+13	9.83E+13	9.75E+13	8.90E+13	7.46E+13	5.61E+13	3.72E+13	2.22E+13	1.34E+13	9.77E+12	8.31E+12	6.65E+12	4.30E+12
2007	1.39E+14	1.48E+14	1.52E+14	1.38E+14	9.60E+13	4.28E+13	7.17E+12	6.80E+12	3.80E+13	8.14E+13	1.12E+14	1.15E+14	1.00E+14	8.99E+13	9.30E+13	9.82E+13	9.16E+13	7.27E+13	5.12E+13	3.53E+13	2.57E+13	1.89E+13	1.24E+13	6.58E+12	2.48E+12	2.38E+10
2008	2.55E+14	9.03E+13	5.35E+11	-1.63E+12	3.49E+13	5.46E+13	4.26E+13	2.81E+13	5.04E+13	1.16E+14	1.82E+14	1.98E+14	1.63E+14	1.23E+14	1.10E+14	1.08E+14	9.25E+13	6.32E+13	3.73E+13	2.46E+13	2.08E+13	1.82E+13	1.34E+13	7.96E+12	3.33E+12	-2.68E+11
2008	n/a	5.27E+13	7.13E+13	5.50E+13	2.84E+13	1.08E+13	6.37E+12	1.28E+13	2.90E+13	5.17E+13	7.33E+13	8.76E+13	9.34E+13	9.07E+13	7.74E+13	5.73E+13	4.24E+13	3.84E+13	3.87E+13	3.41E+13	2.42E+13	1.40E+13	7.86E+12	5.85E+12	5.58E+12	5.22E+12
2008	4.67E+12	1.01E+14	1.32E+14	9.39E+13	3.75E+13	3.29E+12	-3.45E+12	5.36E+12	2.29E+13	4.90E+13	7.96E+13	1.04E+14	1.11E+14	1.04E+14	9.23E+13	8.42E+13	7.81E+13	7.00E+13	5.87E+13	4.58E+13	3.29E+13	2.06E+13	1.04E+13	4.29E+12	2.94E+12	4.92E+12
2008	8.55E+13	7.23E+13	5.99E+13	4.60E+13	3.13E+13	2.12E+13	1.80E+13	1.80E+13	1.66E+13	1.49E+13	2.03E+13	4.00E+13	7.29E+13	1.07E+14	1.28E+14	1.30E+14	1.13E+14	8.62E+13	5.64E+13	3.18E+13	1.70E+13	1.18E+13	1.13E+13	1.06E+13	8.13E+12	4.72E+12
2008	3.45E+14	2.69E+14	1.95E+14	1.25E+14	6.82E+13	3.46E+13	2.10E+13	1.66E+13	1.44E+13	1.59E+13	2.68E+13	4.91E+13	7.85E+13	1.06E+14	1.21E+14	1.21E+14	1.08E+14	8.79E+13	6.58E+13	4.69E+13	3.36E+13	2.52E+13	1.95E+13	1.49E+13	1.10E+13	7.56E+12
2008	1.25E+14	2.09E+14	2.32E+14	1.81E+14	9.57E+13	2.74E+13	-1.07E+09	2.43E+12	1.35E+13	2.37E+13	3.62E+13	5.68E+13	8.57E+13	1.16E+14	1.35E+14	1.37E+14	1.21E+14	9.70E+13	7.39E+13	5.54E+13	4.12E+13	2.95E+13	1.95E+13	1.20E+13	7.97E+12	6.88E+12

Table A.34: Costa Rica ozone concentration (m^{-3})

Costa Rica: Ozone concentration per height increment

Month	Year	75 (km)	76 (km)	77 (km)	78 (km)	79 (km)	80 (km)	81 (km)	82 (km)	83 (km)	84 (km)	85 (km)	86 (km)	87 (km)	88 (km)	89 (km)	90 (km)	91 (km)	92 (km)	93 (km)	94 (km)	95 (km)	96 (km)	97 (km)	98 (km)	99 (km)	100 (km)
4	2005	1.18E+14	6.45E+13	3.01E+13	1.80E+13	1.74E+13	1.79E+13	1.59E+13	1.23E+13	8.59E+12	6.69E+12	9.08E+12	1.73E+13	2.96E+13	4.13E+13	4.83E+13	5.14E+13	5.39E+13	5.59E+13	5.34E+13	4.45E+13	3.26E+13	2.26E+13	1.62E+13	1.20E+13	8.95E+12	6.35E+12
5	2005	4.58E+13	2.87E+13	1.93E+13	1.80E+13	1.89E+13	1.70E+13	1.20E+13	6.72E+12	3.96E+12	5.01E+12	1.02E+13	1.88E+13	2.87E+13	3.70E+13	4.28E+13	4.78E+13	5.29E+13	5.63E+13	5.48E+13	4.76E+13	3.73E+13	2.70E+13	1.88E+13	1.30E+13	9.05E+12	6.14E+12
6	2005	9.62E+13	7.13E+13	4.97E+13	3.23E+13	1.91E+13	1.11E+13	7.77E+12	7.14E+12	7.26E+12	7.99E+12	1.04E+13	1.52E+13	2.24E+13	3.13E+13	4.00E+13	4.62E+13	4.84E+13	4.70E+13	4.35E+13	3.83E+13	3.13E+13	2.32E+13	1.53E+13	9.31E+12	6.07E+12	4.75E+12
7	2005	1.48E+14	9.31E+13	5.33E+13	3.38E+13	2.76E+13	2.65E+13	2.44E+13	1.98E+13	1.43E+13	1.20E+13	1.57E+13	2.38E+13	3.20E+13	3.74E+13	4.08E+13	4.41E+13	4.69E+13	4.73E+13	4.44E+13	3.90E+13	3.22E+13	2.48E+13	1.79E+13	1.24E+13	8.47E+12	5.77E+12
8	2005	1.54E+14	9.51E+13	6.06E+13	5.14E+13	4.95E+13	4.15E+13	2.81E+13	1.60E+13	9.82E+12	9.96E+12	1.50E+13	2.35E+13	3.39E+13	4.34E+13	4.94E+13	5.11E+13	5.04E+13	4.84E+13	4.51E+13	3.99E+13	3.28E+13	2.52E+13	1.82E+13	1.28E+13	9.07E+12	6.49E+12
9	2005	2.51E+14	1.35E+14	5.82E+13	3.11E+13	3.30E+13	3.66E+13	3.02E+13	1.85E+13	1.02E+13	7.84E+12	7.91E+12	1.23E+13	2.04E+13	3.00E+13	3.87E+13	4.48E+13	4.88E+13	5.18E+13	5.35E+13	5.21E+13	4.58E+13	3.59E+13	2.56E+13	1.74E+13	1.18E+13	7.71E+12	4.13E+12
10	2005	2.42E+14	1.44E+14	7.31E+13	3.62E+13	2.24E+13	1.78E+13	1.46E+13	1.08E+13	7.84E+12	7.91E+12	1.23E+13	2.04E+13	3.00E+13	3.87E+13	4.48E+13	4.88E+13	5.18E+13	5.35E+13	5.21E+13	4.58E+13	3.59E+13	2.56E+13	1.74E+13	1.18E+13	7.71E+12	4.13E+12
11	2005	6.06E+13	5.99E+13	5.04E+13	3.27E+13	1.54E+13	5.77E+12	5.22E+12	1.02E+13	1.62E+13	2.13E+13	2.63E+13	3.13E+13	3.43E+13	3.44E+13	3.51E+13	4.06E+13	4.84E+13	5.06E+13	4.33E+13	3.15E+13	2.24E+13	1.78E+13	1.51E+13	1.19E+13	8.63E+12	5.92E+12
12	2005	3.04E+14	1.33E+14	2.90E+13	1.45E+12	1.16E+13	2.23E+13	2.30E+13	1.81E+13	1.29E+13	9.95E+12	1.18E+13	2.04E+13	3.49E+13	5.02E+13	6.04E+13	6.41E+13	6.36E+13	6.06E+13	5.46E+13	4.54E+13	3.52E+13	2.63E+13	1.94E+13	1.41E+13	9.87E+12	6.41E+12
1	2006	8.18E+13	1.23E+14	1.28E+14	9.54E+13	5.57E+13	3.04E+13	2.09E+13	1.81E+13	1.46E+13	1.04E+13	9.63E+12	1.67E+13	3.19E+13	5.09E+13	6.73E+13	7.66E+13	7.81E+13	7.34E+13	6.43E+13	5.21E+13	3.92E+13	2.81E+13	1.97E+13	1.39E+13	9.68E+12	6.35E+12
4	2007	9.88E+13	6.36E+13	3.45E+13	1.58E+13	7.79E+12	6.30E+12	6.36E+12	5.78E+12	4.98E+12	5.10E+12	7.17E+12	1.26E+13	2.31E+13	3.79E+13	5.17E+13	5.79E+13	5.44E+13	4.60E+13	3.94E+13	3.63E+13	3.31E+13	2.68E+13	1.87E+13	1.19E+13	8.10E+12	6.56E+12
5	2007	5.21E+13	4.68E+13	3.97E+13	3.10E+13	2.28E+13	1.60E+13	1.10E+13	7.56E+12	5.52E+12	5.30E+12	7.89E+12	1.43E+13	2.43E+13	3.66E+13	4.95E+13	6.08E+13	6.76E+13	6.88E+13	5.89E+13	4.73E+13	3.58E+13	2.63E+13	1.89E+13	1.33E+13	9.10E+12	5.70E+12
6	2007	1.02E+14	6.30E+13	3.31E+13	1.55E+13	8.17E+12	6.62E+12	6.88E+12	6.69E+12	5.98E+12	6.37E+12	9.77E+12	1.70E+13	2.71E+13	3.84E+13	4.93E+13	5.85E+13	6.37E+13	6.23E+13	5.44E+13	4.31E+13	3.24E+13	2.39E+13	1.72E+13	1.20E+13	8.32E+12	5.96E+12
7	2007	2.27E+13	4.37E+13	5.03E+13	4.10E+13	2.60E+13	1.48E+13	9.96E+12	9.02E+12	9.31E+12	1.00E+13	1.21E+13	1.73E+13	2.75E+13	4.21E+13	5.74E+13	6.81E+13	7.08E+13	6.51E+13	5.36E+13	4.08E+13	3.02E+13	2.30E+13	1.78E+13	1.33E+13	9.19E+12	5.58E+12
8	2007	4.19E+13	2.71E+13	1.81E+13	1.47E+13	1.30E+13	1.05E+13	7.58E+12	4.94E+12	3.31E+12	4.41E+12	1.06E+13	2.22E+13	3.64E+13	4.82E+13	5.47E+13	5.72E+13	5.84E+13	5.76E+13	5.18E+13	4.06E+13	2.82E+13	1.90E+13	1.38E+13	1.09E+13	8.29E+12	5.35E+12
9	2007	9.39E+13	6.42E+13	3.71E+13	1.80E+13	1.01E+13	9.82E+12	1.08E+13	9.66E+12	7.17E+12	6.19E+12	8.78E+12	1.53E+13	2.48E+13	3.63E+13	4.85E+13	5.93E+13	6.55E+13	6.44E+13	5.55E+13	4.25E+13	3.02E+13	2.15E+13	1.61E+13	1.21E+13	8.31E+12	4.57E+12
10	2007	1.19E+14	5.26E+13	1.19E+13	1.08E+12	5.87E+12	1.13E+13	1.18E+13	8.66E+12	5.31E+12	4.22E+12	6.39E+12	1.19E+13	2.10E+13	3.44E+13	5.12E+13	6.78E+13	7.86E+13	7.95E+13	7.05E+13	5.54E+13	3.96E+13	2.67E+13	1.76E+13	1.18E+13	8.20E+12	5.82E+12
11	2007	1.25E+14	5.11E+13	7.02E+12	-3.15E+12	3.98E+12	1.11E+13	1.21E+13	9.22E+12	5.83E+12	3.50E+12	3.40E+12	7.71E+12	1.83E+13	3.42E+13	5.07E+13	6.29E+13	6.91E+13	7.04E+13	6.60E+13	5.49E+13	3.96E+13	2.58E+13	1.68E+13	1.17E+13	8.32E+12	5.10E+12
12	2007	3.50E+14	1.54E+14	2.95E+13	-8.20E+12	4.12E+12	2.20E+13	2.55E+13	1.75E+13	8.48E+12	6.81E+12	1.69E+13	3.93E+13	6.84E+13	9.46E+13	1.10E+14	1.12E+14	1.06E+14	9.50E+13	7.88E+13	6.00E+13	4.26E+13	2.95E+13	2.06E+13	1.47E+13	1.05E+13	7.08E+12
1	2008	6.35E+13	4.71E+13	3.82E+13	3.48E+13	3.04E+13	2.33E+13	1.65E+13	1.14E+13	7.56E+12	6.18E+12	1.12E+13	2.55E+13	4.68E+13	6.83E+13	8.41E+13	9.25E+13	9.35E+13	8.67E+13	7.34E+13	5.70E+13	4.14E+13	2.89E+13	2.01E+13	1.42E+13	1.01E+13	6.98E+12
2	2008	1.49E+14	9.00E+13	4.55E+13	2.26E+13	1.77E+13	1.94E+13	1.85E+13	1.41E+13	1.06E+13	1.15E+13	1.68E+13	2.45E+13	3.43E+13	4.66E+13	6.05E+13	7.32E+13	8.08E+13	7.98E+13	6.96E+13	5.43E+13	3.93E+13	2.76E+13	1.92E+13	1.31E+13	8.96E+12	6.24E+12
3	2008	1.96E+13	2.42E+13	2.47E+13	2.00E+13	1.31E+13	7.48E+12	5.23E+12	5.61E+12	6.38E+12	6.53E+12	7.54E+12	1.29E+13	2.55E+13	4.45E+13	6.34E+13	7.35E+13	7.12E+13	6.11E+13	5.06E+13	4.29E+13	3.63E+13	2.89E+13	2.10E+13	1.41E+13	9.31E+12	6.26E+12
4	2008	2.97E+13	3.44E+13	3.29E+13	2.51E+13	1.62E+13	1.10E+13	9.35E+12	8.73E+12	7.35E+12	6.45E+12	9.48E+12	1.91E+13	3.43E+13	5.07E+13	6.34E+13	6.96E+13	6.94E+13	6.43E+13	5.63E+13	4.68E+13	3.71E+13	2.81E+13	2.04E+13	1.42E+13	9.17E+12	4.77E+12
5	2008	7.22E+13	5.73E+13	4.02E+13	2.29E+13	1.04E+13	5.19E+12	5.21E+12	6.54E+12	7.07E+12	8.13E+12	1.29E+13	2.28E+13	3.57E+13	4.69E+13	5.42E+13	5.86E+13	6.16E+13	6.17E+13	5.69E+13	4.75E+13	3.59E+13	2.50E+13	1.67E+13	1.11E+13	7.77E+12	5.53E+12
6	2008	4.92E+12	2.09E+13	2.83E+13	2.56E+13	1.81E+13	1.21E+13	9.24E+12	7.79E+12	6.17E+12	5.26E+12	7.42E+12	1.40E+13	2.39E+13	3.49E+13	4.56E+13	5.50E+13	6.18E+13	6.38E+13	5.92E+13	4.88E+13	3.56E+13	2.43E+13	1.68E+13	1.22E+13	8.68E+12	5.11E+12
7	2008	4.04E+13	2.97E+13	2.32E+13	2.03E+13	1.78E+13	1.41E+13	1.02E+13	7.28E+12	5.63E+12	6.94E+12	1.28E+13	2.26E+13	3.38E+13	4.34E+13	4.99E+13	5.35E+13	5.44E+13	5.28E+13	4.88E+13	4.27E+13	3.51E+13	2.67E+13	1.87E+13	1.22E+13	7.76E+12	4.68E+12
8	2008	1.96E+14	1.10E+14	5.03E+13	2.35E+13	1.71E+13	1.68E+13	1.44E+13	1.05E+13	7.97E+12	9.24E+12	1.39E+13	2.07E+13	3.03E+13	4.52E+13	6.42E+13	7.81E+13	7.75E+13	6.28E+13	4.43E+13	3.11E+13	2.47E+13	2.14E+13	1.82E+13	1.41E+13	9.82E+12	5.67E+12
9	2008	2.95E+14	1.40E+14	3.68E+13	-7.55E+11	1.45E+12	1.18E+13	1.49E+13	1.15E+13	7.00E+12	5.54E+12	8.13E+12	1.43E+13	2.36E+13	3.60E+13	5.07E+13	6.39E+13	7.07E+13	6.85E+13	5.92E+13	4.71E+13	3.54E+13	2.59E+13	1.86E+13	1.31E+13	8.92E+12	5.61E+12
10	2008	5.88E+13	6.03E+13	5.29E+13	3.83E+13	2.50E+13	1.72E+13	1.28E+13	9.22E+12	6.53E+12	6.57E+12	1.07E+13	1.84E+13	2.87E+13	4.11E+13	5.48E+13	6.58E+13	6.91E+13	6.38E+13	5.40E+13	4.34E+13	3.32E+13	2.37E+13	1.60E+13	1.09E+13	7.84E+12	6.05E+12
11	2008	1.98E+14	8.57E+13	1.65E+13	-1.35E+12	8.43E+12	1.97E+13	2.15E+13	1.68E+13	1.14E+13	8.80E+12	1.03E+13	1.68E+13	2.75E+13	3.97E+13	5.06E+13	5.90E+13	6.30E+13	6.10E+13	5.38E+13	4.41E+13	3.37E+13	2.38E+13	1.59E+13	1.08E+13	8.34E+12	7.33E+12
3	2009	1.34E+14	1.57E+14	1.35E+14	7.89E+13	2.99E+13	1.01E+13	9.93E+12	1.30E+13	1.33E+13	1.72E+13	2.48E+13	3.16E+13	3.33E+13	3.00E+13	2.70E+13	2.97E+13	3.82E+13	4.67E+13	4.81E+13	4.08E+13	2.88E+13	1.74E+13	9.74E+12	6.19E+12	5.21E+12
10	2009	9.28E+13	7.00E+13	4.93E+13	3.16E+13	1.82E+13	1.03E+13	7.32E+12	7.21E+12	7.30E+12	6.63E+12	7.39E+12	1.37E+13	2.74E+13	4.46E+13	5.78E+13	6.29E+13	6.14E+13	5.70E+13	5.08E+13	4.29E+13	3.37E+13	2.46E+13	1.68E+13	1.13E+13	7.99E+12	6.07E+12
1	2010	n/a	5.39E+11	1.38E+12	2.05E+12	2.24E+12	3.25E+12	7.06E+12	1.27E+13	1.59E+13	1.42E+13	1.00E+13	7.33E+12	8.34E+12	1.28E+13	1.84E+13	2.12E+13	2.00E+13	1.70E+13	1.43E+13	1.15E+13	8.06E+12	5.47E+12	4.99E+12	5.19E+12	3.62E+12	n/a
2	2010	n/a	3.56E+13	5.32E+13	4.77E+13	2.90E+13	1.18E+13	3.52E+12	2.56E+12	4.51E+12	7.17E+12	1.04E+13	1.41E+13	1.80E+13	2.23E+13	2.77E+13	3.37E+13	3.75E+13	3.66E+13	3.12E+13	2.40E+13	1.76E+13	1.34E+13	1.10E+13	9.17E+12	6.92E+12	4.20E+12
3	2010	1.25E+14	1.13E+14	8.69E+13	5.33E+13	2.72E+13	1.41E+13	9.03E+12	6.44E+12	4.51E+12	4.25E+12	7.19E+12	1.34E+13	2.10E+13	2.73E+13	3.14E+13	3.43E+13	3.78E+13	4.15E+13	4.29E+13	3.92E+13	3.09E+13	2.14E+13	1.43E+13	1.03E+13	8.01E+12	6.06E+12
4	2010	1.70E+14	1.13E+14	7.20E+13	4.99E+13	3.66E+13	2.57E+13	1.64E+13	9.96E+12	6.99E+12	7.39E+12	1.04E+13	1.49E+13	1.97E+13	2.48E+13	2.98E+13	3.42E+13	3.63E+13	3.55E+13	3.21E+13	2.73E+13	2.25E+13	1.87E+13	1.57E+13	1.25E+13	8.20E+12	3.04E+12
6	2010	1.26E+14	7.38E+13	3.81E+13	2.35E+13	2.14E+13	2.04E+13	1.62E+13	1.10E+13	7.70E+12	7.23E+12	9.45E+12	1.37E+13	1.92E+13	2.55E+13	3.27E+13	4.01E+13	4.57E+13	4.72E+13	4.37E+13	3.64E+13	2.76E+13	1.97E+13	1.40E+13	1.03E+13	7.62E+12	5.20E+12
7	2010	1.01E+14	6.06E+13	4.09E+13	4.26E+13	4.89E+13	3.03E+13	1.48E+13	6.76E+12	7.19E+12	1.24E+13	1.82E+13	2.26E+13	2.55E+13	2.77E+13	2.89E+13	2.89E+13	2.78E+13	2.59E+13	2.35E+13	2.07E+13	1.73E+13	1.36E+13	1.02E+13	7.61E+12	5.74E+12
8	2010	9.14E+13	5.09E+13	2.99E+13	2.93E+13	3.48E+13	3.44E+13	2.67E+13	1.72E+13	1.08E+13	9.54E+12	1.28E+13	1.85E+13	2.43E+13	2.92E+13	3.45E+13	4.09E+13	4.63E+13	4.74E+13	4.25E+13	3.38E+13	2.48E+13	1.81E+13	1.38E+13	1.06E+13	8.00E+12	5.57E+12
9	2010	1.17E+14	1.02E+14	8.19E+13	5.88E+13	3.64E+13	2.06E+13	1.25E+13	9.56E+12	9.15E+12	1.04E+13	1.32E+13	1.80E+13	2.47E+13	3.26E+13	4.03E+13	4.61E+13	4.89E+13	4.79E+13	4.36E+13	3.71E+13	3.00E+13	2.34E+13	1.75E+13	1.26E+13	8.79E+12	5.82E+12
10	2010	1.14E+13	5.38E+13	7.12E+13	5.94E+13	3.46E+13	1.51E+13	7.29E+12	7.06E+12	8.34E+12	8.90E+12	9.93E+12	1.35E+13	2.02E+13	2.86E+13	3.53E+13	3.79E+13	3.77E+13	3.70E+13	3.61E+13	3.29E+13	2.72E+13	2.05E+13	1.49E+13	1.10E+13	8.37E+12	6.41E+12
11	2010	2.93E+12	3.55E+13	5.09E+13	4.48E+13	2.78E+13	1.34E+13	6.58E+12	4.89E+12	4.88E+12	5.62E+12	7.89E+12	1.23E+13	1.82E+13	2.42E+13	2.97E+13	3.49E+13	3.87E+13	3.87E+13	3.37E+13	2.61E+13	1.96E+13	1.59E+13	1.37E+13	1.11E+13	7.74E+12	4.03E+12

Table A.35: Resolute Bay ozone concentration (m^{-3}) (part 1)

Resolute Bay: Ozone concentration per height increment

Year	75 (km)	76 (km)	77 (km)	78 (km)	79 (km)	80 (km)	81 (km)	82 (km)	83 (km)	84 (km)	85 (km)	86 (km)	87 (km)	88 (km)	89 (km)	90 (km)	91 (km)	92 (km)	93 (km)	94 (km)	95 (km)	96 (km)	97 (km)	98 (km)	99 (km)	100 (km)
2000	--	--	7.58E+13	7.34E+13	6.64E+13	5.61E+13	4.69E+13	4.33E+13	4.86E+13	6.25E+13	8.00E+13	9.54E+13	1.06E+14	1.12E+14	1.10E+14	1.00E+14	8.45E+13	6.69E+13	5.11E+13	3.80E+13	2.73E+13	1.88E+13	1.26E+13	8.74E+12	6.55E+12	5.29E+12
2000	--	--	5.94E+13	6.39E+13	6.23E+13	5.32E+13	4.10E+13	3.39E+13	3.96E+13	6.06E+13	9.10E+13	1.20E+14	1.36E+14	1.37E+14	1.25E+14	1.08E+14	8.96E+13	7.24E+13	5.60E+13	4.11E+13	2.88E+13	1.99E+13	1.39E+13	9.87E+12	6.76E+12	4.08E+12
2000	--	--	3.24E+13	4.01E+13	4.15E+13	3.69E+13	3.29E+13	3.75E+13	5.59E+13	8.78E+13	1.27E+14	1.61E+14	1.81E+14	1.81E+14	1.65E+14	1.38E+14	1.09E+14	8.19E+13	6.04E+13	4.41E+13	3.17E+13	2.22E+13	1.53E+13	1.05E+13	7.08E+12	4.50E+12
2000	--	--	4.11E+13	4.37E+13	4.37E+13	4.06E+13	3.94E+13	5.03E+13	8.16E+13	1.31E+14	1.83E+14	2.21E+14	2.33E+14	2.21E+14	1.91E+14	1.55E+14	1.19E+14	8.83E+13	6.47E+13	4.71E+13	3.40E+13	2.41E+13	1.67E+13	1.14E+13	7.58E+12	4.56E+12
2000	--	--	7.58E+13	7.31E+13	6.68E+13	5.73E+13	5.36E+13	7.06E+13	1.15E+14	1.77E+14	2.33E+14	2.63E+14	2.61E+14	2.34E+14	1.94E+14	1.54E+14	1.19E+14	8.98E+13	6.69E+13	4.89E+13	3.50E+13	2.44E+13	1.66E+13	1.12E+13	7.50E+12	4.83E+12
2000	--	--	7.27E+13	8.98E+13	9.33E+13	8.40E+13	7.65E+13	8.85E+13	1.29E+14	1.90E+14	2.47E+14	2.73E+14	2.62E+14	2.25E+14	1.82E+14	1.44E+14	1.14E+14	8.80E+13	6.41E+13	4.43E+13	3.04E+13	2.17E+13	1.61E+13	1.14E+13	6.53E+12	1.55E+12
2000	--	--	9.04E+13	6.67E+13	5.18E+13	4.88E+13	5.89E+13	8.64E+13	1.36E+14	2.00E+14	2.59E+14	2.91E+14	2.86E+14	2.51E+14	2.03E+14	1.55E+14	1.17E+14	8.83E+13	6.67E+13	4.92E+13	3.48E+13	2.38E+13	1.61E+13	1.10E+13	7.58E+12	4.93E+12
2001	1.68E+14	1.22E+14	8.81E+13	6.86E+13	5.62E+13	4.58E+13	3.95E+13	4.28E+13	5.86E+13	8.38E+13	1.12E+14	1.36E+14	1.49E+14	1.49E+14	1.38E+14	1.19E+14	9.62E+13	7.29E+13	5.16E+13	3.54E+13	2.49E+13	1.84E+13	1.38E+13	9.97E+12	6.73E+12	4.10E+12
2001	--	--	8.00E+13	9.10E+13	9.21E+13	8.20E+13	7.31E+13	8.46E+13	1.26E+14	1.86E+14	2.40E+14	2.67E+14	2.60E+14	2.29E+14	1.88E+14	1.46E+14	1.10E+14	8.11E+13	5.91E+13	4.25E+13	3.00E+13	2.09E+13	1.46E+13	1.03E+13	6.95E+12	4.13E+12
2001	--	--	6.27E+13	6.14E+13	5.63E+13	4.74E+13	4.17E+13	5.29E+13	9.09E+13	1.50E+14	2.09E+14	2.45E+14	2.45E+14	2.19E+14	1.82E+14	1.44E+14	1.10E+14	8.23E+13	6.01E+13	4.27E+13	2.96E+13	2.03E+13	1.38E+13	9.47E+12	6.79E+12	5.21E+12
2001	--	--	7.91E+13	7.37E+13	6.70E+13	5.89E+13	5.27E+13	5.64E+13	7.97E+13	1.23E+14	1.70E+14	2.00E+14	1.99E+14	1.76E+14	1.46E+14	1.18E+14	9.54E+13	7.54E+13	5.68E+13	4.07E+13	2.83E+13	1.95E+13	1.36E+13	9.46E+12	6.55E+12	4.40E+12
2001	--	--	8.97E+13	7.81E+13	6.36E+13	4.78E+13	3.67E+13	3.63E+13	4.95E+13	7.37E+13	1.02E+14	1.27E+14	1.42E+14	1.43E+14	1.31E+14	1.11E+14	8.90E+13	6.86E+13	5.12E+13	3.70E+13	2.62E+13	1.81E+13	1.24E+13	8.40E+12	5.80E+12	4.07E+12
2001	--	--	1.15E+14	7.99E+13	5.73E+13	4.90E+13	4.87E+13	5.24E+13	6.21E+13	8.02E+13	1.04E+14	1.27E+14	1.41E+14	1.44E+14	1.34E+14	1.15E+14	9.07E+13	6.76E+13	4.90E+13	3.55E+13	2.60E+13	1.90E+13	1.34E+13	9.03E+12	5.90E+12	3.71E+12
2001	--	--	1.19E+14	1.00E+14	8.30E+13	6.96E+13	6.18E+13	6.41E+13	8.01E+13	1.07E+14	1.36E+14	1.56E+14	1.62E+14	1.54E+14	1.36E+14	1.13E+14	8.95E+13	6.79E+13	5.04E+13	3.70E+13	2.69E+13	1.92E+13	1.34E+13	9.09E+12	6.12E+12	4.03E+12
2001	--	--	9.68E+13	8.01E+13	6.47E+13	5.25E+13	4.67E+13	5.19E+13	7.17E+13	1.04E+14	1.39E+14	1.65E+14	1.73E+14	1.65E+14	1.48E+14	1.26E+14	1.02E+14	7.88E+13	5.82E+13	4.16E+13	2.94E+13	2.08E+13	1.47E+13	1.03E+13	7.04E+12	4.52E+12
2001	--	--	5.62E+13	5.60E+13	5.16E+13	4.33E+13	3.76E+13	4.47E+13	7.22E+13	1.18E+14	1.69E+14	2.09E+14	2.25E+14	2.15E+14	1.86E+14	1.49E+14	1.15E+14	8.64E+13	6.43E+13	4.71E+13	3.36E+13	2.33E+13	1.59E+13	1.08E+13	7.52E+12	5.13E+12
2001	--	--	7.49E+13	7.00E+13	6.24E+13	5.30E+13	4.80E+13	5.76E+13	9.07E+13	1.45E+14	2.04E+14	2.43E+14	2.51E+14	2.29E+14	1.93E+14	1.53E+14	1.18E+14	8.98E+13	6.70E+13	4.89E+13	3.48E+13	2.43E+13	1.67E+13	1.15E+13	7.78E+12	5.06E+12
2001	7.12E+13	6.62E+13	5.99E+13	5.26E+13	4.52E+13	3.87E+13	3.79E+13	5.18E+13	8.77E+13	1.43E+14	2.03E+14	2.45E+14	2.54E+14	2.34E+14	1.97E+14	1.57E+14	1.21E+14	9.23E+13	6.88E+13	5.00E+13	3.56E+13	2.48E+13	1.70E+13	1.17E+13	7.98E+12	5.25E+12
2001	1.01E+14	7.75E+13	5.99E+13	5.02E+13	4.67E+13	4.74E+13	5.40E+13	7.42E+13	1.16E+14	1.74E+14	2.31E+14	2.66E+14	2.67E+14	2.41E+14	2.00E+14	1.57E+14	1.20E+14	9.06E+13	6.72E+13	4.87E+13	3.44E+13	2.39E+13	1.66E+13	1.16E+13	8.00E+12	5.18E+12
2002	7.94E+13	6.18E+13	5.37E+13	5.59E+13	6.18E+13	6.60E+13	7.15E+13	8.95E+13	1.30E+14	1.87E+14	2.43E+14	2.75E+14	2.74E+14	2.47E+14	2.07E+14	1.64E+14	1.26E+14	9.38E+13	6.85E+13	4.91E+13	3.48E+13	2.43E+13	1.67E+13	1.14E+13	7.73E+12	5.02E+12
2002	4.80E+13	4.29E+13	4.13E+13	4.24E+13	4.15E+13	3.66E+13	3.30E+13	4.26E+13	7.48E+13	1.26E+14	1.79E+14	2.14E+14	2.23E+14	2.09E+14	1.81E+14	1.48E+14	1.16E+14	8.76E+13	6.47E+13	4.70E+13	3.36E+13	2.36E+13	1.64E+13	1.12E+13	7.61E+12	4.97E+12
2002	4.88E+13	4.26E+13	3.51E+13	2.74E+13	2.16E+13	1.86E+13	1.95E+13	2.77E+13	4.84E+13	8.41E+13	1.30E+14	1.72E+14	1.96E+14	1.96E+14	1.76E+14	1.46E+14	1.15E+14	8.75E+13	6.47E+13	4.69E+13	3.36E+13	2.38E+13	1.67E+13	1.15E+13	7.79E+12	5.09E+12
2002	4.89E+13	2.83E+13	1.56E+13	1.21E+13	1.27E+13	1.26E+13	1.18E+13	1.42E+13	2.46E+13	4.47E+13	7.32E+13	1.06E+14	1.34E+14	1.49E+14	1.44E+14	1.25E+14	1.01E+14	7.84E+13	5.97E+13	4.45E+13	3.23E+13	2.28E+13	1.58E+13	1.09E+13	7.37E+12	4.73E+12
2002	8.88E+13	6.22E+13	4.18E+13	2.91E+13	2.19E+13	1.72E+13	1.47E+13	1.64E+13	2.52E+13	4.27E+13	6.66E+13	9.23E+13	1.14E+14	1.27E+14	1.28E+14	1.18E+14	9.92E+13	7.79E+13	5.83E+13	4.25E+13	3.05E+13	2.18E+13	1.54E+13	1.07E+13	7.34E+12	4.87E+12
2002	1.29E+14	8.37E+13	5.29E+13	3.93E+13	3.45E+13	3.09E+13	2.84E+13	3.19E+13	4.41E+13	6.16E+13	7.82E+13	9.11E+13	1.02E+14	1.11E+14	1.16E+14	1.12E+14	9.77E+13	7.72E+13	5.67E+13	4.02E+13	2.85E+13	2.06E+13	1.50E+13	1.06E+13	7.19E+12	4.51E+12
2003	8.10E+13	5.15E+13	3.42E+13	3.05E+13	3.23E+13	3.12E+13	2.72E+13	3.01E+13	5.27E+13	9.95E+13	1.59E+14	2.10E+14	2.33E+14	2.24E+14	1.93E+14	1.53E+14	1.16E+14	8.56E+13	6.26E+13	4.58E+13	3.34E+13	2.41E+13	1.71E+13	1.18E+13	7.82E+12	4.70E+12
2003	5.93E+13	4.12E+13	2.96E+13	2.50E+13	2.28E+13	1.91E+13	1.54E+13	1.67E+13	2.83E+13	5.21E+13	8.40E+13	1.15E+14	1.37E+14	1.45E+14	1.42E+14	1.27E+14	1.06E+14	8.29E+13	6.11E+13	4.35E+13	3.07E+13	2.18E+13	1.54E+13	1.09E+13	7.69E+12	5.32E+12
2003	7.12E+13	5.45E+13	4.00E+13	2.93E+13	2.24E+13	1.86E+13	1.79E+13	2.21E+13	3.31E+13	5.03E+13	7.09E+13	9.14E+13	1.09E+14	1.22E+14	1.24E+14	1.16E+14	9.88E+13	7.77E+13	5.79E+13	4.20E+13	3.03E+13	2.17E+13	1.51E+13	1.03E+13	6.99E+12	4.80E+12
2003	1.56E+14	1.22E+14	9.34E+13	7.35E+13	6.25E+13	5.49E+13	4.68E+13	4.17E+13	4.74E+13	6.74E+13	9.69E+13	1.26E+14	1.47E+14	1.54E+14	1.47E+14	1.29E+14	1.04E+14	7.75E+13	5.46E+13	3.80E+13	2.71E+13	1.97E+13	1.38E+13	9.12E+12	6.04E+12	4.53E+12
2004	--	--	3.86E+13	3.89E+13	3.65E+13	3.15E+13	2.74E+13	3.08E+13	4.55E+13	6.77E+13	8.72E+13	9.73E+13	1.01E+14	1.05E+14	1.12E+14	1.13E+14	1.02E+14	8.07E+13	5.70E+13	3.80E+13	2.60E+13	1.93E+13	1.49E+13	1.11E+13	7.51E+12	4.31E+12
2004	--	--	5.73E+13	4.91E+13	4.09E+13	3.40E+13	3.15E+13	3.77E+13	5.45E+13	7.87E+13	1.04E+14	1.25E+14	1.40E+14	1.45E+14	1.40E+14	1.25E+14	1.03E+14	8.00E+13	5.91E+13	4.24E+13	3.02E+13	2.14E+13	1.51E+13	1.05E+13	7.14E+12	4.57E+12
2004	--	--	4.35E+13	3.77E+13	3.18E+13	2.62E+13	2.41E+13	3.25E+13	5.80E+13	9.97E+13	1.47E+14	1.85E+14	2.03E+14	2.01E+14	1.81E+14	1.51E+14	1.19E+14	8.98E+13	6.63E+13	4.83E+13	3.48E+13	2.46E+13	1.71E+13	1.16E+13	7.70E+12	4.74E+12
2004	--	--	6.38E+13	7.42E+13	8.33E+13	8.72E+13	8.71E+13	9.67E+13	1.32E+14	1.92E+14	2.52E+14	2.86E+14	2.84E+14	2.54E+14	2.08E+14	1.55E+14	1.04E+14	6.69E+13	4.85E+13	4.26E+13	3.76E+13	2.79E+13	1.59E+13	6.60E+12	3.38E+12	5.05E+12
2004	--	--	5.69E+13	5.91E+13	5.66E+13	5.06E+13	5.03E+13	6.88E+13	1.14E+14	1.77E+14	2.37E+14	2.70E+14	2.70E+14	2.43E+14	2.03E+14	1.61E+14	1.23E+14	9.20E+13	6.77E+13	4.90E+13	3.46E+13	2.39E+13	1.63E+13	1.12E+13	7.54E+12	4.82E+12
2005	--	--	8.76E+13	7.90E+13	7.08E+13	6.27E+13	5.77E+13	6.74E+13	1.04E+14	1.66E+14	2.28E+14	2.66E+14	2.66E+14	2.37E+14	1.96E+14	1.55E+14	1.19E+14	8.85E+13	6.51E+13	4.74E+13	3.42E+13	2.43E+13	1.70E+13	1.18E+13	7.91E+12	4.81E+12
2005	--	--	6.97E+13	5.91E+13	4.78E+13	3.67E+13	3.09E+13	3.76E+13	6.10E+13	9.70E+13	1.35E+14	1.66E+14	1.82E+14	1.83E+14	1.68E+14	1.42E+14	1.12E+14	8.36E+13	6.10E+13	4.42E+13	3.17E+13	2.23E+13	1.54E+13	1.06E+13	7.19E+12	4.53E+12
2005	--	--	3.65E+13	3.65E+13	3.47E+13	3.14E+13	2.94E+13	3.44E+13	5.12E+13	8.01E+13	1.16E+14	1.49E+14	1.71E+14	1.76E+14	1.62E+14	1.36E+14	1.06E+14	8.00E+13	5.98E+13	4.42E+13	3.16E+13	2.19E+13	1.50E+13	1.04E+13	6.99E+12	4.29E+12
2005	--	--	3.79E+13	2.71E+13	1.82E+13	1.29E+13	1.21E+13	1.70E+13	2.89E+13	4.83E+13	7.31E+13	9.95E+13	1.22E+14	1.35E+14	1.36E+14	1.26E+14	1.07E+14	8.37E+13	6.21E+13	4.44E+13	3.13E+13	2.21E+13	1.55E+13	1.08E+13	7.37E+12	4.63E+12
2005	--	--	3.40E+13	3.57E+13	3.41E+13	2.79E+13	2.12E+13	2.14E+13	3.24E+13	5.28E+13	7.78E+13	1.01E+14	1.16E+14	1.18E+14	1.11E+14	1.01E+14	9.03E+13	7.70E+13	6.10E+13	4.46E+13	3.06E+13	1.99E+13	1.23E+13	7.43E+12	5.25E+12	5.00E+12
2005	--	--	1.26E+14	7.45E+13	4.23E+13	3.20E+13	3.37E+13	3.97E+13	4.96E+13	6.46E+13	8.14E+13	9.45E+13	1.02E+14	1.05E+14	1.07E+14	1.05E+14	9.56E+13	7.79E+13	5.71E+13	3.92E+13	2.68E+13	1.88E+13	1.36E+13	9.76E+12	6.88E+12	4.80E+12
2005	--	--	7.08E+13	6.63E+13	5.81E+13	4.64E+13	3.74E+13	3.99E+13	5.77E+13	8.53E+13	1.13E+14	1.35E+14	1.49E+14	1.54E+14	1.47E+14	1.31E+14	1.07E+14	8.18E+13	5.92E+13	4.20E+13	2.99E+13	2.15E+13	1.54E+13	1.07E+13	7.08E+12	4.36E+12
2005	--	--	5.52E+13	4.89E+13	4.24E+13	3.63E+13	3.39E+13	4.17E+13	6.51E+13	1.03E+14	1.46E+14	1.83E+14	2.03E+14	2.02E+14	1.82E+14	1.50E+14	1.15E+14	8.51E+13	6.19E+13	4.49E+13	3.24E+13	2.30E+13	1.61E+13	1.12E+13	7.54E+12	4.68E+12
2005	--	--	7.30E+13	5.92E+13	4.70E+13	3.79E+13	3.60E+13	4.89E+13	8.24E+13	1.32E+14	1.85E+14	2.23E+14	2.38E+14	2.26E+14	1.95E+14	1.56E+14	1.19E+14	8.88E+13	6.54E+13	4.74E+13	3.38E+13	2.38E+13	1.66E+13	1.15E+13	7.84E+12	5.03E+12
2005	--	--	5.58E+13	5.87E+13	5.87E+13	5.46E+13	5.16E+13	6.27E+13	9.97E+13	1.60E+14	2.24E+14	2.86E+14	2.73E+14	2.47E+14	2.02E+14	1.55E+14	1.16E+14	8.82E+13	6.77E+13	5.09E+13	3.65E+13	2.51E+13	1.70E+13	1.17E+13	8.05E+12	5.31E+12
2005	--	--	8.12E+13	7.00E+13	6.09E+13	5.31E+13	4.87E+13	5.70E+13	8.80E+13	1.41E+14	1.99E+14	2.41E+14	2.53E+14	2.36E+14	2.01E+14	1.60E+14	1.23E+14	9.23E+13	6.84E+13	4.96E+13	3.51E+13	2.42E+13	1.65E+13	1.13E+13	7.63E+12	4.92E+12

Table A. 36: Resolute Bay ozone concentration (m^{-3}) (part 2)

Resolute Bay: Ozone concentration per height increment

Year	75 (km)	76 (km)	77 (km)	78 (km)	79 (km)	80 (km)	81 (km)	82 (km)	83 (km)	84 (km)	85 (km)	86 (km)	87 (km)	88 (km)	89 (km)	90 (km)	91 (km)	92 (km)	93 (km)	94 (km)	95 (km)	96 (km)	97 (km)	98 (km)	99 (km)	100 (km)
2006	--	--	8.23E+13	6.47E+13	5.30E+13	4.74E+13	4.70E+13	5.62E+13	8.29E+13	1.30E+14	1.87E+14	2.35E+14	2.54E+14	2.39E+14	2.01E+14	1.57E+14	1.18E+14	8.75E+13	6.46E+13	4.74E+13	3.43E+13	2.43E+13	1.69E+13	1.15E+13	7.71E+12	4.77E+12
2006	--	--	9.02E+13	9.22E+13	8.73E+13	7.63E+13	7.37E+13	1.00E+14	1.63E+14	2.42E+14	3.03E+14	3.21E+14	2.99E+14	2.56E+14	2.11E+14	1.68E+14	1.29E+14	9.47E+13	6.65E+13	4.51E+13	3.05E+13	2.15E+13	1.62E+13	1.22E+13	8.29E+12	4.45E+12
2006	--	--	3.56E+13	3.36E+13	3.00E+13	2.50E+13	2.18E+13	2.73E+13	4.80E+13	8.45E+13	1.28E+14	1.66E+14	1.85E+14	1.83E+14	1.64E+14	1.37E+14	1.08E+14	8.23E+13	6.06E+13	4.34E+13	3.07E+13	2.16E+13	1.49E+13	1.02E+13	6.86E+12	4.51E+12
2006	--	--	5.82E+12	2.03E+13	2.64E+13	2.30E+13	1.68E+13	1.67E+13	2.77E+13	4.98E+13	7.93E+13	1.09E+14	1.30E+14	1.39E+14	1.33E+14	1.17E+14	9.56E+13	7.50E+13	5.77E+13	4.35E+13	3.15E+13	2.17E+13	1.45E+13	9.72E+12	6.66E+12	4.51E+12
2006	--	--	6.86E+13	4.33E+13	2.61E+13	1.91E+13	2.00E+13	2.61E+13	3.59E+13	4.84E+13	6.28E+13	7.87E+13	9.47E+13	1.07E+14	1.11E+14	1.04E+14	8.87E+13	7.03E+13	5.34E+13	3.98E+13	2.93E+13	2.11E+13	1.47E+13	9.96E+12	6.64E+12	4.30E+12
2006	--	--	5.04E+13	4.22E+13	3.60E+13	3.26E+13	3.26E+13	3.85E+13	5.22E+13	7.16E+13	9.11E+13	1.06E+14	1.17E+14	1.24E+14	1.23E+14	1.14E+14	9.70E+13	7.62E+13	5.62E+13	3.97E+13	2.78E+13	1.97E+13	1.41E+13	1.00E+13	6.89E+12	4.29E+12
2006	--	--	1.12E+14	7.52E+13	4.83E+13	3.45E+13	3.19E+13	3.78E+13	5.05E+13	6.74E+13	8.45E+13	9.95E+13	1.12E+14	1.21E+14	1.24E+14	1.16E+14	9.89E+13	7.64E+13	5.48E+13	3.80E+13	2.66E+13	1.91E+13	1.38E+13	9.78E+12	6.67E+12	4.29E+12
2006	--	--	7.03E+13	5.03E+13	3.50E+13	2.70E+13	2.69E+13	3.54E+13	5.31E+13	7.87E+13	1.08E+14	1.33E+14	1.51E+14	1.58E+14	1.52E+14	1.33E+14	1.07E+14	7.99E+13	5.79E+13	4.17E+13	3.01E+13	2.16E+13	1.52E+13	1.05E+13	7.03E+12	4.43E+12
2006	--	--	2.28E+13	3.64E+13	4.15E+13	3.79E+13	3.33E+13	3.72E+13	5.49E+13	8.52E+13	1.22E+14	1.56E+14	1.81E+14	1.90E+14	1.78E+14	1.50E+14	1.17E+14	8.62E+13	6.31E+13	4.63E+13	3.36E+13	2.37E+13	1.62E+13	1.09E+13	7.47E+12	5.13E+12
2006	--	--	7.67E+13	5.69E+13	4.21E+13	3.49E+13	3.71E+13	5.28E+13	8.53E+13	1.30E+14	1.74E+14	2.05E+14	2.16E+14	2.08E+14	1.86E+14	1.54E+14	1.21E+14	9.02E+13	6.60E+13	4.79E+13	3.46E+13	2.46E+13	1.71E+13	1.18E+13	7.92E+12	5.00E+12
2006	--	--	8.11E+13	6.80E+13	5.38E+13	5.54E+13	7.07E+13	1.07E+14	1.62E+14	2.20E+14	2.61E+14	2.68E+14	2.45E+14	2.03E+14	1.58E+14	1.20E+14	8.95E+13	6.67E+13	4.91E+13	3.52E+13	2.44E+13	1.64E+13	1.10E+13	7.49E+12	5.01E+12	
2006	--	--	5.85E+13	6.64E+13	7.11E+13	7.01E+13	6.68E+13	7.38E+13	1.05E+14	1.60E+14	2.20E+14	2.59E+14	2.63E+14	2.39E+14	2.00E+14	1.59E+14	1.22E+14	9.16E+13	6.69E+13	4.74E+13	3.28E+13	2.27E+13	1.57E+13	1.10E+13	7.47E+12	4.74E+12
2007	--	--	7.63E+13	7.61E+13	7.43E+13	6.97E+13	6.62E+13	7.69E+13	1.14E+14	1.75E+14	2.37E+14	2.73E+14	2.74E+14	2.45E+14	2.03E+14	1.59E+14	1.21E+14	9.14E+13	6.79E+13	4.92E+13	3.46E+13	2.38E+13	1.62E+13	1.10E+13	7.63E+12	5.20E+12
2007	--	--	4.31E+13	4.40E+13	3.96E+13	3.11E+13	2.72E+13	3.84E+13	6.74E+13	1.07E+14	1.48E+14	1.80E+14	1.96E+14	1.91E+14	1.68E+14	1.35E+14	1.03E+14	7.76E+13	5.89E+13	4.42E+13	3.19E+13	2.20E+13	1.49E+13	1.01E+13	6.95E+12	4.70E+12
2007	--	--	2.90E+13	3.71E+13	3.94E+13	3.51E+13	2.97E+13	3.19E+13	4.79E+13	7.75E+13	1.14E+14	1.47E+14	1.67E+14	1.69E+14	1.54E+14	1.27E+14	1.00E+14	7.72E+13	5.87E+13	4.37E+13	3.14E+13	2.18E+13	1.48E+13	1.02E+13	7.05E+12	4.83E+12
2007	--	--	1.91E+13	1.44E+13	1.10E+13	9.34E+12	9.49E+12	1.27E+13	2.12E+13	3.60E+13	5.60E+13	7.74E+13	9.58E+13	1.08E+14	1.13E+14	1.09E+14	9.78E+13	7.99E+13	5.99E+13	4.23E+13	2.92E+13	2.05E+13	1.47E+13	1.05E+13	7.21E+12	4.52E+12
2007	--	--	2.52E+13	2.77E+13	2.79E+13	2.57E+13	2.35E+13	2.45E+13	3.13E+13	4.45E+13	6.22E+13	8.20E+13	1.01E+14	1.16E+14	1.21E+14	1.14E+14	9.70E+13	7.62E+13	5.67E+13	4.11E+13	2.95E+13	2.10E+13	1.48E+13	1.03E+13	7.01E+12	4.52E+12
2007	--	--	1.43E+14	9.23E+13	5.55E+13	3.96E+13	4.28E+13	5.81E+13	7.76E+13	9.52E+13	1.07E+14	1.11E+14	1.11E+14	1.10E+14	1.09E+14	1.04E+14	9.29E+13	7.61E+13	5.69E+13	3.95E+13	2.68E+13	1.88E+13	1.35E+13	9.74E+12	6.66E+12	3.99E+12
2007	--	--	6.55E+13	6.13E+13	5.30E+13	4.11E+13	3.15E+13	3.13E+13	4.46E+13	6.97E+13	9.96E+13	1.26E+14	1.45E+14	1.52E+14	1.46E+14	1.29E+14	1.04E+14	7.89E+13	5.70E+13	4.04E+13	2.86E+13	2.04E+13	1.45E+13	1.01E+13	6.89E+12	4.40E+12
2007	--	--	5.53E+13	5.67E+13	5.50E+13	4.77E+13	3.87E+13	3.99E+13	6.34E+13	1.09E+14	1.64E+14	2.06E+14	2.21E+14	2.08E+14	1.78E+14	1.43E+14	1.12E+14	8.60E+13	6.41E+13	4.62E+13	3.26E+13	2.27E+13	1.58E+13	1.10E+13	7.73E+12	5.45E+12
2007	--	--	6.47E+13	4.91E+13	4.17E+13	4.09E+13	4.25E+13	5.04E+13	7.30E+13	1.10E+14	1.47E+14	1.71E+14	1.78E+14	1.71E+14	1.55E+14	1.35E+14	1.12E+14	8.90E+13	6.77E+13	4.96E+13	3.53E+13	2.42E+13	1.57E+13	9.88E+12	6.68E+12	5.48E+12
2008	--	--	1.79E+12	2.33E+13	3.75E+13	4.08E+13	3.49E+13	2.90E+13	3.53E+13	5.74E+13	8.42E+13	1.02E+14	1.07E+14	1.08E+14	1.10E+14	1.09E+14	9.88E+13	8.06E+13	6.01E+13	4.27E+13	3.01E+13	2.15E+13	1.53E+13	1.08E+13	7.37E+12	4.87E+12
2008	--	--	3.32E+13	3.41E+13	3.16E+13	2.68E+13	2.62E+13	3.90E+13	6.90E+13	1.11E+14	1.53E+14	1.85E+14	2.01E+14	1.99E+14	1.80E+14	1.49E+14	1.16E+14	8.55E+13	6.13E+13	4.36E+13	3.11E+13	2.23E+13	1.59E+13	1.12E+13	7.65E+12	4.79E+12
2008	--	--	3.22E+13	2.57E+13	1.93E+13	1.37E+13	1.17E+13	1.72E+13	3.30E+13	5.76E+13	8.55E+13	1.10E+14	1.28E+14	1.37E+14	1.36E+14	1.23E+14	1.03E+14	8.04E+13	6.07E+13	4.47E+13	3.22E+13	2.26E+13	1.55E+13	1.05E+13	7.00E+12	4.32E+12
2008	--	--	1.40E+13	1.93E+13	1.97E+13	1.63E+13	1.54E+13	2.13E+13	3.27E+13	4.52E+13	5.64E+13	6.69E+13	7.75E+13	8.79E+13	9.59E+13	9.76E+13	9.00E+13	7.42E+13	5.56E+13	3.95E+13	2.81E+13	2.04E+13	1.47E+13	1.02E+13	6.83E+12	4.37E+12
2008	--	--	5.35E+13	5.56E+13	5.38E+13	4.79E+13	4.26E+13	4.39E+13	5.46E+13	7.33E+13	9.59E+13	1.08E+14	1.18E+14	1.33E+14	1.36E+14	1.34E+14	1.20E+14	1.01E+14	7.77E+13	5.63E+13	3.95E+13	2.79E+13	2.02E+13	1.45E+13	1.02E+13	6.89E+12	4.47E+12
2008	--	--	6.96E+13	6.08E+13	5.06E+13	3.98E+13	3.31E+13	3.66E+13	5.19E+13	7.32E+13	9.29E+13	1.08E+14	1.18E+14	1.25E+14	1.25E+14	1.16E+14	9.84E+13	7.68E+13	5.61E+13	3.95E+13	2.76E+13	1.95E+13	1.39E+13	9.82E+12	6.75E+12	4.38E+12
2008	--	--	8.38E+13	6.87E+13	5.59E+13	4.77E+13	4.71E+13	5.69E+13	7.63E+13	9.93E+13	1.18E+14	1.30E+14	1.36E+14	1.31E+14	1.18E+14	9.90E+13	7.64E+13	5.52E+13	3.87E+13	2.74E+13	2.01E+13	1.50E+13	1.08E+13	6.80E+12	2.98E+12	
2008	--	--	2.67E+13	3.09E+13	2.97E+13	2.28E+13	1.56E+13	1.66E+13	3.35E+13	6.74E+13	1.09E+14	1.44E+14	1.62E+14	1.64E+14	1.55E+14	1.37E+14	1.13E+14	8.67E+13	6.30E+13	4.48E+13	3.18E+13	2.26E+13	1.58E+13	1.09E+13	7.28E+12	4.51E+12
2008	--	--	3.51E+13	4.34E+13	4.65E+13	4.43E+13	4.28E+13	5.15E+13	7.86E+13	1.24E+14	1.77E+14	2.21E+14	2.39E+14	2.29E+14	1.99E+14	1.61E+14	1.24E+14	9.28E+13	6.79E+13	4.90E+13	3.51E+13	2.49E+13	1.74E+13	1.20E+13	8.06E+12	5.16E+12
2008	--	--	6.57E+13	6.66E+13	6.09E+13	4.92E+13	4.05E+13	4.80E+13	8.09E+13	1.35E+14	1.93E+14	2.33E+14	2.42E+14	2.22E+14	1.86E+14	1.47E+14	1.14E+14	8.99E+13	7.07E+13	5.31E+13	3.70E+13	2.43E+13	1.59E+13	1.10E+13	7.67E+12	4.85E+12
2008	--	--	7.02E+13	7.53E+13	7.46E+13	6.75E+13	6.31E+13	7.67E+13	1.18E+14	1.78E+14	2.33E+14	2.60E+14	2.55E+14	2.25E+14	1.87E+14	1.50E+14	1.17E+14	8.91E+13	6.44E+13	4.44E+13	3.01E+13	2.09E+13	1.52E+13	1.12E+13	7.83E+12	4.87E+12
2009	--	--	3.17E+13	2.22E+13	1.48E+13	1.10E+13	1.08E+13	1.45E+13	2.32E+13	3.66E+13	5.32E+13	7.16E+13	9.08E+13	1.07E+14	1.13E+14	1.05E+14	8.92E+13	7.10E+13	5.49E+13	4.13E+13	3.00E+13	2.10E+13	1.44E+13	9.92E+12	6.80E+12	4.40E+12
2009	--	--	5.03E+13	4.06E+13	3.14E+13	2.38E+13	2.03E+13	2.37E+13	3.44E+13	4.95E+13	6.49E+13	7.90E+13	9.21E+13	1.04E+14	1.11E+14	1.10E+14	9.89E+13	8.01E+13	5.88E+13	4.05E+13	2.78E+13	1.96E+13	1.42E+13	9.98E+12	6.53E+12	3.70E+12
2009	--	--	6.72E+13	4.96E+13	3.46E+13	2.55E+13	2.61E+13	3.88E+13	6.13E+13	8.60E+13	1.04E+14	1.11E+14	1.11E+14	1.07E+14	1.02E+14	9.51E+13	8.53E+13	7.23E+13	5.71E+13	4.16E+13	2.82E+13	1.81E+13	1.15E+13	7.78E+12	5.72E+12	4.41E+12
2009	--	--	1.10E+14	7.26E+13	4.34E+13	2.71E+13	2.37E+13	3.10E+13	4.62E+13	6.54E+13	8.42E+13	9.89E+13	1.09E+14	1.17E+14	1.20E+14	1.16E+14	1.01E+14	7.99E+13	5.76E+13	3.96E+13	2.74E+13	1.95E+13	1.40E+13	9.81E+12	6.68E+12	4.44E+12
2009	--	--	5.77E+13	4.17E+13	2.81E+13	2.03E+13	2.16E+13	3.32E+13	5.29E+13	7.51E+13	9.44E+13	1.09E+14	1.22E+14	1.31E+14	1.31E+14	1.20E+14	1.01E+14	7.78E+13	5.73E+13	4.12E+13	2.96E+13	2.12E+13	1.49E+13	1.02E+13	6.79E+12	4.28E+12
2009	--	--	4.67E+13	4.27E+13	3.81E+13	3.35E+13	3.06E+13	3.35E+13	4.90E+13	8.12E+13	1.23E+14	1.59E+14	1.77E+14	1.73E+14	1.57E+14	1.34E+14	1.10E+14	8.62E+13	6.54E+13	4.74E+13	3.25E+13	2.14E+13	1.42E+13	9.88E+12	7.04E+12	4.85E+12
2009	--	--	3.68E+13	4.52E+13	4.75E+13	4.32E+13	3.99E+13	5.04E+13	8.33E+13	1.34E+14	1.87E+14	2.22E+14	2.33E+14	2.21E+14	1.92E+14	1.56E+14	1.20E+14	8.99E+13	6.66E+13	4.89E+13	3.55E+13	2.51E+13	1.73E+13	1.16E+13	7.74E+12	4.97E+12
2009	--	--	4.98E+13	5.17E+13	5.42E+13	5.67E+13	6.04E+13	7.29E+13	1.05E+14	1.57E+14	2.13E+14	2.52E+14	2.58E+14	2.36E+14	1.97E+14	1.56E+14	1.19E+14	9.04E+13	6.77E+13	4.95E+13	3.50E+13	2.41E+13	1.64E+13	1.11E+13	7.48E+12	4.72E+12
2009	--	--	6.37E+13	6.93E+13	6.97E+13	6.61E+13	6.39E+13	6.86E+13	8.32E+13	1.08E+14	1.42E+14	1.77E+14	1.99E+14	2.00E+14	1.82E+14	1.52E+14	1.19E+14	8.88E+13	6.44E+13	4.54E+13	3.15E+13	2.18E+13	1.53E+13	1.09E+13	7.60E+12	4.93E+12
2010	--	--	9.75E+13	7.61E+13	5.71E+13	4.26E+13	3.76E+13	5.15E+13	9.03E+13	1.47E+14	2.02E+14	2.35E+14	2.36E+14	2.10E+14	1.71E+14	1.33E+14	1.02E+14	7.91E+13	6.03E+13	4.40E+13	3.06E+13	2.08E+13	1.45E+13	1.03E+13	7.09E+12	4.34E+12
2010	--	--	2.59E+13	3.45E+13	3.94E+13	3.90E+13	3.70E+13	4.21E+13	6.24E+13	9.91E+13	1.43E+14	1.81E+14	2.01E+14	2.00E+14	1.81E+14	1.50E+14	1.17E+14	8.75E+13	6.47E+13	4.77E+13	3.46E+13	2.43E+13	1.62E+13	1.04E+13	6.46E+12	3.79E+12
2010	--	--	5.69E+13	6.39E+13	6.20E+13	4.98E+13	3.68E+13	3.67E+13	5.75E+13	9.61E+13	1.43E+14	1.86E+14	2.13E+14	2.15E+14	1.91E+14	1.53E+14	1.15E+14	8.45E+13	6.32E+13	4.76E+13	3.46E+13	2.36E+13	1.55E+13	1.02E+13	7.09E+12	5.07E+12
2010	--	--	2.40E+13	2.80E+13	2.60E+13	2.04E+13	1.85E+13	2.37E+13	3.33E+13	4.49E+13	6.05E+13	8.31E+13	1.08E+14	1.22E+14	1.17E+14	9.74E+13	7.83E+13	6.58E+13	5.60E+13	4.41E+13	3.09E+13	2.02E+13	1.35E+13	9.72E+12	6.56E+12	3.07E+12
2010	--	--	3.64E+13	3.66E+13	3.63E+13	3.41E+13	3.10E+13	3.30E+13	4.51E+13	6.40E+13	8.12E+13	9.23E+13	9.92E+13	1.04E+14	1.06E+14	9.26E+13	7.66E+13	5.83E+13	4.15E+13	2.84E+13	1.94E+13	1.36E+13	9.65E+12	6.71E+12	4.31E+12	
2010	--	--	4.12E+13	4.40E+13	4.28E+13	3.84E+13	3.57E+13	4.04E+13	5.58E+13	7.87E+13	9.95E+13	1.11E+14	1.16E+14	1.18E+14	1.18E+14	1.13E+14	9.96E+13	7.95E+13	5.81E+13	4.00E+13	2.72E+13	1.88E+13	1.34E+13	9.58E+12	6.66E+12	4.29E+12
2010	--	--	5.76E+13	4.92E+13	4.09E+13	3.32E+13	2.91E+13	3.39E+13	4.99E+13	7.28E+13	9.34E+13	1.06E+14	1.12E+14	1.16E+14	1.19E+14	1.14E+14	9.85E+13	7.66E+13	5.52E+13	3.86E+13	2.71E+13	1.95E+13	1.40E+13	9.83E+12	6.67E+12	4.24E+12
2010	--	--	4.60E+13	4.93E+13	4.94E+13	4.47E+13	3.83E+13	3.80E+13	4.90E+13	6.85E+13	8.94E+13	1.09E+14	1.27E+14	1.42E+14	1.49E+14	1.42E+14	1.20E+14	8.91E+13	6.00E+13	3.90E+13	2.69E+13	2.01E+13	1.53E+13	1.11E+13	7.43E+12	4.53E+12
2010	--	--	4.58E+14	2.61E+14	1.28E+14	8.81E+13	1.18E+14	1.67E+14	2.03E+14	2.28E+14	2.43E+14	2.39E+14	2.15E+14	1.84E+14	1.57E+14	1.30E+14	1.03E+14	8.10E+13	6.76E+13	5.61E+13	4.27E+13	2.80E+13	1.90E+13	6.36E+12	1.88E+12	-2.21E+11
2010	--	--	1.73E+14	1.29E+14	1.16E+14	1.34E+14	1.57E+14	1.68E+14	1.72E+14	1.88E+14	2.19E+14	2.53E+14	2.71E+14	2.60E+14	2.23E+14	1.76E+14	1.34E+14	1.02E+14	7.51E+13	5.25E+13	3.51E+13	2.36E+13	1.68E+13	1.23E+13	8.67E+12	5.49E+12

Table A.37: Socorro ozone concentration (m^{-3}) (part 1)

Socorro: Ozone concentration per height increment

Month	Year	75	76	77	78	79	80	81	82	83	84	85	86	87	88	89	90	91	92	93	94	95	96	97	98	99	100
		(km)	(km)	(km)	(km)	(km)	(km)	(km)	(km)	(km)	(km)	(km)	(km)	(km)	(km)	(km)	(km)	(km)	(km)	(km)	(km)	(km)	(km)	(km)	(km)	(km)	(km)
4	2002	1.30E-14	7.81E+13	4.60E+13	3.42E-13	2.95E+13	2.38E+13	2.00E-13	2.52E-13	3.86E+13	5.15E+13	5.80E-13	6.56E+13	8.59E+13	1.15E-14	1.32E-14	1.25E+14	9.76E+13	6.73E+13	4.54E+13	3.31E+13	2.56E+13	1.92E+13	1.30E+13	8.14E+12	5.53E+12	4.67E+12
5	2002	1.11E+14	9.23E+13	7.67E+13	6.50E+13	5.49E+13	4.42E+13	3.46E+13	3.02E+13	3.48E+13	4.79E+13	6.55E+13	8.25E+13	9.42E+13	9.73E+13	9.18E+13	8.21E+13	7.25E+13	6.34E+13	5.27E+13	4.01E+13	2.78E+13	1.84E+13	1.24E+13	8.70E+12	5.95E+12	3.39E+12
6	2002	2.70E+14	1.87E+14	1.20E+14	7.40E+13	4.58E+13	2.98E+13	2.31E+13	2.52E+13	3.64E+13	5.52E+13	7.74E+13	9.76E+13	1.12E+14	1.18E+14	1.16E+14	1.06E+14	8.91E+13	6.99E+13	5.19E+13	3.72E+13	2.63E+13	1.85E+13	1.30E+13	9.07E+12	5.98E+12	3.33E+12
7	2002	3.83E+14	1.93E+14	6.82E+13	2.75E+13	3.98E+13	5.68E+13	5.41E+13	4.00E+13	3.50E+13	4.86E+13	7.42E+13	9.73E+13	1.09E+14	1.11E+14	1.09E+14	1.03E+14	8.89E+13	7.05E+13	5.34E+13	4.05E+13	3.07E+13	2.24E+13	1.55E+13	1.04E+13	7.03E+12	4.70E+12
8	2002	2.41E+14	1.58E+14	9.80E+13	6.55E+13	4.94E+13	3.88E+13	3.10E+13	3.02E+13	4.04E+13	6.03E+13	8.36E+13	1.04E+14	1.18E+14	1.26E+14	1.25E+14	1.15E+14	9.76E+13	7.63E+13	5.61E+13	4.00E+13	2.83E+13	2.01E+13	1.43E+13	1.01E+13	6.99E+12	4.67E+12
9	2002	1.94E+14	1.25E+14	7.42E+13	4.88E+13	3.95E+13	3.38E+13	2.80E+13	2.69E+13	3.60E+13	5.53E+13	7.99E+13	1.04E+14	1.23E+14	1.31E+14	1.27E+14	1.12E+14	9.02E+13	6.93E+13	5.23E+13	3.93E+13	2.91E+13	2.10E+13	1.46E+13	9.93E+12	6.71E+12	4.48E+12
10	2002	2.11E+14	1.73E+14	1.34E+14	9.93E+13	7.26E+13	5.58E+13	4.81E+13	5.00E+13	6.28E+13	8.59E+13	1.16E+14	1.46E+14	1.68E+14	1.72E+14	1.59E+14	1.33E+14	1.02E+14	7.42E+13	5.28E+13	3.84E+13	2.89E+13	2.18E+13	1.59E+13	1.10E+13	7.37E+12	4.60E+12
11	2002	2.63E+14	1.88E+14	8.22E+13	7.41E+12	-1.45E+13	-5.13E+12	1.32E+13	3.70E+13	6.69E+13	9.40E+13	1.07E+14	1.05E+14	9.62E+13	8.59E+13	7.47E+13	6.22E+13	4.91E+13	3.79E+13	3.02E+13	2.50E+13	2.00E+13	1.47E+13	1.01E+13	7.18E+12	5.56E+12	
3	2003	1.14E+13	4.27E+13	4.97E+13	3.36E+13	1.35E+13	3.33E+12	2.92E+12	6.41E+12	1.11E+13	1.85E+13	3.07E+13	4.61E+13	6.01E+13	6.92E+13	7.33E+13	7.36E+13	7.04E+13	6.29E+13	5.17E+13	3.90E+13	2.78E+13	1.95E+13	1.39E+13	9.99E+12	6.77E+12	3.85E+12
4	2003	3.63E+13	7.88E+13	9.54E+13	7.98E+13	4.73E+13	1.95E+13	7.49E+12	9.08E+12	1.67E+13	2.43E+13	3.05E+13	3.80E+13	4.94E+13	6.40E+13	7.71E+13	8.37E+13	8.13E+13	7.08E+13	5.57E+13	4.03E+13	2.76E+13	1.88E+13	1.32E+13	9.60E+12	6.90E+12	4.65E+12
1	2005	5.58E+13	4.18E+13	3.09E+13	2.38E+13	1.92E+13	1.51E+13	1.09E+13	9.35E+12	1.68E+13	3.74E+13	6.67E+13	9.28E+13	1.07E+14	1.09E+14	1.04E+14	9.79E+13	8.90E+13	7.64E+13	6.07E+13	4.51E+13	3.21E+13	2.27E+13	1.60E+13	1.12E+13	7.82E+12	5.25E+12
2	2005	9.48E+13	6.05E+13	3.51E+13	2.01E+13	1.20E+13	7.72E+12	6.77E+12	9.29E+12	1.53E+13	2.44E+13	3.59E+13	4.96E+13	6.55E+13	8.19E+13	9.38E+13	9.63E+13	8.80E+13	7.28E+13	5.64E+13	4.21E+13	3.09E+13	2.22E+13	1.55E+13	1.07E+13	7.38E+12	5.03E+12
3	2005	4.66E+13	3.64E+13	2.75E+13	2.10E+13	1.75E+13	1.62E+13	1.50E+13	1.35E+13	1.50E+13	2.43E+13	4.22E+13	6.34E+13	8.03E+13	8.91E+13	9.16E+13	8.96E+13	8.33E+13	7.24E+13	5.82E+13	4.36E+13	3.12E+13	2.20E+13	1.55E+13	1.09E+13	7.57E+12	5.02E+12
4	2005	6.44E+13	4.10E+13	2.42E+13	1.68E+13	1.63E+13	1.71E+13	1.61E+13	1.45E+13	1.65E+13	2.44E+13	3.70E+13	5.14E+13	6.52E+13	7.70E+13	8.50E+13	8.70E+13	8.21E+13	7.15E+13	5.77E+13	4.34E+13	3.07E+13	2.10E+13	1.45E+13	1.02E+13	6.89E+12	3.90E+12
5	2005	1.50E+14	8.04E+13	3.32E+13	1.44E+13	1.32E+13	1.53E+13	1.43E+13	1.24E+13	1.47E+13	2.38E+13	3.85E+13	5.49E+13	6.94E+13	8.03E+13	8.73E+13	8.91E+13	8.41E+13	7.22E+13	5.64E+13	4.09E+13	2.88E+13	2.05E+13	1.49E+13	1.07E+13	7.48E+12	4.86E+12
6	2005	1.71E+13	3.21E+13	3.98E+13	3.65E+13	2.50E+13	1.28E+13	5.95E+12	5.81E+12	1.08E+13	1.95E+13	3.17E+13	4.67E+13	6.22E+13	7.50E+13	8.27E+13	8.36E+13	7.78E+13	6.63E+13	5.22E+13	3.87E+13	2.80E+13	2.00E+13	1.43E+13	1.02E+13	7.19E+12	4.94E+12
7	2005	1.17E+14	6.47E+13	2.94E+13	1.45E+13	1.11E+13	1.01E+13	8.54E+12	8.43E+12	1.24E+13	2.17E+13	3.59E+13	5.31E+13	6.98E+13	8.26E+13	8.91E+13	8.85E+13	8.09E+13	6.82E+13	5.33E+13	3.93E+13	2.79E+13	1.95E+13	1.34E+13	9.30E+12	6.65E+12	4.94E+12
8	2005	1.04E+12	1.56E+13	2.57E+13	2.82E+13	2.31E+13	1.48E+13	8.68E+12	7.64E+12	1.07E+13	1.49E+13	1.99E+13	3.02E+13	4.89E+13	7.04E+13	8.39E+13	8.34E+13	7.27E+13	5.89E+13	4.66E+13	3.63E+13	2.74E+13	1.94E+13	1.28E+13	8.04E+12	5.32E+12	4.18E+12
5	2007	1.69E+14	7.52E+13	1.79E+13	3.01E+12	9.09E+12	1.47E+13	1.39E+13	1.24E+13	1.60E+13	2.59E+13	3.98E+13	5.51E+13	7.07E+13	8.55E+13	9.63E+13	9.92E+13	9.23E+13	7.74E+13	5.91E+13	4.21E+13	2.93E+13	2.10E+13	1.55E+13	1.14E+13	7.97E+12	5.12E+12
6	2007	1.98E+14	1.41E+14	9.25E+13	5.63E+13	3.07E+13	1.49E+13	8.39E+12	9.47E+12	1.66E+13	2.89E+13	4.50E+13	6.22E+13	7.75E+13	8.84E+13	9.31E+13	9.03E+13	8.10E+13	6.80E+13	5.41E+13	4.09E+13	2.96E+13	2.09E+13	1.46E+13	1.06E+13	7.43E+12	4.75E+12
7	2007	3.56E+13	4.79E+13	4.93E+13	3.77E+13	2.12E+13	1.00E+13	8.53E+12	1.44E+13	2.33E+13	3.27E+13	4.26E+13	5.32E+13	6.43E+13	7.51E+13	8.32E+13	8.55E+13	8.03E+13	6.85E+13	5.39E+13	4.00E+13	2.90E+13	2.10E+13	1.53E+13	1.10E+13	7.62E+12	4.93E+12
6	2008	1.82E+14	9.18E+13	3.14E+13	8.78E+12	9.70E+12	1.57E+13	1.80E+13	1.81E+13	1.99E+13	2.50E+13	3.32E+13	4.50E+13	6.05E+13	7.68E+13	8.87E+13	9.18E+13	8.52E+13	7.19E+13	5.63E+13	4.17E+13	3.00E+13	2.13E+13	1.51E+13	1.06E+13	7.35E+12	4.80E+12
7	2008	1.46E+14	7.29E+13	2.58E+13	9.48E+12	1.00E+13	1.23E+13	1.13E+13	1.05E+13	1.43E+13	2.47E+13	4.06E+13	5.90E+13	7.73E+13	9.26E+13	1.02E+14	1.02E+14	9.23E+13	7.54E+13	5.68E+13	4.05E+13	2.85E+13	2.03E+13	1.48E+13	1.07E+13	7.41E+12	4.67E+12
8	2008	4.41E+13	3.82E+13	2.84E+13	1.63E+13	6.33E+12	9.51E+11	7.72E+11	6.41E+12	1.78E+13	3.23E+13	4.64E+13	6.08E+13	7.76E+13	9.42E+13	1.02E+14	9.57E+13	7.87E+13	6.09E+13	4.87E+13	4.08E+13	3.32E+13	2.44E+13	1.58E+13	9.39E+12	5.95E+12	4.73E+12
12	2008	7.58E+13	4.95E+13	3.25E+13	2.54E+13	2.23E+13	1.87E+13	1.51E+13	1.55E+13	2.30E+13	3.68E+13	5.35E+13	6.97E+13	8.32E+13	9.26E+13	9.57E+13	9.07E+13	7.90E+13	6.38E+13	4.93E+13	3.75E+13	2.85E+13	2.15E+13	1.56E+13	1.10E+13	7.56E+12	4.98E+12
1	2009	4.82E+13	3.86E+13	2.95E+13	2.26E+13	1.85E+13	1.60E+13	1.45E+13	1.50E+13	1.98E+13	3.05E+13	4.76E+13	6.89E+13	9.01E+13	1.05E+14	1.11E+14	1.04E+14	8.78E+13	6.93E+13	5.29E+13	4.02E+13	3.01E+13	2.19E+13	1.53E+13	1.06E+13	7.17E+12	4.60E+12
2	2009	1.04E+14	4.86E+13	1.43E+13	4.90E+12	8.17E+12	1.18E+13	1.22E+13	1.19E+13	1.47E+13	2.21E+13	3.25E+13	4.37E+13	5.49E+13	6.62E+13	7.65E+13	8.21E+13	7.96E+13	6.94E+13	5.54E+13	4.17E+13	3.03E+13	2.15E+13	1.49E+13	1.02E+13	7.12E+12	5.15E+12
3	2009	3.80E+13	4.57E+13	4.28E+13	3.10E+13	1.89E+13	1.14E+13	8.74E+12	1.07E+13	1.72E+13	2.65E+13	3.62E+13	4.56E+13	5.60E+13	6.82E+13	7.93E+13	8.40E+13	7.92E+13	6.64E+13	5.08E+13	3.73E+13	2.74E+13	2.05E+13	1.52E+13	1.09E+13	7.63E+12	5.02E+12
4	2009	3.25E+13	5.05E+13	4.90E+13	3.07E+13	1.21E+13	3.60E+12	4.17E+12	8.85E+12	1.50E+13	2.23E+13	3.12E+13	4.18E+13	5.34E+13	6.35E+13	6.80E+13	6.45E+13	5.42E+13	4.17E+13	3.19E+13	2.62E+13	2.26E+13	1.88E+13	1.42E+13	9.76E+12	6.49E+12	4.40E+12
5	2009	1.97E+14	1.21E+14	6.65E+13	3.90E+13	2.94E+13	2.57E+13	2.11E+13	1.58E+13	1.39E+13	1.97E+13	3.35E+13	4.96E+13	6.05E+13	6.31E+13	6.16E+13	6.04E+13	5.89E+13	5.35E+13	4.40E+13	3.36E+13	2.49E+13	1.84E+13	1.35E+13	9.70E+12	6.82E+12	4.64E+12
6	2009	9.37E+12	2.15E+13	2.81E+13	2.80E+13	2.31E+13	1.64E+13	1.10E+13	1.00E+13	1.51E+13	2.60E+13	4.13E+13	5.98E+13	7.96E+13	9.54E+13	1.02E+14	9.73E+13	8.49E+13	6.97E+13	5.47E+13	4.12E+13	2.86E+13	2.05E+13	1.42E+13	1.01E+13	6.96E+12	4.04E+12
7	2009	1.46E+14	8.65E+13	4.24E+13	1.95E+13	1.29E+13	1.31E+13	1.36E+13	1.38E+13	1.72E+13	2.73E+13	4.54E+13	6.93E+13	9.37E+13	1.11E+14	1.17E+14	1.11E+14	9.54E+13	7.58E+13	5.67E+13	4.10E+13	2.94E+13	2.11E+13	1.50E+13	1.03E+13	6.92E+12	4.55E+12
8	2009	2.24E+14	1.16E+14	4.02E+13	7.54E+12	3.79E+12	8.48E+12	1.02E+13	9.91E+12	1.39E+13	2.60E+13	4.45E+13	6.49E+13	8.38E+13	9.92E+13	1.09E+14	1.08E+14	9.71E+13	7.87E+13	5.90E+13	4.25E+13	3.04E+13	2.18E+13	1.56E+13	1.10E+13	7.51E+12	4.91E+12
9	2009	5.81E+13	5.37E+13	4.36E+13	2.94E+13	1.72E+13	1.04E+13	8.66E+12	1.09E+13	1.80E+13	3.13E+13	5.10E+13	7.52E+13	9.88E+13	1.15E+14	1.18E+14	1.08E+14	9.02E+13	7.02E+13	5.34E+13	4.07E+13	3.10E+13	2.29E+13	1.60E+13	1.07E+13	7.20E+12	4.83E+12
10	2009	7.88E+13	6.34E+13	4.76E+13	3.37E+13	2.27E+13	1.53E+13	1.17E+13	1.25E+13	1.89E+13	3.22E+13	5.27E+13	7.84E+13	1.03E+14	1.18E+14	1.20E+14	1.09E+14	9.10E+13	7.20E+13	5.47E+13	4.02E+13	2.90E+13	2.07E+13	1.48E+13	1.06E+13	7.47E+12	4.98E+12
11	2009	7.72E+13	7.65E+13	6.40E+13	4.22E+13	2.26E+13	1.24E+13	1.03E+13	1.31E+13	2.03E+13	3.30E+13	5.11E+13	7.24E+13	9.28E+13	1.07E+14	1.11E+14	1.03E+14	8.61E+13	6.67E+13	5.02E+13	3.79E+13	2.87E+13	2.11E+13	1.48E+13	1.01E+13	6.92E+12	4.81E+12
12	2009	1.04E+14	6.53E+13	3.52E+13	1.81E+13	1.21E+13	1.20E+13	1.38E+13	1.64E+13	2.11E+13	2.98E+13	4.43E+13	6.53E+13	8.85E+13	1.05E+14	1.09E+14	9.96E+13	8.44E+13	6.82E+13	5.33E+13	4.00E+13	2.87E+13	1.98E+13	1.35E+13	9.45E+12	6.67E+12	4.47E+12

Table A.38: Socorro ozone concentration (m^{-3}) (part 2)

Socorro: Ozone concentration per height increment

Month	Year	75 (km)	76 (km)	77 (km)	78 (km)	79 (km)	80 (km)	81 (km)	82 (km)	83 (km)	84 (km)	85 (km)	86 (km)	87 (km)	88 (km)	89 (km)	90 (km)	91 (km)	92 (km)	93 (km)	94 (km)	95 (km)	96 (km)	97 (km)	98 (km)	99 (km)	100 (km)
1	2010	7.21E+13	4.44E+13	2.52E+13	1.68E+13	1.53E+13	1.56E+13	1.65E+13	1.98E+13	2.70E+13	3.77E+13	5.28E+13	7.31E+13	9.47E+13	1.09E+14	1.10E+14	9.99E+13	8.46E+13	6.81E+13	5.27E+13	3.94E+13	2.88E+13	2.07E+13	1.45E+13	1.00E+13	6.90E+12	4.69E+12
2	2010	8.67E+13	5.37E+13	2.79E+13	1.34E+13	8.58E+12	8.33E+12	8.94E+12	1.06E+13	1.50E+13	2.29E+13	3.33E+13	4.53E+13	5.82E+13	7.14E+13	8.22E+13	8.68E+13	8.28E+13	7.13E+13	5.64E+13	4.20E+13	3.02E+13	2.13E+13	1.50E+13	1.06E+13	7.53E+12	5.27E+12
3	2010	2.30E+14	1.26E+14	5.13E+13	1.55E+13	7.20E+12	8.75E+12	1.04E+13	1.18E+13	1.57E+13	2.35E+13	3.54E+13	5.07E+13	6.83E+13	8.48E+13	9.50E+13	9.48E+13	8.51E+13	7.06E+13	5.57E+13	4.25E+13	3.11E+13	2.18E+13	1.49E+13	1.03E+13	7.15E+12	4.89E+12
4	2010	4.74E+13	6.97E+13	7.00E+13	4.88E+13	2.43E+13	1.14E+13	1.09E+13	1.70E+13	2.66E+13	3.92E+13	5.37E+13	6.77E+13	7.94E+13	8.88E+13	9.53E+13	9.67E+13	9.05E+13	7.73E+13	6.06E+13	4.47E+13	3.19E+13	2.23E+13	1.53E+13	1.02E+13	6.98E+12	5.01E+12
5	2010	8.77E+13	1.04E+14	9.73E+13	6.91E+13	3.78E+13	1.75E+13	9.66E+12	1.05E+13	1.70E+13	2.77E+13	4.13E+13	5.64E+13	7.16E+13	8.47E+13	9.23E+13	9.19E+13	8.36E+13	6.98E+13	5.43E+13	4.02E+13	2.90E+13	2.09E+13	1.50E+13	1.07E+13	7.47E+12	4.94E+12
6	2010	8.32E+13	6.65E+13	4.66E+13	2.71E+13	1.38E+13	8.04E+12	6.99E+12	8.92E+12	1.46E+13	2.52E+13	3.98E+13	5.64E+13	7.29E+13	8.70E+13	9.58E+13	9.63E+13	8.80E+13	7.35E+13	5.68E+13	4.16E+13	2.96E+13	2.09E+13	1.47E+13	1.04E+13	7.27E+12	4.98E+12
7	2010	2.17E+13	2.16E+13	1.99E+13	1.69E+13	1.35E+13	1.07E+13	9.09E+12	1.04E+13	1.65E+13	2.83E+13	4.45E+13	6.28E+13	8.03E+13	9.41E+13	1.02E+14	1.01E+14	9.18E+13	7.65E+13	5.91E+13	4.33E+13	3.10E+13	2.20E+13	1.55E+13	1.07E+13	7.24E+12	4.78E+12
8	2010	1.08E+14	6.46E+13	3.48E+13	2.12E+13	1.64E+13	1.34E+13	1.05E+13	1.07E+13	1.74E+13	3.09E+13	4.87E+13	6.73E+13	8.40E+13	9.66E+13	1.02E+14	9.97E+13	8.87E+13	7.28E+13	5.60E+13	4.12E+13	2.95E+13	2.09E+13	1.47E+13	1.03E+13	7.22E+12	4.97E+12
9	2010	8.41E+13	4.82E+13	2.45E+13	1.55E+13	1.43E+13	1.35E+13	1.18E+13	1.27E+13	1.97E+13	3.39E+13	5.40E+13	7.69E+13	9.75E+13	1.10E+14	1.12E+14	1.03E+14	8.96E+13	7.32E+13	5.65E+13	4.16E+13	2.99E+13	2.14E+13	1.55E+13	1.11E+13	7.77E+12	5.12E+12
10	2010	4.98E+13	5.07E+13	4.63E+13	3.63E+13	2.49E+13	1.59E+13	1.09E+13	1.17E+13	2.02E+13	3.68E+13	5.90E+13	8.25E+13	1.02E+14	1.14E+14	1.14E+14	1.04E+14	8.85E+13	7.17E+13	5.59E+13	4.21E+13	3.07E+13	2.19E+13	1.54E+13	1.07E+13	7.40E+12	4.81E+12
11	2010	9.30E+13	5.39E+13	2.81E+13	1.74E+13	1.45E+13	1.25E+13	1.00E+13	1.01E+13	1.58E+13	2.77E+13	4.41E+13	6.17E+13	7.71E+13	8.74E+13	9.09E+13	8.80E+13	8.00E+13	6.81E+13	5.41E+13	4.04E+13	2.89E+13	2.05E+13	1.47E+13	1.06E+13	7.44E+12	4.87E+12
12	2010	1.68E+14	1.08E+14	5.80E+13	2.54E+13	1.13E+13	9.54E+12	1.24E+13	1.70E+13	2.53E+13	3.88E+13	5.60E+13	7.28E+13	8.56E+13	9.33E+13	9.56E+13	9.24E+13	8.33E+13	6.95E+13	5.38E+13	3.91E+13	2.76E+13	1.93E+13	1.36E+13	9.53E+12	6.54E+12	4.22E+12
1	2011	6.26E+13	5.60E+13	4.58E+13	3.24E+13	1.98E+13	1.16E+13	9.88E+12	1.54E+13	2.70E+13	4.04E+13	5.12E+13	5.90E+13	6.76E+13	7.86E+13	8.74E+13	8.81E+13	7.95E+13	6.60E+13	5.22E+13	3.98E+13	2.91E+13	2.06E+13	1.43E+13	9.96E+12	6.73E+12	4.07E+12
2	2011	9.72E+13	5.84E+13	3.02E+13	1.58E+13	1.18E+13	1.20E+13	1.18E+13	1.10E+13	1.33E+13	2.15E+13	3.52E+13	5.19E+13	6.92E+13	8.48E+13	9.42E+13	9.28E+13	8.09E+13	6.40E+13	4.85E+13	3.70E+13	2.84E+13	2.11E+13	1.47E+13	9.65E+12	6.38E+12	4.54E+12
3	2011	1.03E+14	8.02E+13	5.60E+13	3.31E+13	1.74E+13	1.22E+13	1.55E+13	2.21E+13	2.85E+13	3.35E+13	3.80E+13	4.52E+13	5.79E+13	7.41E+13	8.65E+13	8.76E+13	7.74E+13	6.22E+13	4.81E+13	3.67E+13	2.77E+13	2.02E+13	1.45E+13	1.02E+13	7.05E+12	4.60E+12
4	2011	1.44E+14	7.26E+13	2.56E+13	8.51E+12	9.43E+12	1.35E+13	1.45E+13	1.48E+13	1.91E+13	2.91E+13	4.26E+13	5.52E+13	6.37E+13	6.80E+13	6.95E+13	6.92E+13	6.60E+13	5.85E+13	4.74E+13	3.57E+13	2.60E+13	1.89E+13	1.34E+13	9.29E+12	6.54E+12	4.96E+12
5	2011	1.01E+14	7.89E+13	5.42E+13	3.10E+13	1.63E+13	1.09E+13	1.07E+13	1.21E+13	1.50E+13	2.01E+13	2.66E+13	3.23E+13	3.55E+13	3.68E+13	3.84E+13	4.06E+13	4.15E+13	3.93E+13	3.42E+13	2.78E+13	2.16E+13	1.63E+13	1.19E+13	8.52E+12	5.99E+12	4.10E+12
6	2011	8.28E+13	3.99E+13	1.55E+13	1.14E+13	1.54E+13	1.62E+13	1.26E+13	9.11E+12	1.05E+13	1.77E+13	2.84E+13	3.89E+13	4.69E+13	5.14E+13	5.24E+13	5.04E+13	4.65E+13	4.16E+13	3.62E+13	3.01E+13	2.37E+13	1.78E+13	1.30E+13	9.56E+12	6.95E+12	4.79E+12
7	2011	1.44E+14	8.18E+13	3.87E+13	1.93E+13	1.47E+13	1.43E+13	1.31E+13	1.17E+13	1.26E+13	1.75E+13	2.69E+13	3.99E+13	5.45E+13	6.80E+13	7.68E+13	7.82E+13	7.19E+13	6.06E+13	4.77E+13	3.60E+13	2.63E+13	1.88E+13	1.33E+13	9.23E+12	6.44E+12	4.47E+12
8	2011	1.17E+14	6.74E+13	3.20E+13	1.51E+13	1.07E+13	1.02E+13	9.29E+12	8.81E+12	1.21E+13	2.14E+13	3.56E+13	5.14E+13	6.48E+13	7.38E+13	7.78E+13	7.70E+13	7.16E+13	6.23E+13	5.05E+13	3.85E+13	2.79E+13	1.97E+13	1.38E+13	9.75E+12	6.87E+12	4.67E+12
9	2011	9.77E+13	6.43E+13	3.76E+13	2.22E+13	1.62E+13	1.36E+13	1.12E+13	1.08E+13	1.69E+13	3.07E+13	4.98E+13	6.84E+13	8.17E+13	8.78E+13	8.75E+13	8.28E+13	7.49E+13	6.46E+13	5.25E+13	4.01E+13	2.92E+13	2.08E+13	1.48E+13	1.06E+13	7.36E+12	4.71E+12
10	2011	2.94E+13	3.87E+13	3.94E+13	3.02E+13	1.79E+13	9.43E+12	7.09E+12	1.02E+13	1.85E+13	3.27E+13	5.22E+13	7.41E+13	9.30E+13	1.04E+14	1.05E+14	9.65E+13	8.25E+13	6.68E+13	5.19E+13	3.90E+13	2.84E+13	2.01E+13	1.39E+13	9.64E+12	6.79E+12	4.81E+12
11	2011	8.62E+13	5.60E+13	3.12E+13	1.57E+13	9.30E+12	8.78E+12	1.07E+13	1.36E+13	1.83E+13	2.69E+13	4.03E+13	5.68E+13	7.32E+13	8.55E+13	9.08E+13	8.77E+13	7.76E+13	6.38E+13	4.97E+13	3.72E+13	2.72E+13	1.96E+13	1.41E+13	1.02E+13	7.11E+12	4.50E+12
12	2011	2.70E+13	3.21E+13	3.15E+13	2.48E+13	1.65E+13	1.24E+13	1.35E+13	1.74E+13	2.28E+13	3.19E+13	4.71E+13	6.77E+13	8.89E+13	1.04E+14	1.07E+14	9.93E+13	8.53E+13	6.99E+13	5.50E+13	4.13E+13	2.94E+13	2.03E+13	1.41E+13	9.96E+12	7.11E+12	4.89E+12
1	2012	4.37E+13	3.81E+13	3.10E+13	2.34E+13	1.85E+13	1.72E+13	1.77E+13	1.79E+13	1.83E+13	2.13E+13	3.01E+13	4.61E+13	6.58E+13	8.13E+13	8.60E+13	8.05E+13	6.97E+13	5.77E+13	4.58E+13	3.50E+13	2.62E+13	1.95E+13	1.44E+13	1.04E+13	7.35E+12	4.85E+12
2	2012	1.91E+13	7.12E+13	8.55E+13	6.14E+13	2.77E+13	8.17E+12	5.65E+12	1.10E+13	1.73E+13	2.51E+13	3.97E+13	6.29E+13	8.72E+13	1.01E+14	9.92E+13	8.76E+13	7.29E+13	5.99E+13	4.96E+13	4.05E+13	3.11E+13	2.20E+13	1.44E+13	9.33E+12	6.59E+12	5.25E+12
3	2012	4.40E+13	6.02E+13	6.06E+13	4.52E+13	2.58E+13	1.25E+13	7.16E+12	6.72E+12	9.38E+12	1.58E+13	2.64E+13	3.96E+13	5.24E+13	6.19E+13	6.68E+13	6.68E+13	6.23E+13	5.44E+13	4.48E+13	3.48E+13	2.57E+13	1.86E+13	1.35E+13	9.87E+12	7.08E+12	4.62E+12
4	2012	9.59E+13	7.20E+13	4.97E+13	3.26E+13	2.29E+13	1.90E+13	1.72E+13	1.64E+13	1.80E+13	2.36E+13	3.32E+13	4.60E+13	6.05E+13	7.31E+13	7.87E+13	7.53E+13	6.56E+13	5.44E+13	4.38E+13	3.42E+13	2.56E+13	1.84E+13	1.30E+13	9.11E+12	6.47E+12	4.52E+12
5	2012	1.02E+12	4.80E+13	6.92E+13	6.09E+13	3.89E+13	2.09E+13	1.36E+13	1.51E+13	2.33E+13	3.88E+13	6.17E+13	8.88E+13	1.13E+14	1.27E+14	1.26E+14	1.12E+14	9.13E+13	7.13E+13	5.46E+13	4.06E+13	2.87E+13	1.90E+13	1.21E+13	7.86E+12	5.62E+12	4.36E+12

Table A.39: Yellowknife ozone concentration (m^{-3}) (part 1)

Yellowknife: Ozone concentration per height increment

Month	Year	75 (km)	76 (km)	77 (km)	78 (km)	79 (km)	80 (km)	81 (km)	82 (km)	83 (km)	84 (km)	85 (km)	86 (km)	87 (km)	88 (km)	89 (km)	90 (km)	91 (km)	92 (km)	93 (km)	94 (km)	95 (km)	96 (km)	97 (km)	98 (km)	99 (km)	100 (km)
6	2002	3.59E+11	1.36E+14	1.79E+14	1.34E+14	7.13E+13	3.85E+13	3.54E+13	4.42E+13	5.67E+13	7.84E+13	1.15E+14	1.59E+14	1.91E+14	1.97E+14	1.80E+14	1.51E+14	1.21E+14	9.40E+13	7.01E+13	4.95E+13	3.22E+13	1.90E+13	1.03E+13	5.23E+12	2.26E+12	8.85E+10
7	2002	3.72E+14	3.05E+14	2.38E+14	1.67E+14	9.32E+13	3.58E+13	1.05E+13	1.60E+13	4.27E+13	8.36E+13	1.31E+14	1.70E+14	1.91E+14	1.92E+14	1.78E+14	1.55E+14	1.28E+14	9.95E+13	7.26E+13	4.97E+13	3.14E+13	1.84E+13	1.06E+13	6.51E+12	3.67E+12	7.90E+11
8	2002	2.90E+14	2.19E+14	1.41E+14	7.36E+13	3.54E+13	2.54E+13	2.85E+13	3.57E+13	4.73E+13	6.57E+13	9.12E+13	1.23E+14	1.58E+14	1.85E+14	1.91E+14	1.73E+14	1.38E+14	1.01E+14	7.06E+13	4.99E+13	3.58E+13	2.52E+13	1.65E+13	9.84E+12	6.18E+12	5.15E+12
3	2003	-1.09E+10	2.69E+12	3.02E+12	2.18E+12	5.78E+12	1.88E+13	3.69E+13	4.64E+13	4.03E+13	3.01E+13	3.40E+13	5.49E+13	7.82E+13	9.02E+13	9.16E+13	9.03E+13	8.87E+13	8.23E+13	6.76E+13	4.71E+13	2.75E+13	1.36E+13	6.01E+12	2.47E+12	7.97E+11	-5.20E+10
4	2003	2.95E+14	1.31E+14	3.33E+13	8.79E+12	1.69E+13	2.09E+13	1.33E+13	4.20E+12	4.41E+12	1.66E+13	3.56E+13	5.27E+13	6.24E+13	6.64E+13	6.91E+13	7.11E+13	6.84E+13	5.95E+13	4.71E+13	3.55E+13	2.66E+13	1.99E+13	1.41E+13	8.67E+12	3.99E+12	2.12E+11
5	2003	6.24E+14	3.39E+14	1.35E+14	3.69E+13	1.46E+13	1.92E+13	2.10E+13	1.76E+13	2.01E+13	3.55E+13	5.87E+13	7.73E+13	8.56E+13	8.91E+13	9.45E+13	9.93E+13	9.59E+13	8.16E+13	6.10E+13	4.10E+13	2.61E+13	1.71E+13	1.26E+13	9.65E+12	5.58E+12	4.52E+10
6	2003	7.83E+14	5.05E+14	2.99E+14	1.79E+14	1.18E+14	8.18E+13	5.50E+13	3.58E+13	3.11E+13	4.43E+13	6.89E+13	9.52E+13	1.17E+14	1.32E+14	1.35E+14	1.25E+14	1.04E+14	7.87E+13	5.64E+13	3.94E+13	2.77E+13	2.00E+13	1.49E+13	1.11E+13	7.67E+12	4.23E+12
7	2003	4.62E+14	3.63E+14	2.46E+14	1.27E+14	4.85E+13	2.36E+13	2.97E+13	3.92E+13	4.35E+13	5.10E+13	7.11E+13	1.02E+14	1.30E+14	1.43E+14	1.35E+14	1.15E+14	9.29E+13	7.46E+13	5.95E+13	4.51E+13	3.15E+13	2.11E+13	1.47E+13	1.09E+13	8.03E+12	5.31E+12
8	2003	1.94E+10	1.28E+14	1.64E+14	1.18E+14	5.91E+13	2.86E+13	2.20E+13	2.50E+13	3.41E+13	5.14E+13	7.62E+13	1.04E+14	1.28E+14	1.41E+14	1.38E+14	1.22E+14	1.00E+14	7.79E+13	5.81E+13	4.19E+13	2.98E+13	2.14E+13	1.55E+13	1.13E+13	7.94E+12	5.16E+12
9	2003	4.12E+14	2.40E+14	1.24E+14	6.93E+13	4.29E+13	2.47E+13	1.54E+13	2.18E+13	4.63E+13	8.26E+13	1.17E+14	1.39E+14	1.46E+14	1.40E+14	1.28E+14	1.13E+14	9.61E+13	7.86E+13	6.10E+13	4.49E+13	3.18E+13	2.20E+13	1.53E+13	1.07E+13	7.50E+12	5.04E+12
10	2003	1.25E+14	6.74E+13	3.09E+13	1.90E+13	1.88E+13	1.83E+13	1.60E+13	1.86E+13	3.13E+13	5.07E+13	6.96E+13	8.73E+13	1.08E+14	1.28E+14	1.36E+14	1.23E+14	9.77E+13	7.12E+13	5.22E+13	4.01E+13	3.10E+13	2.26E+13	1.50E+13	9.46E+12	6.46E+12	5.34E+12
11	2003	2.26E+13	2.30E+13	2.32E+13	2.19E+13	1.76E+13	1.16E+13	8.30E+12	1.47E+13	3.51E+13	6.59E+13	9.54E+13	1.15E+14	1.24E+14	1.27E+14	1.20E+14	9.88E+13	6.98E+13	4.53E+13	3.33E+13	3.01E+13	2.69E+13	1.96E+13	1.09E+13	4.73E+12	1.71E+12	2.47E+11
12	2003	1.36E+14	9.44E+13	6.31E+13	4.35E+13	3.01E+13	1.86E+13	1.09E+13	1.40E+13	3.34E+13	6.75E+13	1.08E+14	1.45E+14	1.70E+14	1.76E+14	1.61E+14	1.34E+14	1.03E+14	7.65E+13	5.70E+13	4.31E+13	3.24E+13	2.34E+13	1.57E+13	9.13E+12	3.96E+12	-1.54E+11
1	2004	2.71E+13	2.34E+13	1.93E+13	1.64E+13	1.63E+13	1.82E+13	2.03E+13	2.55E+13	4.22E+13	7.71E+13	1.25E+14	1.69E+14	1.90E+14	1.81E+14	1.51E+14	1.18E+14	9.38E+13	7.68E+13	6.22E+13	4.76E+13	3.38E+13	2.24E+13	1.42E+13	9.16E+12	6.71E+12	5.81E+12
2	2004	1.93E+13	3.35E+13	3.48E+13	2.53E+13	1.64E+13	1.43E+13	1.75E+13	2.46E+13	3.88E+13	6.33E+13	9.52E+13	1.25E+14	1.41E+14	1.39E+14	1.23E+14	1.01E+14	7.84E+13	5.79E+13	4.08E+13	2.74E+13	1.74E+13	1.05E+13	5.78E+12	2.74E+12	9.34E+11	-7.97E+10
3	2004	4.62E+10	4.93E+13	6.59E+13	5.23E+13	3.30E+13	2.21E+13	1.80E+13	1.62E+13	1.64E+13	2.22E+13	3.93E+13	6.94E+13	1.04E+14	1.28E+14	1.32E+14	1.19E+14	9.79E+13	7.46E+13	5.39E+13	3.80E+13	2.66E+13	1.81E+13	1.14E+13	6.90E+12	5.02E+12	5.09E+12
4	2004	1.52E+14	1.01E+14	6.54E+13	4.69E+13	3.86E+13	3.31E+13	2.67E+13	2.09E+13	2.19E+13	3.44E+13	5.60E+13	7.86E+13	9.69E+13	1.11E+14	1.20E+14	1.18E+14	1.03E+14	8.08E+13	5.91E+13	4.26E+13	3.12E+13	2.27E+13	1.55E+13	9.76E+12	6.27E+12	4.91E+12
5	2004	2.17E+14	1.29E+14	7.16E+13	5.58E+13	6.40E+13	6.91E+13	5.84E+13	4.04E+13	3.10E+13	3.74E+13	5.42E+13	7.23E+13	8.86E+13	1.05E+14	1.18E+14	1.20E+14	1.06E+14	7.94E+13	5.18E+13	3.24E+13	2.36E+13	2.07E+13	1.80E+13	1.36E+13	8.84E+12	4.95E+12
6	2004	1.45E+14	7.84E+13	4.19E+13	3.78E+13	4.47E+13	4.37E+13	3.57E+13	3.51E+13	5.02E+13	7.37E+13	9.34E+13	1.08E+14	1.24E+14	1.40E+14	1.46E+14	1.34E+14	1.09E+14	8.02E+13	5.59E+13	3.70E+13	2.30E+13	1.39E+13	9.53E+12	8.08E+12	6.94E+12	5.18E+12
7	2004	-1.78E+11	7.61E+12	2.01E+13	3.69E+13	5.35E+13	6.32E+13	5.90E+13	4.32E+13	3.22E+13	4.26E+13	7.01E+13	9.27E+13	9.52E+13	8.61E+13	8.12E+13	8.23E+13	7.89E+13	6.56E+13	4.76E+13	3.22E+13	2.26E+13	1.71E+13	1.33E+13	9.99E+12	7.28E+12	5.27E+12
8	2004	6.34E+11	7.51E+13	1.12E+14	1.06E+14	7.87E+13	5.00E+13	3.02E+13	2.45E+13	3.64E+13	6.32E+13	9.63E+13	1.27E+14	1.50E+14	1.60E+14	1.53E+14	1.34E+14	1.08E+14	8.25E+13	6.12E+13	4.47E+13	3.24E+13	2.32E+13	1.64E+13	1.08E+13	5.42E+12	-2.66E+10
9	2004	2.68E+12	2.04E+13	3.52E+13	4.22E+13	3.83E+13	2.70E+13	1.67E+13	1.51E+13	2.53E+13	4.64E+13	7.46E+13	1.05E+14	1.32E+14	1.40E+14	1.44E+14	1.22E+14	9.38E+13	6.91E+13	5.19E+13	4.03E+13	3.12E+13	2.30E+13	1.60E+13	1.08E+13	7.44E+12	5.16E+12
10	2004	1.69E+14	1.11E+14	6.60E+13	3.89E+13	2.78E+13	2.57E+13	2.58E+13	2.65E+13	3.30E+13	5.43E+13	9.38E+13	1.40E+14	1.74E+14	1.82E+14	1.65E+14	1.37E+14	1.09E+14	8.43E+13	6.37E+13	4.64E+13	3.26E+13	2.25E+13	1.57E+13	1.11E+13	7.64E+12	4.72E+12
11	2004	7.40E+12	1.60E+13	2.27E+13	2.57E+13	2.30E+13	1.45E+13	6.45E+12	1.10E+13	3.63E+13	7.67E+13	1.17E+14	1.45E+14	1.63E+14	1.70E+14	1.63E+14	1.40E+14	1.09E+14	8.11E+13	6.01E+13	4.41E+13	3.02E+13	1.82E+13	9.77E+12	5.46E+12	4.41E+12	5.10E+12
12	2004	2.60E+13	4.21E+13	4.80E+13	4.17E+13	2.98E+13	2.05E+13	1.92E+13	2.86E+13	5.07E+13	8.47E+13	1.22E+14	1.50E+14	1.62E+14	1.59E+14	1.45E+14	1.24E+14	9.97E+13	7.70E+13	5.79E+13	4.25E+13	3.05E+13	2.14E+13	1.52E+13	1.09E+13	7.65E+12	5.04E+12
1	2005	9.55E+13	6.21E+13	3.64E+13	2.17E+13	1.57E+13	1.27E+13	1.04E+13	1.41E+13	3.21E+13	6.79E+13	1.13E+14	1.51E+14	1.69E+14	1.68E+14	1.54E+14	1.33E+14	1.09E+14	8.42E+13	6.21E+13	4.39E+13	3.01E+13	2.01E+13	1.27E+13	7.28E+12	3.20E+12	-2.48E+10
2	2005	7.87E+13	4.84E+13	2.38E+13	1.08E+13	9.95E+12	1.45E+13	1.63E+13	1.32E+13	1.09E+13	1.94E+13	4.45E+13	8.09E+13	1.14E+14	1.30E+14	1.20E+14	9.39E+13	6.62E+13	4.95E+13	4.33E+13	3.91E+13	3.05E+13	1.87E+13	8.28E+12	2.69E+12	2.16E+12	4.73E+12
3	2005	3.11E+14	1.63E+14	6.50E+13	2.50E+13	1.87E+13	2.02E+13	2.00E+13	2.19E+13	3.45E+13	6.19E+13	9.94E+13	1.32E+14	1.43E+14	1.28E+14	9.95E+13	7.89E+13	7.33E+13	7.21E+13	6.33E+13	4.60E+13	2.80E+13	1.63E+13	1.12E+13	9.24E+12	7.47E+12	5.13E+12
4	2005	4.79E+13	3.37E+13	2.16E+13	1.44E+13	1.23E+13	1.20E+13	1.06E+13	8.67E+12	1.02E+13	1.92E+13	3.70E+13	6.25E+13	9.26E+13	1.20E+14	1.31E+14	1.21E+14	9.48E+13	6.77E+13	4.88E+13	3.83E+13	3.12E+13	2.37E+13	1.56E+13	8.69E+12	4.85E+12	3.76E+12
5	2005	1.14E+14	4.53E+13	7.12E+12	2.77E+12	1.30E+13	1.96E+13	1.93E+13	1.98E+13	2.91E+13	4.89E+13	7.30E+13	9.11E+13	9.76E+13	9.64E+13	9.46E+13	9.33E+13	8.80E+13	7.53E+13	5.73E+13	3.96E+13	2.66E+13	1.88E+13	1.42E+13	1.08E+13	7.59E+12	4.53E+12
6	2005	8.32E+13	1.86E+14	2.11E+14	1.55E+14	7.63E+13	2.79E+13	1.81E+13	3.03E+13	5.21E+13	7.91E+13	1.07E+14	1.29E+14	1.44E+14	1.50E+14	1.46E+14	1.31E+14	1.09E+14	8.50E+13	6.27E+13	4.41E+13	3.00E+13	2.06E+13	1.47E+13	1.06E+13	7.08E+12	3.69E+12
7	2005	1.95E+12	8.23E+13	1.41E+14	1.61E+14	1.37E+14	8.61E+13	3.82E+13	1.96E+13	3.32E+13	6.38E+13	9.39E+13	1.13E+14	1.20E+14	1.22E+14	1.25E+14	1.26E+14	1.20E+14	1.02E+14	7.64E+13	4.91E+13	2.69E+13	1.38E+13	9.34E+12	8.90E+12	7.92E+12	5.34E+12
8	2005	8.44E+11	1.58E+13	3.52E+13	5.30E+13	5.66E+13	4.30E+13	2.66E+13	2.58E+13	4.72E+13	8.44E+13	1.26E+14	1.62E+14	1.81E+14	1.81E+14	1.66E+14	1.43E+14	1.16E+14	8.99E+13	6.63E+13	4.65E+13	3.05E+13	1.82E+13	1.02E+13	6.58E+12	5.48E+12	5.24E+12
9	2005	1.45E+14	9.72E+13	5.76E+13	3.07E+13	1.84E+13	1.13E+13	1.06E+13	1.41E+13	2.59E+13	4.80E+13	7.58E+13	1.01E+14	1.18E+14	1.27E+14	1.30E+14	1.23E+14	1.07E+14	8.54E+13	6.44E+13	4.71E+13	3.38E+13	2.39E+13	1.64E+13	1.10E+13	7.46E+12	5.27E+12
10	2005	3.11E+14	1.59E+14	5.70E+13	1.49E+13	8.62E+12	8.61E+12	5.28E+12	9.17E+12	3.45E+13	8.22E+13	1.37E+14	1.76E+14	1.87E+14	1.75E+14	1.50E+14	1.23E+14	9.82E+13	7.76E+13	6.06E+13	4.63E+13	3.39E+13	2.38E+13	1.63E+13	1.11E+13	7.65E+12	5.05E+12
11	2005	1.72E+14	9.12E+13	3.83E+13	2.00E+13	2.13E+13	2.44E+13	2.53E+13	3.15E+13	4.70E+13	6.39E+13	7.17E+13	7.27E+13	8.11E+13	1.02E+14	1.21E+14	1.25E+14	1.11E+14	8.85E+13	6.62E+13	4.80E+13	3.43E+13	2.42E+13	1.69E+13	1.16E+13	7.79E+12	5.01E+12
12	2005	3.72E+13	4.78E+13	4.78E+13	3.76E+13	2.68E+13	2.25E+13	2.44E+13	2.97E+13	3.81E+13	5.08E+13	6.78E+13	8.82E+13	1.11E+13	1.30E+14	1.37E+14	1.27E+14	1.05E+14	8.07E+13	6.05E+13	4.55E+13	3.35E+13	2.30E+13	1.41E+13	7.84E+12	4.94E+12	4.52E+12

Table A.40: Yellowknife ozone concentration (m^{-3}) (part 2)

Yellowknife: Ozone concentration per height increment

Month	Year	75 (km)	76 (km)	77 (km)	78 (km)	79 (km)	80 (km)	81 (km)	82 (km)	83 (km)	84 (km)	85 (km)	86 (km)	87 (km)	88 (km)	89 (km)	90 (km)	91 (km)	92 (km)	93 (km)	94 (km)	95 (km)	96 (km)	97 (km)	98 (km)	99 (km)	100 (km)
1	2006	1.99E+14	1.46E+14	9.99E+13	6.42E+13	3.85E+13	2.04E+13	1.11E+13	1.66E+13	4.02E+13	7.46E+13	1.04E+14	1.17E+14	1.21E+14	1.24E+14	1.25E+14	1.18E+14	1.02E+14	8.08E+13	5.95E+13	4.17E+13	2.89E+13	2.06E+13	1.51E+13	1.10E+13	7.43E+12	4.24E+12
2	2006	1.27E+14	6.62E+13	3.07E+13	2.58E+13	3.53E+13	4.14E+13	3.85E+13	3.49E+13	4.13E+13	6.01E+13	8.55E+13	1.11E+14	1.30E+14	1.39E+14	1.31E+14	1.11E+14	8.57E+13	6.26E+13	4.47E+13	3.37E+13	2.78E+13	2.31E+13	1.75E+13	1.17E+13	7.31E+12	4.53E+12
3	2006	3.58E+12	5.88E+13	7.84E+13	6.16E+13	3.40E+13	1.56E+13	8.80E+12	9.17E+12	1.64E+13	3.29E+13	5.74E+13	8.51E+13	1.10E+14	1.25E+14	1.26E+14	1.14E+14	9.49E+13	7.62E+13	5.96E+13	4.44E+13	3.07E+13	1.98E+13	1.27E+13	8.66E+12	6.34E+12	4.67E+12
4	2006	3.00E+14	1.45E+14	4.47E+13	8.73E+12	6.79E+12	9.93E+12	9.00E+12	8.06E+12	1.22E+13	2.14E+13	3.17E+13	4.14E+13	5.35E+13	7.12E+13	8.99E+13	9.98E+13	9.49E+13	7.76E+13	5.53E+13	3.51E+13	2.16E+13	1.54E+13	1.33E+13	1.15E+13	8.25E+12	4.08E+12
5	2006	2.35E+14	1.52E+14	9.58E+13	7.21E+13	6.29E+13	5.03E+13	3.30E+13	2.09E+13	2.01E+13	2.73E+13	3.64E+13	4.63E+13	6.04E+13	7.91E+13	9.40E+13	9.52E+13	8.25E+13	6.43E+13	4.90E+13	3.86E+13	3.09E+13	2.34E+13	1.56E+13	9.12E+12	5.59E+12	4.79E+12
6	2006	2.89E+14	2.46E+14	2.05E+14	1.60E+14	1.10E+14	6.99E+13	5.02E+13	4.91E+13	5.99E+13	7.72E+13	9.71E+13	1.15E+14	1.27E+14	1.30E+14	1.25E+14	1.11E+14	9.26E+13	7.34E+13	5.65E+13	4.28E+13	3.15E+13	2.18E+13	1.38E+13	8.29E+12	5.79E+12	5.43E+12
7	2006	1.78E+12	7.62E+13	1.13E+14	1.04E+14	7.40E+13	5.49E+13	5.60E+13	6.73E+13	7.68E+13	8.00E+13	8.17E+13	9.00E+13	1.06E+14	1.20E+14	1.23E+14	1.15E+14	9.99E+13	8.23E+13	6.38E+13	4.65E+13	3.25E+13	2.26E+13	1.60E+13	1.13E+13	7.74E+12	4.85E+12
8	2006	1.17E+14	9.78E+13	7.45E+13	5.16E+13	3.70E+13	3.17E+13	2.97E+13	2.76E+13	2.96E+13	4.10E+13	6.02E+13	8.09E+13	1.00E+14	1.19E+14	1.34E+14	1.35E+14	1.19E+14	9.19E+13	6.51E+13	4.51E+13	3.21E+13	2.33E+13	1.67E+13	1.14E+13	7.58E+12	4.82E+12
9	2006	2.68E+12	1.60E+13	2.55E+13	2.83E+13	2.38E+13	1.50E+13	6.84E+12	5.13E+12	1.42E+13	3.39E+13	5.91E+13	8.27E+13	9.92E+13	1.06E+14	1.02E+14	8.85E+13	6.99E+13	5.24E+13	4.04E+13	3.26E+13	2.46E+13	1.55E+13	7.01E+12	2.23E+12	1.84E+12	4.40E+12
11	2006	4.77E+13	2.36E+13	9.44E+12	4.99E+12	4.40E+12	6.51E+12	1.40E+13	2.47E+13	3.02E+13	2.65E+13	1.92E+13	1.57E+13	1.63E+13	1.87E+13	2.55E+13	3.99E+13	5.62E+13	6.26E+13	5.31E+13	3.30E+13	1.37E+13	2.75E+12	4.30E+11	2.13E+12	3.50E+12	3.42E+12
12	2006	3.42E+13	4.18E+13	3.97E+13	2.81E+13	1.52E+13	8.48E+12	7.99E+12	1.12E+13	1.85E+13	3.17E+13	4.89E+13	6.28E+13	6.80E+13	6.76E+13	6.84E+13	7.02E+13	6.63E+13	5.36E+13	3.75E+13	2.51E+13	1.76E+13	1.28E+13	9.51E+12	7.38E+12	5.70E+12	4.02E+12
1	2007	1.04E+13	6.68E+12	4.43E+12	3.17E+12	1.87E+12	1.29E+12	4.25E+12	1.32E+13	2.75E+13	4.38E+13	6.17E+13	8.54E+13	1.14E+14	1.33E+14	1.26E+14	9.84E+13	7.03E+13	5.46E+13	4.66E+13	3.88E+13	2.97E+13	2.09E+13	1.32E+13	7.41E+12	4.02E+12	2.41E+12
2	2007	3.89E+14	1.51E+14	9.32E+12	-2.20E+13	8.50E+11	2.11E+13	2.09E+13	1.08E+13	3.63E+12	2.68E+12	5.16E+12	8.70E+12	1.24E+13	1.53E+13	1.70E+13	1.90E+13	2.25E+13	2.61E+13	2.70E+13	2.40E+13	1.80E+13	1.13E+13	6.01E+12	2.73E+12	1.02E+12	5.26E+10
12	2007	2.44E+11	5.63E+12	1.16E+13	1.48E+13	1.74E+13	1.88E+13	1.49E+13	9.49E+12	6.78E+12	2.24E+13	4.67E+13	6.27E+13	5.74E+13	3.65E+13	1.72E+13	9.91E+12	1.21E+13	1.57E+13	1.61E+13	1.39E+13	1.16E+13	1.02E+13	9.16E+12	7.99E+12	6.55E+12	4.71E+12	2.45E+12	-4.19E+10
4	2008	2.83E+11	4.88E+12	1.13E+13	1.74E+13	1.88E+13	1.49E+13	9.49E+12	6.78E+12	7.95E+12	1.27E+13	2.17E+13	3.58E+13	5.36E+13	6.98E+13	7.90E+13	8.03E+13	7.60E+13	6.76E+13	5.50E+13	3.91E+13	2.36E+13	1.27E+13	7.93E+12	6.40E+12	4.16E+12	-9.11E+09
5	2008	3.86E+14	2.33E+14	1.26E+14	6.88E+13	3.81E+13	2.07E+13	1.63E+13	2.49E+13	4.32E+13	6.78E+13	9.41E+13	1.15E+14	1.26E+14	1.27E+14	1.24E+14	1.16E+14	1.01E+14	8.17E+13	6.10E+13	4.32E+13	2.96E+13	2.00E+13	1.30E+13	7.86E+12	4.24E+12	1.63E+12
6	2008	5.28E+11	8.72E+13	1.52E+14	1.73E+14	1.44E+14	9.25E+13	5.38E+13	4.23E+13	5.35E+13	7.63E+13	1.04E+14	1.30E+14	1.48E+14	1.52E+14	1.42E+14	1.25E+14	1.05E+14	8.47E+13	6.50E+13	4.76E+13	3.38E+13	2.35E+13	1.62E+13	1.12E+13	7.72E+12	5.12E+12
7	2008	5.25E+14	4.22E+14	3.09E+14	1.97E+14	1.11E+14	6.11E+13	4.21E+13	4.32E+13	5.96E+13	8.67E+13	1.17E+14	1.42E+14	1.59E+14	1.63E+14	1.54E+14	1.35E+14	1.12E+14	8.86E+13	6.77E+13	4.97E+13	3.53E+13	2.44E+13	1.67E+13	1.14E+13	7.84E+12	5.27E+12
8	2008	1.37E+14	2.11E+14	2.19E+14	1.58E+14	8.12E+13	3.24E+13	2.09E+13	3.38E+13	5.70E+13	8.24E+13	1.06E+14	1.27E+14	1.44E+14	1.53E+14	1.51E+14	1.37E+14	1.15E+14	9.00E+13	6.69E+13	4.81E+13	3.41E+13	2.40E+13	1.68E+13	1.17E+13	7.96E+12	5.21E+12
9	2008	1.27E+14	7.31E+13	4.05E+13	2.99E+13	2.67E+13	2.10E+13	1.36E+13	1.18E+13	2.20E+13	4.54E+13	7.63E+13	1.07E+14	1.32E+14	1.48E+14	1.51E+14	1.39E+14	1.15E+14	8.69E+13	6.32E+13	4.57E+13	3.30E+13	2.36E+13	1.65E+13	1.13E+13	7.63E+12	4.86E+12
10	2008	1.44E+14	1.01E+14	6.28E+13	3.37E+13	1.68E+13	9.89E+12	8.07E+12	9.30E+12	1.74E+13	3.88E+13	7.49E+13	1.18E+14	1.53E+14	1.68E+14	1.61E+14	1.39E+14	1.11E+14	8.49E+13	6.40E+13	4.75E+13	3.44E+13	2.43E+13	1.69E+13	1.13E+13	6.27E+12	1.33E+12
11	2008	1.23E+14	8.16E+13	5.07E+13	3.31E+13	2.41E+13	1.86E+13	1.57E+13	2.06E+13	4.12E+13	7.96E+13	1.26E+14	1.63E+14	1.77E+14	1.70E+14	1.47E+14	1.19E+14	9.42E+13	7.56E+13	6.18E+13	4.90E+13	3.59E+13	2.37E+13	1.40E+13	7.90E+12	5.42E+12	5.19E+12
12	2008	1.55E+14	1.12E+14	7.22E+13	4.18E+13	2.59E+13	2.20E+13	2.26E+13	2.58E+13	3.85E+13	6.67E+13	1.06E+14	1.44E+14	1.66E+14	1.48E+14	1.24E+14	9.91E+13	7.78E+13	5.99E+13	4.48E+13	3.23E+13	2.25E+13	1.55E+13	1.08E+13	7.56E+12	5.03E+12	
1	2009	1.43E+13	5.63E+13	7.04E+13	5.75E+13	3.83E+13	2.82E+13	2.76E+13	3.23E+13	4.27E+13	6.21E+13	9.09E+13	1.24E+14	1.52E+14	1.66E+14	1.59E+14	1.36E+14	1.08E+14	8.32E+13	6.31E+13	4.72E+13	3.45E+13	2.43E+13	1.65E+13	1.11E+13	7.64E+12	5.29E+12
2	2009	4.03E+13	6.40E+13	6.54E+13	4.55E+13	2.21E+13	9.17E+12	8.06E+12	1.38E+13	2.36E+13	4.04E+13	6.92E+13	1.08E+14	1.45E+14	1.64E+14	1.59E+14	1.36E+14	1.08E+14	8.21E+13	6.08E+13	4.39E+13	3.12E+13	2.18E+13	1.47E+13	9.38E+12	6.43E+12	5.54E+12
3	2009	2.88E+13	3.10E+13	3.18E+13	3.07E+13	2.71E+13	2.01E+13	1.23E+13	9.99E+12	2.06E+13	4.74E+13	8.48E+13	1.19E+14	1.36E+14	1.36E+14	1.26E+14	1.14E+14	9.99E+13	8.26E+13	6.36E+13	4.61E+13	3.23E+13	2.25E+13	1.60E+13	1.14E+13	8.05E+12	5.36E+12
4	2009	-1.07E+11	1.39E+13	2.14E+13	2.21E+13	1.87E+13	1.29E+13	6.78E+12	4.26E+12	9.38E+12	2.30E+13	4.22E+13	6.34E+13	8.39E+13	9.85E+13	1.01E+14	9.06E+13	7.50E+13	6.19E+13	5.24E+13	4.35E+13	3.34E+13	2.35E+13	1.56E+13	1.03E+13	7.16E+12	4.96E+12
5	2009	3.44E+13	6.46E+13	8.53E+13	8.76E+13	7.20E+13	5.03E+13	3.45E+13	3.01E+13	3.86E+13	5.90E+13	8.66E+13	1.13E+14	1.28E+14	1.31E+14	1.25E+14	1.17E+14	1.05E+14	8.68E+13	6.59E+13	4.68E+13	3.26E+13	2.30E+13	1.63E+13	1.14E+13	7.81E+12	5.29E+12
6	2009	3.75E+14	1.61E+14	4.23E+13	2.67E+13	5.36E+13	6.89E+13	6.56E+13	6.50E+13	8.04E+13	1.05E+14	1.25E+14	1.36E+14	1.43E+14	1.45E+14	1.37E+14	1.19E+14	9.79E+13	7.79E+13	6.08E+13	4.59E+13	3.31E+13	2.26E+13	1.44E+13	8.85E+12	5.99E+12	5.23E+12
7	2009	3.18E+14	1.76E+14	1.14E+14	1.22E+14	1.34E+14	1.07E+14	5.95E+13	3.25E+13	4.23E+13	7.78E+13	1.16E+14	1.41E+14	1.49E+14	1.48E+14	1.42E+14	1.31E+14	1.13E+14	8.85E+13	6.49E+13	4.57E+13	3.21E+13	2.30E+13	1.67E+13	1.20E+13	8.27E+12	5.03E+12
8	2009	2.31E+14	1.12E+14	4.12E+13	2.45E+13	3.23E+13	3.88E+13	3.96E+13	4.41E+13	5.99E+13	8.48E+13	1.10E+14	1.30E+14	1.44E+14	1.52E+14	1.51E+14	1.40E+14	1.19E+14	9.33E+13	6.81E+13	4.77E+13	3.32E+13	2.34E+13	1.66E+13	1.17E+13	8.04E+12	5.17E+12
9	2009	9.51E+13	1.24E+14	1.17E+14	7.73E+13	3.22E+13	6.37E+12	2.68E+12	1.28E+13	3.01E+13	5.06E+13	7.04E+13	8.75E+13	1.04E+14	1.22E+14	1.36E+14	1.36E+14	1.19E+14	9.18E+13	6.44E+13	4.40E+13	3.09E+13	2.25E+13	1.63E+13	1.15E+13	7.64E+12	4.97E+12
10	2009	4.23E+13	6.36E+13	6.67E+13	4.96E+13	2.57E+13	9.20E+12	5.57E+12	1.53E+13	3.78E+13	6.79E+13	9.49E+13	1.10E+14	1.15E+14	1.16E+14	1.18E+14	1.17E+14	1.07E+14	8.86E+13	6.65E+13	4.68E+13	3.22E+13	2.25E+13	1.60E+13	1.15E+13	8.10E+12	5.47E+12
11	2009	1.33E+14	9.70E+13	6.75E+13	4.83E+13	3.74E+13	3.01E+13	2.42E+13	2.23E+13	3.06E+13	5.53E+13	9.68E+13	1.45E+14	1.82E+14	1.92E+14	1.74E+14	1.40E+14	1.07E+14	8.15E+13	6.30E+13	4.81E+13	3.52E+13	2.45E+13	1.65E+13	1.11E+13	7.56E+12	5.07E+12
12	2009	2.72E+14	1.99E+14	1.30E+14	7.49E+13	4.22E+13	3.29E+13	4.15E+13	6.77E+13	1.15E+14	1.73E+14	2.16E+14	2.28E+14	2.11E+14	1.83E+14	1.57E+14	1.33E+14	1.05E+14	7.27E+13	4.47E+13	3.00E+13	2.62E+13	2.44E+13	1.95E+13	1.22E+13	5.21E+12	-3.13E+11

Curriculum Vita

Name	Reynold E. Sukara
Education	MSc. Physics, expected 2013 University of Western Ontario London, Ontario MSc. Geophysics, 2011 University of Western Ontario London, Ontario Hon. BSc. Geology, 2009 The University of Western Ontario London, Ontario
Awards	Integrating Atmospheric Chemistry and Physics from Earth to Space (IACPES) NSERC CREATE Scholarship (issuing institution: York University), 2011-2013 Northern Scientific Training Program, Indian and Northern Affairs Canada, 2011 Graduate Thesis Research Award, 2009, 2011, 2012 The Faculty of Science Teaching Assistant Award, 2010 Faculty of Science Entrance Scholarship, 2009
Related Work Experience	Graduate Research Assistant, 2011-2013 Department of Physics & Astronomy, The University of Western Ontario London, Ontario Teaching Assistant, 2011-2013 Department of Physics & Astronomy, The University of Western Ontario London, Ontario Graduate Research Assistant, 2009-2011 Earth Science Department, The University of Western Ontario London, Ontario Teaching Assistant, 2009-2011 Earth Science Department, The University of Western Ontario London, Ontario

Refereed Journal Articles

Sukara, R. E., Secco, R. E. (2012) *Viscosity of liquid sulfur at 4.5 GPa in the L and L' regions,* High Pressure Research: An International Journal, 32 (4), 451-456

Non-refereed Publications

Sukara, R. E. (2011) *Viscosity of Sulfur at 4.5 GPa and in the L and L' Liquid Regions*, MSc Thesis, The School of Graduate and Postdoctoral Studies, Western University, pp. 144

Sukara, R. E. (2010) *The Geodynamo: Origin of Earth's Magnetic Field*, Western Graduate Geoscience Reviews, Western University

Sukara, R. E. (2009) *Petrography and geochemistry of suevites from the Popigai Impact structure (Russia)*, Undergraduate Honours Thesis, Earth Science Department, Western University, pp. 102

Conference Proceedings

Sukara, R. E. and Hocking, W.K. (2013) *Mesospheric Ozone Determination from the Radar Meteor Echo Duration*, IACPES Symposium, York University, Toronto, Jun 10-14, 2013

Sukara, R. E. and Hocking, W.K. (2013) *Mesospheric Ozone Determination from the Radar Meteor Echo Duration*, DASP Conference, Kingston, Feb 17-20, 2013

Secco*, R. A., **Sukara, R. E.** (2012) *Viscosity of liquid sulfur at 4.5 GPa in the L and L' regions,* 50th EHPRG Meeting, September 16 - 21, 2012, Thessaloniki, Greece

Sukara, R. E. (2012) *Study of Overdense Meteors and the Secondary Ozone Layer Using VHF Meteor Radars*, IACPES Symposium, York University, Toronto, Aug 10, 2012

Osinski, G.R., **Sukara, R.E.**, Grieve, R.A.F. (2010) "Suevites" of the Popigai Impact Structure, Russia: (Mis)understood?, 41st Lunar and Planetary Science Conference, held March 1-5, 2010 in The Woodlands, Texas. LPI Contribution No. 1533, p.2171

Sukara R. E. and Osinski G. R. (2009) Origin of suevites at the Popigai impact structure, Russia (abstract #GA32B-03), Eos, Transactions, American Geophysical Union, 90(22), Joint Assembly Supplement, Toronto, Ontario, May 27 2009